ISSN 0021-9673

VOL. 511 JULY 6, 1990
COMPLETE IN ONE ISSUE

JOURNAL OF CHROMATOGRAPHY

INTERNATIONAL JOURNAL ON CHROMATOGRAPHY, ELECTROPHORESIS AND RELATED METHODS

ELSEVIER

JOURNAL OF CHROMATOGRAPHY

Scope. The *Journal of Chromatography* publishes papers on all aspects of chromatography, electrophoresis and related methods. Contributions consist mainly of research papers dealing with chromatographic theory, instrumental development and their applications. The section *Biomedical Applications*, which is under separate editorship, deals with the following aspects: developments in and applications of chromatographic and electrophoretic techniques related to clinical diagnosis or alterations during medical treatment; screening and profiling of body fluids or tissues with special reference to metabolic disorders; results from basic medical research with direct consequences in clinical practice; drug level monitoring and pharmacokinetic studies; clinical toxicology; analytical studies in occupational medicine.

Submission of Papers. Papers in English, French and German may be submitted, in three copies. Manuscripts should be submitted to: The Editor of *Journal of Chromatography*, P.O. Box 681, 1000 AR Amsterdam, The Netherlands, or to: The Editor of *Journal of Chromatography, Biomedical Applications*, P.O. Box 681, 1000 AR Amsterdam, The Netherlands. Review articles are invited or proposed by letter to the Editors. An outline of the proposed review should first be forwarded to the Editors for preliminary discussion prior to preparation. Submission of an article is understood to imply that the article is original and unpublished and is not being considered for publication elsewhere. For copyright regulations, see below.

Subscription Orders. Subscription orders should be sent to: Elsevier Science Publishers B.V., P.O. Box 211, 1000 AE Amsterdam, The Netherlands, Tel. 5803 911, Telex 18582 ESPA NL. The *Journal of Chromatography* and the *Biomedical Applications* section can be subscribed to separately.

Publication. The *Journal of Chromatography* (incl. *Biomedical Applications*) has 37 volumes in 1990. The subscription prices for 1990 are:

J. Chromatogr. (incl. *Cum. Indexes, Vols. 451–500*) + *Biomed. Appl.* (Vols. 498–534):
Dfl. 6734.00 plus Dfl. 1036.00 (p.p.h.) (total *ca.* US$ 3885.00)

J. Chromatogr. (incl. *Cum. Indexes, Vols. 451–500*) only (Vols. 498–524):
Dfl. 5616.00 plus Dfl. 756.00 (p.p.h.) (total *ca.* US$ 3186.00)

Biomed. Appl. only (Vols. 525–534):
Dfl. 2080.00 plus Dfl. 280.00 (p.p.h.) (total *ca.* US$ 1180.00).

Our p.p.h. (postage, package and handling) charge includes surface delivery of all issues, except to subscribers in Argentina, Australia, Brasil, Canada, China, Hong Kong, India, Israel, Malaysia, Mexico, New Zealand, Pakistan, Singapore, South Africa, South Korea, Taiwan, Thailand and the U.S.A. who receive all issues by air delivery (S.A.L. — Surface Air Lifted) at no extra cost. For Japan, air delivery requires 50% additional charge; for all other countries airmail and S.A.L. charges are available upon request. Back volumes of the *Journal of Chromatography* (Vols. 1–497) are available at Dfl. 195.00 (plus postage). Claims for missing issues will be honoured, free of charge, within three months after publication of the issue. Customers in the U.S.A. and Canada wishing information on this and other Elsevier journals, please contact Journal Information Center, Elsevier Science Publishing Co. Inc., 655 Avenue of the Americas, New York, NY 10010. Tel. (212) 633-3750.

Abstracts/Contents Lists published in Analytical Abstracts, ASCA, Biochemical Abstracts, Biological Abstracts, Chemical Abstracts, Chemical Titles, Chromatography Abstracts, Clinical Chemistry Lookout, Current Contents/Life Sciences, Current Contents/Physical, Chemical & Earth Sciences, Deep-Sea Research/Part B: Oceanographic Literature Review, Excerpta Medica, Index Medicus, Mass Spectrometry Bulletin, PASCAL-CNRS, Pharmaceutical Abstracts, Referativnyi Zhurnal, Science Citation Index and Trends in Biotechnology.

See inside back cover for Publication Schedule, Information for Authors and information on Advertisements.

0021-9673/90/$03.50

CONTENTS

(Abstracts/Contents Lists published in Analytical Abstracts, ASCA, Biochemical Abstracts, Biological Abstracts, Chemical Abstracts, Chemical Titles, Chromatography Abstracts, Current Contents/Life Sciences, Current Contents/Physical, Chemical & Earth Sciences, Deep-Sea Research/Part B: Oceanographic Literature Review, Excerpta Medica, Index Medicus, Mass Spectrometry Bulletin, PASCAL-CNRS, Referativnyi Zhurnal and Science Citation Index)

(Continued overleaf)

(Continued overleaf)

(Continued overleaf)

In articles with more than one author, the name of the author to whom correspondence should be addressed is indicated in the article heading by a 6-pointed asterisk (*)

Selective Sample Handling and Detection in High-Performance Liquid Chromatography

Journal of Chromatography Library, 39

part A

edited by **R.W. Frei**†, *Free University, Amsterdam, The Netherlands, and* **K. Zech**, *Byk Gulden Pharmaceuticals, Konstanz, FRG*

Part A of this two-volume project attempts to treat the sample handling and detection processes in a liquid chromatographic system in an integrated fashion. The need for more selective and sensitive chromatographic methods to help solve the numerous trace analysis problems in complex samples is undisputed. However, few workers realize the strong interdependence of the various steps - sample handling, separation and detection - which must be considered if one wants to arrive at an optimal solution. By introducing a strong element of selectivity and trace enrich- ment in the sample preparation step, fewer demands are placed on the quality of the chromatography and often a simple UV detector can be used. By using a selective detection mode, i.e. a reaction detector, the sample handling step can frequently be simplified and more easily automated. The impact of such a "total system" approach on handling series of highly complex samples such as environmental specimens or biological fluids can be easily imagined.

Contents: 1. On-line sample handling and trace enrichment in liquid chromatography. The determination of organic compounds in water samples. 2. Determination of drugs and their metabolites in biological samples by fully automated HPLC with on-line solid-liquid extraction and pre-column switching. 3. Immobilization of compounds for selective interaction with analytes in liquid chromatography. 4. Design and choice of suitable labelling reagents for liquid chromatography. 5. Photodiode array detection and recognition in high-performance liquid chromatography. 6. Electrochemical techniques for detection in HPLC. 7. Solid-phase reactors in high-performance liquid chromatography. 8. Commercial aspects of post-column reaction detectors for liquid chromatography. Subject Index.

1988 xii + 458 pages
US$ 123.00 / Dfl. 240.00
ISBN 0-444-42881-X

part B

edited by **K. Zech**, *Byk Gulden Pharmaceuticals, Konstanz, FRG, and* **R.W. Frei**†, *Free University, Amsterdam, The Netherlands*

Part B completes the treatment of the handling, separation and detection of complex samples as an integrated, interconnected process. On the basis of this philosophy the editors have selected those contributions which demonstrate that optimal sample preparation leads to a simplification of detection or reduced demands on the separation process. Throughout the book emphasis is on chemical principles with minimum discussion of the equipment required - an approach which reflects the editors' view that the limiting factor in the analysis of complex samples is an incomplete knowledge of the underlying chemistry rather than the hardware available. This lack of knowledge becomes more evident as the demands for lower detection limits grow, as solving complex matrix problems requires a greater understanding of the chemical interaction between the substance to be analysed and the stationary phase.

Contents: I. Preconcentration and Chromatography on Chemically Modified Silicas with Complexation Properties. II. Sample Handling in Ion Chromatography. III. Whole Blood Sample Clean-Up for Chromatographic Analysis. IV. Radio-Column Liquid Chromatography. V. Modern Post-Column Reaction Detection in High-Performance Liquid Chromatography. VI. New Luminescence Detection Techniques. VII. Continuous Separation Techniques in Flow-Injection Analysis. Subject Index.

1989 xii + 394 pages
US$ 136.00 / Dfl. 265.00
ISBN 0-444-88327-4

Written by experienced practitioners, these volumes will be of interest to investigators in many areas of application, including environmental scientists and those active in the clinical, pharmaceutical and bioanalytical fields.

For more information, please write to:

Elsevier Science Publishers
P.O. Box 211, 1000 AE Amsterdam, The Netherlands
P.O. Box 882, Madison Square Station, New York, NY 10159, USA

ANNOUNCING....

INTERNATIONAL ION CHROMATOGRAPHY SYMPOSIUM 1990

September 30 - October 3, 1990
Hotel del Coronado
San Diego, CA

Program Chairman:

Paul R. Haddad
The University of New South Wales
New South Wales, Australia

Scientific Committee:

Guenther K. Bonn
Innsbruck University
Innsbruck, Austria

Richard M. Cassidy
University of Saskatchewan
Saskatoon, Saskatchewan, Canada

James S. Fritz
Iowa State University
Ames, Iowa USA

Douglas T. Gjerde
Sarasep, Inc.
Santa Clara, California USA

Petr Jandik
Waters Chromatography Division
Milford, Massachusetts USA

John D. Lamb
Brigham Young University
Provo, Utah USA

Donald J. Pietrzyk
University of Iowa
Iowa City, Iowa USA

Gabriella Schmuckler
Technion
Haifa, Israel

Hamish Small
Consultant
Leland, Michigan USA

John Stillian
Dionex Corporation
Sunnyvale, California USA

Plenary Lecture:

"Twenty" Years of Ion Chromatography
by
Hamish Small

Separation methods:

Suppressed and Non-Suppressed IC
Ion-Interaction Chromatography
Capillary Electrophoresis
HPLC of Metal Chelates and Organometallics
Alternate Technology for Inorganic Ions

Application areas:

Environmental	Industrial
Food and Plant Materials	Clinical
Ultra-pure Water	Pharmaceutical
Industrial Hygiene	Biochemical

For program details and registration information, write or call:

Century International, Inc.
P.O. Box 493
Medfield, MA 02052 USA
508/359-8777
508/359-8778 (FAX)

JOURNAL OF CHROMATOGRAPHY

VOL. 511 (1990)

JOURNAL *of* CHROMATOGRAPHY

INTERNATIONAL JOURNAL ON CHROMATOGRAPHY,
ELECTROPHORESIS AND RELATED METHODS

ELSEVIER
AMSTERDAM — OXFORD — NEW YORK — TOKYO

J. Chromatogr., Vol. 511 (1990)

0021-9673/90/$03.50

Printed in The Netherlands

Journal of Chromatography, 511 (1990) 1–15
Elsevier Science Publishers B.V., Amsterdam

CHROM. 22 384

Theoretical study of the effect of a difference in column saturation capacities for the two components of a binary mixture on their elution band profiles and separation in non-linear chromatography

M. ZOUBAÏR EL FALLAH, SADRODDIN GOLSHAN-SHIRAZI and GEORGES GUIOCHON*
**Department of Chemistry, University of Tennessee, Knoxville, TN 37966-1600 and Division of Analytical Chemistry, Oak Ridge National Laboratory, Oak Ridge, TN, 37831-6120 (U.S.A.)*
(Received December 14th, 1989)

ABSTRACT

The elution profiles of large samples of binary mixtures are determined using the classical competitive Langmuir isotherm equations, with different values of the column saturation capacities for the two components. It is shown that the elution profile of an incompletely separated binary band system depends on the ratio of the two loading factors rather than on the relative concentrations of the feed. The ratio of the two column loading capacities is as important as the relative composition in determining the two band profiles. Thus, if the column saturation capacity is lower for the first-eluted component than for the second, the displacement effect will appear to be smaller than would be predicted on the basis of the feed composition. Conversely, the tag-along effect will appear to be more important. The reverse is true if the column saturation capacity is larger for the first-eluted component than for the second.

INTRODUCTION

In previous publications[1–5], we considered in detail the influence of the relative retentions of the two components of a binary mixture and of various experimental conditions (*e.g.*, sample size, relative concentrations of the feed, mobile phase velocity, column efficiency) on the separation of high concentration bands in preparative chromatography. These theoretical studies were performed using competitive Langmuir isotherms to account for the interactions between the two bands during their progressive separation and assuming that the column saturation capacities for the two components are equal.

Recently, experimental data have been presented suggesting that the competition between the two components of a binary mixture results in band profiles that depend considerably on the relative column saturation capacity[6]. The theory of the

0021-9673/90/$03.50

ideal model of chromatography[7] show that the relative intensities of the displacement and the tag-along effects in this model depend on the ratio of the loading factors of the two components, not on the relative composition of the feed[8]. We show here that the semi-ideal model supports the same results. We also demonstrate that conclusions regarding the validity of the Langmuir competitive isotherm model cannot be derived merely from the qualitative consideration of the pattern of interfering bands for a series of mixtures with different relative compositions.

THEORY

Competitive equilibrium isotherms

The use of Langmuir isotherms to account for experimental data in phase equilibria is extremely convenient. Langmuir isotherms are most often in excellent agreement with the results of measurements made for the adsorption equilibrium of pure compounds in normal- or reversed-phase chromatographic systems[9–11]. In the few cases where significant, systematic disagreement has been reported, a bi-Langmuir isotherm was found to be satisfactory[12,13]. In the case of competitive equilibria, however, the situation is more complex.

First, the theoretical basis of the Langmuir isotherms has been established in the case of gas or vapor adsorption, where there is no matrix adsorption. The fraction of the surface that is not covered by the adsorbate is really free, *i.e.*, bare. Even in gas chromatography there is not much adsorption of the carrier gas. The extension to the case of liquid–solid equilibria is not straightforward because, even with a pure solute, there is competition between the solute and the solvent for adsorption[14].

In the case of competitive adsorption of two components, the Langmuir binary isotherm model is thermodynamically correct only if the molecules of the two components occupy the same surface area on the adsorbent surface (*i.e.*, have the same "footprint") and the column saturation capacity is the same for both compounds[15]. Otherwise, the Gibbs–Duhem relationship is not satisfied. This condition is generally not fulfilled, although in many practical cases we are interested in the separation of closely related compounds and the ratio of their column saturation capacities will not be very different from unity. Unrelated compounds which interfere in a given chromatographic system can usually be separated easily in a different system.

In spite of these theoretical reservations, it turns out that in many practical cases the Langmuir isotherm model gives an acceptable fit of the experimental data. The quality of this fit can be deceptive, however. When isotherms are determined using the classical frontal analysis method for a binary mixture[16] or the "simple wave" method[17], the data obtained at constant feed composition and variable feed sample size are well accounted for by the Langmuir competitive model, although the variation with the feed composition of the coefficients obtained by a least-squares fit of the data to the Langmuir model does not agree well with the prediction of this model[11,17]. In most practical cases, it seems that the Langmuir model is no more than a satisfactory or fair first-order approximation to the real competitive isotherms, especially when the column saturation capacities of the two components are different.

The considerable practical advantage of the competitive Langmuir isotherms, which explains the great popularity of this model, is that the numerical values of all the

coefficients are those for the pure compound isotherms. Only the experimental determination of the single-component isotherms is required, which is considerably simpler than that of the competitive isotherms. As the Langmuir competitive isotherm is an acceptable approximation which is easy to estimate, its use as an empirical model is justified in general investigations such as the present one.

Computer calculations

The calculations reported and discussed here are based on the same principles as for our previous results using the semi-ideal model of chromatography[1–5,18]. We use the system of two partial differential equations stating the mass balance of the two components of a binary mixture, with the assumption of an ideal model (*i.e.*, the column efficiency is infinite). This system, completed with a set of isotherm equations, is solved numerically, and the values of the time and space increments are adjusted to account for the finite column efficiency, a licit calculation procedure[19–21]. In the cases where a comparison has been possible, experimental studies show excellent agreement between the profiles simulated for a pure compound and those recorded experimentally[22,23]. In the case of a binary mixture, excellent agreement is obtained when the exact competitive isotherm is used[17].

In all the following, the calculations were performed for a column having 5000 theoretical plates. The injection profile is assumed to be rectangular. The ratio of the concentrations of the two components in the feed was varied from 1:8 to 8:1. The isotherms are competitive Langmuir equations [*i.e.*, $Q_i = a_iC_i/(1 + b_1C_1 + b_2C_2)$].

For the sake of simplicity in the symbols, we define as RX the ratio of the values of X for the two components of the binary mixture studied (*i.e.*, $RX = X_2/X_1$). Thus:

$$RC_0 = C_2^0/C_1^0 \tag{1a}$$

$$RQ_s = Q_{s,2}/Q_{s,1} \tag{1b}$$

$$RL_f = L_{f,2}/L_{f,1} = RC_0/RQ_s \tag{1c}$$

where $L_{f,1}$ and $L_{f,2}$ are the individual loading factors of the first- and second-eluted components of the mixture, respectively, C_1^0 and C_2^0 are the concentrations of the first and second components in the feed, respectively, and $Q_{s,1}$ and $Q_{s,2}$ are the column saturation capacities for the lesser and more strongly retained components, respectively. The loading factor is the ratio of the sample size to the column saturation capacity. The column saturation capacity of a component i is equal to the ratio of its individual equilibrium isotherm parameters, a_i and b_i multiplied by the volume of the stationary phase.

In order to study the effect of a difference between the column saturation capacities for a given relative feed composition, RC_0, we vary the saturation capacity of either component with respect to that of the other component, which is kept constant in any given series of calculations. The saturation capacity ratio, RQ_s, is varied between 0.5 and 2, which covers the most useful range of values. This is achieved by changing the parameter b in the isotherm equation of one component, while a_1. a_2 and the b coefficient of the other component remain constant in all the calculations. Thus, the isotherm slopes at infinite dilution for the two solutes and their ratio, the relative retention, are not modified in the process.

Obviously, when RQ_s is smaller than 1, the saturation capacity of the second component is smaller than that of the first and the pure compound isotherms intersect. It has been shown, however, that this intersection has no direct physical meaning[11,24]. The planes $(Q_1, C_1, 0)$ and $(Q_2, 0, C_2)$ have nothing in common, except the vertical axis, and the coordinates of the intersection of the isotherms depend on the unit chosen for the concentrations. The real question is rather what the intersection curve of the two surfaces, $Q_1 = f_1(C_1, C_2)$ and $Q_2 = f_2(C_1, C_2)$ is and whether it is contained in the vertical plane of the equation $a_1C_1 = a_2C_2$, as predicted by the Langmuir model of competitive adsorption[11,24]. A more detailed investigation of this problem and its practical consequences is in progress and will be reported later[24].

The influence of the ratio of the column saturation capacities of the two compounds on the degree of band interference can be studied by computer simulation, as described previously[19], but theoretical considerations based on the properties of the analytical solution of the ideal model[8] help in the understanding of the results. The program used for the calculation of band profiles was written in Pascal and run on the VAX-8900 of the University of Tennessee Computer Center. The calculation of a complete set of profiles lasts *ca.* 5 min.

Properties of the displacement effect

The intensity of the displacement effect can be measured by the ratio of the concentrations of the first component in the front side and in the rear side of the second shock, $C_{1,A'}$ and $C_{1,M}$, respectively[7,8]. Using the ideal model, we have shown recently[8] that the ratio of these two concentrations is given by

$$C_{1,A'}/C_{1,M} = 1 + RL_f \tag{2a}$$

Hence

$$C_{1,A'}/C_{1,M} = 1 + RC_0/RQ_s \tag{2b}$$

Therefore, it is only when the column saturation capacities of the two components are equal that the intensity of the displacement effect depends simply on the relative feed composition, increasing with increasing relative concentration of the second component in the feed. On the other hand, at constant value of the relative feed composition, the loading factor ratio and the intensity of the displacement effect decrease with increasing value of the column saturation capacity ratio, RQ_s. Hence, the intensity of the displacement effect increases with decreasing column saturation capacity for the second component and/or with increasing column saturation capacity for the first.

The solution of the ideal model of chromatography in the case of a binary mixture with Langmuir competitive isotherms[7] permits a quantitative description of the displacement effect. It has been shown that the retention time of the second shock, $t_{f,2}$, is given by an equation which can be rewritten as follows, assuming the width of the injection pulse to be small, and the root r_1 of eqn. 22 in ref. 7 to be equal to $1/RC_0$, as shown in ref. 8:

$$t_{f,2} = t_0\left[1 + k'_{0,2} \cdot \frac{RL_f + 1}{RL_f + 1/\alpha}(1 - \sqrt{L'_f})^2\right] \tag{3}$$

where t_0 is the column dead time, $k'_{0,2}$ is the retention factor of the second component (at infinite dilution), α ($= a_2/a_1$) is the relative retention and L'_f is the adjusted loading factor, given by the equation[7]

$$L'_f = \left(1 + \frac{RQ_s}{\alpha RC_0}\right)\frac{n_2}{Q_{s,2}(1-\varepsilon)SL} \tag{4a}$$

or

$$L'_f = L_{f,2}\left(1 + \frac{1}{\alpha RL_f}\right) = L_{f,2} + \frac{L_{f,1}}{\alpha} \tag{4b}$$

where n_2 is the amount of second component injected and $(1-\varepsilon)SL$ accounts for the volume of packing in the column. Replacing L'_f in eqn. 3 by its value in eqn. 4 shows that the retention time of the second shock depends on the column dead time, the ratio of the two loading factors, the loading factor for the second component and the coefficients a_1 and a_2 of the equilibrium isotherms. According to eqns. 3 and 4, the retention time of the second shock depends strongly on $(1 - \sqrt{L'_f})^2$. L'_f in turn depends on both RQ_s and $Q_{s,2}$, so the discussion of the influence of the column saturation capacity on the resolution between the two bands must consider separately the influence of $Q_{s,1}$ and $Q_{s,2}$.

There are two simple ways to decrease RQ_s. We can either decrease $Q_{s,2}$ at constant $Q_{s,1}$ or increase $Q_{s,1}$ at constant $Q_{s,2}$. In the latter case, when we increase $Q_{s,1}$, $L_{f,1}$ and hence L'_f decrease (eqn. 4b). The retention time of the second front increases (eqn. 3) and the resolution between the two bands improves, while the intensity of the displacement effects increases. In the former case, when we decrease $Q_{s,2}$, $L_{f,2}$ and hence L'_f increase (eqn. 4b). The retention time of the second front decreases (eqn. 3) and the resolution between the two bands deteriorates, although the intensity of the displacement effect increases.

In summary, the intensity of the displacement effect always increases with decreasing ratio of the column saturation capacities, but the separation (and hence the production rate and/or the recovery yield) can either improve or deteriorate. The separation will improve with increasing column saturation capacity for either the first or the second component.

For a given chromatographic system and for mixtures of the same compounds, but with different compositions, the intensity of the displacement effect depends on the relative composition. It can be shown that in the mixed zone, where the two components coexist, their concentration profiles are simply related to RQ_s. Eqns. 43 and 44 in ref. 7 can be rewritten as

$$C_1 = \frac{FQ_{s,1}}{k'_{0,1}(1 + RL_f)}\left(\sqrt{\frac{1 + RL_f}{1 + \alpha RL_f}\cdot\frac{k'_{0,1}t_0}{t - t_0}} - 1\right) \tag{5}$$

where F [$= (1-\varepsilon)/\varepsilon$] is the phase ratio and ε the packing porosity and

$$C_2 = \frac{FQ_{s,2}}{k'_{0,2}(1 + 1/RL_f)}\left(\sqrt{\frac{1 + RL_f}{RL_f + 1/\alpha}\cdot\frac{k'_{0,2}t_0}{t - t_0}} - 1\right) \tag{6}$$

The practical importance of the mixed zone depends largely on the ratio C_2/C_1. The larger the latter is, the smaller is the relative magnitude of this zone and the higher are the recovery yields. This ratio depends essentially on RL_f:

$$\frac{C_2}{C_1} = \frac{RC_0}{\alpha} \cdot f(RL_f) \tag{7}$$

where $f(RL_f)$ represents the ratio of the two terms in parentheses at the end of eqns. 5 and 6, respectively. As α is close to unity in most practical cases, the ratio $f(RL_f)$ varies only slowly with RL_f. Note that if $\alpha = 1$, there is no separation and C_2/C_1 becomes equal to RC_0.

Properties of the tag-along effect

The tag-along effect is a consequence of the influence of the local concentration of the first component on the velocity associated with a concentration of the second component[7,8]. Further, the velocity associated with a given concentration of the second component when pure is lower than the limit of the velocity associated with the same concentration of the second component, but in the presence of the first component, when the concentration of this first component tends towards zero. Thus, a plateau appears on the rear of the second component profile when the concentration of the first component becomes zero[7].

The width, Δt, of the plateau is given by the following equation[8]:

$$\Delta t = \frac{1 + RL_f}{(\alpha RL_f + 1)^2}(k'_{0,2} - k'_{0,1})t_0 \tag{8}$$

where $k'_{0,1}$ and $k'_{0,2}$ are the column capacity factors of the first and the second components, respectively, at infinite dilution. The intensity of the tag-along effect depends on the loading factor ratio and on the difference between the retention factors of the two components at infinite dilution. In the calculations reported here, the retention factors of the two components at infinite dilution are kept constant so the intensity of the tag-along effect depends only on RL_f.

RESULTS AND DISCUSSION

Both the displacement and the tag-along effects have been observed, the former in preparative liquid chromatography when the column is overloaded for a high production rate[6,25,26] and the latter in detailed investigations of individual band profiles[27]. An experimental study of the influence of the ratio of column saturation capacities for the two components has been presented[6]. Based on the theoretical conclusions reported above, we discuss the results of numerical calculations made using the semi-ideal model of chromatography[1,18–21].

Study of the displacement effect

With Langmuir equilibrium isotherms the velocity associated with a certain concentration of a compound[28] increases with increasing concentration of this

compound. Hence the front of each elution band must be a shock in the ideal model and a shock layer in practice, because of the smoothing effect of a finite mass transfer kinetics.

The displacement effect is due to the fact that the concentration of each compound in the stationary phase is a function of the mobile phase concentrations of all the other components. The appearance of the second shock (a positive jump in the concentration of the second component) at the rear of the first component band causes a negative shock in the concentration of the first-eluted solute[7]. Alternately, we know that, with a convex isotherm, the velocity associated with a certain concentration of the first component increases with increasing concentration of the second component. Only high concentrations of the first component can move faster than the concentration of the first component which moves with the front of the second component[7].

As shown in the Theory section, the intensity of the displacement effect depends on the ratio of the column saturation capacities. Increasing RQ_s can be done either by decreasing $Q_{s,1}$ (as done in Fig. 1a and b) or by increasing $Q_{s,2}$ (*i.e.*, decreasing b_2, as done in Fig. 2a–e).

Influence on the displacement effect of a change in the column saturation capacity of the first component

In this case, we increase RQ_s by decreasing $Q_{s,1}$. Then L'_f increases, as $L_{f,1}$

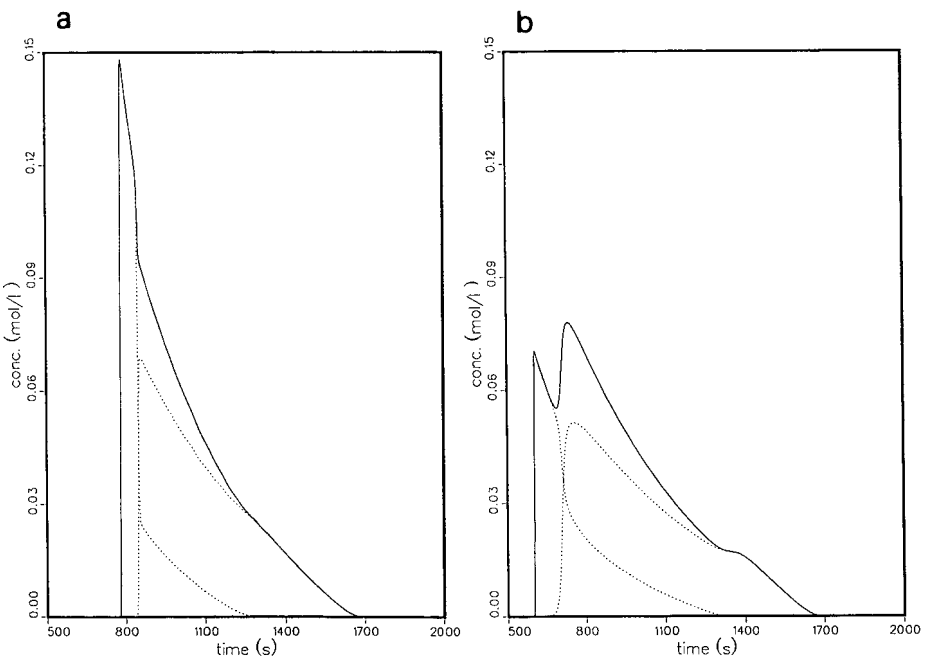

Fig. 1. Influence of the loading factor ratio on the intensity of the displacement effect and the separation between bands. Effect of the column saturation capacity for the first component. Chromatograms calculated for a binary mixture of constant composition (RC_0 = 2.0, 1:2 mixture) for columns of different saturation capacity for the first component. Langmuir competitive isotherms (a_1 = 24, a_2 = 28.8, b_1 = 4.8, α = 1.20, $Q_{s,2}$ = 5.0). Constant sample size: 0.40 mmol of second component ($L_{f,2}$ = 9.7%) and 0.20 mmol of first component. (a) RQ_s = 0.5, RL_f = 4.0, $L_{f,1}$ = 2.4%; (b) RQ_s = 2.0, RL_f = 1.0, $L_{f,1}$ = 9.7%.

increases and $L_{f,2}$ remains constant. RL_f also decreases and the intensity of the displacement effect weakens. The retention time of the second shock decreases (eqn. 3) and the separation deteriorates. C_1 decreases more slowly with increasing time at lower values of $Q_{s,1}$. The change in the individual elution profiles is illustrated in Fig. 1a and b.

In this series of calculations, the feed composition (C_1°/C_2°) is kept constant and equal to 1/2. The sample size is kept constant and the loading factor for the second component remains equal to 9.7%. From Fig. 1a to Fig. 1b RQ_s increases from 0.5 to 2 and RL_f decreases from 4.0 to 1.0. As predicted by theory, the displacement effect decreases and the separation becomes worse, as demonstrated by the longer, more important tail of the first component band behind the second shock.

For real columns, the reduction in the recovery yield and production rate due to the lesser degree of separation of the bands is enhanced by the consequences of a less strong displacement effect. The front of the second component band and the rear shock layer of the first component band are less steep (compare Fig. 1a and b). Hence kinetic effects reinforce the negative consequences of thermodynamic effects.

Influence on the displacement effect of a change in the column saturation capacity of the second component

In this case, we increase RQ_s by increasing $Q_{s,2}$, at constant sample size. L_f' decreases since $L_{f,2}$ decreases and $L_{f,1}$ is constant (eqn. 4b) and the retention time of the second component front increases (eqn. 3). The intensity of the displacement effect decreases. C_2 increases slowly with increasing $Q_{s,2}$ (eqn. 6). The change in the two individual profiles is illustrated in Fig. 2a–e. In this series of calculations, the relative feed composition (C_1°/C_2°) is kept constant and equal to 1/8. The sample size is also kept constant and the loading factor for the first component remains equal to 0.725%. From Fig. 2a to Fig. 2e RQ_s increases from 0.5 to 2 and RL_f decreases from 16.0 to 4.0.

When RQ_s increases at constant RC_0, RL_f decreases (eqn. 1c) and the decrease in both solute concentrations along the profile in the mixed zone is faster, while the mixed zone becomes narrower. As the sample size and the elution time of the second component tail are constant, the throughput remains constant in Fig. 2a–e. As $Q_{s,2}$ is increased, however, $L_{f,2}$ and hence L_f' decrease (see eqn. 4) and the degree of band overlap decreases, and the production rates and recovery yields of both components increase with increasing column saturation capacity for the second component from Fig. 2a ($RQ_s = 0.5$) to Fig. 2e ($RQ_s = 2$), although the intensity of the displacement effect decreases. This result is easily explained by the decreasing degree of column overloading when the sample size is kept constant while the column saturation capacity for the second component is increased.

From Fig. 2a to Fig. 2e, while RQ_s increases at constant RC_0, the steep front of the second component band recedes (the retention time increases from 820 to 1180 s). In the same time, the end of the first component tail moves only from 1220 to 1260 s, but the retention time of the first front increases from 790 to 1080 s. The velocity of the concentration shocks and/or shock layers decreases with decreasing value of the loading factor ratio (16.0 for Fig. 2a, 8.0 for Fig. 2c, 4.0 for Fig. 2e), but the effect is more important for the second component (the column saturation capacity of which is increasing) than for the first one (the column saturation capacity of which remains constant). The second shock, moving in the rear of the first band and displacing it,

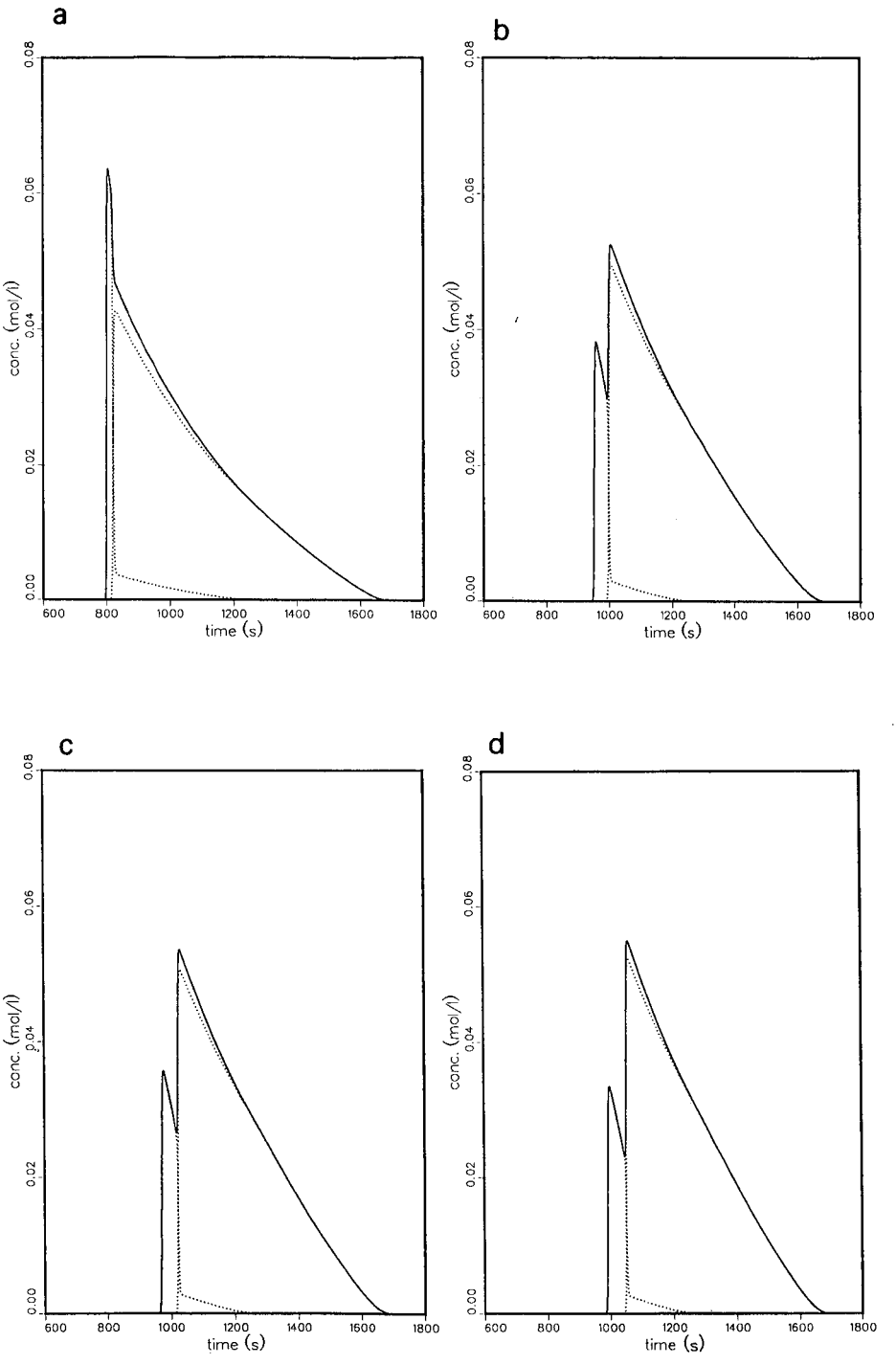

Fig. 2

(*Continued on p. 10*)

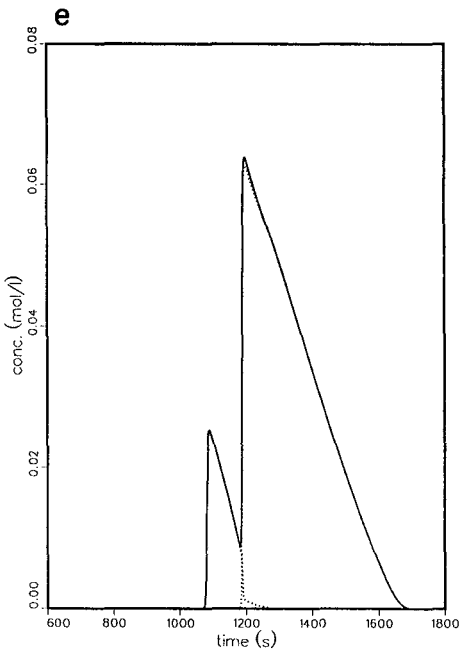

Fig. 2. Influence of the loading factor ratio on the intensity of the displacement effect and the separation between bands. Effect of the column saturation capacity for the second component. Chromatograms calculated for a binary mixture of constant composition (RC_0 = 8.0, 1:8 mixture) for columns of different saturation capacity for the second component. Langmuir competitive isotherms (a_1 = 24; a_2 = 28.8, b_1 = 4.8, α = 1.20, $Q_{s,1}$ = 5.0). Constant sample size: 0.030 mmol of the first component ($L_{f,1}$ = 0.725%) and 0.24 mmol of the second component. (a) RQ_s = 0.50, RL_f = 16.0, $L_{f,2}$ = 11.6%; (b) RQ_s = 0.91, RL_f = 8.80, $L_{f,2}$ = 6.4%; (c) RQ_s = 1.0, RL_f = 8.0, $L_{f,2}$ = 5.8%; (d) RQ_s = 1.11, RL_f = 7.21, $L_{f,2}$ = 5.23%; (e) RQ_s = 2.0, RL_f = 4.0, $L_{f,2}$ = 2.9%.

becomes farther and farther from the first shock. The degree of band overlap decreases. As the second shock moves more slowly and the mixed zone narrows, the concentration of the more retained solute at the front of the second shock becomes higher. These effects can be observed in Fig. 2a–e.

Displacement effect at constant column saturation capacity

At constant RQ_s, the intensity of the displacement effect increases with increasing relative concentration of the second component, *i.e.*, with increasing RC_0, as shown by comparing Figs. 2e, 3a and 3b. In these figures, the degree of band overlap increases with decreasing RC_0, from 8 (Fig. 2e) to 4 (Fig. 3a) and 2 (Fig. 3b), the displacement effect decreases and the tag-along effect (see next section) increases.

All these results illustrate the importance of the ratio of the loading factor for the two components and demonstrate the effect of this ratio on the intensity of the displacement effect.

Study of the tag-along effect

When RL_f becomes small compared with $1/\alpha$ (and thus with 1), the width of the plateau increases and tends towards $(k'_{0,2} - k'_{0,1})\, t_0$ (see eqn. 8). At low values of RL_f,

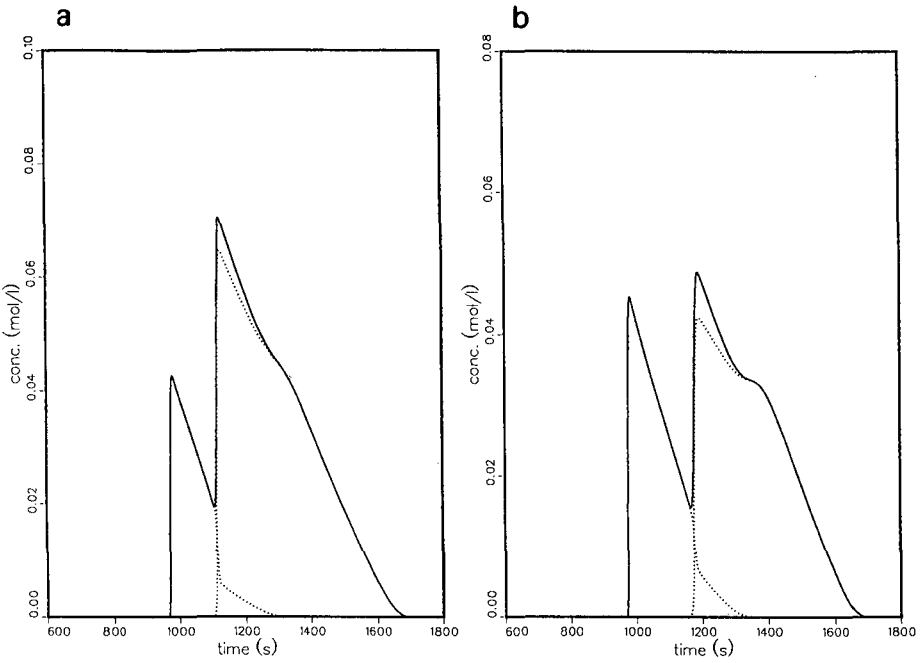

Fig. 3. Influence of the loading factor ratio on the intensity of the displacement effect. Effect of the relative concentration of the feed. Chromatograms calculated for columns of constant saturation capacities (RQ_s = 2.0, Q_1 = 5.0, Q_2 = 10) and with a binary mixture of variable composition. Same Langmuir competitive isotherms as for Fig. 1. See Fig. 1a, RC_0 = 8, RL_f = 4. (a) RC_0 = 4.0 (1:4 mixture), RL_f = 2.0 ($L_{f,1}$ = 1.81%), sample amount: 0.452 mmol, $L_{f,2}$ = 3.62%. (b) RC_0 = 2.0 (1:2 mixture), RL_f = 1.0 ($L_{f,1}$ = 2.42% = $L_{f,2}$), sample amount 0.361 mmol.

it is proportional to $[1 + (1 - 2/\alpha)RL_f](k'_{0.2} - k'_{0.1})t_0$. Under these conditions, the displacement effect is negligible.

When RL_f becomes very large the tag-along effect vanishes. The length of the plateau is proportional to $1/RL_f$ at large values of the loading factor ratio (see eqn. 8). In Fig. 2e, RL_f is equal to 4 and the tag-along effect is already insignificant. In contrast, in Fig. 4a–c RL_f increases from 0.5 to 2. All these figures exhibit a strong tag-along effect with a feed relative concentration of 1. The width of the plateau decreases progressively with increasing loading factor ratio, while the displacement effect increases.

At a fixed value of RQ_s, the loading factor ratio is proportional to the relative composition of the feed (see eqn. 1c) and the intensity of the tag-along effect increases with decreasing relative concentration of the second component[1]. This effect is illustrated in Fig. 5a–c, where the relative concentration of the second component decreases from 1/2 to 1/8 and the loading factor ratio decreases from 0.25 to 0.0625, for a constant ratio RQ_s equal to 2.0. If we compare Figs. 4a and 5a–c, we see that the length of the plateau increases progressively, as expected, and tends towards a limit which is nearly achieved in Fig. 5c.

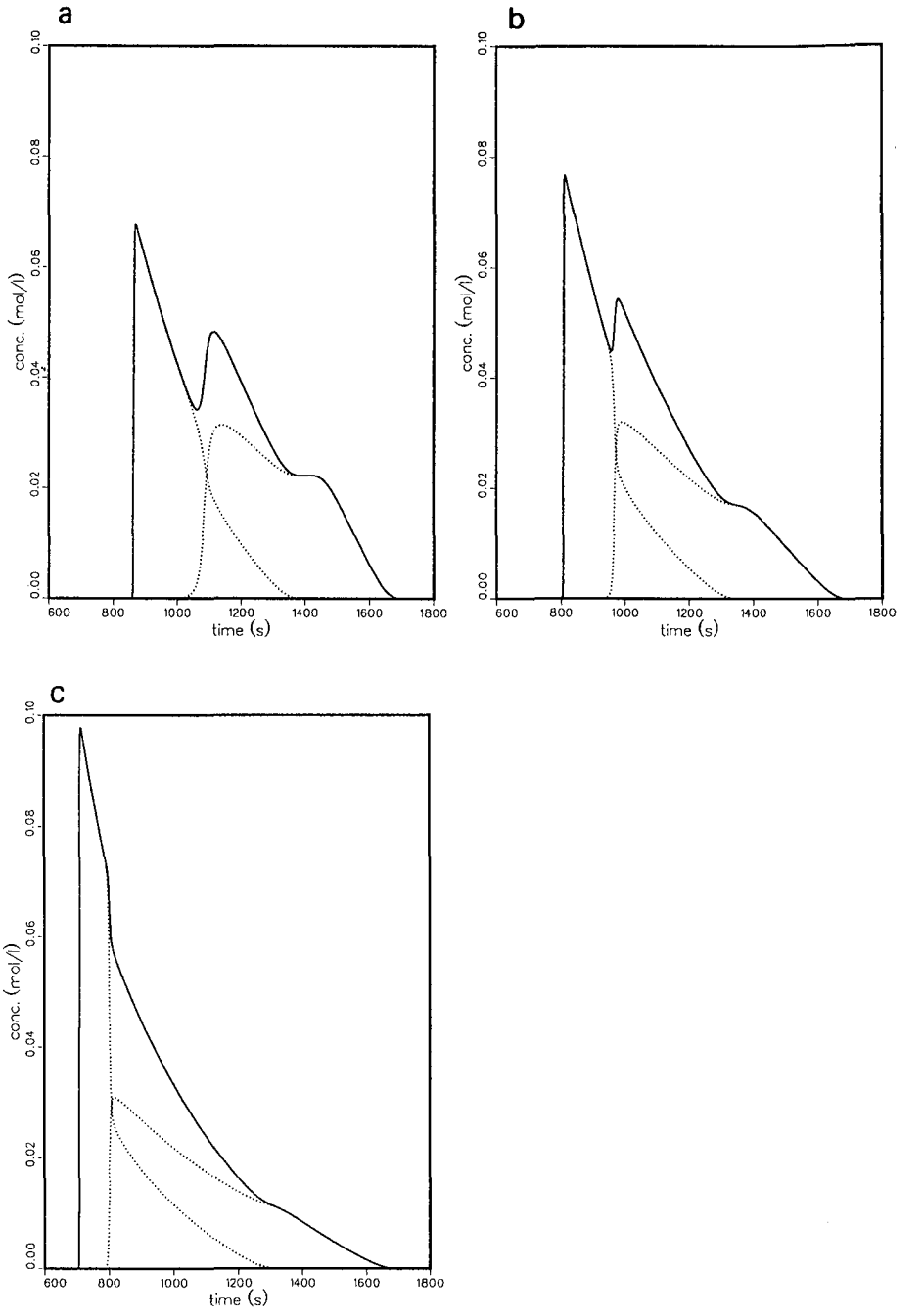

Fig. 4. Influence of the loading factor ratio on the intensity of the tag-along effect. Effect of the column saturation capacity for the second component. Chromatograms calculated for a binary mixture of constant composition (RC_0 = 1.0, 1:1 mixture) for columns of different saturation capacities for the second component. Same Langmuir competitive isotherms as for Fig. 1. Constant sample size: 0.483 mmol ($L_{f,1}$ = 4.83%). (a) RQ_s = 2.0, RL_f = 0.50, $L_{f,2}$ = 2.42%; (b) RQ_s = 1.0, RL_f = 1.0, $L_{f,2}$ = 4.83%; (c) RQ_s = 0.50, RL_f = 2.0, $L_{f,2}$ = 9.66%.

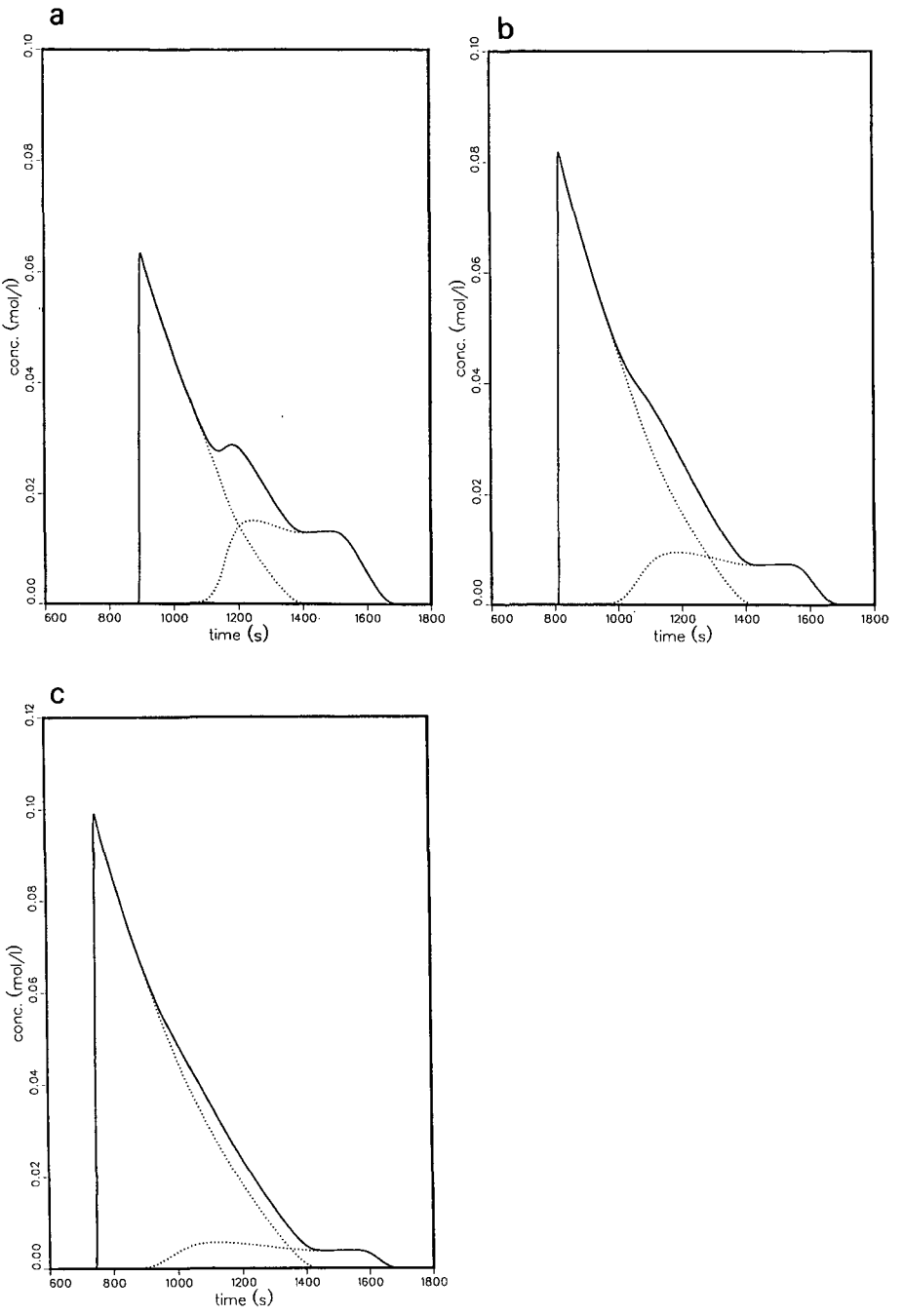

Fig. 5. Influence of the loading factor ratio on the intensity of the tag-along effect. Effect of the relative concentration of the feed. Chromatograms calculated for columns of constant saturation capacities (RQ_s = 2.0, Q_1 = 5.0, Q_2 = 10) and with a binary mixture of variable composition. Same Langmuir competitive isotherms as for Fig. 1. See Fig. 4a, RC_0 = 1, RL_f = 0.50. (a) RC_0 = 0.50 (2:1 mixture), RL_f = 0.25 ($L_{f,1}$ = 4.83%), sample amount 0.362 mmole, $L_{f,2}$ = 1.21%; (b) RC_0 = 0.25 (4:1 mixture), RL_f = 0.125 ($L_{f,1}$ = 7.25%), sample amount 0.453 mmol, $L_{f,2}$ = 0.91%; (c) RC_0 = 0.125 (8:1 mixture), RL_f = 0.0625 ($L_{f,1}$ = 9.67%), sample amount 0.544 mmol, $L_{f,2}$ = 0.60%.

CONCLUSION

The intensities of the displacement and the tag-along effects have been shown to be controlled by the loading factor ratio of the two components in the case of a binary mixture separation, not merely by the relative concentrations of the two components of the feed. The intensities of these two effects vary in opposite directions when the loading factor ratio is changed at constant total column loading. When the saturation capacity of the first-eluted component is lower than that of the more retained component, the intensity of the displacement effect is depressed whereas the intensity of the tag-along effect is increased, compared with the case where the column has the same saturation capacity for the two components. The inverse case produces the opposite variations: the intensity of the tag-along effect is less important and that of the displacement effect is enhanced if the column saturation capacity is lower for the second component than for the first.

The existence of a difference between the column saturation capacities of the two components to be separated has to be considered in any optimization procedure. Of special importance is a judicious choice of the stationary phase, which must take into account not only the relative retentions of the two components at low concentration, but also the dependence of the column saturation capacities for the two compounds and their ratio on the experimental conditions[29]. The influence of this ratio on the production rate at fixed purity may be important. It depends in a large part on the composition of the feed.

Finally, when the ratio of the column saturation capacities, RQ_s, is less than unity, the two single-component equilibrium isotherms plotted in the same graph intersect. As long as the mobile phase concentrations used are lower than those corresponding to this intersection point, the chromatograms obtained are those described here. Displacement chromatography can be achieved with a suitable displacer and no special problem arises from this "isotherm intersection". When concentrations higher than those corresponding to the intersection point are involved in an experiment, some theoretical and practical difficulties may arise. A detailed discussion of this interesting but complex problem will be reported soon[24]. The conclusions of the IAS model derived from single component Langmuir isotherms and those of the conventional binary competitive Langmuir isotherms are somewhat different. They will be compared.

ACKNOWLEDGEMENTS

This work was supported in part by Grant CHE-8901382 of the National Science Foundation and by the cooperative agreement between the University of Tennessee and the Oak Ridge National Laboratory.

REFERENCES

1 G. Guiochon and S. Ghodbane, *J. Phys. Chem.*, 92 (1988) 3682.
2 S. Ghodbane and G. Guiochon, *J. Chromatogr.*, 440 (1988) 9.
3 S. Ghodbane and G. Guiochon, *J. Chromatogr.*, 444 (1988) 275.
4 S. Ghodbane and G. Guiochon, *J. Chromatogr.*, 450 (1988) 27.
5 S. Ghodbane and G. Guiochon, *J. Chromatogr.*, 452 (1988) 209.

6 G. B. Cox and L. R. Snyder, *J. Chromatogr.*, 483 (1989) 95.
7 S. Golshan-Shirazi and G. Guiochon, *J. Phys. Chem.*, 93 (1989) 4143.
8 S. Golshan-Shirazi and G. Guiochon, *Anal. Chem.*, 62 (1990) 217.
9 J. Frenz and Cs. Horváth, *AIChE J.*, 31 (1985) 400.
10 J. E. Eble, R. L. Grob, P. E. Antle and L. R. Snyder, *J. Chromatogr.*, 384 (1987) 45.
11 J. X. Huang and G. Guiochon, *J. Colloid Interface Ci.*, 128 (1989) 577.
12 R. J. Laub, *ACS Symp. Ser.*, No. 297 (1986) 1.
13 J. X. Huang, J. V. H. Schudel and G. Guiochon, *J. Chromatogr.*, 504 (1990) 335.
14 E. sz. Kováts, in F. Bruner (Editor), *The Science of Chromatography*, Elsevier, Amsterdam, 1985, p. 205.
15 T. Le Van and M. D. Vermeulen, *J. Phys. Chem.*, 85 (1981) 3247.
16 J. M. Jacobson, J. H. Frenz and Cs. Horvath, *Ind. Eng. Chem. Res.*, 26 (1987) 43.
17 Z. Ma, A. M. Katti and G. Guiochon, *J. Phys. Chem.*, in press.
18 G. Guiochon, S. Golshan-Shirazi and A. Jaulmes, *Anal. Chem.*, 60 (1988) 1856.
19 B. Lin, Z. Ma, S. Golshan-Shirazi and G. Guiochon, *J. Chromatogr.*, 500 (1989) 185.
20 B. Lin, Z. Ma and G. Guiochon, *J. Chromatogr.*, 484 (1989) 83.
21 M. Czok and G. Guiochon, *Anal. Chem.*, 62 (1990) 189.
22 S. Golshan-Shirazi, S. Ghodbane and G. Guiochon, *Anal. Chem.*, 60 (1988) 2630.
23 S. Golshan-Shirazi and G. Guiochon, *Anal. Chem.*, 60 (1988) 2634.
24 S. Golshan-Shirazi and G. Guiochon, in preparation.
25 J. Perry, paper presented at the VIth International Symposium on Preparative Chromatography, Washington, DC, May 1989.
26 J. Newburger and G. Guiochon, *J. Chromatogr.*, 484 (1989) 153.
27 A. M. Katti and G. Guiochon, *J. Chromatogr.*, 499 (1990) 25.
28 B. Lin, S. Golshan-Shirazi, Z. Ma and G. Guiochon, *Anal. Chem.*, 60 (1988) 2647.
29 J. X. Huang, J. V. H. Schudel and G. Guiochon, *J. Prep. Chromatogr.*, in press.

Journal of Chromatography, 511 (1990) 17–33
Elsevier Science Publishers B.V., Amsterdam

CHROM. 22 402

Simultaneous optimization of variables influencing selectivity and elution strength in micellar liquid chromatography

Effect of organic modifier and micelle concentration

JOOST K. STRASTERS, EMELITA D. BREYER, ANDREW H. RODGERS[a] and MORTEZA G. KHALEDI*

North Carolina State University, Department of Chemistry, P.O. Box 8204, Raleigh, NC 27695 (U.S.A.)

(First received October 9th, 1989; revised manuscript received February 20th, 1990)

ABSTRACT

Previously, the simultaneous enhancement of separation selectivity with elution strength was reported in micellar liquid chromatography (MLC) using the hybrid eluents of water–organic solvent–micelles. The practical implication of this phenomenon is that better separations can be achieved in shorter analysis times by using the hybrid eluents. Since both micelle concentration and volume fraction of organic modifier influence selectivity and solvent strength, only an investigation of the effects of a simultaneous variation of these parameters will disclose the full separation capability of the method, *i.e.* the commonly used sequential solvent optimization approach of adjusting the solvent strength first and then improving selectivity in reversed-phase liquid chromatography is inefficient for the case of MLC with the hybrid eluents. This is illustrated in this paper with two examples: the optimization of the selectivity in the separation of a mixture of phenols and the optimization of a resolution-based criterion determined for the separation of a number of amino acids and small peptides.

The large number of variables involved in the separation process in MLC necessitates a structured approach in the development of practical applications of this technique. A regular change in retention behavior is observed with the variation of the surfactant concentration and the concentration of organic modifier, which enables a successful prediction of retention times. Consequently interpretive optimization strategies such as the iterative regression method are applicable.

INTRODUCTION

During recent years, the number of applications of reversed-phase high-

[a] Present address: University of New Orleans, Department of Chemistry, New Orleans, LA 70148, U.S.A.

0021-9673/90/$03.50

performance liquid chromatography (RP-HPLC), has been greatly extended by the use of secondary chemical equilibria in the mobile phase[1,2]. The use of these equilibria is mostly aimed at an enhancement of selectivity, and examples include ion-suppression, ion-pairing, complexation and use of micelles. One of the consequences of the use of additional equilibria is an extension of the number of parameters influencing the retention and selectivity observed in the chromatographic process. The chromatographer will only be able to exploit the full potential of the implemented separation mechanisms, if a systematic approach is available to describe or examine the effect of all important parameters involved. The results of such an investigation can then be used to predict the optimal conditions for a given separation problem.

A rigorous analysis of the chemical principles of the effect of secondary equilibria on the separation has been used to derive the setpoint for the optimal separation of one pair of components[2,3]. However, in practical applications it is necessary to consider the interactions of the parameter related to the secondary equilibrium with other parameters: for instance a change in organic modifier concentration will influence the dissociation constants of the solutes. Furthermore, different regions of the parameter space will often be associated with different critical peak-pairs, necessitating an analysis involving all components.

In a previous paper[4], we reported the simultaneous enhancement of separation selectivity and solvent strength in micellar liquid chromatography (MLC) using hybrid eluents of water–micelles–organic solvents. This selectivity enhancement occurs systematically, *i.e.* peak separation increases monotonically with volume fraction of organic solvent added to micellar eluents. This phenomenon in MLC was attributed to the existence of competing equilibria and/or the compartmentalization of solutes and organic modifier by micelles which have a great influence on the solvent strength parameter, S [*i.e.* slope of log capacity factor (k') *vs.* volume fraction of organic modifier (φ_{org})]. This phenomenon was observed for different groups of ionic and nonionic compounds with a variety of functional groups and for both anionic and cationic micellar eluents. The generality of the simultaneous selectivity enhancement with elution strength in hybrid systems indicates that the possible cause(s) is (are) not the same as the typical solvent selectivity effect in hydro–organic mobile phases, as the latter is only observed for a limited group of compounds which selectively interact with a given solvent. In fact, it has been shown recently that although maximum selectivity can be observed at intermediate solvent strength values in certain ternary or quaternary hydro–organic mixtures and for selected compounds, the general trend is higher selectivity at lower eluent strength[5].

There are two general approaches for optimization of solvent strength and selectivity in RP-HPLC with conventional hydro–organic eluents. Snyder and co-workers[6–8] have shown that adequate resolution can be achieved by varying the concentration of the organic modifier in the mobile phase. This method is only suitable for simple samples that contain components of different molecular size or dissimilar chemical functionality[6]. However, in cases where this method is applicable, good separations can be achieved with a few initial experiments[6–8]. The change in band spacing as a result of an increase in organic modifier concentration in hydro–organic RP-HPLC is usually not possible for samples that contain solutes with equal (or close) S values or when there is a strong correlation between S values and the corresponding retention[6–8]. As a consequence, most approaches in RP-HPLC with respect to

a systematic improvement of the isocratic separation of more complex mixtures are based on the following steps[6–11]: first the required elution strength is determined, preferably by means of a gradient. Then the selectivity of the mobile phase is varied, *e.g.* by changing the type of organic modifier, keeping the overall elution strength constant. Recently, the selectivity effect of the weak solvent (*i.e.* water) in ternary/quaternary hydro–organic eluents, was discussed[5]. However, in order to describe this effect for a given sample, a number of additional experiments will be required for the optimization of the ternary/quaternary mobile phases. As described below, the most important implication of the simultaneous increase of selectivity with solvent strength in MLC is that sequential optimization of solvent strength and selectivity is not effective and a more structured approach is required due to the complex nature of the retention process.

Optimization of the selectivity has received much attention in the literature and excellent reviews are available[8–10]. One differentiates between two types of procedures: (a) non-interpretive strategies which make no assumptions on the individual retention behavior of the components and solely evaluate the quality of the observed chromatograms, thus avoiding the need for peak-tracking; (b) interpretive optimization strategies which model the retention behavior of the individual components, thus requiring fewer experiments to derive an acceptable separation. However, specific information on the retention of all components is essential. Although most of these optimization strategies have been developed for standard RP-HPLC, a number of applications in ion-pairing chromatography have been described[12–16]. In most of these cases the addition of anionic or cationic surfactant is aimed at selectively decreasing the elution strength of the mobile phase for the ionic compounds, while keeping the retention of the uncharged solutes constant, as indicated in a recent review of optimization strategies in ion-pairing chromatography by Low *et al.*[17]

However, when the concentration of surfactant is further increased (*i.e.* when working above the critical micelle concentration, CMC), the retention mechanisms involved change dramatically as compared to ion-pairing chromatography. The presence of the micellar pseudo-phase enables additional partitioning of solutes between the stationary and the mobile phase, either because of electrostatic interaction with the charged outer-layer of the micelles and/or because of hydrophobic interactions with the lipophilic interior, thus influencing both the retention of neutral and ionized species. It is because of this dualistic influence on the retention of different solutes that strong changes in selectivity are observed in response to the variation of different parameters[4,18–20]. Obviously, one of the major parameters influencing retention is the concentration of the micellar pseudo-phase, equal to the total concentration of surfactant minus the CMC. Models described in the literature[21,22] indicate a linear relation between the inverse of the capacity factor, k', and the micelle concentration $[M]$:

$$k' = \frac{P_{SW} \cdot \Phi}{v \cdot (P_{MW} - 1) \cdot [M] + 1} \tag{1}$$

P_{MW} and P_{SW} represent distribution coefficients describing the partitioning of the solute between aqueous and micellar phase and aqueous and stationary phase respectively, v is the molar volume of the micellar pseudo-phase and Φ is the

chromatographic phase ratio. A number of parameters can be varied to influence the elution characteristics: in addition to the concentration, the charge of the headgroup and the length of the hydrophobic chain are factors related to the surfactant. Traditionally, only low concentrations of organic modifier are used (*e.g.* 3% propanol) to influence the column efficiency[23–26]. Only recently, the influence of the type and concentration of the organic modifier on the selectivity was described[4,20]. Because of the role of the electrostatic interactions, the pH is an important parameter to direct the retention of protonated species[27], for instance in the case of amino acids and peptides[28]. The ionic strength of the mobile phase will influence the elution as well, again depending on the combination of hydrophobic and electrostatic interactions[27]. Apart from the effect of the temperature on efficiency[23], the influence of this variable on the separation has not yet been examined systematically.

It is the aim of this paper to demonstrate that a sequential approach, *i.e.* an initial determination of the elution strengh followed by the optimization of the selectivity, is not feasible in the case of MLC and that the complex retention behavior necessitates a combined examination of the influence of the independent parameters involved. In this first investigation, we concentrate on two parameters which cause a large change in retention and selectivity and which are easy to vary: the concentration of the surfactant [either myristyltrimethylammonium bromide (CTAB) or sodium dodecyl sulfate (SDS)] and the concentration of the organic modifier, 2-propanol.

EXPERIMENTAL

In order to examine the changes in selectivity caused by a change in concentration of both organic modifier and micellar pseudo-phase, the retention times of two mixtures, a set of fifteen phenols and a set of thirteen amino acids and small peptides, were collected using reversed-phase columns.

The initial experiments regarding the phenol mixture were performed on a 5-μm particle LiChroCart C_{18} column (Merck, Darmstadt, F.R.G.), 12.5 cm × 4 mm I.D. The column was thermostated at 40°C and the flow was 1 ml/min. The column dead volume (0.67 ml) was measured by making multiple injections of water samples. A silica precolumn was employed to saturate the mobile phase with silicates and to protect the analytical column. The chromatographic equipment consisted of a dual-pump system (Model 2350, ISCO, Lincoln, NE, U.S.A.) and a V^4 absorbance detector set at 254 nm (ISCO), controlled by Chemresearch Chromatographic Data Management/System Controller software (ISCO) running on a PC-88 Turbo Personal Computer (IDS, Paramount, CA, U.S.A.). The analysis of the mixture was performed on the same instrument, using two identical LiChroCart columns as described above, and operating with a flow of 1.5 ml/min. In this case the dead volume was 1.40 ml.

The compositions of the mobile phase, the identities of the solutes and the observed capacity factors are listed in Table I. The solutes and the surfactant, CTAB, were obtained from Aldrich (Milwaukee, WI, U.S.A.). The surfactant solution was prepared by dissolving the required amount in doubly distilled deionized water and filtering through a 0.45-μm nylon filter. The ionic strength was adjusted by adding phosphate buffer (pH 7) such that the total buffer concentration of the final solution was 0.05 *M*. After adding the required amount of organic modifier, 2-propanol (Fisher Scientific, Pittsburgh, PA, U.S.A.), the pH was adjusted to 7.

TABLE I

THE CONCENTRATION OF THE SURFACTANT, [CTAB], AND THE PERCENTAGE OF 2-PROPANOL, USED IN THE CHROMATOGRAPHIC EXPERIMENTS REGARDING THE MIXTURE OF FIFTEEN PHENOLS

In addition the identities and capacity factors k' of the solutes are listed.

Mobile phase						
[CTAB], *M*		0.04	0.04	0.08	0.12	0.12
% 2-Propanol		0.0	10.0	5.0	0.0	10.0
Components				k'		
1	4-Benzamidephenol	4.7	1.9	2.3	2.2	1.2
2	4-Hydroxybenzyl alcohol	7.2	2.5	3.1	3.9	1.6
3	4-Hydroxyphenemethyl alcohol	11.4	3.4	4.3	5.4	2.0
4	4-Hydroxybenzylcyanide	20.1	5.9	7.0	8.3	3.4
5	4-Hydroxyacetophenone	29.0	9.5	9.9	10.9	4.4
6	Phenol	29.9	11.6	11.2	12.7	6.0
7	4-Hydroxybenzaldehyde	31.4	11.8	11.2	10.8	4.9
8	4-Fluorophenol	37.8	15.1	13.4	14.5	6.8
9	4-Methylphenol	43.6	18.4	15.3	16.4	8.1
10	4-Hydroxypropiophenone	50.7	19.3	16.5	17.3	7.5
11	4-Nitrophenol	63.8	29.7	22.0	17.5	10.2
12	4-Isopropylphenol	73.4	32.9	23.8	27.1	12.9
13	4-Hydroxybenzophenone	75.5	35.5	24.2	22.2	11.3
14	4-Hydroxydiphenylmethane	77.4	37.8	24.8	26.0	13.5
15	4-*tert.*-Butylphenol	86.8	38.2	27.7	32.6	14.9

All experiments regarding the amino acid–peptide mixture were performed on the same chromatographic system, using two identical columns in series with a total dead volume of 1.40 ml and with the detector set at 210 nm. The compositions of the mobile phase, the identities of the solutes and the capacity factors are listed in Table II. The solutes and the surfactant, SDS, were obtained from Sigma (St. Louis, MO, U.S.A.). The flow-rate was varied between 0.7 and 1.5 ml/min (dictated by the pressure limit of the system). The final analysis of the mixture was run at 1 ml/min. The preparation of the mobile phase was identical to the one described above with the following exceptions: the molarity of phosphate ions in the final solution was 0.02 *M*, and the pH was adjusted to 2.5.

The software to evaluate the separation at different mobile phase compositions was based on an extended version of the iterative regression optimization strategy[26,27] implemented by means of the Turbo-Pascal compiler version 4.0 (Borland, Scotts Valley, CA, U.S.A.). The program runs on a DeskPro 286 (COMPAQ Computer Corporation, Houston, TX, U.S.A.), equipped with a 80287 coprocessor, 640 kByte of conventional and 1 MByte of expanded memory, and an Enhanced Graphics Adapter with color monitor. The simulated chromatograms are based on a Gaussian peak-shape, using the plate-count and dead-volume observed in the chromatographic experiments.

TABLE II

THE CONCENTRATION OF THE SURFACTANT, [SDS], AND THE PERCENTAGE OF 2-PROPANOL, USED IN THE CHROMATOGRAPHIC EXPERIMENTS REGARDING THE MIXTURE OF THIRTEEN AMINO ACIDS–PEPTIDES

In addition the identities and capacity factors k' of the solutes are listed.

Mobile phase							
[SDS], *M*			0.1	0.1	0.25	0.4	0.4
% 2-Propanol			0.0	15.0	7.5	0.0	15.0
Components			k'				
1	Ala–Tyr	(AY)	5.5	3.2	1.7	1.4	0.9
2	Tyr	(Y)	11.3	3.0	2.4	2.9	1.1
3	Asp–Phe	(DF)	16.5	7.9	4.2	3.9	1.9
4	Leu–Tyr	(LY)	17.0	6.0	3.6	4.3	1.5
5	Gly–Leu–Tyr	(GLY)	18.3	6.9	3.7	4.3	1.5
6	Met	(M)	25.1	4.4	4.1	6.6	1.8
7	Trp	(W)	30.1	9.9	6.0	7.1	2.5
8	Arg	(R)	38.0	14.8	6.8	7.4	2.6
9	Leu–Trp	(LW)	49.3	15.1	8.3	11.3	3.2
10	Lys–Phe	(KF)	52.1	44.7	13.2	10.5	5.4
11	Gly–Phe–Leu	(GFL)	81.3	26.6	14.1	17.7	5.1
12	Phe–Phe	(FF)	81.5	21.8	12.6	18.2	4.6
13	Arg–Phe	(RF)	85.3	50.8	16.7	17.5	6.3

RESULTS AND DISCUSSION

In order to predict the properties of a chromatogram, such as the retention times and selectivities of the solutes that will be observed at a given mobile phase composition, we used the iterative regression optimization strategy originally described by Drouen *et al.*[29] and extended by Van Renesse *et al.*[30]. This is an interpretive optimization method which was also applied in ion-pairing chromatography[12,14]. First, the retention of all individual compounds in a mixture is modeled as a linear function of the variable(s) using a minimum number of initial experiments. For instance, in the case of one variable situation, φ_{org}, a linear model of ln k' *vs.* φ_{org} is derived on the basis of two initial values of φ_{org}. The parameter space for a given optimization is encompassed by the initial parameter values. Then, the retention of the solutes at mobile phase compositions other than those used in the actual measurements within the parameter space will be predicted through interpolation of the assumed linear model of ln k' *vs.* parameter(s). Based on the predicted retention values of all the compounds in the mixture, the quality of separation at all mobile phase compositions within the parameter space is calculated and an optimum is predicted. If the observed quality of the separation at the predicted optimum composition is not satisfactory, more experiments will have to be performed (*i.e.* through an iterative process) in order to locate the global optimum in the parameter space. The success or failure of finding the optimum parameter values with a minimum number of initial experiments would depend on the correctness of the linearity assumption of the model. In the case of

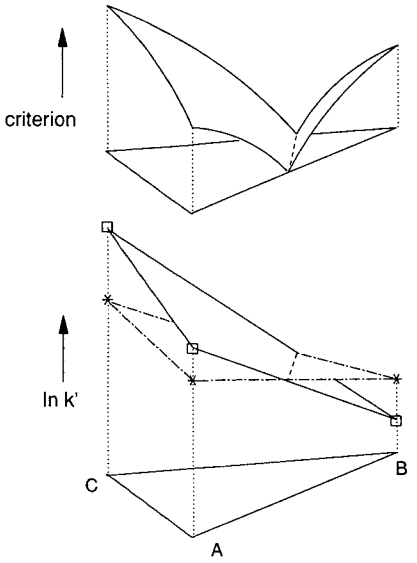

Fig. 1. An example of the retention-planes of a two component mixture, predicting the retention ln k' in the parameter space defined by mobile phase compositions A, B and C (lower part). The quality of the predicted chromatograms is expressed by means of a criterion, resulting in the response surface displayed in the top figure.

MLC, excellent agreement between the predicted and observed optimum chromatograms was observed with a minimum number of experiments as shown below. This is attributed to the regular change in retention behavior as a function of the variables. In this case we are dealing with two parameters, the concentration of surfactant and of 2-propanol respectively, and consequently the linear model will consist of a plane fitted through the retention data observed in three initial chromatograms. The three chromatograms are selected such that they are enclosing the parameter space currently under investigation. The model is then used to predict the retention of the component at a point located within this parameter space. This process is repeated for all components in a mixture, and the quality of the resulting estimated chromatograms is expressed by means of a suitable criterion. Fig. 1 shows an example with two components.

On the basis of a theoretical derivation using the solubility parameter concept, it was found that the relation between ln k' and the concentration of organic modifier in RP-HPLC is in fact quadratic[31] and the assumed linearity will only hold over a limited range of compositions. To compensate for deviations from linearity in the selected parameter space, further refinement of the model using additional measurements is usually required in an actual optimization in conventional RP-HPLC with hydro–organic eluents. In the case of MLC only a small range of organic modifier concentrations is examined and we can expect that deviations from linearity will be limited. The actual relation between the capacity factor and micelle concentration is given in eqn. 1. However, due to the fact that all examined micelle concentrations are of the same order of magnitude, only small deviations from linearity will be observed in relations between ln k' and $[M]$.

In order to derive an unambiguous definition of the examined parameter space[14], the retention is determined at five mobile phase compositions as indicated in Tables I and II: four measurements at the corners of the selected two-dimensional parameter-space and one measurement in the center. The square parameter space consists of four triangle subspaces. A separate linear model is determined for each of the four subspaces defined by three of the five measurements, *i.e.* two corner points and the central point. The extreme values of the parameters are dictated by the practical limitations of the chromatographic system: the lower surfactant concentration must be well above the CMC (*ca.* 8 m*M* for SDS and 0.9 m*M* for CTAB at ambient temperatures and without organic modifier) and must be strong enough to cause elution of all components. The upper surfactant concentration is determined by a combination of the solubility of the surfactant, the viscosity of the resulting mobile phase and degradation of the efficiency at higher concentrations. The organic modifier concentration is limited to a maximum of *ca.* 15% propanol to ensure the integrity of the micelles.

First we are concerned with a general description of the observed selectivity over the full parameter space, and the initial five compositions will suffice. However, in order to derive practical separations additional measurements in the areas of interest must be checked against the applied model and if necessary the model must be refined. The following discussion will first focus on the phenol mixture, followed by a description of the results regarding the amino acid–peptide mixture.

Elution strength

As expected, a decrease in retention time was observed when either the surfactant concentration (and hence the micelle concentration) or the concentration of organic modifier is increased. This is illustrated in Fig. 2 for 4-*tert.*-butylphenol: the mobile phase compositions where the same retention is expected on the basis of the linear interpolation are connected, resulting in "iso-retention" (dashed) lines. It is obvious that when both micelle and modifier concentration are increased, the respective effects will be combined and an even shorter retention is observed. In this way the retention of 4-*tert.*-butylphenol decreases from a capacity factor of 87.8 in the

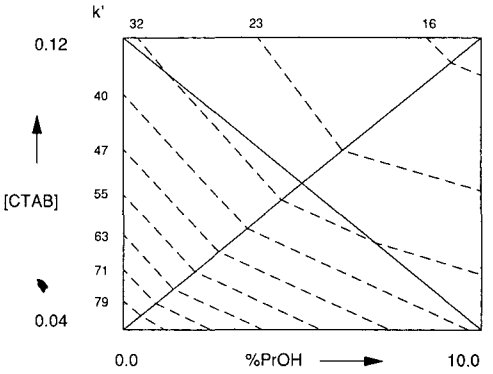

Fig. 2. The capacity factor of 4-*tert.*-butylphenol, *k'*, as a function of the surfactant concentration [CTAB] (*M*) and the percentage of 2-propanol, %PrOH. The dashed lines connect points defined by equal capacity factors. The solid lines connect the measured compositions thus defining the retention planes.

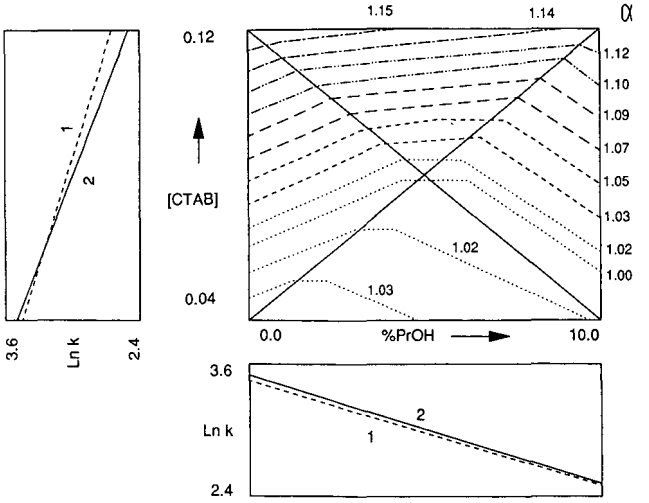

Fig. 3. Retention, ln k', of phenol (1) and 4-hydroxybenzaldehyde (2) as a function of the 2-propanol concentration (%PrOH) at 0.04 *M* CTAB (lower frame) and as a function of the surfactant concentration [CTAB] (*M*) at 0% 2-propanol (upper left frame). The selectivity α of the two components as a function of both surfactant and 2-propanol concentration: the dashed lines connect points with identical selectivity (upper right frame).

lower left corner (0.04 *M* CTAB, 0% 2-propanol) to 14.8 in the upper right corner (0.12 *M* CTAB, 10% 2-propanol).

Selectivity

Although the above trend is observed for all components, it must be stressed that the amount of reduction will not be the same, thus resulting in the desired change in selectivity. This is further illustrated by examining the changes in selectivity, α, which is defined as the ratio of the capacity factors of two components where numerator and denominator are selected such that the resulting value is larger than 1. Fig. 3 shows the effect of varying surfactant and propanol concentration on the selectivity of phenol and 4-hydroxybenzaldehyde: when the propanol concentration is increased a general decrease in selectivity is observed, due to a similar change in retention (lower frame of Fig. 2). However, by increasing the surfactant concentration an increase in selectivity is observed due to the fact that 4-hydroxybenzaldehyde shows a stronger drop in retention than phenol. Although the selectivity goes through a minimum as the two components coelute somewhere between 0.04 and 0.12 *M* CTAB, the final separation in 0.12 *M* CTAB is clearly superior to the ones observed at other mobile phase compositions.

The reverse is observed when the retention behavior of 4-hydroxy-propiophenone and 4-nitrophenol is examined (Fig. 4): a reduction of the selectivity occurs when the surfactant concentration is increased, since the two components are coeluting in 0.12 *M* CTAB. When the 2-propanol concentration is increased from 0 to 10% the selectivity increases, since the reduction in retention of 4-hydroxy-propiophenone is stronger than the change in retention of 4-nitrophenol.

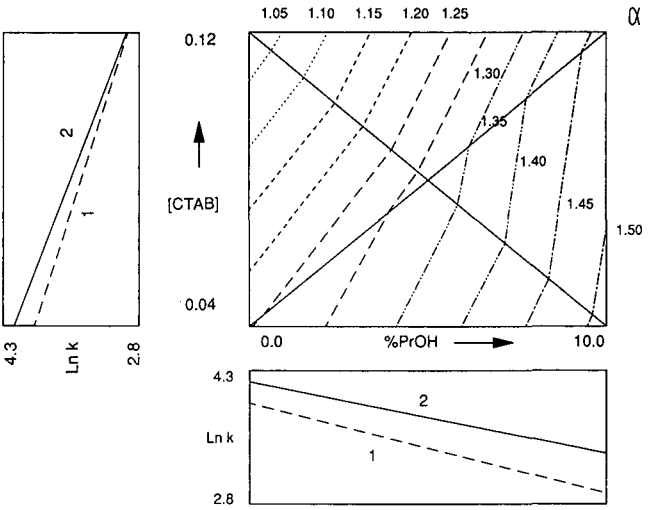

Fig. 4. Retention, ln k', of 4-hydroxypropiophenone (1) and 4-nitrophenol (2) as a function of the 2-propanol concentration at 0.04 *M* CTAB (lower frame) and as a function of the surfactant concentration [CTAB] (*M*) at 0% 2-propanol (upper left frame). The selectivity α of the two components as a function of both surfactant and 2-propanol concentration: the dashed lines connect points with identical selectivity (upper righ frame).

Simultaneous evaluation of selectivity and elution strength

Apparently in MLC different components react in different ways to changes in concentration of surfactant and/or organic modifier. In this way the chromatographer is supplied with additional tools to refine a separation and optimize the selectivity for a given multi-component mixture. However, the described advantage can only be exploited to the fullest when both parameters are simultaneously taken into account, *i.e.* by only using the surfactant or the organic modifier concentration, or varying one after optimizing the other, a better separation can be easily missed. This is generally true for other HPLC methods where co-optimization of the variables is necessary, *e.g.* [ion pair] and pH in ion-pair LC as demonstrated by Kong *et al.*[32].

It is possible that in MLC the optimal selectivity is observed when mobile phase compositions are used with a higher elution strength, depending on the components involved. Although this will complicate the design of an efficient optimization strategy, the gain in control over the separation can be considerable and will outweigh this disadvantage. As an example, the chromatograms of the mixture of fifteen phenols at the five mobile phase compositions are displayed in Fig. 5 (the chromatograms were simulated on the basis of the retention data in Table I). The best overall separation (in terms of selectivity) is observed in chromatogram E, which also happens to be the chromatogram with the minimum overall retention time. The other chromatograms show a severe coelution of a larger number of components. This is further emphasized in Fig. 6, showing the minimum selectivity which will be observed in chromatograms of the fifteen-component mixture recorded at different mobile phase compositions. The maximum values of this minimum selectivity are observed in the upper right corner, *i.e.* in the region with high elution strength.

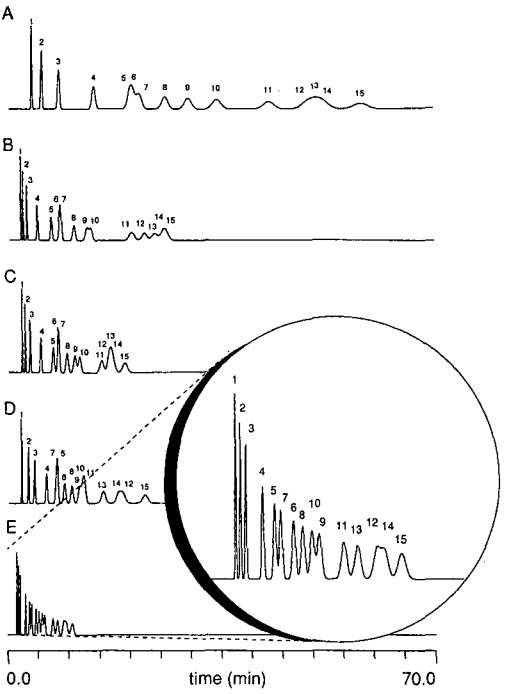

Fig. 5. Five simulated chromatograms using retention data of the fifteen components from Table I and assuming 2500 plates and equal areas for all components. Mobile phase compositions: (A) 0.04 *M* CTAB, 0% 2-propanol; (B) 0.04 *M* CTAB, 10% 2-propanol; (C) 0.08 *M* CTAB, 5% 2-propanol; (D) 0.12 *M* CTAB, 0% 2-propanol; (E) 0.12 *M* CTAB, 10% 2-propanol.The identification numbers of the solutes refer to Table I.

Optimization of selectivity

As can be observed in Fig. 5, showing the simulated chromatograms for the phenol mixture, the best selectivity for this mixture is observed at high micelle and propanol concentrations. However, the resolution of components 12 and 14 is still

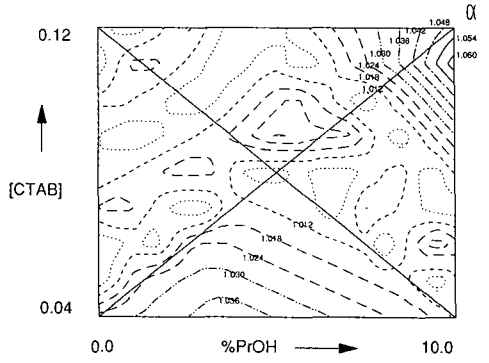

Fig. 6. A contourplot indicating the minimum selectivity that will be observed in chromatograms of the fifteen-component mixture described in Table I, when recorded at different mobile phase compositions. The lines connect points with equal minimum selectivity.

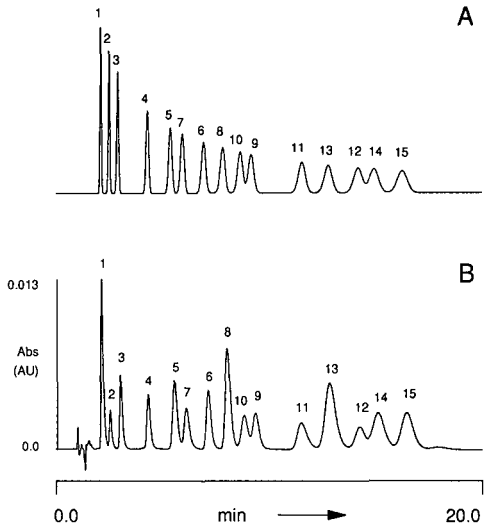

Fig. 7. Chromatograms of the fifteen-component mixture recorded at 0.11 *M* CTAB and 10% 2-propanol. (A) The chromatogram predicted on the basis of the linear retention model used in the optimization, assuming 4500 plates and equal areas for all components. (B) The measured chromatogram using two 12.5-cm columns and a flow of 1.5 ml/min. (for further details see Experimental section). The numbering refers to table I.

insufficient. In order to better resolve these two peaks, we examined the minimum α plot (for the fifteen-component mixture) over the full parameter space (Fig. 6). Apparently, a maximum value for the minimum selectivity in the chromatograms will be observed at 0.11 *M* CTAB and 10% 2-propanol. In order to test the accuracy of the predicted optimum, a chromatographic experiment with the fifteen-component mixture was performed at the above mobile phase composition. To increase the resolution, a two-column system was used, resulting in an average plate-count of 4500. The increase in retention time was partially compensated for by operating at 1.5 ml/min.

Both the predicted and observed chromatograms are shown in Fig. 7. The change in mobile phase composition has indeed improved the selectivity of components 12 and 14 without deteriorating the selectivity of the other separations (observed minimum selectivity 1.066). Furthermore, the observed retention data (Fig. 7B) correspond well with the predicted capacity factors (Fig. 7A), indicating that the assumed linear model is reasonable. Additionally, it will be unlikely that a better selectivity will be observed anywhere within the examined parameter space. In order to derive a truly optimal separation other parameters, such as pH, must be involved in the optimization procedure (in fact the five initial experiments originated from a parallel investigation into the application of MLC in quantitative structure–activity relationship studies of phenols, which requires experimental circumstances different from those more suited for a separation problem).

The amino acid–peptide mixture

In the foregoing discussion we concentrated on the observed selectivity in the

various chromatograms to stress the lack of correlation between elution strength and selectivity in MLC. However, the use of selectivity as an optimization criterion has a number of disadvantages, one of which is the fact that the observed separation (resolution) is determined by a combination of selectiviy, retention and efficiency. However, other optimization criteria which express the goal of the chromatographer in a better way can also be used without changing the overall optimization strategy[11]. This is illustrated by optimizing the separation of thirteen amino acids and small peptides using iterative regression design and a resolution based criterion (Table II). In this case the normalized resolution product r (ref. 29), was chosen as the optimization criterion which aims at an even distribution of all peaks over the available separation space:

$$r = \prod_{i=1}^{n-1} R_{s_{i+1,i}} \Big/ \left[\sum_{i=1}^{n-1} R_{s_{i+1,i}} / (n-1) \right]^{n-1} \qquad (2)$$

where $R_{s_{i+1,i}}$ represents the resolution between peaks $i+1$ and i out of a total of n components. Since the product of all observed (expected) resolutions is used, coelution will effectively cause the criterion to drop to zero. On the other hand, extremely long chromatograms with a number of unnecessarily large resolution values will also be represented by low criterion values. This criterion has its own disadvantages: due to the normalization, a very short chromatogram with all

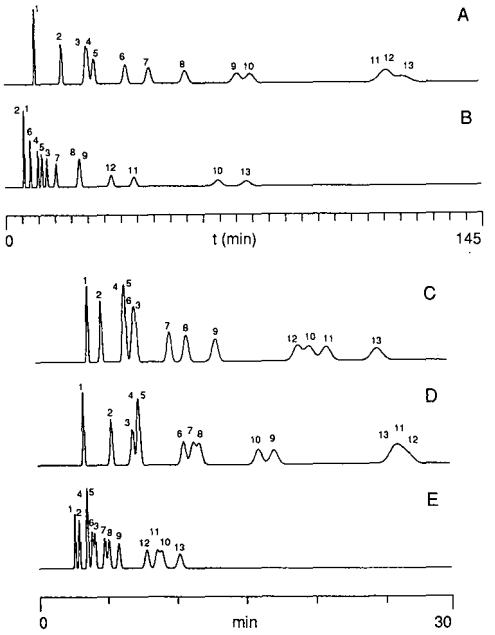

Fig. 8. Five simulated chromatograms using retention data of the thirteen components from Table II and assuming 4000 plates and equal areas for all components. Mobile phase compositions: (A) 0.1 *M* SDS, 0% 2-propanol; (B) 0.1 *M* SDS, 15% 2-propanol; (C) 0.25 *M* SDS, 7.5% 2-propanol; (D) 0.4 *M* SDS, 0% 2-propanol; (E) 0.4 *M* SDS, 15% 2-propanol. The identification numbers of the solutes refer to Table II.

components evenly distributed will still be heavily favored, even if the maximum observed resolution is small. If this is the case, only an increase of the plate-count will provide the desired separation (*not* a decrease of the solvent strength due to the effect on selectivity as described above). Alternatively, a response surface related to a different criterion can be examined.

The initial chromatograms are displayed in Fig. 8, and observations similar to those made for the phenol mixture are apparent: either increase in micelle concentration or increase in organic modifier concentration will decrease the overall retention, but will influence different solutes in different ways. This is best seen by looking at components 6, 11 and 12, showing a much stronger change in retention with varying conditions than the surrounding components, causing numerous cases of coelution and peak-crossings in intermediate mobile phase compositions. A satisfactory separation can only be found through a systematic search of the parameter space, as displayed in Fig. 9A. In this case (Fig. 9A) the predicted optimum criterion value is located at an intermediate elution strength at 0.16 *M* SDS and 12% 2-propanol. The predicted chromatogram at this composition is shown in Fig. 10A, showing an almost full separation of all components. Although the reduction in analysis time (not included in the criterion and consequently not considered in a systematic way in this optimization) is not as dramatic as in the previous example (Fig. 7), the chromatogram still shows a threefold reduction as compared to the chromatogram at 0.1 *M* SDS. What is more important however, is the fact that the actual chromatogram recorded at the specified mobile phase composition (Fig. 10B) is almost identical to the predicted one (Fig. 10A), with the exception of the last two components which show a slightly lower retention than predicted (resulting in a slightly lower criterion value of 0.170 instead of 0.175). This means that the response surface, predicted on the basis of the first five experiments, will hardly change when the new data point is included in the modeling, resulting in the same location for the optimum. A stable response surface is indicative of a reliable optimum, and no further experiments are necessary to further refine the location of the optimal mobile phase composition. Consequently, the regular retention behavior observed in these MLC

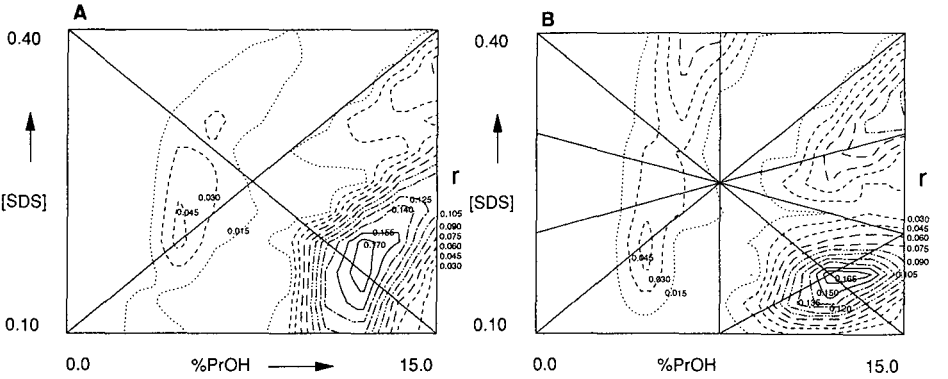

Fig. 9. A contourplot indicating the normalized resolution product *r* that will be observed in chromatograms of the thirteen-component mixture described in Table II, when recorded at different mobile phase compositions. The lines connect points with equal criterion values. (A) The response surface on the basis of five measurements. (B) The response surface on the basis of twelve experiments.

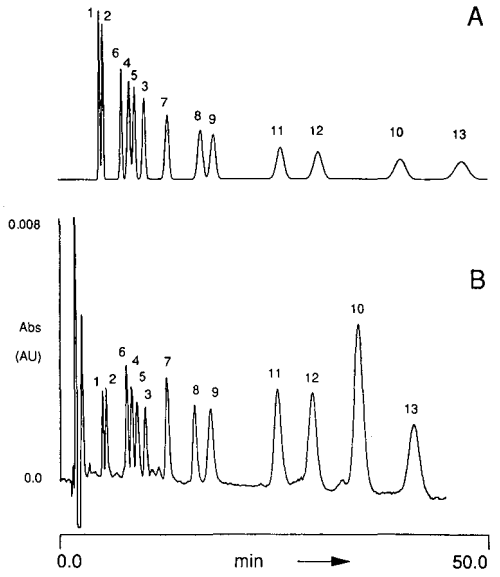

Fig. 10. Chromatograms of the thirteen-component mixture at 0.16 *M* SDS and 12% 2-propanol. (A) The chromatogram predicted on the basis of the linear retention model used in the optimization, assuming 4000 plates and equal areas for all components. (B) The measured chromatogram (further details in experimental section). The numbering refers to Table II.

examples, which is responsible for the stability of the response surface, enables an optimization on the basis of a relatively small number of experiments. As a final proof, Fig. 9B displays the response surface observed when a larger number of chromatograms is measured and included in the retention modeling, one of them the actual optimum displayed in Fig. 10B. The additional data-points are used to define a finer grid of triangles over the parameter-space, resulting in a more accurate response surface. Although a number of secondary, local, maxima are slightly more prominent, the important characteristics of the response surface such as location, criterion value and stability of the global optimum remain aproximately the same.

CONCLUSION

The two examples described in the previous section illustrate the following points:

Due to the complex retention mechanisms involved, a separate optimization of elution strength and selectivity in MLC is inefficient. In fact, it is observed that an increase in elution strength can coincide with an enhancement of the selectivity. Since the concentration of surfactant and organic modifier both influence the above factors, it is essential that a variation of these two parameters is examined simultaneously.

Although retention and selectivity vary strongly with varying concentrations of surfactant and/or organic modifier, the observed changes are very regular and are well described by a simple linear model with ln k' as dependent variable. As a consequence, it is possible to predict the retention behavior of the solutes on the basis of a limited

number of experiments (in the above examples five), even though these experiments are relatively far apart in the parameter space. In this way it is easy to estimate the likelihood of finding the desired separation, defined by the applied criterion, within the selected parameter space, thus reducing the required effort with respect to actual experiments.

The major drawback of practical separations applying MLC still is the low chromatographic efficiency caused by the resistance to mass transfer in the processes involving the micelles and the with surfactant modified stationary phase. This is especially important when the increased micelle concentrations cause a decrease in plate count, resulting in a varying efficiency over the parameter space. In this respect it is worthwhile to examine the inclusion of the expected efficiency and peak shape in the expression of the chromatographic quality in order to reduce the problem as much as possible, for instance by applying the adjusted resolution equations described by Schoenmakers *et al.*[33]. In addition to improvements in the chromatographic efficiency, inclusion of additional parameters such as pH and temperature will further increase possibility of harnessing the separation power supplied by secondary equilibria.

ACKNOWLEDGEMENTS

The authors gratefully acknowledge the financial support by the National Institutes of Health (GM 38738). Acknowledgement is also made to the donors of the Petroleum Research Funds administered by the American Chemical Society.

REFERENCES

1 B. L. Karger, J. N. LePage and N. Tanaka, in Cs. Horváth (Editor), *High Performance Liquid Chromatography: Advances and Perspectives*, Vol. 1, Academic Press, New York, 1980, p. 113.
2 J. P. Foley and W. E. May, *Anal. Chem.*, 59 (1987) 102.
3 J. P. Foley and W. E. May, *Anal. Chem.*, 59 (1987) 110.
4 M. G. Khaledi, J. K. Strasters, A. H. Rodgers and E. D. Breyer, *Anal. Chem.*, 62 (1990) 130–136.
5 P. M. J. Coenegracht, H. J. Metting, A. K. Smilde and P.J. M. Coenegracht-Lamers, *Chromatographia*, 27 (1989) 135.
6 L. R. Snyder, M. A. Quarry and J. L. Glajch, *Chromatographia*, 24 (1987) 33.
7 M. A. Quarry, R. L. Grob, L. R. Snyder, J. W. Dolan and M. P. Rigney, *J. Chromatogr.*, 384 (1984) 163.
8 L. R. Snyder, J. L. Glajch and J. J. Kirkland, *Practical HPLC Method Development*, Wiley, New York, 1988, Ch. 2 and 4.
9 P. J. Schoenmakers, *Optimization of Chromatographic Selectivity, a Guide to Method Development*, Elsevier, Amsterdam, 1986.
10 J. C. Berridge, *Techniques for the Automated Optimization of HPLC Separations*, Wiley, Chichester, 1985.
11 P. R. Haddad and S. Sekulic, *J. Chromatogr.*, 392 (1987) 65.
12 H. A. H. Billiet, A. C. J. H. Drouen and L. de Galan, *J. Chromatogr.*, 316 (1984) 231.
13 A. P. Goldberg, E. Nowakowska, P. E. Antle and L. R. Snyder, *J. Chromatogr.*, 316 (1984) 241.
14 H. A. H. Billiet, J. Vuik, J. K. Strasters and L. de Galan, *J. Chromatogr.*, 384 (1987) 153.
15 P. M. J. Coenegracht, N.V. Tuyen, H. J. Metting and P.J. M. Coenegracht-Lamers, *J. Chromatogr.*, 389 (1987) 351.
16 J. K. Strasters, F. Coolsaet, A. Bartha, H. A. H. Billiet and L. de Galan, *J. Chromatogr.*, 499 (1990) 523.
17 G. K.-C. Low, A. Bartha, H. A. H. Billiet and L. de Galan, *J. Chromatogr.*, submitted for publication.
18 P. Yarmchuk, R. Weinberger, R. F. Hirsch and L. J. Cline Love, *Anal. Chem.*, 54 (1982) 2233.
19 D. W. Armstrong and G. Y. Stine, *Anal. Chem.*, 55 (1983) 2317.
20 M. G. Khaledi, *Anal. Chem.*, 60 (1988) 876.

21 D. W. Armstrong and F. Nome, *Anal. Chem.*, 53 (1981) 1662.
22 M. Arunyanart and L. J. Cline Love, *Anal. Chem.*, 56 (1984) 1557.
23 J. G. Dorsey, M. T. DeEchegaray and J. S. Landy, *Anal. Chem.*, 55 (1983) 924.
24 P. Yarmchuck, R. Weinberger, R. F. Hirsch and L. J. Cline Love, *J. Chromatogr.*, 283 (1984) 47.
25 D. W. Armstrong, T. J. Ward and A. Berthod, *Anal. Chem.*, 58 (1986) 579.
26 M. F. Borgerding, R. L. Williams, W. L. Hinze and F. H. Quinn, *J. Liq. Chromatogr.*, 12 (1989) 1367.
27 M. Arunyanart and L. J. Cline Love, *Anal. Chem.*, 57 (1985) 2837.
28 A. H. Rodgers, J. K. Strasters and M. G. Khaledi, in preparation.
29 A. C. J. H. Drouen, H. A. H. Billiet, P. J. Schoenmakers and L. de Galan, *Chromatographia*, 16 (1982) 48.
30 A. van Renesse, J. K. Strasters, H. A. H. Billiet and L. de Galan, *Thirteenth Symposium on Column Liquid Chromatography,* June 26 and 27, 1989, Abstracts, 1989, p. 218.
31 P. J. Schoenmakers, H. A. H. Billiet and L. de Galan, *Chromatographia*, 205 (1982) 205.
32 R. C. Kong, B. Schock and S. N. Deming, *J. Chromatogr.*, 199 (1980) 307–316.
33 P. J. Schoenmakers, J. K. Strasters and A. Bartha, *J. Chromatogr.*, 458 (1988) 355.

Journal of Chromatography, 511 (1990) 35–47
Elsevier Science Publishers B.V., Amsterdam

CHROM. 22 399

Important parameters in liquid chromatography–continuous-flow fast atom bombardment mass spectrometry

P. KOKKONEN
TNO–CIVO Institutes, P.O. Box 360, 3700 AJ Zeist, and Division of Analytical Chemistry, Center for Bio-Pharmaceutical Sciences, P.O. Box 9502, 2300 RA Leiden (The Netherlands)
E. SCHRÖDER
Finnigan MAT GmbH, Barkhausenstrasse 2, 2800 Bremen 14 (F.R.G.)
W. M. A. NIESSEN* and U. R. TJADEN
Division of Analytical Chemistry, Center for Bio-Pharmaceutical Sciences, P.O. Box 9502, 2300 RA Leiden (The Netherlands)
and
J. VAN DER GREEF
TNO-CIVO Institutes, P.O. Box 360, 3700 AJ Zeist, and Division of Analytical Chemistry, Center for Bio-Pharmaceutical Sciences, P.O. Box 9502, 2300 RA Leiden (The Netherlands)
(First received December 12th, 1989; revised manuscript received February 26th, 1990)

ABSTRACT

Continuous-flow fast atom bombardment (CF-FAB) is an attractive technique of interfacing reversed-phase high-performance liquid chromatography and mass spectrometry (LC–MS). Some of the important parameters affecting the performance of CF-FAB were studied. The wettability of the CF-FAB target and liquid film properties on the surface of the CF-FAB target play an important role in obtaining stable performance in LC–CF-FAB-MS. The wettability of the target can be improved by an acid treatment. The thermal conductivity of the CF-FAB target material together with the flow-rate and the mobile phase composition influence the liquid film properties of the target. The optimum supply rate of glycerol is observed to be 0.3 μl/min for LC–CF-FAB-MS under the studied conditions. Some bioanalytical examples of LC–CF-FAB-MS are shown.

INTRODUCTION

Continuous-flow fast atom bombardment (CF-FAB) is an important development in the rapidly growing research field of interfacing high-performance liquid chromatography and mass spectrometry (LC–MS). The reason for this is the improved performance of CF-FAB compared with conventional FAB and the possibility of using FAB as an ionization method in LC–MS. FAB is made available to on-line LC–MS applications by using either a frit-FAB interface, as described first by Ito *et al.*[1], or a direct introduction type of interface, as described by Caprioli *et al.*[2]. The

0021-9673/90/$03.50

TABLE I

SYSTEMS INVESTIGATED

Parameter	*System A*	*System B*	*System C*	*System D*	*FIA I*	*FIA II*
Pump	Pharmacia	Pharmacia	LKB	LKB	LDC/Milton Roy	LKB
Mobile phase[a]	TFA–Gly–ACN–H_2O	TFA–Gly–ACN–H_2O	TFA–Gly–ACN–H_2O	Gly–ACN–buffer	Gly–ACN–H_2O	TFA–Gly–MeOH
Composition (%, w/w)	0.26:10:30:59.74	0.25:10:30:59.75	0.25:9.9:29.8:60.05	10.2:41.4:48.4	10:30:60	0.28:10.1:89.62
LC flow-rate (ml/min)	1.0	1.0	1.2	1.0	5–7	500
Injector (μl)	20	20	20	20	0.5	20
Column	Techopak	Techopak	Techopak	PRP-1	–	–
Split capillary	19 cm × 200 μm I.D.	19 cm × 200 μm I.D.	44 cm × 150 μm I.D.	20 cm × 220 μm I.D.	–	40 cm × 200 μm I.D.
CF-FAB capillary	85 cm × 75 μm I.D.	85 cm × 75 μm I.D.	75 cm × 75 μm I.D.	80 cm × 75 μm I.D.	100 cm × 75 μm I.D.	80 cm × 75 μm I.D.
Splitting ratio	1:180	1:200	1:170	1:160	–	1:74
CF-FAB flow-rate (μl/min)	6	5	7	6	5–7	6
Mass spectrometer	MAT 8200	MAT 8200	MAT 90	MAT 90	MAT 90	MAT 90
Source temperature (°C)	40	40	60	75	40	40
Cold trap	No	No	Yes	Yes	No	Yes
Wick	No	No	Yes	Yes	Yes	Yes

[a] TFA = trifluoroacetic acid; Gly = glycerol; ACN = acetonitrile; MeOH = methanol; buffer = 0.1 *M* ammonium acetate (pH 8.3) and H_2O = water.

latter interface is usually referred to as the continuous-flow FAB or the dynamic FAB interface, and is the topic of this paper.

In CF-FAB, the maximum flow-rate is *ca.* 10 μl/min, leading to the necessity to split the eluent after conventional LC columns (3–4.6 mm I.D.). As a result, the concentration detection limits are increased by a factor of 50–100. Miniaturization of the LC system, *e.g.*, to 1 mm I.D. columns, reduces the splitting ratio but does not improve the concentration limits, because the injection volume in microbore systems is decreased correspondingly.

Despite the mentioned difficulties, impressive results have been reported with a broad variety of compounds[1–15]: bile acids[1,13], peptides[2–8], dansylated amino acids[3], antibiotics[4,14], oligosaccharides[9], drugs[10], glucosinolates[11], non-ionic detergents[12], polyethylene glycol oligomers[14] and herbicides[15]. In these applications, either flow-injection analysis (FIA)[1–3,5,6,8,9,13,14] or packed fused-silica capillary[1,4,9,12–15], microbore[3,4,6] or conventional bore[7,10,11] columns have been used.

Although the applicability of the CF-FAB method has been studied intensively by various groups, little attention has been paid to a systematic study of the key parameters determining the performance of CF-FAB, both from a mass spectrometric point of view and as an LC–MS interface. In this work, some of the important parameters of CF-FAB were investigated, such as the target material and conditions enhancing the wettability and liquid film properties of the target. Some illustrative examples of CF-FAB applied in LC–MS are given.

EXPERIMENTAL

Liquid chromatography

The six different experimental set-ups that have been used are summarized in Table I and are referred to in the text as systems A–D and FIA I and II. In systems A–D conventional-bore LC columns in combination with a splitter were used. FIA was performed using either a 0.5-μl injector (FIA I) and a low flow-rate or a 20-μl injector (FIA II) and a high flow-rate in combination with a splitter.

The LC system consisted of either a Pharmacia (Uppsala, Sweden) P-3500 pump, an LKB (Bromma, Sweden) 2150 pump or an LDC/Milton Roy (Riviera Beach, FL, U.S.A.) MicroMetric metering pump and a Rheodyne (Berkeley, CA, U.S.A.) Model 7125 (20-μl) or a Model 7410 (0.5-μl) injection valve.

For the determination of dextromethorphan in plasma (systems A–C), a Techopak reversed-phase C_{18} column (15 cm × 3.9 mm I.D., packed with 10-μm material) (HPLC Technology, Macclesfield, U.K.) was used. A laboratory-packed PRP-1 (Hamilton, Reno, NV, U.S.A.) column (10 cm × 3.9 mm I.D.) with 10-μm particles was used for the determination of erythromycin 2′-ethylsuccinate in plasma (system D). The temperature of the column and the stainless-steel capillaries (systems A–D) was kept at 56°C in order to reduce the viscosity of the mobile phase.

The eluent from the LC column (systems A–D) and from FIA II was directed to a laboratory-made splitting device described in detail elsewhere[10]. FIA I and the splitter were connected to a Finnigan MAT (Bremen, F.R.G.) prototype CF-FAB probe by means of a 75-μm I.D. fused-silica capillary, the so-called CF-FAB capillary.

Mass spectrometry

The CF-FAB probe was fitted to either a Finnigan MAT 8200 or a Finnigan MAT 90 double-focusing mass spectrometer, operating at 3 and 5 kV, respectively. Both instruments were equipped with a FAB gun (Ion Tech, Teddington, U.K.) using xenon and producing a beam of neutral atoms with 5–8 kV energy. The FAB spectra were recorded in the positive ion mode by scanning from 20 to 1000 with a scan speed of 1 s per decade.

In the MAT 90 instrument an exchangeable ion volume with a wick was applied. The exchangeable ion volume reduces contamination problems. The wick was prepared from compressed paper and positioned at the bottom of the ion volume. Additional vacuum pumping at the ion source housing was obtained with a liquid nitrogen trap. In the MAT 8200 instrument there was no possibility of using an exchangeable ion volume, a wick or a cold trap.

Acid treatment of the target

Four different metal targets were used at the CF-FAB probe, *viz.*, stainless-steel, copper, nickel and silver. The stainless-steel target was pretreated with concentrated hydrochloric acid for 30 min. The target was washed in an ultrasonic bath with both water and methanol for 15 min and subsequently air dried. The nickel and silver targets were pretreated with concentrated nitric acid for 15 min and washed as described above. The copper target was quickly washed with 30% hydrochloric acid and subsequently rinsed with water.

Reagents

Dextromethorphan hydrobromide, erythromycin, erythromycin 2′-ethylsuccinate and erythromycin d_5-2′-ethylsuccinate were obtained from the Research Center of Orion Pharmaceutica (Espoo, Finland). Vindesine was supplied by Dr. D. E. M. M. Vendrig (Department of Pharmaceutical Analysis, Faculty of Pharmacy, University of Utrecht, The Netherlands).

Trifluoroacetic acid, hydrochloric acid, nitric acid, methanol, hexane, ammonium acetate, ammonia, iodomethane and diethyl ether were supplied by E. Merck (Darmstadt, F.R.G.). Glycerol (98% pure) was purchased from Lamers & Pleuger ('s-Hertogenbosch, The Netherlands), sodium carbonate and potassium carbonate (AnalaR) from BDH (Poole, U.K.), triethylamine by Pierce (Rockford, IL, U.S.A.) and acetonitrile (ChromAR) from Promochem (Wesel, F.R.G.). The pH of the ammonium acetate buffer was adjusted with concentrated ammonia solution. Water was distilled before use.

The mobile phase was prepared by weighing the solvents. It was filtered and degassed ultrasonically before use. The mobile phase was prepared daily in order to avoid bacterial growth.

Sample preparation

Stock solutions containing 15 mg of dextromethorphan hydrobromide were prepared in 10 ml of water. Plasma samples containing 1.8 μg/ml of dextromethorphan were prepared by adding the appropriate amount in 50 μl of water to 2.0 ml of blank human plasma. The sample pretreatment procedure, consisting of a liquid–liquid extraction step, has been described in detail elsewhere[10].

Stock solutions of erythromycin 2′-ethylsuccinate (1.18 mg/ml) and erythromycin d_5-2′-ethylsuccinate (1.30 mg/ml) were prepared in acetonitrile. Duplicate plasma samples containing 0.25, 0.49, 0.98, 2.5, 4.9 and 9.8 μg/ml of erythromycin 2′-ethylsuccinate were prepared by adding the appropriate amount of erythromycin 2′-ethylsuccinate in 50 μl of acetonitrile to 2.0 ml of blank human plasma; 13 μg of d_5-erythromycin 2′-ethylsuccinate in 50 μl of acetonitrile was added to the samples as an internal standard. After rapid mixing, 200 μl of saturated sodium carbonate solution and 5.0 ml of diethyl ether were added. The tubes were gently shaken on a horizontal shaker for 15 min. After centrifugation for 5 min (1000 *g*), 4.0 ml of the organic layer were separated and evaporated to dryness in a gentle stream of helium at 30°C. The residue was dissolved in 50 μl of acetonitrile. An aliquot of 20 μl was injected onto the HPLC column (system D).

Methylation of dextromethorphan

Methylation of dextromethorphan was performed according to Kidwell *et al.*[16]. To 950 μl of water 10 mg of potassium carbonate and 2.5 μg of the dextromethorphan in 50 μl of water were added. After mixing for 30 s, 250 μl of methanol and 50 μl of iodomethane were added. The mixture was heated at 60°C for 5 min until the solution was homogeneous and 20 μl of the sample were injected onto the FIA II system.

RESULTS AND DISCUSSION

CF-FAB target

In LC–CF-FAB-MS the sample from the LC column or from the flow-injection system is introduced to the CF-FAB target via a fused-silica capillary. The sample in a glycerol matrix is bombarded at the target with a beam of 5–8-kV xenon atoms to produce ions which are mass analysed. A schematic diagram of the CF-FAB target is given in Fig. 1. The positioning of the fused-silica capillary at the target tip is an important aspect in producing a homogeneous film of the mobile phase on the target. If the tip of the capillary protrudes too much, droplets of the mobile phase are formed on the surface of the target and unstable vaporization of the mobile phase takes place. When the tip of the capillary protrudes *ca.* 0.5 mm out of the surface of the target, it is possible to obtain a good liquid film. With the help of an adjustment screw in the CF-FAB probe the positioning of the tip is simplified. Compressed paper at the

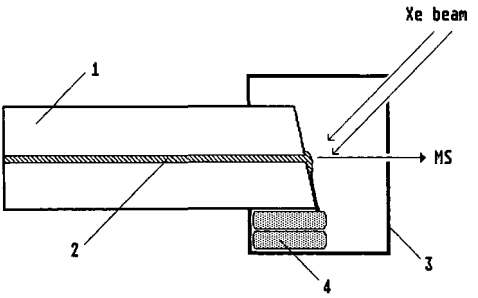

Fig. 1. Schematic diagram of the CF-FAB target with an exchangeable ion volume. 1 = CF-FAB target; 2 = CF-FAB capillary; 3 = exchangeable ion volume; 4 = wick.

bottom of the ion volume, the so-called wick, is used to collect the excess of mobile phase from CF-FAB target to prevent droplet formation at the CF-FAB target and to maintain a liquid film of the mobile phase on the target.

The wettability of the target is a key factor for the stable performance of the LC–CF-FAB-MS system. Treatment of the target surface with a concentrated acid roughens the surface of the target and thereby enchances the wettability. The roughness is maintained longer when an acid is also included in the mobile phase, *e.g.*, 0.2% trifluoroacetic acid (TFA). The wick in combination with the correctly adjusted capillary tip and the acid-treated target improve the liquid film properties, resulting in improved stability of the chemical background ions.

Stainless-steel[1,9–11,13], copper[2,10], gold[3,4,6] and silver[12] have been used as target and frit materials in CF-FAB. Takeuchi *et al.*[14] compared the performances of stainless-steel, silver, glass, paper and PTFE as frit materials. They concluded that the highest intensities for the analyte are observed when stainless-steel and silver frits are used, and that this is due to the good wettability of these materials by glycerol. Nickel, silver, copper and stainless-steel have been tested as target materials in our laboratory. The performance of the target material was evaluated with respect to the stability of the baseline by monitoring the intensities of protonated glycerol (*m/z* 93) and protonated acetonitrile (*m/z* 42). A typical example of a background signal is given in Fig. 2 (FIA I, with an acid-treated nickel target). When nickel, silver or copper are used as target materials, good stability of the background ions is achieved after a few minutes. The latter takes up to 15 min with a stainless-steel target. The observed good liquid film properties are probably due to the good thermal conductivity of these target materials resulting in enhanced evaporation of the mobile phase. A disadvantage of the nickel target is that the time-consuming roughening had to be done every 2 h to maintain the wettability of the target and consequently the stability of the baseline. The silver and copper targets are difficult to use in practice because of the strong clustering of copper and silver ions (no TFA can be used for the latter material). The best long-term stability was obtained with the acid-treated stainless-steel target. Although it takes more time to achieve stability of the baseline with a stainless-steel target, its performance can be maintained for the whole working day. The roughness of the stainless-steel target has to be renewed daily. So far stainless-steel is preferred as the most useful target material, but there is still a need for inert target materials, with good thermal conductivity and wettability.

The analytical performances of the copper and stainless-steel targets were compared by studying the within-run precision of the LC–CF-FAB-MS method for the determination of dextromethorphan in plasma. The plasma samples were spiked with 1.8 μg/ml of dextromethorphan, corresponding to 5–7 ng introduced into the mass spectrometer after splitting. The protonated molecule of dextromethorphan at *m/z* 272 and the protonated glycerol cluster at *m/z* 277 were recorded in the selected ion monitoring mode. In Table II the relative standard deviations for 5–6 measurements of the peak areas are summarized. By using the acid-treated copper target (system A) a better precision is obtained than by using the untreated stainless-steel target (system B). However, the performance of the stainless-steel target is improved when the wick and the cold trap are used after acid treatment of the target (system C).

TABLE II

WITHIN-RUN PRECISION OF THE PEAK AREAS FOR DETERMINATION OF DEXTROMETHORPHAN IN HUMAN PLASMA BY MEANS OF LC–CF-FAB-MS WITH A COPPER AND A STAINLESS-STEEL TARGET

Plasma spiked with 1.8 μg/ml of dextromethorphan.

Target	*n*	*Relative standard deviation (%)*	*Conditions*
Copper	5	13	No wick No cold trap Acid-treated target System A
Stainless-steel	5	24	No wick No cold trap Non-treated target System B
	6	15	Wick Cold trap Acid-treated target System C

Mobile phase

In CF-FAB glycerol is generally used as the ionization matrix, because of its good solubility properties and its low vapour pressure. In CF-FAB usually 5–20% of glycerol is added to the mobile phase of the LC system in either the pre-column[1–6,8–15] or post-column mode[7]. For the frit-FAB approach, Takeuchi *et al.*[14] reported that the optimum supply rate of glycerol in the mobile phase is 0.1 μl/min, which means 10% (v/v) of glycerol in the mobile phase at a flow-rate of 1 μl/min and 5% (v/v) at 2 μl/min. In the frit approach, glycerol and solute are left on the surface of the frit, while the other solvents immediately evaporate from the surface of the frit[1,9,13,14]. In CF-FAB, the mobile phase is constantly directed to the CF-FAB target and the surface layer is renewed at the rate of the mobile phase flow. When conventional FAB, frit-FAB and CF-FAB are compared, the disturbing background and chemical noise derived from the glycerol are greatly reduced in the latter two instances and the most in the continuous-flow approach.

To study the optimum supply rate of glycerol for CF-FAB, the within-run precision in flow injection (FIA II) of dextromethorphan as a test compound was investigated by adding different amounts of glycerol to the mobile phase. A sample containing 40 ng of dextromethorphan in water was injected, which corresponds to 500 pg introduced into the mass spectrometer. In Table III the relative standard deviations of the peak areas are summarized. The content of trifluoroacetic acid was constant during the measurements and only the ratio of glycerol and methanol was changed. When 1–2.3% (w/w) of glycerol is used in the mobile phase, a moderate precision is achieved for these injections of dextromethorphan, but after some time the baseline becomes very unstable and it is impossible to obtain reproducible results. This

TABLE III

INFLUENCE OF SUPPLY RATE OF GLYCEROL ON WITHIN-RUN PRECISION OF FLOW INJECTION OF DEXTROMETHORPHAN

Injected amount 40 ng (500 pg in the mass spectrometer after splitting). For conditions, see text. FIA II with an acid-treated stainless-steel target.

Amount of glycerol in mobile phase		*CF-FAB flow-rate (μl/min)*	*Supply rate of glycerol (μl/min)*	*Relative standard derivation (‰)*	*n*
% (w/w)	*% (v/v)*[a]				
1.0	0.6	5.6	0.03	26	8
2.3	1.5	5.3	0.08	27	4
5.0	3.2	5.5	0.18	19	6
6.9	4.4	6.1	0.27	9	9
10.1	6.6	6.5	0.43	19	8

[a] Made up as % (w/w), recalculated in % (v/v).

is probably due to a lack of glycerol on the target, resulting in an unstable liquid film on the target.

The best overall performance under thes experimental conditions (FIA II) was obtained with 7% (w/w) of glycerol in the mobile phase, indicating that the optimum supply rate of glycerol is 0.3 μl/min for CF-FAB, which is three times higher than that in the frit approach. From this result it can be calculated that for 1% (v/v) of glycerol in the mobile phase, the optimum flow-rate is *ca.* 30 μl/min, for 5% (v/v) 6 μl/min and for 10% (v/v) 3 μl/min. However, it must be pointed out that the stability of the system depends not only on the supply rate of glycerol, but also on the applied mobile phase composition, the evaporation rate of that mobile phase and the pumping capacity of the mass spectrometer. A mobile phase containing only trifluoroacetic acid, methanol and glycerol as used in this experiment (FIA II) is especially suitable for the desorption step in phase-system switching (PSS) experiments reducing the flow-rate[10] and for general FIA procedures. The key parameters are the fast baseline stabilization due to the good liquid film properties of this mobile phase, the fast evaporation rate of methanol and the absence of water.

The influence of the flow-rate on the baseline stability of CF-FAB is illustrated in Fig. 2. With 5 μl/min irregular acetonitrile evaporation within the CF-FAB capillary and droplet formation from glycerol on the target took place, resulting in a very unstable baseline. At 7 μl/min the evaporation of acetonitrile took place from a stable liquid film on the target surface. As a result, a very stable baseline with low glycerol (cluster) intensity can be obtained under the latter conditions.

The ion-source temperature affects the evaporation rate of the components of the mobile phase. When the flow-rate or the water content of the mobile phase is changed, the ion-source temperature has to be optimized. Generally, an ion-source temperature of 40–45°C is used for non-aqueous mobile phases and up to 80°C for mobile phases containing high percentages of water in order to prevent freezing of the solvents on the target.

In CF-FAB, typically reversed-phase mobile phases, *e.g.*, methanol, acetonitrile, water and mixtures thereof, are used. In a solvent mixture containing 10% of glycerol,

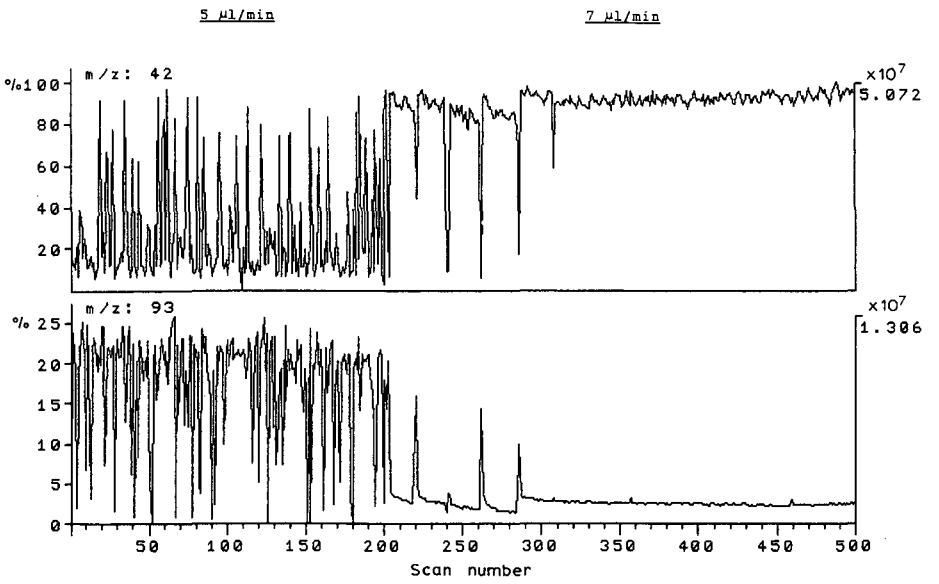

Fig. 2. Influence of flow-rate on the baseline stability of the LC–CF-FAB-MS system. Reconstructed mass chromatograms at *m/z* 42 for protonated acetonitrile (top) and at *m/z* 93 for protonated glycerol (bottom). FIA I (see Table I) with an acid-treated nickel target.

only up to 45% of acetonitrile can be mixed. Higher acetonitrile percentages result in an emulsion. With methanol–water–glycerol mixtures these problems are absent: these solvents can be mixed in any required composition. The composition of the solvent mixture influences the stability and the time required to obtain stable conditions after installing the probe. It is more difficult to achieve a stable performance with high water contents, because of the increased amount of vapour. The cold trap improves the pumping capacity of the mass spectrometer and, by that means, the overall performance and stability of the system.

One of the difficulties in LC–MS interfacing is the limitation to the buffers that can be used in the mobile phase. The applied buffers have to be volatile. Trifluoroacetic acid has been used with excellent results to adjust the pH of the mobile phase, to improve and maintain the wettability of the CF-FAB target and also to enhance the sensitivity for particular analytes. In order to study the possibilities of using the volatile ammonium acetate buffer in the mobile phase, a method for the determination of erythromycin 2'-ethylsuccinate in human plasma using LC–CF-FAB-MS has been developed.

Application: erythromycin 2'-ethylsuccinate in plasma

Erythromycin is a macrolide antibiotic. To improve the pharmacokinetic and pharmaceutical properties of erythromycin, several 2'-esters have been synthesized. Because these esters are antibacterially inactive, it is important that an analytical method is capable of separating erythromycin and its esters. Only a few LC methods have been published for the determination of erythromycin and erythromycin

esters[17,18] in biological fluids. The determinations are based on coulometric[17] and UV detection[18]. Erythromycin 2'-ethylsuccinate has also been determined in human plasma by FAB-MS[19]. A method for the determination of erythromycin 2'-ethylsuccinate in plasma using LC–CF-FAB-MS has been developed. The separation of erythromycin and erythromycin 2'-ethylsuccinate is achieved by applying a polymer-based stationary phase and a mobile phase that contains ammonium acetate, glycerol and acetonitrile. A good separation of erythromycin and its 2'-ethylsuccinate ester is obtained. Erythromycin d_5-2'-ethylsuccinate is used as an internal standard for the determination of erythromycin 2'-ethylsuccinate.

Selected ion monitoring chromatograms of the protonated molecule of erythromycin 2'-ethylsuccinate and internal standard at *m/z* 862 and 867 are given in Fig. 3. The plasma samples were spiked with 9.8 μg/ml of erythromycin 2'-ethylsuccinate (corresponding to 40 ng introduced into the mass spectrometer) and 6.5 μg/ml of erythromycin d_5-2'-ethylsuccinate (26 ng introduced). The protonated molecule of erythromycin at *m/z* 734 was also monitored. The blank plasma is free from an interfering background at the *m/z* values monitored. The linearity (ratio of peak area of analyte and internal standard *vs.* concentration) of the method was checked in the range 0.25–9.8 μg/ml of erythromycin 2'-ethylsuccinate in plasma. The calibration graph is linear over this range, corresponding to 1–39 ng of erythromycin 2'-ethylsuccinate introduced into the mass spectrometer. The determination limit with a signal-to-noise ratio of 10:1 is *ca.* 0.25 μg/ml in the selected ion monitoring mode. The recovery of the extraction method was calculated to be 81% at the 5 μg/ml level by comparing the peak areas obtained from extracted spiked plasma samples and from extracted blank samples, to which erythromycin 2'-ethylsuccinate was added after extraction.

The within-run precision of the method was studied by analysing spiked plasma samples containing 5 μg/ml of erythromycin 2'-ethylsuccinate. The relative standard

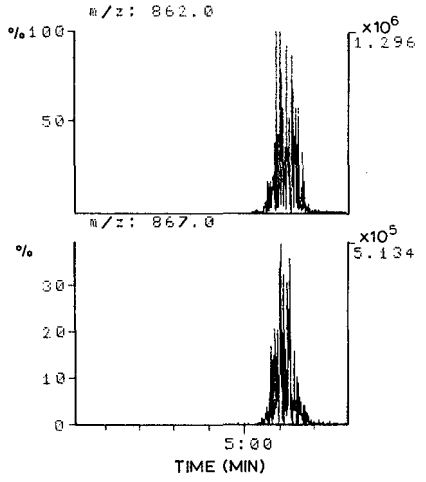

Fig. 3. Selected ion monitoring chromatograms of protonated erythromycin 2'-ethylsuccinate (upper trace, *m/z* 862) and protonated erythromycin d_5-2'-ethylsuccinate (lower trace, *m/z* 867). Plasma was spiked with 9.8 μg/ml of erythromycin 2'-ethylsuccinate and 6.5 μg/ml of erythromycin d_5-2'-ethylsuccinate. System D (see Table I) with an acid-treated stainless-steel target.

deviation of the peak areas is 19% for five measurements. Because there is a high buffer concentration [48% (w/w) of 0.1 *M* ammonium acetate] in the mobile phase, only a moderate precision of the method is achieved. However, when a dilute ammonium acetate buffer is used, the method can be applied to the determination of erythromycin 2′-ethylsuccinate. In spite of the mandatory splitting, the sensitivity of the method is sufficient for typical concentration levels of erythromycin 2′-ethylsuccinate in human plasma[19]. It can be concluded that ammonium acetate can be used in the mobile phase with LC–CF-FAB-MS while sufficient selectivity of the LC system is achieved.

Sample solution

In LC, the solvent of the sample solution usually influences both the sensitivity of the method and the chromatographic peak shape. In CF-FAB in the FIA mode, the solvent plug injected is expected to affect the ionization as a result of its influence on the liquid film at the target surface. The latter effect is demonstrated in Fig. 4, in which the reconstructed total ion current chromatogram (RIC, *m/z* 20–1000) and the reconstructed mass chromatograms of the protonated acetonitrile (*m/z* 42) and protonated dextromethorphan (*m/z* 272) are given. When the peak from a replicate injection (without splitting) of a sample containing 11 ng of dextromethorphan in aqueous solution elutes to the surface of the target, the liquid film of the target is disturbed for a few seconds and a decrease in the intensity of the protonated acetonitrile is observed.

In FIA, when small flow-rates (5–7 μl/min) are used, a 0.5- or 1.0-μl injector is usually applied without a splitter. However, the use of such an injector is very critical and readily causes extra peak broadening. The peak broadening of dextromethorphan in Fig. 4 resulted from the use of a 0.5-μl injector. Better peak shapes have been obtained using a 20-μl injector in combination with a high flow-rate and a splitting

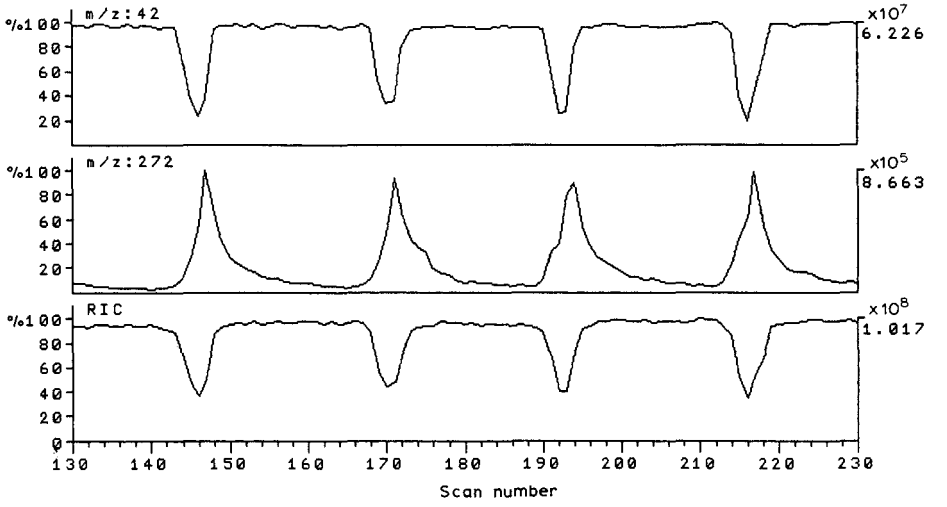

Fig. 4. Influence of the replicate injection of 11 ng of dextromethorphan in water on the baseline stability of the LC–CF-FAB-MS system. Reconstructed total ion current chromatogram (RIC, *m/z* 20–1000) and reconstructed mass chromatograms of protonated acetonitrile (*m/z* 42) and protonated dextromethorphan (*m/z* 272). FIA I (see Table I) with an acid-treated nickel target.

device. When a column between the pump and the injector is used, additional pulse damping is provided. This is shown in Fig. 5 for the flow injection of 960 ng of vindesine, a vinca alkaloid, corresponding to 13 ng of vindesine introduced into the mass spectrometer after splitting. In order to show the baseline stability, the reconstructed selected ion monitoring chromatogram obtained by adding traces of the protonated vindesine and the glycerol background at *m/z* 754 and 737 is given. Under these experimental conditions good peak shapes and stable performance are achieved.

Preformed ions of drugs in complex mixtures have been shown to enhance sensitivity in secondary ion mass spectrometry[16,20]. These methods include derivatization, *e.g.*, with Girard reagents or methylation. A fixed charge is introduced into the molecule before ionization and preformed ions are desorbed from the surface of the conventional FAB probe. To study the effect of preionization in CF-FAB, preprotonation and methylation were compared. A sample containing 40 ng of dextromethorphan (500 pg in the mass spectrometer after splitting, FIA II) was injected as an acidic aqueous solution of pH 2, well below the pK_a of dextromethorphan, which is 8.3. These results were compared with those obtained for 40 ng of methylated dextromethorphan. Single ion monitoring chromatograms of the protonated molecule of dextromethorphan, the protonated glycerol cluster $[3M + H]^+$ and methylated dextromethorphan at *m/z* 272, 277 and 286, respectively, were recorded. When dextromethorphan is methylated, a fixed charge is introduced into the molecule. The derivatization procedure is apparently not completed, because after methylation underivatized dextromethorphan was found. The protonated and methylated dextromethorphan showed similar responses. As a conclusion there does not seem to be any significant difference in sensitivity between a fixed charge or preprotonation for this compound in LC–CF-FAB-MS.

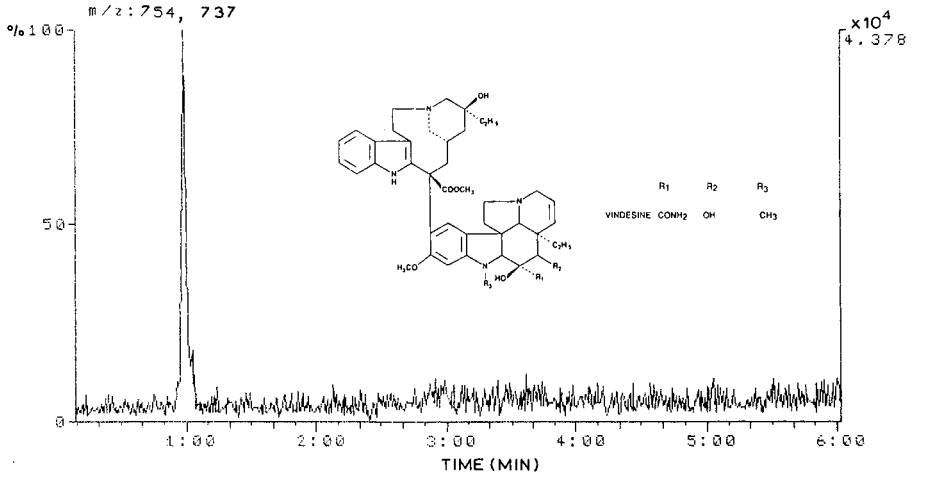

Fig. 5. Reconstructed selected ion monitoring chromatogram obtained by adding the signals corresponding to protonated vindesine (*m/z* 754) and the protonated glycerol cluster (*m/z* 737). The amount injected was 960 ng of vindesine (13 ng in the mass spectrometer). FIA II (see Table I) with an acid-treated stainless-steel target.

REFERENCES

1 Y. Ito, T. Takeuchi, D. Ishii and M. Goto, *J. Chromatogr.*, 346 (1985) 161.
2 R. M. Caprioli, T. Fan and J. S. Cottrell, *Anal. Chem.*, 58 (1986) 2949.
3 A. E. Ashcroft, J. R. Chapman and J. S. Cottrell, *J. Chromatogr.*, 394 (1987) 15.
4 A. E. Ashcroft, *Org. Mass Spectrom.*, 22 (1987) 754.
5 R. M. Caprioli, W. T. Moore and T. Fan, *Rapid Commun. Mass Spectrom.*, 1 (1987) 15.
6 R. M. Caprioli, *Biomed. Environ. Mass Spectrom.*, 16 (1988) 35.
7 D. E. Games, S. Pleasance, E. D. Ramsey and M. A. McDowall, *Biomed. Environ. Mass Spectrom.*, 15 (1988) 179.
8 J. A. Page, M. T. Beer and R. Lauber, *J. Chromatogr.*, 474 (1989) 51.
9 Y. Ito, T. Takeuchi, D. Ishii, M. Goto and T. Mizuno, *J. Chromatogr.*, 391 (1987) 296.
10 P. Kokkonen, W. M. A. Niessen, U. R. Tjaden and J. van der Greef, *J. Chromatogr.*, 474 (1989) 59.
11 P. Kokkonen, J. van der Greef, W. M. A. Niessen, U. R. Tjaden, G. J. ten Hove and G. van de Werken, *Rapid Commun. Mass Spectrom.*, 3 (1989) 102.
12 T. Takeuchi, S. Watanabe, N. Kondo, M. Goto and D. Ishii, *Chromatographia*, 25 (1988) 523.
13 Y. Ito, T. Takeuchi, D. Ishii, M. Goto and T. Mizuno, *J. Chromatogr.*, 358 (1986) 201.
14 T. Takeuchi, S. Watanabe, N. Kondo, D. Ishii and M. Goto, *J. Chromatogr.*, 435 (1988) 482.
15 A. C. Barefoot, R. W. Reiser and S. A. Cousins, *J. Chromatogr.*, 474 (1989) 39.
16 D. A. Kidwell, M. M. Ross and R. J. Colton, *Biomed. Mass Spectrom.*, 12 (1985) 254.
17 P. Kokkonen, H. Haataja and S. Välttilä, *Chromatographia*, 24 (1987) 680.
18 C. Stubbs, J. M. Haigh and I. Kanfer, *J. Pharm. Sci.*, 74 (1985) 1126.
19 P. Ottoila and J. Taskinen, *Biomed. Environ. Mass Spectrom.*, 14 (1987) 659.
20 D. A. Kidwell, M. M. Ross and R. J. Colton, *Int. J. Mass Spectrom. Ion Processes*, 78 (1987) 315.

Journal of Chromatography, 511 (1990) 49–58
Elsevier Science Publishers B.V., Amsterdam

CHROM. 22 410

Theoretical aspects of the chromatographic analysis of heterogeneous polymers

L. Z. VILENCHIK
Indiana Purdue University, School of Science, Department of Chemistry, 1125 E. 38th Street, Indianapolis, IN 46205-2810 (U.S.A.)
(First received December 13th, 1989; revised manuscript received March 2nd, 1990)

ABSTRACT

A method for the chromatographic analysis of heterogeneous polymers is proposed and theoretically confirmed. Such polymers include block and random copolymers, oligomers and polymers with functional groups. The basis of this procedure is the combined use of two main variants of liquid chromatography, size-exclusion and adsorption chromatography. The experimental data are treated by the methods of the theory of distributions. This procedure makes it possible to determine the molecular weight distribution of heterogeneous polymers and their compositional distribution and the distribution of functional groups. The possibility of using the adsorption variant of liquid chromatography under both isocratic and gradient conditions is considered.

INTRODUCTION

The quantitative analysis of heterogeneous polymers should include the determination of their molecular weight distribution (MWD) and composition. In the case of block copolymers this involves the determination of the MWD of each block, and for random copolymers this requires the determination of the weight fraction of each component of the copolymer. For example, for a molecule of a random copolymer with n_A units of component A and n_B units of component B, the molecular weight is

$$M_{AB} = n_A m_A + n_B m_B \quad (1)$$

where m_A is the weight of monomer A and m_B that of monomer B, and the degree of polymerization is

$$N = n_A + n_B \quad (2)$$

More generally, for a copolymer consisting of k components,

0021-9673/90/$03.50

$$M_\Sigma = \sum_{i=1}^{k} n_i m_i = \sum_{i=1}^{k} M_i \tag{3}$$

where $M_i = n_i m_i$ is the net weight of the ith component in a molecule of the heteropolymer. Complete analysis of the heteropolymer requires that we find the distribution $W_i(M_i)$ for each ith component. The chromatographic behavior of polymers or oligomers with adsorption-active groups is determined by the number of these groups.

Many workers have investigated this problem (*e.g.*, refs. 1–8). Particularly relevant to this study are recent results obtained by Mori[7,8] by means of combined size-exclusion[9] and adsorption[10] chromatography. They used a calibration graph of copolymer composition *versus* retention volume. This procedure is possible only under the unusual circumstances where samples with known composition and molecular weight are available. This paper represents a theoretical attempt to determine the MWD and composition of heteropolymers using the more limited data typically available.

In size-exclusion chromatography (SEC), macromolecules are separated according to their hydrodynamic volume[11]. This separation results from a decrease in the entropy of macromolecules when they pass from the channels of the mobile phase of the chromatographic column into the pores of a stationary phase[12].

In the adsorption form of liquid chromatography (LAC), additional retention is observed. The elution of macromolecules in this instance is determined not only by entropy changes but also the enthalpy changes which they undergo in the interphase transition. The reason for the enthalpy changes is the energetic interaction between the macromolecules and the stationary phase matrix. The magnitude of this interaction is proportional to the number of adsorbing units of the chain. For an adsorbing homopolymer it is a degree of polymerization[13]. In the case of heterogeneous polymers, it is possible that only one kind of unit interacts with the packing. Therefore, the magnitude of this interaction is proportional to the number of such units, n_i, in the macromolecule.

Consequently, the chromatograms obtained by SEC shown distributions of the macromolecules of the sample according to size, whereas in LAC the chromatograms reflect both this size distribution and also the number, n_i, of the adsorbing monomer residues in the macromolecule. As will be show below, if the chromatograms of a heteropolymer obtained by SEC and LAC methods are considered together, distribution theory makes it possible to distinguish the contributions due to the size of macromolecules from those related to their energetic interaction with the packing and hence to obtain distributions according to both molecular weight and compostion.

The problem ultimately reduces to a search for the law of the distribution of a random variable which is a function of two other random variables, the distribution laws of which are known. These three interrelated random variables are the hydrodynamic size, $R_\eta \approx (\bar{M}[\eta])^{1/3}$, of the macromolecules, the net weight, M_i, of the adsorbing monomers, *i.e.*, all monomers of the heteropolymer component taking part in adsorption interaction with the packing matrix, and the chromatographic elution time, t_a ($\bar{M}$ is here an average molecular weight and $[\eta]$ is the intrinsic viscosity of the heteropolymer).

The chromatogram of the sample, $F_1(t_e)$, obtained under pure SEC conditions in which the variable t_e is replaced with R_η [with the aid of the universal calibration dependence[11] $t_e = f(R_\eta)$] yields the distribution $\tilde{F}_1(R_\eta)$ according to the hydrodynamic size of macromolecules R_η (ref. 14).

The distribution in time, t_a, of the elution of macromolecules from the column under the conditions of an adsorption chromatographic experiment is a joint law of the distribution of the variables R_η and M_i (where i corresponds to the adsorbing monomers). This distribution is directly represented by the corresponding chromatogram $F_2[t_a(R_\eta, M_i)]$. Mathematically we can change this classification and consider the variable M as a function of the variables t_a and R_η. Then the law of the distribution of M_i will be the joint distribution of the variables R_η and t_a.

This law is unknown and must be determined, that is, we have to determine the distributions according to the net weight of each ith kind of the adsorbing monomers of the investigated heterogeneous polymers. When it is found, the overall distribution of molecular weight and composition in the sample may be calculated.

THEORETICAL

The interrelationship between the three random variables t_a, R_η and M_i requires the application of conditional distribution laws[15]. From the experimental standpoint, the simplest determination of this law can be carried out for the variable t_a under the condition that R_η takes some fixed values. For this purpose, the heterogeneous sample should be divided into fractions with the aid of SEC. The average molecular size in each fraction will be R_η. Subsequently, each fraction will undergo chromatography on the same column (or a second identical column) but in another eluent, so that the conditions of LAC would be fulfilled successively for each component of the investigated heteropolymer. The family of chromatograms obtained in this manner gives the density of the conditional distribution function $F_2(t_a|R_\eta)$.

The law of joint distribution for a system of two random variables, t_a and R_η, may be expressed through the density of the distribution functions of these variables as follows:

$$F(t_a, R_\eta) = \tilde{F}_1(R_\eta)F_2(t_a/R_\eta) \tag{4}$$

Then the distribution law of a random variable M_i which may be regarded as a function of the values t_a and R_η is given by

$$W_i(M_i) = \frac{\partial}{\partial M_i} \int_{R_1}^{R_2} dR_\eta \int_{t_0}^{t_a} dt \cdot F(t, R_\eta) = \int_{R_1}^{R_2} dR_\eta \cdot \frac{\partial t_a (M_i, R_\eta)}{\partial M_i} \cdot \tilde{F}_1(R_\eta)F_2(t_a|R_\eta) \tag{5}$$

The function $\tilde{F}_1(R_\eta)$ is obtained from the chromatogram $F_1(t_e)$ by replacing the variables according to the universal calibration of a given chromatographic system, and $W(M)$ is the function density of distribution according to the net weight of the adsorbing monomers.

Before determining the function $t_a = t_a(M_i, R_\eta)$, the following remark should be

made. When an adsorption interaction between the polymer and the packing exists,it is not always possible to carry out chromatographic experiments under isocratic conditions even if the polymer–packing interaction energies are close to the critical value[10,13]. Hence, it is often necessary to use gradient chromatography[16]. Bearing this in mind, the function t_a (M_i, R_η) will be determined for the more general case of gradient conditions, whereas for isocratic conditions a particular form of this function will be obtained.

The coefficient of interphase distribution of macromolecules may be regarded as their principal characteristic. It is written as the ratio of solution concentrations in the stationary phase, C_{st}, and mobile phase, C_m, of the column and reflects the ratio of probabilities of the existence of molecules in each of these phases[14]:

$$K_d = \frac{C_{st}}{C_m} = \frac{v_m}{v_{st}} \cdot \frac{W_{st}}{W_m} \tag{6}$$

where W_{st} and W_m are the probabilities of the existence of molecules in the stationary and the mobile phases and v_m and v_{st} are the volumes of the mobile phase and stationary phase of the column, respectively. It is easy to show the correctness of eqn. 6, because the number of solute molecules distributed between the phases of the column is as follows:

$$\begin{aligned} n_m &= nW_m \\ n_{st} &= nW_{st} \\ n_m + n_{st} &= n \end{aligned} \tag{7}$$

where n_m and n_{st} are the numbers of solute molecules in the mobile and stationary phase, respectively, and n is the total number of the solute molecules in the column.

Under equilibrium conditions, each of these probabilities W_m and W_{st} is determined in a standard manner by the value of the free energy of the molecules G, the macromolecules being considered as independent thermodynamic systems:

$$W_m = \frac{v_m \exp(-G_m)}{v_m \exp(-G_m) + v_{st} \exp(-G_{st})} \tag{8a}$$

$$W_{st} = \frac{v_{st} \exp(-G_{st})}{v_m \exp(-G_m) + v_{st} \exp(-G_{st})} \tag{8b}$$

where G_m and G_{st} are in units of kT, where k is Boltzmann's constant and T is the absolute temperature.

As the concentration of the solute is $C_m = n_m/v_m$ in the mobile phase and $C_{st} = n_{st}/v_{st}$ in the stationary phase, we obtain for their ratio eqn. 6. Substituting expressions 8 into eqn. 6, we obtain the distribution coefficient K_d as uniquely given by the change in the free energy of macromolecules, $\Delta G = G_{st} - G_m$, during interphase transitions:

$$K_d = \exp[-(G_{st} - G_m)] = \exp[-\Delta G] \tag{9}$$

The value of ΔG is the sum of the entropy and enthalpy changes which the macromolecules undergo in the course of the chromatographic process:

$$\Delta G = \Delta H - T\Delta S \tag{10}$$

When the macromolecules enter the packing pores in the absence of energetic interactions, *i.e.*, in SEC, only the entropy changes. This leads to the following change in the free energy:

$$\Delta G_1 = -T\Delta S \tag{11}$$

In the same pores, when an energetic interaction exists (this occurs in LAC), the enthalpy, ΔH, changes simultaneously with the entropy. An additional change in entropy ΔS_2 related to the interaction also occurs. As a result, the interphase free energy of macromolecules undergoes an additional change by the quantity

$$\Delta G_2 = \Delta H - T\Delta S_2 \tag{12}$$

The corresponding total change in energy is given by the sum

$$\Delta G = \Delta G_1 + \Delta G_2 \tag{13}$$

Hence, the value of the distribution coefficient may be written as the product of two factors (see, *e.g.*, ref. 17):

$$K_d = \exp(-\Delta G_1)\exp(-\Delta G_2) \equiv k_A k_G \tag{14}$$

Here $k_G = \exp(-\Delta G_1)$ is the distribution coefficient under the conditions of SEC and $k_A = \exp(-\Delta G_2)$ reflects the addition to k_G related to adsorption interaction with the same packing.

In accordance with the adsorption theory of macromolecules[13,18], for homopolymers the value of ΔG_2 is proportional to molecular weight M. Therefore, we may assume that the change in free energy, ΔG_2, in adsorption chromatography is proportional to the net weight, M_i, of the units of the heteropolymer which can interact with the packing matrix. Hence, the fulfillment of the following approximate equality will be considered valid:

$$\Delta G_2 \approx \varepsilon M_i \tag{15}$$

where ε characterizes the value of the polymer–packing adsorption interaction in the given solvent from the standpoint of both enthalpy and entropy changes which the macromolecule undergoes during adsorption.

It is clear that the free energy, ΔG, of the macromolecules on transport into the pore can either increase or decrease. It will increase if the decrease in enthalpy is insufficient to compensate for the decrease in entropy, in this case we have $\Delta G > 0$ and $K_d < 1$. The free energy of the macromolecule will decrease when the decrease in enthalpy is greater than that in entropy; then we have $\Delta G < 0$ and $K_d > 1$. The former

case should be classified as SEC complicated by weak adsorptions; the latter is proper LAC.

The situation in which the changes in enthalpy and entropy are equal and mutually compensating deserves particular attention. In this case $\Delta G = 0$ and $K_d = 1$. Hence, regardless of the ratio of the dimensions of the pore and the macromolecule, the latter can exist either in the pore or in the mobile phase with equal probability of an appropriate compensating enthalpy change occurring. This means that when appropriate conditions are chosen, a large macromolecule can enter a small pore, if it can be located in the pore, by changing its "geometry" and "creeping" along its walls. This case corresponds to so-called critical conditions and value ε designated by ε_{cr}.

In 1979, Skvortsov and Gorbunov[19] propounded the use of chromatography under critical conditions for the analysis of block copolymers. According to their idea, the chromatographic system for this purpose should be designed in such a manner that one component of the block copolymer undergoes chromatography by the SEC mechanism and the other component is chromatographed by the LAC mechanism at $\varepsilon = \varepsilon_{cr}$. As a result, the retention time for a block copolymer will be determined only by the size its components, which are not going to have any adsorption interaction with the packing.

Unfortunately, no experimental verification has appeared, perhaps because of the difficulty in obtaining reproducible chromatography under critical conditions. Therefore, in our work an approach is propounded in which the chromatographic experiments have to be carried out under LAC conditions when $|\varepsilon|$ is greater than $|\varepsilon_{cr}|$ but is close to the critical value.

In the general case with gradient chromatographic conditions, it is possible to vary the value of ε according to the linear law

$$\begin{aligned} \varepsilon(t_a) &= \varepsilon_0 - \beta t_a \quad \text{at} \quad t_a \leqslant \varepsilon_0/\beta \\ \varepsilon(t_a) &= 0 \qquad\quad \text{at} \quad t_a \geqslant \varepsilon_0/\beta \end{aligned} \tag{16}$$

where β is slope of this dependence and t_a is the retention time under the conditions of the adsorption chromatographic experiment.

Usually this variation of the value of ε is attained by variation of the solvent composition, in which the fraction of the more adsorption-active (with packing) component increases in the solvent with time. Simultaneously, this component of the solvent is chosen so that it is the stronger solvent for the adsorbing units of the heteropolymer. As a result, ε decreases and the rate of motion of the solute along the column increases:

$$U(t_a) = \frac{u_0}{1 + (v_{st}/v_m)K_d(t_a)} \tag{17}$$

where u_0 is the elution rate, and K_d varies according to following law:

$$\begin{aligned} K_d &= k_G \exp[\varepsilon_0 M_i - \beta M_i(t_a - \tau)] \quad \text{at} \quad t_a \leqslant (\varepsilon_0 - \varepsilon_{cr})/\beta + \tau \\ K_d &= k_G \exp(\varepsilon_{cr}) = 1 \qquad\qquad\quad \text{at} \quad t_a \geqslant (\varepsilon_0 - \varepsilon_{cr})/\beta + \tau \end{aligned} \tag{18}$$

where τ, the lag time, represents the delay between initiating the gradient and arrival of the gradient at the position of the solute in the column at time t_a.

We saw that macromolecules of any molecular weigh M may have a distribution coefficient K_d of unity if the energy of their adsorption interaction is equal to a critical value ε_{cr}. As the value of K_d for a solvent is also unity, then beginning with time $t_a = (\varepsilon_0 - \varepsilon_{cr})/\beta + \tau$, when $\varepsilon(t_a) = \varepsilon_{cr}$, both the solute and solvent begin to move with equal velocity $\bar{u}$:

$$\bar{u} = \frac{u_0}{1 + v_{st}/v_m} \tag{19}$$

For the lag time τ the following expression is correct:

$$\tau = \frac{1}{\bar{u}} \int_0^{t_a} u(t)\, dt \tag{20}$$

where $u(t)$ is determined by eqns. 17 and 18.

Finally, using eqns. 16–20 and the universal calibration $R_\eta = f(t_e)$ in SEC, we can write the following equation connecting the values of the retention time t_a of a solute, the net weight of its adsorbing monomers M_i and the size of the macromolecules R_η:

$$L = \int_0^{t_a} u(t)\, dt \tag{21}$$

where $L = u_0 t_0$ is the length of the column and t_0 is the column dead time.

A rigorous solution of eqn. 21 is possible only by computer. For an analytical solution, we use the well known approximate expression for retention time in gradient chromatography[20,21]. In our terminology we can write

$$t_a = \frac{1}{\beta M_i} \log [2.3\, k_G \beta M_i (t_1/t_0 - 1) \exp(\varepsilon_0 M_i) + 1] + t_e + \tau \tag{22}$$

where t_1 is the retention time in SEC for small molecules which corresponds to a value $K_d = 1$. In addition, we have $(t_1/t_0 - 1) = v_{st}/v_m$.

Eqn. 22 makes it possible to find the function $\partial t(M_i, R)/\partial M_i$ contained in the definition of the density of distribution $W_i(M_i)$ of the net weight of the adsorbing monomers in molecules of the investigated polymer:

$$\frac{\partial t(M_i, R_\eta)}{\partial M_i} = \frac{1}{\beta M_i} \left\{ \frac{\varepsilon_{0,i} M_i + 1}{M_i + 1/[2{,}3\, k_G \beta t_e \exp(\varepsilon_{0,i} M_i)\, (t_1 - t_0)/t_0]} - \frac{1}{M_i} \log [2.3\, k_G \beta t_e M_i \exp(\varepsilon_{0,i} M_i)\, (t_1 - t_0)/t_0 + 1] \right\} \tag{23}$$

Hence, the function of density $W_i(M_i)$ of a heteropolymer is given by

$$W_i(M_i) = \int_{t_a}^{t_0} F_1(t_e) F_{2i} \left(\frac{1}{\beta M_i} \log [2.3\, k_G \beta M_i \exp(\varepsilon_{0,i} M_i)\, (t_1/t_0 - 1)\, t_e + 1] + \right.$$
$$\left. + t_e + \tau | f^{-1}(t_e) \right) \frac{\partial t(M_i, R_\eta)}{\partial M_i} \cdot \mathrm{d}t_e \qquad (24)$$

where $F_1(t_e)$ is the chromatogram of the sample investigated under SEC conditions, $F_{2,i}(t_a | R_\eta)$ is the family of chromatograms obtained in LAC for the fractions of the samples eluted in SEC at different fixed times t_e, $f^{-1}(t_e)$ is the function inverse to the universal calibration and $\varepsilon_{0,i}$ is the initial (at the initial moment $t = 0$) characteristic of the energy of interaction between the sorbent and the adsorbing component of the heteropolymer (denoted by subscript i).

The density of the distribution function $W_j(M_j)$ of any other jth kind of adsorbing monomers of the heteropolymer is obtained in a similar manner (in this instance it is necessary to choose an eluent composition such that only the jth kind of monomers will be adsorbed on this packing). The density of the function of the random value M, which is the sum of independent random values M_i[15], is

$$W(M) = \frac{\partial}{\partial M} \int \ldots \int_{\mathrm{D}} \prod_{i=1}^{n} W_i(M_i)\, \mathrm{d}M_i \qquad (25)$$

where D is the range of determination of the function $W_i(M_i)$.

In the case of a two-component copolymer, eqn. 25 becomes

$$W(M) = \frac{\partial}{\partial M} \int \int W_1(M_1)\, W_2(M_2)\, \mathrm{d}M_1\, \mathrm{d}M_2 =$$
$$\int W_1(M - M_2)\, W_2(M_2)\, \mathrm{d}M_2 \qquad (26)$$

DISCUSSION

In order to carry out the above scheme of chromatographic analyses of heteropolymers, preliminary calibration experiments should be made with homopolymers of each of the monomer units contained in the heteropolymer under investigation. The purpose of these experiments is to determine the constants $\varepsilon_{0,i}$ characterizing the polymer–sorbent interaction. For this purpose, the sample of each (ith) homopolymer is first chromatographed under SEC conditions and separated into fractions (8–10 fractions) according to hydrodynamic size. Subsequently, each of these fractions undergoes chromatography under the appropriate LAC conditions with a suitable gradient (*e.g.*, a linear gradient with the coefficient β_i). In other words, for each ith component the functions $F_1(t_e)$ and $F_{2,i}(t_a, M_i)$ contained in eqn. 24 are found. Eqn. 24 is solved with a computer (*e.g.*, by the least-squares

method) with respect to the parameter $\varepsilon_{0,i}$, completing the calibration. Now a similar procedure is carried out with the sample being analyzed. It is divided into fractions by SEC, and each fraction is eluted under the LAC conditions k times (according to the number of components of the heteropolymer). These conditions are varied each time precisely repeating those of the corresponding calibration on experiments.

The selection of adequate conditions for the gradient LAC of heteropolymers seems possible, according to the work of Mori[7,8]. The selection of adequate conditions includes the choice of packing, solvent and temperature. This choice is determined by the relationship of energetic interactions in the formation of four pairs of contacts: polymer–solvent, polymer–packing, packing–solvent and solvent–solvent. Contact of a polymer segment with the adsorption surface occurs only if it is energetically more favourable than the interactions of the polymer and the packing with the solvent. In this instance interactions with the solvent should be eliminated, *i.e.*, desolvation of the solvent from both the polymer segments and the adsorption sites of the packing should occur. The greater the preference of polymer adsorption on a given packing at a given temperature, the greater is the number of the adsorption sites that will not be occupied by contacts with the solvent, and the higher is the mean statistical value of the energy of interaction between a polymer segment and the packing. Therefore, by variation of solvent and temperature we can obtain either SEC or LAC for different components of an investigated heteropolymer.

The proposed method contains two assumptions. The first, as mentioned above, is the extension of eqn. 15 to heteropolymers, *i.e.*, the proportionality of the change in the free energy during the adsorption of macromolecules to the net weight of the units of monomer in the macromolecule interacting with the packing matrix. The second assumption is that under the same conditions the proportionality coefficient in eqn. 15 is identical for the heteropolymer and the corresponding homopolymer. In other words, it is assumed that the values of $\varepsilon_{0,i}$ are identical in the calibration and principal experiments. Here the possible change in the magnitude of adsorption interactions between the polymer unit and the packing and the related entropy losses due to the screening of this interaction by units of other components of the heteropolymer are neglected. This screening can lead to a decrease in the effective value of $\varepsilon_{0,i}$ in comparison with that determined in the calibration experiment. The validity of neglecting the possibility of screening the adsorption interaction must be subjected to further experimental tests.

It is clear that both assumptions are correct if the fraction of the adsorbing component of the heteropolymer is not very small in each its macromolecules. Otherwise, these assumptions can be checked by carrying out the chromatographic experiments with different model copolymers (block, graft, etc.). First conditions for SEC and LAC are chosen in these experiments for each homopolymer of the given copolymer, then values of ε are determined using eqns. 14 and 15 under conditions of isocratic chromatography. Subsequently, similar experiments are carried out with the model copolymer, and calculated values of ε should be compared. The same assumptions were also made implicitly by Skvortsov and Gorbunov[19].

CONCLUSIONS

The proposed method of quantitative analysis is suitable for heteropolymers of any structure, including block and random copolymers and polymers and oligomers with functional groups.

This method uses chromatography with one detector. However, it should be noted that the composition and the MWD of heteropolymers can be determined by using chromatography with two detectors, *e.g.*, a refractometer and a spectrophotometer, connected in series. The refractometer is sensitive to all components of the heteropolymer. The spectrophotometer should be tuned to the characteristic wavelength of one component only. The analysis of signals from both detectors permits the determination of the composition, the MWD and some other characteristics of the heteropolymer. Early work in this field was carried out by Anderson *et al.*[22] and Lechermeier *et al.*[23]. If we use a viscometer as the second detector we can determine the MWD of a heteropolymer by means of SEC using universal calibration according to Benoit, but for characterizing the composition of a heteropolymer one should use some additional speculations about the size of its macromolecules.

REFERENCES

1 S. Mori, *J. Chromatogr.*, 194 (1980) 163.
2 S. T. Balke and R. D. Patel, *J. Polym. Sci., Polym. Lett. Ed.*, 18 (1980) 453.
3 G. Glöckner, J. H. M. van den Berg, N. L. Meijerink, T. G. Scholte and R. Koningsveld, *Macromolecules*, 17 (1984) 962.
4 V. V. Nesterov, V. D. Krasikov, E. V. Chubarova, B. G. Belenkii and L. D. Turkova, *Vysokomol. Soedin., Ser. A*, 24 (1982) 1330.
5 B. G. Belenkii and E. S. Gankina, *J. Chromatogr.*, 141 (1987) 13.
6 S. G. Entelis, V. V. Evreinov and A. I. Kuzaev, *Reaktsionno-Sposobnye Oligomery*, Khimiya, Moscow, 1985.
7 S. Mori, *Anal. Chem.*, 60 (1988) 1125.
8 S. Mori, *Appl. Polym. Sci. Appl. Polym. Symp.*, 43 (1989) 65.
9 J. E. Moore, *J. Polym. Sci. Part A-2*, (1964) 835.
10 B. G. Belenkii, E. S. Gankina, M. B. Tennikov and L. Z. Vilenchik, *Dokl. Akad. Nauk SSSR*, 231 (1976) 1147.
11 Z. Grubisic, P. Rempp and H. Benoit, *J. Polym. Sci.*, 135 (1967) 753.
12 E. F. Casassa, *J. Polym. Sci., Part B5*, (1967) 773.
13 E. A. DiMarzio and R. J. Rubin, *J. Chem. Phys.*, 55 (1971) 4318.
14 B. G. Belenkii and L. Z. Vilenchik, *Modern Liquid Chromatography of Macromolecules*, Elsevier, Amsterdam, 1983.
15 W. Feller, *An Introduction to Probability Theory and Its Applications*, Vol. I, Wiley, New York, 1968.
16 P. Jandera and J. Churacek, *Gradient Elution in Column Liquid Chromatography (Journal of Chromatography Library*, Vol. 31), Elsevier, Amsterdam, 1988.
17 J. V. Dawkins, *J. Liq. Chromatogr.*, 1 (1978) 279.
18 T. M. Birshtein, *Macromolecules*, 12 (1979) 715.
19 A. M. Skvortsov and A. A. Gorbunov, *Vysokomol. Soedin., Ser. A*, 21 (1979) 339.
20 J. P. Larmaun, J. J. DeStefano, A. P. Goldber, R. W. Stout, L. R. Snyder and M. A. Stadalius, *J. Chromatogr.*, 255 (1983) 163.
21 L. R. Snyder and M. A. Stadalius, in Cs. Horváth (Editor), *High-Performance Liquid Chromatography*, Vol. 4, Academic Press, New York, 1986.
22 J. N. Anderson, S. K. Baczek, H. E. Adams and L. E. Vescelius, *J. Appl. Polym. Sci.*, 19 (1975) 2255.
23 G. Lechermeier, C. Pillot, J. Gole and A. Revillion, *J. Appl. Polym. Sci.*, 19 (1975) 1979.

Journal of Chromatography, 511 (1990) 59–68
Elsevier Science Publishers B.V., Amsterdam

CHROM. 22 357

Separation of simple ions by gel chromatography

I. Simple model of separation for single-salt systems

TAKESHI FUKUDA*, NORIYUKI KOHARA, YOSHIHIKO ONOGI[a] and HIROSHI INAGAKI[b]
Institute for Chemical Research, Kyoto University, Uji, Kyoto 611 (Japan)
(Received January 15th, 1990)

ABSTRACT

The chromatographic separation of simple ions by a polymer gel in water was modelled as a liquid–liquid partition process. The model consists of two "homogeneous" phases, a mobile phase of pure eluent and a stationary (gel) phase of a structureless concentrated polymer solution with a few electric charges fixed within it. Thermodynamic considerations and a simplifying approximation yielded a simple description of single-salt systems, which accounted for the chromatographic behaviour of simple ions at low and high concentrations in a systematic fashion. The introduced notion of "intrinsic distribution coefficients" of ions proved to be useful. The main mechanism of the separation of simple ions is suggested to be the difference in the thermodynamic stabilities of individual ions in the two phases, rather than involving size-exclusion and adsorption effects.

INTRODUCTION

Gel chromatography, so designated by Determann[1], is a method for separating molecules into different species by use of a polymer gel. Its basic principle is generally considered to be a size-exclusion effect exerted by the porous gel matrix. This form of liquid chromatography has developed into a particularly useful tool for separating macromolecules according to their size. In the field of synthetic polymers, it is more commonly termed gel permeation chromatography (GPC)[2].

It is also known that certain non-electrolytic polymer gels are capable of separating simple ions in an aqueous medium[3,4]. The basic mechanism of simple-ion separation has been assumed to be a GPC effect arising from the size difference of

[a] Present address: Department of Polymer Chemistry, Faculty of Engineering, Kyoto University, Sakyo-ku, Kyoto 606, Japan.
[b] Present address: Faculty of Home Economics, Mukogawa Women's University, Ikebiraki-cho, Nishinomiya, Hyogo 663, Japan.

0021-9673/90/$03.50

(hydrated) ions. However, a number of examples exsist that cannot be explained in terms of the size effect or the size effect alone.

According to Yoza[3], possible "side effects" include ion exclusion, adsorption, counter-ion effects and others. Ion exclusion is a Donnan effect exerted by a usually small number of ionic charges often incorporated in the (basically) neutral gel matrix for aqueous use. Pecsok and Saunders[4] and Kadokura *et al.*[5] have discussed this problem on a quantitative basis. "Side effects" that cause retardation of a sample solute in the column for a longer period than expected for its size have been often ascribed to chemical or physical adsorption. In some instances, adsorption or sorption[4] has been claimed to be a major mechanism, rather than a side effect, of simple-ion separation by a polymer gel[4,6–8]. The counter-ion effect has been phenomenologically treated by Saunders and Pecsok[6]. More recently, Shibukawa *et al.*[9] modelled simple-ion separation as a combined effect of size exclusion and partition, the latter involving the counter-ion effect and all other possibly operative effects.

These previous results seemed to us to suggest that the major mechanism of separation might be neither size exclusion nor adsorption. We then attempted to model the gel chromatography of simple ions like a liquid–liquid partition process: our model consists of two "homogeneous" phases, a mobile phase of pure eluent and a stationary phase of a polymer gel through which simple ions are assumed to migrate freely. We assume no particular structure for the gel phase, viewing it as if it were a concentrated polymer solution. Hence, in this model, ions are partitioned between the two phases according to their intrinsic thermodynamic stability in each phase. The counter-ion effect is automatically taken into account by postulating electrical neutrality in the two phases. To simplify the theoretical formulation and to make direct comparisons of theory and experiment feasible, we introduce the assumption that the activity coefficients of the individual ions are equal in the two phases. This is admittedly a crude approximation, but at the cost of rigour it provides a simple and new insight into the problem. It will be shown here that the model is capable of systematically describing experimental results for single-salt systems with fair precision. The simplicity of the model is particularly useful for treating more complicated systems like mixed-salt systems, which will be the subject of a separate report[10].

THEORETICAL

We let a cation 1 of the type K^{+z_1} and an anion 2 of the type A^{-z_2} be distributed between a mobile phase of volume V_m and a stationary (gel) phase of volume V_g, and assume V_m and V_g to be constant (Fig. 1). In Fig. 1, N_i and N_i' denote the total numbers of ion i (= 1 or 2) in the mobile and the gel phases, respectively. Hereafter a prime denotes the gel phase, and numbers are mole-based. As most polymer gels for aqueous use are more or less electrically charged, we assume that a total N_g' of *negative* charges are fixed in the gel phase.

The chemical potential μ_i of each ion in each phase is given by

$$\mu_i = \mu_i^0 + RT \ln a_i + (-1)^i F z_i \psi \tag{1}$$

$$\mu_i' = \mu_i'^0 + RT \ln a_i' + (-1)^i F z_i \psi' \tag{2}$$

Mobile Phase (m)	Stationary Phase (g)
volume: V_m	volume: V_g
cations: N_1	cations: N_1'
anions: N_2	anions: $N_2' + N_g'$

Fig. 1. Schematic representation of the model (see text for details).

where μ_i^0 and $\mu_i'^0$ are the standard chemical potentials, a_i and a_i' are the activities, z_i is the charge number of the ion, ψ and ψ' are the electrostatic potentials and R, T and F are the gas constant, the absolute temperature and the Faraday constant, respectively. At equilibrium $\mu_i = \mu_i'$, and we have

$$\Delta\mu_1^0 + RT \ln (a_1'/a_1) - Fz_1\Delta\psi = 0 \tag{3}$$

$$\Delta\mu_2^0 + RT \ln (a_2'/a_2) + Fz_2\Delta\psi = 0 \tag{4}$$

with

$$\Delta\mu_i^0 \equiv \mu_i'^0 - \mu_i^0 \tag{5}$$

$$\Delta\psi \equiv \psi' - \psi \tag{6}$$

We now introduce the already-mentioned approximation that the activity coefficients of the ions are equal in the two phases, *i.e.*,

$$a_i'/a_i = c_i'/c_i \tag{7}$$

where c_i and c_i' are the concentrations given by

$$c_i = N_i/V_m \tag{8}$$

$$c_i' = N_i'/V_m \tag{9}$$

Eliminating $\Delta\psi$ from eqns. 3 and 4 and using eqns. 7–9, we obtain

$$k_1^{1/z_1}k_2^{1/z_2} = (k_1^0)^{1/z_1}(k_2^0)^{1/z_2} \tag{10}$$

with

$$k_i \equiv N_i'/N_i \tag{11}$$

$$k_i^0 \equiv (V_g/V_m) \exp (-\Delta\mu_i^0/RT) \tag{12}$$

We shall call k_i as given by eqn. 11 the "distribution coefficient". It is more common to define the distribution coefficient by c_i'/c_i, but we prefer our definition for the sake of

simpler descriptions and easier correlation with experiments (see below). If we write $c_i'/c_i \equiv K_i$, we have the relationship

$$K_i = (V_m/V_g)\, k_i \tag{13}$$

The conditions of electrical neutrality are

$$z_1 N_1 = z_2 N_2 \tag{14}$$

$$z_1 N_1' = z_2 N_2' + N_g' \tag{15}$$

Eqns. 10–12, 14 and 15 lead to

$$(k_2 + g_2)^{1/z_1} k_2^{1/z_2} = (k_{12}^0)^{(1/z_1 + 1/z_2)} \tag{16}$$

$$k_1 = k_2 + g_2 \tag{17}$$

with

$$g_2 \equiv N_g'/(z_2 N_2) \tag{18}$$

$$k_{12}^0 \equiv (k_1^0)^{z_2/(z_1+z_2)} (k_2^0)^{z_1/(z_1+z_2)} \tag{19}$$

Thus eqns. 16 and 17 give k_1 and k_2 as a function of k_1^0, k_2^0 and g_2.

When the number of gel-fixed charges is negligibly small in comparison with the number of free charges, or in the limit of $g_2 \to 0$, we have

$$k_1 = k_2 = k_{12}^0 \tag{20}$$

Eqns. 19 and 20 are the central relationship to be examined in this paper. Referring to eqn. 12, we see that k_i^0 is a constant related to the difference in the standard chemical potentials of the individual ions in the two phases, and we may properly call k_{12}^0 the "intrinsic" distribution coefficient of the ion (in a particular system). k_{12}^0 as defined by eqn. 19 is the distribution coefficient of a 1–2 salt, *i.e.*, a salt comprising ions 1 and 2, in the absence of the fixed-charge effect. Saunders and Pecsok[6] have empirically given the distribution coefficient of a 1–2 salt as a charge-weighted algebraic mean of the individual cation and anion contributions. Eqn. 19 indicates that the arithmatic mean may be preferable theoretically.

When the fixed-charge effect is important, or g_2 is non-zero, k_1 and k_2 become dependent on solute concentration. As we have assumed the fixed charges to be negative or $g_2 > 0$, it generally holds that $k_1 > k_{12}^0 > k_2$ (see eqns. 16 and 17). This has been discussed by Pecsok and Saunders[4] and more extensively by Kadokura *et al.*[5]. Their theoretical results regarding the fixed-charge effect are essentially the same as ours, but our equations describe the effect in a more general form.

EXPERIMENTAL

Chromatographic-grade chemicals and highly deionized water were used throughout. The gel column used was a glass tube, 300 mm × 15 mm I.D., packed with Sephadex G-10 gel (Pharmacia). It was placed concentrically in a larger glass tube with thermostated water circulated through the gap to maintain the system at 20.0 ± 0.5°C. An ERMA Model ERC-7520 differential refractometer was used as a detector. A flow-rate of 1 ml/min was maintained by use of a peristaltic pump.

The void volume of the column was estimated using the conventional GPC mode with a series of poly(ethylene glycol) (PEG) samples (Wako). The exclusion limit of the column was of the order of a few hundreds in PEG molecular weight, and thus we regarded the elution volume of the PEG with a nominal molecular weight of 20 000 as equal to the void volume, which was 14.6 ml. In the following discussion, we shall identify this volume with the mobile phase volume V_m. In the context of our model, the gel phase volume V_g may be given by the bed volume minus V_m, which is about 28 ml, but this value itself is of no direct importance in the following analysis. With conventional notation, the elution volume V_e can be represented by

$$V_e = V_m + KV_g \tag{21}$$

with K defined as previously. Eqns. 11, 13 and 21 give

$$k = (V_e - V_m)/V_m \tag{22}$$

i.e., k is formally independent of V_g. This is one of the reasons why we prefer k to K or otherwise defined distribution coefficients. Of course, the value of V_g will become important if one wishes to go into greater detail than we do here.

Chromatographic runs with salt samples were carried out by the equilibrium saturation mode of Sebille *et al.*[11], *i.e.*, we used the sample solution as the eluent and injected a small amount of pure water as a "probe". The amount of water injected ranged from 0.05 to 0.2 ml. The higher the sample concentration, the smaller was the amount of water sufficient for sample detection. Usually, passage of two to three column volumes of the sample solution was sufficient to bring the column system to equilibrium prior to each run.

RESULTS AND DISCUSSION

Concentration dependence and fixed charge effect

The equilibrium saturation mode has the advantage over the conventional mode that it allows us to determine the distribution coefficient as a function of concentration with little theoretical and experimental ambiguity[5,11]. First, once the column system has been equilibrated with the sample eluent, the composition of the mobile phase is always equal to that of the eluent. Second, owing to the usually small size of the pure solvent injected as a probe, the internal equilibrium is little perturbed.

Fig. 2 shows the chromatograms for sodium chloride solutions obtained using this mode. There is a set of negative peaks showing a lack of the salt. These peaks, which are fairly sharp and symmetrical, correspond to the elution volumes of the anion

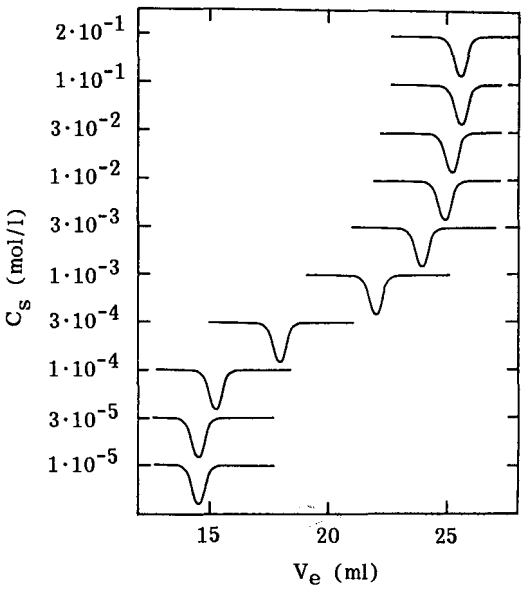

Fig. 2. Chromatograms for Cl^- at different NaCl concentrations, C_s.

Cl^- but not of the cation Na^+, as our gel has negative fixed charges or cation-exchanging ability[8]. An additional experiment is necessary to observe cation elution volumes[5]. Each baseline level corresponds to the salt concentration in the mobile phase, C_s, which in this example is equal to the Cl^- concentration in that phase, *i.e.*, $C_s = N_2/V_m$. When C_s is sufficiently smaller than the fixed-charge density, the sample salt can hardly enter the gel phase because of the relatively high population of the counter ions bound in the gel phase, and hence it is eluted with V_e close to V_m. On the other hand, when C_s is large enough, the fixed charges have no important effect, and the sample salt, freely distributed between the two phases, is eluted at the position V_e^0 characteristic of the salt. At intermediate concentrations, V_e takes intermediate values between V_m and V_e^0.

In Fig. 3, values of k_2 for sodium chloride and sodium sulphate solutions are plotted against C_s. The points are experimental values and the curves show eqns. 16 and 18 with $N_g'/V_m = 7.0 \cdot 10^{-4}$ mol/l and $k_{12}^0 = 0.75$ (NaCl) or 0.35 (Na_2SO_4). The good agreement between theory and experiment suggests the validity of the present treatment and also confirms the previous work[5]. Moreover, the new finding that the elution behaviour of the two salts with k_{12}^0 values very different from each other can be described in terms of the common number of fixed charges N_g' suggests that size exclusion is not the main mechanism of separation in these systems; if salts of different sizes penetrate the gel phase to different extents, the effective numbers of fixed charges which they "feel" should be different.

We carried out chromatographic runs for some salts at higher concentrations, *e.g.*, $C_s \approx 1$ mol/l, and observed that V_e is substantially the same as those in the 0.1 mol/l range. This implies that the present model, despite the crude approximation of equal activity coefficients, works unexpectedly well at least in a practically important range of concentrations.

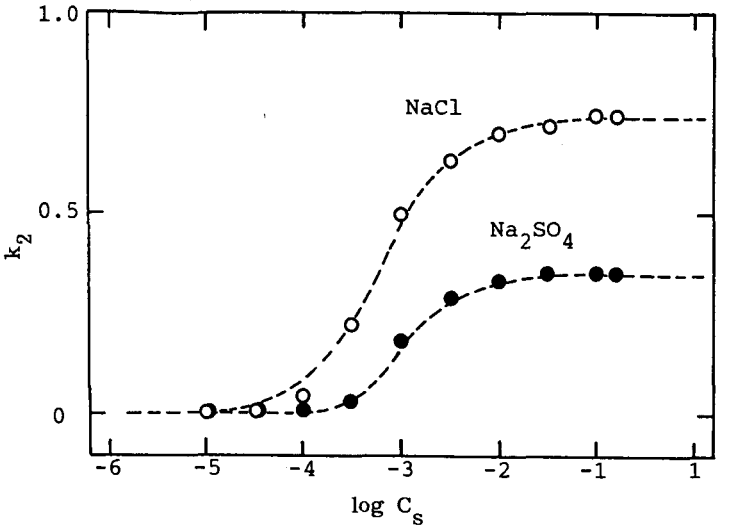

Fig. 3. Anion distribution coefficient k_2 as a function of salt concentration C_s (in mol/l).

Behaviour at high concentrations

We now turn to the main problem. As we have seen, the fixed-charge effect becomes unimportant at concentrations higher than about 0.1 mol/l (Fig. 3). Thus we regarded k_2 at $C_s = 0.2$ mol/l as equal to k_{12}^0. Values of k_{12}^0 thus determined for various sodium and chlorine compounds are listed in Table I. It can be seen that k_{12}^0 differs among sodium compounds and also among chlorides.

According to eqn. 19, k_{12}^0 is given by the arithmetic mean of the intrinsic distribution coefficients k_1^0 and k_2^0 of the individual ions. Hence, knowing the value of k_i^0 for a standard ion, *e.g.*, Cl^-, we can calculate the k_1^0 values of various cations from the k_{12}^0 values of the corresponding chlorides by use of eqn. 19, and $k_{Na^+}^0$ value so calculated and the experimentally determined k_{12}^0 values of the sodium salts may subsequently be used to evaluate the k_2^0 values of various anions. However, there is no

TABLE I

DISTRIBUTION COEFFICIENTS OF SIMPLE ELECTROLYTES IN A SEPHADEX G-10 COLUMN

Salt	k_{12}^0	*Salt*	k_{12}^0	*Salt*	k_{12}^0
NaF	0.563	$AlCl_3$	0.563	KCl	0.792
NaCl	0.750	$BaCl_2$	1.01	LiCl	0.764
NaBr	0.917	$CaCl_2$	0.840	$MgCl_2$	0.694
NaI	1.48	$CdCl_2$	0.910	NH_4Cl	0.771
Na_2SO_4	0.354	$CoCl_2$	0.771	$NiCl_2$	0.750
$NaNO_2$	0.883	$CuCl_2$	0.778	$PbCl_2$	1.59
$NaNO_3$	1.01	$CsCl_2$	0.771	RbCl	0.759
NaSCN	1.87	$FeCl_3$	0.632	$ZnCl_2$	0.944
NaOH	1.43	HCl	0.924		

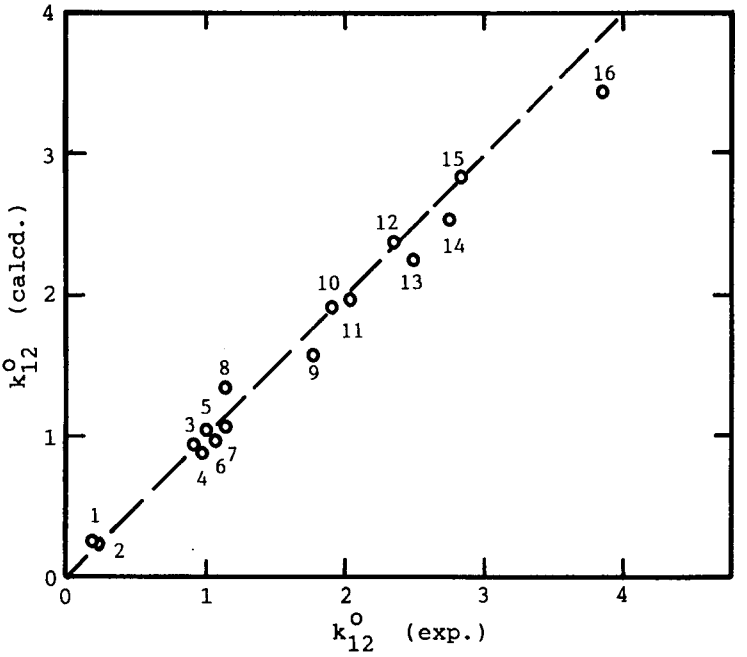

Fig. 4. Comparison of experimental and calculated distribution coefficients k^0_{12} for (1) $CuSO_4$, (2) $MgSO_4$, (3) LiBr, (4) $Al(NO_3)_3$, (5) $LiNO_3$, (6) KBr, (7) KNO_3, (8) $Cd(NO_3)_2$, (9) KI, (10) NH_4SCN, (11) KSCN, (12) $Pb(NO_3)_2$, (13) CdI_2, (14) BaI_2, (15) $Ca(SCN)_2$ and (16) $Ba(SCN)_2$.

direct method for determining k_i^0, as an ion never behaves independently of its counter ion. We propose to assume k_{Cl^-} to be unity. It can be easily shown that results such as those given in Fig. 4 are independent of the choice of the standard. The relative orders of k_i^0 among anions and among cations, respectively, are also independent of this choice. Comparison of a cation k_1^0 and an anion k_2^0 is obviously meaningless, however.

TABLE II

INTRINSIC DISTRIBUTION COEFFICIENTS OF SIMPLE IONS (SEPHADEX G-10)

It is assumed that $k^0_{Cl^-} = 1$.

Anion	k_2^0	*Cation*	k_1^0	*Cation*	k_1^0
SO_4^{2-}	0.140	Al^{3+}	0.100	Ca^{2+}	0.593
F^-	0.563	Fe^{3+}	0.160	Cs^+	0.594
Cl^-	(1)	Mg^{2+}	0.334	NH_4^+	0.594
NO_2^-	1.38	Ni^{2+}	0.423	K^+	0.627
Br^-	1.49	Co^{2+}	0.445	Cd^{2+}	0.806
NO_3^-	1.81	Cu^{2+}	0.471	Zn^{2+}	0.841
OH^-	3.64	Na^+	0.563	H^+	0.854
I^-	3.89	Rb^+	0.576	Ba^{2+}	1.04
SCN^-	6.21	Li^+	0.584	Pb^{2+}	4.01

Table II lists the values of k_i^0 determined in this way. Of all the cations listed, k_1^0 is the smallest for Al^{3+} and the largest for Pb^{2+}, and of all the anions listed, k_2^0 is the smallest for SO_4^{2-} and the largest for SCN^-.

We can now use eqn. 19 and the k_i^0 values in Table II to predict the k_{12}^0 value of an arbitrary 1–2 salt. Fig. 4 shows a comparison of the predicted and experimental values of k_{12}^0 for various non-sodium, non-chloride salts. The agreement is generally satisfactory.

Comparison with other gel systems

We have seen that the present model describes well the experimental results for the Sephadex G-10 system. Fig. 5 compares the k_2^0 values of typical anions for Sephadex G-10 with those for two other gels, Sepharon 300 (Pharmacia) and Extex HG-7 (Japan Exlan, Okayama, Japan). Sepharon is based on a water-soluble polymer, poly(hydroxyethyl methacrylate). The chemical structure of Extex is unreported; it has a low affinity towards water and excellent mechanical strength. The Sepharon data were taken from Borăk[12] and the Extex data were obtained by us using the same procedure as for the Sephadex system. Despite the differences in the physico-chemical properties of the gels, linear relationships are observed in Fig. 5, which supports the general validity of the present model.

To conclude, the main mechanism of simple-ion separation by a polymer gel in water is suggested to be the difference in the thermodynamic stabilities of the individual ions in the mobile and gel phases. Both size-exclusion and adsorption concepts are basically inconsistent with the experimental results. The trend in the gel chromatographic separation of ions is in general agreement with that in their water–oil partition behaviour[13], which supplements our conclusion.

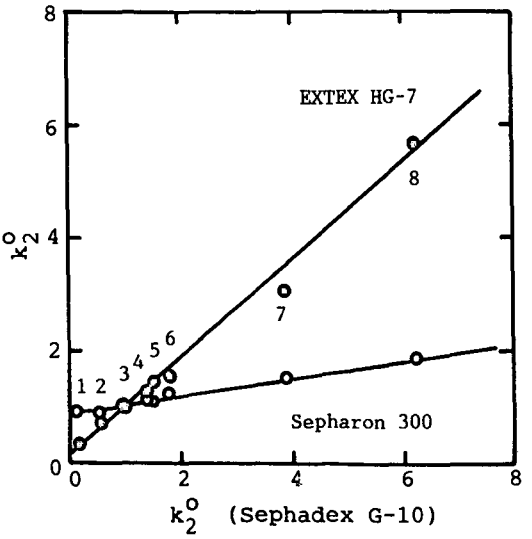

Fig. 5. Comparison of gels with respect to the anion distribution coefficients k_2^0 of (1) SO_4^{2-}, (2) F^-, (3) Cl^-, (4) NO_2^-, (5) Br^-, (6) NO_3^-, (7) I^- and (8) SCN^-; $k_{Cl^-}^0$ is assumed to be unity in all instances.

ACKNOWLEDGEMENT

We thank Professor S. Kihara of the Institute for Chemical Research, Kyoto University, for valuable comments.

REFERENCES

1 H. Determann, *Angew. Chem., Int. Ed. Engl.*, 3 (1964) 608.
2 J. C. Moore, *J. Polym. Sci., Part A*, 2 (1964) 835.
3 N. Yoza, *J. Chromatogr.*, 86 (1975) 325.
4 R. L. Pecsok and D. Saunders, *Sep. Sci.*, 3 (1968) 325.
5 S. Kadokura, T. Miyamoto and H. Inagaki, *Polym. J.*, 14 (1982) 993.
6 D. Saunders and R. L. Pecsok, *Anal. Chem.*, 40 (1968) 44.
7 B. Z. Egan, *J. Chromatogr.*, 34 (1968) 382.
8 H. Ortner and O. Pacher, *J. Chromatogr.*, 71 (1972) 55.
9 M. Shibukawa, N. Ohta and R. Kuroda, *Anal. Chem.*, 53 (1981) 1620.
10 T. Fukuda, N. Kohara and T. Miyamoto, in preparation.
11 B. Sebille, N. Thuaud and J. P. Tillement, *J. Chromatogr.*, 180 (1979) 103.
12 J. Borăk, *J. Chromatogr.*, 153 (1978) 69.
13 S. Kihara and M. Matsui, *Hyomen*, 23 (1985) 694.

Journal of Chromatography, 511 (1990) 69–78
Elsevier Science Publishers B.V., Amsterdam

CHROM. 22 448

Glucose-silica, an improved medium for high-pressure gel filtration chromatography

HUEY G. LEE and HARRY W. JARRETT*
Department of Biochemistry, School of Medicine, 800 Madison Avenue, University of Tennessee, Memphis, TN 38138 (U.S.A.)
(First received December 14th, 1989; revised manuscript received March 13th, 1990)

ABSTRACT

Glucose was covalently coupled to aminopropyl derivatized silica of various pore sizes. The reaction most likely involved Schiff's base formation between the aldehyde of glucose and the amine on the silica which was then reduced with $NaCNBH_3$. This glucose-silica behaved as a nearly ideal molecular sieving support for the high-pressure gel filtration chromatography of proteins and was superior in performance to many currently available supports.

INTRODUCTION

Gel filtration is size-exclusion chromatography that uses aqueous solvents and hydrophylic packings. Low-pressure gel filtration media such as dextrans, agaroses and polyacrylamides have been used both preparatively and analytically. High-pressure gel filtration chromatography (HPGFC)[1] should have enhanced resolution and reduced time requirements. The enhanced resolution necessarily means that much less quantity of sample would be needed for analytical purpose.

In recent years, HPGFC has been used extensively. Researchers have used the technique for quick isolation and analysis of proteins of interest. A rapid, sensitive protein assay employing HPGFC has recently been described[1]. More recently, Massom *et al.*[2] have described a HPGFC method useful for studying ligand binding by proteins. While the applications of HPGFC are potentially extensive and powerful, it is also clear that current media are less than ideal. Several of the current supports have pressure limitations well below the capabilities of modern chromatographs. To obtain supports capable of withstanding high pressures, macroporous silicas have commonly been used. To minimize the interactions of silica itself and its ionizable silanols with the sample, the silica surface is often chemically modified with some hydrophilic silanizing reagent such as the glycidiol-3-oxypropyl moiety. Even so, currently available columns, silica-based or non-silica-based, often show mixed-mode chromatographic behavior consistent with some interactions between the applied

0021-9673/90/$03.50

sample and either the support surface or the hydrophilic modifying group attached to it[2–9].

By coupling glucose to aminopropyl-silica, five hydroxyl groups are added to the silica surface. As a result, hydrophilicity is enhanced on the surface and mobile solutes are further protected from interacting with the silica. Columns prepared from glucose-silica were compared to many of the existing HPGFC columns and showed improved performance.

EXPERIMENTAL

Chromatography

The Chromatograph was a Gilson 9000 autoanalytical system outfitted with a Jasco UVDEC detector, a Tandy 3000HD computer, and the Gilson 714 software for data collection and analysis. Chromatography was at room temperature (20°C) throughout.

Preparation of glucose-silica

The starting material was 7-μm spherical 3-aminopropyl-silica of various porosities. When available, these were obtained from Alltech (Deerfield, IL, U.S.A.); otherwise, they were synthesized from 7-μm Macherey-Nagel (Düren, F.R.G.) silicas of the appropriate pore size as follows: 10 g silica were refluxed 4–6 h in 20% (w/v) 3-aminopropyltrimethoxysilane (Petrarch, Bristol, PA, U.S.A.) in toluene. The derivatized silica was then thoroughly washed with toluene, then methanol, and dried at 60°C overnight.

Glucose-silica was prepared by reacting 5 ml (1 mmol) of 0.2 *M* D-glucose, 10 m*M* sodium phosphate, pH 6.8, and 126 mg (2 mmol) $NaCNBH_3$ per gram of aminopropyl-silica. The mixture was constantly stirred at 60°C for 5 h. The reacted resin was then washed with water, acetone, and then dried at 60°C. The dried glucose-silica was then tested with Cd–ninhydrin[10] and was typically found to lack any detectable unreacted amines.

Initially, the disappearance of glucose from the reaction mixture was measured with the anthrone reagent[11] to follow the progress of the reaction. However, control reactions lacking in silica also showed a decrease in measurable glucose with time, albeit at a slower rate and to a lesser extent. Presumably, this was due to a slow reduction by $NaCNBH_3$ of glucose to sorbitol. While such controls allow the coupling reaction to be followed qualitatively, the method is cumbersome and an alternative procedure was developed.

In order to study the reaction rate more accurately, approximately 600 000 cpm of [3-^{3}H]D-glucose (New England Nuclear, Boston, MA, U.S.A.) was added to the 5 ml reaction mixture. At various times, 0.2-ml portions of the reaction mixture were removed and mixed with 0.8 ml of 0.1 *M* hydrochloric acid to immediately terminate the reaction. After a brief centrifugation, duplicate 0.4-ml portions of the supernatant were mixed with 5 ml of scintillation fluid and the amount of [^{3}H]glucose determined using a Packard Tri-Carb 4640 scintillation counter. Silicas, recovered from the centrifugation during the time course study were washed thoroughly and tested with the Cd–ninhydrin reagent.

Column testing

Glucose-silica supports of 60, 100, 300 and 500 Å pore sizes were made as described and packed into 100 × 4.6 mm I.D. columns. The mobile phase was 100 m*M* sodium sulfate, 20 m*M* sodium phosphate, pH 6.8 and the flow-rate was 1 ml/min throughout. For comparison, 100 × 4.6 mm I.D. columns of RoGel P (70 Å pore), SynchroPak GPC (60 Å), Macrosphere GPC (60 Å), and a 250 × 4.6 mm I.D. Macrosphere R (20 Å pore) column were obtained from Alltech and also tested under the same conditions. A 300 × 7.5 mm I.D. BioSil TSK-125 column (Bio-Rad Labs., Richmond, CA, U.S.A.) was also compared under the same conditions except that it was necessary to reduce the flow-rate to 0.7 ml/min to maintain a backpressure of less than 30 bar as suggested by the manufacturer.

Proteins with a wide range of molecular weights were used to test the columns. Low-molecular-weight tryptophan (mol.wt. 204) was used as a marker for total excluded column volume. The individual proteins were typically made up as 1 mg/ml stock solutions and various mixtures were then prepared. Each protein was also injected individually onto the various columns to confirm the identity of each peak in a mixture. The injection volume was 5 μl and detection was by absorption at 220 nm throughout.

A 300 × 6.2 mm I.D. column of 100 Å pore glucose-silica was also packed for comparison to the TSK column. For this comparison, the protein test mixture supplied by Bio-Rad with the TSK column was used.

To characterize the pH resistance of the various supports, the underivatized silica, aminopropyl-silica and glucose-silica from the same base silica and porosity were treated with different pH buffers for 2 h. After 2 h, the samples were centrifuged, the supernatants were removed, and the dissolved silica content was determined by the molybdate method[12] using a commercially available kit (Chemets, Calverton, VA, U.S.A.). To further investigate the pH stability of the glucose-silica, 100 ml of the pH 10 buffer (60 column volumes) was flowed at 1 ml/min through a 300-Å glucose-silica column (100 × 4.6 mm I.D.). Chromatograms obtained before and after the high pH treatment were compared.

RESULTS

The reaction used to prepare glucose-silica is depicted in Fig. 1. The chemistry used is mild and simple to carry out. The aldehyde moiety of D-glucose presumably reacts with the primary amine on aminopropyl-silica to produce a Schiff's base. The Schiff's base is then reduced by $NaCNBH_3$, a reductant which is relatively specific for Schiff's bases[13]. A temperature of 60°C was found to be optimal for this reaction.

Using [^{3}H]glucose as a radiotracer, it was found that 0.25 mmol of the D-glucose coupled per gram of the 300 Å pore aminopropyl-silica and 0.55 mmol/g for the 100-Å aminopropyl-silica. The reaction was found to follow (pseudo)first order kinetics and the half-time of the reaction was 26 min for the 300-Å and 28 min for the 100-Å resin with an average of 27 min overall (Fig. 2). Therefore, the 5-h reaction time used should allow the reaction to be about 99.9% complete.

The completion of the reaction was confirmed by the Cd–ninhydrin test. It was found that glucose-silica showed no color change in the Cd–ninhydrin reagent while the parent aminopropyl-silica appeared intensely orange-red in color following Cd–

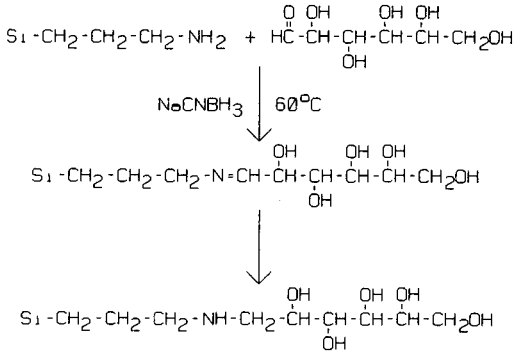

Fig. 1. A reaction overview. The amine of the aminopropyl-silica presumably forms a Schiff's base with the aldehyde of the D-glucose which is then reduced with sodium cyanoborohydride[13]. The two steps occur in a continuous fashion at 60°C in the presence of glucose and the reducing agent $NaCNBH_3$.

ninhydrin reaction. Cd–ninhydrin typically gives the same orange-red color with other primary amines (glycine, ethanolamine) tested. The addition of Cd to the ninhydrin reagent gives a more stable color than the typical purple color obtained with ninhydrin alone[10]. The progress of the reaction could also be following with Cd–ninhydrin during the time course shown in Fig. 2: silicas from short reaction time gave the characteristic orange-red color which progressively diminished until, as the glucose reaction reached completion, a pure white silica was observed.

The glucose-silica columns (60, 100, 300 and 500 Å) were tested with protein sizes ranging from immunoglobulin M (mol.wt. 1 000 000) to melittin (mol.wt. 2848). Fig. 3 shows the plots of molecular weight *vs.* retention time for the various pore sizes

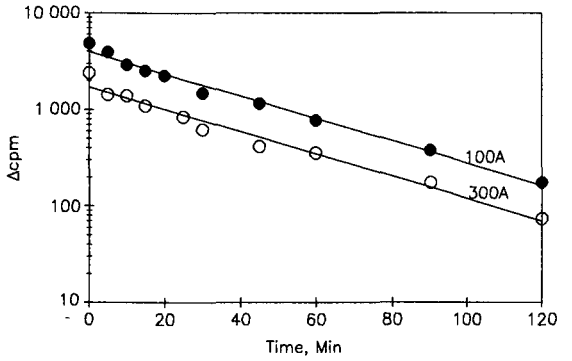

Fig. 2. Coupling of D-glucose to aminopropyl-silica follows (pseudo)first order kinetics. [^{3}H]Glucose was used to trace the coupling of glucose to two different pore size (100 Å and 300 Å) AP-silicas. The cpm remaining in the supernatant after reaction for a day was considered to represent the reaction endpoint and has been subtracted from the data (Δcpm). The semilogarithmic plot of Δcpm as a function of time was fit reasonably well by (pseudo)first order kinetics; the line shown was derived from the equation for a first order process. The average half-time of the reaction with either silica was 27 min. The difference in the vertical location of the curves is due to the greater quantity of the glucose coupled to the 100-Å resin as compared to the 300-Å resin which has a lower surface area and presumably, less aminopropyl groups to react.

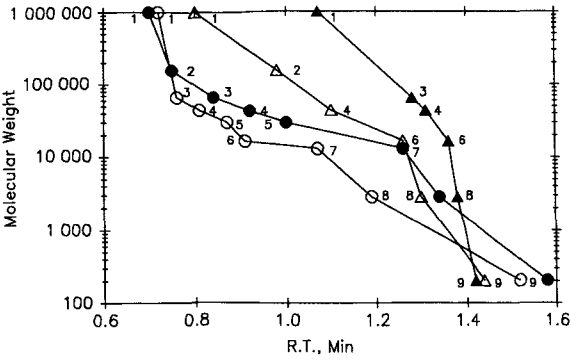

Fig. 3. Molecular weight *versus* retention time (R.T.) of various pore sizes. The proteins tested are indicated by the numbers. Proteins: 1 = immunoglobulin M (mol.wt. 1 000 000); 2 = immunoglobulin G (IgG) (156 000); 3 = bovine serum albumin (66 300); 4 = ovalbumin (44 000); 5 = carbonic anhydrase (30 000); 6 = bovine brain calmodulin (16 700); 7 = cytochrome *c* (13 000); 8 = bee venom melittin (2848). Number 9 is the amino acid tryptophan (204). Glucose-silica columns (100 × 4.6 mm I.D.) of different pore sizes are represented by open circles (60 Å), closed circles (100 Å), open triangles (300 Å) and closed triangles (500 Å).

and demonstrates the ability of glucose-silica to resolve proteins of different size classes. As expected, columns with larger pores were capable of resolving larger proteins.

As illustrated in Fig. 4, the performance of the 60-Å glucose-silica column was compared to four other commercial HPGFC columns: RoGel P, Macrosphere GPC 60, SynchroPak GPC 60 and Macrosphere GPC-R. When a mixture of three proteins

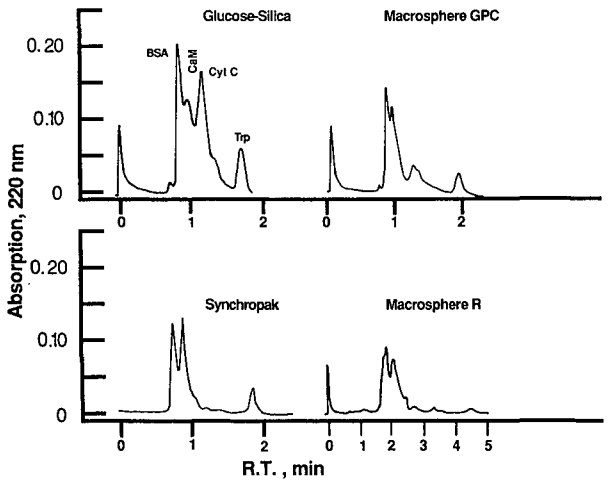

Fig. 4. A comparison of glucose-silica with other HPGFC columns. A mixture containing three proteins and Trp was injected onto four different columns: 60 Å pore glucose-silica, Macrosphere GPC 60 ("GPC"), SynchroPak GPC 60 and Macrosphere/R GPC ("R"). All columns were 100 × 4.6 mm I.D. except the last which was 250 × 4.6 mm I.D. All chromatograms are shown to the same scale and may be compared for protein recovery as well.

[bovine serum albumin (BSA), calmodulin (CaM) and cytochrome *c* (Cyt C)] and Trp was injected onto the columns, both the SynchroPak GPC 60 and the Macrosphere/R GPC could not resolve all four constituents in the mixture, yielding three and two peaks, respectively (Fig. 4). No peaks were observed at all with the RoGel column suggesting that this column bound all components of the mixture applied to it (data not shown). The glucose-silica column could not only separate all the constituents into four distinct peaks, it also gave the highest recovery of injected protein. The chromatograms shown (Fig. 4) are plotted to the same scale and represent the same amount of sample injected. The eye confirms the result obtained by integration that the glucose-silica column gave greater peak areas indicating that more of the applied protein elutes from the column.

Although the Macrosphere GPC 60 was able to resolve all the components in the above mixture, the chromatography of the individual proteins in the mixture demonstrated that retention time was not strictly dependent on protein size with this column. In fact, the Macrosphere GPC 60 support apparently has a strong repulsive interaction with the acidic protein CaM as shown in Fig. 5. As shown by this figure, calmodulin (mol. wt. 16 700) actually elutes before carbonic anhydrase (30 000) from the Macrosphere GPC column while they elute in the proper order from glucose-silica and at a retention time wholly consistent with each protein's molecular weight (see also Fig. 3).

A similar phenomenon was also observed with the TSK column. Again, calmo-

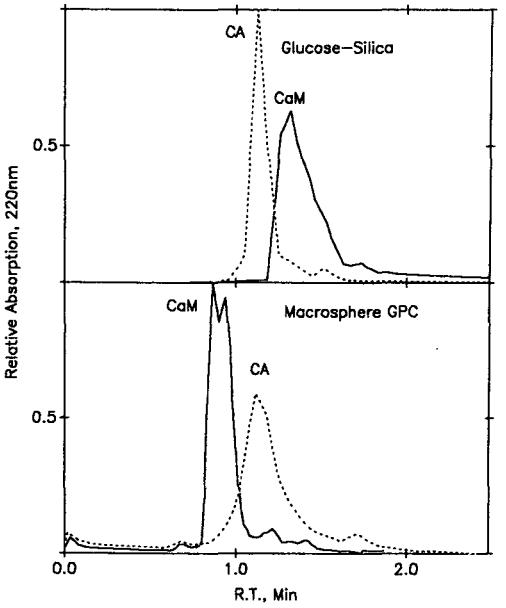

Fig. 5. Calmodulin behaves differently on glucose-silica and Macrosphere GPC 60. Samples of calmodulin (CaM) and carbonic anhydrase (CA) were injected onto the glucose-silica and the Macrosphere GPC 60 columns. CA, being a much larger protein than CaM, was observed to come off the glucose-silica column earlier than CaM, as expected. However, the Macrosphere GPC 60 demonstrated the reverse order of elution.

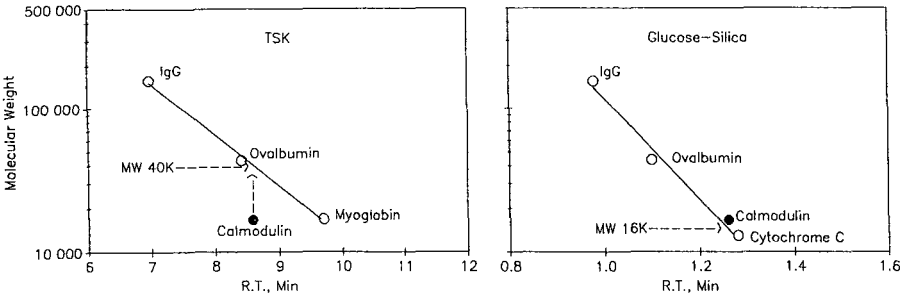

Fig. 6. Calmodulin's behavior on TSK is also unusual. CaM, a strongly acidic protein, behaved as though it were a 40 000 (40 K) molecular weight protein on the TSK column, while the glucose-silica gave a retention time for calmodulin more consistent with its true molecular weight. The apparent molecular weight calculated from the standard curve for calmodulin is indicated.

dulin was found to elute too soon for its small size. The acidic calmodulin behaved as though it were a 40 000 molecular weight protein on the TSK column (Fig. 6). In contrast, the glucose-silica column, once calibrated with the same standard proteins gave a molecular weight for calmodulin of 16 000, which is entirely consistent with its actual molar mass of 16 700 (ref. 14).

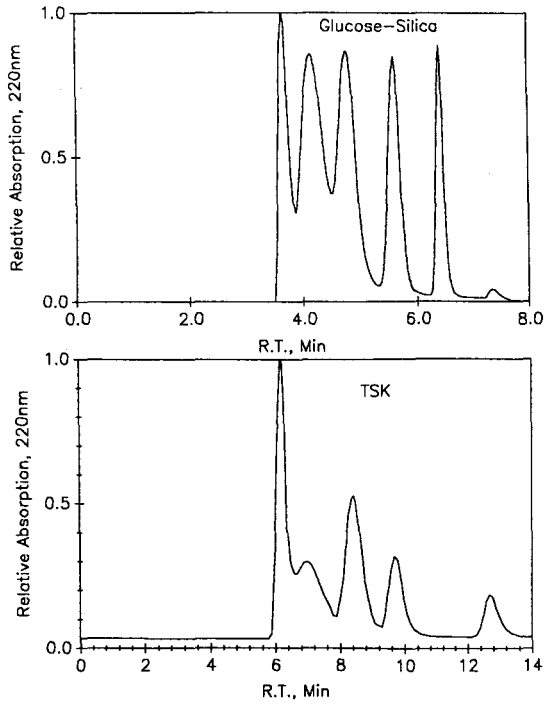

Fig. 7. Glucose-silica compared to TSK. The test mixture supplied by Bio-Rad with the TSK column was better resolved on glucose-silica. The test mixture contained, in order of elution, "protein aggregate", thyroglobulin (670 000), IgG, ovalbumin, myoglobulin (17 000), and vitamin B_{12} (1350).

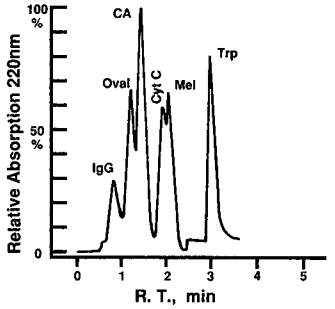

Fig. 8. Coupling two columns of different pore sizes extends the range of glucose-silica. Two 100 × 4.6 mm I.D. glucose-silica columns of different pore sizes (100 Å and 300 Å) were connected, outlet to inlet, with a short piece of tubing. A 10-μl mixture of five proteins and Trp was separated by the tandem-connected 100-Å and 300-Å columns connected together at the flow-rate of 1 ml/min. The last peak (Trp) appeared at approximately 3 min after the injections. Oval = Ovalbumin; Mel = melittin.

Furthermore, a 300 × 6.2 mm I.D. glucose column, though smaller than the TSK column 300 × 7.5 mm I.D., was capable of resolving all six components of the Bio-Rad protein standard test mixture while the TSK column could not (Fig. 7). The comparison also showed that the glucose column gave sharper peaks than the TSK column could. The glucose column clearly is superior to the TSK in resolving power as well as the ability to give correct molecular weights for acidic proteins like calmodulin.

To investigate whether a combination of pore sizes might extend the range of the glucose-silica column, a mixture of five proteins and Trp was injected onto two tandem-connected 100-Å and 300-Å glucose-silica columns. As shown in Fig. 8, all constituents were well resolved in 3 min at the flow-rate of 1 ml/min. This clearly demonstrated the powerful separation ability of glucose-silica as an HPGFC support.

Finally, glucose-silica was shown to possess strong resistance to high-pH solutions, as compared to the aminopropyl-silica and underivatized silica from which it

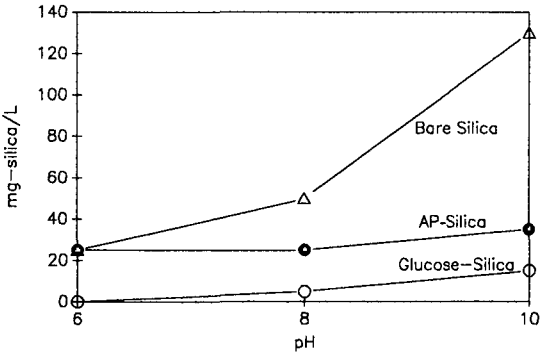

Fig. 9. Low pH sensitivity of the glucose-silica. Underivatized silica, 3-aminopropyl (AP)-silica and glucose-silica were treated with pH 6, 8 and 10 buffers (50 m*M* each in Tris, imidazole and boric acid titrated to the desired pH) for 2 h. The mixtures were then centrifuged and the supernatants removed for determination of dissolved silica. The glucose-silica resin showed strong pH resistance as compared to the 3-aminopropyl-silica and the bare silica.

was made (Fig. 9). For example, the pH 10 buffer dissolved only 0.01% of the glucose-silica in 2 h, as opposed to 0.13% for the bare silica. In a separate experiment, the chromatograms obtained before and after 100 ml of the pH 10 buffer (60 column volumes) flowed through the 300-Å column (100 × 4.6 mm I.D.) revealed no detectable difference in the resolution or peak area of the injected proteins (data not shown). The result suggested that the glucose on the silica surface may sterically block the pH sensitive silane linkage. A similar pH stability has been observed for a sterically blocked silica-based support in a reversed-phase column[15]. Thus, the pH stability of glucose-silica makes for a pH stable column. This could be an invaluable property if high pH mobile phases were necessary to an experiment.

DISCUSSION

A simple way of coupling glucose to macroporous silicas has been described. Fig. 1. represents only the presumed mechanism since the final product was only partially characterized chemically. The chromatographic behavior of the support is more germain and was the focus of the presented experiment. The resulting support proved to be superior to many commercially available HPGFC supports. The small 100 × 4.6 mm I.D. glucose-silica columns used for most of the studies here were sufficient to give good separation because of the high resolution of glucose-silica. A larger column is capable of even higher resolution (Figs. 7 and 8). All the tests performed have demonstrated that Glucose-Silica columns behave consistently with basic proteins (*e.g.*, melittin, lysozyme), acidic proteins (*e.g.*, calmodulin), and with large (immunoglobulin M) and small (melittin, cytochrome *c*) proteins. The glucose must nearly completely shielded the silica from interacting with the mobile phase and the solutes it contains as demonstrated by these results with various proteins and the demonstrated pH stability relative to silica. Glucose-silica appears to represent a significant improvement upon existing HPGFC supports.

ACKNOWLEDGEMENTS

We would like to thank Mr. Larry Massom for technical assistance and Dr. Steve Marshall for the gift of [^{3}H]glucose. Mr. William Foster at Alltech/Applied Science kindly packed the glucose-silica columns. We would also like to thank Miguel Carrion (Lederle Laboratories, Pearl River, NY, U.S.A.) for his help with the anthrone reaction and for helpful discussion. This work was supported in part by NSF (DMB 8996229) and NIH (GM 43609).

REFERENCES

1 V. A. Fried, M. E. Ando and A. J. Bell, *Anal Biochem.*, 146 (1985) 271–276.
2 L. Massom, H. Lee and H. W. Jarrett, *Biochemistry*, 29 (1990) 671–681.
3 W. Kopaciewicz and F. E. Regnier, *Anal Biochem.*, 126 (1982) 8–16.
4 B. Johansson and J. Gustavsson, *J. Chromatogr.*, 457 (1988) 205–213.
5 I. Martin and Ü. Lille, *J. Chromatogr.*, 466 (1989) 339–345.
6 B. Anspach, H. U. Gierlich and K. K. Unger, *J. Chromatogr.*, 443 (1988) 45–54.
7 S. C. Goheen, *J. Liq. Chromatogr.*, 22 (1988) 1221–1228.
8 N. Hirata, M. Kasai, Y. Yanagihara and K. Noguchi, *J. Chromatogr.*, 434 (1988) 71–82.

9 Q. C. Meng, Y. F. Chen, L. J. Delucas and S. Oparil, *J. Chromatogr.*, 445 (1988) 29–36.
10 W. J. Dryer and E. Bynum, *Methods Enzymol.*, 11 (1967) 32–39.
11 D. W. Vomhof, J. Truitt and T. C., Tucker, *J. Chromatogr.*, 21 (1966) 335–337.
12 *Methods for Chemical Analysis of Water and Wastes,* National Technical Information Service, Springfield, VA, 1983, Method 370.1.
13 R. F. Borch, M. D. Bernstein and H. D. Durst, *J. Am. Chem. Soc.*, 93 (1971) 2897–904.
14 D. M. Watterson, F. Sharief and T. C. Vanaman, *J. Biol. Chem.*, 255 (1980) 962–971.
15 J. L. Glajch and J. J. Kirkland, *LC·GC*, 8 (1990) 140.

Journal of Chromatography, 511 (1990) 79–88
Elsevier Science Publishers B.V., Amsterdam

CHROM. 22 414

Preparation and comparison of a pentafluorophenyl stationary phase for reversed-phase liquid chromatography

EDIT CSATÓ, NÁNDOR FÜLÖP and GYULA SZABÓ*
"Frédéric Joliot Curie" National Research Institute for Radiobiology and Radiohygiene, P.O. Box 101, H-1775 Budapest (Hungary)
(First received August 1st, 1988; revised manuscript received March 5th, 1990)

ABSTRACT

A pentafluorophenyl stationary phase was prepared for reversed-phase liquid chromatography. The amount of organic moiety bonded on a silica support was determined from thermogravimetric curves of modified silica gel. The specific surface area of the gel was obtained from nitrogren sorption measurements at 77 K. The retention behaviour of solutes on a column packed with this gel was examined and compared with that on a commercially available phenylmethyl column. The capacity factors of the solutes were normalized to unit surface area of the support (k'/S_{BET}) and compared with the k'/S_{BET} values for 52 different solutes in an isoeluotropic system. It was observed that the pentafluorophenyl stationary phase exhibited specific fluorine–fluorine interactions and showed enhanced retention not only of fluorine-containing compounds but also of some other halogen-containing solutes.

INTRODUCTION

Although reversed-phase high-performance liquid chromatography (RP-HPLC) is more widely used than the normal-phase mode and improvements are still being made, the former has generally been considered to be less selective than the latter with respect to changes in retention due to steric factors associated with the solutes and changes in the type of solvents in the mobile phase. The major factor in retention in RP-HPLC is solvophobic interaction[1], which is less polar and gives lower steric selectivity compared with polar adsorption in normal-phase chromatography.

The present practice in RP-HPLC is that a preliminary attempt at separation on a C_{18} stationary phase with a certain composition of an aqueous mobile phase is followed by a change in the eluent composition in order to optimize the k' values and the separation. The use of tetrahydrofuran and solvents other than methanol or acetonitrile was shown to be useful[2–4]. If the desired separation is not obtained, one can try other commercially available stationary phases such as C_8 or phenyl. Organic functional groups other than octadecylsilyl (ODS) have been bonded to silica. An aryl ether bonded phase was prepared and used for the RP-HPLC of nitroaromatic

0021-9673/90/$03.50

compounds[5]. Amino acids and peptides were separated using a bonded peptide stationary phase[6]. Several other organic bonded phases have been tried in attempts to increase the selectivity of the stationary phase by using very long alkyl[7], organomercury(II) species[8], alkyl, aryl, aralkyl and alicyclic structures[9] and cyclodextrin[10] in the stationary phase.

Recently, highly fluorinated RP-HPLC stationary phases have been introduced[11–16] but few studies have been reported.

Berendsen *et al.*[12] directly compared a heptadecafluorodecyldimethyl (HFD) support with its hydrocarbonaceous analogue, a decyl (C_{10}) bonded phase. Only eleven solutes were used in the study. Billiet *et al.*[11] used a wider variety of the test solutes but compared an HFD column with an octadecyl-bonded silica (ODS) column. The chromatographic difference between decyl- and an octadecyl-bonded phases was concluded to be insignificant. They found the HFP-bonded phase to have an increased selectivity over the octadecyl-bonded phase for esters, ketones and fluoro-substituted solutes. Sadek and Carr[17] extended the number of solutes tested in order to compare directly the chromatographic characteristics of the HFD- and C_{10}-bonded phases. In addition, two other fluorinated phases, heptafluoroisopropoxypropyldimethyl (HFIPD) and pentafluorophenydimethyl (PFP), were evaluated under the same mobile phase conditions as for the HFD and C_{10} phases in an attempt to compare all four phases qualitatively. They found that the selectivity of the solutes is completely different on the hydrocarbon and fluorocarbon decyl columns.

In this work, we prepared a pentafluorophenyl-bonded stationary phase for RP-HPLC. The silica gel was modified with pentafluorophenyldimethylchlorosilane. The purpose was to examine the retention behaviour of the solutes on a column packed with a pentafluorophenyl-modified silica gel stationary phase and to compare it with a commercially available phenylmethyl phase in RP-HPLC. We used a phenyl phase as a reference to eliminate the effects of phenyl groups present in the stationary phase. This paper describes some details of the chromatograhic properties of the PFP phase. Both specific effects and the general separation power were considered.

EXPERIMENTAL

Equipment

Chromatographic separations were carried out with a Varian 8500 solvent delivery system, a Model 7125 sample injector (Rheodyne, Berkely, CA, U.S.A.) and a Varian Model 635 UV–VIS monitor. The gel was packed in a 120 × 4. 0 mm I.D. stainless-steel tube by Bio-Separation Technologies (Budapest, Hungary). The thermal studies were performed with a MOM (Budapest, Hungary) Derivatograph-3427. The BET surface area of silica gels was determined with a sorptometer made in the Department for Physical Chemistry, Technical University of Budapest (Hungary).

Materials

A reference phenylmethyl phase column (5 μm; 120 × 4.0 mm I.D.) was obtained from Bio-Separation Technologies. Separon SGX Si-100 (5 μm) was purchased from Laboratorní Přístoje (Prague, Czechoslovakia). Pentafluorophenyldimethylchlorosilane was obtained from Fluka (Buchs, Switzerland). Methanol was of liquid chromatographic grade (Merck, Darmstadt, F.R.G.). All fluorinated solutes

were kindly provided by Chemical Works of Budapest (Hungary). All other chemicals were obtained from commercial sources and used without purification.

Chromatography

The test solutes were dissolved in methanol at a concentration of 0.1 mg/ml. Typically 10 μl were injected. The flow-rates were usually 1 ml/min. Sample peaks were detected at 254 nm.

Preparation of pentafluorophenyl stationary phase packing

The preparation of the PFP stationary phase packing was based on Unger's procedure[18]. A 10-g amount of dried silica gel was mixed of pentafluorophenyldimethylchlorosilane in anhydrous toluene and refluxed in a sealed flask. The reaction was complete within 8 h. The PFP-modified silica gel was filtered and washed successively with toluene, methanol, water and methanol. The solid phase was kept at 353 K for several hours under vacuum. Residual hydroxy groups were deactivated by treating the solid material with 10% of trimethylchlorosilane in toluene. A 4-g amount of this deactivated PFP-bonded silica gel for packing was suspended and sonicated in 50 ml of isopropyl alcohol. The supernatant was decanted after standing for 20 min. The packing material was again resuspended in 40 ml of isopropyl alcohol and transferred to the packing reservoir. The packing pump used was a Haskel 122. Packing was performed at 47 MPa with methanol as the pressurizing and washing solvent. A 120 × 4.0 mm I.D. stainless steel column was used.

Analysis of prepared PFP- and reference phenylmethyl-modified silica gels

The amount of organic moiety bound on the silica support was determined from the thermogravimetric analysis (TGA) curves of modified silica gels[19]. The specific surface areas of the gels (S_{BET}) before and after grafting were obtained from nitrogen sorption measurements at 77 K.

Preparation of isoeluotropic system

The term isoeluotropic system was introduced by Schoenmakers *et al.*[20] for mobile phases of different composition that yield (on average) equal retention times on a given RP-HPLC stationary phase. The retention of the examined solutes was expressed in terms of their capacity factor (k'). In order to eliminate the influence of the specific surface area of the investigated support, we used k'/S_{BET} instead of k'. The validity of this approach has been demonstrated[21–23]. The eluotropic strength of such a mixture can be expressed as the volume fraction of the corresponding binary mixture

TABLE I

CHARACTERISTICS OF SILICA GELS USED

Functional group bonded	*Particle size (μm)*	*Specific surface area, S_{BET} (m^2/g)*	*Mean pore diameter (nm)*	*Surface concentration μmol/m^2*	*Carbon (%)*
Phenylmethylhydroxysilyl	5	397	10	3.6	13.0
Pentafluorophenyldimethylsilyl	5	389	10	3.5	12.5

TABLE II

SUMMARY OF RETENTION DATA OBTAINED ON THE REFERENCE PHENYLMETHYL AND ON THE PENTAFLUOROPHENYL COLUMNS

The values of ln k'_0, slope, their standard errors (S.E.) and correlation coefficient (r) were obtained using eqn. 1.

Solute	*Phenylmethyl column*					*Pentafluorophenyl column*				
	ln k'_0	*S.E.*	*Slope*	*S.E.*	*r*	*ln* k'_0	*S.E.*	*Slope*	*S.E.*	*r*
Aniline	2.419	0.243	−4.546	0.448	−0.981	1.973	0.362	−4.208	0.668	−0.953
m-Cresol	3.836	0.245	−6.214	0.452	−0.989	3.421	0.287	−5.702	0.530	−0.983
Nitrobenzene	4.546	0.260	−6.271	0.480	−0.988	3.864	0.402	−5.785	0.741	−0.968
Methyl benzoate	6.021	1.065	−8.145	1.969	−0.901	4.957	0.319	−6.978	0.588	−0.986
Bromobenzene	5.975	0.298	−7.783	0.551	−0.99	5.241	0.327	−7.117	0.604	−0.986
p-Xylene	6.493	0.341	−8.265	0.629	−0.988	5.901	1.058	−7.282	1.952	−0.881
4-Chloro-3-nitro-α,α,α-trifluorotoluene	7.071	0.349	−9.228	0.643	−0.99	6.673	0.374	−8.677	0.690	−0.987
2-Chloro-α,α,α-trifluorotoluene	7.593	0.626	−9.696	1.105	−0.981	7.269	2.378	−8.74	4.972	−0.779
n-Propylbenzene	7.683	0.608	−9.441	1.073	−0.981	7.108	0.599	−8.921	1.057	−0.979

of methanol in water (φ_M). When another stationary phase is used the retention will change. However, this effect can be nullified by changing the mobile phase composition.

Let us consider the capacity factor per unit specific surface area of the gel, $k'/S_{BET} \times 10^3 = 12.87$, obtained for bromobenzene in the binary mixture methanol–water (55:45) ($\varphi_M^{Ph} = 0.55$) on a reference phenylmethyl (Ph) column. Using a PFP stationary phase the same k'/S_{BET} value is obtained with the mobile phase methanol–water (49:51) ($\varphi_M^{PFP} = 0.49$). The value of φ_M^{PFP} that corresponds to φ_M^{Ph} will be different for different solutes. The RP-HPLC system phenylmethyl/methanol (φ_M^{Ph})–water and PFP phase/methanol (φ_M^{PFP})–water can be referred to as an isoeluotropic system. An arbitrary solute is than expected to yield similar k'/S_{BET} values in both systems.

RESULTS AND DISCUSSION

Analysis of stationary phase

The amount of organic moiety bound on the silica support was determined by TGA. The maximum surface concentrations of the bonded Si–aryl groups are given in Table I. The specific surface areas of the gels were obtained from nitrogen sorption measurements at 77 K. It was assumed that the starting silica had a specific surface area of 535 m^2/g (Laboratorní Přístoje). These measurements (see Table I) demonstrate a considerable reduction in S_{BET} values on the modified silica supports of *ca.* 25–28% of the starting gel.

Polarity of columns

Retention data of ten solutes were obtained on two columns, one filled with phenylmethyl stationary phase (as reference) and the other with the pentafluorophenyl (PFP) phase. We used mixtures of methanol and water at 5% composition intervals, from 40 to 70% methanol. In Table II. $\ln k'_0$ values and standard errors of the $\ln k'$ data are presented, using the following linear equation to relate $\ln k'$ with the mobile phase composition, φ:

$$\ln k' = \ln k'_0 - p_2\varphi \tag{1}$$

where φ is the volume fraction of organic solvent in the water–organic solvent mixture, k'_0 represents the capacity factor of a solute with pure water as a mobile phase and p_2 is a constant for a given solute–eluent combination. Ln k'_0 and p_2 were obtained from least-squares approximation of the generally convex $\ln k'$ *vs.* φ curve by a straight line over the interval examined. Table II also gives standard errors of $\ln k'$ from the straight line. It can be seen from Table II that the values obtained for $\ln k'_0$ on the PFP column are considerably smaller than those obtained with the phenylmethyl column, wich illustrates that with the same mobile phase composition, the retention will decrease on the PFP phase. In order to elute a solute from the PFP column with the same k' as observed on the phenylmethyl column, a mobile phase must be used that contains less methanol and, hence, more water. Consequently, PFP behaves as a less retentive stationary phase than the phenylmethyl stationary phase. We tried to exclude other factors (silica gel, pore volume, carbon content, type of chlorosilane modifier and column length that could play a dominant role in the separation of solutes by

TABLE III

ANALYSIS OF THE SELECTIVITY OF DIFFERENT PHASES FOR 52 DIFFERENT TYPES OF SOLUTES IN THE ISOELUOTROPIC SYSTEM

Least-squares analysis of the data was used. The values of the intercept (a), slope (b) and correlation coefficient (r) were obtained using eqn. 2.

Solutes	a	b	r
Fluorinated (16 compounds)	−0.92	1.39	0.87
Haogenated (26 compounds)	−1.50	1.30	0.87
Halogenated other than fluorinated (10 compounds)	−0.45	1.15	0.91
Polar (19 compounds)	0.24	0.85	0.92
Apolar (7 compounds)	0.58	1.07	0.85

RP-HPLC. We guessed that this effect might be due to the fluorination because the perfluorocarbon molucules have both a relatively high dipole moment of the C–F groups of 189 D and low polarizability indices compared with those of hydrocarbons.

Specific effect

The retention behaviour of PFP bonded silica gel was examined and compared with commercially available phenylmethyl-bonded silica gel. The capacity factors of the solutes were normalized to unit surface area of the support, k'/S_{BET}, for 52 very different solutes in an isoeluotropic system were calculated from an anisoelutropic system. We compared the k'/S_{BET} value of bromobenzene ($k'/S_{BET} \times 10^3 = 12.87$) in a binary system of methanol ($\varphi_M^{Ph} = 0.55$)–water (55:45) on a reference phenylmethyl phase. Using the PFP phase the same retention values could be achieved with the mobile phase methanol ($\varphi_M^{PFP} = 0.49$)–water (49:51). Systematic increases in selectivity on the PFP column would be manifested by a slope of the plot of k'/S_{BET} of the PFP phase *versus* that of the phenylmethyl phase (reference) of greater than unity. We applied least-squares analysis of the data.

$$k'/S_{BET_{PFP}} = a + bk'/S_{BET_{Ph}} \quad (2)$$

The 52 solutes that were examined were divided into five groups according to their chemical properties. The results are given in Table III. With fluorinated and halogenated compounds the slopes are greater than unity, for the non-apolar group they are about unity, which is evident from the isoeluotropic system, but for the polar groups they are less than unity. The correlation coefficients are only 0.85–0.92 because of scatter of the data points about the line. We conclude that the PFP phase shows an improved selectivity for halogenated and particularly fluorinated compounds.

We defined the specific effect on the PFP phase in the isoeluotropic system as the deviation from the line of

TABLE IV

SPECIFICITY OF THE PENTAFLUOROPHENYL COLUMN FOR FLUORINATED COMPOUNDS

Specificity for solute *i* eluted from the PFP phase relative to the isoeluotropic system with the phenylmethyl (Ph) phase was obtained using eqn. 4.

Solute	$k'/S_{BET_{PFP}} \times 10^3$ *[methanol–water (44:51)]*	$k'/S_{BET_{Ph}} \times 10^3$ *[methanol–water (55:45)]*	S_i
Bromobenzene	12.877	12.877	0.00
3-Amino-α,α,α-trifluorotoluene	7.118	6.221	0.897
2-Hydroxy-α,α,α-trifluorotoluene	7.327	6.221	1.106
3-Amino-α,α,α-trifluorotoluene	8.374	6.549	1.825
4-Hydroxy-α,α,α-trifluorotoluene	9.631	6.549	3.082
2-Chloro-5-amino-α,α,α-trifluorotoluene	12.877	10.258	2.619
4-Chloro-3,5-dinitro-α,α,α-trifluorotoluene	15.075	13.097	1.978
2-Chloro-3,5-dinitro-α,α,α-trifluorotoluene	16.540	14.514	2.026
α,α,α-Trifluorotoluene	20.620	14.079	6.541
2-Chloro-5-nitro-α,α,α-trifluorotoluene	23.030	19.208	3.822
4-Chloro-3-nitro-α,α,α-trifluorotoluene	25.020	17.244	7.776
2,4-Dichloro-5-amino-α,α,α-trifluorotoluene	26.171	20.191	5.980
4-Chloro-α,α,α-trifluorotoluene	27.427	20.628	6.799
2-Chloro-α,α,α-trifluorotoluene	32.452	22.030	10.422
3-Bromo-α,α,α-trifluorotoluene	39.362	25.757	13.605
2,4-Dichloro-α,α,α-trifluorotoluene	48.156	33.833	14.323
5-Bromo-2-chloro-α,α,α-trifluorotoluene	52.553	40.818	11.735

$$k'/S_{\mathrm{BET}_{\mathrm{PFP}}} = k'/S_{\mathrm{BET}_{\mathrm{Ph}}} \tag{3}$$

In this case, specificity should be defined for a solute *i* as

$$S_i = k'/S_{\mathrm{BET}_{\mathrm{PFP}}} - k'/S_{\mathrm{BET}_{\mathrm{Ph}}} \tag{4}$$

TABLE V

SPECIFICITY OF THE PENTAFLUOROPHENYL COLUMN FOR HALOGENATED COMPOUNDS

Specificity for solute *i* eluted from the PFP phase relative to the isoeluotropic system with the phenylmethyl (Ph) phase was obtained using eqn. 4.

Solute	$k'/S_{BET_{PFP}} \times 10^3$ *[methanol–water (49:51)]*	$k'/S_{BET_{Ph}} \times 10^3$ *[methanol–water (55:45)]*	S_i
Bromobenzene	12.877	12.877	0.00
2-Chloroaniline	4.606	4.584	0.022
2,4-Dinitrochlorobenzene	7.224	9.275	−2.051
Chlorobenzene	11.829	10.913	0.916
1,4-Dichlorobenzene	17.377	17.244	0.133
1,3-Dichlorobenzene	18.216	17.462	0.754
Bromotoluene	19.052	20.736	−1.684
1,2-Dichlorobenzene	20.309	18.334	1.973
1,2,5-Trichlorbenzene	29.095	28.814	0.281
1,2,4-Trichlorobenzene	29.523	28.814	0.709

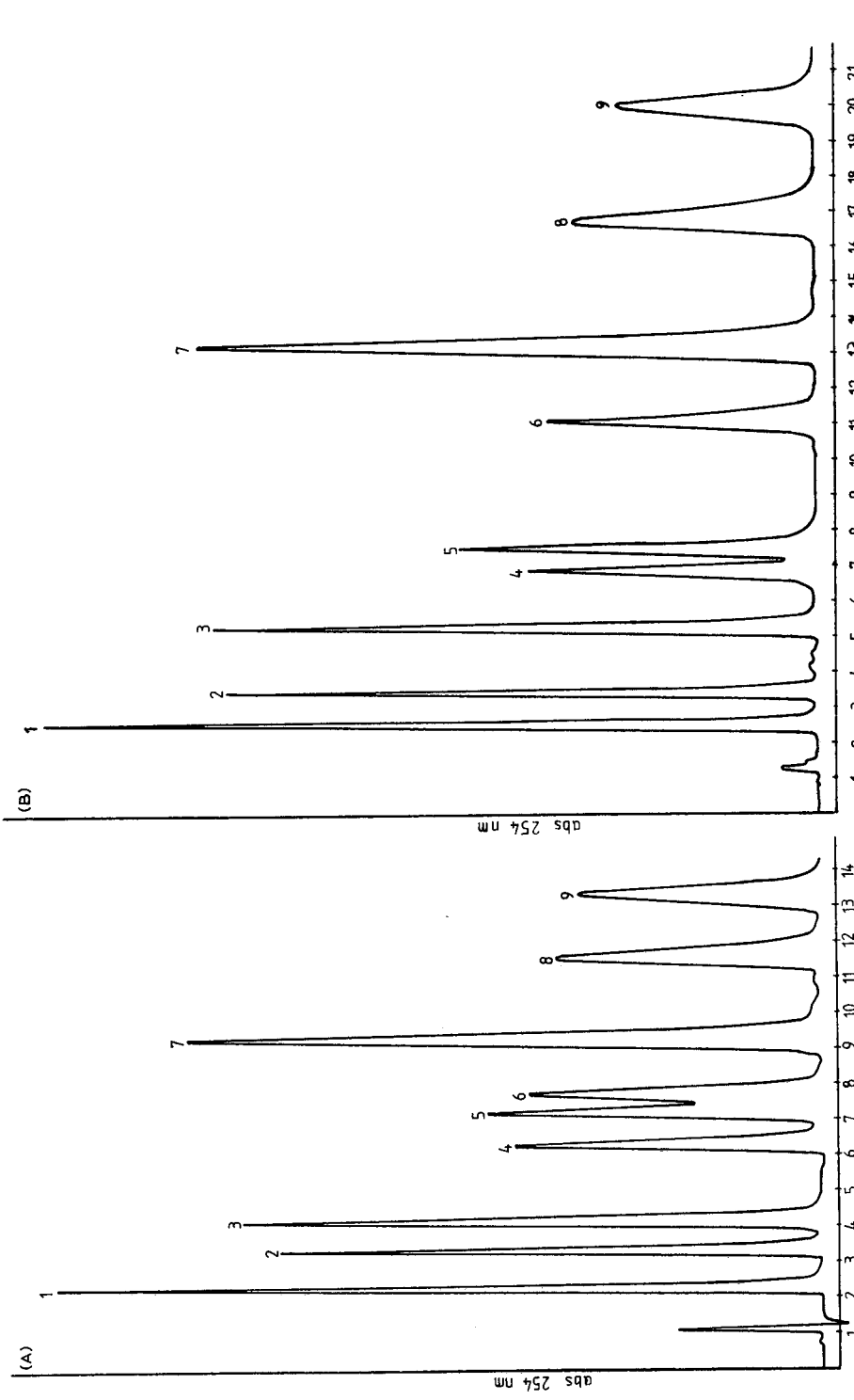

Fig. 1. (A) Separation of test solutes on phenylmethyl phase. Mobile phase, methanol–water (55:45, v/v); flow-rate, 1 ml/min; detection, UV (254 nm); temperature ambient. (B) Separation of test solutes on PFP phase. Conditions as in A, except mobile phase, methanol–water (49:51, v/v). Peaks: 1 = phenol; 2 = 2-chloroaniline; 3 = 2-amino-α,α,α-trifluorotoluene; 4 = chlorobenzene; 5 = bromobenzene; 6 = α,α,α-trifluorotoluene; 7 = 4-chloro-3-nitro-α,α,α-trifluorotoluene; 8 = 2-chloro-α,α,α-trifluorotoluene; 9 = 3-bromo-α,α,α-trifluorotoluene.

TABLE VI

SPECIFICITY OF THE PENTAFLUOROPHENYL COLUMN FOR POLAR COMPOUNDS

Specificity for solute *i* eluted from the PFP phase relative to the isoeluotropic system with the phenylmethyl (Ph) phase was obtained using eqn. 4.

Solute	$k'/S_{BET_{PFP}} \times 10^3$ *[methanol–water (49:51)]*	$k'/S_{BET_{Ph}} \times 10^3$ *[methanol–water (55:45)]*	S_i
Bromobenzene	12.877	12.877	0.000
p-Nitrophenol	1.570	2.182	−0.612
o-Nitrophenol	2.513	4.348	−1.835
o-Nitroamiline	2.827	3.054	−0.227
m-Nitroaniline	3.035	3.492	−0.457
p-Nitroaniline	4.291	5.019	−0.728
1,4-Dinitrobenzene	4.291	5.456	−1.65
1,2-Dinitrobenzene	5.967	8.731	−2.764
Nitrobenzene	6.909	7.203	−0.294
2,4-Dinitrofluorobenzene	7.013	9.603	−2.590
2,4-Dichlorobenzene	7.224	9.275	−2.051
Phenol	2.721	2.399	0.322
m-Cresol	4.397	3.709	0.688
Anisole	6.176	7.311	−1.135
1-Naphthol	7.746	8.293	−0.547
Aniline	2.198	2.182	0.016
2-Chloroaniline	4.606	4.584	0.022
Benzaldehyde	3.977	5.020	−1.043
Acetophenone	6.070	5.894	0.176

because this result is positive when the specific interaction between the solute and the PFP phase causes a specific retardation. The fluorinated solutes show a strong specific effect on the PFP phase (see Table IV), but the specificity is not limited to only these molecules. We observed specific interactions between the chlorinated compounds and the fluorinated phase (see Table V). It can be seen from Table IV that the PFP phase preferentally retains the fluoro-substituted solutes *vs.* the phenylmethyl phase. We guess that this is due to the "like prefers like" effect. Sadek and Carr[17] generally found stronger retardation of more polar, non-ionizable groups (NO_2, OH, etc.) (see Table VI) for nitro-substituted solutes, but for other groups our results are the same. A clear illustration of the specific effect occurring in the PFP system is provided by the chromatograms in Fig. 1.

Two chromatograms were obtained in an isoeluotropic system. The chromatogram in Fig. 1A corresponds to a methanol–water (55:45) mobile phase on the phenylmethyl column and Fig. 1B shows the elution of the same mixture of substances on the isoeluotropic PFP system with methanol–water (49:51) mobile phase. The solutes are numbered in order of appearance. It is evident that the PFP phase (B) is the better stationary phase for fluorinated ad chlorinated substances. The order of appearance of solutes did not change but the retention times in Fig. 1B are is longer than those in Fig. 1A. We observed a strong specific retardation for fluorinated and mild specificity for chlorinated compounds.

Stationary phase with a pentafluorophenyl functional group have been shown to have some merit such as increased retentivity and widely different selectivity for

halogenated substances *vs.* the phenylmethyl phase. It can be a good alternative to a phenyl phase, and the complementary use of such stationary phases with commercially available phases will increase the capability of RP-HPLC.

ACKNOWLEDGEMENTS

We are grateful to Dr. R. M. Cassidy for helpful discussions and revision of the manuscript, to Chemical Works of Budapest for the gift of different fluorinated solutes and to Mrs. É. Szakács and Miss Zs. Horváth for technical work.

REFERENCES

1 Cs. Horváth, W. Melander and I. Molnár, *J. Chromatogr.*, 125 (1976) 129.
2 N. Tanaka, H. Goodell and B. L. Karger, *J. Chromatogr.*, 158 (1978) 233.
3 R. M. McCormic and B. L. Karger, *J. Chromatogr.*, 199 (1980) 259.
4 E. Roggendorf and R. Spatz, *J. Chromatogr.*, 204 (1981) 263.
5 T. A. Mourey and S. Siggia, *Anal. Chem.*, 51 (1979) 763.
6 E. S. Kikta and E. Grushka, *J. Chromatogr.*, 135 (1977) 367.
7 C. S. Little, A. D. Dale and M. E. Evans, *J. Chromatogr.*, 153 (1978) 543.
8 J. Chmielowiec, *J. Chromatogr. Sci.*, 19 (1981) 269.
9 N. Tanaka,Y. Tokuda, K. Iwaguchi and M. Araki, *J. Chromatogr.*, 239 (1982) 761.
10 P. W. Armstrong and W. Demoud, *J. Chromatogr. Sci.*, 22 (1984) 411.
11 H. A. H. Billiet, P. J. Schoenmakers and L. de Galan, *J. Chromatogr.*, 218 (1981) 443.
12 G. E. Berendsen, K. A. Pikaart, C. Olieman and L. de Galan, *Anal. Chem.*, 52 (1980) 1990.
13 A. Haas, J. Köhler and H. Hemetsberger, *Chromatographia*, 14 (1981) 341.
14 F. M. Rabee and E. T. Butts, *LC, Mag. Liq. Chromatogr. HPLC*, 1 (1983) 42.
15 W. Ecknig, B. Trugg, R. Radeglia and U. Gross, *Chromatographia*, 16 (1982) 178.
16 W. Ecknig, K. Metzner, I. Nehls and Z. Stanke, *J. Chromatogr.*, 204 (1981) 29.
17 P. C. Sadek and P. W. Carr, *J. Chromatogr.*, 288 (1984) 25.
18 K. K. Unger, *Porous Silica (Journal of Chromatography Library*, Vol. 16), Elsevier, Amsterdam, 1979, p. 120.
19 C. Fulche, M. A. Cromwell, R. Baylics, K. B. Holland and J. R. Jerozek, *Anal. Chim. Acta*, 129 (1981) 29.
20 P. J. Schoenmakers, H. A. H. Billiet and L. de Galan, *J. Chromatogr.*, 185 (1979) 179.
21 K. K. Unger, N. Becker and P. Roumeliotis, *J. Chromatogr.*, 125 (1976) 115.
22 B. W. Sands, Y. S. Kim and I. L. Bass, *J. Chromatogr.*, 360 (1986) 353.
23 Z. Suprynowicz, J. Rayss, A. L. Dawidowicz and R. Lodkowski, *Chromatographia*, 20 (1985) 677.

Journal of Chromatography, 511 (1990) 89–95
Elsevier Science Publishers B.V., Amsterdam

CHROM. 22 400

Characteristics of ovomucoid-conjugated columns in the direct liquid chromatographic resolution of racemic compounds

TOSHINOBU MIWA*, HIROFUMI KURODA and SHIGERU SAKASHITA
Eisai Co., Ltd., Pharmaceutical Research Laboratory, Takehaya machi 1-chome, Kawashima cho, Hashima gun, Gifu 501-61 (Japan)
and
NAOKI ASAKAWA and YASUO MIYAKE
Eisai Co., Ltd., 4th Research Department, 1-3, Tokodai 5-chome, Tsukuba-shi, Ibaragi 300-26 (Japan)
(First received November 29th, 1989; revised manuscript received February 20th, 1990)

ABSTRACT

The chiral recognition properties of ovomucoid-conjugated columns were investigated. Trypsin slightly affected the chiral recognition characteristics of the column. Neuraminidase treatment of ovomucoid columns altered their acidic solute retention properties. Deglycosylated ovomucoid-conjugated columns dit not resolve racemic chlorpheniramine or ketoprofen. A sugar chain is essential for the exibition of chiral recognition ability for ovomucoid.

INTRODUCTION

Recent studies on liquid chromatographic chiral resolution showed that the unique characteristics of chromatography using protein-bonded stationary phases make it a useful analytical method[1]. These columns have been employed for the chiral resolution of a large number of compounds, almost all of which have pharmaceutical importance[1]. The chiral resolution mechanism of proteins is still not clear, although some apparent mechanisms involving racemic solutes and low-molecular-weight ligand-conjugated columns have been proposed[2].

Interest has been shown in the contribution of the physiologically important binding part of proteins to chiral resolution. Albumin [bovine serum albumin (BSA)]-conjugated column[3] and α1-acid glycoprotein columns[4] were developed on the basis of the idea that those serum proteins which take part in enantioselective drug transport *in vivo* must also have a chiral recognition capacity in their immobilized state. However, interacting sites capable of participating in the three-point-holding mechanism of chiral recognition[2] are abundant in large protein molecules, together with a few physiologically active sites. From this point of view, it could be said that almost

0021-9673/90/$03.50

all proteins could be enantioseparators, so that more efforts should be made to find proteins with the property of chiral recognition. We have already reported that egg-white avidin, well known as a biotin acceptor, is capable of chiral recognition of acidic compounds[5]. The chiral resolution capacity of the avidin-conjugated column was strongly affected by biotin, the physiological ligand of the protein. This result strongly suggests that the chiral resolution capacity of a protein is closely related to its physiological effect.

Ovomucoid, which is characterized by a high sugar content and trypsin inhibition, has been used as an enantioselective ligand[1]. The objective of this study was to elucidate the relationship between the physiological effect and the enantioselectivity of ovomucoid. We investigated the chiral recognition properties of ovomucoid-conjugated columns treated with trypsin or neuraminidase, and also prepared a deglycosylated ovomucoid-conjugated column to elucidate the absence of enantioselective activity.

EXPERIMENTAL

Apparatus

A Shimadzu LC-6A pump equipped with an SPD-6A variable-wavelength UV monitor and an SCL-6A automatic sample injector was used. The ovomucoid-conjugated columns used is commercially available as Ultron ES-OVM from Shinwa Kako (Kyoto, Japan). We also prepared an ovomucoid-conjugated column as reported previously[6].

Chemicals

Ketoprofen, *m*-$(C_6H_5CO)C_6H_4CH(CH_3)COOH$, from Nihon Bulk Yakuhin (Osaka, Japan) and chlorpheniramine maleate from Kowa (Nagoya, Japan) were used. Trypsin (type III) and neuraminidase (type X) were purchased from Sigma (St. Louis, MO, U.S.A.). Trifluoromethanesulphonic acid (TFMS) was obtained from Wako (Osaka, Japan). All other chemicals were of analytical-reagent grade or higher quality.

The buffer used in all instances was 20 m*M* potassium phosphate buffer.

Adsorption of trypsin to Ultron ES-OVM and elimination of trypsin from the column.

Trypsin (300 mg) was suspended in 100 ml of the buffer (pH 6.0) at 4°C. This suspension was stored overnight at 4°C, then centrifuged at 3000 *g* for 10 min. The total absorbance of the supernatant was 380 at 280 nm. This solution was passed through an Ultron ES-OVM column (150 mm × 4.6 mm I.D.) at 4°C at a flow-rate of 0.6 ml/min, then the column was washed with the buffer (pH 6.0). The total absorbance recovered in the eluate was 312. The adsorbed trypsin was eluted with a solution of 0.25 *M* sodium chloride in the buffer (pH 6.0).

Enzymatic modification of the ovomucoid-conjugated column by neuraminidase

Ten units of neuraminidase were dissolved in the buffer (pH 5.5) and the resulting solution was recycled at 30°C in the ovomucoid-conjugated column (150 mm × 4.6 mm I.D.) for 4.5 h at a flow-rate of 0.9 ml/min. The recycled solution was passed through an Amicon YM5 filter and sialic acid was determined spectrophotometrically using resorcinol[7].

Chemical deglycosylation of ovomucoid and preparation of deglycosylated ovomucoid-conjugated column

Chemical deglycosylation was performed according to the method of Edge *et al.*[8]. This method was also applied with ovomucoid by Gu *et al.*[9]. Briefly, 12.5 ml of anisole and 25 ml of trifluoromethanesulphonic acid were mixed and cooled to 0°C in ice. Ovomucoid (1 g) was dissolved in the mixture and nitrogen was bubbled into the solution for 2 h with magnetic stirring at 0°C. The reaction mixture was diluted with 75 ml of diethyl ether cooled to −40°C, then 120 ml of ice-cold 50% aqueous pyridine were added. The aqueous phase was washed with diethyl ether, dialysed against water and lyophilized.

Sodium dodecylsulphate–polyacrylamide gel electrophoresis (SDS-PAGE) was performed in 15% acrylamide gel.

The conjugation of deglycosylated ovomucoid to silica gel was performed in the same way as native ovomucoid conjugation[6].

RESULTS

A chromatogram of chlorpheniramine maleate on the Ultron-ES OVM (OVM column) is shown in Fig. 1. The trypsin-adsorbed OVM (Try-OVM) column still exhibited chiral recognition of chlorpheniramine, although its retention capacity decreased markedly (Fig. 2). Desorption of trypsin from the column was performed with 0.25 *M* sodium chloride in the buffer (pH 6.0). The trypsin-desorbed OVM (dTry-OVM) column showed the same retention and separation for chlorpheniramine enantiomers as the OVM column.

The neuraminidase treatment liberated 0.48 mg of sialic acid. The enzyme-treated (NT-OVM) column and the OVM column showed the same retention and

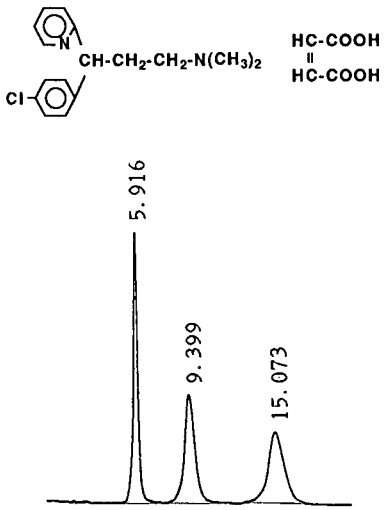

Fig. 1. Chromatogram of chlorpheniramine maleate on the Ultron ES-OVM column. Mobile phase, 20 m*M* potassium phosphate (pH 6.2) containing 12% ethanol; flow-rate, 1.2 ml/min. The elution order is maleic acid, (+)-chlorpheniramine and (−)-chlorpheniramine. Number at peaks indicate retention times in min.

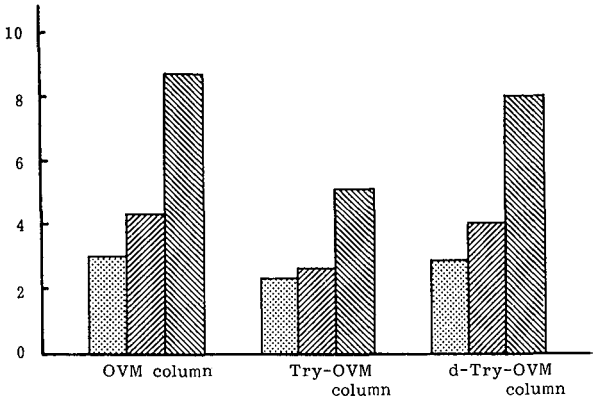

Fig. 2. Retention profile change in the ovomuocid-conjugated (OVM) column by trypsin adsorption. Chlorpheniramine maleate was chromatographed on an OVM columns, a trypsin-adsorbed OVM (Try-OVM) column and the same column trypsin-desorbed (dTry-OVM column). Boxes: left, maleic acid; centre, (+)-chlorpheniramine; right, (−)-chlorpheniramine. The ordinate shows the capacity factor.

separation of racemic chlorpheniramine (Fig. 3); on the other hand, the capacity factor of maleic acid on the NT-OVM column was reduced to 80% of that on the OVM column. Racemic ketoprofen was still resolved by the NT-OVM column, showing two thirds of the capacity factors of the OVM column (Fig. 4).

Chemically deglycosylated ovomucoid migrated faster than native ovomucoid in SDS-PAGE, as shown in Fig. 5. This result coincides with that of Gu *et al.*[9] Deglycosylated ovomucoid was conjugated to succinimide-activated aminopropylsilica gel, which had also been used for the immobilization of native ovomucoid. The effects of the mobile phase pH on the retention of solutes on the deglycosylated ovomucoid-conjugated (dG-OVM) column are shown in Table I. The dG-OVM column did not show chiral recognition of chlorpheniramine and ketoprofen. Chlorpheniramine was strongly retained on the dG-OVM column concurrently with a decrease in the mobile phase pH; this behaviour was the opposite of that of the OVM column.

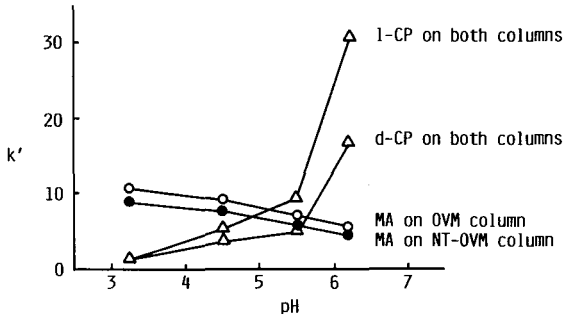

Fig. 3. pH–retention profiles for maleic acid (MA) and (±)-chlorpheniramine (CP) on ovomucoid-conjugated (OVM) column and neuraminidase-treated ovomucoid (NT-OVM) column). ○ = Maleic acid on OVM column; ● = maleic acid on NT-OVM column, △ = chlorpheniramine on OVM and NT-OVM columns. Mobile phase, 20 m*M* potassium phosphate containing 10% ethanol; column temperature, 25°C.

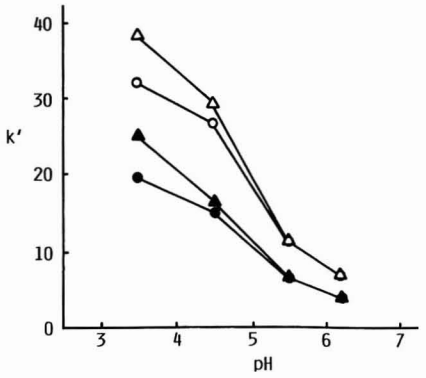

Fig. 4. Influence of pH on the retention of ketoprofen (KP) enantiomers. ○,△ = Ketoprofen enantiomers on ovomucoid-conjugated (OVM) column; ●,▲ = ketoprofen enantiomers on neuraminidase-treated ovomucoid (NT-OVM) column. Mobile phase, 20 m*M* potassium phosphate containing 12% ethanol; column temperature, 25°C.

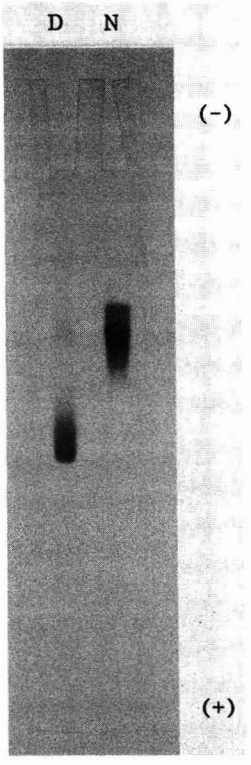

Fig. 5. SDS-PAGE of native ovomucoid (N) and deglycosylated ovomucoid (D). Acrylamide concentration, 15%.

TABLE I

EFFECTS OF pH ON THE RETENTION (k') OF CHLORPHENIRAMINE MALEATE AND KETOPROFEN ON DEGLYCOSYLATED OVOMUCOID-CONJUGATED COLUMN

Racemic resolution of chlorpheniramine and ketoprofen was not achieved. Mobile phase, 20 m*M* potassium phosphate containing 10% ethanol; column temperature, 25°C.

pH	k'		
	Maleic acid	*Chlorpheniramine*	*Ketoprofen*
3.5	0.439	7.23	9.09
4.5	0.602	6.01	12.6
5.5	1.17	4.65	6.80
6.2	1.97	3.66	4.40

The highest capacity for ketoprofen was observed at pH 4.5, but the OVM column retained the compound more strongly at lower pH.

DISCUSSION

Chicken ovomucoid is a triplicate imprinting polymer of a Kazal-type inhibitor, although 1 mol of it inhibits 1 mol of trypsin.[10] Molecular biological studies have shown that ovomucoid is composed of three tandem homologous domains.[11] The trypsin-binding site is located in the second domain, and the proteinase inhibition effects of the first and third domains are almost zero.[11] The objective of this study was to elucidate the chiral recognition properties of proteins, as this may lead to the discovery of new chiral resolution columns. The abundant data on physiological and molecular biological aspects of ovomucoid suggests that this protein could be a suitable material for investigating the chiral recognition properties of proteins.

The chiral recognition of the column was not influenced by trypsin, as Fig. 2 shows. The separation factor (k' ratio) of (±)-chlorpheniramine on this column was not changed by trypsin adsorption. This result suggests that the trypsin-inhibiting site of ovomucoid Arg89–Ala located in domain II was almost unrelated to the differentiation of chlorpheniramine enantiomers. However, the decrease in the capacity factor (k') of solutes on the trypsin-adsorbed column demonstrates that bound ligands could interfere with achiral protein–solute interactions. There are major differences between avidin-conjugated columns and OVM columns regarding the effects of ligands. The chiral resolution ability of the avidin column was eliminated by biotin[5]. The difference between the two columns may be attributed to the K_a values: that for ovomucoid-trypsin is *ca.* $1 \cdot 10^{10}$ l/mol and that of avidin–biotins, $1 \cdot 10^{15}$ l/mol. However, a more important cause of the difference is the conformational change of the proteins, including the sugar chain. We consider that biotin–avidin interaction results in a conformational change, whereas trypsin–ovomucoid interactions does not.

The effect of neuraminidase, which eliminates sialic acid, is interesting. In this experiment, the conjugated ovomucoid was treated with neuraminidase and the chromatographic parameters of maleic acid, ketoprofen and chlorpheniramine were in-

vestigated. The NT-OVM column showed a lower retention of the acidic solutes than the OVM column, although the capacity factor and chiral separation of amines was not affected at all. The chiral resolution of ketoprofen also was not changed. These results imply that the sialic acid of ovomucoid participates in a non-specific retention of acidic solutes. We believe from the results of this experiment that columns with interesting characteristics could be developed even for protein bonded phases by some modification procedure.

Chemical deglycosylation of ovomucoid through TFMS treatment did not alter its trypsin inhibition effect[9], which shows the constancy of its active centre during this treatment. The disappearance of the chiral recognition ability of the dG-OVM column (Table I) indicates that the enantioselectivity of proteins is not attributable to their physiological effect, as we have discussed in relation to the action of trypsin. The pH-retention property of the dG-OVM column for chlorpheniramine and maleic acid was opposite to that of the native OVM column. The dG-OVM column behaves like a counter-ion-exchange column for the above two compounds in the pH range in which these solutes are dissociated. The pH–k' relationship of ketoprofen on the dG-OVM column also suggests the above-mentioned characteristics of the column. The strong hydrophobic interaction which was observed in the OVM column against ketoprofen (Fig. 4) was not recognized in the dG-OVM column. It is clear that the sugar chain of ovomucoid is essential for its enantiospecific interaction with solutes.

REFERENCES

1 S. Allenmark, in A. M. Krstulovic (Editor), *Chiral Separation by HPLC,* Wiley, New York, 1988, p. 285.
2 W. H. Pirkle, T. C. Pochapsky, G. S. Mahler and P. E. Field, *J. Chromatogr.*, 348 (1985) 89.
3 S. Allenmark, B. Bomgren and H. Boren, *J. Chromatogr.*, 264 (1983) 63.
4 J. Hermansson, *J. Chromatogr.*, 269 (1983) 71.
5 T. Miwa, T. Miyakawa and Y. Miyake, *J. Chromatogr.*, 457 (1988) 227.
6 T. Miwa, M. Ichikawa, M. Tsuno, T. Hattori, T. Miyakawa and Y. Miyake, *Chem. Pharm. Bull.*, 35 (1987) 682.
7 L. Svennerholm, *Biochim. Biophys. Acta,* 24 (1957) 604.
8 A. S. B. Edge, C. R. Faltytnek, L. Hof, L. E. Reichert, Jr., and P. Weber, *Anal. Biochem.*, 118 (1981) 131.
9 J. Gu, T. Matsuda, R. Nakamura, H. Ishiguro, I. Ohkubo, M. Sasaki and N. Takahashi, *J. Biochem.*, 106 (1989) 66.
10 M. B. Rhodes, M. Bennett and R. E. Feeney, *J. Biol. Chem.*, 235 (1960) 1686.
11 I. Kato, J. Schrode, W. J. Kohr and M. Laskowski, Jr., *Biochemistry,* 26 (1987) 193.

Journal of Chromatography, 511 (1990) 97–107
Elsevier Science Publishers B.V., Amsterdam

CHROM. 22 398

Analytical and preparative resolution of enantiomers of prostaglandin precursors and prostaglandins by liquid chromatography on derivatized cellulose chiral stationary phases

LARRY MILLER* and CARA WEYKER
Chemical Development Department, G.D. Searle & Co., 4901 Searle Parkway, Skokie, IL 60077 (U.S.A.)
(First received December 5th, 1989; revised manuscript received February 9th, 1990)

ABSTRACT

Analytical methods were developed for the separation of the enantiomers of four cyclopentenone precursors of prostaglandins. The resolution obtained is correlated with the chemical environment around the chiral center of the cyclopentenones. The analytical methods were scaled up to preparative loadings and the chromatographic parameters were varied to determine their effect on the preparative separations. The correlation between analytical resolution and preparative resolution was also investigated. In addition to the precursors, the preparative resolution of the enantiomers of a synthetic prostaglandin analogue was investigated.

INTRODUCTION

Cyclopentenones are important intermediates for numerous natural products including prostaglandins[1,2]. They contain one or more chiral carbon(s) and can exist as enantiomers. There are two approaches to obtaining enantiomerically pure chemicals. These are (1) asymmetric synthesis of the desired isomer and (2) resolution of a racemic mixture into individual isomers. Various synthetic methods to produce optically pure cyclopentenones have been developed[3–5]. Methods for the resolution of a racemic mixture include recrystallization of diastereomeric salts, formation of diastereomeric derivatives followed by chromatographic resolution on an achiral stationary phase, or direct chromatographic resolution of enantiomers using a chiral stationary phase or a chiral mobile phase additive. Only a limited amount of work using liquid chromatography for the resolution of prostaglandins and their precursors has been published[6,7]. Direct resolution of the enantiomers of a prostaglandin and it's precursors using liquid chromatography on a chiral stationary phase was attempted at both analytical and preparative loadings.

Enisoprost (Fig. 1) is an E_1 type prostaglandin analogue. It was first synthesized in 1979 in the medicinal chemistry laboratories of G. D. Searle & Co. The present

0021-9673/90/$03.50

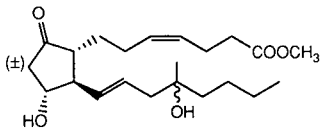

Fig. 1. Structure of enisoprost.

synthesis of enisoprost results in the formation of four isomers (Fig. 2). Since the 11*R*,16*S*-isomer was needed for testing purposes, an attempt was made to synthesize this isomer. Enisoprost is produced by coupling the β side chain to the cyclopentenone containing the α side chain (Fig. 3)[8]. Enisoprost can be derived from any of four different cyclopentenone derivatives (Fig. 4)[9]. An asymmetric synthesis of the beta side chain was easily developed[10]. The asymmetric synthesis of the cyclopentenone was significantly more difficult and time consuming, therefore preparative liquid chromatography was investigated to isolate the desired enantiomer from a racemic mixture.

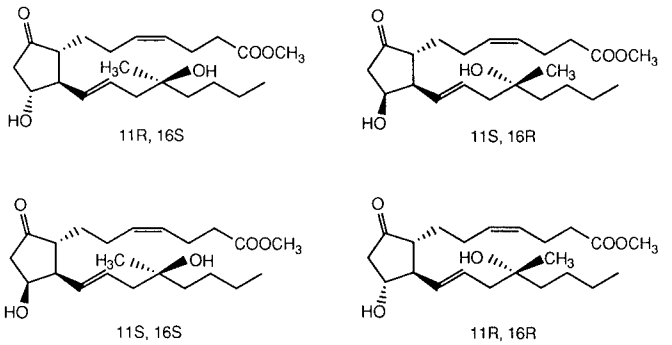

Fig. 2. Structures of four isomers of enisoprost.

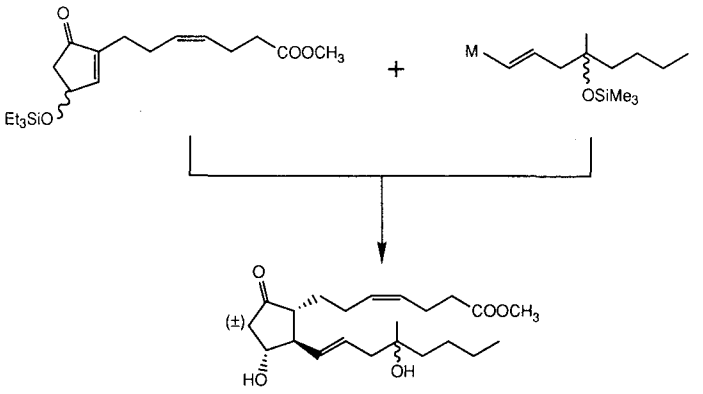

Fig. 3. Synthesis of enisoprost. Et = Ethyl; Me = methyl.

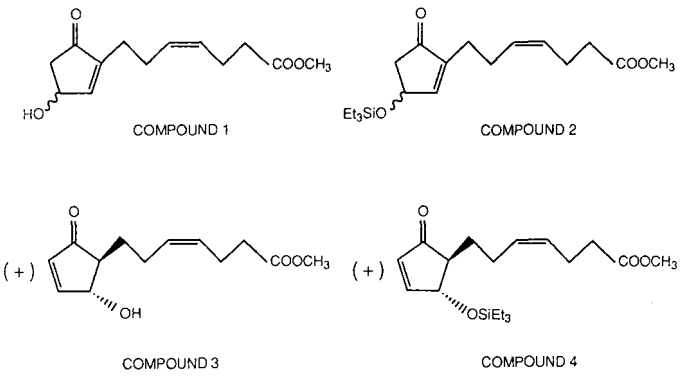

Fig. 4. Structures of four cyclopentenone precursors, compounds **1–4**.

In this paper we will report on the use of liquid chromatography for the enantiomeric resolution of cyclopentenone derivatives and a prostaglandin analogue. Analytical high-performance liquid chromatography (HPLC) methods were developed using derivatized cellulose stationary phases. In addition, the preparative resolution of these compounds will be discussed.

EXPERIMENTAL

Materials

The chiral stationary phases used for these studies were obtained from Daicel (Tokyo, Japan) through J. T. Baker (Phillipsburgh, NJ, U.S.A.) as prepacked analytical (250 × 4.6 mm I.D.) and preparative columns (500 × 10 mm I.D. and 500 × 20 mm I.D.). The prostaglandin precursors were synthesized in the Chemical Development or Preclinical Research laboratories of G. D. Searle & Co. (Skokie, IL, U.S.A.). The solvents were reagent grade or better and obtained from a variety of sources.

Equipment

The analytical chromatograph consisted of a Waters Assoc. (Milford, MA, U.S.A.) Model 590 solvent-delivery system and a U6K injector or Waters intelligent sample processor, a Kratos (Ramsey, NJ, U.S.A.) Model 783 variable-wavelength detector, a Linear (Hackensack, NJ, U.S.A.) Model 585 recorder and a Digital (Equipment Corp.) VAX 11/785 computer with Searle chromatography data system.

The preparative chromatograph consisted of two Beckman (Berkeley, CA, U.S.A.) Model 101 pumps with preparative heads, a Model 165 variable-wavelength detector with a 5-mm semi-preparative flow-cell, a Model 450 data system/controller and a Kipp & Zonen (Delft, The Netherlands) Model BD41 two-channel recorder. A Rheodyne (Cotati, CA, U.S.A.) Model 7125 syringe loading sample injector equipped with a 10-ml loop (Valco, Houston, TX, U.S.A.) was used. The column effluent was fractionated using a Gilson (Middleton, WI, U.S.A.) Model FC220 fraction collector.

RESULTS AND DISCUSSION

Analytical HPLC

Analytical HPLC methods for the enantiomer separation of the four cyclopentenones shown in Fig. 4 were developed using a Chiralcel OC column. Chiralcel OC (Fig. 5) is a phenylcarbamate derivative of cellulose which is adsorbed on silica gel. Cellulose-based phases have mobile phase restrictions since certain solvents can dissolve the cellulose. The manufacturer of these columns recommends the use of alkanes with low percentages (<40%) of alcohols as polar modifiers. The analytical HPLC separations for compounds **1–4** are shown in Fig. 6. Table I summarizes the

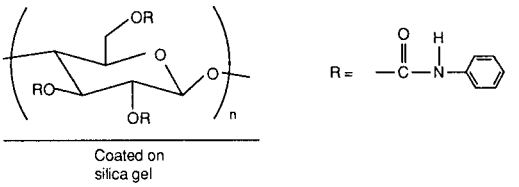

Fig. 5. Structure of Chiralcel OC packing.

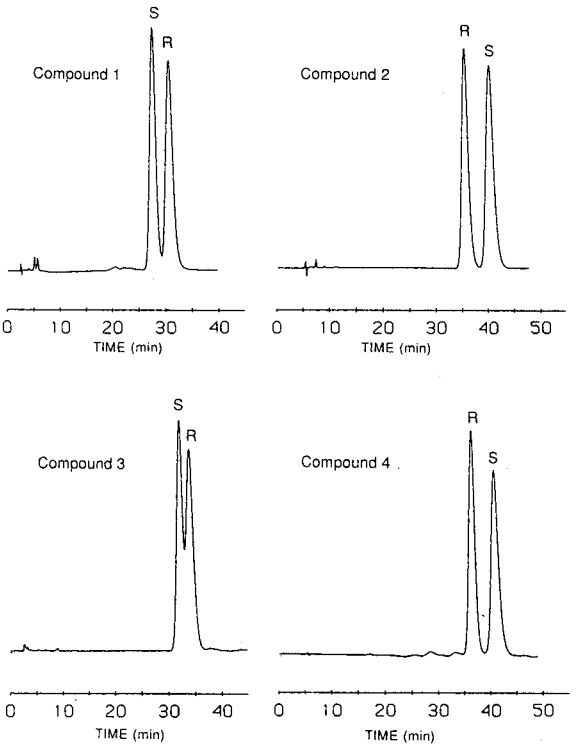

Fig. 6. Analytical HPLC separation of compounds **1–4**. Analysis conducted on Chiralcel OC column (250 × 4.6 mm I.D.), detection at 215 nm, 0.1 a.u.f.s. Mobile phase, flow-rate: compound **1**, hexane–isopropanol (85:15, v/v), 1.0 ml/min; compound **2** and **4**, hexane–isopropanol (99:1, v/v), 0.5 ml/min; compound **3**, hexane–isopropanol (90:10, v/v), 1.0 ml/min.

TABLE I

VALUES FOR ANALYTICAL SEPARATION OF ENANTIOMERS FOR COMPOUNDS **1–4**

See Fig. 6 for HPLC conditions.

Compound	k'_1 [a]	k'_2 [b]	α	R_s
1	9.65	10.82	1.12	1.3
2	5.47	6.33	1.16	1.9
3	11.35	12.06	1.06	0.7
4	5.64	6.43	1.14	1.7

[a] Capacity factor for first-eluting enantiomer.
[b] Capacity factor for second-eluting enantiomer.

capacity factors (k'), separation factor (α), and resolution (R_s) for the enantiomer separation of these four compounds.

Further analytical method development was done using compound **2**. Using a Chiralcel OC column, mobile phases of hexane with various alcohols were investigated. The percentage of alcohol present in the mobile phase was varied such that the capacity factors remained approximately constant. The results of these experiments are summarized in Table II. These data show that various straight chain alcohols have no significant effect on resolution. Branched alcohols gave reduced resolution compared to their straight chain analogues.

Different types of derivatized cellulose packings were investigated for the separation of the enantiomers of compound **2**. The derivatized cellulose packings used are shown in Fig. 7. Results are summarized in Table III. These results show that Chiralcel OC packing gave the largest resolution for compound **2**.

Chiral separations occur in liquid chromatography through the formation of diastereomeric complexes between the solute and the chiral stationary phase. With cellulose-based chiral phases these complexes are formed through attractive interactions such as hydrogen bonding, π–π and dipole interactions. One major difference with cellulose-based phases is that the chiral discriminator is located in the cavities or

TABLE II

EFFECT OF POLAR MODIFIER ON ANALYTICAL SEPARATION OF ENANTIOMERS OF COMPOUND **2**

HPLC conditions: Chiralcel OC (250 × 4.6 mm I.D.); flow-rate, 0.5 ml/min; non-polar solvent, hexane; detection, 215 nm, 0.2 a.u.f.s.

Polar modifier (%)	k'_1 [a]	k'_2 [b]	α	R_s
Ethanol (0.4)	6.01	7.13	1.19	2.3
n-Propanol (0.65)	5.79	6.85	1.18	2.1
n-Butanol (1.0)	5.08	6.07	1.19	2.2
Isopropanol (1.0)	5.47	6.33	1.16	1.9
tert.-Butanol	5.67	6.52	1.15	1.5

[a] Capacity factor for first-eluting enantiomer.
[b] Capacity factor for second-eluting enantiomer.

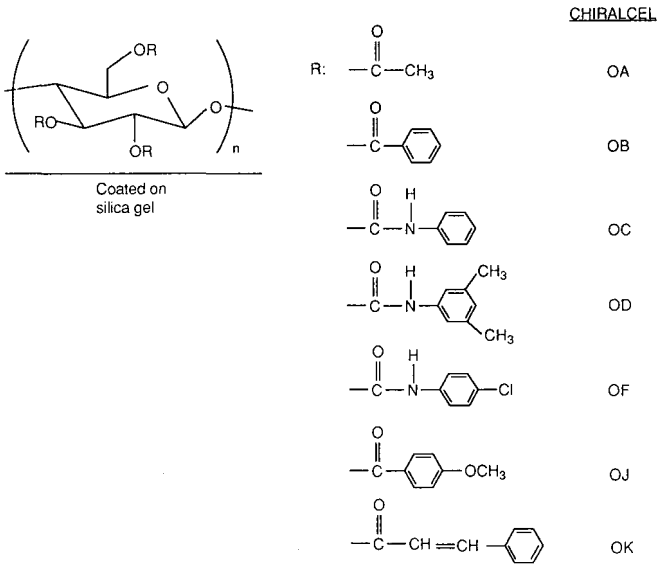

Fig. 7. Structures of various Chiralcel packings.

ravines of the cellulose[11]. In an attempt to understand the chiral mechanism, the effect of differing silyl protecting groups on the separation of the enantiomers of compound **2** was investigated. The protecting groups and the results obtained are summarized in Table IV. The distances for the protecting group are measured from the ether oxygen to the outermost hydrogen. For non-spherical protecting groups, two distances are given. Volume measurements use the outermost distance as the diameter of the protecting group. These data indicate that the bulky diphenyl methyl protecting group causes loss of chiral discrimination. This appears related to the inability of this compound to enter into the cavity of the cellulose and interact with the chiral

TABLE III

EFFECT OF CHIRAL STATIONARY PHASE ON ANALYTICAL SEPARATION OF ENANTIOMERS OF COMPOUND **2**

HPLC conditions: mobile phase, hexane–isopropanol (99:1, v/v); flow-rate, 0.5 ml/min; detection, 215 nm, 0.2 a.u.f.s.

Chiralcel packing	k'_1[a]	k'_2[b]	α	R_s
OA	1.57	1.57	1	0
OB	3.34	4.10	1.20	0.6
OC	5.47	6.33	1.16	1.9
OD	3.20	3.70	1.16	1.6
OF	>10	>10	–	–
OJ	2.78	2.99	1.08	0.8
OK	4.82	5.35	1.11	0.8

[a] Capacity factor for first eluting enantiomer.
[b] Capacity factor for second eluting enantiomer.

TABLE IV

EFFECT OF PROTECTING GROUP ON ANALYTICAL SEPARATION OF ENANTIOMERS OF COMPOUND **2**

HPLC conditions: Chiralcel OC (250 × 4.6 mm I.D.); mobile phase, hexane–isopropanol (99:1, v/v), flow-rate, 0.5 ml/min; detection 215 nm, 0.2 a.u.f.s.

Protecting group	*Distance (Å)*[b]	*Volume (Å³)*[c]	k'_1[d]	k'_2[e]	α	R_s
$(C_6H_5)_2CH_3Si$–[a]	2.5, 5.8	202.3	6.8	6.8	1.0	0
$((CH_3)_2CH)_3Si$–	3.1	193.1	4.2	4.8	1.14	1.4
$(CH_3)_2[(CH_3)_3C]Si$–	2.5, 3.9	142.9	3.4	4.0	1.18	1.7
$(CH_3CH_2)_3Si$–	3.9	144.2	5.5	6.3	1.16	1.9

[a] Flow-rate 1.0 ml/min.
[b] Distance to outer hydrogen(s).
[c] Volume for protecting group measured using distance to outermost hydrogen as diameter.
[d] Capacity factor for first eluting enantiomer.
[e] Capacity factor for second eluting enantiomer.

discriminator. Similar results using 4-hydroxy-2-cyclopentenone derivatives have been previously reported[12].

Preparative HPLC

When developing an analytical method for scale-up to preparative, it is desirable to have an analytical resolution greater than 2 and a k' for the desired compound of less than 5. Table I shows that for compounds **1–4**, the resolution was between 0.7 and 1.9 and the k' ranged from 5.6 to 12.1. A k' of less than 5 is desired because of shorter run times and a corresponding increase in the throughput (g/h of pure chemical) for the purification.

Column eluent was monitored with a UV detector. The increased sample load either reduced or destroyed altogether the separation seen on the preparative chromatogram. Because of this, individual fractions were analyzed using analytical HPLC to determine enantiomeric content. A plot of enantiomer content *versus* fraction number is shown in Fig. 8.

To determine the feasibility of isolating gram quantities of chiral cyclopentenone the analytical separations reported in Fig. 6 were scaled up to preparative loadings. A 500 × 10 mm I.D. column containing approximately 25 g of stationary phase was used for preparative method development. This is approximately a nine-fold increase in column volume compared to the analytical column. A direct scale-up of the analytical methods would allow an injection of only 0.2 mg of a racemic mixture. This sample size was much too small to produce the required amount of chemical. Experiments were undertaken to determine the effect of increasing sample size on the separation. Column loadings of 1, 2 and 4 mg sample per gram of packing were investigated. Preparative loadings greater than 4 mg sample per gram packing were not investigated due to the small degree of separation seen analytically and the need to keep the isolated yields as high as possible. Loadings less than 1 mg sample per gram of packing were not investigated since they would be inefficient to purify gram quantities of material.

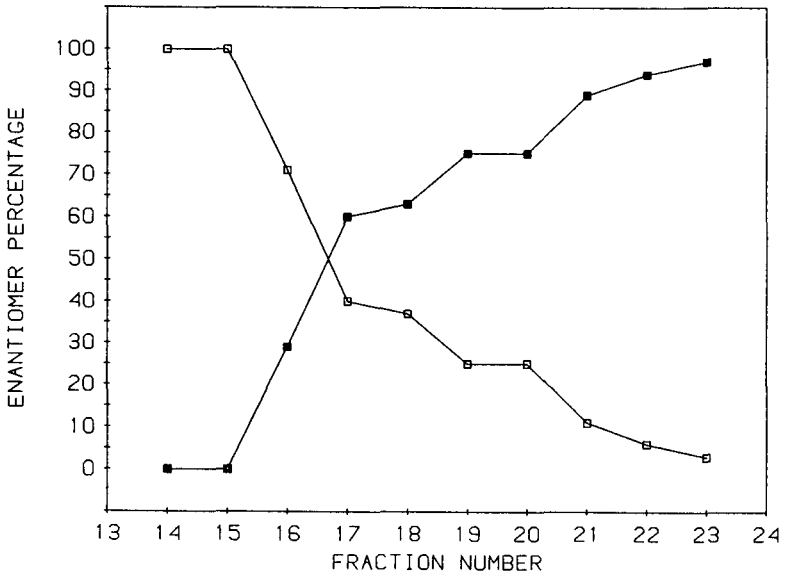

Fig. 8. Enantiomeric purity of individual fractions collected from preparative purification of compound **4**. Purification conducted on Chiralcel OC (500 × 10 mm I.D.) containing approximately 25 g of packing. Loading of 2 mg sample per gram of packing, a mobile phase of hexane–isopropanol (99:1, v/v) and a flow-rate of 4 ml/min was used. Each fraction contains 8 ml. Purification yielded 30% of available first enantiomer (>99.5%) and no second-eluting enantiomer. □ = *R*-enantiomer; ■ = *S*-enantiomer.

From these preparative loading experiments it was determined that the first eluting enantiomer could be isolated pure for three of the four compounds. The compound which showed no separation preparatively, compound **3**, also exhibited the poorest resolution in the analytical HPLC method. The results of these experiments are summarized in Table V. These data show that as loading increases, the amount of first enantiomer produced per hour increases even though the percentage of enantiomer isolated decreases. This results in a method with greater throughput. This is just one of the many trade-offs that must be negotiated when developing an efficient preparative liquid chromatographic method. Another benefit of a larger sample size is that the sample is more concentrated in the column eluent and therefore less solvent needs to be removed to recover the product.

Preparative method development showed that no significant amount of second eluting enantiomer could be isolated at any of the column loadings attempted. In order to isolate the second eluting enantiomer a series of purifications was needed. Each purification would remove a portion of the first eluting enantiomer. The overlap material from each purification, which was enriched in the second eluting enantiomer, would then be repurified to remove additional first eluting enantiomer. This process would be repeated until second eluting enantiomer of sufficient purity was obtained. This approach was used to isolate the second eluting enantiomer of compound **2**. One gram of a racemic mixture was originally chromatographed through multiple injections on a Chiralcel OC column (500 × 20 mm I.D.). From the first purification 270 mg of first-eluting enantiomer were obtained. The fractions containing the

TABLE V

RESULTS OF PREPARATIVE EXPERIMENTS FOR COMPOUNDS 1–4

HPLC conditions: Chiralcel OC (500 × 10 mm I.D.) containing approximately 25 g of packing; flow-rate, 4 ml/min for compounds **2** and **4**, 8 ml/min for compounds **1** and **3**.

Compound	*Mobile phase (hexane–isopropanol)*	*Loading (mg/g)*	*First eluting enantiomer*[a]		
			Percent[b] *isolated*	*mg per injection*	*mg per hour*
1	85:15	1	63	7.9	15.8
	85:15	2	35	8.9	17.8
	85:15	4	18	9.6	19.2
1	90:10	1	56	7.0	14.0
	90:10	2	39	9.8	19.6
	90:10	4	34	17.0	34.0
2	99:1	1	35	4.4	8.8
	99:1	2	35	8.9	17.8
	99:1	4	37	19.0	38.0
3	85:15	1	0	–	–
	85:15	2	0	–	–
	85:15	4	0	–	–
4	99:1	1	38	5.0	10.0
	99:1	2	30	7.5	15.0
	99:1	4	29	14.6	29.2

[a] No second-eluting enantiomer isolated.
[b] Purity of first enantiomer > 99.5%.

second-eluting enantiomer were combined, dried and repurified. This procedure of purification, solvent removal and repurification was repeated two times to generate a 391-mg sample which contained 95% of the second eluting enantiomer. This sample was then purified to produce 200 mg of second enantiomer. Using this series of four purifications, 270 mg of first-eluting enantiomer (>99.5%) and 200 mg of second-eluting enantiomer (>98%) were isolated. This represents recoveries of 54 and 40%, respectively. Since the remaining enantiomerically impure chemical from these series of chromatographic purifications was very close to a racemic mixture, it could be rerun through another series of purifications, if desired, to isolate more of the individual enantiomers.

Preparative resolution of prostaglandin enantiomers

The preparative resolution of the 11*R*,16*S*- and the 11*S*,16*R*-enantiomers of enisoprost (Fig. 2) was investigated. The analytical separation for these two enantiomers is shown in Fig. 9. This method was scaled up to preparative loadings and the percentage of isopropanol present in the mobile phase varied. The results of these experiments are summarized in Table VI. These results show that both enantiomers could be isolated at all loadings and isopropanol percentages attempted. The α value for this separation is 1.29. This is much better than the α value for the separation of the

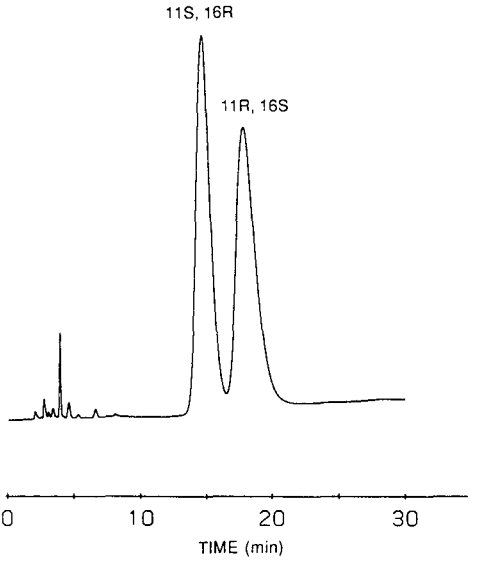

Fig. 9. Analytical HPLC separation of 11*S*,16*R*- and 11*R*,16*S*-enantiomers of enisoprost. Analysis conducted on Chiralcel OC column (250 × 4.6 mm I.D.) with a mobile phase of hexane–isopropanol (85:15, v/v). A flow-rate of 0.5 ml/min and detection at 215 nm, 0.1 a.u.f.s. was used.

prostaglandin precursors (see Table I) and because of this a larger amount of chemical could be isolated at the preparative loadings attempted.

CONCLUSION

Analytical and preparative HPLC can be used for the direct resolution of the enantiomers of prostaglandins and their precursors. Using cellulose-based phases,

TABLE VI

PREPARATIVE RESOLUTION OF 11*R*,16*S*- AND 11*S*,16*R*-ENANTIOMERS OF ENISOPROST

HPLC conditions: Chiralcel OC (500 × 10 mm I.D.) containing approximately 25 g of packing; flow-rate 8 ml/min.

Mobile phase (hexane–isopropanol)	*Loading (mg/g)*	*First enantiomer*[a]		*Second enantiomer*[a]	
		(%)[b]	*weight (mg)*	*(%)*[b]	*weight (mg)*
85:15	1	72	9.0	49	6.1
90:10	1	83	10.6	61	7.7
	2	76	19.1	31	7.8
	4	38	19.3	16	8.2
95:5	1	82	10.4	58	7.4
	2	73	18.8	35	9.1

[a] Purity > 99.5%.
[b] Percent of enantiomer available.

changing the alcohol in the mobile phase has very little effect on the separation, although branched alcohols reduce the separation obtained with their straight chain analogues. The degrees of separation obtained is related to the ability of the molecule to interact with the stationary phase and "fit" into the cellulose cavity. The analytical separation is directly related to the resolution obtained at preparative loadings.

ACKNOWLEDGEMENTS

The authors wish to thank John Adamek, Helga Bush, Terry Kosobud, Paul Collins and Konrad Kohler for their technical support. The compounds were provided by chemists in the Synthesis Development group at G. D. Searle & Co.

REFERENCES

1 A. J. H. Klunder, W. B. Huizinga, P. J. M. Sessink and B. Zwanenburg, *Tetrahedron Lett.*, 28 (1987) 357.
2 Y. Okamoto, R. Aburatani, M. Kawashima, K. Hatada and N. Okamura, *Chem. Lett.*, (1986) 1767.
3 R. Noyori and M. Suzuki, *Angew. Chem., Int. Ed. Engl.*, 23 (1984) 847.
4 G. Stork and M. Isobe, *J. Am. Chem. Soc.*, 97 (1975) 6260.
5 M. Asami, *Tetrahedron Lett.*, 26 (1985) 5803.
6 Y. Okamoto, R. Aburatani, M. Kawashima, K. Hatada and N. Okamura, *Chem. Lett.*, (1986) 1767.
7 L. Miller, H. Bush, *J. Chromatogr.*, 484 (1989) 337–345.
8 P. W. Collins, E. Z. Dajani, R. Pappo, A. F. Gasiecki, R. G. Bianchi and E. M. Woods, *J. Med. Chem.*, 26 (1983) 786.
9 J. H. Dygos, J. P. Adamek, K. A. Babiak, J. R. Behling, J. R. Medich, J. S. Ng and J. J. Wieczorek, in preparation.
10 A. L. Campbell, K. A. Babiak, J. R. Behling and J. S. Ng, *U.S. Pat.*, 4 785 124 (1988).
11 I. W. Wainer, *Trends Anal. Chem.*, 6 (1987) 125.
12 Y. Okamoto, R. Aburatani, M. Kawashima, K. Hatada and N. Okamura, *Chem. Lett.*, (1986) 1767.

Journal of Chromatography, 511 (1990) 109–114
Elsevier Science Publishers B.V., Amsterdam

CHROM. 22 392

Direct separation and optimization of timolol enantiomers on a cellulose tris-3,5-dimethylphenylcarbamate high-performance liquid chromatographic chiral stationary phase[a]

HASSAN Y. ABOUL-ENEIN* and M. RAFIQUL ISLAM

Drug Development Laboratory, Radionuclide and Cyclotron Operations, King Faisal Specialist Hospital and Research Centre, P.O. Box 3354, Riyadh (Saudi Arabia)

(First received November 28th, 1989; revised manuscript received February 13th, 1990)

ABSTRACT

A high-performance liquid chromatographic method was developed for the direct resolution and optimization of the separation of timolol enantiomers. The method involves the use of a cellulose tris-3,5-dimethylphenylcarbamate chiral stationary phase (OD-Chiralcel) column. The effects of concentration of 2-propanol, various aliphatic alcohols and diethylamine in the mobile phase and column temperature on the retention and enantioselectivity of timolol enantiomers were studied. The maximum resolution factor obtained was 4.00 when using the solvent system hexane–2-propanol (95:5) containing 0.4% (v/v) diethylamine at 5°C.

INTRODUCTION

Timolol maleate, (*S*)-(−)-1-(*tert.*-butylamino)-3-[(4-morpholino-1,2,5-thiadiazol-3-yl)oxy]-2-propanol maleate (Fig. 1), is a β-adrenergic blocking agent and is used for the treatment of essential hypertension, ocular hypertension and chronic, open-angle glaucoma, including aphakia. Timolol eye drops are widely used for the treatment of glaucoma. Although timolol, like all β-adrenoceptor antagonist, is contraindicated in patients with asthma, its inadvertent administration as eye drops to such patients continues to have severe and even fatal consequences[1]. Richards and Tattersfield[2] reported that the (*R*)-(+)-timolol enantiomer, L-714,465 was considerably less potent as a β-adrenoceptor antagonist in animals than the clinically used (*S*)-(−)-timolol enantiomer, but only slightly less potent in reducing intraocular pressure. The (*R*)-(+)-timolol enantiomer is 49 times less potent than (*S*)-(−)-timolol on β_2-adrenoceptor in animals and thirteen times less potent in constricting the airways of normal subjects, yet it is only four times less potent in reducing intraocular pressure in

[a] Presented at the *41st Pittsburgh Conference and Exposition, New York, March 5–9th, 1990*, Abstract No. 834.

0021-9673/90/$03.50

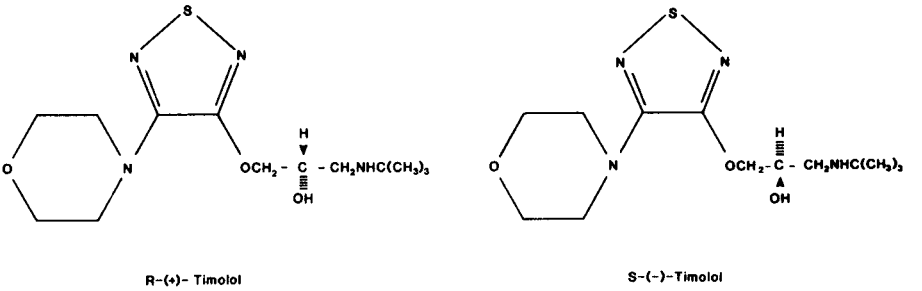

Fig. 1. Absolute configuration of (*R*)-(+)-timolol and (*S*)-(−)-timolol.

man[3]. These findings suggested that (*R*)-(+)-timolol might be a safer alternative for the treatment of glaucoma with less systemic side-effects than the (*S*)-(−)-enantiomer when applied as eye drops (in concentrations ranging between 0.25 and 4.0%), as it has a smaller bronchoconstricting effect.

A number of cellulose-based high-performance liquid chromatographic (HPLC) chiral stationary phases (CSPs) have been developed and are now commercially available[4,5]. This paper reports the direct separations of timolol enantiomers on a cellulose tris-3,5-dimethylphenylcarbamate column (OD-Chiralcel) without any derivatizations (Fig. 2). The effects of 2-propanol, various aliphatic alcohols, temperature and diethylamine concentration on resolution of timolol are discussed.

EXPERIMENTAL

Apparatus

The liquid chromatographic system consisted of a Waters Model M-45 pump, a U6K injector and a Lamda-Max Model 480 LC UV detector operated at 224 nm. A Chiralcel OD analytical column (25 cm × 0.46 cm I.D.) (Daicel Chemical Industries, Tokyo, Japan) containing cellulose tris-3,5-dimethylphenylcarbamate coated on silica gel of particle size 10 μm was used.

Chemicals

(*R*)-(+)-timolol (Lot No. L-714,465-001E015) and (*S*)-(−)-timolol (Lot No. L-714,503-01T12) were kindly supplied by Merck Sharp & Dohme (NJ, U.S.A.) HPLC-grade hexane was obtained from Fisher Scientific (NJ, U.S.A.), HPLC-grade 2-propanol from Romil (U.K.), diethylamine from BDH (Poole, U.K.) and HPLC-

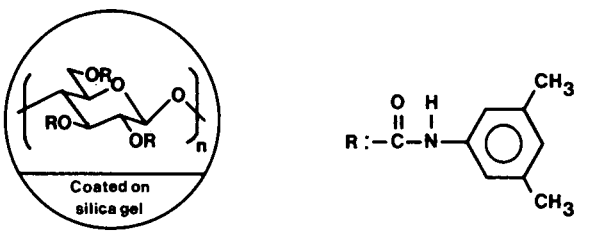

Fig. 2. The structure of the Chiralcel OD chiral stationary phase used.

grade 2-butanol, 1-butanol, 1-pentanol and 1-propanol, from Aldrich (WI, U.S.A.).

RESULTS AND DISCUSSION

To the best of our knowledge, no work has been reported on the direct resolution of timolol using a chiral stationary phase column. We have studied the separation of timolol enantiomers using a Chiralcel OD column. This cellulose-based chiral phase has been used successfully to separate directly several β-adrenergic blockers, *e.g.*, alprenolol, oxyprenolol, propranol, pindolol and atenolol[6]. The mobile phase consists of a mixture of hexane, 2-propanol and diethylamine. A chromatogram of the enantiomeric separation of timolol is shown in Fig. 3. A comparison of the chromatograms and capacity factors of (*R*)-(+)-timolol (Fig. 4a) and (*S*)-(−)-timolol (Fig. 4b) indicated that the peak that eluted with a lower capacity factor was that of the former enantiomer and the peak with a higher capacity factor was that of the latter. The maximum resolution (*R*) obtained was 4.00.

Effects of mobile phase on retention and stereoselectivity

The capacity factors (k'), separation factors (α) and resolutions (R_s) of solutes can be regulated over a wide range by the addition of an alcohol. The influence of the concentration of 2-propanol and other aliphatic alcohols in the mobile phase on the separation of timolol enantiomers was thoroughly studied.

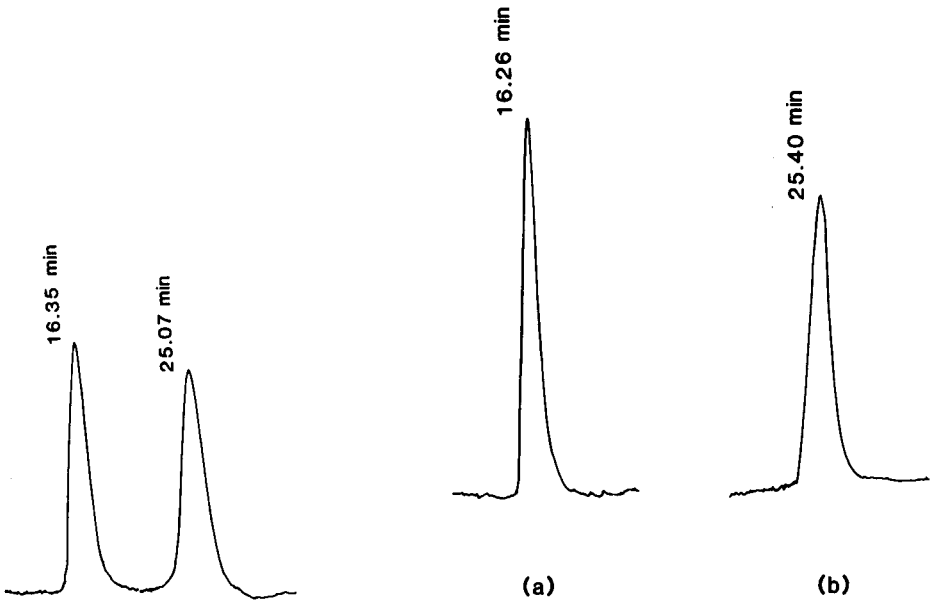

Fig. 3. HPLC separation of timolol maleate enantiomers. Column: Chiralcel OD (250 mm × 4.6 mm I.D.); mobile phase, hexane–2-propanol–diethylamine (95:5:0.4); flow-rate, 0.7 ml/min; chart-speed, 0.5 cm/min; temperature, 5°C; pressure, 250 p.s.i.; sample amount, 10 nmol; detector: UV (224 nm); sensitivity, 0.01 a.u.f.s.

Fig. 4. Chromatograms of (a) (*R*)-(+)- and (b) (*S*)-(−)-timolol maleate. Sample amount, 5 nmol. Other conditions as in Fig. 3.

TABLE I

EFFECT OF THE 2-PROPANOL CONTENT IN MOBILE PHASE ON CAPACITY FACTOR, SEPARATION FACTOR AND RESOLUTION IN THE SEPARATION OF TIMOLOL ENANTIOMERS

Conditions: column, Chiralcel OD (250 × 4.6 mm I.D.); mobile phase, hexane–2-propanol with 0.4% (v/v) diethylamine; temperature, 5°C; flow-rate, 0.7 ml/min.

Parameter[a]	*2-Propanol concentration (%, v/v)*				
	0	*5*	*10*	*15*	*20*
k'_1	No elution	4.58	2.32	1.78	1.51
k'_2	No elution	7.56	3.59	2.48	1.98
α	No elution	1.65	1.55	1.39	1.31
R_s	No elution	4.00	3.05	1.98	1.44

[a] k'_1 = capacity factor of 1st-eluted compound; k'_2 = capacity factor of 2nd-eluted compound; α = separation factor; R_s = resolution.

Effects of 2-propanol concentration

Concentrations of 0–20% 2-propanol in the mobile phase were investigated (Table I). Timolol enantiomers did not elute from the column when a mobile phase without any modifier was used. An increase in 2-propanol concentration resulted in a corresponding decrease in retention. The change in α is significant (1.3–1.6), providing almost twice the contribution to R_s at 5% 2-propanol, as compared to addition of 20% 2-propanol.

Effects of straight- and branched-chain aliphatic alcohols

The effects of the structure of the polar mobile phase modifier were investigated using a series of primary and secondary alcohols. The changes in k' and R_s observed with a series of primary and secondary alcohols (1-propanol, 2-propanol, 1-butanol, 2-butanol, 1-pentanol and 2-pentanol) are presented in Table II. An increase in the chain length of the alkyl group of the primary alcohol increased k', but the effect on α was not significant. Thus, a better resolution was obtained using 1-butanol as a modifier in the mobile phase. On the other hand, the use of the branched-chain

TABLE II

EFFECT OF DIFFERENT PRIMARY AND SECONDARY ALIPHATIC ALCOHOLS IN THE MOBILE PHASE ON CAPACITY FACTOR, SEPARATION FACTOR AND RESOLUTION IN THE SEPARATION OF TIMOLOL ENANTIOMERS

Conditions as in Table I and mobile phase [hexane–2-propanol (95:5, v/v) containing 0.4% (v/v) diethylamine].

Parameter[a]	*1-Propanol*	*2-Propanol*	*1-Butanol*	*2-Butanol*	*1-Pentanol*	*2-Pentanol*
k'_1	1.66	2.34	1.78	2.86	3.40	4.42
k'_2	1.83	3.32	2.27	4.06	3.60	6.99
α	1.17	1.42	1.27	1.42	1.07	1.58
R_s	0.449	2.47	1.20	2.37	0.30	2.92

[a] See Table I

TABLE III

EFFECT OF DIETHYLAMINE CONTENT IN MOBILE PHASE ON CAPACITY FACTOR SEPARATION FACTOR AND RESOLUTION IN THE SEPARATION OF TIMOLOL ENANTIOMER

Conditions as in Table I, except the mobile phase [hexane–2-propanol (95:5, v/v)] contained different concentrations of diethylamine.

Parameter[a]	*Diethylamine concentration (%, v/v)*				
	0	*0.1*	*0.4*	*0.7*	*1.0*
k'_1	No separation	4.41	4.58	4.24	4.24
k'_2	No separation	7.14	7.56	7.01	7.09
α	No separation	1.62	1.65	1.65	1.67
R_s	No separation	2.95	4.00	3.85	4.32

[a] See Table I.

alcohols as modifiers in the mobile phase gave a significantly better resolution than straight-chain alcohols. Both primary and secondary alcohols yield largers k' values for higher-molecular-weight alcohols, whereas the α values do not change mucht with the larger alcohols. However, a better resolution was obtained using 2-propanol as a modifier in the mobile phase. There is a single point of interaction between the hydroxyl hydrogen on the alcohol and the carbonyl oxygen of the CSP, while the solute competes with the modifier for hydrogen-bonding sites on the CSP. This competition takes place at both chiral and achiral sites on the CSP[7]. This does not preclude interactions between the modifier and the solute, which appears to play a lesser role in the determination of the chromatographic parameters.

Effects of diethylamine concentration in the mobile phase

The effects of diethylamine concentration are shown in Table III. No separation was obtained without diethylamine present. The resolution factor ($R_s = 4.32$) did improve in the presence of 1% (v/v) diethylamine as suggested by the manufacturer[7]. In order to prevent the detrimental effect of the basic mobile phase on the stationary phase, as contained ester groups were present in the packing material, only

TABLE IV

EFFECT OF TEMPERATURE ON CAPACITY FACTOR, SEPARATION FACTOR AND RESOLUTION IN THE SEPARATION OF TIMOLOL ENANTIOMERS

Conditions as in Table I, except temperature and mobile phase [hexane–2-propanol (95:5, v/v) containing 0.4% (v/v) diethylamine].

Parameter[a]	*Temperature (°C)*				
	5	*10*	*15*	*23*	*30*
k'_1	4.58	4.35	4.08	3.96	3.77
k'_2	7.56	6.97	6.23	5.72	5.35
α	1.65	1.60	1.53	1.44	1.42
R_s	4.00	3.46	2.94	2.88	2.55

[a] See Table I.

0.4% (v/v) diethylamine was used, and gave a reasonably improved resolution factor ($R_s = 4.0$).

Effect of temperature

Optimization of the separation at different temperatures was studied (Table IV). It was found that chiralcel OD is sensitive to any small changes in temperature. The resolution increased about 1.57-fold when the temperature was decreased from 30 to 5°C. The existence of both simultaneous and stepwise binding is supported by the effect of temperature on stereochemical resolution. An increase in temperature resulted in a corresponding increase in the conformational mobility of the solute, which destabilized the solute–CSP complex and reduced the stereoselectivity[8].

CONCLUSION

Direct separation of timolol enantiomers was achieved using a Chiralcel OD column with hexane–2-propanol (95:5) containing 0.4% (v/v) diethylamine at 5°C. The maximum R_s obtained could be due to the chiral recognition mechanism explained by Wainer and Stiffen[8]. As the maximum R_s was obtained using this column, it could possibly be used for the preparative separation and optical purity determination of the drug. This technique can also be used for the determination of the (*R*)-(+)- and (*S*)-(−)-enantiomers of timolol in biological fluids, which is currently under study.

ACKNOWLEDGEMENT

The authors thank the administration of the King Faisal Specialist Hospital and Research Centre for their continuous support to the drug development research programme.

REFERENCES

1 F. T. Fraunfelder and A. F. Barker, *N. Engl. J. Med.*, 311 (1984) 1441.
2 R. Richards and A. E. Tattersfield, *Br. J. Clin. Pharmacol.*, 20 (1985) 459–462.
3 R. Richards and A. E. Tattersfield, *Br. J. Clin. Pharmacol.*, 24 (1987) 485–491.
4 A. Ichida, T. Shibata, I. Okamoto, Y. Yuki, H. Namikoshi and Y. Toga, *Chromatographia*, 19 (1984) 280–284.
5 Y. Okamoto, M. Kawashima, K. Yamamoto and K. Hatada, *Chem. Lett.*, (1984) 739–742.
6 Y. Okamoto, M. Kawashima, R. Aburatani, K. Hatada, T. Nishiyama and M. Matsuda, *Chem. Lett.*, (1986) 1237–1240.
7 *Instruction Sheet, Chiralcel OA, OB, OC, OJ, OK*, Daicel Chemical Industries, CA.
8 I. W. Wainer and R. M. Stiffen, *J. Chromatogr.*, 411 (1987) 139–151.

Journal of Chromatography, 511 (1990) 115–121
Elsevier Science Publishers B.V., Amsterdam

CHROM. 22 421

Ligand-exchange chromatography of α-trifluoromethyl-α-amino acids on chiral sorbents

S. V. GALUSHKO*, I. P. SHISHKINA, V. A. SOLOSHONOK and V. P. KUKHAR
Institute of Bioorganic Chemistry, Academy of Sciences of the Ukrainian SSR, 252660 Kiev 94 (U.S.S.R.)
(First received August 7th, 1989; revised manuscript received February 23rd, 1990)

ABSTRACT

The chromatographic behaviour of some α-trifluoromethyl-α-aminoacids on L-proline- and L-hydroxyproline sorbents was studied. The retention and selectivity parameters of the separation of amino acid enantiomers on the sorbents were determined. The introduction of a CF group led to an increased selectivity in the separation of amino acid enantiomers on a proline sorbent and to a decreased selectivity on a hydroxyproline sorbent.

INTRODUCTION

The bioactivity of synthetic analogues of natural compounds depends primarily on the enantiomer used, so it is important to find optimum conditions for obtaining individual enantiomers and to develop methods for controlling their enantiomeric purity. Fluoroamino acids (FAA) have high biological activity[1], but few studies have been devoted to the enantiomer analysis of FAA. The separation of some FAA by ligand-exchange chromatography has been described[2]. A method for controlling the enantiomeric purity of α-trifluoromethylalanine (α-CF_3Ala) by reversed-phase liquid chromatography with a chiral mobile phase has been developed[3]. No data concerning the ligand-exchange chromatography of α-trifluoromethyl-α-amino acids (α-CF_3AA) on chiral sorbents have been reported.

The aims of this work were to determine the optimum conditions for the ligand-exchange chromatography (LEC) of α-CF_3AA enantiomers and to compare the selctivities of separation of the α-CF_3AA and their natural analogues on L-proline and L-hydroxyproline sorbents.

EXPERIMENTAL

Chromatographic conditions

The experiments were performed on an LKB (Bromma, Sweden) liquid chromatographic system consisting of a Model 2150 high-performance liquid chromatographic (HPLC) pump, a Model 2152 LC controller, a Model 7410 injector,

0021-9673/90/$03.50

a Model 2151 variable-wavelength monitor operated at wavelength 225 nm and a Model 2220 recording integrator. The columns used were (i) a proline column with chiral ProCu = Si100 Polyol (L-Proline covalently bound to Si100 Polyol, 5 μm), 250 × 4.6 mm I.D. (Serva, Heidelberg, F.R.G.), (ii) a hydroxyproline column with Nucleosil Chiral-1 (L-hydroxyproline covalently bound to Nucleosil 120, 5 μm), 250 × 4.0 mm I.D. (Macherey-Nagel, Düren, F.R.G.) and (iii) a Microbe glass column with Chiral ProCu = Si100 Polyol (5 μm), slurry packed, 100 × 1.0 mm I.D. The mobile phase was $0.1 \cdot 10^{-3}$–$5 \cdot 10^{-3}$ *M* copper sulphate solution at a flow-rate of 1.0 ml/min (i, ii) or 0.03 ml/min (iii).

Materials

α-Trifluoromethyl-α-amino acids and villardine were obtained as described[4,5]. Natural amino acids were supplied by Reakhim (Moscow, U.S.S.R.). Copper sulphate and hydrochloric acid (analytical-reagent grade) were used as received. Water was doubly distilled and filtered for HPLC use.

RESULTS AND DISCUSSION

In isocratic LEC the ligand (A) is usually chemically bonded to the surface of a sorbent and the mobile phase contains a constant concentration of metal ions (M). When a certain amount of another ligand (B) is introduced into the mobile phase, a mixed complex $(MAB)_s$ is formed on the surface. The capacity factor of the ligand B can be defined as follows:

$$k' = \varphi \cdot \frac{[MAB]_s}{[B]_m + [MB]_m + \ldots + [MB_n]_m} \tag{1}$$

where φ is the phase ratio and m and s represent the concentrations in the mobile phase and on the sorbent surface, respectively.

The formation of a mixed complex on the surface can be represented by

$$\begin{aligned} &(MA)_s + (B)_m \rightleftharpoons (MAB)_s \\ &K_1[MA]_s[B]_s = [MAB]_s \end{aligned} \tag{2}$$

where K_1 is the equilibrium constant. The concentration of a metal ion in the mobile phase (C_M) is usually much higher than that of the ligand B (C_B), and we can assume that in the mobile phase a complex MB exists:

$$\begin{aligned} &(M)_m + (B)_m \rightleftharpoons (MB)_m \\ &K_2[M]_m[B]_m = [MB]_m \end{aligned} \tag{3}$$

When the complex MB is weakly dissociated, $[MB]_m \gg [B]_m$ and

$$k' = \varphi \cdot \frac{[MAB]_s}{[MB]_m} \tag{4}$$

As $C_M \gg C_B$, it can be assumed that $[M]_m \approx C_M$, and using eqns. 2 and 3, eqn. 4 can be written as follows:

$$k' = \varphi \cdot \frac{K_1[MA]_s}{K_2 C_M}$$

When the ions of metal are in abundance and the complex formed, $(MA)_s$, is strong, almost all the surface ligands are bonded in the complex $(MA)_s$; therefore, the concentration of this complex increases insignificantly with increase in the concentration of M ions in the mobile phase. Taking into account that $[MA]_s \gg [MAB]_s$, one can assume $[MA]_s \approx$ constant, and then

$$K' = \frac{Q}{C_M}$$

where $Q = (K_1[MA]_s)/K_2$. Hence a plot of k' *vs.* $1/C_M$ is a straight line of slope Q passing through the origin. Q is a constant for a given column and ligand B. Plots of k' *vs.* $1/C_M$ for several amino acids are shown in Fig. 1. As can be seen, the deflection from a straight line is observed only with a low concentration of Cu^{2+} ions in the mobile phase (lower than $5 \cdot 10^{-4}$ *M*), *i.e.*, when the condition $C_M \gg C_B$ is not satisfied. The values of Q can be determined when the columns are tested. Knowing the Q values, the capacity factors of enantiomers can be calculated exactly under various conditions of metal ions in the mobile phase.

These experiments have shown that the enantiomers of α-CF_3AA can be successfully separated on chiral sorbents containing proline and hydroxyproline. The efficiency of the columns is so high that the separation is easily achieved even at ambient temperature (Fig. 2). The optimum concentrations of Cu^{2+} ions in the mobile phase are $1 \cdot 10^{-3}$–$5 \cdot 10^{-3}$ *M*. For poorly retained 3,3,3-trifluoroalanine and α-trifluoromethylalanine it is preferable to use a mobile phase with a low Cu^{2+} concentration, whereas for α-CF_3Phe it is necessary to use a mobile phase with a Cu^{2+} concentration not lower than $5 \cdot 10^{-3}$ *M*. The chromatographic behaviour of α-trifluoromethylphenylglycine differs greatly from that of other α-CF_3AA. The retention and selectivity of separation of α-trifluoromethylphenylglycine enantiomers are so great that it is necessary to use a mobile phase with a higher concentration of H^+ ions and the separation should be carried out at 45–55°C. An eluent of composition A–B = 75:25 or 50:50, where A is $5 \cdot 10^{-3}$ *M* $CuSO_4$ containing ethanol (10%, v/v) and B is $5 \cdot 10^{-3}$ *M* $CuSO_4$(pH 3.0; HCl) are optimum for the separation of enantiomers of α-trifluoromethylphenylglycine (Fig. 3). The selectivity of separation (α) is about 3.5, *i.e.*, the conditions are suitable for both enantiomeric analysis and preparative work.

There is a great difference in the retention and selectivity of separation of the amino acid enantiomers on proline and hydroxyproline sorbents (Table I). Si100 Polyol is a polyol derivative containing propylglycerol groups. The surface area of Si100 Polyol (matrix of proline sorbent) is higher than that of Nucleosil Chiral-1 (300 and 200 m^2/g, respectively) and the retention of amino acids on the proline column is higher than that on the hydroxyproline column. The α-CF_3 group exerts a consider-

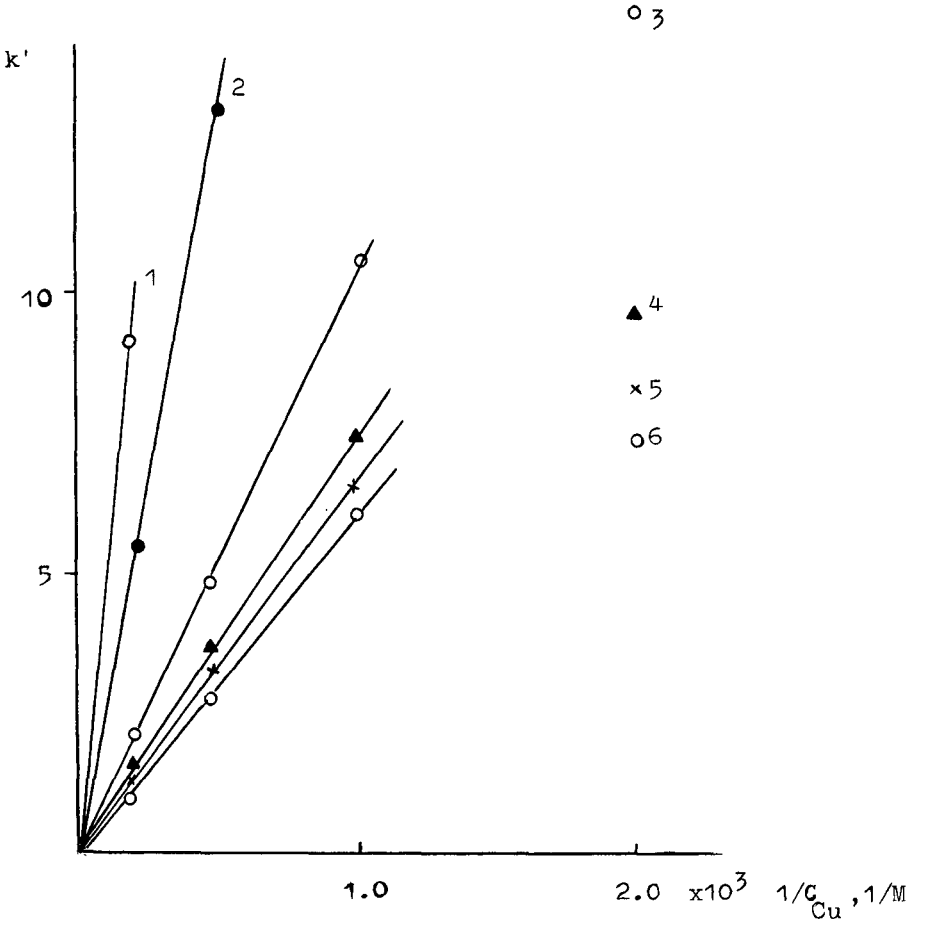

Fig. 1. Effect of $CuSO_4$ concentration on capacity factors: 1 = L-α-CF_3Phe; 2 = D-α-CF_3Phe; 3 = L-α-CF_3Ala; 4 = L-3,3,3-trifluoroalanine; 5 = D-α-CF_3Ala; 6 = D-3,3,3-trifluoroalanine. Microbore glass column (100 × 1.0 mm I.D.) with chiral ProCu = Si100 Polyol, 5 μm; flow-rate, 0.01 ml/min.

able influence on both the retention and the selectivity of the separation of amino acid enantiomers. The retention of α-CF_3AA is much higher than that of natural amino acids. The change in the free energy of sorption when the CF_3 group is introduced is 1.2–2.5 kJ/mol on the proline column and 0.8–4.4 kJ/mol on the hydroxyproline column (Table I). These results imply that the stability of mixed complexes (ProCu B) for α-CF_3AA is higher than that for natural amino acids. The differences in the selectivity of the separation of enantiomers on proline and hydroxyproline columns is considerable (Table II). On the proline column the selectivity of separation of α-CF_3-AA enantiomers is much higher than that of natural amino acids. For example, for Leu, Nle and Ala no separation of enantiomers takes place, whereas for α-CF_3-AA the separation is excellent. The situation is different with the hydroxyproline column; the selectivity of separation of α-CF_3-AA enantiomers is lower than that of the natural

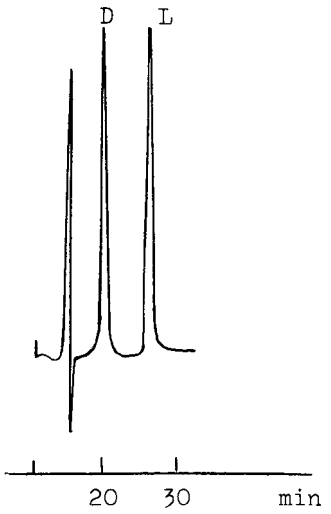

Fig. 2. Separation of enantiomers of α-CF_3-alanine. Column, Si 100 Polyol Chiral Pro-Cu, 5 μm (250 × 4.6 mm I.D.); mobile phase, $5 \cdot 10^{-3}$ *M* $CuSO_4$; flow-rate, 1 ml/min; temperature, ambient; wavelength, 225 nm.

compounds. In most instances the selectivity of separation on the hydroxyproline column is higher than that on the proline column. For example, whereas on the proline column there is no separation of Leu, Nle, Nva or Ala, the separation is excellent on the hydroxyproline column. However, the separation of α-CF_3Ala and α-CF_3Asp enantiomers is not possible on the hydroxyproline column, whereas it is easily achieved on the proline column. In addition, the separation of α-CF_3Asp, Phe and α-CF_3Phe is

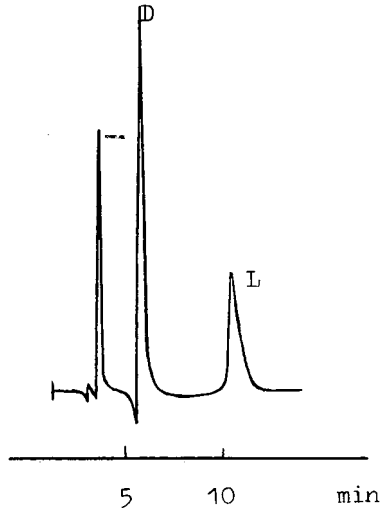

Fig. 3. Separation of enantiomers of α-CF_3-phenylglycine. Column, Nucleosil Chiral-1, 5 μm (250 × 4 mm I.D.); mobile phase, A–B (75:25), where A = $5 \cdot 10^{-3}$ *M* $CuSO_4$–10% (v/v) ethanol and B = $5 \cdot 10^{-3}$ *M* $CuSO_4$ (pH 3.0, HCl); flow-rate, 1 ml/min; temperature, 50°C.

TABLE I

SELECTIVITY PARAMETERS FOR THE SEPARATION OF L-AMINO ACIDS

Compound	$\Delta(\Delta G)^a$ *(kJ/mol)*	
	Proline column	*Hydroxyproline column*
α-CF_3Phe–Phe	1.26	0.84
α-CF_3Nle–Nle	1.66	1.81
α-CF_3Ala–Ala	1.63	2.88
α-CF_3Nva–Nva	2.46	2.99
α-CF_3Leu–Leu	2.24	2.72
α-CF_3Asp–Asp	2.04	4.43

[a] $\Delta(\Delta G) = RT \ln \alpha$.

more selective on the proline column. Replacing the benzene ring in Phe for the hydrophilic heterocycle of uracil [villardine(uracilylalanine) natural alkaloid[5]] leads to a considerable decrease in the retention and selectivity of separation of enantiomers on the proline column and to a complete loss of selectivity on the hydroxyproline column. Enantioselectivity may by caused by coordination and hydrophobic interactions and also hydrogen bonds between ligands[6]. As in our case ethanol added to the mobile phase (0.5–50%, v/v) has no effect on the selectivity of enantiomer separation, we can assume that hydrophobic interactions have no appreciable effect on this process.

The results obtained enable optimum conditions and a sorbent for the complete separation of amino acid enantiomers to be chosen.

TABLE II

SEPARATION OF AMINO ACID ENANTIOMERS ON PROLINE AND HYDROXYPROLINE SORBENTS

Mobile phase, $5 \cdot 10^{-3}$ *M* $CuSO_4$; temperature, 20°C.

Compound	*Proline column*		*Hydroxyproline column*	
	k'_L	α^a	k'_L	α^a
Phe	16.8	2.0	3.7	1.8
Leu	5.8	1.0	1.4	2.1
Ala	4.3	1.0	0.5	1.7
Nle	7.3	1.0	3.8	1.9
Nva	4.2	1.0	1.6	2.4
Asp	2.5	1.0	0.5	1.0
α-CF_3Phe	28.0	6.0	5.2	1.3
α-Trifluoroaminobutyric acid	7.6	1.5	3.2	1.6
α-CF_3Nle	14.3	1.5	7.9	1.9
3,3,3-Trifluoroalanine	5.1	1.3	1.2	2.4
α-CF_3Nva	11.7	1.4	4.8	1.8
α-CF_3Ala	8.3	1.8	1.6	1.0
α-CF_3Leu	14.3	1.6	4.7	2.0
α-CF_3Asp	5.7	1.6	3.0	1.2
Villardine	6.2	1.2	0.5	1.0

[a] $\alpha = k'_L k'_D$.

REFERENCES

1 C. T. Walsh, *Annu. Rev. Biochem.*, 53 (1984) 493.
2 J. R. Guerson and M. J. Adam, *J. Chromatogr.*, 325 (1985) 103.
3 I. W. Keller and B. I. Hamilton, *Tetrahedron Lett.*, 27 (1986) 1249.
4 V. A. Soloshonok, I. I. Herus, Yu. L. Yagupolskii and V. P. Kukhar, *Zh. Org. Khim.*, 23 (1987) 1441.
5 Yu. I. Shwatchkin and M. P. Azarova, *Zh. Obshch. Khim.*, 34 (1964) 407.
6 P. Roumeliotus, K. Unger, A. Kurganov and V. Davankov, *J. Chromatogr.*, 225 (1983) 51.

Journal of Chromatography, 511 (1990) 123–130
Elsevier Science Publishers B.V., Amsterdam

CHROM. 22 403

Isocratic hydrophobic interaction chromatography of dansyl amino acids

Correlation of hydrophobicity and retention parameters

JOANNE GEHAS and DONALD B. WETLAUFER*
Department of Chemistry and Biochemistry, University of Delaware, Newark, DE 19716 (U.S.A.)
(First received January 3rd, 1990; revised manuscript received February 27th, 1990)

ABSTRACT

Hydrophobic interaction chromatography of the dansyl derivatives of 20 common amino acids has been carried out, and the dependence of log k' (k' = capacity factor) on the ammonium sulfate concentration in the mobile phase determined. Linear relationships above 0.2 M ammonium sulfate are found. For the amino acid derivatives studied, the slopes of the equation relating retention (log k') to salt concentration (M_s) in the mobile phase (log $k' = mM_s + b$) correlate well with other measures of amino acid hydrophobicity.

INTRODUCTION

Hydrophobic interaction chromatography (HIC) is commonly utilized for protein separations[1–4]. However, the influence of analyte structure on retention in HIC is not yet well understood. Although structure–retention relationships have been discussed extensively in reversed-phase studies[5–10], there have been few reports on similar studies in HIC[11,12].

Because it should be easier to examine the effect of the mobile phase and of solute structure on retention in HIC if small molecules are employed, we have undertaken a study of dansyl amino acid derivatives under HIC conditions that are conventionally applied for protein separations. Retention parameters are reported as a function of ammonium sulfate concentration in the mobile phase. The relationship between retention parameters in HIC and a solute's contact area with the stationary phase are discussed.

EXPERIMENTAL

Materials

A kit of dansyl amino acids was obtained from Mann Research Labs. (New

0021-9673/90/$03.50

York, NY, U.S.A.). Dansyl amide was obtained from Sigma (St. Louis, MO, U.S.A.). Ammonium sulfate (ultrapure grade) was obtained from Schwarz-Mann Biotech (Cleveland, OH, U.S.A.). All other reagents were of A.C.S. analytical-reagent grade.

Methods

The chromatographic system consisted of two Waters Model M6000A pumps, a Rheodyne Model 7125 injection valve, a 150 × 4.6 mm I.D. SynChropak propyl hydrophobic interaction column (SynChrom, Lafayette, IN, U.S.A.) with 6.5-μm particle packing, and a Hewlett-Packard (Avondale, PA, U.S.A.) Model 3390A reporting integrator. The column dead time was determined by water injection.

Mobile phases were prepared with high-purity HPLC-grade water obtained in-house with a Millipore (Bedford, MA, U.S.A.) Milli-Q water purification system as follows: Mobile phase A: 2.1 *M* ammonium sulfate, 0.02 *M* potassium phosphate monobasic, adjusted to pH 6.0 with a sodium hydroxide solution. Mobile phase B: 0.02 *M* potassium phosphate monobasic, adjusted to pH 6.0 with a sodium hydroxide solution.

The composition of the mobile phase was controlled by a Waters Model 660 solvent programmer. Stock solutions of each dansyl amino acid were prepared using high-purity HPLC-grade water (unbuffered) at a concentration *ca.* 1.0 mg/ml. Mobile phases and stock solutions were filtered through a Millipore HA (0.45 μm) filter and stored at 4°C when not in use. A 20-μl injection loop was used for all injections (approximately 20 μg per injection). The dansyl amino acids were detected at 254 nm using a Waters Lambda-Max Model 480 spectrophotometer. The flow-rate was 2.0 ml/min throughout the study. The chromatographic column was maintained at 30.0 ± 0.2°C with a circulating water jacket.

RESULTS AND DISCUSSION

In isocratic HIC, the log of the capacity factor, k', is linearly related to the salt concentration (M_s) in the mobile phase[13].

$$\log k' = \log k'_0 + mM_s \tag{1}$$

This equation is derived from the linear relationship of the log of the retention factor to the surface tension of the mobile phase[14] and from the linear relationship between surface tension and salt concentration[15]. The Setschenow equation for the salting-out of non-polar compounds from aqueous solution is of a similar form[16].

Melander and Horváth[13] have discussed the linear relationship in HIC between k' and M_s. However, at low salt concentrations, deviations from linearity are observed due to electrostatic effects. Above a certain salt concentration (which is dependent on the solute), concomitant ionic shielding suppresses the electrostatic interactions, and $\log k'$ then becomes a linear function of M_s. They propose that the slope of eqn. 1, m, is dependent on the non-polar contact area between the solute and the stationary phase or the molecular contact area upon binding.

Eqn. 1 is analogous to the equation in reversed-phase chromatography (RPC) relating $\log k'$ to the organic volume fraction in the mobile phase, φ.

$$\log k' = \log k'_0 + S\varphi \tag{2}$$

Analogous to the m values in HIC, S values are presumed to reflect the magnitude of the non-polar contact area between the solute and the hydrocarbon ligands of the stationary phase. S values for polypeptides are usually larger than those for small solutes[17]. For example, Terabe *et al.*[18] have studied the RPC of peptides and found that the larger the peptide molecule, the steeper the slope in eqn. 2. These findings also support a direct relationship of the slope to the non-polar contact area of the solute with the stationary phase.

It has been suggested that slope values in HIC are generally smaller than in RPC due to the weaker interaction of the solute with the stationary phase in HIC[19]. This is a difficult comparison to make, since not only are ammonium sulfate and its organic solvent counterpart likely to have different incremental solvent powers, but also the conventional concentration scales for HIC (molar or molal) and RPC (% organic component) are different. Moreover, stationary phases for RPC are more non-polar than those for HIC, both in the size and the packing density of the surface moieties. Finally, in contrast with HIC, RPC solvent systems usually denature proteins, thereby exposing a larger protein contact area. Any quantitative comparison of HIC and RPC retention parameters should take these differences into account. We will not pursue it further here.

Others have given interpretations of the slope and intercept values in eqn. 1. Zaslavsky *et al.*[20] discuss the relationship between the partition coefficient, K (which is linearly related to k') and ionic strength, as it relates to the measurement of the hydrophobicity of the amino acid side chains partitioning in a two-phase system. The slope (m) reflects the effect of ionic strength on the transfer of a given compound and the intercept (log k'_0) is the relative hydrophobicity of a substance at zero ionic strength. In another paper[21] they propose that the slope reflects the overall effect of ionic strength on a system of given ionic composition of all the ionogenic groups on the surface and that the intercept (log k'_0) is related to both the overall relative

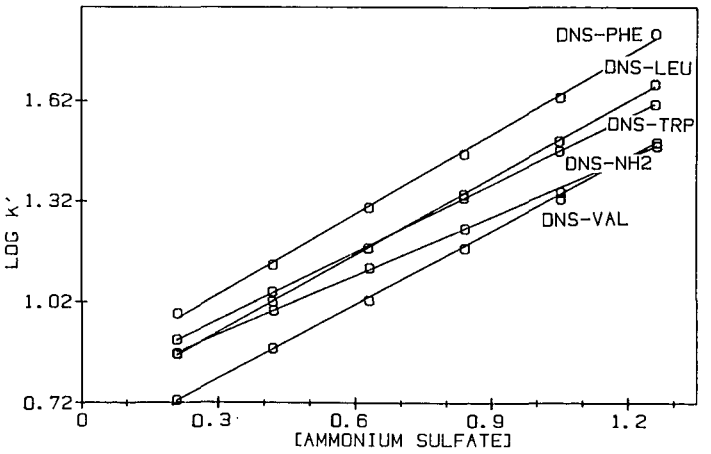

Fig. 1. Retention of dansylamide and dansylated amino acids on a SynChropak propyl column as a function of ammonium sulfate molar concentration. DNS-VAL = Dansyl valine; DNS-NH2 = dansyl amide; DNS-TRP = dansyl tryptophan; DNS-LEU = dansyl leucine; DNS-PHE = dansyl phenylalanine.

hydrophobicity of surface groups at zero ionic strength and the total number of equivalent CH_2 groups on the surface. Harnisch *et al.*[22] state that, in the RP-HPLC context, the slope is not only affected by solute–solvent and solute–stationary phase interactions, but also by solute size and structure.

For the dansyl amino acid derivatives, isocratic data were acquired with mobile phases ranging in concentration from 0.21 to 1.26 *M* ammonium sulfate. Fig. 1 gives an example of the plots of log *k versus* M_s for a few of the more non-polar dansyl amino acid derivatives (phenylalanine, tryptophan, valine and leucine), with dansyl amide included for comparison purposes.

From comparison of the retention order in isocratic elutions at 0.4 and at 1.0 *M* ammonium sulfate, it is evident that retention order changes with salt concentration. Therefore, it is misleading to infer the hydrophobicity of one solute relative to that of another from their retention order at any single salt concentration. Braumann *et al.*[23] have also pointed out that k' is not a good parameter to describe the hydrophobic nature of a solute since compounds with the same k' at a given mobile phase composition do not necessarily exhibit the same retention mechanism as inferred from the different values of slope (m in eqn. 1).

Table I gives the slope (m) and intercept (log k'_0) calculated from 0.21 to 1.26 *M* ammonium sulfate from eqn. 1. The dansyl derivative for lysine is in parentheses

TABLE I

LINEAR REGRESSION ANALYSIS OF $\log k' = \log k'_0 + mM_s$

Linear regression from 0.21 to 1.26 *M* ammonium sulfate, $n = 6$; correlation coefficient > 0.996.

Dansyl derivative	*Slope (m)*	*Intercept (log k'_0)*
Phe	0.79388	0.80400
Ile	0.78844	0.81400
Leu	0.76394	0.70133
Tyr	0.74694	1.02930
Val	0.73374	0.57253
Met	0.73320	0.37960
Pro	0.67565	0.49040
Trp	0.67007	0.76533
Lys[a]	0.66299	0.22320
Ala	0.61524	0.21880
Amide	0.59932	0.74600
Thr	0.59565	0.12320
Cys	0.58912	0.71200
Gln	0.57565	0.07773
Gly	0.56136	0.42907
Ser	0.55510	0.16500
Glu	0.53544	−0.02453
Asn	0.52871	0.01773
His[b]	0.51605	0.25320
Arg	0.49578	−0.01573
Asp	0.46993	−0.03887

[a] Derivatized on ε-nitrogen, not on α-nitrogen.
[b] Partially ionized at pH 6.0.

because it is derivatized on the ε-nitrogen rather than on the α-nitrogen as are the other dansyl derivatives. Because of this, it should not be directly compared to the other dansyl derivatives. It also should be noted that dansyl histidine is expected to be partially ionized in the mobile phase (buffered at pH 6.0). The pK_2 of dansyl histidine, though not readily available, is probably a few tenths of a unit higher than that of histidine itself ($pK_2 = 6.0$), based on a simple electrostatic argument.

Slope values (m) of all the dansyl derivatives examined have been ranked in order from largest to smallest in Table I and show an interesting trend. The amino acids that are commonly thought of as hydrophobic (phenylalanine, isoleucine, leucine, valine, methionine and tryptophan) have large slope values, while the more hydrophilic amino acids (aspartic acid, glutamic acid, asparagine, glutamine and arganine) have small slope values. Thus, the slope value, reflecting the solute's non-polar contact area with the stationary phase, appears to correlate with that what is generally accepted to be the relative hydrophobicity (relative polarity) of the amino acid.

It has already been pointed out that the isocratic retention order changes for the dansyl amino acid derivatives at different salt concentrations. For this reason, the slope value (m), rather than retention time, is taken to be a better determinant of a solute's relative hydrophobicity. To set up a quantitative scale of hydrophobicity for the amino acids from the retention behavior of their derivatives, it is assumed that the dansyl group makes a constant contribution to the behavior of all the derivatives.

The relative order of the slopes (m) shown in Table I correlates well with other published scales of amino acid hydrophobic parameters. Many such scales have been published[24–31]. These relative scales of amino acid hydrophobicity are based largely on data from liquid–liquid partition experiments or statistical data based on the appearance of amino acid residues in the interior *versus* the exterior of proteins of known three-dimensional structure. An extensive review of many scales of amino acid hydrophobicity is given by Cornette *et al.*[32]. However, in order to directly compare published hydrophobic parameters with the slope values in Table I, all of the amino acid values within a particular scale have been reassigned values such that the most hydrophobic amino acid of the group is assigned a value of -10.0 and the most hydrophilic amino acid of the group is assigned a value of 10.0. The remaining amino acids in each group are scaled proportionally.

Table II shows the scaled values of the dansyl amino acids based on the slope values of Table I (Lys, the ε-derivative, is not used in the correlation or the t-tests even though it appears in Table I). For comparison purposes, the intercept data ($\log k'_0$) have been scaled proportionally, along with two published hydrophobicity scales. One is based on octanol–water partition data[24] and the other on surface tension data[25]. The correlation coefficients between the scaled slope data from this study and the other scales are listed as well as the results of a paired t-test (comparing an experimental scale with the slope values from this study) at the 98% confidence interval. The t-test is important because two particular scales may show a good correlation ($r \geq 0.75$) but fail the paired t-test because the differences between the values assigned for each amino acid may be significant between the two scales chosen to be compared. As can be seen from Table II, there appears to be good agreement between the slope values and the two independent scales of amino acid relative hydrophobicities. Other published scales have also been found to show a good correlation with the slope data given here and their correlation coefficients are given in Table III (all values have been scaled

TABLE II

CORRELATIONS BETWEEN HIC PARAMETERS (EQN. 1, TABLE I) AND HYDROPHOBICITY SCALES

All scales have been normalized to range from −10.0 to 10.0 (most hydrophobic to most hydrophilic). See text.

Amino acid	*Slope (m)*	*Intercept (log k'_0)*	*Octanol–water*[a]	*Surface tension*[b]
Phe	−10.0	−5.8	−7.2	−9.0
Ile	−9.7	−6.0	−7.2	−8.5
Leu	−8.2	−3.9	−6.6	−10.0
Tyr	−7.1	−10.0	−2.1	−8.3
Val	−6.3	−1.4	−3.7	−3.1
Met	−6.3	2.2	−3.7	−2.4
Pro	−2.7	0.1	−0.6	1.3
Trp	−2.4	−5.1	−10.0	−6.6
Ala	1.0	5.2	1.9	7.2
Thr	2.2	7.0	2.2	4.8
Cys	2.6	−4.1	−5.6	5.3
Gln	3.5	7.8	5.2	10.0
Gly	4.4	1.2	3.8	8.8
Ser	4.7	6.2	4.0	5.8
Glu	6.0	9.7	7.7	6.5
Asn	6.4	8.9	7.5	9.4
His	7.2	4.5	3.0	7.9
Arg	8.4	9.6	10.0	7.9
Asp	10.0	10.0	8.5	7.2
Correlation coefficient	1.00	0.827	0.853	0.917
Paired *t*-test (98% C.I.)[d]		Do not reject[c]	Do not reject	Do not reject

[a] Ref. 24.

[b] Ref. 25.

[c] There is no significant difference between the paired values of the amino acids between the scale in question and the slope values.

[d] C.I. = Confidence interval.

proportionally as before for direct comparison). The high correlation between this retention-based scale and independently derived scales for hydrophobicity supports the assumption that the non-amino acid structural components of the dansyl derivatives contribute additively and independently to their chromatographic retention.

The slope values are used instead of the intercept values for the comparison to the other scales of relative amino acid hydrophobicity because the slope values for a particular dansyl amino acid did not vary significantly with chromatographic column usage, but the intercept values slowly decreased to lower values with continued column use. In other words, column degradation did not change the solute's contact area with the stationary phase, but did change the strength of the interaction systematically at all ammonium sulfate concentrations, including the zero intercept. Because of this, slope values are considered here to be more reliable than intercept values in comparing our data to parameters obtained by other investigators.

TABLE III

CORRELATION OF LITERATURE SCALES WITH SLOPE SCALE (TABLES I AND II)

Scale type	*Ref.*	*Correlation coefficient*
Octanol–water distribution	24	0.853
ΔG_{CH_2} from solution to air–aqueous interface	25	0.917
ΔG_{CH_2} from dilute aqueous solution to the vapor phase	26	0.680
Based on previously published tables	27	0.794
Combination of previously published tables	28	0.779
Average surrounding hydrophobicity	29	0.791
Fractional aqueous solvent exposure in proteins	30	0.718
Optimal matching hydrophobicities	31	0.926

Braumann *et al.*[23] have recommended the use of the intercept (the RPC capacity factor at 100% aqueous mobile phase) as a better measure of hydrophobicity than the use of the capacity factor (retention order), but go on to state that the slope as well as the intercept is largely dependent on the hydrophobic surface area of the solute. Minick *et al.*[33] argue, that in RPC the slope is a more reliable measure of the hydrophobic properties of a solute than the intercept.

Even with the small systematic error in intercept, a good correlation exists between the slope values (m) and intercept values ($\log k'_0$) in this study (Table II, $n = 19$, $r = 0.827$). This suggests that the slope and the intercept are dependent variables, both reflecting similar molecular properties of the solute.

However, the effect of salt on retention is not the only parameter to be considered in determining a solute's retention in HIC. In an HIC study of the retention of lysozymes isolated from related bird spcies, Fausnaugh and Regnier[11] find that pH affects the intercept of $\log k'$ *versus* molality plots, but not the slope. This is taken to indicate that the contact surface area is not altered, but the ionization state of the amino acids in the contact surface area modifies the intercept (the strength of the association of the solute with the stationary phase). Similarly, our studies on the hydrophobic interaction chromatography of small molecules[12] showed that while adenosine and adenosine 5'-monophosphate (AMP) appear to have parallel plots of $\log k'$ *versus* salt concentration in the mobile phase, AMP has a much lower intercept ($\log k'_0$). Heinitz *et al.*[34], in a study of the retention characteristics of proteins in HIC and ion-exchange chromatography, also find that electrostatic interactions appear to influence retention at the high ionic strengths used in HIC.

Therefore, it is apparent that both hydrophobicity and hydrophilicity affect HIC retention. A theoretical framework that can adequately express the combined influence of both a solute's hydrophobic and hydrophilic structural components on chromatographic retention remains to be developed.

ACKNOWLEDGEMENTS

This work was initiated with a Biomedical Research Grant from the NIH Division of Research Resources, and supported in its final stages by the National Science Foundation (grant CHE-8707592).

REFERENCES

1 D. L. Gooding, M. N. Schmuck, M. P. Nolan and K. M. Gooding, *J. Chromatogr.*, 359 (1986) 331.
2 S. C. Goheen and S. C. Engelhorn, *J. Chromatogr.*, 317 (1984) 55.
3 N. T. Miller, B. Feibush and B. L. Karger, *J. Chromatogr.*, 316 (1984) 519.
4 L. A. Kennedy, W. Kopaciewicz and F. E. Regnier, *J. Chromatogr.*, 359 (1986) 73.
5 M. Kunitani, D. Johnson and L. R. Snyder, *J. Chromatogr.*, 371 (1986) 313.
6 A. W. Purcell, M. I. Aguilar and M. T. W. Hearn, *J. Chromatogr.*, 476 (1989) 113.
7 J.-X. Huang, W. S. P. Bouvier, J. D. Stuart, W. R. Melander and Cs. Horváth, *J. Chromatogr.*, 330 (1985) 181.
8 R. Kalizsan, *Quantitative Structure–Chromatographic Retention Relationships*, Wiley, New York, 1987.
9 R. Kalizsan, *Chromatography*, 2, No. 5 (1987) 19.
10 C. T. Mant, T. W. L. Burke, J. A. Black and R. S. Hodges, *J. Chromatogr.*, 458 (1988) 193.
11 J. L. Fausnaugh and F. E. Regnier, *J. Chromatogr.*, 359 (1986) 131.
12 J. Gehas and D. B. Wetlaufer, *J. Chromatogr.*, 477 (1989) 249.
13 W. R. Melander and Cs. Horváth, *Arch. Biochem. Biophys*, 183 (1977) 200.
14 Cs. Horváth, W. R. Melander and I. Molnar, *J. Chromatogr.*, 125 (1976) 129.
15 G. Heydweiller, *Ann. Phys.*, 33 (1910) 145.
16 F. A. Long and W. F. McDevit, *Chem. Rev.*, 51 (1952) 119.
17 M.-I. Aguilar, A. N. Hodder and M. T. W. Hearn, *J. Chromatogr.*, 327 (1985) 115.
18 S. Terabe, H. Nishi and T. Ando, *J. Chromatogr.*, 212 (1981) 295.
19 N. T. Miller and B. L. Karger, *J. Chromatogr.*, 326 (1985) 45.
20 B. Yu. Zaslavsky, N. M. Mestechkina, L. M. Miheeva and S. V. Rogozhin, *J. Chromatogr.*, 240 (1982) 21.
21 B. Yu. Zaslavsky, L. M. Miheeva and S. V. Rogozhin, *Biochim. Biophys. Acta*, 588 (1979) 89.
22 M. Harnish, H. J. Möckel and G. Schulze, *J. Chromatogr.*, 282 (1983) 315.
23 T. Braumann, G. Weber and L. H. Grimme, *J. Chromatogr.*, 261 (1983) 329.
24 J. Fauchere and V. Pliska, *Eur. J. Med. Chem.*, 18 (1983) 369.
25 H. B. Bull and K. Breese, *Arch. Biochem. Biophys.*, 161 (1974) 665.
26 R. Wolfenden, L. Andersson, P. M. Cullis and C. C. B. Southgate, *Biochemistry*, 20 (1981) 849.
27 T. P. Hopp and K. R. Woods, *Proc. Natl. Acad. Sci. U.S.A.*, 78 (1981) 3824.
28 J. Kyte and R. F. Doolittle, *J. Mol. Biol.*, 157 (1982) 105.
29 P. Manavalan and P. K. Ponnuswamy, *Nature (London)*, 275 (1978) 673.
30 G. D. Rose, A. R. Geselowitz, G. J. Lesser, R. H. Lee and M. H. Zehfus, *Science (Washington, D.C.)*, 229 (1985) 834.
31 R. M. Sweet and D. Eisenberg, *J. Mol. Biol.*, 171 (1983) 479.
32 J. L. Cornette, K. B. Cease, H. Margalit, J. L. Spouge, J. A. Berzofsky and C. DeLisi, *J. Mol. Biol.*, 295 (1987) 659.
33 D. J. Minick, J. J. Sabatka and D. A. Brent, *J. Liq. Chromatogr.*, 10 (1987) 2565.
34 M. L. Heinitz, L. Kennedy, W. Kopaciewicz and F. E. Regnier, *J. Chromatogr.*, 443 (1988) 173.

Journal of Chromatography, 511 (1990) 131–136
Elsevier Science Publishers B.V., Amsterdam

CHROMSYMP. 1876

Simultaneous high-performance liquid chromatographic determination of amino acids in a dried blood spot as a neonatal screening test[a]

F. MORETTI, M. BIRARELLI, C. CARDUCCI , A. PONTECORVI and I. ANTONOZZI*
Genetic–Metabolic Disease Section, Department of Experimental Medicine, University "La Sapienza", Via dei Sabelli 108, 00185 Rome (Italy)
(First received June 25th, 1989; revised manuscript received February 2nd, 1990)

ABSTRACT

A new screening test on dried blood spots for inherited disorders of amino acid metabolism using reversed-phase high-performance liquid chromatography (RP-HPLC) is described. The method allows the simultaneous analysis of fourteen different amino acids; among these, seven whose blood levels are increased in the most important amino acid disorders have been determined. The procedure requires a preliminary extraction of the amino acids from 9-mm autoclaved dried blood spots by sonication in phosphate-buffered saline. A precolumn *o*-phthaldialdehyde–3-mercaptopropionic acid derivatization is then followed by analysis of the amino acids by RP-HPLC. Blood-spots levels of histidine (His), tyrosine (Tyr), valine (Val), methionine (Met), isoleucine (Ile), phenylalanine (Phe) and leucine (Leu) can be determined in a single 15-min run, including column washing and regeneration. The minimum detectable amount of each amino acid is 0.5 pmol with a linear dose–response range between 1 and 100 μM. The recovery for all amino acids is greater than 70% except for Met (66%). Up to 20 000 samples/year can be processed on a single automated analytical line resulting in an estimated cost of about US$ 0.25/sample. The multiple diagnostic capacity, the low cost and the possibility of complete automation of the method make it suitable for primary perinatal screening of amino acid disorders.

INTRODUCTION

Since 1963, bacterial inhibition assay has been the method of choice for the screening of inherited disorders of amino acid metabolism[1]. The main disadvantage of this test is the inability to detect simultaneously more than one amino acid disorder

[a] Presented at the *13th International Symposium on Column Liquid Chromatography, Stockholm, June 25–30, 1989*. The majority of the papers presented at this symposium have been published in *J. Chromatogr.*, Vols. 506 and 507 (1990).

0021-9673/90/$03.50

together with the lack of a precise quantification of the levels of the amino acid tested. The possibility of complete automation of the analytical procedure combined with low operating cost represents another necessary characteristic in order to keep the cost/benefit ratio of a screening programme low.

Several methods have been investigated with the purpose of establishing a test suitable for multiple screening of inherited amino acid disorders with high specificity and sensitivity, and the capacity to determine blood amino acid levels accurately; thin-layer[2] and ion-exchange chromatography[3,4] have been the most frequently used methods.

More recently, promising high-performance liquid chromatographic (HPLC) methods for amino acid analysis have been developed. Several techniques, based on precolumn amino acid derivatization in association with reversed-phase (RP) HPLC analysis, have recently been described[5–8].

In this paper we present a micromethod based on precolumn *o*-phthaldialdehyde derivatization of amino acids that allows the RP-HPLC separation of fourteen amino acids; the levels of seven of them (histidine, tyrosine, valine, methionine, isoleucine, phenylalanine and leucine) which are increased in the most frequent aminoacidopathies, were determined after direct extraction from 9-mm dried blood spots.

EXPERIMENTAL

L-Amino acid crystalline salts and *o*-phthaldialdehyde (OPA) were obtained from Sigma (St. Louis, MO, U.S.A.), HPLC-grade solvents from Carlo Erba (Milan, Italy) and 3-mercaptopropionic acid (3-MPA) from Merck (Darmstadt, F.R.G.). The HPLC system consisted of a Pharmacia-LKB (Uppsala, Sweden) 2152 automated gradient controller and two Pharmacia-LKB 2150 HPLC pumps, a Rheodyne (Berkeley, CA, U.S.A.) injector equipped with a 20-μl loop, a Violet (Rome, Italy) T-55 temperature controller, a Kontron (Zurich, Switzerland) SFM 25 spectrofluorimeter, a Kontron 460 autosampler and a Shimadzu (Kyoto, Japan) C-R3A integrator.

Dried blood spots of 9 mm diameter were autoclaved at 120°C for 3.5 min and amino acids eluted by sonication for 1 h in 200 μl of phosphate-buffered saline (PBS) of pH 7.2. The eluate was then subjected to a two-step derivatization procedure: first, 4 μl of OPA–3-MPA [25 mg of OPA in 4.5 ml of methanol plus 0.5 ml of 50 m*M* borate buffer (pH 9.5) plus 50 μl of 3-MPA] were added to 20 μl of the eluate in 100 μl of 50 m*M* borate buffer (pH 9.5); after incubation for 1 min at room temperature, 76 μl of 0.1 m*M* phosphate buffer (pH 6.5) were added followed by the immediate injection of 20 μl of the solution into the HPLC system.

A Spherisorb ODS-2 (3 μm) column (15 cm × 0.46 cm I.D.) was used in conjunction with a Spherisorb ODS-2 (5 μm) guard column (5 cm × 0.46 cm I.D.) (Phase Separations, Waddinxveen, The Netherlands). Both columns were maintained at a constant temperature of 35°C. The flow-rate was 0.8 ml/min and the mobile phase consisted of solvent A, 12 m*M* phosphate buffer (pH 7.2), and solvent B, acetonitrile–water (70:30), mixed according to the scaled composition profile shown in Fig. 1.

RESULTS

Under the experimental conditions used, a good separation of threonine (Thr), histidine (His), citrulline (Cit), alanine (Ala), taurine (Tau), arginine (Arg), tyrosine (Tyr), valine (Val), methionine (Met), isoleucine (Ile), phenylalanine (Phe), ornithine (Orn), leucine (Leu) ad lysine (Lys) was achieved in 13 min (Fig. 1). Among these compounds, our interest is mainly on the determination of the amino acids whose levels are increased in the more frequent aminoacidopathies, *viz.*, His, Tyr, Val, Met, Ile, Phe and Leu.

Different analytical conditions were tested to establish the most efficient extraction of the various amino acids from dried blood spots; the autoclaving time, elution volume and elution time were examined. The minimum autoclaving time required for complete protein fixation to the paper discs was 3.5 min. The extraction of the amino acids from the paper discs was independent of the volume of the eluent in the range 150–400 l, and sonication for longer than 1 h lowered the amino acid recovery, probably because of their degeneration. For a similar reason the eluted amino acids must be kept at 4°C before the derivatization step.

The sensitivity of the method allowed the detection of 0.5 pmol of each amino acid. The dose–response relationship for the seven amino acids in the range 1–100 μM showed a correlation coefficient of greater than 0.999 for all the amino acids tested (Fig. 2).

The recovery of the method was evaluated by adding different amounts of a standard mixture of the various amino acids to a blood sample with known amino

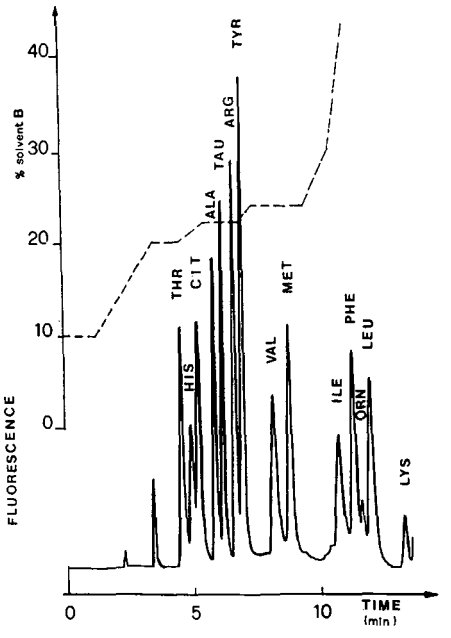

Fig. 1. Chromatogram of a 50 μM standard solution showing the separation of fourteen amino acids. Fluorescence: excitation 270 nm, emission 475 nm.

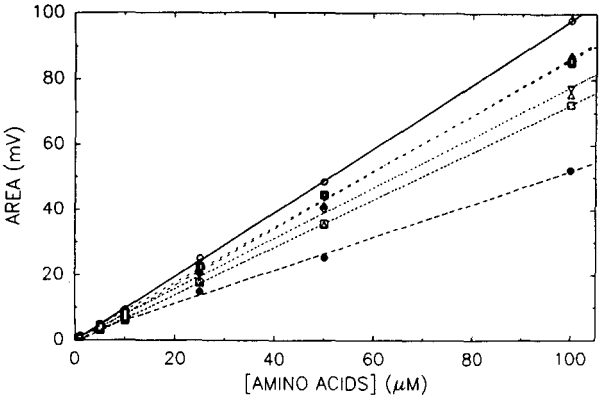

Fig. 2. Linear regression analysis between amino acid concentration and area in mV for (○) Tyr, (●) His, (△) Val, (▲) Met, (□) Ile, (■) Phe and (▽) Leu. The linear correlation coefficients ranged from $r = 0.9990$ for His to 0.9998 for Leu.

acid concentration, followed by spotting on 9-mm paper discs, extraction and analysis as described previously. The mean percentage recovery for each amino acid was calculated at five different concentrations (50, 100, 200, 500 and 1000 μM). The

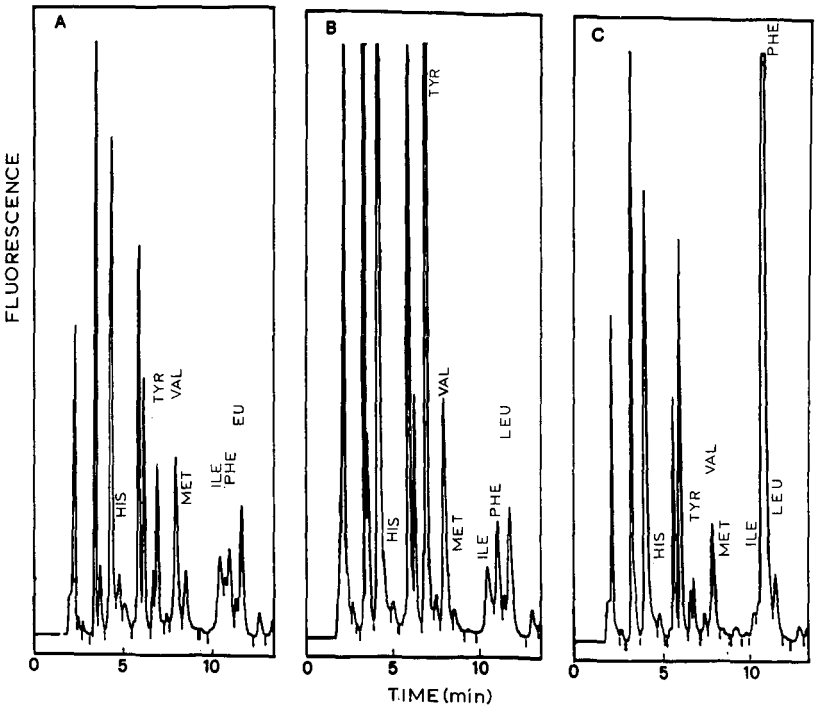

Fig. 3. Chromatograms obtained from (A) a normal newborn and newborns affected by (B) neonatal hypertyrosinaemia (Tyr = 472 μM) and (C) phenylketonuria (Phe = 594 μM). Fluorescence: excitation 270 nm, emission 470 nm.

recovery did not vary significantly in the concentration range investigated; the mean recoveries were His 70 ± 6, Tyr 76 ± 8, Val 87 ± 9, Met 66 ± 6, Ile 97 ± 5, Phe 77 ± 7 and Leu 91 ± 4% (mean ± S.D. for ten determinations at each concentration).

The method was field tested by analysing dried blood spots obtained from a perinatal multiple screening programme for inherited metabolic diseases. As shown in Fig. 3, a good discrimination among controls, phenylketonuric and hypertyrosinaemic newborns was achieved.

DISCUSSION

The basic requirements in a screening programme for inherited diseases are to keep the costs low together with the possibility of screening a wider range of diseases. It is impossible to obtain such a compromise with the traditional bacterial inhibition assay. Inherited disorders of amino acid metabolism have a very different incidence among the neonatal population, from about 1:10 000 for phenylketonuria[9], the most common amino acid disease, to 1:226 000 for maple syrup urine disease[10] and 1:354 000 for homocystinuria[11]. Disorders with such a low incidence are generally not included in screening programmes because of a low cost/benefit ratio.

The micromethod described here allows the simultaneous separation of different amino acids starting from a 9-mm dried blood spot. The method in fact also allows the determination of several other amino acids. It is therefore theoretically possible to screen the neonatal population simultaneously for a wide range of amino acid disorders such as phenylketonuria, tyrosinaemia, maple syrup urine disease, homocystinuria, histidinaemia, urea cycle disorders, hyperornithinaemia and hyperlysinaemia, resulting in an overall probability of detection of an amino acid disorder in at least 17 out of 100 000 newborns screened, without considering neonatal hypertyrosineaemia.

Other HPLC methods applied to amino acid analysis starting from dried blood spots described so far have been oriented towards the identification of tyrosine and phenylalanine[12,13]. These methods are time consuming and cumbersome when applied to large numbers of samples. Most of them require a two-step extraction of the sample by elution of the whole blood from the paper disc followed by amino acid extraction[12–14].

The proposed method allows the direct extraction of amino acids from a large number of dried spots at the same time and the analysis of each sample by HPLC in a total period of 15 min including column washing and regeneration. This accomplishment is important as previously reported methods had analysis times ranging from 8[12] to 20 min[13] for Tyr and Phe or about 80 min for 18 amino acids[14]. The use of an autosampler linked to the analytical line allows more than 90 samples/day to be processed with an estimated cost for each sample of about US$ 0.25.

REFERENCES

1 R. Guthrie and A. Susi, *Pediatrics*, 32 (1963) 338.
2 K. Adriaenssens, R. Van Heule and M. Van Belle, *Clin. Chim. Acta*, 15 (1967) 362.
3 M. Bonnafè, C. Charpentier and A. Lemmonier, in J. Laturaze, J. Chouteau, J. C. Serre and A. Favier (Editors), *Les Aminoacidopathies*, Domain de la Merci, Grenoble, 1972, p. 196.
4 I. Antonozzi, G. Santagata and R. Tofani, *Ricerca*, 12 (1982) 507.

5 C. Fonck, S. Frutiger and G. J. Hughes, *J. Chromatogr.*, 370 (1986) 339.
6 Y. Watanabe and K. Imai, *Anal. Biochem.*, 116 (1981) 471.
7 I. Betnér and P. Foldi, *Chromatographia*, 22 (1986) 381.
8 T. A. Graser, H. G. Godel, S. Albers, P. Foldi and P. Furst, *Anal. Biochem.*, 151 (1985) 142.
9 I. Antonozzi, R. Dominici, F. Monaco and M. Andreoli, *J. Endocrinol. Invest.*, 4 (1980) 357.
10 E. W. Naylor, in H. Bickel, R. Guthrie and G. Hammersen (Editors), *Neonatal Screening for Inborn Errors of Metabolism,* Springer, Berlin, 1980, p. 19.
11 D. H. H. Pullon, in H. Bickel, R. Guthrie and G. Hammersen (Editors), *Neonatal Screening for Inborn Errors of Metabolism,* Springer, Berlin, 1980, p. 29.
12 J. L. Rudy, J. C. Rutledge and L. S. Lewis, *Clin. Chem.*, 33 (1987) 1152.
13 R. A. Roesel, P. R. Blankenship and F. A. Hommes, *Clin. Chim. Acta,* 156 (1986) 91.
14 Y. Watanabe and K. Imai, *J. Chromatogr.*, 309 (1984) 279.

Journal of Chromatography, 511 (1990) 137–145
Elsevier Science Publishers B.V., Amsterdam

CHROM. 22 321

Bioanalysis of the peptide des-enkephalin-γ-endorphin

On-line sample pretreatment using membrane dialysis and solid-phase isolation

D. S. STEGEHUIS, U. R. TJADEN* and J. VAN DER GREEF
Division of Analytical Chemistry, Center for Bio-Pharmaceutical Sciences, University of Leiden, P.O. Box 9502, 2300 RA Leiden (The Netherlands)
(First received July 18th, 1989; revised manuscript received December 18th, 1989)

ABSTRACT

Des-enkephalin-γ-endorphin is a neuroleptic endogenous peptide that is active in the central nervous system in extremely low concentrations. The pharmacokinetics of this peptide could not be studied in detail as a bioanalytical method for determining endogenous levels of this peptide in biological matrices was not available. Liquid chromatography with fluorescence reaction detection in principle offers sufficient sensitivity for this application, provided that a selective sample pretreatment can be performed. The development of a pretreatment method for plasma samples is described. After protein precipitation with trichloroacetic acid, high-molecular-weight compounds are removed using on-line continuous-flow dialysis. After dialysis, polar low-molecular-weight compounds, including those containing amino functions, are removed by solid-phase isolation, while simultaneously the analyte is concentrated. By means of valve switching the pretreatment system is coupled on-line to the liquid chromatographic system. With the developed system it is possible to determine des-enkephalin-γ-endorphin in plasma in the range 10–100 ng/ml.

INTRODUCTION

Des-enkephalin-γ-endorphin (DEγE) or β-endorphin(6–17) is an endogenous non-opoid γ-type endorphin and may be considered as a neuroleptic-like compound in the central nervous system with antipsychotic activity in schizophrenic patients[1,2]. It is active in very low concentrations. The uptake by the brain of this neuropeptide appears to be relatively low; a maximum of *ca.* 2% of an intravenously administered dose has been reported[3]. The disappearance of DEγE from plasma after an intravenous injection can be described by a one-compartment model and the resulting half-life is about 2 min. Degradation products of DEγE in plasma are formed by carboxypeptidase and aminopeptidase activity[3,4]. The main metabolites are β-en-

0021-9673/90/$03.50

dorphin(7–17) and β-endorphin(8–17)[5]. The exact working mechanism of DEγE cannot be investigated until a bioanalytical method is available for determining endogenous levels of this peptide in biological matrices.

For more detailed pharmacokinetic studies there is a need for a selective and sensitive bioanalytical method. Plasma samples contain low concentrations of the analyte peptide in combination with high concentrations of interfering compounds that are similar to the analyte, that degrade it and interfere with the bioanalysis. Plasma levels down to the sub-ng/ml range have to be measured. A method based on post-column derivatization with *o*-phthaldialdehyde (OPA) and fluorescence detection is in principle sensitive enough for this application. However, a selective pretreatment method is required, which can only be achieved by combining a number of pretreatment steps. So far no bioanalysis permitting the determination of DEγE in plasma in the low-ng/ml range has been described, apart from a radioimmuno assay method[3].

This paper describes a method that uses deproteination of the sample with trichloroacetic acid in order to stabilize the samples, continuous-flow dialysis to remove interfering compounds with a molecular weight above 10 kDa and an on-line solid-phase isolation (SPI) on XAD-2 between the dialysis and the liquid chromatographic (LC) step to concentrate the analyte. All manipulations can be automated, except the stabilization step, which has to be performed as soon as possible after the sample is taken. The LC system consists of a reversed-phase C_{18} column and an acetonitrile and phosphate buffer gradient.

EXPERIMENTAL

Equipment

The continuous-flow system consisted of a Skalar (Breda, The Netherlands) Model 1 autosampler with solvent flux tubing and a Skalar Model 202 peristaltic pump. The polystyrene autosampler tubes had a volume of 3.5 ml. The dialysis was performed with a Skalar Model 5275 70-cm Perspex dialysis block equipped with a Type C cellulose membrane. The precolumn was a stainless-steel cartridge (3.0 cm × 2.0 mm I.D.) packed manually with XAD-2 in methanol under reduced pressure. The valve-switching system was a MUST (Spark Holland, Emmen, The Netherlands) equipped with two six-port switching valves (Model 7001; Rheodyne, Berkeley, CA, U.S.A.).

Injections were performed with a Rheodyne fixed-volume (100 μl) Model 7125 injection valve. The LC gradient system consisted of two dual-piston high-pressure pumps (Spectroflow 400; Kratos, Ramsey, NJ, U.S.A.) controlled by an SF 450 programmer (Kratos). A laboratory-made hogh-pressure mixing device with an internal volume of about 400 μl and equipped with a stirring magnet was applied to mix the effluent of the two pumps. The analytical column was a glass cartridge (10 cm × 3.0 mm I.D.) packed with Chromospher C_{18} (5-μm particles) (Chrompack, Middelburg, The Netherlands). The post-column derivatization device consisted of a Model P-35 high-pressure pump (Pharmacia, Uppsala, Sweden). A stainless-steel reaction coil (4 μm I.D.) was spirally wound with O.D. *ca.* 2 cm and an internal volume of *ca.* 0.6 ml. A stainless-steel dead-volume mixing device (Upchurch Scientific, Oak Harbor, WA, U.S.A.) was applied for mixing of the effluent and the derivatization

reagent. Fluorescence detection was performed with a Perkin-Elmer (Beaconsfield, U.K.) LS-4 detector using an excitation wavelength of 334 nm, an emission wavelength of 455 nm and a slit width of 5 nm. Chromatograms were recorded with an electronic integrator (Model C-R3A; Shimadzu, Kyoto, Japan).

Materials

DEγE was donated by Organon International (Oss, The Netherlands). Trichloroacetic acid was obtained from Baker Chemicals (Deventer, The Netherlands), mercaptoethanol and *o*-phthaldialdehyde from Fluka (Buchs, Switserland) and LC-grade acetonitrile from Rathburn (Walkerburn, U.K.). The phosphate buffers were composed of different volumes of 0.01 mol/l phosphoric acid and 0.01 mol/l disodium hydrogenphosphate (Brocacef, Maarsen, The Netherlands). The borate buffers were mixtures of 0.1 mol/l sodium tetraborate and 0.01 mol/l sodium hydroxide (Merck, Darmstadt, F.R.G.). Deionized water (Milli-Q water purification system; Millipore, Bedford, MA, U.S.A.) and capped polopropylene vials (Greiner, Alphen a/d Rijn, The Netherlands) were used for all peptide-containing solutions. Amberlite XAD-2 (Rohm and Haas, Philadelphia, PA, U.S.A.) with a particle size range of 20–30 μm was applied. Prefabricated normal-phase, reversed-phase and ion-exchange precolumns (Analytichem, Harbor City, CA, U.S.A.) were used.

Protein precipitation

The protein precipitation experiments were performed with 1-ml plasma samples spiked with 1 ng/ml of the analyte. The plasma sample was mixed with 2 ml of methanol, ethanol or acetonitrile or with 300 μl of trichloroacetic acid or perchloric acid. After vortex mixing for 10 s the mixtures were centrifuged for 10 min (2500 *g*) and subsequently the supernatant was transferred to the polypropylene autosampler vials and analysed by the described system. Some samples were analysed immediately and others after 3 h or after 3 days. The deproteinated samples were stored after centrifugation at −10°C.

On-line dialysis

The on-line dialysis experiments were performed with the deproteinated plasma samples. The pH of the supernatant (650 μl) was adjusted to 5.7 with 350 μl of 0.1 mol/l borate buffer in the autosampler vials. The whole sample was transported to the dialysis block. The inside diameters of the tubing were chosen to result in a flow of the donor (sample) stream of 0.32 ml/min and with a flow-rate of 0.42 ml/min of the acceptor (water) stream. The donor stream was segmented with air at 0.16 ml/min. The system was used in the countercurrent mode. In this way the dialysis took about 15 min. The acceptor stream was loaded on the XAD-2 column in about 3 min.

Solid-phase isolation

XAD-2 was used in an on-line trapping and isolation column. The column was used as an interface between the dialysis system and the LC system. By switching the MUST unit the sample was transferred from one system to the other.

Chromatographic system and detection

Chromatography was performed with a C_{18} analytical column in combination

with gradient elution. Eluent A was 0.05 mol/l phosphate buffer (pH 2.4) and eluent B was 0.05 mol/l phosphate buffer (pH 2.4)–acetonitrile (50:50, v/v). A step gradient was applied: 2 min 15% B, 2 min 40% B, 6 min 75% B and finally 2 min 15% B. With 15% B the analyte did not elute from the XAD-2; with 40% B the analyte was eluted from the XAD-2 to the analytical column.

The reagent solution for the post-column OPA derivatization consisted of 2 ml of borate buffer (pH 9.5), 9 mg of OPA and 300 μl of mercaptoethanol. The flow in the post-chromatographic derivatization unit was 0.75 ml/min and was established by an eluent flow-rate of 0.5 ml/min and a reagent flow-rate of 0.25 ml/min.

RESULTS AND DISCUSSION

The peptide DEγE is unstable in enzyme-containing matrices. Therefore, the first priority is the enzyme deactivation by deproteination in order to stabilize the analyte concentration in the sample. Another important aspect during the bioanalytical procedure is to avoid the use of glass vessels because DEγE is adsorbed to polar surfaces such as glass.

The molecular weight of DEγE is 1304 so it can be separated from all high-molecular-weight compounds by ultrafiltration or dialysis. In this study, the possibilities of on-line continuous-flow dialysis were investigated[6]. The advantages of this method are an absolute cut-off value at molecular weight 10 000 and the fact that the method can be performed on-line, which is advantageous with respect to reproducibility and labour intensity.

DEγE possesses two primary amino functions and two carboxylic acid functions. The isoelectric point is at pH 5.7. These characteristics combined with its polarity and hydrophobicity make it possible to separate the peptide from the remaining low-molecular-weight compounds using SPI and LC. As the post-column OPA derivatization is specific for primary amino-containing compounds, the sample has to be purified to remove these as much as possible. With respect to the strong dilution that takes place during the dialysis, the most suitable purfication step is a solid-phase isolation using a reversed-phase material such as XAD-2. The preconcentration column can be installed in a valve switching unit and the sample can be loaded on the XAD-2 and introduced automatically into the LC system where it is eluted by an acetonitrile gradient[7].

Sample stabilization

Deproteination of 1 ml of plasma by adding 2 ml of an organic solvent such as methanol, ethanol and acetonitrile appeared not to be sufficient for complete inhibition of the enzyme activity. Even immediately after such a protein precipitation, degradation of DEγE could be observed. A few minutes after deproteination the recovery had been reduced to about 5%, and decreased further as a function of time.

Precipitation with either 1 mol/l perchloric acid (PCA) or 1 mol/l trichloroacetic acid (TCA) appeared to be superior to the former method. With neither precipitating agent was any analyte degradation observed, but addition of TCA resulted in more precipitate while the supernatant was more transparent. The amount of interfering compounds was minimal after deproteination with TCA.

A sample of 1 ml of plasma deproteinated by adding 300 μl of 1 mol/l TCA was

stable after 3 h and even after 3 days no degradation of the analyte was observed. TCA has only a limited buffer capacity, so pH adjustments are facile. In addition, there will be no problem with respect to the compatibility with the dialysis, which should be a problem after deproteination with organic solvents (the cellulose membrane dissolves in organic solvents). The recovery of the analyte after the precipitation with TCA is about 85%. The loss is probably due to inclusion in the precipitate and adsorption on precipitated matrix compounds. This was confirmed by assaying samples that were spiked after enzyme deactivation, but before the vortex mixing and centrifugation. Possible decreases in recovery appeared to be due to precipitation and adsorption and not to degradation.

On-line dialysis

The system was equipped with a cellulose membrane with a molecular mass resistance of 10 000 Da. The recovery of the analyte is determined by the contact time between the donor and the acceptor stream (the actual dialysis time). This contact time depends on the flow of the donor and acceptor stream and whether the concurrent or the countercurrent mode is applied. In the concurrent mode the donor and acceptor streams flow in the same direction and, assuming equal flow-rates, equilibrium can be obtained between the donor and acceptor streams. After an infinite dialysis time the theoretical maximum recovery of 50% can be achieved. In the countercurrent mode the donor and acceptor streams flow in opposite directions. In this way the dialysis can be exhausting, resulting in a recovery of 100%. Unfortunately, increasing the recovery of the analyte by prolonging the contact time between the donor and acceptor streams does not result in an improved selectivity, as the ratio between the analyte and background is constant at all recoveries.

Air segmentation of the donor stream is performed to avoid contamination of subsequent samples, to limit sample dispersion and to optimize the flow pattern towards the membrane by convective mixing in each liquid compartment. This is not of importance for the acceptor stream because it is concentrated after the dialysis on the trapping column.

The influence of the ionic strength and the pH on the dialysis was investigated. The best results were obtained when both the donor and the acceptor streams had minimum ionic strength. If a significant difference in ionic strength exists between the donor and acceptor streams this results in a water flow through the membrane, resulting in pressure irregularities which influence the flow and thereby the dialysis time. Buffer solutions with molarities varying from 0.001 to 0.1 were used as donor and acceptor streams while the recovery of DEγE was monitored. The influence of pH was caused by the charge of the analyte. DEγE is an ampholite with five possible charge stages. At pH < 2 it is charged $2+$, at about pH 4 the charge is $1+$, the isoelectric point is at pH 5.7, at about pH 8 it is charged $1-$ and at pH > 11 it is charged $2-$. Because there are polarizable functions present on the membrane the dialysis should be performed at the isoelectric point of the analyte (pH 5.7). In this case adsorptions and electric repulsions will be minimized (Fig. 1). This was done with buffer solutions of different pH so that the recovery of DEγE could be determined at all its possible charge stages. At the optimum solvent composition the concurrent and countercurrent modes were compared just like segmented and unsegmented donor and acceptor streams. Although dialysis is normally a time-consuming procedure, on-line dialysis applying

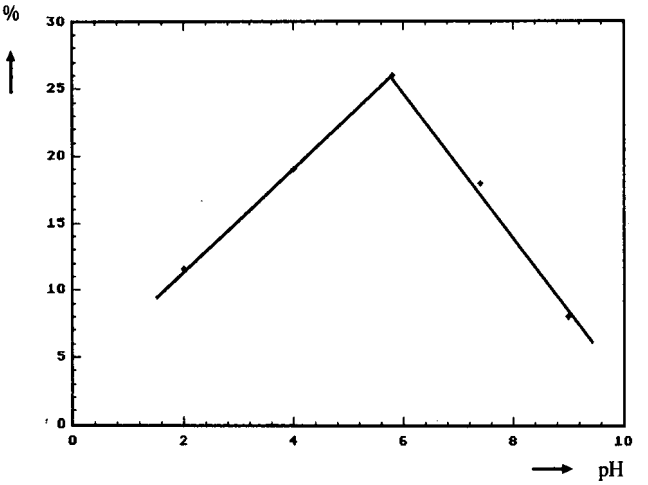

Fig. 1. Recovery of DEγE as a function of the pH of the donor stream in the continuous-flow dialysis system.

a continuous-flow system permits the reproducible removal of proteins in about 15 min with a recovery of the peptide of 25%, applying optimum conditions, *i.e.*, use of the countercurrent mode, an air-segmented donor stream, minimum ionic strength of the donor and acceptor streams and dialysis at the isoelectric point of the analyte peptide (pH 5.7). The overall recovery, determined by assaying a standard solution of DEγE, by performing the complete sample pretreatment, *i.e.*, on-line dialysis, solid-phase isolation and heart-cutting of the gradient run, was 25.0 ± 0.9%, independent of the concentration range studied (10 ng/ml–5 μg/ml). When the dialysis took place at a sample pH of 2, caused by addition of TCA, the recovery was only 12%.

Solid-phase isolation

In principle, on-line dialysis is not compatible with LC because of the relatively large dilution inherent to on-line dialysis. Therefore, preconcentration of the sample should be executed before it can be analysed using LC. In fact, the solid-phase isolation is the interface between the (strongly diluting) dialysis and the (small injection volume demanding) chromatography.

Our objective was to combine precolumn concentration of the dialysed sample and removal of most of the low-molecular-weight compounds containing a primary amino group such as amino acids and biogenic amines that can interfere with the final detection. In order to use the precolumn for this purpose the analyte should be adsorbed on the sorbent, whereafter most of the interfering compounds are eluted from the column and finally the analyte is selectively eluted from the precolumn. The most important parameters are the breakthrough volume (this volume should be large enough to concentrate the sample after the dialysis and to wash the column without losing the analyte) and the elution volume (the amount of solvent needed to elute the analyte). The breakthrough volume should be as large as possible while the elution volume should be minimal.

To find the most suitable column material for the solid-phase isolation a number

of normal-phase, reversed-phase and ion-exchange materials were investigated. The polymeric neutral resin XAD-2 appeared to be most suitable in combination with the on-line dialysis system, as the capacity ratio of the analyte on the precolumn is sufficiently high ($k' > 10$) to concentrate the aqueous 10 ml of the dialysed sample. The capacity factor of DEγE was determined on this material by loading an aqueous sample of DEγE on the XAD-2 column and eluting it with different percentages of acetonitrile (Fig. 2). The elution of the analyte could be done in a small fraction of about 0.5 ml with a mixture of phosphate buffer containing at least 15% of acetonitrile (Fig. 2). This fraction was directly eluted to the analytical column. The hydrophobic reversed-phase material XAD-2 in a precolumn of length 3.0 cm is able to concentrate the acceptor stream fraction of about 10 ml and to isolate the analyte from most of the amino acids without influencing the elution profile.

Total system

Apart from the off-line enzyme deactivation step, which must be performed as soon as possible after blood sampling, the other steps of the sample pretreatment were combined in an on-line system (Fig. 3). Deproteinated samples are transported to the dialysis system by means of a peristaltic pump.

After removal of the macromolecules, the sample is concentrated on the XAD-2 column, where interfering low-molecular-weight compounds are removed to a considerable extent. Subsequently the analyte-containing fraction is eluted to the analytical column where it is separated from related compounds, derivatized in the post-column mode and detected by fluorescence detection. Using this method, the analysis of one sample takes about 45 min. Because the total procedure is performed in the on-line mode, the method has minimum labour requirements.

With continuous analyses every 30 min, samples can be analysed during 24 h a day. As in most continuous-flow systems the reproducibility is an advantage. At a level of 250 ng/ml DEγE in plasma the relative standard deviation (R.S.D.) was 2.7%

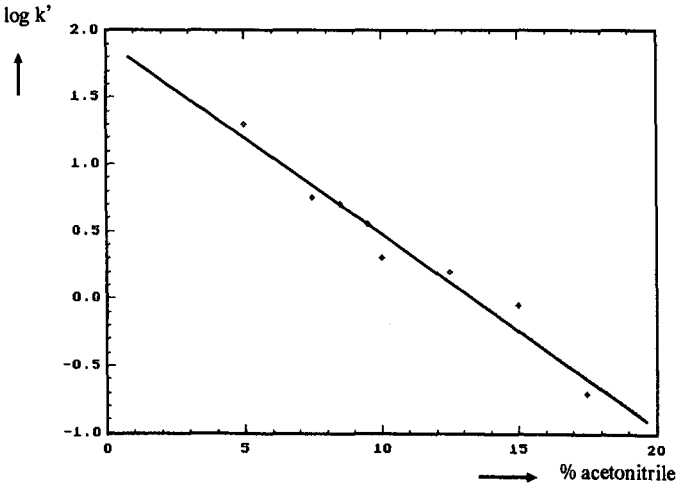

Fig. 2. Capacity ratios (k') for DEγE on the 30 mm × 2 mm I.D. XAD-2 precolumn as a function of the acetonitrile content of the mobile phase.

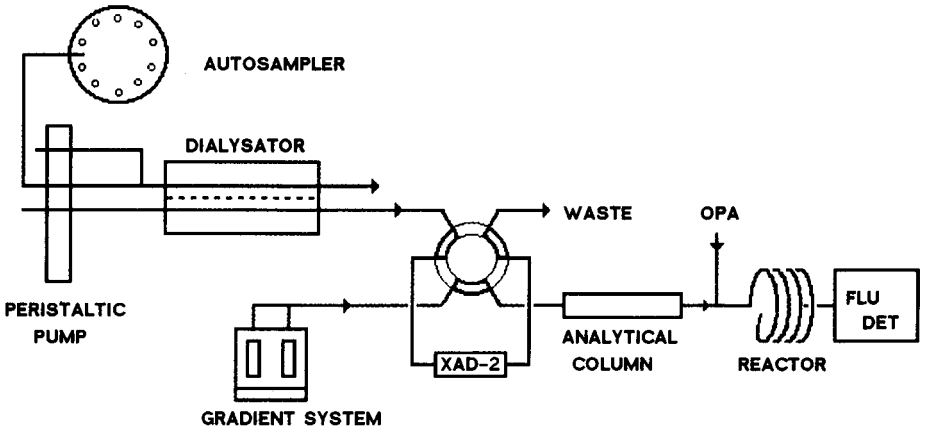

Fig. 3. Scheme of total pretreatment procedure. FLU DET = Fluorescence detector.

(n = 5), which is acceptable for this type of analysis. At lower levels (50 ng/ml DEγE) the R.S.D. was 5.9% (n = 5). Some results are shown in Fig. 4.

The large hump in the chromatograms, also in the chromatogram of an aqueous solution without DEγE (see Fig. 4A), is caused by the acetonitrile gradient, which is present even when freshly distilled acetonitrile is used. In our opinion this phenomenon is caused by the gradient elution of strongly hydrophobic compounds that are adsorbed from the mobile phase and previously injected samples, and that are in fact enriched in the so-called on-column mode. It must be emphasized that all constituents of the mobile phase were of high analytical purity and that the water used was highly purified. Fig. 4B shows the chromatogram obtained from a plasma sample spiked with

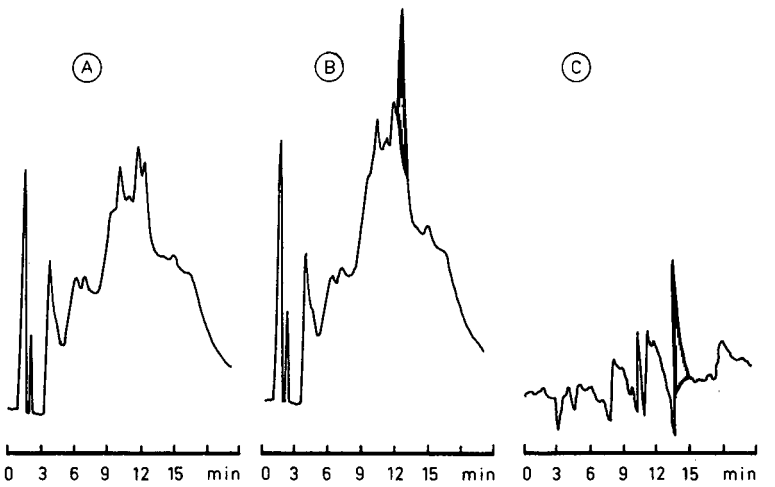

Fig. 4. Chromatograms of plasma samples treated according to the described procedure. (A) Blank plasma; (B) plasma spiked with 100 ng/ml DEγE; (C) differential chromatogram of plasma spiked with 10 ng/ml DEγE and blank plasma. Injection volume, 500 μl of plasma. For other conditions, see text.

100 ng/ml of DEγE. Apparently smaller amounts cannot be determined, but by applying electronic background subtraction with the integrator a differential trace is obtained, as shown in Fig. 4C. In this instance the blank gradient run (Fig. 4A) is subtracted from the chromatogram obtained from a plasma sample spiked with 10 ng/ml of DEγE.

In spite of the hump in the baseline, a calibration graph could be generated without any problem in the concentration range 10–500 ng/ml DEγE in plasma. A typical calibration graph, represented by the equation $y = 2.47x + 14.6$ with a correlation coefficient of 0.9991, where x and y are the concentration in ng and the peak height in arbitrary units, respectively, was generated by analysing blank plasma samples spiked in the concentration range mentioned above. In the spiked samples and blank it is shown that the method is selective enough for this concentration range (10–100 ng/ml).

CONCLUSIONS

The method described, based on continuous-flow dialysis, solid-phase isolation, LC separation and fluorescence reaction detection with OPA, permits the measurement of plasma samples containing DEγE down to 10–100 ng/ml. To lower this detection limit the selectivity of the sample pretreatment procedure would have to be increased by applying methods with greater selectivity at higher recoveries, *e.g.*, gel filtration or electrophoresis. The sensitivity of detection may then be further increased by using laser-induced fluorescence detection[8]. Further work in these directions is in progress.

REFERENCES

1 D. de Wied, *Trends Neurosci.*, 2 (1979) 79.
2 W. M. A. Verhoeven, J. M. van Ree, A. Heezius van Bentum, D. de Wied and H. M. van Praag, *Arch. Gen. Psychiatry*, 39 (1982) 648.
3 J. C. Verhoef, H. Scholtens, E. G. Vergeer and A. Witter, *Peptides*, 6 (1985) 467.
4 D. de Wied, J. M. van Ree and H. M. van Gerven, *Life Sci.*, 26 (1980) 1575.
5 P. S. L. Janssen, J. W. van Nispen, P. A. T. A. Melgers and R. L. A. E. Hamelinck, *Chromatographia*, 21 (1986) 461.
6 U. R. Tjaden, E. A. de Bruijn, R. A. M. van der Hoeven, C. Jol, J. van der Greef and H. Lingeman, *J. Chromatogr.*, 420 (1986) 53.
7 U. R. Tjaden, D. S. Stegehuis, H. J. E. M. Reeuwijk, H. Lingeman and J. van der Greef, *Analyst (London)*, 113 (1987) 171.
8 C. M. B. van den Beld, H. Lingeman, G. J. van Ringen, U. R. Tjaden and J. van der Greef, *Anal. Chim. Acta*, 205 (1988) 15.

Journal of Chromatography, 511 (1990) 147–153
Elsevier Science Publishers B.V., Amsterdam

CHROM. 22 430

Separation of human apolipoproteins A-IV, A-I and E by reversed-phase high-performance liquid chromatography on a TSK Phenyl-5PW column

TIM TETAZ* and ELAINE KECORIUS
Baker Medical Research Institute, Commercial Road, Prahran, Melbourne, Victoria 3181 (Australia)
BORIS GREGO
Applied Biosystems, 26 Harker Street, Burwood, Victoria 3125 (Australia)
and
NOEL FIDGE
Baker Medical Research Institute, Commercial Road, Prahran, Melbourne, Victoria 3181 (Australia)
(First received November 14th, 1989; revised manuscript received March 5th, 1990)

ABSTRACT

A method has been developed for the rapid separation of the medium-molecular-weight apolipoproteins A-IV, A-I and E by high-performance liquid chromatography. Separations were achieved using a commercially available column of very low hydrophobicity (TSK Phenyl-5PW) in the reversed-phase mode rather than the conventional mode of hydrophobic interaction. Delipidated apolipoproteins were dissolved in 20 m*M* orthophosphoric acid (pH 2.3), applied to the column which was pre-equilibrated with the same buffer, and eluted with an increasing gradient of acetonitrile. Purified apolipoproteins were identified by a combination of sodium dodecyl sulphate–polyacrylamide gel electrophoresis, amino acid analysis and N-terminal sequence analysis. In one step the method can be used to separate the major human chylomicron apolipoproteins A-IV, A-I and E, following preliminary removal of apolipoprotein A-II and the C apolipoproteins by size-exclusion chromatography.

INTRODUCTION

Purification of the various plasma apolipoproteins (apo) has enabled investigation of their structure and function and consequently the assignment of physiological roles to many of them[1]. Of special interest to this laboratory has been the separation of the medium-molecular-weight apolipoproteins, apo A-IV, apo A-I and apo E. These proteins have traditionally been purified by a series of steps including size exclusion, anion exchange or chromatofocussing[2–6], usually in the presence of denaturants such as urea or guanidinium hydrochloride. However, none of these techniques alone produces satisfactory purification of apolipoproteins and most lipoprotein labora-

0021-9673/90/$03.50

tories use preparative gel electrophoresis as a final step to obtain homogeneous preparations of apolipoproteins, particularly when these proteins are needed for antibody production or functional investigations. More recently, two groups[7,8] have described the application of reversed-phase high-performance liquid chromatography (RP-HPLC) to the separation of apolipoproteins. These groups have used standard reversed-phase columns of high hydrophobicity (C_{18}) in order to separate apo A-IV from apo A-I (ref. 8) or apo A-I from apo E (ref. 7). In our hands, the use of such columns does not allow the efficient separation of apo A-IV, apo A-I and apo E in a single chromatographic step. We have, however, developed a method which achieves such a separation by the unconventional use of a column (TSK Phenyl-5PW) of much lower hydrophobicity than the standard C_8 or C_{18} reversed-phase columns. This method is of particular use in the separation of the components of human lymph chylomicrons.

EXPERIMENTAL

Reagents

High-purity reagents (HPLC grade) were used throughout. Water and acetonitrile were purchased from Mallinckrodt, while orthophosphoric acid and trifluoroacetic acid (TFA) were obtained from Merck and Pierce Chemicals, respectively.

HPLC columns

TSK Phenyl-5PW columns (75 mm × 7.5 mm I.D.) were purchased from Toyo Soda (Japan). The packing material consists of a 10-μm porous (1000 Å pore size) hydroxylated polyether support with a low density of covalently bound surface phenyl groups. μBondapak C_{18} (P/N 27324, 300 mm × 3.9 mm I.D.) and Activon RP300 C_8 (30 mm × 4.6 mm I.D.) columns were purchased from Beckman (Australia) and Applied Biosystems (Australia), respectively. The packing material for these two columns consists of porous spherical silica particles (10 μm diameter for μBondapak, 7 μm diameter for RP300) to which are covalently bonded C_{18} or C_8 alkyl chains.

HPLC methodology

Reversed-phase separations were performed on a Hewlett-Packard HP1090 HPLC system equipped with a Rheodyne sample injector (2-ml loop) and a diode array detector. Solvent A was 20 m*M* H_3PO_4 in water (pH 2.3) and solvent B was 20 m*M* H_3PO_4 in acetonitrile–water (60:40). Purified apolipoproteins were dissolved or diluted in solvent A and applied to the column at flow-rates of 1.35 ml/min (TSK Phenyl-5PW) or 0.5 ml/min (μBondapak, RP300). Column temperature was maintained at 45°C. Elution of proteins was effected by a linear (50 min) gradient from solvent A to solvent B. Protein elution was monitored simultaneously at 215 nm, 254 and 280 nm. Fractions were collected on a Cygnet fraction collector (Iscom).

Purification of apolipoproteins

Apolipoprotein A-I was purified from delipidated human high-density lipoprotein by ion-exchange chromatography in 6 *M* urea on DEAE-Sephacel[6]. Apolipoproteins A-IV and E were isolated from delipidated human lymph chylomicrons by preparative sodium dodecyl sulphate–polyacrylamide gel electrophoresis (SDS-PAGE) and electroelution[9].

Analytical methods

Samples for SDS-PAGE were run on 8–20% polyacrylamide gels and stained with Coomassie blue, using a Phastgel system (Pharmacia).

For amino acid analysis, samples were transferred to WISP vials (Waters Assoc.) containing 4 nmol of amino-guanidino propionic acid hydrochloride (AGPA) as an internal standard. Gas-phase hydrolysis was performed for 24 h at 110°C by the method described by Meltzer *et al.*[10] except that thioglycolic acid was omitted. Separation and quantitation of amino acids were performed on a Beckman System 6300 high-performance analyzer.

Amino acid sequences were determined using an Applied Biosystems Model 470A protein sequencer, equipped with an on-line Model 120A PTH analyzer.

RESULTS AND DISCUSSION

TSK Phenyl-5PW columns are designed for use in hydrophobic interaction chromatography (HIC) rather than for RP-HPLC. While HIC and RP-HPLC columns both contain stationary phases which consist of hydrophobic groups covalently bonded to hydrophilic supports, the HIC columns contain hydrophobic groups which are packed at a lower density[11]. It might thus be expected that the use of a HIC column for the reversed-phase separation of very hydrophobic proteins, such as apolipoproteins, might lead to improved separation of these proteins. To test this hypothesis, purified apolipoproteins A-IV, A-I and E were applied to a TSK Phenyl-5PW column and eluted with an increasing gradient of acetonitrile, as described in Methods. The resulting chromatograms are shown in Fig. 1A–C. Apolipoproteins A-IV and A-I eluted as single peaks with retention times of 10.1 and 17.2 min, respectively. Apolipoprotein E eluted as two peaks, with retention times of 21.7 and 23.9 min. The separation of a mixture of apolipoproteins A-IV, A-I and E is shown in Fig. 1D. The identity and purity of individual peaks from Fig. 1D were confirmed by amino acid analysis (Table I), SDS-PAGE (Fig. 2) and N-terminal sequencing of the first 10 amino acids. In a single step, purified apolipoproteins A-IV, A-I and E were obtained with yields in excess of 95% (as determined by amino acid analysis).

In contrast, we have found that poor separation of apolipoproteins A-IV, A-I and E resulted when these proteins were run on standard RP-HPLC columns under the same conditions as used for the separation on TSK Phenyl-5PW. The results of an attempted separation of these proteins on a standard C_8 RP-HPLC column (RP300, Activon, 30 × 4.6 mm) are shown in Fig. 3. Apolipoproteins A-IV, A-I and E eluted very late in the gradient with retention times of 37.9, 39.0 and 39.1 min respectively (Fig. 3, A–C). A mixture of these three proteins chromatographed as a single peak (Fig. 3D). Very similar results were obtained by using a μBondapak C_{18} column (P/N 27324, 300 × 3.9 mm), with apolipoproteins A-IV and A-I eluting with retention times of 43.9 and 45.2 min, respectively. Apo E eluted as two peaks, with retention times of 45.2 and 47.2 min (chromatograms not shown).

Two other groups have reported on the purification of apolipoproteins by RP-HPLC. Hughes *et al.*[7] described a RP-HPLC system with the capacity to separate apo A-I from apo E, although apo E eluted in several broad peaks and the chromatography of apo A-IV was not examined in that study. Weinberg *et al.*[8] used

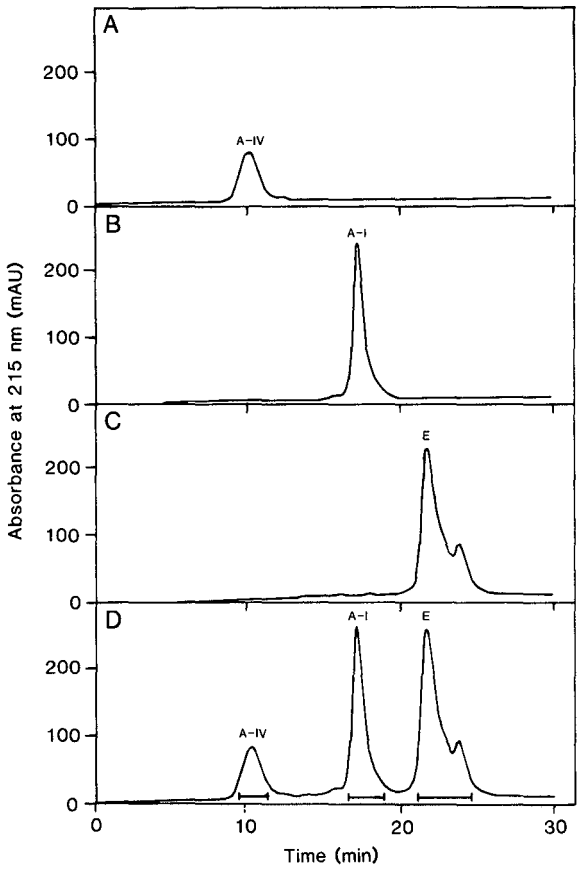

Fig. 1. RP-HPLC chromatograms of apolipoprotein separations on a TSK Phenyl-5PW column. Gradient conditions were as described in the text. Apolipoproteins A-IV (A, 30 μg), A-I (B, 50 μg) and E (C, 50 μg) were applied to the column separately (A–C) and as a mixture (D). Fractions were collected as indicated (|——|).

RP-HPLC to successfully separate apo A-IV from apo A-I, but in our hands that system does not separate apo A-I from apo E (date not shown). In both of the above procedures high concentrations of acetonitrile were used in the mobile phase, with very shallow gradients on standard C_{18} columns. Apart from the improved separation, RP-HPLC of apolipoproteins A-IV, A-I and E on the TSK Phenyl-5PW column has other advantages over the above methods. The lower concentration of acetonitrile needed for elution and the shorter residence times on the column may favour recovery of biological activity[11], while the steeper gradient elution might be expected to yield more reproducible separations of proteins[11].

The use of the hydrophilic ion-pairing reagent phosphoric acid as a mobile phase modifier has often been found to decrease column retention times for peptides and proteins in RP-HPLC and hence lead to sharper peaks[12]. In agreement with this, we have found that replacing phosphoric acid with TFA in our reversed-phase system leads to markedly increased retention times and lower resolution for apolipoprotein

TABLE I

AMINO ACID COMPOSITION[a] OF PURIFIED APOLIPOPROTEINS

Amino acid	*Expected*[b]			*Obtained (Fig. 1D)*		
	A-IV	*A-I*	*E*	*A-IV*	*A-I*	*E*
Asx[c]	36	21	12	36.8	21.6	12.9
Threonine	13	10	11	11.6	8.1	9.0
Serine	18	15	14	12.9	9.7	8.9
Glx[c]	92	46	71	104.4	52.5	80.0
Proline	12	10	8	11.0	9.8	8.5
Glycine	15	10	17	17.6	11.2	18.2
Alanine	30	19	35	32.5	20.1	35.9
Cysteine	0	0	1	ND[d]	ND	ND
Valine	19	13	22	19.3	13.7	22.7
Methionine	5	3	7	2.1	1.7	5.0
Isoleucine	5	0	2	4.8	0	2.1
Leucine	53	37	37	55.4	39.6	39.6
Tyrosine	6	7	4	5.1	5.5	3.3
Phenylalanine	11	6	3	11.1	6.3	3.3
Histidine	8	5	2	8.5	5.2	2.1
Lysine	28	21	12	28.4	21.4	12.5
Tryptophan	1	4	7	ND[d]	ND	ND
Arginine	24	16	34	23.0	16.7	34.9

[a] Expressed as number of residues per molecule.

[b] Theoretical values obtained from Swissprot data base (University of Geneva, Geneva, Switzerland).

[c] Asx = Asparagine plus aspartate; Glx = glutamine plus glutamate.

[d] ND = Not determined.

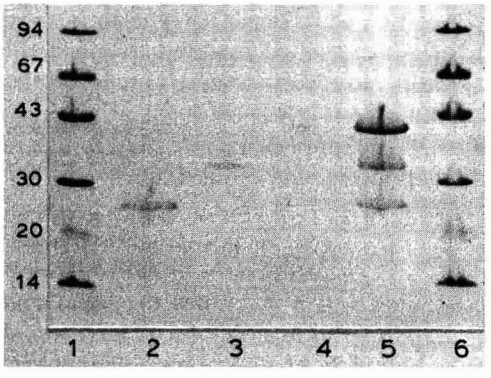

Fig. 2. Analysis of fractions from the TSK Phenyl-5PW column by SDS-PAGE and Coomassie staining. Sample loading buffer includes β-mercaptoethanol. Lanes 1 and 6 contain molecular weight standards (mol.wt. $\times 10^{-3}$). Lane 5 contains a mixture of apo A-IV, apo A-I and apo E. Lanes 2 (apo A-I) and 3 (apo E) and 4 (apo A-IV) correspond to the fractions collected as shown in Fig. 1D.

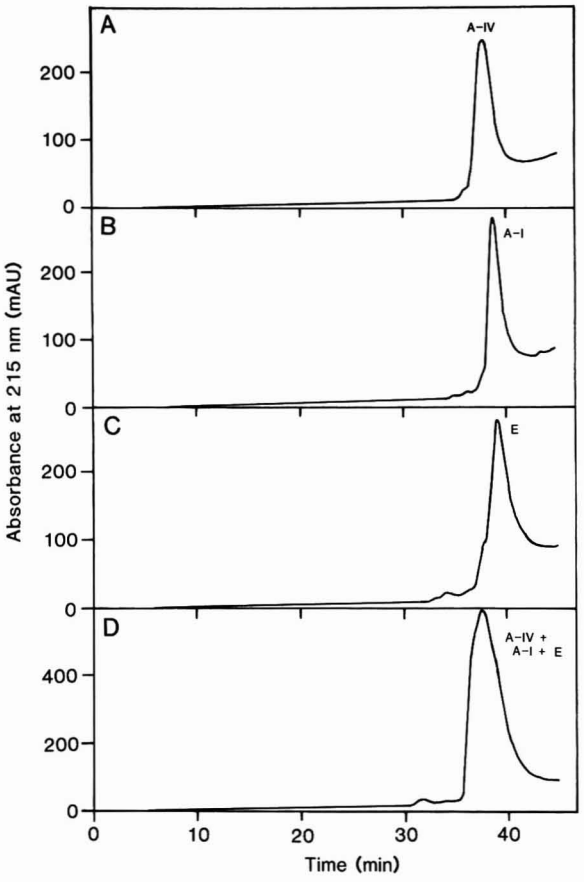

Fig. 3. RP-HPLC chromatograms of apolipoprotein separations on an Activon RP300 (C_8) column. Gradient conditions were as described in the text. Apolipoprotein samples were as described for Fig. 1.

separations (data not shown), and we therefore recommend the use of phosphoric acid as a mobile phase modifier. Another factor which has been found to affect the retention times of proteins in RP-HPLC is temperature: an increase in temperature usually leads to decreased retention[11]. In agreement with this also, we have observed that lowering the column temperature from 45°C to ambient temperature results in a significant increase in retention time for apolipoproteins A-IV, A-I and E (to 18.4, 23.3 and 26.4 min, respectively) on the TSK Phenyl-5PW column under the gradient conditions used, with some loss of resolution although the peaks are still separated baseline to baseline.

In conclusion, we have described a method which facilitates the rapid and efficient separation of apolipoproteins A-IV, A-I and E. Furthermore, we have found that the method is of particular use in the separation of the apolipoprotein components of human lymph chylomicrons, provided that the insoluble B apolipoprotein, apo A-II and C apolipoproteins are first removed by size-exclusion chromatography since some of the C apolipoproteins co-elute with apo A-IV and apo A-II coelutes with apo A-I (data not shown). An example of such a separation is shown in Fig. 4, which illustrates

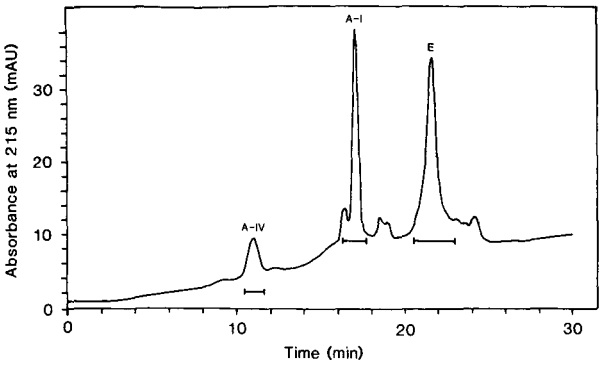

Fig. 4. Analytical RP-HPLC separation of the apolipoprotein components of human lymph chylomicrons on a TSK Phenyl-5PW column. Gradient conditions were as described in the text. The sample applied to the column was a fraction from the size-exclusion chromatography of delipidated human lymph chylomicrons on a Sephacryl S-300 column. Fractions were collected as indicated (|———|).

the analytical separation of apolipoproteins A-IV, A-I and E which were contained in a fraction obtained by size-exclusion chromatography of delipidated human lymph chylomicrons through Sephacryl S-300 equilibrated with 4 *M* guanidinium hydrochloride in 50 m*M* Tris–HCl pH 8.0. This type of gel filtration is the most widely reported technique used to isolate apolipoproteins from plasma or lymph triglyceride-rich lipoproteins[2,13], but never provides a satisfactory separation of the medium-molecular-weight apolipoproteins which are often the subject of investigation. However, as shown in Fig. 4, the method described in this paper achieves their isolation; the identity and purity of individual peaks from Fig. 4 were confirmed by SDS-PAGE, amino acid analysis and N-terminal sequencing.

ACKNOWLEDGEMENTS

The authors wish to thank John Morrison and Charles Allan (Baker Medical Research Institute, Victoria, Australia) and Christian Ehnholm (National Public Health Institute, Helsinki, Finland) for samples of purified apolipoproteins A-I and A-IV. This research was partially supported by a grant from the National Heart Foundation of Australia.

REFERENCES

1 R. W. Mahley, T. L. Innerarity, S. C. Rall and K. H. Weisgraber, *J. Lipid Res.*, 25 (1984) 1277.
2 C. L. Bisgaier, O. P. Sachdev, L. Megna and R. M. Glickman, *J. Lipid Res.*, 26 (1985) 11.
3 R. B. Weinberg and M. S. Spector, *J. Lipid Res.*, 26 (1985) 26.
4 R. Vercaemst, J. Bury and M. Rosseneu, *J. Lipid Res.*, 25 (1984) 876.
5 W. März and W. Gross, *J. Clin. Chem. Clin. Biochem.*, 21 (1983) 459.
6 M. C. Cheung and J. J. Albers, *J. Clin. Invest.*, 60 (1977) 43.
7 T. A. Hughes, M. A. Moore, P. Neame, M. F. Medley and B. H. Chung, *J. Lipid Res.*, 29 (1988) 363.
8 R. Weinberg, C. Patton and B. DaGue, *J. Lipid Res.*, 29 (1988) 819.
9 T. Ohta, N. H. Fidge and P. J. Nestel, *J. Biol. Chem.*, 259 (1984) 14888.
10 N. M. Meltzer, G. I. Tous, S. Gruber and S. Stein, *Anal. Biochem.*, 160 (1987) 356.
11 P. H. Corran, in R. W. A. Oliver (Editor), *HPLC of Macromolecules*, IRL Press, Oxford, 1989, p. 127.
12 C. A. Bishop, in W. S. Hancock (Editor), *Handbook of HPLC for the Separation of Amino Acids, Peptides and Proteins*, Vol. 1, CRC Press, Boca Raton, FL, 1986, p. 153.
13 E. Dvorin, W. W. Mantulin, M. F. Rohde, A. M. Gotto, Jr., H. J. Pownall and B. C. Sherrill, *J. Lipid Res.*, 26 (1985) 38.

Journal of Chromatography, 511 (1990) 155–166
Elsevier Science Publishers B.V., Amsterdam

CHROM. 22 364

Naphthalene- and anthracene-2,3-dialdehyde as precolumn labelling reagents for primary amines using reversed- and normal-phase liquid chromatography with peroxyoxalate chemiluminescence detection

P. J. M. KWAKMAN*, H. KOELEWIJN, I. KOOL, U. A. Th. BRINKMAN and G. J. DE JONG
Department of Analytical Chemistry, Free University, De Boelelaan 1083, 1081 HV Amsterdam (The Netherlands)

(First received October 31st, 1989; revised manuscript received January 30th, 1990)

ABSTRACT

Naphthalene-2,3-dialdehyde (NDA) and anthracene-2,3-dialdehyde (ADA) were applied as pre-column labelling reagents for the peroxyoxalate chemiluminescence detection of primary amines. The advantages of these labels are the selective derivatization reaction with primary amines and the good chemiluminescence properties. A serious disadvantage is the formation of cyanide-induced side-products which are major interferences in reversed-phase chromatography. For normal-phase chromatography, the excess of reagent was removed by adding a polar amine after derivatization, with subsequent extraction of the labelled analyte with an apolar solvent. The detection limit for NDA-labelled fluvoxamine, an anti-depressant, was in the low femtomole range in standard solutions and in urine samples. For ADA-labelled analytes difficulties were obtained with linearity in peroxyoxalate chemiluminescence detection, probably owing to oxidation of the derivative by hydrogen peroxide.

INTRODUCTION

In high-performance liquid chromatography (HPLC), the detection of analytes containing a primary amine functional group is routinely carried out in many laboratories with detection limits in the low nanogram range. Well known fluorescence derivatization reagents such as *o*-phthalaldehyde (OPA), fluorescamine and 5-dimethylaminonaphthalene-1-sulphonyl chloride (dansyl chloride) can be used for the sensitive detection of these types of compounds[1–3]. In order to obtain lower detection limits, a new label was recently synthesized, naphthalene-2,3-dialdehyde (NDA); the reaction is based on the selective isoindole formation of primary amines similar to the reaction with OPA[4,5]. The fluorescence quantum yield of these benzisoindole derivatives is about 0.5–0.6 in aqueous solvents[6] and very low detection limits (0.2–1 fmol) can be obtained using an argon-ion laser as light source[7]. The same principle

0021-9673/90/$03.50

was applied by Beale and co-workers[8,9], who used 3-benzoyl-2-quinolinecarboxaldehyde, a fluorogenic reagent yielding derivatives with absorption maxima compatible with the 442-nm line of the He–Cd laser.

Peroxyoxalate chemiluminescence (CL) has been shown to be a highly sensitive detection principle for HPLC, yielding detection limits in the low femtomole and even attomole range[10–13]. Therefore, CL may be regarded as a serious competitor for laser-induced fluorescence detection in HPLC. Recently it has been reported that NDA derivatives can conveniently be detected by the peroxyoxalate CL detection system[14,15]. Hayakawa *et al.*[15] compared dansyl, 4-fluoro-7-nitrobenzoxadiazole (NBD-F) and NDA derivatization with peroxyoxalate CL detection, and found that NDA derivatives could be detected ten times more sensitively than dansyl derivatives and more than 50 times better than NBD-F derivatives.

The aim of this study was to investigate the applicability of NDA and anthracene-2,3-dialdehyde (ADA) as labels for reversed- and normal-phase HPLC with peroxyoxalate CL detection. The emission wavelengths of ADA derivatives are expected to be above 550 nm. As published in a previous paper dealing with a rhodamine label, long-wavelength emitters are favourable for peroxyoxalate CL detection[16], because a 550-nm emission cut-off filter will reduce the noise caused by the CL background. Further, the fluorescence and CL characteristics of ADA and NDA derivatives were compared. The determination of the anti-depressant fluvoxamine in urine is shown as an example.

EXPERIMENTAL

Chemicals

HPLC-grade solvents were purchased from Baker (Deventer, The Netherlands) and bis(2,4,6-trichlorophenyl) oxalate (TCPO) and bis(2,4-dinitrophenyl) oxalate (DNPO) from Fluka (Buchs, Switzerland). Bis(2-nitrophenyl) oxalate (2-NPO) was synthesized as described[17]. NDA and ADA were obtained from Molecular Probes (Eugene, OR, U.S.A.). Fluvoxamine {5-methoxy-1-[4-(trifluoromethyl)phenyl]-1-pentanone(*E*)-O-(2-aminoethyl)oxime} was supplied by Duphar (Weesp, The Netherlands) and amphetamine by Aldrich (Brussels, Belgium); Fig. 1 shows the structures of both analytes. Lissamine Rhodamine B sulphonyl chloride was purchased from Kodak (Weesp, The Netherlands) and 5-dimethylaminonaphthalene-1-sulphonyl chloride from Aldrich. Perylene-3-sulphonate was synthesized by P. de Wit (Department of Organic Chemistry, University of Amsterdam, The Netherlands[18]). All other chemicals were of analytical-reagent grade.

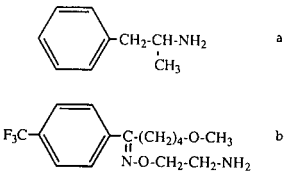

Fig. 1. Structural formulae of (a) amphetamine and (b) fluvoxamine.

High-performance liquid chromatography

In the reversed-phase systen, the mobile phase was delivered by a Gilson Model 302 pump equipped with a Gilson Model 308 manometric module (Gilson, Villiers-le-Bel, France). A laboratory-made six-port injection valve with a 25-μl loop was used for the introduction of samples onto a 150 × 3.1 mm I.D. analytical column packed by a slurry technique with 5-μm LiChrosorb RP-18 (Merck, Darmstadt, F.R.G.). Reversed-phase HPLC was carried out with acetonitrile–imidazole buffer (2.5 m*M*, pH 7.0) (75:25, v/v) as eluent at a flow-rate of 0.5 ml/min.

In the normal-phase system, a Gilson 302 pump with a laboratory-made membrane-type pulse damper was used to deliver the HPLC mobile phase. A laboratory-made six-port injection valve with a 35-μl loop was used for injection onto a 250 × 3.1 mm I.D. 5-μm LiChrosorb Si 60 (Merck) silica column. Chromatography of standard solutions was carried out using a mobile phase of dichloromethane containing 0.3% methanol at a flow-rate of 0.5 ml/min. For urine samples 0.2% methanol was used in the mobile phase.

Detection system

The reversed-phase system was essentially the same as that described in a previous paper[16]. Hydrogen peroxide and 2-NPO dissolved in acetonitrile at final concentrations of 50 and 5 m*M*, respectively, were mixed just before use and added to the column effluent with a pulseless Isco (Lincoln, NE, U.S.A.) μLC-500 syringe pump. The mobile phase (0.5 ml/min) and the reagent stream (0.2 ml/min) were mixed with a standard Valco T-piece immediately before the detector. A Kratos (Ramsey, NJ, U.S.A.) FS 970 fluorescence detector (with the lamp turned off) equipped with a 2π steradian mirror, a laboratory-made 50-μl flow cell and a 418-nm emission cut-off filter (NDA) or a 550-nm filter (ADA) was used for detection.

The set-up for the normal-phase system is shown in Fig. 2. A laboratory-made pulseless syringe pump delivered a mixture of 50 m*M* hydrogen peroxide and 0.5 m*M* triethylamine in acetonitrile–dichloromethane (1:1, v/v) at a flow-rate of 0.1 ml/min. A second laboratory-made syringe pump delivered 5 m*M* TCPO in dichloromethane, also at a flow-rate of 0.1 ml/min. A Kratos FS 980 fluorescence detector, with the lamp

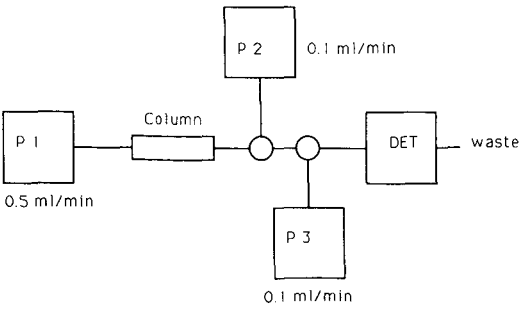

Fig. 2. Experimental set-up for normal-phase HPLC with peroxyoxalate CL detection. P1 = Dichloromethane containing 0.2–0.3% methanol, flow-rate 0.5 ml/min; P2 = 50 m*M* hydrogen peroxide + 0.5 m*M* triethylamine in acetonitrile–dichloromethane (1:1, v/v), flow-rate 0.1 ml/min; P3 = 5 m*M* TCPO in dichloromethane, flow-rate 0.1 ml/min; DET = Kratos FS 980 fluorescence detector with the lamp turned off.

turned off, equipped with a standard 25-μl flow cell and a 418-nm (NDA) or a 550-nm (ADA) emission cut-off filter was used for detection.

Derivatization of primary amines with NDA or ADA

The derivatization procedure is a modification of that described by de Montigny *et al.*[4]. Standard solutions of amines were prepared in 0.02 *M* borate buffer (pH 9.5). To 500 μl of amine solution, 100 μl of a 10 m*M* sodium cyanide solution in borate buffer (pH 9.5) were added and, subsequently, 500 μl of a 0.1 m*M* NDA or ADA solution in methanol. After reaction for 20 min at ambient temperature, a 25-μl aliquot was injected onto the reversed-phase HPLC system. For the normal-phase HPLC system, after derivatization 100 μl of 0.1 *M* glycine in borate buffer (pH 9.5) were added to the reaction mixture and allowed to react for 10 min. The relatively apolar derivative was extracted with 500 μl of toluene–hexane (1:1, v/v); 400 μl of the toluene–hexane layer were diluted with 800 μl of dichloromethane and a 35-μl aliquot was injected onto the silica column.

Analysis of urine samples

To 8 ml of urine, 2 ml of a borate buffer (0.1 *M*, pH 9.5) were added. After filtration through a 0.2-μm disposable filter, derivatization was carried out as described in the previous section, the only exception being the concentration of NDA (1 m*M* instead of 0.1 m*M*). For fluvoxamine analysis, 7 ml of urine (+ 2 ml of borate buffer) were spiked with 1 ml of a fluvoxamine solution and treated in the same way.

RESULTS AND DISCUSSION

Derivatization reaction

Derivatization conditions. In their derivatization procedures for primary amines with NDA, de Montigny *et al.*[4] used 50 μl of sample solution and a total amount of 450 μl of reagent solution (borate buffer, cyanide and NDA). In this study, a distinctly larger volume of sample was used (500 μl). The conversion was still quantitative with a reaction time of only 20 min at room temperature for both NDA and ADA and for the model compound amphetamine (see reaction scheme in Fig. 3). In agreement with the data reported by de Montigny *et al.*[4], we found that the NDA derivatives are very stable. After extraction into toluene–hexane (1:1) no decrease in signal intensity was found even after 8 h. ADA derivatives, however, were found to be relatively unstable, probably owing to oxidation of one of the aromatic rings. About a 50% loss in signal was observed after 4 h. Therefore, ADA derivatives had to be injected within 30 min after derivatization (3–4% loss). The stability of the ADA derivatives in the aqueous solvent used for reversed-phase HPLC was found to be similar.

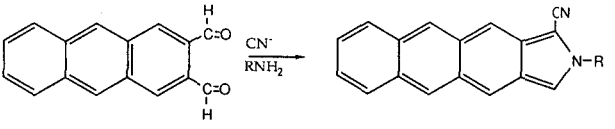

Fig. 3. Derivatization reaction of ADA with primary amines.

Side-product formation. In both reversed- and normal-phase HPLC various unknown peaks appeared in the chromatograms when analysing blank and standard amphetamine solutions after derivatization. These interfering peaks present severe problems at low analyte concentrations (10^{-8}–10^{-9} *M*), as illustrated in Fig. 4. Surprisingly, injection of the reagent (NDA or ADA) itself did not cause any interferences; these only occurred after mixing the reagent with borate buffer and cyanide. Roach and Harmony[7] mentioned the possible formation of benzoin condensation side-products. It is known that cyanide can induce the condensation of two aromatic aldehydes to form an α-hydroxyketone[19]. As two neighbouring aldehyde groups are present in NDA and ADA, many condensation products are, in principle, possible.

The formation of interferences in derivatization procedures seems to present a general problem in trace-level analysis. Many workers have only demonstrated the high sensitivity of their CL detection systems with commercially available derivatives, *e.g.*, with dansyl derivatives of amino acids[20,21]. Others probably carried out the derivatization at high analyte concentration and then prepared a series of diluted test solutions. In some instances, such as in the derivatization of catcholamines with fluorescamine[22] and thiols with N-[4-(6-dimethylamino-2-benzofuranyl)phenyl]male-

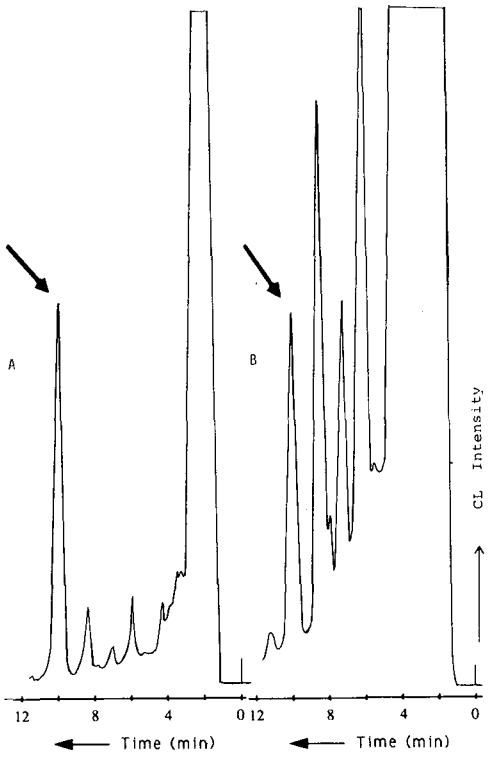

Fig. 4. Reversed-phase HPLC of (A) 10^{-7} *M* and (B) 10^{-8} *M* amphetamine derivatized with ADA and detected by peroxyoxalate CL. The amphetamine ADA derivative is indicated by an arrow. Mobile phase: acetonitrile–water (70:30, v/v), containing 2.5 m*M* imidazole. For other conditions, see Experimental.

imide (DBPM)[23], the final sample solution could be injected directly after derivatization onto an HPLC column without dilution. In actual practice, however, the problem often is that the reagent, at a concentration of 1.0 or 0.1 m*M*, is *ca.* 10^5–10^6 times in excess when derivatizing analyte concentrations of 10^{-8} or 10^{-9} *M*. This means that 0.1% of reagent impurities and side-products can cause severe interferences in trace-level studies. Dilution of the reagent generally is not possible as it will cause a large increase in reaction time. For a reaction that is carried out in, *e.g.*, 10 min the reaction rate will probably decrease 10-fold or more on diluting the analyte 10^3–10^4-fold and the reagent 10-fold[24].

In the case of peroxyoxalate CL detection of NDA and ADA derivatives, the selectivity of the chemical excitation process can be used to reduce the interferences caused by side-products. This is illustrated in Fig. 5 in which the same derivatization reaction, after reversed-phase HPLC, is monitored by fluorescence and CL detection. It can be clearly seen that the sensitivity of CL detection is higher and that the selectivity also is much better in the case of CL detection (see, *e.g.*, ref. 25). Unfortunately, for both NDA and ADA derivatives of amphetamine in reversed-phase HPLC the interfering peaks still start to dominate the chromatogram at the 10^{-8} *M* level even with standard solutions, so that real trace-level analysis cannot be carried out.

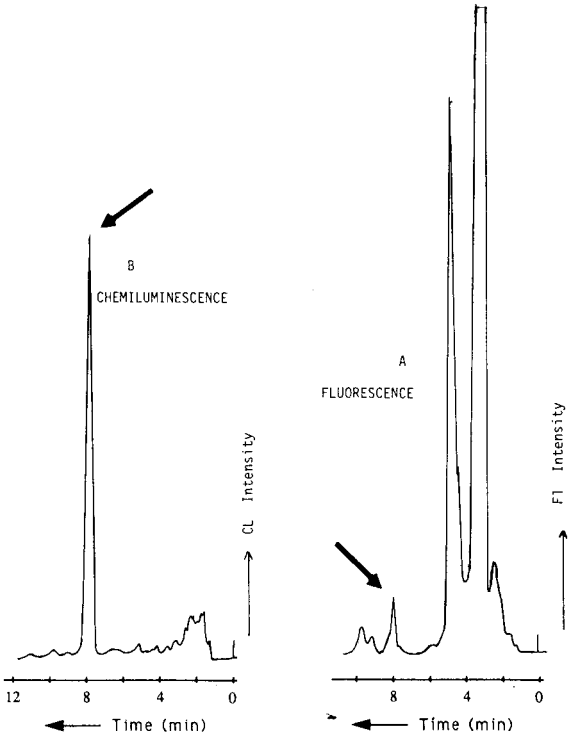

Fig. 5. Reversed-phase HPLC of a 10^{-6} *M* ADA-labelled amphetamine solution detected by (A) fluorescence and (B) chemiluminescence. The amphetamine ADA derivative is indicated by an arrow. Mobile phase: acetonitrile–water (75:25, v/v), containing 2.5 m*M* imidazole. For other conditions, see Experimental.

For normal-phase HPLC studies, the excess of reagent, and part of the interfering products, were removed by means of a simple liquid–liquid extraction. The excess of reagent can be separated from the analyte by adding a small amount (100 μl of a 0.1 *M* solution) of a very polar amine, *e.g.*, glycine, with subsequent extraction of the derivative of the analyte into an apolar organic phase [toluene–hexane (1:1, v/v)]. After extraction with toluene only, various interfering peaks were still visible in the chromatogram; an extraction with hexane only resulted in relatively clean chromatograms with, however, a slight decrease in recovery. A 1:1 mixture of both solvents gave the best results. After adding dichloromethane, the organic layer can be injected directly onto a normal-phase column. In this way a much cleaner chromatogram can be obtained and low-level derivatization of primary amines of medium polarity with peroxyoxalate CL detection becomes possible (see Fig. 6). If the same procedure is carried out with fluorescence detection, with excitation at 260 nm, the chromatogram still contains a large interfering band from t_0 to about 16 min. Obviously, the naphthalene-type side-products fluoresce relatively well, but seem to have poor CL characteristics. This again demonstrates well the superiority of peroxyoxalate CL over fluorescence detection.

In principle, a similar purification method can be carried out for a reversed-phase system. After the derivatization, addition of a very apolar amine, such as

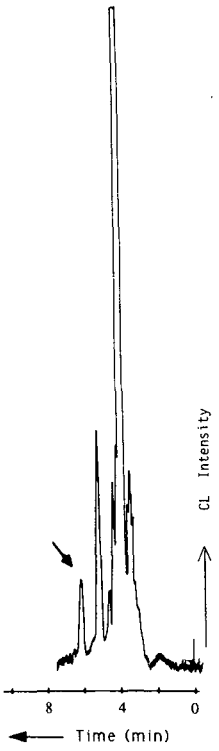

Fig. 6. Normal-phase HPLC of $1 \cdot 10^{-9}$ *M* fluvoxamine derivatized with NDA (indicated by an arrow). Mobile phase: dichloromethane containing 0.3% methanol. For other experimental conditions, see Fig. 2.

n-heptylamine, will allow the extraction of the excess of reagent into an apolar solvent. This was not useful for a fluvoxamine NDA derivative as it was co-extracted with the *n*-heptylamine NDA derivative into the organic solvent. However, for more polar amines, such as amino acids, this approach seems very promising, but was not investigated here.

Optimization of CL conditions

Reversed-phase HPLC. The CL detection system was the same as described in previous paper[16]. The oxalate, 2-NPO, and hydrogen peroxide were mixed in acetonitrile just before use and were added to the column eluate with a pulseless syringe pump. The CL reaction rate is then mainly determined by the pH of the mobile phase and the presence of a catalyst, often imidazole or triethylamine. Surprisingly, we found that the imidazole concentration (10 m*M*) used with rhodamine-labelled chlorophenols[16] was too high for the NDA and ADA derivatives. Varying the imidazole concentration from 10 to 0.5 m*M* resulted in an optimum at 2.5 m*M*, with a gain in signal-to-noise (S/N) ratio of about one order of magnitude. On carrying out further optimization studies, we found that the half-life of the CL signal for the NDA and ADA derivatives differed significantly from that of other well known chemiluminophores[26]. The results are summarized in Table I.

It is surprising that the three chemiluminophores rhodamine sulphonate, perylene sulphonate and dansylated ethanolamine all have comparable CL half-lives of 10–15 s, which are substantially different from the 1.5-s half-lives found for the NDA and ADA derivatives of ethanolamine (the latter amine was selected as a model compound at this stage because of the short retention time of its NDA and ADA derivatives). Interestingly, under the present conditions the half-life of the CL background (measured in the stopped-flow mode) was found to be over ten times higher than that of the latter two compounds. This means that with an appropriate volume of the flow cell a large fraction of the signal produced by the NDA and ADA derivatives can be measured while only a relatively low background signal is measured. The residence time in the flow cell should then be of the same order of magnitude as the half-life of the derivative. In the present system with a volume of *ca.* 2 μl between the T-piece and the flow cell and a total flow-rate of 700 μl/min, it takes 0.15 s from the T-piece to the detector and, subsequently, the CL signal is measured during *ca.* 4 s in

TABLE I

CL HALF-LIVES OF CHEMILUMINOPHORES IN REVERSED-PHASE HPLC

Conditions for all chemiluminophores: 2.5 m*M* imidazole in mobile phase, acetonitrile–water (75:25, v/v); 5 m*M* 2-NPO and 50 m*M* hydrogen peroxide added in acetonitrile at a flow-rate of 0.2 ml/min. The half-lives were measured by switching a valve, inserted just before the detector, realizing an immediate stopped-flow; the decay time was then recorded from the maximum to 50% intensity. In order to minimize injection artifacts, all experiments were carried out under reversed-phase HPLC conditions as described above. For further details, see Experimental.

Chemiluminophore	*Half-life (s)*	*Chemiluminophore*	*Half-life (s)*
Rhodamine sulphonate	13	Ethanolamine NDA	1.5
Perylene sulphonate	10	Ethanolamine ADA	1.5
Dansylated ethanolamine	11	CL background	19

the 50-μl flow cell. This means that these conditions are suitable for the efficient discrimination between the analyte signal and the background signal, clearly illustrating that the CL half-life plays an important role in the optimization of the S/N ratio. Another aspect is that a comparison of the sensitivity of two different chemiluminophores with the same HPLC system is not possible if their CL half-lives differ too much. In practice this will not often be a real problem as labelling procedures are carried out with one label at a time.

Normal-phase HPLC. In a previous study dealing with normal-phase HPLC and peroxyoxalate CL detection, relatively large amounts of acetonitrile and methanol were present in the mobile phase[16]. Therefore, the addition of hydrogen peroxide could be performed with a so-called perhydrit reactor, which contains hydrogen peroxide held on a urea support. With NDA and ADA derivatives of fluvoxamine, however, mobile phases consisting of chloroform or dichloromethane with a low content of methanol (0.2–0.3%) as modifier were used. In these solvents the solubility of hydrogen peroxide of the perhydrit is much too low; therefore, other methods of hydrogen peroxide addition had to be developed. A solution of aqueous hydrogen peroxide in acetonitrile (100 m*M*) was mixed with the same volume of triethylamine in dichloromethane (1 m*M*) and added to the column eluate with a pulseless syringe pump (flow-rate 0.1 ml/min). Final concentrations of hydrogen peroxide higher than 50 m*M* did not increase the S/N ratio and therefore this concentration was used for all further experiments. The concentration of triethylamine was varied between 20 and 0.1 m*M*; 0.5 m*M* was found to be the optimum, with a gain in S/N ratio by a factor of about 30. This triethylamine concentration is in sharp contrast with the 100 m*M* utilized in the normal-phase system described by Nozaki *et al.*[27]. This can probably be explained by the faster CL kinetics of NDA derivatives compared with dansyl derivatives (see above) and perhaps also by the use of different solvents. The oxalate, TCPO, was dissolved in dichloromethane and added with a second syringe pump (see Fig. 2), at a flow-rate of 0.1 ml/min. Varying the TCPO concentration between 1 and 10 m*M* showed 5 m*M* to be the optimum concentration.

In normal-phase HPLC all initial studies were carried out with both ADA and NDA derivatives of fluvoxamine. However, we found a strange non-linear behaviour for the ADA derivatives in flow-injection analysis and in normal-phase HPLC. This was observed with all possible combinations of the oxalates DNPO, 2-NPO and TCPO and the catalysts imidazole and triethylamine. Fluorescence batch experiments showed that the ADA derivatives, in contrast with NDA derivatives, are unstable in the presence of hydrogen peroxide (*ca.* 90% loss in 30 min). Obviously, the ADA derivatives are rapidly oxidized during the CL reaction, which essentially agrees with the observations made during optimization of the reaction conditions (see above). NDA derivatives, however, are more stable in the presence of hydrogen peroxide and, therefore, in all further experiments NDA was used. With NDA derivatives, good linearity was found with TCPO and triethylamine.

Analytical data and application

Comparison of CL and fluorescence detection. The Kratos FS 980 fluorescence detector is equipped with a deuterium lamp and, based on the excitation spectra of the present derivatives, excitation wavelengths of 260 nm (NDA; 252 nm in ref. 4) and 280 nm (ADA) were selected. These wavelengths should be used if a real comparison

has to be made between fluorescence and CL sensitivity with the Kratos detector. However, in fluorescence analysis better selectivity will be achieved if excitation is carried out in the visible region, *viz.*, at about 420 nm (maxima at about 414 and 438 nm for NDA derivatives of amino acids in ref. 4). A xenon lamp with high intensity in the visible region may well offer the best compromise with regard to sensitivity and selectivity.

The results are summarized in Table II. It should be emphasized that in three out of the four cases tested (for the exception, see below), it was not possible to derivatize low analyte concentrations (10^{-9} *M*) because of the presence of large interfering peaks or the instability of the derivatives as discussed in the previous sections. Therefore, relatively concentrated (*ca.* 10^{-6} *M*) solutions were diluted 10–1000-fold to measure the S/N ratios. From the data in Table II one can conclude that, under ideal conditions, CL detection is at least an order of magnitude more sensitive than fluorescence detection, but there is little difference between normal- and reversed-phase HPLC and an ADA or an NDA derivative. The better sensitivity of CL compared with fluorescence detection is in agreement with the results of Hayakawa *et al*[15]. Their better detection limits may be ascribed to the different detector optics, a larger flow cell volume and different composition of the final CL solvent. However, the aspect of overriding importance is that only in the case of NDA derivatives analysed by normal-phase HPLC with CL detection was direct derivatization of a 10^{-9} *M* solution possible (see Fig. 6). In other words, this is the only technique which is applicable to real-sample trace-level analyses.

Linearity and application. Using normal-phase HPLC with CL detection the linearity of the total procedure was measurd in the range $5 \cdot 10^{-7}$–$5 \cdot 10^{-10}$ *M* fluvoxamine. Good linearity was obtained over the whole range ($n = 8$, $r = 0.998$). As an application, Fig. 7 shows the analysis of a urine sample spiked with $5 \cdot 10^{-9}$ *M* fluvoxamine and the corresponding blank. The urine was filtered and, after adjustment of the pH with a borate buffer, was analysed without further treatment. Therapeutic

TABLE II

CL AND FLUORESCENCE DETECTION LIMITS (S/N = 3) FOR NDA AND ADA DERIVATIVES

For reversed-phase HPLC amphetamine was used as a model compound (see Table I); for normal-phase HPLC fluvoxamine was used (see Fig. 2).

Mode of operation	*Detection limit (fmol)*	
	NDA	*ADA*
Chemiluminescence		
Reversed-phase	4	2
Normal-phase	5	—[a]
Fluoresence		
Reversed-phase	100[b]	100[c]
Normal-phase	40[b]	80[c]

[a] Not determined because of non-linear behaviour (see text).
[b] Emission cut-off filter of 418 nm, $\lambda_{exc.} = 260$ nm.
[c] Emission cut-off filter of 550 nm, $\lambda_{exc.} = 280$ nm.

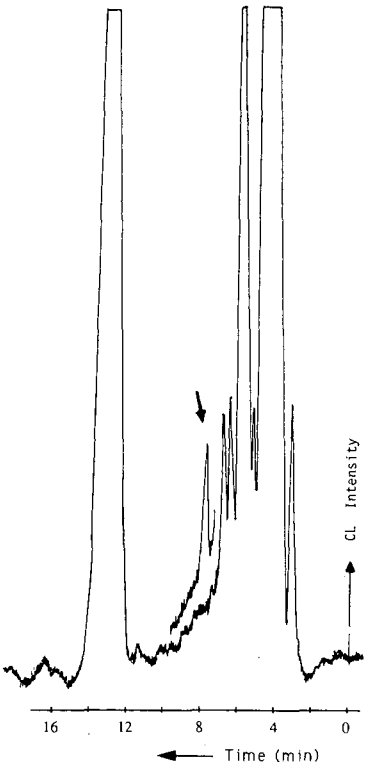

Fig. 7. Normal-phase HPLC of blank urine and a urine spiked with $5 \cdot 10^{-9}$ *M* fluvoxamine (indicated by an arrow), both derivatized with NDA. Mobile phase: dichloromethane containing 0.2% methanol. For other conditions, see Fig. 2 and Experimental.

levels of fluvoxamine in plasma are in the range 10^{-7}–10^{-8} *M*, that is, the sensitivity of the present system is obviously satisfactory for bioanalysis. As there are many primary amine-type compounds in urine, the concentration of NDA had to be increased from 0.1 to 1.0 m*M* and even with this reagent concentration the recovery was not quantitative, as can be seen by comparing peak heights (and concentrations) in Figs. 6 and 7. However, the fluvoxamine NDA derivative could still be linearly detected over at least two orders of magnitude (10^{-7}–10^{-9} *M*). Further optimization of the method is necessary for the routine analysis of real samples.

CONCLUSIONS

In normal-phase HPLC with peroxyoxalate CL detection, NDA can be used as a sensitive label for the detection of primary amines if the excess of reagent is removed from the mixture by adding a concentrated glycine solution after the derivatization step. With the anti-depressant fluvoxamine as analyte, a detection limit of 5 fmol is obtained, with good linearity in the range 10^{-6}–10^{-9} *M*. The practicability of the procedure is shown by the determination of $5 \cdot 10^{-9}$ *M* fluvoxamine in urine. In

contrast to NDA, ADA is not a promising label. ADA derivatives decompose fairly rapidly, especially in the presence of hydrogen peroxide.

In this study, CL detection was shown to be 10–50-fold more sensitive than fluorescence detection, which is in agreement with data reported by Hayakawa *et al.*[15]. In addition, the selectivity is distinctly better with the CL technique. Although other workers[7] using laser fluorescence detection have reported better detection limits (0.2–1 fmol) than those achieved in this work, the use of peroxyoxalate CL detection will often be preferable because of the relatively low cost of the detection system and the higher selectivity of the chemical excitation process.

ACKNOWLEDGEMENT

This work was financially supported by the Dutch Foundation of Technical Sciences (NWO/STW) under grant No. 700-349-1301.

REFERENCES

1 D. R. Knapp, *Handbook of Analytical Derivatization Reactions*, Wiley, New York, 1977.
2 L. A. Sternson, in R. W. Frei and J. F. Lawrence (Editors), *Chemical Derivatization in Analytical Chemistry*, Plenum Press, New York, 1981, p. 138.
3 K. Imai and T. Toyo'oka, in R. W. Frei and K. Zech (Editors), *Selective Sample Handling and Detection in High-Performance Liquid Chromatography*, Part A, Elsevier, Amsterdam, 1988, Ch. 4.
4 P. de Montigny, J. F. Stobaugh, R. S. Givens, R. G. Carlson, K. Srinivasachar, L. A. Sternson and T. Higuchi, *Anal. Chem.*, 59 (1987) 1096.
5 R. G. Carlson, K. Srinivasachar, R. S. Givens and B. Matuszewski, *J. Org. Chem.*, 51 (1986) 3978.
6 B. Matuszewski, R. S. Givens, K. Srinivasachar, R. G. Carlson and T. Higuchi, *Anal. Chem.*, 59 (1987) 1102.
7 M. C. Roach and M. D. Harmony, *Anal. Chem.*, 59 (1987) 411.
8 S. C. Beale, J. C. Savage, D. Wiesler, S. M. Wietstock and M. Novotny, *Anal. Chem.*, 60 (1988) 1765.
9 S. C. Beale, Y.-Z. Hsieh, J. C. Savage, D. Wiesler and M. Novotny, *Talanta*, 36 (1989) 321.
10 K. Imai and R. Weinberger, *Trends Anal. Chem.*, 4 (1985) 170.
11 K. Imai, A. Nishitani and Y. Tsukamoto, *Chromatographia*, 24 (1987) 77.
12 G. J. de Jong and P. J. M. Kwakman, *J. Chromatogr.*, 492 (1989) 319.
13 K. Kobayashi and K. Imai, *Anal. Chem.*, 52 (1980) 424.
14 T. Kawasaki, O. S. Wong, K. Imai, T. Higuchi, R. S. Givens, J. F. Stobaugh and T. Kuwana, presented at the *10th International Symposium on Column Liquid Chromatography, San Francisco, CA, May 1986*, abstract No. 3511.
15 K. Hayakawa, K. Hasegawa, N. Imaizumi, O. S. Wong and M. Miyazaki, *J. Chromatogr.*, 464 (1989) 343.
16 P. J. M. Kwakman, J. G. J. Mol, D. A. Kamminga, R. W. Frei, U. A. Th. Brinkman and G. J. de Jong, *J. Chromatogr.*, 459 (1988) 139.
17 A. G. Mohan and N. J. Turro, *J. Chem. Educ.*, 51 (1974) 528.
18 H. Cerfontain, K. Laali and H. J. A. Lambrechts, *Recl. Trav. Chim. Pays-Bas*, 102 (1983) 210.
19 A. L. Ternay, *Contemporary Organic Chemistry*, Saunders, Philadelphia, PA, 2nd ed., 1979, p. 743.
20 K. Miyaguchi, K. Honda and K. Imai, *J. Chromatogr.*, 303 (1984) 173.
21 W. Baeyens, J. Bruggeman and B. Lin, *Chromatographia*, 27 (1989) 191.
22 S. Kobayasi, J. Sekino, K. Honda and K. Imai, *Anal. Biochem.*, 112 (1981) 99.
23 K. Nakashima, C. Umekawa, S. Nakatsuji, S. Akiyama and R. S. Givens, *Biomed. Chromatogr.*, 3 (1989) 39.
24 W. Morozowich and M. J. Cho, in T. Kiyoshi and W. Morozowich (Editors), *GLC and HPLC Determination of Therapeutic Agents, Part 1* (*Chromatographic Science Series*, Vol. 9), Marcel Dekker, New York, 1978.
25 K. W. Sigvardson, J. M. Kennish and J. W. Birks, *Anal. Chem.*, 56 (1984) 1096.
26 K. Honda, K. Miyaguchi and K. Imai, *Anal. Chim. Acta*, 177 (1985) 103.
27 O. Nozaki, Y. Ohba and K. Imai, *Anal. Chim. Acta*, 205 (1988) 255.

Journal of Chromatography, 511 (1990) 167–176
Elsevier Science Publishers B.V., Amsterdam

CHROMSYMP. 1873

Simultaneous measurement of L-DOPA, its metabolites and carbidopa in plasma of Parkinsonian patients by improved sample pretreatment and high-performance liquid chromatographic determination[a]

C. LUCARELLI*, P. BETTO, G. RICCIARELLO and M. GIAMBENEDETTI
Istituto Superiore di Sanità, V. le Regina Elena 299, 00161 Rome (Italy)
C. CORRADINI
Istituto di Cromatografia del CNR, Area della Ricerca di Roma, P.O. Box 10, 00016 Monterotondo Stazione (Italy)
F. STOCCHI
I Clinica Neurologica, Università "La Sapienza", V. le Dell'Università 30, 00185 Rome (Italy)
and
F. BELLIARDO
Dipartimento Scienza e Tecnologia del Farmaco, Università di Torino, Turin (Italy)
(First received June 25th, 1989; revised manuscript received February 1st, 1990)

ABSTRACT

A procedure is described for the determination of L-3,4-dihydroxyphenylalanine (L-DOPA), its metabolites and carbidopa (CD) in plasma of Parkinsonian patients by high-performance liquid chromatography with dual working-electrode coulometric electrochemical detection. An efficient sample preparation scheme is presented for the isolation of L-DOPA, its metabolites and the catecholamines from the same plasma aliquot. After a simple deproteinization with methanol containing 2% of 0.5 *M* perchloric acid and evaporation of the solvent, L-DOPA, its metabolites and CD were separated with a 5-μm Nucleosil C_{18} column. Catecholamines were extracted from the supernatant of the deproteinized plasma by ion exchange on small columns and adsorption on alumina. Recoveries were close to 100% for L-DOPA, its metabolites and CD and 70% for catecholamines. The use of the same mobile phase for the concurrent assay of L-DOPA, its metabolites and catecholamines considerably increased the throughput of samples in the chromatographic system. The dual-electrode coulometric detector afforded peak identification by comparing current ratios. Monitoring of data from patients under L-DOPA therapy is reported.

[a] Presented at the *13th International Symposium on Column Liquid Chromatography, Stockholm, June 25–30, 1989*. The majority of the papers presented at this symposium have been published in *J. Chromatogr.*, Vols. 506 and 507 (1990).

0021-9673/90/$03.50

INTRODUCTION

Since L-3,4-dihydroxyphenylalanine (L-DOPA) alone or in combination with carbidopa (CD), a peripheral decarboxylase inhibitor (PDD), was introduced for the treatment of Parkinson's disease, there have been many studies on its metabolism and pharmacokinetics that have greatly improved the dosage form of the drug.

Many methods have been developed for the determination of these compounds and their metabolites in biological materials, such as spectrophotometric[1], fluorimetric[2,3], gas chromatographic[4,5], radioenzymatic[6,7] and high-performance liquid chromatographic (HPLC) methods with ultraviolet[8,9], fluorescence[10–12] and electrochemical detection (ED)[10,12–29]. Most of these methods evaluated only a few of the interesting catechol compounds, although there is general agreement on the assumption that the complete profile is more informative in diseases involving abnormalities of catecholamine metabolism. In fact, only the simultaneous monitoring of L-DOPA, 3-O-methyl-DOPA (OMD), dopamine (DA), 3-4-dihydroxyphenylacetic acid (DOPAC), norepinephrine (NE) and epinephrine (E) in plasma allows the study of the genesis of fluctuations in motor performance occurring in Parkinsonian patients undergoing long-term L-DOPA treatment[30]. In this regard, the role of L-DOPA metabolites (particularly OMD) that compete with the drug for the use of the blood–brain carriers is very important[31].

A new pro-drug, L-DOPA methyl ester (L-DOPA ME), is now in experimental use on patients with Parkinson's disease. The advantages of this pro-drug are its high solubility and low acidity[32], so that the drug can be diluted in small volumes of water and administered orally, intravenously or intraduodenally. The clinical effects of this drug are very similar to those obtained with standard L-DOPA but the dosage required are higher. This results in a higher production of OMD[32] and for this reason it is crucial to determine the OMD plasma level in treated patients. The measurement of CD is necessary to ensure that peripheral interfences remain minimal.

The two major problems involving the determination of these compounds are the very low levels of free catecholamines with respect to the amounts of L-DOPA and OMD and the difficult separation of OMD and CD in clinical samples. In previous work[12] these problems were overcome by using a weak cation-exchange column to extract the catecholamines and a double detection system for the determination of OMD and CD. In this paper we report an easy and inexpensive way to shorten the analysis time by an improved plasma prepurification procedure. A complete separation of all compounds is obtained by using an optimized mobile phase composition of appropriate pH. Moreover, the use of two detectors is not required, which is important in terms of cost and simplicity of the method.

The sample preparation simply includes deproteinization with cold methanol solution containing 2% of 0.5 *M* perchloric acid followed by centrifugation. An aliquot (200 μl) of the supernatant is used to measure L-DOPA, OMD, DOPAC and CD. The other part, employed for catecholamine determination, must be purified using a short column of CM-Sephadex and alumina adsorption. The two portions were analysed using the same chromatographic conditions. Detection was performed with a coulometric detector.

EXPERIMENTAL

Materials

Norepinephrine (NE), epinephrine (E), dopamine (DA), DOPAC and N-methyldopamine (NMDA, internal standard) were purchased from Sigma (St. Louis, MO, U.S.A.). L-DOPA and CD were gifts from Merck Sharp & Dohme (Darmstadt, F.R.G.). 1-Octanesulphonic acid sodium salt (OSA) and ethylene glycol-O,O′-bis-(2-aminoethyl-N,N,N′,N′-tetraacetic acid (EGTA) were purchased from Fluka (Buch s, Switzerland). Methanol (HPLC grade) and all other chemicals, of analytical-reagent grade, were obtained from Carlo Erba (Milan, Italy). CM-Sephadex C-25 was purchased from Pharmacia (Uppsala, Sweden) and acid alumina AG-4 from Bio-Rad Labs. (Richmond, CA, U.S.A.). All solvents used in the HPLC system were solubilized with distilled water treated with a Milli-Q system (Millipore, Milford, MA, U.S.A.). The two anticoagulant–antioxidant solutions tested for sample treatment contained EGTA and reduced glutathione[12,33] or EDTA and sodium metabisulphite[26].

High-performance liquid chromatography

The HPLC system consisted of a Model M-45 solvent delivery system (Waters–Millipore, Bedford, MA, U.S.A.) and a Model 7125 injector (equipped with a 100-μl loop). The column was reversed-phase Nucleosil C_{18} (12.5 cm × 4.6 mm I.D.), particle size 5 μm (Macherey, Nagel & Co., Duren, F.R.G.). The Coulochem 5100 A electrochemical detection system (ESA, Bedford, MA, U.S.A.) had a 5011 A analytical cell. The potentials were +0.25 V for the first electrode and −0.35 V for the second. The detector gain was set to 6000 for the first electrode and 20 000 for the second with a full-scale sensitiviy of 1.7 and 0.5 nA, respectively. Chromatograms were analysed with a Chemresearch chromatographic data management computer (ISCO; Lincoln, NE, U.S.A.) monitoring both detector signals. The mobile phase consisted of 0.013 *M* sodium acetate containing 100 mg/l of OSA (ion-pairing reagent), 200 mg/l of disodium EDTA and 15% of methanol (organic modifier) (pH 2.82). The elution of the compounds was carried out isocratically at room temperature with a flow-rate of 0.8 ml/min.

Sample separation

Blood samples from patients receiving L-DOPA were drawn by venipuncture and collected in tubes containing 50 μl of EGTA–reduced glutathione solution and immediately centrifuged (2000 *g*, 5 min, 4°C). The supernatants were stored at −80°C prior to the analysis.

Samples were allowed to thaw at room temperature and a plasma aliquot (1 ml) was spiked with 50 μl of internal standard solution (NMDA, 80 ng/ml). Deproteinization was performed by adding three volumes of ice-cold methanol containing 2% of 0.5 *M* perchloric acid and centrifugation (4000 g, 3 min, 4°C). A volume of 0.2 ml of the supernatant (first aliquot) was aspired and was evaporated to dryness under vacuum and the residue was dissolved in 0.2 ml of the mobile phase. A 5–50-μl volume of the solution was injected into the chromatographic system for the determination of L-DOPA, DOPAC, OMD and CD. Isolation of catecholamines (NE, E, DA) was carried out in the remaining supernatant (second aliquot) according to the previously published method[12]. A 3-ml volume of 0.1 *M* phosphate buffer (pH 7) was added to

the solution and the mixture was poured onto a CM-Sephadex C-25 column (2 cm × 0.5 cm I.D.). Before use the column was washed with 5 ml of 0.1 *M* hydrochloric acid and 10 ml of distilled water and buffered with 10 ml of 0.1 *M* phosphate buffer (pH 7). After the sample had passed through, the column was washed with 5 ml of distilled water. The catecholamines were eluted with 3 ml of 1.5 *M* perchloric acid, collecting the effluent in conical tubes with caps. A 2-ml volume of 1.5 *M* Tris buffer (pH 9.3) containing 0.06 *M* EDTA and 20 mg of acid-washed alumina[34] was added to the solution. The tube was vortex mixed for 2 min on a whirlmixer, the supernatant removed by vacuum aspiration and the alumina washed three times with 1 ml of water. The catecholamines were eluted with 100 μl of 0.1 *M* acetic acid, vortex mixed for 2 min, allowed to settle and centrifuged at 3000 *g* for 2 min. The supernatant was removed and 25 μl were injected.

RESULTS AND DISCUSSION

As catechols are liable to oxidize[35], antioxidants such as sodium metabisulphite or reduced glutathione are commonly added to blood together with the anticoagulants, before the preparation of plasma. We compared two different anticoagulant–antioxidant pairs, EGTA–reduced glutathione and EDTA–metabisulphite, and no significant differences were observed. We preferred to use EGTA–reduced glutathione as these constituents have been demonstrated to produce negligible chromatographic interferences on the front peaks.

The sample pretreatment for measuring the compounds of main clinical interest such as L-DOPA, OMD, DOPAC and CD is faster than that used previously, as proteins are simply separated by centrifugation and the drying solvent (methanol) is highly volatile. Moreover, the extract is more concentrated, which is particularly useful in detecting CD, the plasma level of which is often lower than the detection limit. Deproteinization by addition of trichloroacetic acid, perchloric acid, acetonitrile, methanol and methanol containing 2% of 0.5 or 1.0 *M* perchloric acid was examined. The use of methanol containing 2% of 0.5 *M* perchloric acid to prepare protein-free samples from the plasma gave highly reproducibile recoveries of L-DOPA, its metabolites and CD. It was necessary to evaporate the supernatant to dryness in order to obtain unaltered chromatographic characteristics. The recovery was determined by comparing the peak heights of known amounts of standards added to a pool of plasma from healthy subjects carried through the assay procedures with those resulting from the analysis of the same amount of standard stock solution. As reported in Table I, satisfactory recoveries were obtained with good relative standard deviations (R.S.D.). Table I also gives the regression equations of amount of catechol added *versus* amount found. The regression coefficient is indicative of the recovery and the intercept corresponds to a good approximation to the endogenous concentration.

Several approaches can be used to improve the chromatographic separation of catechols by the reversed-phase ion-pairing technique as a fine balance must be obtained between ion-pairing reagent, organic solvent and pH. The pH of the mobile phase can perhaps provide a means of separating the various substances as it can modify the charges of functional groups. On increasing the pH the retention times of the carboxylic acids and amino acid catechols decreased[35]. The retention time of OMD and CD is the most sensitive to modest pH manipulations in the range 2.75–3.0,

TABLE I

RECOVERY AND REGRESSION LINES OF CATHECHOLS OBTAINED BY STANDARD ADDITION TO A NORMAL PLASMA POOL

The values represent the means of five experiments at three different concentrations. The recovery of L-DOPA, DOPAC, OMD, CD and NMDA[a] was obtained after deproteinization and evaporation steps; the recovery of NE, DA, E and NMDA[b] was obtained after extraction by weak cation exchange and subsequent adsorption on alumina. The internal standard (NMDA) was used in both methods.

Compound	*Recovery (mean ± S.D.)*	*Relative standard deviation (%)*	*Concentration range*[c]	*Regression equation*[d]	*r*
L-DOPA	100.0 ± 7.3	6.7	10–40	$y = 0.853x + 2.028$	0.9999
DOPAC	93.3 ± 4.6	4.6	10–40	$y = 0.889x + 0.954$	0.9968
NMDA[a]	94.4 ± 4.5	4.8	20–80	$y = 0.915x + 0.099$	0.9978
OMD	150.0 ± 5.1	5.1	400–1600	$y = 1.000x + 2.520$	0.9992
CD	93.2 ± 1.6	1.7	200–800	$y = 0.892x + 0.056$	0.9997
NE	74.5 ± 4.5	6.0	152–1249	$y = 0.525x + 160.7$	0.9719
E	68.9 ± 3.3	4.8	15–855	$y = 0.679x + 7.38$	0.9997
DA	69.1 ± 4.2	6.1	13–889	$y = 0.704x + 12.28$	0.9968
NMDA[b]	66.0 ± 5.2	5.2	400–1600	$y = 0.668x - 1.27$	0.9990

[a] NMDA internal standard used for the determination of L-DOPA, DOPAC, OMD, CD.

[b] NMDA internal standard used for the determination of NE, E, DA.

[c] L-DOPA, DOPAC,NMDA[a], OMD and CD are expressed in ng/ml and NE, E, DA and NMDA[b] in pg/ml.

[d] x = added amount of L-DOPA, DOPAC, OMD, CD, NMDA[a] (expressed as ng/ml) and NE, E, DA, NMDA[b] (expressed as pg/ml); y = found amount.

whereas the retention times of amines were not influenced. Fig. 1 shows the effect of pH on the retention times of the compounds in the acidic range. For OMD and CD, optimum separation was obtained at a mobile phase pH of 2.82, and these conditions allowed the simultaneous separation of all the analytes tested without prolonging their retention times too much.

DA was normally detected in the second aliquot, purified by CM-Sephadex C-25 and alumina (see *Sample separation*). When the DA plasma concentration was particularly high it could also be found in the first aliquot, that used to measure L-DOPA, OMD, DOPAC and CD. For this reason, the chromatogram (Fig. 2A) illustrating resolution of standard mixture of L-DOPA and its metabolites also includes DA. As an effect of pharmacological treatment, the plasma levels of L-DOPA, OMD and (sometimes) DOPAC can be 1000–10 000 times higher than that of the other compounds. Fig. 2B shows a chromatogram of an extract from a plasma sample from a Parkinsonian patient after administration of a dose of L-DOPA and CD. As some peaks of interest were out of the range the extract was diluted 20-fold and re-injected (Fig. 2C).

Fig. 3 shows the separation of the catecholamines (A) in a standard mixture and (B) in the plasma extract analysed in Fig. 2. The results demonstrate that all compounds are conveniently separated and can be determined avoiding the previously necessary double detection system. With the chromatographic conditions used in this method, OMD can also be easily detected with the coulometric detector using a higher sensitivity than that employed in the previous work[12] (a gain of 20 000 *vs.* a gain of

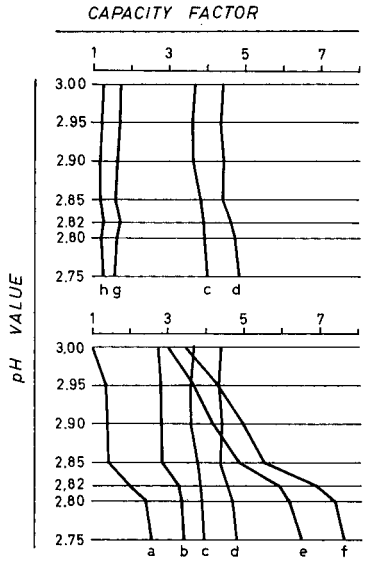

Fig. 1. Influence of pH on the capacity factor of (top) (h) NE, (g) E, (d) NMDA and (c) DA (bottom) (a) L-DOPA, (b) DOPAC, (c) DA, (e) OMD and (f) CD. Column, Nucleosil C_{18}, 5 μm; mobile phase, 0.013 *M* acetate containing 100 mg/l of OSA, 200 mg/l of disodium EDTA and 15% of methanol; flow-rate, 0.8 ml/min. DA was included in both groups as it is often concentrated enough to be detectable in the aliquot used for L-DOPA and the other main compounds (OMD, DOPAC and CD).

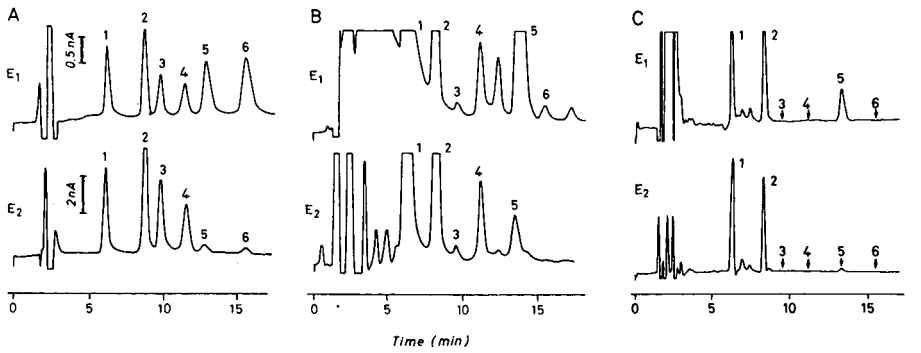

Fig. 2. Chromatograms of (1) L-DOPA, (2) DOPAC, (3) DA, (4) NMDA, (5) OMD and (6) CD after injection of (A) 10 μl of standard solution containing 0.2 ng each of L-DOPA, DOPAC, DA and NMDA, 8.0 ng of OMD and 0.8 ng of CD; (B) 20 μl of the solution obtained after deproteinization of plasma from a patient under L-DOPA therapy containing 2.5 ng of L-DOPA, 2.6 ng of DOPAC and 91.8 ng of OMD; and (C) the same extract as analysed in (B) diluted 20-fold. Chromatogram B does not allow the quantificaton of DA as its peak is not completely resolved and sited on the trailing side of the large tailing peaks of L-DOPA and DOPAC. Column, Nucleosil C_{18}, 5 μm; mobile phase, 0.013 *M* sodium acetate containing 100 mg/l of OSA, 200 mg/l of disodium EDTA and 15% of methanol (pH 2.82). The potential applied was +0.20 V at the first electrode (upper part of the chromatogram) and −0.35 V at the second (lower part). The detector gain was set to 6000 for the first electrode and to 20 000 for the second, with a full-scale sensitivity of 1.7 and 0.5 nA, respectively.

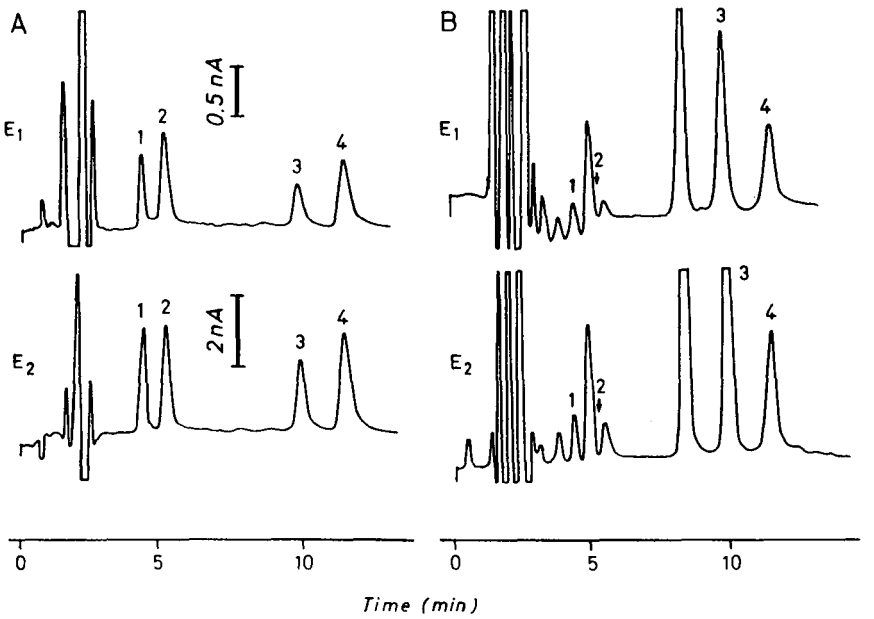

Fig. 3. Chromatograms of (1) NE, (2) E, (3) DA and (4) NMDA after injection of (A) 10 μl of standard solution containing 0.1 ng each of NE and E, 0.2 ng each of DA and NMDA and (B) 25 μl of alumina extract of plasma obtained from a patient under L-DOPA therapy containing 0.05 ng of NE and 0.9 ng of DA. Other details as in Fig. 2.

TABLE II

REPRODUCIBILITY OF THE METHOD

Between- and within-assay reproducibility. A plasma sample was spiked with known amounts of L-DOPA, its metabolites, CD and catecholamines.

Compound	*Concentration*[c]	*Within-assay R.S.D. (%)*[d]	*Between-assay R.S.D. (%)*[d]
L-DOPA	18.2	5.5	6.7
DOPAC	38.3	4.1	5.8
NMDA[a]	747.2	3.3	4.2
OMD	855.1	5.6	5.9
CD	370.4	5.7	6.1
NE	292.1	4.9	5.3
E	156.1	4.8	5.5
DA	151.7	5.9	6.8
NMDA[b]	278.1	5.2	6.3

[a] NMDA internal standard used for the determination of L-DOPA, DOPAC, OMD, CD (deproteinization and evaporation steps).

[b] NMDA internal standard used for the determination of NE, E, DA (cation exchange and alumina extraction).

[c] L-DOPA, DOPAC, NMDA[a], OMD and CD are expressed in ng/ml and NE, E, DA and NMDA[b] in pg/ml.

[d] Within-assay $n = 6$; between-assay $n = 20$; 5 runs.

TABLE III

REVERSIBILITY RATIOS OF CATECHOLS

The values represent the ratios of the detector responses (oxidation current/reduction current) of L-DOPA, its metabolites, catecholamines and CD. Results are means ± S.D. of ten experiments. E: plasma level was not detectable under our experimental conditions.

Compound	*Standards*	*Plasma*
L-DOPA	0.98 ± 0.05	1.02 ± 0.05
DOPAC	0.77 ± 0.06	0.74 ± 0.03
NMDA	0.93 ± 0.05	0.90 ± 0.03
OMD	6.07 ± 0.17	5.89 ± 0.21
CD	11.18 ± 0.38	11.45 ± 0.43
NE	0.68 ± 0.04	0.71 ± 0.05
E	1.01 ± 0.1	–
DA	0.76 ± 0.06	0.78 ± 0.05

5000) where the compound can only be detected spectrofluorimetrically. The use of a dual electrode system constitutes a powerful tool for optimizing selectivity because the potential of each electrode can be controlled independently. This permits oxidizable and reducible sustances to be detected simultaneously. For our determinations, the oxidation potential was kept as low as possible in order to minimize the background noise and to reduce the interference of the large amounts of OMD normally present in plasma from patients on L-DOPA therapy with the determination of CD, taking advantage of the fact that OMD is not readily oxidized at low potential[10].

The reproducibility of the method, evaluated from multiple analysis of a pooled plasma samples, is satisfactory. Table II gives the between- and within-assay reproducibilities.

TABLE IV

L-DOPA, ITS METABOLITES, CD AND CATECHOLAMINE PLASMA LEVELS IN A PARKINSONIAN PATIENT RECEIVING A CONTINUOUS INTRAJEJUNAL INFUSION OF L-DOPA ME

Each value represents the mean of three determinations. Infusion rate = 180 mg/h plus oral CD 25 mg every hour. CD levels are constistently higher than the minimum amound detectable after the administration of a further 25 mg of the drug (240 min). E: plasma level was not detectable under our experimental conditions.

Time (min)	*L-DOPA (μg/ml)*	*DOPAC (μg/ml)*	*OMD (μg/ml)*	*CD (ng/ml)*	*DA (ng/ml)*	*NE (ng/ml)*
0	0.1 ± 0.01	n.d.[a]	5.2 ± 0.2	n.d.[a]	73.0 ± 6.1	0.5 ± 0.03
20	19.7 ± 0.8	4.5 ± 0.2	5.5 ± 0.3	26 ± 1.6	28.3 ± 1.7	1.6 ± 0.10
40	9.9 ± 0.3	4.7 ± 0.1	6.7 ± 0.2	28 ± 1.5	17.2 ± 1.2	0.5 ± 0.02
60	5.9 ± 0.2	2.8 ± 0.2	8.5 ± 0.3	34 ± 2.4	12.0 ± 0.9	n.d.[a]
180	6.3 ± 0.4	0.5 ± 0.3	8.7 ± 0.3	39 ± 2.6	1.2 ± 0.1	0.2 ± 0.01
300	5.2 ± 0.2	0.4 ± 0.3	8.7 ± 0.6	60 ± 3.4	4.7 ± 0.3	0.5 ± 0.03
420	5.6 ± 0.3	0.4 ± 0.2	12.4 ± 0.4	58 ± 4.5	2.6 ± 0.2	0.6 ± 0.04
540	3.4 ± 0.2	0.3 ± 0.1	10.2 ± 0.4	41 ± 3.2	4.5 ± 0.9	0.9 ± 0.04
660	4.5 ± 0.4	0.3 ± 0.2	16.4 ± 0.7	57 ± 2.1	5.2 ± 0.2	0.4 ± 0.03

[a] n.d. = not detectable (< 5 ng/ml for CD and 0.5 ng/ml for catecholamines).

TABLE V

L-DOPA, ITS METABOLITES AND CATECHOLAMINE PLASMA LEVELS IN A PARKINSONIAN PATIENT RECEIVING A CONTINUOUS INTRAVENOUS INFUSION OF L-DOPA

Each value represents the mean of three determinations. CD levels below the minimum amount detectable could be due to the incomplete inhibition of PDD. Infusion rate = 60 mg/h plus oral CD (25 mg 4-hourly). E: plasma level was not detectable under our experimental conditions.

Time (min)	*Plasma level (ng/ml)*					
	L-DOPA	*DOPAC*	*OMD*	*CD*	*DA*	*NE*
0	128 ± 8	7.8 ± 0.6	6845 ± 444	n.d.[a]	0.133 ± 0.011	0.075 ± 0.005
30	2529 ± 164	9.8 ± 0.8	7219 ± 288	n.d.	0.231 ± 0.011	0.152 ± 0.007
60	2233 ± 179	20.6 ± 1.1	7330 ± 513	n.d.	0.436 ± 0.030	0.164 ± 0.013
90	2470 ± 185	25.3 ± 2.3	5843 ± 351	n.d.	0.608 ± 0.048	0.194 ± 0.009
120	2771 ± 150	32.2 ± 1.4	7498 ± 440	n.d.	0.562 ± 0.035	0.177 ± 0.012

[a] n.d. = not detectable (< 5 ng/ml for CD and 0.5 ng/ml for the catecholamines).

Two approaches were used to establish the peak identification. Initially, the peaks were identified on the basis of liquid chromatographic retention behaviour and co-injection with standard compounds. Later, the identity of the separated compounds was tested by recording both the first detector response (E_1, oxidation current) and the second (E_2, reduction current). Comparison of the detector response ratios obtained with standard compounds and plasma samples can confirm peak identity and purity[36,37]. The detector response ratios of standard compounds and of plasma samples are given in Table III. In the case reported in Fig. 3, the peak with a position close to the retention time of standard E (arrow 2) could be easily mistaken for endogenous E, as a small shift of the peak might occur. The comparison of the detector response ratios allowed us to avoid an incorrect identification.

Assuming a signal-to-noise ratio of at least 3, the detection limits of the assay described in this paper were 10, 10, 10, 10, 100 and 40 pg for L-DOPA, DOPAC, DA, NMDA, OMD and CD, respectively.

The continuous intrajejunal administration of L-DOPA ME provided constant blood levels of L-DOPA (Table IV), very similar to the continuous intravenously administered standard L-DOPA (Table V).

From the data in Table IV, it can be seen that the plasma OMD levels in patients receiving L-DOPA ME, even if high, remained constant as soon as they reached the steady state (360 min). The plasma CD levels could be a useful means of monitoring the inhibition of PDD. The higher CD levels detectable after 240 min could indicate complete inhibition of PDD after the administration of another 25 mg of the drug. Table V reports CD levels below the minimum amount detectable, perhaps owing to the incomplete inhibition of PDD.

ACKNOWLEDGEMENT

The authors are grateful to Amelia Raspa for assistance in the language revision.

REFERENCES

1 T. A. Hare and W. H. Vogel, *Biochem. Med.*, 4 (1970) 277.
2 F. Eichorn, A. Rutenberg and E. Kott, *Clin. Chem.*, 17 (1971) 296.
3 S. Fahn, A. L. N. Prasard and R. Delesie, *Anal. Biochem.*, 46 (1972) 557.
4 K. Imai, N. Arizumi, M. Wang, S. Yoshine and Z. Tamura, *Chem. Pharm. Bull.*,20 (1972) 2436.
5 J. R. Watson and R. C. Lawrence, *J. Chromatogr.*, 103 (1975) 63.
6 G. Zurcher and M. D. Prada, *J. Neurochem.*, 33 (1979) 631.
7 M. J. Brown and C. T. Dollery, *Br. J. Clin. Pharmacol.*, 11 (1981) 79.
8 J. Mitchell and C. J. Coscia, *J. Chromatogr.*, 145 (1978) 295.
9 J. Seki, Y. Arakawa, K. Imai, Z. Tamura, S. Yoshine, Y. Mizuno, K. Yamada, M. Matsue and H. Narabayashi, *Chem. Pharm. Bull.*, 29 (1981) 789.
10 T. Ishimitsu and S. Hirose, *J. Chromatogr.*, 337 (1985) 239.
11 M. Lee, H. Nohta, K. Ohtsubo, B. Yoo and Y. Ohkura, *Chem. Pharm. Bull.*, 29 (1981) 789.
12 P. Betto, G. Ricciarello, M. Giambenedetti, C. Lucarelli, S. Ruggeri and F. Stocchi, *J. Chromatogr.*, 459 (1988) 341.
13 R. M. Riggin, R. L. Alcorn and P. T. Kissinger, *Clin. Chem.*, 22 (1976) 782.
14 C. R. Freed and P. A. Asmus, *J. Neurochem.*, 32 (1979) 163.
15 A. Shum, G. R. Van Loon and M. J. Sale, *Life Sci.*, 31 (1982) 459.
16 E. Nissinen and J. Taskinen, *J. Chromatogr.*, 231 (1982) 459.
17 R. C. Causon and M. J. Brown, *J. Chromatogr.*, 277 (1983) 115.
18 S. Ito, T. Kato, K. Maruta and K. Fujita, *J. Chromatogr.*, 311 (1984) 154.
19 M. F. Beers, M. Stern, H. Hurtig, G. Melvin and A. Scarpa, *J. Chromatogr.*, 336 (1984) 380.
20 D. S. Goldstein, R. Stull, R. Zimlichman, P. D. Levinson, H. Smith and H. R. Keiser, *Clin. Chem.*, 30 (1984) 380.
21 T. Ishimitsu and S. Hirose, *Anal. Biochem.*, 150 (1985) 300.
22 A. Baruzzi, M. Contin, F. Albani and R. Riva, *J. Chromatogr.*, 375 (1986) 165.
23 M. A. Mena, V. Murodas, E. Bazan, J. Reiriz and J. G. de Yebenes, *Adv. Neurol.*, 45 (1986) 481.
24 C. R. Benedict, *J. Chromatogr.*, 385 (1987) 369.
25 J. M. Cederbaum, R. Williamson and H. Kutt, *J. Chromatogr.*, 415 (1987) 393.
26 Y. Michotte, M. Moors D. Delen, P. Herregodts and G. Ebinger, *J. Pharm. Biomed. Anal.*, 5 (1987) 659.
27 C. Lucarelli, P. Betto, M. Giambenedetti, G. Ricciarello, S. Ruggeri and F. Stocchi, *Giorn. Ital. Chim. Clin.*, 12 (1987) 223.
28 A. Premel-Cabic and P. Allain, *J. Chromatogr.*, 434 (1988) 187.
29 G. Eisenhofer, K. Kirk, I. J. Kopin and D. S. Goldstein, *J. Chromatogr.*, 431 (1988) 156.
30 C. D. Marsden, J. D. Parkes and S. Fahn (Editors), *Movement Disorders, Fluctuations, Disability in Parkinson's Disease— Clinical Aspects*, Butterworth, Guildford, 1981, pp. 96–112.
31 J. G. Nutt, W. R. Woodward and J. L. Andersen, *Ann. Neurol.*, 18 (1987) 537.
32 F. Stocchi, S. Ruggeri, A. Carta, N. P. Quinn, P. Jenner, R. J. Coleman, M. Bragoni, C. D. Bragoni, C. D. Marsden and A. Agnoli, in R. H. Bellmaker, M. Sandler, A. Dohlstrom, (Editors), *Progress in Catecholamine Research. Part C: Clinical Aspects, New Strategies in the Treatment of Parkinson's Disease*, A. R. Liss, New York, 1989, pp. 13–17.
33 B. M. Eriksson and B. A. Persson, *J. Chromatogr.*, 228 (1982) 143.
34 A. H. Anton and D. F. Sayre, *J. Pharmacol. Exp. Ther.*, 138 (1962) 360.
35 B. Kagedal and D. S. Goldstein, *J. Chromatogr.*, 429 (1988) 177.
36 J. Dutrieu and Y. A. Delmotte, *Fresenius Z. Anal. Chem.*, 314 (1983) 416.
37 M. E. Hall, B. J. Hoffer and G. A. Gerhardt, *LC · GC Int., Mag. Chromatogr. Sci.*, 2 (1989) 54.

Journal of Chromatography, 511 (1990) 177–183
Elsevier Science Publishers B.V., Amsterdam

CHROM. 22 429

High-performance liquid chromatographic method for the determination of dansyl-polyamines[a]

SUBHASH C. MINOCHA*, RAKESH MINOCHA[b] and CHERYL A. ROBIE[c]
Department of Plant Biology, University of New Hampshire, Durham, NH 03824-3597 (U.S.A.)
(First received May 3rd, 1989; revised manuscript received March 2nd, 1990)

ABSTRACT

This paper describes a fast reliable, and a sensitive technique for the separation and quantification of dansylated polyamines by high-performance liquid chromatography. Using a small 33 × 4.6 mm I.D., 3 μm particle size, C_{18} reversed-phase cartridge column and a linear gradient of acetonitrile–heptanesulfonate (10 *mM*, pH 3.4), at a flow-rate of 2.5 ml/min, the retention time for different polyamines was: N^8-acetyl-spermidine, 1.79 min; N^1-acetylspermidine, 1.82 min; putrescine, 2.26 min; cadaverine, 2.43 min; heptanediamine, 2.83 min; spermidine, 3.42 min; and spermine, 4.41 min. With an additional column regeneration time of 3–4 min, the complete cycle per sample took less than 8 min at room temperature. Using a fluorescence detector, the lower limit of detection was less than 1 pmol per 6 μl injection volume. The fluorescence response was linear up to 200 pmol per 6 μl for each polyamine. The method is suitable for separation of polyamines from animal, plant and fungal sources.

INTRODUCTION

The ubiquitous occurrence and psysiological importance of the polyamines in living systems has led to the development of a variety of analytical techniques for their separation and quantification. Thin-layer chromatography (TLC), thin-layer electrophoresis, gas chromatography and high-performance liquid chromatography (HPLC) have all been used[1]. The most widely used method of derivatization for quantifiation is dansylation[2–5]. Other methods of derivatization include benzoylation, tosylation, and dabsylation[6–10]. As compared to the separation of dansylated polyamines by TLC and quantification by fluorimetry[11,12], HPLC allows both a lower detection limit and a wider range of linearity[3,4,11,13–15]. Separation by HPLC

[a] Scientific contribution number 1669 from the New Hampshire Agricultural Experiment Station
[b] Present address: Louis C. Wyman Forestry Sciences Laboratory, Northeastern Forest Experiment Station, Durham, NH 03824, U.S.A.
[c] Present address: Biotechnica International Inc., 85 Bolton Street, Cambridge, MA 02140, U.S.A.

0021-9673/90/$03.50

generally involves a reversed-phase column and an isocratic or a gradient elution system using either water–methanol or water–acetonitrile as the solvent[14–18]. Further improvements in separation can be achieved by the use of an ion-pairing reagent such as octanesulfonic acid or heptanesulfonic acid.

Since a number of reliable protocols for separation of polyamines by HPLC are available, further improvements are directed mainly at decreasing the elution time and increasing the sensitivity and resolution of the technique. Protocols available at present generally require an elution time of 15–90 min depending upon the column and the solvent system. If a column regeneration time of 5–15 min per run is included, it takes at least 20–30 min for each sample. In a recent paper, Walter and Geuns[18] reported a relatively fast separation of dansylated polyamines by HPLC with a total elution time of about 5 min, using a 10-cm reversed-phase column and an isocratic solvent mixture at 50°C. At room temperature, the elution time was more than 10 min. Unfortunately, little information was provided on the parameters of separation and quantification such as the types of polyamines that can be separated, the limits of detection and the range of linearity, etc.

Using a smaller and a more efficient column, combined with a gradient elution, we have developed a rapid and a sensitive method of separation and quantification of dansylated polyamines from different sources. The method allows a complete elution of dansyl-polyamines in less than 5 min at room temperature. With a 3–4 min column regeneration time, the complete cycle per sample takes about 8 min. The elution time can be further reduced or the back pressure can be lowered at higher column temperatures. The limits of detection are less than 1 pmol per 6 μl injection volume, with a linearity of up to 200 pmol for each polyamine in the mixture. The method is suitable for the separation of polyamines from plant, animal and fungal sources[19,20].

EXPERIMENTAL

Materials

Dansyl chloride and all polyamine and acetylpolyamine standards were purchased from Sigma (St. Louis, MO, U.S.A.). Acetone, toluene (Photrex grade), HPLC-grade methanol and acetonitrile were supplied by J. T. Baker (Phillipsburg, NJ, U.S.A.).

Extraction and dansylation of polyamines

Polyamines were extracted from various tissues and dansylated following modifications of the procedure of Smith and Davies[4]. Stock solutions of the various compounds were made in 5% perchloric acid and diluted to obtain the necessary final concentrations. Aliquots (50 μl) of each solution or the centrifuged tissue extract were placed in 1.0-ml Reactivials (Pierce, Rockford, IL, U.S.A.) containing 100 μl of a saturated sodium carbonate solution. A 100-μl volume of dansyl chloride solution in acetone (10 mg/ml) was added to each vial. The vials were capped tightly and incubated in the dark in a water bath at 60°C for 1 h. A 50-μl volume of proline (100 mg/ml) was added to the reaction mixture to remove excess dansyl chloride. After an additional 30 min incubation, acetone was evaporated from each vial by spinning under vacuum for 2 min in SpeedVac Evaporator (Savant, Farmingdale, NY, U.S.A.). A 400-μl volume of toluene was then added to the solution and each vial was

vortex-mixed for 30 s. The vials were centrifuged at 500 *g* for 2 min. After the aqueous and organic phases had separated, 200 μl of the toluene layer were transferred to an Eppendorf tube. Toluene was completely evaporated in the SpeedVac and the residue dissolved in 1 ml of methanol or acetonitrile.

HPLC apparatus

The liquid chromatographic system consisted of a Perkin-Elmer series 400 pump, a Rheodyne injector valve fitted with a 6-μl loop, a Perkin-Elmer Pecosphere-3 × 3 CR C_{18}, 33 × 4.6 mm I.D. cartridge column (3 μm particle size), and a fluorescence detector (LS-1, Perkin-Elmer). The excitation and emission wavelengths were set at 340 and 510 nm, respectively. Peak areas were calculated using a LCI-100 integrator (Perkin-Elmer).

A helpful hint: When heptanesulfonate solution was left in the bottle for several days, the growth of microorganisms (not identified) in the connecting tubes caused problems with chromatography. The inclusion of 10% (v/v) acetonitrile in the heptanesulfonate solution eliminated this problem. Appropriate adjustments should be made in the gradient profile to achieve the desired concentrations at each step.

RESULTS AND DISCUSSION

Isocratic vs. gradient elution

The first important objective of the study was to obtain a clean separation of the three major polyamines (putrescine, spermidine and spermine) within as short a time as possible. Based on information in the literature, a reversed-phase C_{18} column was used with (1) an isocratic or (2) a linear gradient elution system. In order to achieve a faster elution time, while also maintaining peak resolution, a 3-μm, 33-mm column was selected for separation. The isocratic solvent system of water–acetonitrile (28:72) used by Walter and Geuns[18] produced an unsatisfactory separation of the three polyamines with this column. Whereas putrescine and spermidine eluted within 2 min, with distinct but overlapping peaks, spermine did not elute until 7.2 min (Fig. 1A). Increasing the column temperature, as suggested by the authors, did reduce the total elution time, while at the same time making the peaks of putrescine and spermidine even less distinct. A significant improvement in separation as well as elution time was seen when water was replaced by a 10 m*M* solution of heptanesulfonate, pH 3.4. The elution times for putrescine, spermidine and spermine were 1.34, 4.05 and 5.83 min, respectively (Fig. 1B). Furthermore, all three peaks were well-separated. Increasing the concentration of acetonitrile to 90% in heptanesulfonate caused a faster separation of the compounds but resulted in poor resolution of the peaks.

A much faster and cleaner separation of the three polyamines was obtained by using a linear gradient of acetonitrile and heptanesulfonate with the parameters shown in Table I. Retention times of 1.84, 2.61 and 3.28 min, were seen for putrescine, spermidine and spermine, respectively (Fig. 1C). A flow-rate of 2.5 ml/min was found to be optimal for separation. At this flow-rate the back pressure ranged from 45 bar at 100% acetonitrile to 110 bar at 50% acetonitrile. When a mixture of histamine and seven polyamines (including two of the acetyl derivatives and heptanediamine, a commonly used internal standard) was injected, the separation was unsatisfactory using the above gradient. A modification of the gradient profile as shown in Table II

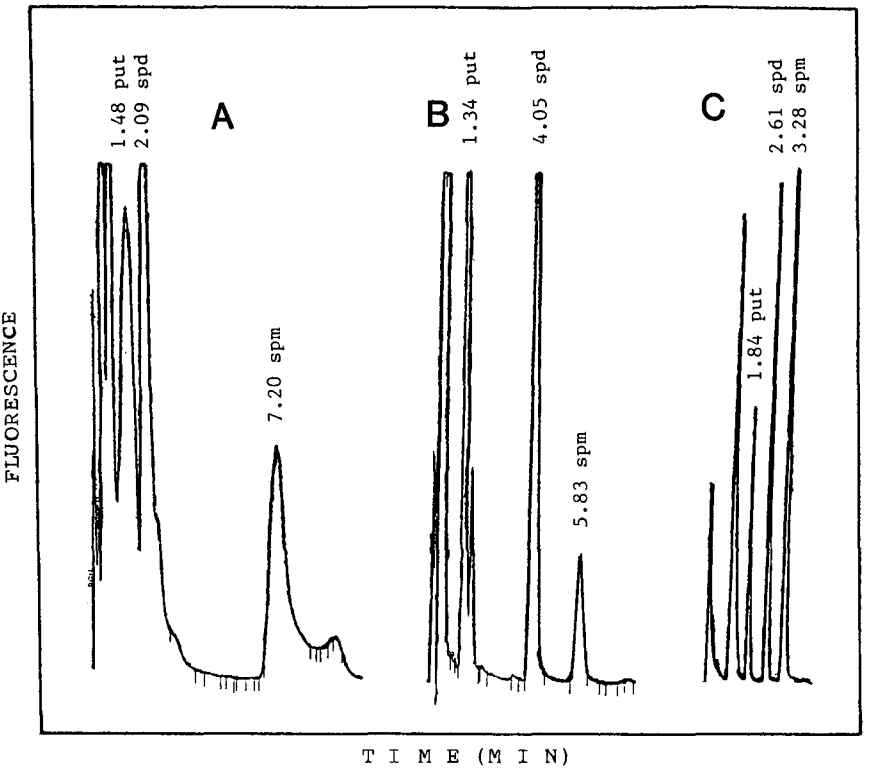

Fig. 1. Separation of standard dansyl polyamines on a 3-μm, 3.3-cm Pecosphere C_{18} reversed-phase column using an isocratic or a gradient elution. Each injection (6-μl loop) contained the equivalent of 50 pmol each of putrescine (put), spermidine (spd) and spermine (spm). Flow-rate was 2.5 ml/min. The fluorescence detector was set at 340 nm and 510 nm for absorption and emission, respectively. The solvent systems were: (A) isocratic with acetonitrile–water (72:28); (B) isocratic with acetonitrile–heptanesulfonate, 10 m*M*, pH 3.4 (72:28); (C) linear gradient of acetonitrile and heptanesulfonate. Parameters of the gradient are given in Table I.

TABLE I

GRADIENT PROFILE OF THE SOLVENT FOR THE SEPARATION OF DANSYLATED PUTRESCINE, SPERMIDINE AND SPERMINE

Step	*Time*[a]	*Acetonitrile (%)*	*Heptanesulfonate (%)*[b]
1	0.1	50	50
2	1.5	80	20
3	2.0	100	0
4	1.0	100	0
5	0.1	50	50
6	2.0	50	50

[a] Time is not cumulative from the start of the run.
[b] Heptanesulfonate concentration: 10 m*M*, pH 3.4.

TABLE II

GRADIENT PROFILE OF SOLVENT FOR THE SEPARATION OF DANSYL-POLYAMINES AND THEIR ACETYL DERIVATES

Solvent A = 100% acetonitrile; solvent B = heptanesulfonate (10 m*M*, pH 3.4)-acetonitrile (90:10).

Step	*Time*[a]	*Solvent A (%)*	*Solvent B (%)*
0	0.1	40	60
1	2.0	70	30
2	3.3	100	00
3	2.0	100	00
4	0.1	40	60
5	1.0	40	60

[a] Time is not cumulative from the start of the run.

resulted in a clean separation of all the compounds. The retention times for various compounds were as follows: N^8-acetylspermidine, 1.79 min; N^1-acetylspermidine, 1.82 min; putrescine, 2.26 min; cadaverine, 2.43 min; heptanediamine, 2.83 min; spermidine, 3.42 min; and spermine, 4.41 min (Fig. 2). Histamine eluted in two peaks (0.86 and 1.36 min) and did not interfere with the peaks of other polyamines. Including a column cleaning and regeneration time of 3–4 min, the total time per sample was about 8 min. The identity of each peak was confirmed by running each compound separately as well as by spiking the mixture individually with each compound. Using the above method, it was not possible to clearly separate N^1- and N^8-acetylspermidines. However, further modification of the gradient resulted in an excellent separation of these two derivatives, but it took a total of about 15 min per sample[21].

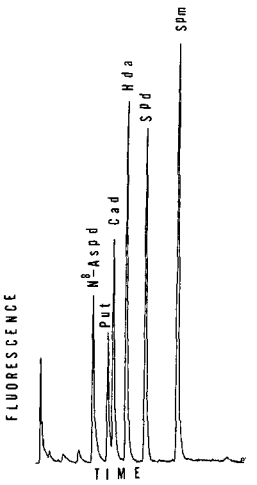

Fig. 2. Separation of a mixture of seven dansyl-polyamines with the gradient profile of the solvent presented in Table II. Each sample contained the equivalent of 20 pmol of each compound per 6 μl injection. N^8-Aspd = N^8-Acetylspermidine; Put = putrescine; Cad = cadaverine; Hda = heptanediamine; Spd = spermidine; Spm = spermine.

The retention time for each peak was highly repeatable for samples run on the same day (average standard error less than 2%), although it varied slightly from one day to another. Increased flow-rate resulted in somewhat faster elution but increased back pressure (*e.g.* at 3.0 ml/min, the pressure was about 130 bar); decrease flow-rate had the opposite effects. Raising the column temperature to 50°C, while maintaining the flow-rate at 2.5 ml/min, lowered the back pressure by 25–35% and decreased the total elution time to 2.65 min, but produced poor resolution.

Quantification of dansylated polyamines

Both the peak height and the peak area have been used for quantification of polyamines and other compounds separated by HPLC. The selection of the method depends largely on the mode of integration and the range of concentrations. Peak areas were used to determine the quantities of polyamines in the present study. The range of linearity for accurate quantification was from 1 to 200 pmol per injection (6-μl loop). The detection limit for putrescine (the least sensitive of the three major polyamines with respect to fluorescence) was at least an order of magnitude lower than 1 pmol, however, the increased noise-to-signal ratio affected the accuracy of quantification at lower concentrations. Concentrations higher than 200 pmol were not tested. A similar correlation between concentration and peak area was also observed for heptanediamine, making it suitable for use as an internal standard[19,20].

Analysis of biological samples

Extracts from a variety of sources including animal, plant, and fungal tissues were tested for separation of dansylated polyamines using the above chromatographic conditions. All parameters of pump (gradient profile), detector, and integrator were kept constant for comparison. In each case excellent separation and quantification of the three polyamines was obtained using heptanediamine as an internal standard[19,20].

CONCLUSION

In conclusion, we have developed a fast, sensitive, and highly quantitative technique for the analysis of dansylated polyamines. The technique is suitable for quantification over a wide range of concentrations of polyamines from a variety of sources. Separation of the three common polyamines is achieved in less than 3.5 min, a complex mixture containing acetylpolyamines and an internal standard (*e.g.* heptanediamine) can all be separated within about 5 min. This is a considerable improvement over previously published separation times of 15–90 min[3,4,9,10,14,15,17,18]. The cartridge column used here is very efficient and inexpensive as compared to larger columns. Fast separation also results in considerable saving of solvents and allows a large number of samples to be run within a normal working day. The method is suitable for the analysis of polyamines as well as their acetyl derivatives from a variety of biological samples in conjunction with the use of an internal standard[19,20].

ACKNOWLEDGEMENTS

The authors are thankful to Carol A. Macomber for her technical help with HPLC.

REFERENCES

1 H. Tabor and C. W. Tabor (Editors), *Methods Enzymol.*, 94 (1983) 1–497.
2 F. L. Vandermark, G. J. Schmidt and W. Slavin, *J. Chromatogr. Sci.*, 16 (1978) 465.
3 N. Seiler, B. Knogden and F. Eisenbiss. *J. Chromatogr.*, 145 (1978) 29.
4 M. A. smith and P. J. Davies, *Plant Physiol.*, 78 (1985) 89.
5 M. P. Kabra, H. K. Lee, W. P. Lubich and L. J. Marton, *J. Chromatogr.*, 380 (1986) 19.
6 R. Sugiura, T. Hayashi, S. Kawai and T. Ohno. *J. Chromatogr.*, 110 (1975) 385.
7 J. W. Redmond and A. Tseng, *J. Chromatogr.*, 170 (1979) 479.
8 J.-K. Lin and C.-C. Lai, *J. Chromatogr.*, 227 (1982) 369.
9 P. Koski, I. M. Helander, M. Sarvas and M. Vaara, *Anal. Biochem.*, 164 (1987) 261.
10 P. P. C. Lin, *Plant Physiol.*, 74 (1984) 975.
11 N. Seiler, in J. M. Gaugas (Editor) *Polyamines in Biomedical Research*, Wiley, New York, 1980, pp. 435–461.
12 N. Seiler and M. Wiechmann, *Hoppe-Seyler's Z. Physiol. Chem.*, 348 (1967) 1285.
13 N. Seiler and B. Knogden, *J. Chromatogr.*, 221 (1980) 227.
14 M. A. Desiderio, P. Davalli and A. Perin, *J. Chromatogr.*, 419 (1987) 285.
15 M. I. Escribano and M. E. Ligaz, *Plant Physiol.*, 87 (1988) 519.
16 N. Seiler, *Methods Enzymol.*, 94 (1983) 10–25.
17 H. E. Flores and A. W. Galston, *Plant Physiol.*, 69 (1982)) 701.
18 H. J.-P. Walter and J. M. C. Geuns, *Plant Physiol.*, 83 (1987) 232.
19 A. J. Khan and S. C. Minocha, *Plant Cell Physiol.*, 30 (1989) 655.
20 N. S. Papa, A. J. Khan, A. I. Samuelsen and S. C. Minocha, *Plant Physiol.*, in press.
21 A. G. Marsh and C. W. Walker, personal communication.

Journal of Chromatography, 511 (1990) 185–194
Elsevier Science Publishers B.V., Amsterdam

CHROM. 22 419

Determination of 4,4′-methylenedianiline in hydrolysed human urine using liquid chromatography with UV detection and peak identification by absorbance ratio

A. TILJANDER and G. SKARPING*
Department of Occupational and Environmental Medicine, University Hospital, S-221 85 Lund (Sweden)
(First received November 6th, 1989; revised manuscript received February 19th, 1990)

ABSTRACT

A liquid chromatographic method using multi-wavelength UV detection (258 and 285 nm) is presented for the determination of 4,4′-methylenedianiline (MDA) in hydrolysed human urine. The method is based on hydrolysis under strongly acidic conditions followed by derivatization with pentafluoropropionic anhydride. The perfluoro fatty acid amide derivative formed was analysed on a bonded octadecylsilyl column using isocratic elution with acetonitrile–water (67:33, v/v) as mobile phase. The overall recovery for urine samples containing 115 μg/l of MDA was 97 ± 3%. The calibration graph was linear in the investigated range (12–122 μg/l) with a correlation coefficient of 0.998. The precision was 2.3% for urine samples containing 122 μg/l and the detection limit was 8 μg/l. The chromatograms were evaluated using a combination of retention time data and absorbance ratio by the simultaneous monitoring of the wavelengths 285 and 258 nm. The absorbance ratio (285/258 nm) was virtually constant (0.28 ± 0.04) in the range 78–10 000 μg/l. The precision for the absorbance ratio was 6.1% for urine samples containing 124 μg/l and the lowest amount of MDA to give an absorbance ratio was 50 μg/l.

The procedure for the hydrolysis of urine spiked with MDA and N,N′-diacetyl-MDA and urine from skin-exposed workers was studied under strongly acidic, weakly acidic and basic conditions. MDA was found in hydrolysed urines from skin-exposed epoxy resin workers in the concentration range 8–700 μg/l.

INTRODUCTION

4,4′-Methylenedianiline (MDA) is a commercially important aromatic diamine used as an intermediate in the preparation of isocyanates, epoxy resins, polyurethanes and rubber chemicals[1,2]. MDA has been reported to be hepatoxic in dogs[3], rats[4,5] and humans[6,7]. In the Ames test, MDA has been found to be mutagenic[8] and it has been reported to be carcinogenic in rats and mice[9]. MDA has low volatility, but has been found to absorb readily through the skin[10]. The monitoring of MDA in biolog-

0021-9673/90/$03.50

ical fluids from exposed persons[11,12] is therefore of major importance. MDA-related metabolites such as N-acetyl-MDA and N,N'-diacetyl-MDA, have been found in urine[8,11,12]. Several techniques have been developed for the determination of MDA in matrices such as air-sampling solutions[13–16], blood[17,18] and urine[11,12,18–22]. For the determination of MDA in urine gas chromatography–mass spectrometry (GC–MS) has been used with detection limits ranging from 1 to 10 μg/l[11,12,18–21]. The determination of underivatized MDA using high-performance liquid chromatography (HPLC) with UV and electrochemical detection has been reported, with detection limits of total amounts of 32 and 3 ng, respectively[22].

Multi-wavelength detection has been demonstrated to provide specific and reliable evaluation of complicated chromatograms originating from biological samples. The use of absorbance-ratio measurements for peak identification and for peak purity is also feasible with this technique[23–26].

In this paper, a method is described for the determination of MDA in hydrolysed human urine using derivatization with pentafluoropropionic anhydride (PFPA) or heptafluorobutyric anhydride (HFBA) and reversed-phase HPLC with UV detection. The use of absorbance-ratio measurements for low concentrations of MDA in urine was investigated. The procedure for the hydrolysis of urine from skin-exposed workers was studied under strongly acidic and basic conditions.

EXPERIMENTAL

Equipment

The HPLC system consisted of a Waters 600 multi-solvent delivery system (Millipore–Waters, Milford, MA, U.S.A.), a Waters 712 WISP with variable injection volume, a Waters 490 programmable multi-wavelength detector, a three-channel SE 130 recorder (ABB Goerz, Vienna, Austria) and a Shimadzu (Kyoto, Japan) C-R3A integrator. The mobile phase was acetonitrile–water (67:33, v/v) and the injection volume was 50 μl. Absorption spectra were recorded on a Shimadzu UV-260 UV–visible recording spectrophotometer. For separation of phases a Model 3E-1 centrifuge (Sigma, Harz, F.R.G.) was used. For enrichment and evaporation a vacuum desiccator connected to an aspiration pump was employed. The vacuum desiccator was equipped with an electrically heated oven. The water was produced in Milli-Q apparatus (Millipore, Bedford, MA, U.S.A.).

Columns

Reversed-phase HPLC columns of stainless steel were used: Spherisorb S5 ODS-1 Excel (20 cm × 3.2 mm I.D.), Spherisorb S5 ODS-2 Excel (20 cm × 3.2 mm I.D.) and Hypersil 5-ODS Excel (20 cm × 3.2 mm I.D.) from Hichrom (Reading, U.K.), Apex II octadecyl (25 cm × 4.6 mm I.D.) from Jones Chromatography (Hengoed, U.K.); and Nucleosil 5 C_{18} (20 cm × 3 mm I.D.) from Macherey-Nagel (Düren, F.R.G.).

Chemicals

MDA and acetic anhydride were purchased from Aldrich (Beerse, Belgium), PFPA and HFBA from Pierce (Rockford, IL, U.S.A.), sodium hydroxide and hydrochloric acid from Merck (Darmstadt, F.R.G.), acetonitrile, methanol and toluene of

HPLC grade from Lab-Scan (Dublin, Ireland) and ethanol from Kemetyl (Stockholm, Sweden).

Synthesis

N,N′-Diacetyl-MDA. A 150-ml volume of an aqueous solution containing 7.5 ml of acetonitrile and 1.6 g of sodium hydroxide was added to a solution containing 10 g of MDA and 10 ml of methanol. Acetic anhydride (50 ml) was added dropwise. After 15 min the solution was heated in a water-bath at 80°C for 15 min, then cooled to room temperature. The crystals formed were filtered and washed with water and then with methanol. The crystals were dried in an incubator at 40°C.

MDA–perfluoro fatty acid amide derivatives. A 17.5-g amount of PFPA was added to a solution containing 5.0 g of MDA and 90 ml of toluene. The mixture was heated slowly to 70°C, then cooled and evaporated to dryness on a rotating evaporator. The residue was recrystallized from ethanol–water (7:1) and the crystals were filtered and washed with the same mixture. The crystals obtained were dried in a vacuum desiccator. The MDA–HFBA derivative was synthesized in an analogous way.

Preparation of standard solutions

Stock solutions of MDA were prepared in 0.1 *M* HCl at the 1 g/l level and diluted with 0.1 *M* HCl to the appropriate concentrations. A stock solution of N,N′-diacetyl-MDA was prepared in methanol and diluted with 0.1 *M* HCl to the desired concentrations. Stock solutions of MDA–perfluoro fatty amide derivatives were prepared in ethanol at the 1 g/l level and further dilutions were made with acetonitrile–water (67:33, v/v). The stock solutions were stable for more than 10 weeks without any noticeable degradation when stored in a refrigerator.

Sampling

A 2-ml volume of 6 *M* HCl per 100 ml of urine was added to the urine samples. The acidified urine samples were stored in a refrigerator until analysis.

Work-up procedure

A 1.2-ml volume of 6 *M* HCl was added to a 0.8-ml urine sample in a 10-ml test-tube, equipped with a PTFE cap. The test-tube was heated at 98°C for 2 h and then cooled to room temperature. A 3-ml volume of toluene and 4 ml of saturated NaOH solution were added to the test-tube. The mixture was shaken for 10 min and then centrifuged at 1500 *g* for 10 min. A 2-ml aliquot of the organic phase was separated and transferred to a new test-tube, 20 μl of PFPA or HFBA were added to the organic phase and the solution was shaken for 10 min. A 1-ml volume of the organic phase was transferred to a new test-tube and the toluene and the excess of derivatization reagent were removed by evaporation in a vacuum desiccator at 30°C. The residue was dissolved in 0.7 ml of the mobile phase.

RESULTS AND DISCUSSION

Standards

The identities of the MDA–perfluoro fatty acid amide derivatives and N,N′-

diacetyl-MDA were confirmed by GC–MS. The purities were determined using HPLC with UV detection and capillary GC with thermionic specific detection and found to be better than 99%. The purities were further confirmed by elemental analysis; the experimental values for carbon, hydrogen, nitrogen and oxygen did not differ by more than 0.2% from the calculated values.

Work-up procedure

Hydrolysis. The urine samples were acidified according to the sampling procedure.

The hydrolysis procedure was studied for urine samples from unexposed persons with a spiked concentration of 130 μg/l of MDA. The hydrolysis were performed under strongly acidic, weakly acidic and basic conditions. For strongly acidic conditions 0.8 ml of urine sample was mixed with 1.2 ml of 6 *M* HCl. For weakly acidic conditions 2 ml of urine sample alone were used. For basic conditions 1 ml of 10 *M* NaOH was added to 1 ml of urine sample. The urine samples were hydrolysed at 98°C and the hydrolysis time was varied between 15 min and 7 days. The work-up procedure was then performed and one determination with duplicate injections was made for each time and condition.

No losses were found under strongly acidic and basic conditions (Fig. 1A) for a hydrolysis time of 0.25–16 h. However, with hydrolysis under basic conditions for 2 days or more, more than 20% was lost. With hydrolysis under weakly acidic conditions the losses were unacceptable (> 50%).

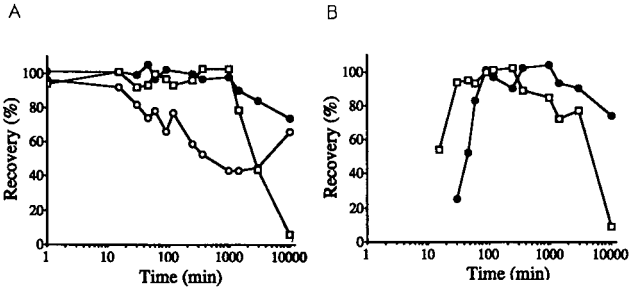

Fig. 1. Recovery of MDA–PFPA derivative in worked-up urine *versus* time. Urine sample spiked with (A) 130 μg/l of MDA and (B) 130 μg/l of N,N′-diacetyl-MDA. (●) Strongly acidic conditions; (○) weakly acidic condition; (□) basic conditions.

The hydrolysis procedure was also studied for urine samples with a spiked concentration of 130 μg/l of N,N′-diacetyl-MDA using the same procedure as for MDA-spiked urine samples. The recovery of MDA in N,N′-diacetyl-MDA-spiked urine under strongly acidic and basic conditions (Fig. 1B) showed a plateau, representing *ca.* 100% recovery, between 1 and 16 h and between 0.5 and 8 h, respectively. With basic conditions a prolonged hydrolysis time resulted in a decreased recovery.

The hydrolysis procedure was also studied for urine samples originating from three skin-exposed workers, using the same procedure as for MDA-spiked urine samples. The largest amount of MDA found for each urine was assumed to represent a 100% recovery. For each time and condition an average was calculated from the

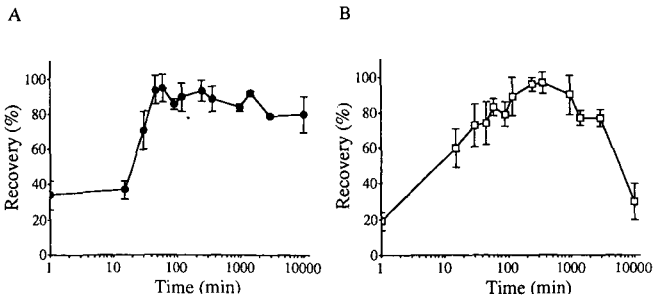

Fig. 2. Recovery of MDA from urine from three exposed workers (251, 545 and 645 μg/l) *versus* hydrolysis time under (A) strongly acidic and (B) basic conditions. The average recovery and the range are plotted.

three different urine samples (Fig. 2). Under strongly acidic conditions the amount of MDA found increased to a plateau, which virtually reached a maximum after 45 min. Within experimental error it was not possible to determine whether the recovery decreased if the hydrolysis time was prolonged. With hydrolysis under basic conditions the amount of MDA found reached a maximum much later than under strongly acidic conditions. It was also demonstrated that the amount of MDA found decreased if the hydrolysis time was prolonged to more than 16 h.

Extraction of MDA. The recovery for the extraction of MDA into the organic phase was *ca.* 100%, irrespective of whether 5 *M* or saturated sodium hydroxide solution was added to the hydrolysed urine sample. The foaming tendency was found to be less pronounced when saturated sodium hydroxide solution was used. For separations of phases it was necessary to centrifuge the urine samples.

Evaporation. Evaporation to dryness was performed in order to enrich the sample, to remove the excess of derivatization reagent and the acid formed and to choose a suitable solvent for the subsequent HPLC analysis. No losses were found in the evaporation step.

Chromatography

Choice of derivatization reagents. Initial attempts to determine underivatized MDA by HPLC with UV detection gave a bad resolution relative the urine matrices. Considerable efforts were made to clean up the sample without sample losses. However, in analyses for MDA at the μg/l level, these attempts were unsuccesful. The chromatograms obtained using either PFPA or HFBA as derivatization reagents were very similar. For the problems related to the matrix no differences were found. One of the advantages with MDA–perfluoro fatty amide derivatives is that the mobile phase did not need to be buffered to minimize absorption, which eliminated the problems due to salt precipitation in the HPLC system.

Choice of chromatographic conditions. The capacity factors (k') for the MDA–PFPA and MDA–HFBA derivatives were recorded for aqueous acetonitrile (Table I) to determine the optimum chromatographic conditions. Aqueous acetonitrile was found to be better than aqueous methanol owing to the k' values and the better resolution between the biological matrix and the MDA–PFPA and MDA–HFBA derivatives. Aqueous acetonitrile as the mobile phase also required a lower pressure and gave a better resolution.

TABLE I

RETENTION TIMES, t_R (min), AND CAPACITY FACTORS (k') FOR INVESTIGATED SUBSTANCES ON A 5-μm NUCLEOSIL C_{18} PACKING

Conditions: column, Nucleosil 5 C_{18} (20 cm × 3 mm I.D.); flow-rate, 1.0 ml/min; mobile phase, acetonitrile–water with various volume ratios.

Derivative	*Acetonitrile–water (v/v)*									
	85:15		*80:20*		*75:25*		*70:30*		*65:35*	
	t_R	k'	t_R	k'	t_R	k'	t_R	k'	t_R	k'
MDA–PFPA	4.6	1.8	5.5	2.4	6.5	3.2	8.8	4.8	13.5	7.2
MDA–HFBA	5.4	2.3	7.0	3.3	9.1	4.9	13.5	7.8	22.7	12.9

For low water contents in the mobile phase the MDA–PFPA and MDA–HFBA derivatives eluted fairly rapidly. The k' values increased with increasing water content, which reflects the dominant influence of the non-polar parts of the MDA–perfluoro fatty acid amide derivatives on retention. As expected, an increased chain length of the alkyl group on the derivatization reagent gave an increased retention (Table I). No significant differences in the chromatographic matrices could be seen between strongly acidic and basic conditions at their respective plateaux.

Choice of columns. Columns packed with 5-μm octadecylsilyl particles supplied by different manufacturers were tested. Significantly different k' values and resolutions relative to the matrices were obtained. The Apex II octadecyl column gave the best resolution relative to the matrices (Fig. 3). No endogenous peaks from the urine extract interfered in the analysis.

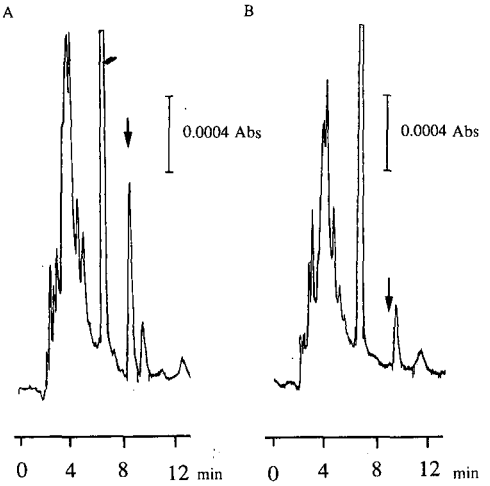

Fig. 3. Chromatograms of urine samples. (A) MDA–PFPA derivative from a urine sample from an exposed worker. The peak corresponds to a concentration of 220 μg/l. (B) Chromatogram from an unexposed worker. Conditions: Column, Apex II octadecyl; eluent, acetonitrile–water (67:33, v/v); flow-rate, 1 ml/min; injection volume, 50 μl; UV detection (258 nm); time constant, 1.0 s.

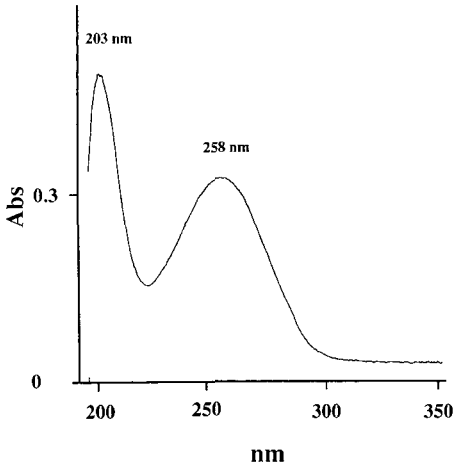

Fig. 4. Absorbance spectra of MDA–PFPA derivative, diluted with acetonitrile, at a concentration of 2.12 mg/l. Conditions: slit, 0,5 nm; speed, 95 nm/min; path length, 1.0 cm.

Detection

Absorbance maxima of the MDA–PFPA and MDA–HFBA derivatives were found at 203 and 258 nm (Fig. 4). The signal-to-noise ratio for the MDA–PFPA and MDA–HFBA derivatives were optimum and the same at 258 nm.

Absorbance ratio

The low concentrations of MDA in complex matrices such as urine samples from exposed persons necessitate sensitive detection and appropriate work-up procedures. More than ten urine samples were worked up as described under Experimental and no interfering peaks were found, although the matrix varied greatly from sample to sample. However, it could not be disregarded that the urine samples could possibly contain co-eluting UV-absorbing compounds originating from the diet, medication, etc. The use of a more selective determination was therefore examined to ensure peak identity and peak purity. Detection wavelengths of 258 and at 285 nm were applied simultaneously and the absorbance ratios between these wavelengths were monitored. The absorbance ratio was 0.28 ± 0.04 (95% confidence, $n = 7$) when the MDA concentration was varied between 78 and 10 000 μg/l (Fig. 5). On injecting

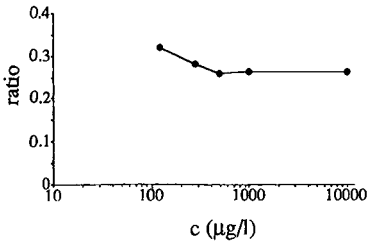

Fig. 5. Absorbance ratio (285/258 nm) *versus* concentration (c) of MDA. Each point on the graph represents the average of six measurements of the absorbance ratio.

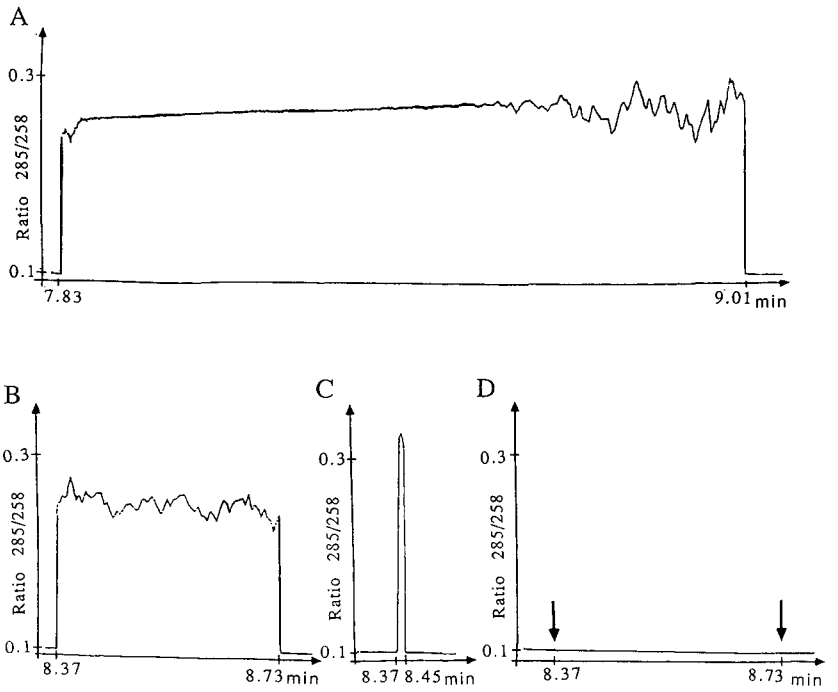

Fig. 6. Ratio chromatograms obtained monitoring of the absorbance ratio (285/258 nm). (A) Standard solution of MDA–PFPA at a concentration of 10 mg/l; (B) urine sample originating from an exposed worker at a concentration of 220 μg/l; (C) MDA-spiked urine sample at a concentration of 75 μg/l; (D) urine sample from an unexposed person. Chromatographic conditions as in Fig. 3 and ratio min, 0.1; absorbance threshold, 0.0001.

urine samples containing 124 μg/l of MDA the precision for the absorbance ratio was 6.1% (n = 14). The shape of the ratio chromatogram for low concentrations was noisy, especially at the peak start and the peak end. The ratio measurements were, of course, impossible when the absorbance approached the detection limit. An absorbance threshold of 0.0001 was therefore used for the two wavelengths in the ratio determination. The limit for ratio monitoring was 50 μg/l of MDA and was set by the absorbance at the least sensitive wavelength, 285 nm. The absorbance ratios were the same for diluted MDA–PFPA derivative, spiked urine and urine from exposed workers (Fig. 6). This confirms the identification and the peak purity. The absorbance ratio was therefore used as an extra quality measurement.

Quantitative analysis

Recovery. The overall recovery was studied for eight urine samples containing 115 μg/l of MDA. The peak areas obtained were compared with a standard. The recovery was 97 ± 3% (95% confidence, n = 14).

Calibration graph. Eight different concentrations of MDA in urine and urine blanks were prepared according to the work-up procedure. For each concentration, two determinations with duplicate injections were made. The calibration graph for

the investigated range of 12–122 μg/l of MDA was linear with a correlation coefficient of 0.998 ($n = 8$; $y = 120x - 344$).

Detection limit. The detection limit, defined as the concentration in a urine sample giving a signal equal to the blank signal plus three standard deviations[27], was 8 μg/l of MDA. No interfering peaks appeared when urine samples from ten persons were examined.

Precision. Eight urine samples containing 122 μg/l of MDA were analysed. The relative standard deviation of the MDA peak area was 2.3%.

CONCLUSIONS

The method developed for assessing occupational exposure to MDA provides the selective and sensitive determination of MDA at the 8–10 000 μg/l level using HPLC with UV detection. Multi-wavelength detection and ratio chromatograms were demonstrated to give the selective determination of MDA in human urine. The use of a derivatization procedure with perfluoro-fatty acid anhydrides produced stable derivatives resolved from the urine matrices. The low detection limit achieved together with the opportunity to use ratio detection gave safer quantification and identification.

ACKNOWLEDGEMENTS

The authors are indebted to Professor Staffan Skerfving, Head of the Department of Occupational and Environmental Medicine, for his interest in this work. They also gratefully acknowledge the Swedish Work Environment Fund (AMFO 88-0161) for financial support.

REFERENCES

1 World Health Organization, *Evaluation of the Carcinogenic Risk of Chemicals to Humans* (*IARC Monographs*, Vol 39), IARC, Lyon, 1986, p. 347.
2 M. Grayson (Editor), *Kirk-Othmer Encyclopedia of Chemical Technology*, Vol 2, Wiley-Interscience, Toronto, 1978, p. 338.
3 W. B. Deichmann, W. E. MacDonald, M. Coplan, F. Woods and E. Blum, *Toxicology*, 11 (1978) 185.
4 S. Fukushima, M. Shibata, T. Hibino, T. Yoshimura, M. Hirose and N. Ito, *Toxicol. Appl. Pharmacol.*, 48 (1979) 145.
5 G. Pludro, K. Karlowski, M. Mankowska, H. Woggon and W.-J. Uhde, *Acta Pol. Pharm.*, 26 (1969) 352.
6 D. B. McGill and J. D. Motto, *N. Engl. J. Med.*, 291 (1974) 278.
7 H. Kopelman, P. J. Scheuer and R. Williams, *Q. J. Med.*,. 35 (1966) 553.
8 K. Tanaka, T. Ino, T. Sawahata, S. Marui, H. Igaki and H. Yashima, *Mutat. Res.*, 143 (1985) 11.
9 E. K. Weisburger, A. S. K. Murthy, H. S. Lilja and J. C. Lamb, IV, *J. Natl. Cancer Inst.*, 72 (1984) 1457.
10 S. R. Cohen, *Arch. Dermatol.*, 121 (1985) 1022.
11 J. Cocker, W. Gristwood and H. K. Wilson, *Br. J. Ind. Med.*, 43 (1986) 620.
12 J. Cocker, L. C. Brown, H. K. Wilson and K. Rollins, *J. Anal. Toxicol.*, 12 (1988) 9.
13 G. Skarping, L. Renman and M. Dalene, *J. Chromatogr.*, 270 (1983) 207.
14 G. Skarping, C. Sangö and B. E. F. Smith, *J. Chromatogr.*, 208 (1981) 313.
15 G. Skarping, L. Renman and B. E. F. Smith, *J. Chromatogr.*, 267 (1983) 315.
16 C. C. Anderson and E. C. Gunderson, SRI International Project PYD-8963, Final Report SRI 8963-021.

17 M. Tortoreto, P. Catalani, M. Bianchi, C. Blonda, C. Pantarotto and S. Paglialunga, *J. Chromatogr.*, 262 (1983) 367.
18 M. J. Avery, *J. Chromatogr.*, 488 (1989) 470.
19 A. Tiljander, G. Skarping and M. Dalene, *J. Chromatogr.*, 479 (1989) 144.
20 R. M. Riggin, C. C. Howard, D. R. Scott and R. L. Hedgecoke, *J. Chromatogr. Sci.*, 21 (1983) 321.
21 C. Rosenberg and H. Savolainen, *J. Chromatogr.*, 358 (1986) 385.
22 P. Trippel-Schulte, J. Zeiske and A. Kettrup, *Chromatographia*, 22 (1986) 138.
23 D. J. Reuland and W. A. Trinler, *Forensic Sci. Int.*, 37 (1988) 37.
24 P. C. White, A. Etherington and T. Catterick, *Forensic Sci. Int.*, 37 (1988) 55.
25 K. H. Law and N. P. Das, *J. Chromatogr.*, 388 (1987) 225.
26 N. A. Hall, G. W. Lynes and N. M. Hjelm, *Clin. Chem.*, 34 (1988) 1041.
27 J. C. Miller and J. N. Miller, *Statistics for Analytical Chemistry*, Ellis Horwood, Chichester, 1984.

Journal of Chromatography, 511 (1990) 195–221
Elsevier Science Publishers B.V., Amsterdam

CHROM. 22 454

Neutral, alkaline and difference ultraviolet spectra of secondary metabolites from *Penicillium* and other fungi, and comparisons to published maxima from gradient high-performance liquid chromatography with diode-array detection

R. RUSSELL M. PATERSON*
CAB International Mycological Institute, Ferry Lane, Kew, Surrey TW9 3AF (U.K.)
and
CARLOS KEMMELMEIER
Fundacao Universidade Estadual de Maringa, Campus Universitario, Av. Colombo, 3690-(DDD 0442) Maringa (Brazil)
(First received September 19th, 1989; revised manuscript received March 19th, 1990)

ABSTRACT

The ultraviolet spectra of 6 predominantly secondary metabolites from filamentous fungi which, *inter alia*, are useful in the identification of the compounds after chromatography, were obtained in neutral (methanol) and alkaline solvents. Difference spectra were obtained by subtracting the neutral from the alkaline spectrum for each metabolite, using the spectrophotometer software. The data and method are of use in differentiating metabolites with similar chromophores. A database of the maxima was stored on a microcomputer for flexible storage, retrieval and updating of information. These data are compared to those published previously, obtained by diode-array detection using gradient high-performance liquid chromatography, which indicated that changes in solvent concentrations of the gradient affect the spectra of some metabolites. This could cause misidentification of chemosyndromes and metabolites which have been claimed to be of use in fungal chemotaxonomy.

INTRODUCTION

Fungal secondary metabolites are important because of the wide range of biological activities which the compounds can elicit. The effects can be beneficial (*e.g.* antibiotics) or detrimental (*e.g.* mycotoxins). Additional methods are required in the search to find new drugs, insecticides[1,2], herbicides, etc. derived from fungi, and to detect both established and potential mycotoxins. A concomitant need is to refine the species concepts in some groups of fungi to ensure that published work can be repeated

0021-9673/90/$03.50

with similar strains, and biochemical characters can contribute to this[3]. Towards this end, secondary metabolites have been increasingly emphasised as additional characters in fungal systematics[4].

Chromatography is often used to separate, and UV spectroscopy to identify, fungal secondary metabolites[5]. Spectra can be obtained from metabolites removed from (a) thin-layer chromatography (TLC) or preparative layer chromatography (PLC) plates[1] or (b) fractions from preparative high-performance liquid chromatography (HPLC); both these procedures permit additional analysis of the compounds to be made. Diode-array detection (DAD) with HPLC[6,7], and the recently developed technology to take UV spectra of spots on TLC plates[8] for the identification of fungal compounds, increasingly establishes the link between UV spectroscopy and chromatography.

The utility of UV spectroscopy can be increased for certain classes of compounds by comparing spectra of metabolites in neutral to those in strongly alkaline solvents, and subtracting the neutral from the alkaline spectrum to obtain a difference spectrum[9,10]. Difference curves are characteristic only of the ionizable elements of compounds and can be used to give quantitative and qualitative information on the compounds in mixtures. Also, the data and method are useful for the differentiation of metabolites with similar chromophores. Advantages are provided over absorption curves for the analyses of ionizable chromophores when the absorbing units are present either as parts of the molecule or in mixtures of various molecules. The method was primarily developed for the determination of phenolic components in lignin, but other ionizable chromophores which are ammenable to this technique are unsaturated systems containing, for example, enolic, carboxcylic and amino groups.

Difference curves permit the study of separate chromophores in complex mixtures without the need for physical separation and will be useful for the rapid determination of distinctive compounds in crude extracts of fungi. The technique will be useful in the identification of both fungi and compounds which the fungus has produced. Also, the UV spectra of certain metabolites which have similar UV spectra in neutral solvents can sometimes be differentiated by the UV spectra in alkaline solvents and/or the difference spectra.

A wide range of fungal metabolites has been used as taxonomic characters in *Penicillium*[3], and rapid and convenient methods are required to identify the metabolites. Frisvad and Filtenborg[4] published a list of TLC characteristics of selected secondary metabolites useful for systematic purposes in that genus. A standardized TLC database has also been made available on 80 identified and 27 unidentified fungal metabolites[11], and HPLC data bases have also been published[12]. Gradient HPLC–DAD of 182 secondary metabolites was published by Frisvad and Thrane[6], and the method was used to identify biosynthetically related metabolites on the basis of similar chromophores, which was claimed to be useful in the chemotaxonomy of fungi. References 6 and 12 are particularly useful in the identification of peaks obtained from HPLC of fungal extracts in other laboratories[2].

This paper provides the neutral, alkaline and difference spectra of 6 metabolites to assist in the identification of secondary metabolites with biological activity and those useful in taxonomy. These data are compared with the maxima published for the same metabolites obtained from gradient HPLC–DAD[6], to assess the validity of the methods used in refs. 6 and 7 for the identification of chromophores and metabolites of use in fungal systematics.

EXPERIMENTAL

Metabolites and purity

These were obtained from a collection of pure fungal metabolites held at CAB International Mycological Institute (Kew, U.K.). Purity of the metabolites was established before analysis as detailed in ref. 11, and 48 of the metabolites were also re-analysed for purity after UV analysis by both TLC systems. Six metabolites were analysed by HPLC[2] and assessed as pure, except for xanthocillin which has four peaks (also seen in ref. 6) which probably represent the methyl and dimethyl ether derivatives of xanthocillin; the spectral data are included in Tables I and II. UV spectra in methanol of some of the metabolites considered here have been published[5], and the spectra were compared to the maxima in ref. 6 (Table III).

UV spectra

All UV spectra were determined using a Philips PU8700 Series UV–VIS spectrophotometer. Spectra in the neutral solvent were obtained in HPLC-grade methanol; alkaline spectra were obtained by adding two drops of 2 *M* sodium hydroxide solution to the cuvette using a Pasteur pipette[13]. Difference spectra were obtained by using the graphic system of the spectrophotometer to subtract the neutral from the alkaline spectra. Molar extinction coefficients (ε) were not calculated because the metabolites were not weighed with a sufficiently sensitive weighing balance.

RESULTS AND DISCUSSION

Fig. 1 gives neutral, alkaline and difference spectra of some representative so-called acid, neutral and alkaloid metabolites with either two, three, four or five maxima in methanol. Table I provides the wavelength maxima of the neutral, alkaline and difference spectra for all metabolites. The spectra of the alkaloids cyclopenin and cyclopenol provide an example of the utility of the difference curves in differentiating between compounds with similar chromophores. Cyclopenin is converted into cyclopenol by cyclopenin *m*-hydroxylase which catalyses the addition of a hydroxyl group onto the phenyl ring. The UV maximum of cyclopenin is 289 nm, whereas that for cyclopenol is 282 nm, and both spectra are similar. However, the difference spectra of the two compounds are clearly different and can be used to differentiate between these similar compounds more effectively. Another example is that of the related compounds 3,5-dimethyl-6-methoxyphthalide and 3,5-dimethyl-6-hydroxyphthalide where the difference spectra are more distinct than the UV spectra in methanol. Other examples can be observed readily in Table II which lists the metabolites in order of increasing wavelength of the maxima, thereby listing together those metabolites with similar chromophores and enabling the rapid identification of spectra from unknown metabolites. Also, in some cases peaks were obtained with the alkaline and/or difference spectra where only end absorption was observed in methanol (*i.e.* hadacidin, canadensolide and β-nitropropionic acid), thus providing more information which can be used to identify these metabolites.

The UV maxima of the metabolites in methanol published here are compared to those published by Frisvad and Thrane[6], in an acetonitrile (with trifluoroacetic acid) and water solvent gradient, and to the methanol spectra of Cole and Cox[5] (Table III).

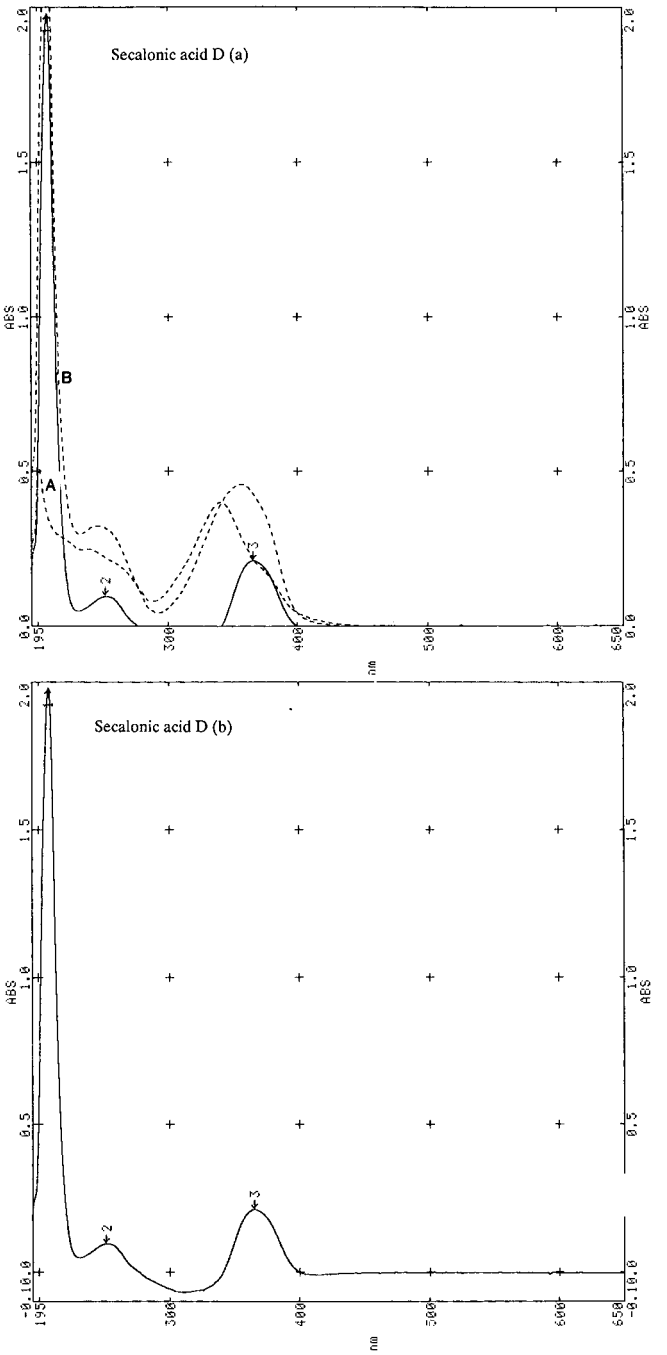

Fig. 1.

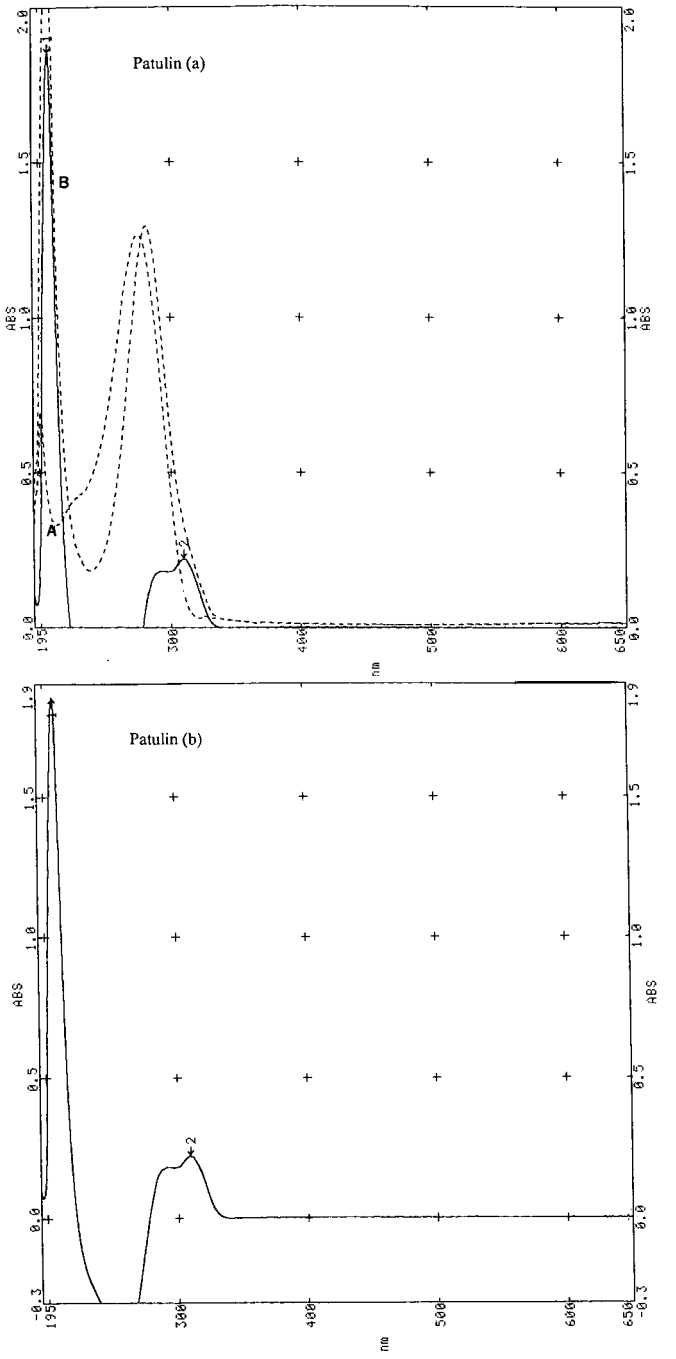

Fig. 1.

(Continued on p. 200)

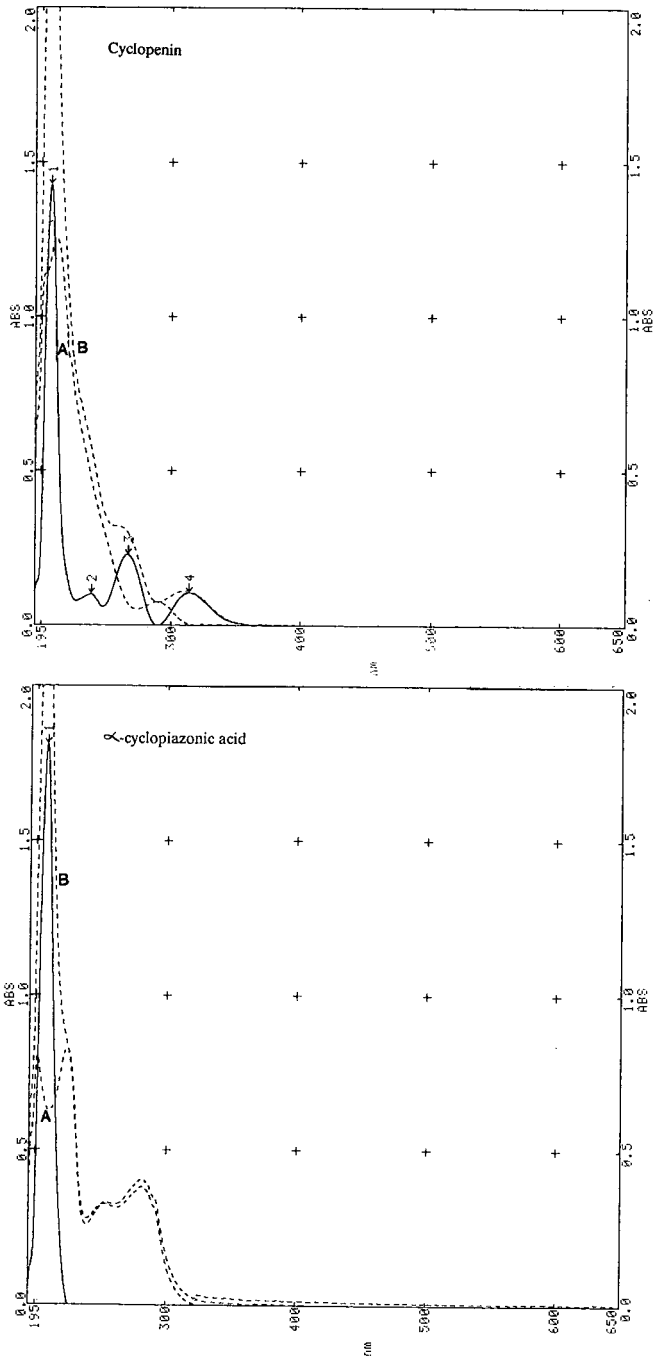

Fig. 1.

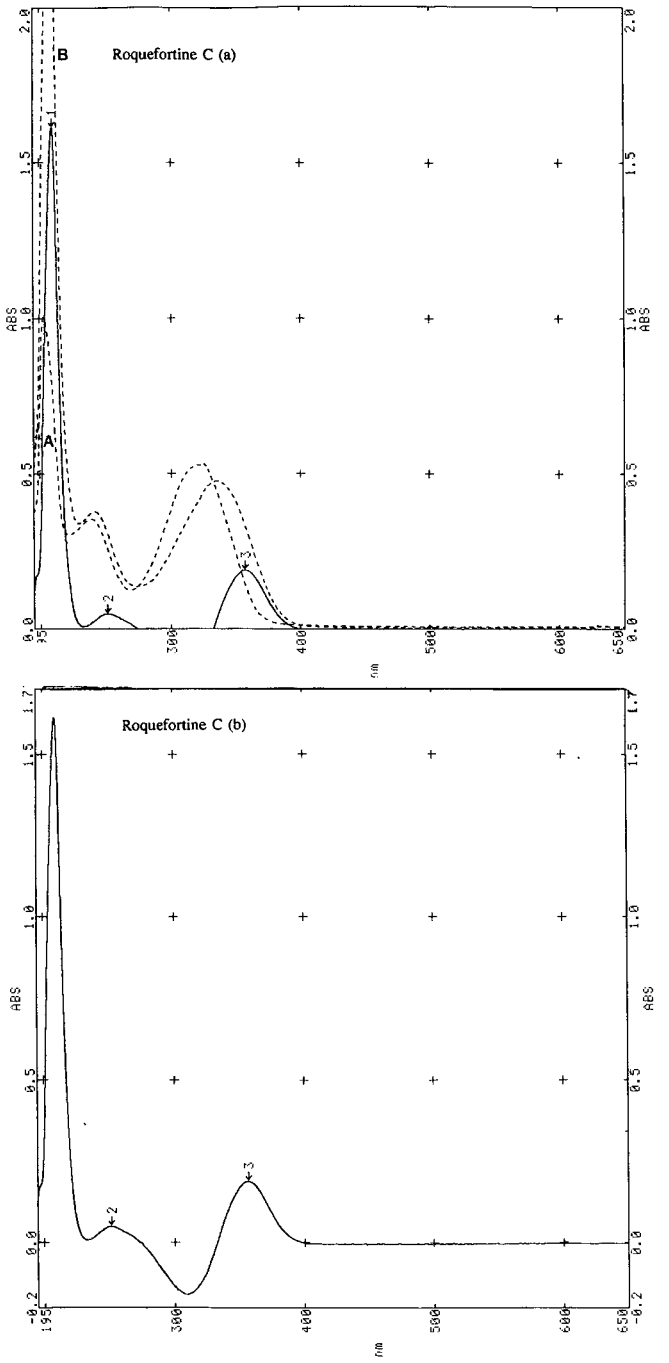

Fig. 1.

(Continued on p. 202)

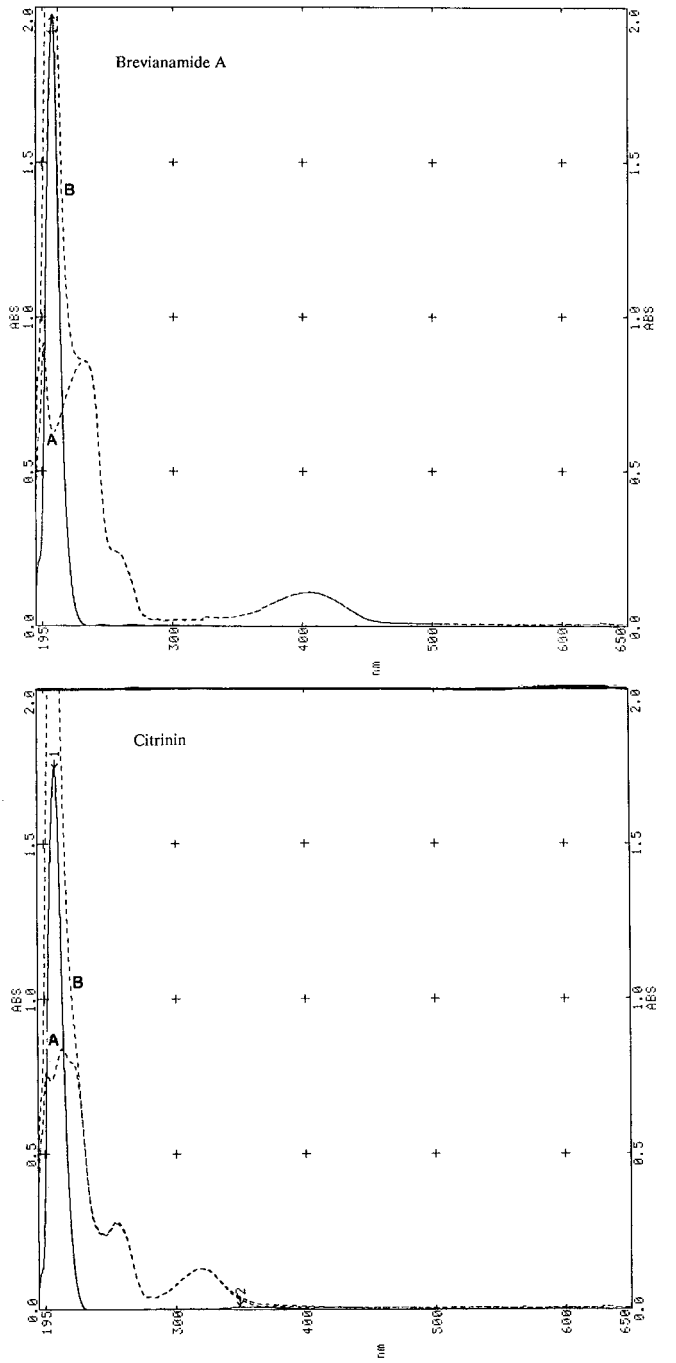

Fig. 1.

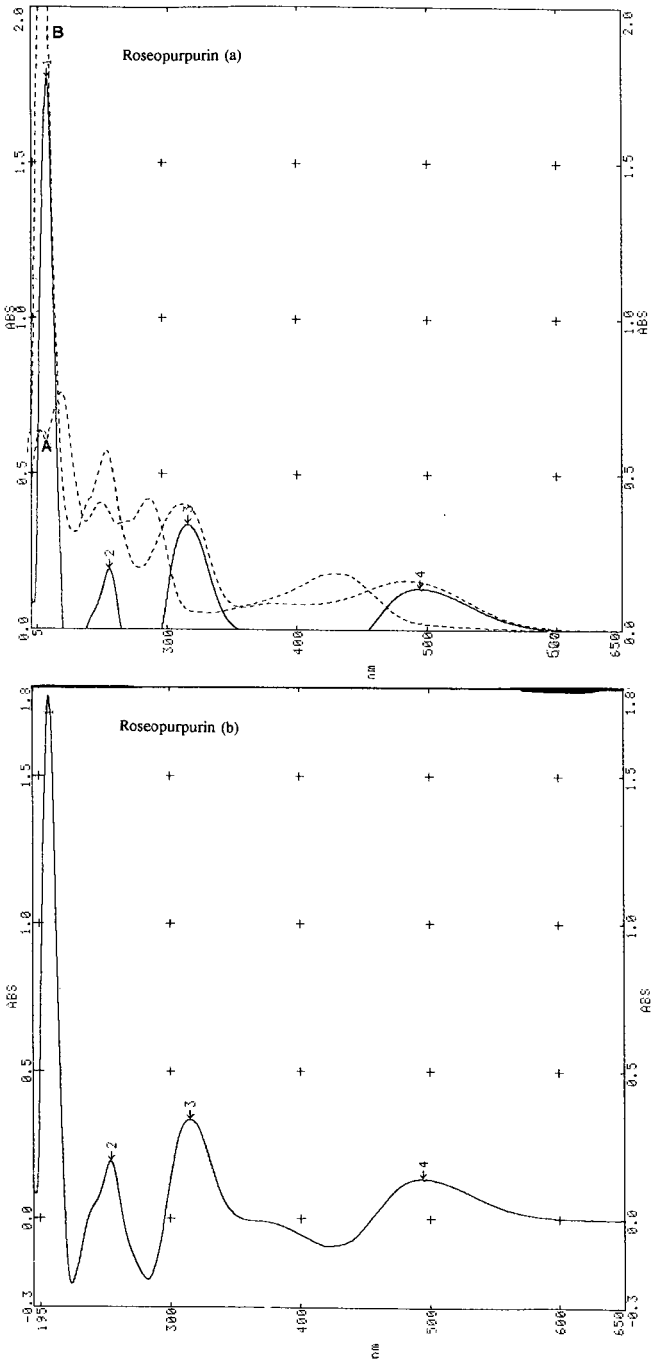

Fig. 1.

(Continued on p. 204)

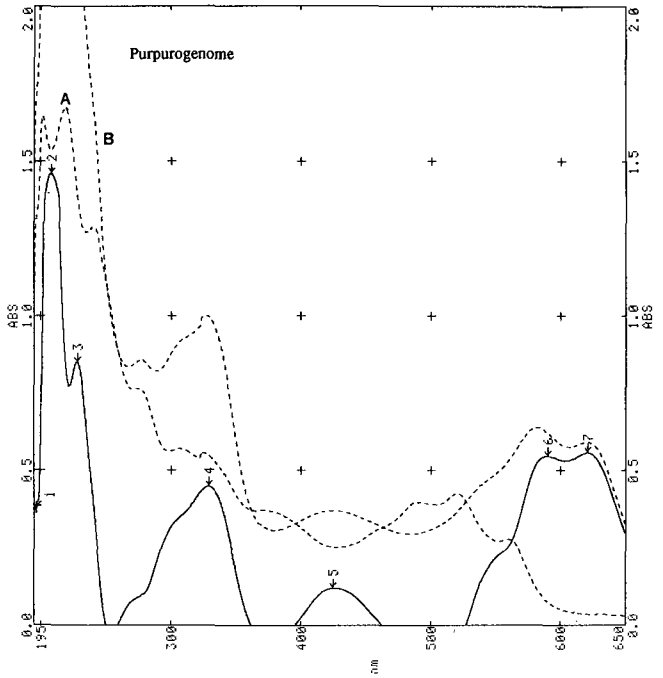

Fig. 1. Spectra of selected metabolites. Metabolites with one maximum are secalonic acid D (acid), patulin (neutral) and cyclopenin (alkaloid); two maxima are α-cyclopiazonic acid (acid), roquefortine C (neutral) and brevianamide A (alkaloid); three maxima is citrinin (acid); four maxima is roseopurpurin; five maxima is purpurogenome. (a) UV spectrum in methanol (dashed line A), plus sodium hydroxide (dashed line B) and difference spectrum (solid line), (b) = Difference spectrum alone.

An estimate of the similarity in the wavelength maxima for each metabolite is provided in Table IV. Although there was similarity to most of the maxima given by Frisvad and Thrane[6], the following was observed: (a) what were considered maxima by Frisvad and Thrane[6] are sometimes only shoulders or small peaks in the data obtained here (*e.g.* canescin, dipicolonic acid, etc.; Table III); (b) some maxima reported in ref. 6 were not observed in the new data set, and *vice versa* (*e.g.* carolic acid, chaetoglobosin C, etc.; Table III); (c) maxima had different values for the same metabolites (*e.g.* 3,5-dimethyl-6-hydroxyphthalide, fulvic acid, etc.; Table III). This indicates considerable differences in the two data sets, and not slight differences as observed by Frisvad and Thrane[6] when comparing their data to those of Cole and Cox[5].

The similarity in the data appears to be correlated with the retention indices of the metabolites[6] and consequently the particular solvent composition in which they were dissolved at the time of elution. The largest discrepancy between the present results and those of Frisvad and Thrane[6] occur at retention indices (*I*) of between 1000 and 1299 (Table IV). The differences which occurred in this range are, for example: the chaetoglobosin C peak at 252 nm in ref. 6 was not observed in the present study or in ref. 5, and shoulders and small peaks were observed here rather than the maxima as given in ref. 6; the α-cyclopiazonic acid shoulder at 253 nm was observed in the present

TABLE I

MAXIMA (AS ASSESSED BY THE SPECTROPHOTOMETER COMPUTER) OF THE SECONDARY METABOLITES IN METHANOL, METHANOL PLUS TWO DROPS OF 2 *M* SODIUM HYDROXIDE AND DIFFERENCE SPECTRA

λ = Wavelength; A = absorbance.

Metabolite		*Methanol*		*Sodium hydroxide*		*Difference*	
		λ (nm)	A	λ (nm)	A	λ (nm)	A
Aurofusarin	(1)	201.1	0.413	207.3	2.168	207.5	1.931
(4.0 μg ml^{-1})	(2)	253.7	0.189	251.4	0.199		
Austdiol	(1)	201.7	0.761	208.1	2.276	208.5	1.763
(4.0 μg ml^{-1})	(2)	256.4	0.517	256.3	0.445	312.0	0.042
	(3)	380.0	0.853	380.0	0.756	407.6	0.037
Brefeldin A	(1)	203.6	1.584	209.1	2.518	209.6	1.107
(9.0 μg ml^{-1})							
Brevianamide A	(1)	200.9	0.917	207.8	2.607	207.9	1.977
(3.2 μg ml^{-1})	(2)	232.0	0.859	405.6	0.110		
	(3)	406.2	0.113				
Canadensic acid	(1)	202.9	0.903	208.4	2.138	208.9	1.475
(10.0 μg ml^{-1})							
Canadensolide	(1)	203.3	0.849	207.8	2.618	208.0	1.811
(6.6 μg ml^{-1})	(2)					244.1	0.527
Canescin	(1)	200.1	0.516	206.6	2.235	206.7	1.897
(1.6 μg ml^{-1})	(2)	247.3	1.053	257.9	0.920	244.0	−0.347
	(3)	327.4	0.147	284.0	0.329	258.5	0.536
	(4)			313.0	0.315	285.7	0.183
	(5)					309.0	0.212
Carlosic acid	(1)	199.8	0.551	206.7	2.439	206.7	2.220
(4.0 μg ml^{-1})	(2)	230.9	0.870	230.9	0.892	256.8	0.073
	(3)	265.8	0.963	264.6	1.002		
Carolic acid	(1)	196.5	0.432	206.0	2.273	206.0	1.783
(4.0 μg ml^{-1})	(2)	205.6	0.490	233.6	0.675	248.1	0.360
	(3)	230.2	0.574	256.0	0.883		
	(4)	269.1	0.972				
Chaetoglobosin C	(1)	202.2	1.347	209.9	2.989	209.9	1.961
(2.8 μg ml^{-1})	(2)	221.3	1.273				
Cinnamic acid	(1)	203.2	0.889	207.7	2.364	207.9	1.590
(1.8 μg ml^{-1})	(2)	215.2	0.773	267.2	0.819	242.0	0.082
	(3)	221.0	0.633				
	(4)	269.7	0.829				
Citrinin	(1)	201.3	0.764	208.5	2.514	208.2	1.742
(3.2 μg ml^{-1})	(2)	213.7	0.840	254.5	0.277		
	(3)	254.6	0.283	319.8	0.132		
	(4)	320.1	0.131				
Compactin	(1)	198.7	0.573	206.9	2.515	206.9	2.083
(6.6 μg ml^{-1})	(2)	229.5	1.154	229.5	1.149	240.6	0.006
	(3)	236.7	1.265	236.7	1.247	249.2	0.023
	(4)	245.1	0.836	245.1	0.832		

(Continued on p. 206)

TABLE I *(continued)*

Metabolite		*Methanol*		*Sodium hydroxide*		*Difference*	
		λ (nm)	*A*	*λ (nm)*	*A*	*λ (nm)*	*A*
Cyclopaldic acid	(1)	202.3	1.296	206.4	2.483	207.6	1.593
(5.0 μg ml^{-1})	(2)	243.9	1.080	393.3	0.076	298.3	0.071
	(3)					398.6	0.069
Cyclopenin	(1)	212.0	1.255	208.2	2.626	207.7	1.427
(4.8 μg ml^{-1})	(2)	288.8	0.076	312.8	0.111	239.3	0.102
	(3)					267.3	0.229
	(4)					314.5	0.106
Cyclopenol	(1)	203.1	1.405	208.8	2.592	209.5	1.620
(1.8 μg ml^{-1})	(2)	281.6	0.095			308.7	0.072
α-Cyclopiazonic acid	(1)	201.3	0.806	207.9	2.456	208.0	1.812
(3.2 μg ml^{-1})	(2)	224.5	0.828	253.6	0.327	250.8	−0.004
	(3)	281.6	0.407	281.8	0.382		
Cytochalasin H	(1)	202.9	1.058	208.9	2.322	209.5	1.479
(3.3 μg ml^{-1})							
Desacetylpebrolide	(1)	201.5	0.986	206.5	2.247	206.9	1.805
(11.9 μg ml^{-1})	(2)	229.6	0.794	229.6	0.786		
Dehydrocanadensolide	(1)	200.6	0.386	212.9	2.910	213.4	2.629
(40 μg ml^{-1})							
Dehydrocarolic acid	(1)	199.6	0.666	206.8	2.483	206.8	1.896
(9.0 μg ml^{-1})	(2)	244.1	0.806	247.1	1.024	248.1	0.225
	(3)	285.6	0.861	300.8	0.476	317.0	0.154
Desmethoxyviridiol	(1)	201.1	0.491	207.2	2.356	207.5	2.011
(1.6 μg ml^{-1})	(2)	248.2	0.530	232.8	0.484	292.8	0.655
	(3)	318.9	0.265	293.5	0.793	368.9	0.098
	(4)			368.9	0.107	459.5	0.198
	(5)			460.8	0.198		
3,5-Dimethyl-6-	(1)	208.7	1.299	207.3	2.411	207.1	1.126
-hydroxyphthalide	(2)	242.4	0.236	224.4	1.159	225.1	0.896
(1.6 μg ml^{-1})	(3)	312.8	0.151	247.2	0.240	253.5	0.163
	(4)			351.2	0.251	351.4	0.235
3,5-Dimethyl-6-	(1)	207.9	1.835	210.2	2.448	211.7	0.682
-methoxyphthalide	(2)	239.8	0.398	240.4	0.383		
(1.6 μg ml^{-1})	(3)	300.0	0.180	300.0	0.173		
Dipicolonic acid	(1)	202.6	1.319	206.5	2.177	207.6	1.300
(10.0 μg ml^{-1})	(2)	269.7	0.269	269.9	0.296	279.0	0.035
Duclauxin	(1)	201.3	0.898	207.1	2.672	194.4	0.261
(not determined)	(2)	232.1	0.872	240.5	0.788	207.3	1.880
	(3)			319.5	0.541	252.9	0.089
	(4)			415.6	0.170	322.0	0.358
	(5)					415.7	0.119
Epoxysuccinate	(1)	200.8	0.393	207.6	2.058	207.7	1.768
(40.0 μg ml^{-1})							
(29) Ergosterol	(1)	201.7	0.974	206.4	2.229	207.0	1.544
(10.0 μg ml^{-1})	(2)	271.9	0.615	271.8	0.621		
	(3)	282.1	0.638	282.1	0.644		
	(4)	293.8	0.379	293.8	0.388		

TABLE I *(continued)*

Metabolite		*Methanol*		*Sodium hydroxide*		*Difference*	
		λ (nm)	*A*	*λ (nm)*	*A*	*λ (nm)*	*A*
Ethisolide (3.3 μg ml^{-1})	(1)	201.3	0.689	208.0	2.216	208.2	1.712
Frequentin (3.3 μg ml^{-1})	(1)	198.9	0.769	207.3	2.693	207.1	2.122
	(2)	231.5	1.286	227.2	1.183	252.1	0.066
	(3)	288.8	0.213	312.8	0.636	314.1	0.510
Fulvic acid (3.3 μg ml^{-1})	(1)	200.7	0.631	207.8	2.340	207.9	1.882
	(2)	376.3	0.307	368.9	0.351	246.5	0.075
	(3)					266.8	0.072
	(4)					358.0	0.052
Gentisic acid (3.3 μg ml^{-1})	(1)	202.5	0.950	208.1	2.321	208.1	1.426
	(2)	327.6	0.170	330.4	0.144	252.5	0.053
	(3)					364.3	0.032
Gentisyl alcohol (4.0 μg ml^{-1})	(1)	202.7	1.164	207.7	2.350	208.5	1.760
	(2)	296.8	0.205	268.3	0.476	266.0	0.449
	(3)					321.0	0.058
Glauconic acid (4.0 μg ml^{-1})	(1)	203.2	0.877	207.7	2.283	207.9	1.462
Gliotoxin (8.0 μg ml^{-1})	(1)	202.6	1.016	208.5	2.408	209.1	1.666
	(2)	268.3	0.295	267.2	0.300		
Griseofulvin (16.0 μg ml^{-1})	(1)	196.5	0.642	208.4	2.156	206.6	1.688
	(2)	212.7	0.769	232.9	0.704	259.9	−0.002
	(3)	233.1	0.724	251.8	0.737	299.2	0.012
	(4)	251.7	0.744	288.1	1.361		
	(5)	287.9	1.376				
Griseophenone C (2.8 μg ml^{-1})	(1)	205.3	1.796	207.5	2.655	209.2	1.018
	(2)	296.1	0.683	302.4	0.611	246.2	0.471
	(3)			380.8	0.190	311.1	0.103
	(4)					389.9	0.164
Hadacidin (4.0 μg ml^{-1})	(1)	204.1	0.990	207.2	2.650	207.3	1.681
	(2)					237.5	0.747
5′-Hydroxyasperentin (4.8 μg ml^{-1})	(1)	201.1	0.740	208.1	2.373	207.7	1.587
	(2)	216.1	0.940	246.2	0.421	242.9	0.299
	(3)	268.8	0.577	310.8	1.114	313.2	0.933
	(4)	301.3	0.252				
m-Hydroxybenzoic acid (1.8 μg ml^{-1})	(1)	207.7	1.589	209.1	2.581	209.9	1.020
	(2)	297.3	0.146	312.0	0.120	218.5	0.900
	(3)					249.7	0.179
	(4)					320.7	0.091
p-Hydroxybenzoic acid (4.0 μg ml^{-1})	(1)	202.9	1.315	208.9	2.455	209.9	1.527
	(2)	252.2	0.899	276.0	1.098	286.1	0.954
Hydroxyisocanadensic acid (4.4 μg ml^{-1})	(1)	200.1	0.494	207.7	2.326	207.7	1.985
	(2)	225.2	0.452				
Itaconic acid (4.0 μg ml^{-1})	(1)	202.8	0.880	208.1	2.202	208.7	1.519

(Continued on p. 208)

TABLE I *(continued)*

Metabolite		*Methanol*		*Sodium hydroxide*		*Difference*	
		λ (nm)	*A*	*λ (nm)*	*A*	*λ (nm)*	*A*
Kojic acid	(1)	200.4	0.780	206.7	2.576	206.6	1.874
(4.0 μg ml^{-1})	(2)	217.5	0.906	226.9	1.405	229.2	0.841
	(3)	270.4	0.501	314.4	0.337	315.7	0.322
Lapidosin	(1)	199.8	0.575	207.4	2.449	207.4	1.970
(3.3 μg ml^{-1})	(2)	229.1	0.570	259.5	0.683	257.6	0.341
	(3)	320.2	0.551	305.4	0.619	303.4	0.103
	(4)					359.5	0.171
Lichexanthone	(1)	201.1	0.723	207.7	2.479	207.9	1.890
(4.0 μg ml^{-1})	(2)	241.7	0.621	240.0	0.586	271.3	0.081
	(3)	307.2	0.373	306.1	0.312	375.3	0.038
6-Methylsalicylic acid	(1)	209.7	0.969	209.3	2.344	209.1	1.376
(1.6 μg ml^{-1})	(2)	311.0	0.124	300.8	0.114	290.6	0.017
Monorden	(1)	201.9	1.062	207.0	2.541	207.3	1.561
(4.0 μg ml^{-1})	(2)	266.4	0.526	253.6	0.573	248.6	0.199
	(3)			275.0	0.633	277.7	0.134
	(4)			318.9	0.354	324.0	0.231
Mycelianamide	(1)	201.6	0.745	208.2	2.305	208.7	1.881
(4.0 μg ml^{-1})	(2)	231.2	0.239	328.9	0.398	276.6	0.017
	(3)	324.2	0.406			357.9	0.127
Mycophenolic acid	(1)	201.9	0.949	208.1	2.497	207.9	1.633
(3.2 μg ml^{-1})	(2)	215.8	0.997	345.3	0.176	229.4	0.480
	(3)	250.1	0.226			262.5	0.025
	(4)	305.9	0.115			345.3	0.151
β-Nitropropionic acid	(1)	201.5	0.645	207.1	2.340	207.5	1.880
(4.0 μg ml^{-1})	(2)			236.0	0.467	237.8	0.423
Norlichexanthone	(1)	201.0	0.840	207.3	2.513	207.5	1.867
(3.3 μg ml^{-1})	(2)	241.3	0.797	237.6	0.690	247.7	−0.025
	(3)	311.1	0.468	266.4	0.462	267.0	0.232
	(4)			360.5	0.728	362.9	0.653
Orsellenic acid	(1)	200.6	0.800	207.1	2.432	206.9	1.719
(1.6 μg ml^{-1})	(2)	217.5	1.017	275.6	0.477	236.8	0.237
	(3)	259.2	0.411			277.4	0.357
	(4)	300.0	0.176				
Palitantin	(1)	198.5	0.761	206.6	2.674	206.5	2.082
(4.9 μg ml^{-1})	(2)	232.0	1.430	231.7	1.396	251.0	0.012
Patulin	(1)	200.7	0.700	207.4	2.226	207.7	1.852
(3.2 μg ml^{-1})	(2)	275.7	1.263	281.4	1.293	309.4	0.221
Paxilline	(1)	199.2	0.568	206.8	2.523	206.8	2.039
(1.6 μg ml^{-1})	(2)	230.5	0.940	230.1	0.938		
	(3)	281.6	0.201	280.1	0.204		
Penicillic acid	(1)	200.7	0.656	208.7	2.583	208.5	2.051
(3.2 μg ml^{-1})	(2)	224.8	0.800			251.5	0.087
Penitrem A	(1)	200.9	0.701	206.7	2.356	206.8	1.771
(7.4 μg ml^{-1})	(2)	234.9	0.666	234.6	0.662		
	(3)	301.9	0.215	301.6	0.215		

TABLE I *(continued)*

Metabolite		*Methanol*		*Sodium hydroxide*		*Difference*	
		λ (nm)	*A*	*λ (nm)*	*A*	*λ (nm)*	*A*
Phoenicin	(1)	200.7	0.872	207.2	2.785	207.2	2.014
(4.0 μg ml^{-1})	(2)	217.6	0.829	269.1	0.666	287.0	0.093
	(3)	261.6	0.821	527.3	0.123	577.9	0.053
	(4)	492.8	0.105				
PR-Toxin	(1)	201.5	0.920	208.3	2.479	208.7	1.952
(4.6 μg ml^{-1})	(2)	247.5	0.653	248.3	0.621	402.7	0.027
	(3)			400.3	0.054		
Purpurogenone	(1)	201.9	1.647	203.5	3.008	195.9	0.381
(20.0 μg ml^{-1})	(2)	219.5	1.674	278.2	0.859	208.5	1.462
	(3)	241.4	1.291	327.3	1.001	228.3	0.851
	(4)			423.5	0.370	329.2	0.450
	(5)	519.5	0.424	581.6	0.639	424.9	0.119
	(6)			621.9	0.592	590.6	0.546
	(7)					621.9	0.557
2-Pyruvoylamino-	(1)	211.2	0.920	206.9	2.467	206.9	1.563
benzamide	(2)	248.0	0.460	309.9	0.278	236.8	0.064
(4.0 μg ml^{-1})	(3)	301.3	0.228			321.9	0.127
Roquefortine B	(1)	202.2	0.937	207.0	2.359	207.3	1.527
(4.0 μg ml^{-1})	(2)	223.7	1.234	281.1	0.272		
	(3)	281.9	0.272				
Roquefortine C	(1)	203.1	1.005	208.9	2.406	209.6	1.614
(4.8 μg ml^{-1})	(2)	238.6	0.355	241.8	0.380	251.6	0.050
	(3)	324.1	0.536	336.5	0.477	357.0	0.189
Roseopurpurin	(1)	201.0	0.648	207.8	2.396	207.7	1.773
(4.0 μg ml^{-1})	(2)	218.5	0.760	253.8	0.576	255.0	0.193
	(3)	248.3	0.407	311.7	0.402	315.6	0.336
	(4)	285.7	0.419	482.8	0.160	494.3	0.134
	(5)	429.6	0.183				
Rubratoxin B	(1)	202.3	0.956	208.2	2.319	208.7	1.539
(3.2 μg ml^{-1})							
Rugulovasine A	(1)	203.6	1.069	207.7	2.503	207.7	1.450
(4.0 μg ml^{-1})	(2)	221.2	1.183	287.0	0.231		
	(3)	287.2	0.229				
Secalonic acid D	(1)	201.1	0.511	207.9	2.329	208.1	1.980
(4.0 μg ml^{-1})	(2)	340.8	0.400	247.2	0.324	251.7	0.097
	(3)			356.0	0.459	364.9	0.211
Scytalone	(1)	200.7	0.704	207.1	2.280	207.0	1.717
(1.6 μg ml^{-1})	(2)	221.3	0.710	252.0	0.264	225.7	−0.061
	(3)	282.1	0.651	330.4	1.226	250.0	0.191
	(4)					332.1	1.039
Spinulosin	(1)	210.4	0.529	206.5	2.218	206.5	1.709
(1.6 μg ml^{-1})	(2)	301.1	0.317	330.5	0.612	332.5	0.466
Sterigmatocystin	(1)	201.9	0.736	206.9	2.568	207.1	1.871
(2.0 μg ml^{-1})	(2)	246.4	0.839	240.0	0.885	238.5	0.089
	(3)	326.5	0.398	324.0	0.355	274.7	0.041
	(4)					389.7	0.031

(Continued on p. 210)

TABLE I *(continued)*

Metabolite		*Methanol*		*Sodium hydroxide*		*Difference*	
		λ (nm)	*A*	*λ (nm)*	*A*	*λ (nm)*	*A*
Stipitatic acid	(1)	200.1	0.738	207.1	2.543	207.2	1.977
(1.6 μg ml^{-1})	(2)	263.0	1.602	264.4	1.454	282.8	0.456
	(3)	324.1	0.190	333.8	0.284	333.8	0.112
	(4)	369.1	0.237			404.8	0.017
Terrestric acid	(1)	201.3	0.569	206.1	2.288	206.3	1.764
(1.6 μg ml^{-1})	(2)	228.5	0.365	254.1	0.805	248.6	0.429
	(3)	272.6	0.924				
Viomellein	(1)	200.7	0.562	207.7	2.426	207.9	2.009
(4.0 μg ml^{-1})	(2)	222.4	0.448	264.5	0.483	316.2	0.019
	(3)	264.1	0.537	382.4	0.140	548.2	0.056
	(4)	380.3	0.154	528.5	0.073		
Viridicatum toxin	(1)	201.2	0.580	207.7	2.277	208.1	1.951
(not determined)	(2)	235.2	0.223	280.1	0.263		
	(3)	283.2	0.289	440.8	0.092		
	(4)	449.6	0.086				
Xanthocillin	(1)	201.1	0.792	208.1	2.524	208.5	2.009
(4.0 μg ml^{-1})	(2)	346.4	0.405	251.2	0.454	266.6	0.249
	(3)			338.4	0.443	335.2	0.065
	(4)			410.4	0.390	416.1	0.359

TABLE II

METABOLITES LISTED BY INCREASING WAVELENGTH (nm) OF MAXIMA

In lists 2–8 end absorption peaks have been omitted.

Methanol	*Sodium hydroxide*	*Difference*	*Metabolite*
(1) End absorption only			
200.6	212.9	213.4	Dehydrocanadensolide
200.8	207.6	207.7	Epoxysuccinate
201.3	208.0	208.2	Ethisolide
202.3	208.2	208.7	Rubratoxin B
202.8	208.1	208.7	Itaconic acid
202.9	208.4	208.9	Canadensic acid
202.9	208.9	209.5	Cytochalasin H
203.2	207.7	207.9	Glauconic acid
203.6	209.1	209.6	Brefeldin A
(2) Difference peak only			
		237.5	Hadacidin
		244.1	Canadensolide
(3) Sodium hydroxide and difference peak only			
	236.0	237.8	β-Nitropropionic acid

TABLE II *(continued)*

Methanol	*Sodium hydroxide*	*Difference*	*Metabolite*
(4) One maximum in methanol			
221.3	–	–	Chaetoglobosin C
224.8	–	251.5	Penicillic acid
225.2			Hydroxyisocanadensic acid
229.6	229.6		Desacetylpebrolide
232.0	231.7	251.0	Palitantin
232.1	240.5 319.5 415.6	207.3 252.9 322.0 415.7	Duclauxin
243.9	393.3	298.3 398.6	Cyclopaldic acid
247.5	248.3 400.3	272.1 402.7	PR-Toxin
252.2	276.0	286.1	*p*-Hydroxybenzoic acid
253.7	251.4		Aurofusarin
266.4	253.6 275.0 318.9	248.6 277.7 324.0	Monorden
268.3	267.2		Gliotoxin
269.7	269.9	279.0	Dipicolonic acid
275.7	281.4	309.4	Patulin
281.6		308.7	Cyclopenol
288.8	312.8	239.3 267.3 314.5	Cyclopenin
296.1	302.4 380.8	246.2 311.1 389.9	Griseophenone C
296.8	268.3	266.0 321.0	Gentisyl alcohol
297.3	312.0	218.5 249.7 320.7	*m*-Hydroxybenzoic acid
301.1	330.5	332.5	Spinulosin
311.0	300.8	290.6	6-Methylsalicylic acid
327.6	330.4	252.5 364.3	Gentisic acid
340.8	247.2 356.0	251.7 364.9	Secalonic acid D
346.4	251.2 338.4 410.4	266.6 335.2 416.1	Xanthocillin

(Continued on p. 212)

TABLE II *(continued)*

Methanol	*Sodium hydroxide*	*Difference*	*Metabolite*
376.3	368.9	246.5 266.8 358.0	Fulvic acid
(5) Two maxima in methanol			
217.5 270.4	226.9 314.4	229.2 315.7	Kojic acid
221.3 282.3	252.0 330.4	225.7 250.0 332.1	Scytalone
221.2 287.2	287.0		Rugulovasine A
223.7 281.9	281.1		Roquefortine B
224.5 281.6	253.6 281.8	250.8	α-Cyclopiazonic acid
228.5 272.6	254.1	248.6	Terrestric acid
229.1 320.2	259.5 305.4	257.6 303.4 359.5	Lapidosin
230.9 265.8	230.9 264.6	256.8	Carlosic acid
230.5 281.6	230.1 280.1		Paxilline
231.5 288.8	227.2 312.8	252.1 314.1	Frequentin
231.2 324.2	328.9	276.6 357.9	Mycelianamide
232.0 406.2	405.6		Brevianamide A
234.9 301.9	234.6 301.6		Penitrem A
238.6 324.1	241.8 336.5	251.6 357.0	Roquefortine C
239.8 300.0	240.4 300.0		3,5-Dimethyl-6-methoxyphthalide
241.3 311.1	237.6 266.4 360.5	247.7 267.0 362.9	Norlichexanthone
241.7 307.2	240.0 306.1	271.3 375.3	Lichexanthone
242.4 312.8	224.4 247.2 351.2	225.1 253.5 351.4	3,5-Dimethyl-6-hydroxyphthalide

TABLE II *(continued)*

Methanol	*Sodium hydroxide*	*Difference*	*Metabolite*
244.1	247.1	248.1	Dehydrocarolic acid
285.6	300.8	317.0	
246.4	240.0	238.5	Sterigmatocystin
326.5	324.0	274.7	
		389.7	
247.3	257.9	244.0	Canescin
327.4	284.0	258.5	
	313.0	285.7	
		309.0	
248.2	309.9	236.8	2-Pyruvoylaminobenzamide
301.3		321.9	
248.2	232.8	292.8	Desmethoxyviridiol
318.9	293.5	368.9	
	368.9	459.5	
	460.8		
256.4	256.3	312.0	Austdiol
380.0	380.0	407.6	
(6) Three maxima in methanol			
205.6	233.6	248.1	Carolic acid
230.2	256.0		
269.1			
213.7	254.5		Citrinin
254.6	319.8		
320.1			
215.2	267.2	242.0	Cinnamic acid
221.0			
269.7			
215.8	345.3	229.4	Mycophenolic acid
250.1		262.5	
305.9		345.3	
216.1	246.2	242.9	5′-Hydroxyasperentin
268.8	310.8	313.2	
301.3			
217.5	275.6	236.8	Orsellenic acid
259.2		277.4	
300.0			
217.6	269.1	287.0	Phoenicin
261.6	527.3	577.9	
492.8			
222.4	264.5	316.2	Viomellein
264.1	382.4	548.2	
380.3	528.5		
229.5	229.5	240.6	Compactin
236.7	236.7	249.2	
245.1	245.1		

(Continued on p. 214)

TABLE II *(continued)*

Methanol	*Sodium hydroxide*	*Difference*	*Metabolite*
235.2	280.1		Viridicatum toxin
283.2	440.8		
449.6			
263.0	264.4	282.8	Stipitatic acid
324.1	333.8	333.8	
369.1		404.8	
271.9	271.8	258.7	Ergosterol
282.1	282.1	268.1	
293.8	293.8	279.3	
		291.6	
(7) Four maxima in methanol			
212.7	232.9	259.9	Griseofulvin
233.1	251.8	299.2	
251.7	288.1		
287.9			
218.5	253.8	255.0	Roseopurpurin
248.3	311.7	315.6	
285.7	482.8	494.3	
429.6			
(8) Five maxima in methanol			
219.5	278.2	208.5	Purpurogenome
241.4	327.3	228.3	
324.2	423.5	329.2	
519.5	581.6	424.9	
	621.9	590.6	
		621.9	

TABLE III

COMPARISON OF UV DATA OF THE PRESENT STUDY WITH THOSE OF THE SAME METABOLITES IN FRISVAD AND THRANE[6] AND COLE AND COX[5]

x = Wavelength taken from the listed maxima and y = wavelength directly from the spectrum provided in Cole and Cox. sh, sm = Shoulder and small peak, respectively, which were determined by visual inspection of spectra and not printed by the spectrophotometer in the present study. B = Assessment of similarity of data determined by only considering genuine maxima in the present study; C = assessment of similarity of data determined by also comparing shoulders and small peaks in the present data to maxima in ref. 6. + = Very similar/identical; − = obvious difference. 1, 2 = Peaks with highest and second highest absorption value. e = End absorption. I = retention index[6].

Metabolite	*I*	*Present*	*Ref. 6*	*Ref. 5*	*B*	*C*
Austdiol	702	201.7[2]	e	204[2]	+	+
		256.4	256[2]	255		
		380.0[1]	378[1]	379[1]		
Brevianamide A	865	200.9[1]			−	+
		232.0[2]	234[1]			
		255sh	254			
		406.2	404[2]			

TABLE III *(continued)*

Metabolite	*I*	*Present*	*Ref. 6*	*Ref. 5*	*B*	*C*
Canescin	907–994	200.1[2]			–	+
		247.3[1]	247[1]			
		280sm	279[2]			
		290sm	289			
		327.4	331			
Carlosic acid	692	199.8			+	+
		230.9[2]	230[2]			
		265.8[1]	263[1]			
Carolic acid	676	196.5			–	–
		205.6				
		230.2[2]	230[2]			
		269.1[1]	263[1]			
Chaetoglobosin C	1174	202.2[1]		212sh	–	–
		221.3[2]	222[1]	223[1]		
			253[2]			
		290sh	280	280		
		295sm	289	292sm		
Citrinin	919	201.3[2]			–	–
		213.7[1]	220[1]	218[1]		
		220sh		220sh		
			235			
		254.6		252[2]		
		320.1	329[2]	319		
Cyclopaldic acid	843	202.3[1]			–	–
		243.9[2]	244[1]			
		285sh	272[2]			
			326			
				x *y*		
Cyclopenin	864	212.0[1]	211[1]	211[1] 215[1]	+	+
		288.8[2]	288[2]	290 290		
				x *y*		
Cyclopenol	779	203.1[1]	211[1]	218[1]	+	+
		281.6	282	285 285		
α-Cyclopiazonic acid	1148	201.3[2]	e[1]	210sh	–	–
		224.5[1]	222[1]	225[1]		
		253sh				
		281.6	279[2]			
		291sh	288	290[2]		
Dehydrocarolic acid	678	199.6			+	+
		244.1[2]	245[1]			
		285.6[1]	294[2]			
Desacetylpebrolide	902	201.5[1]	e[1]		–	+
		229.6[2]	231[2]			
		272sm	273			
3,5-Dimethyl-6-hydroxyphthalide	901	208.7[1]	206[1]		+	+
		242.4[2]	240[2]			
		312.8	298			
Dipicolonic acid	677	202.6[1]			–	+
		220sm	220[2]			
		269.7[2]	271[1]			

(Continued on p. 216)

TABLE III *(continued)*

Metabolite	*I*	*Present*	*Ref. 6*	*Ref. 5*	*B*	*C*
Duclauxin	1142	201.3			–	–
		232.1	224[1]			
			264[2]			
			320			
			342			
Ethisolide	730	201.3	205		+	+
Frequentin	910	198.9[2]	e[1]		+	+
		231.5[1]	230[2]			
		288.8	292			
Fulvic acid	942	200.7[1]	202[1]		–	–
			230			
		330sh	338			
		376[2]	388[2]			
Gentisyl alcohol	662	202.7[1]			–	+
		223sh	220[1]			
		296.8[2]	290[2]			
Gliotoxin	848	202.6[1]			–	–
			216[1]			
		268.3[2]	267			
				x *y*		
Griseofulvin	990	196.5			+	+
		212.7[2]	210[2]	212[1]		
		233.1	234	236[2] 238sh		
		251.7	250	252		
		287.9[1]	292[2]	291[1] 290[1]		
			328	324 328sh		
Griseophenone C	945	205.3[1]			–	+
		220sh	220[1]			
		296.1[2]	296			
		340sh	334			
Hadacidin	674	204.1	210		+	+
5′-Hydroxyasperentin	828	201.1[2]			+	+
		216.1[1]	215[1]			
		268.8	266[2]			
		301.3	299			
Hydroxyisocanadesic acid	771	200.1[1]	e[2]		+	+
		225.2[2]	225[1]			
Kojic acid	676	200.4[2]			+	+
		217.5[1]	220[1]	220[1]		
		270.4	267[2]	270		
Lapidosin	914	199.8[1]	215		–	–
		229.1[2]	236			
			278[2]			
		320.2	322			
Lichexanthone	1382	201.1[1]	e[1]		–	+
		241.1[2]	240[2]			
		307.2	307			
		335sh	334			

TABLE III *(continued)*

Metabolite	*I*	*Present*	*Ref. 6*	*Ref. 5*	*B*	*C*
6-Methylsalicylic acid	802	209.7[1]	204[1]		–	–
		237.9sm	240[2]			
		311.0[2]	303			
Monorden	928	201.9[1]			–	–
			215[1]			
		266.4[2]	274[2]			
Mycelianamide	1181	201.6[1]			–	–
			210[1]			
		231.2	229			
		324.2[2]	317[2]			
Mycophenolic acid	984	201.9[2]		*x* *y*	+	+
		215.8[1]	217[1]	217 220[1]		
		250.1[2]	249[2]	249 252[2]		
		305.9	302	304 306		
Norlichexanthone	1008	201.0[1]	202[1]		–	–
		241.3[2]	240[2]			
			266			
		311.1	312			
			346			
Orsellenic acid	746	200.6[2]			+	+
		217.5	213[1]			
		259	256[2]			
		300.0	296			
Palitantin	887	198.5			+	+
		232.0[1]	230			
Patulin	684	200.7		*x* *y*	+	+
		275.7[1]	275	269 275		
Paxilline	1287	199.2[2]		*x* *y*	+	+
		230.5[2]	229[1]	230[1] 229[1]		
		281.6	280	281 280		
Penicillic acid	717	200.7		*x* *y*	+	+
		224.8[1]	226	221 225		
Penitrem A	1331	200.9[1]		*x* *y*	+	+
			210[1]	212		
		234.9[2]	234[1]	233[1] 235sh		
		301.9	290[2]	295 292		
Phoenicin	705	200.7[1]	e[2]		–	–
		217.6[2]				
		261.6	267[1]			
		492.8	435			
PR-Toxin	820	201.5[1]			+	+
		247.5	248	249(ethanol)		

(Continued on p. 218)

TABLE III *(continued)*

Metabolite	*I*	*Present*	*Ref. 6*	*Ref. 5*	*B*	*C*
Purpurogenone	1191	201.9[2]	201[1]		–	–
		219.5[2]				
		241.4	250[2]			
		265sm	265			
		310sm	308			
			389			
		485sm	499			
		519.5				
			530			
		560sm				
2-Pyruvoylaminobenzamide	767	211.2[1]	210[1]		–	–
		248.0[2]	236			
		301.3	306[2]			
Roquefortine B	674, 694	202.2[2]		212sh	–	+
		223.7[1]	223[1]	220[1]		
		275sh	275	275sh		
		281.9	280[2]	280		
		290sm	289	290sm		
Roquefortine C	928	203.1[1]	206[2]	209[1]	–	–
		238.6	232	238		
		324[2]	304[1]	328[2]		
Roseopurpurin	869	201.0[2]			–	–
		218.5[1]	210[1]			
		248.3	248			
			267			
			278			
		285.7	284[2]			
		429.6	434			
Rugulovasine A	724	203.6[2]			–	+
		221.2[1]	220[1]	224[1]		
		287.2	284[2]	284sm		
		290sh	290	290		
Scytalone	723	200.7[2]	e[1]		–	+
		221.3[1]	230			
		282.1	282[2]			
		320sh	315			
Secalonic acid D	1176	201.1[1]			–	–
			220[1]	220sh		
		240sh	248	242		
		340.8	334[2]	346		
Spinulosin	707	210.4[1]	e	210[1]	+	+
		301.1	294[1]	294		
Sterigmatocystin	1100	201.9[2]	208[1]	210[2]	–	+
		230sh	232	232sh		
		246.4[1]	246[2]	246[1]		
		326.5	324	326		
Stipatic acid	693	200.1[2]			–	+
		263.0[1]	258[1]			
		324.1	334			
		369.1	358[2]			

TABLE III *(continued)*

Metabolite	*I*	*Present*	*Ref. 6*	*Ref. 5*	*B*	*C*
Terrestric acid	738	201.3[2]	e		+	+
		228.5[1]	230[2]			
		272.9	272[1]			
Viomellein	1234,1246	200.7[1]		*x*	–	–
		222.4	222[2]	225[2]		
		264.1[2]	263[1]	264[1]		
			298			
		380.3	374	395		
Viridicatum toxin	1200	201.2[1]	e[1]		–	–
		235.2	241[2]	238[2]		
		283.2[2]	283	280		
			325	325sh		
			330			
			349	345sh		
		449.6	431	430		
Xanthocillin	201.1[1]				Not compared	
(four peaks by HPLC)	225sm		218[1]			
			235			
	240sh		240			
			252			
	295sh		295[1]			
			327[2]			
	346		348[2]			
			370[2]			
			371			

study but not in ref. 6, and a maximum was recorded in ref. 6 but only a shoulder was obtained in present study; duclauxin peaks at 224, 320 and 342 nm in ref. 6 are missing in the present study and the mycelianamide peak at 210 nm in ref. 6 is missing in the present study; norlichexanthone peaks at 266 and 346 nm in ref. 6 are missing in the present data; etc. (Table III).

TABLE IV

PERCENTAGE OF METABOLITES WHICH HAVE VIRTUALLY IDENTICAL/IDENTICAL UV SPECTRAL DATA IN THE PRESENT STUDY AND IN FRISVAD AND THRANE

B, C as for Table III; n = number of metabolites; I = retention index.

I[5]	n	*B (%)*	*C (%)*
600–699	11	54	91
700–799	12	67	83
800–899	9	44	56
900–999	11	27	54
1000–1099	1	0	0
1100–1199	7	0	14
1200–1299	3	33	33
1300–1399	2	50	100

The variation in the data at both the lower and higher *I* values, where the solvent composition was the same or most similar, can be explained by the different solvent systems used in ref. 6 and the methanol used here. However, the increase in variation observed at the intermediary *I* values is probably due to the changes in solvent composition and especially the large pH decreases which would result from the increasing concentrations of trifluoroacetic acid used in the gradient[6].

The use of UV spectra obtained by gradient HPLC–DAD to indicate biosynthetic relatedness of metabolites from similarity of chromophores, and hence their taxonomic value in fungi, has been recommended[6,7]. However, it has been indicated here that misidentification of metabolites and chemosyndromes and consequently erroneous use of the data in systematics on the basis of similar UV maxima as determined by gradient HPLC–DAD could occur; spectra with similar UV maxima need not have similar chromophores, and dissimilar UV maxima could be from similar chromophores, especially if the metabolites exhibit large differences in *I* by gradient HPLC–DAD as in ref. 6. The effect of solvent compositions on UV spectra used in HPLC–DAD merits further investigation in view of these findings. The solvent system developed by Paterson and Kemmelmeier[2] might be more suitable for the purpose of chromophore comparison and fungal chemotaxonomy by HPLC–DAD than those used in refs. 6 and 7, as the system does not contain an acidic component and large pH changes would not occur.

UV spectra are useful for the identification of metabolites, and additional characteristic information is provided by the difference spectra. These data can be of value, for example, in the further characterization of spots removed from TLC or PLC plates[1]. If gradient solvent DAD systems are used in HPLC, the solvent is not uniform throughout and conditions for taking the spectra could be different at different stages of the gradient depending on the construction of the gradient. As indicated here, this might cause difficulties in the identification of compounds by UV absorption, particularly where large pH changes occur in the solvent because of the chosen gradient.

ACKNOWLEDGEMENTS

This work was supported by EC grant to C.K. (No. 007732) for science and technology cooperation between the EEC and Brazil. We thank Dr. L. Fellows, Royal Botanic Gardens (Kew, U.K.) for use of chromatography equipment, Professor D. L. Hawksworth (Director, CMI) for critical reading of the manuscript and Ms. G. Godwin for art work.

REFERENCES

1 R. R. M. Paterson, M. S. J. Simmonds, C. Kemmelmeier and W. M. Blaney, *Mycol. Res.*, 94 (1990) 538–542.
2 R. R. M. Paterson and C. Kemmelmeier, *J. Chromatogr.*, 483 (1989) 153–168.
3 P. D. Bridge, D. L. Hawskworth, Z. Kozakiewicz, A. H. S. Onions, R. R. M. Paterson, M. J. Sackin and P.H.A. Sneath, *J. Gen. Microbiol.*, 135 (1989) 2941–2966.
4 J. C. Frisvad and O. Filtenborg, *Appl. Environ. Microbiol.*, 46 (1983) 1301–1310.
5 R. J. Cole and R. H. Cox, *Handbook of Toxic Fungal Metabolites*, Academic Press, New York, London, 1981.

6 J. C. Frisvad and U. Thrane, *J. Chromatogr.*, 404 (1987) 195–214.
7 J. C. Frisvad, *Bot. J. Linn. Soc.*, 99 (1989) 81–95.
8 O. Filtenborg and J. C. Frisvad, in R. A. Samson and J. I. Pitt (Editors), *Modern Concepts in Penicillium and Aspergillus Classification*, Plenum Press, New York, London, 1990, in press.
9 G. Aulin-Erdtman, *Chem. Ind.*, May 21 (1955) 581–582.
10 G. Aulin-Erdtman and R. Sanden, *Acta Chem. Scand.*, 22 (1968) 1187–1209.
11 R. R. M. Paterson, *J. Chromatogr.*, 368 (1986) 249–264.
12 J. C. Frisvad, *J. Chromatogr.*, 392 (1987) 333–347.
13 J. B. Harbourne, *Phytochemical Methods*, Chapman & Hall, London, 1973.

Journal of Chromatography, 511 (1990) 223–231
Elsevier Science Publishers B.V., Amsterdam

CHROMSYMP. 1903

Ion chromatographic determination of plasma oxalate in healthy subjects, in patients with chronic renal failure and in cases of hyperoxaluric syndromes[a]

MICHELE PETRARULO*, ORNELLA BIANCO, MARTINO MARANGELLA, SERGIO PELLEGRINO and FRANCO LINARI
Laboratory of Renal Stone Disease, Ospedale Mauriziano Umberto I, Largo Turati 62, Turin (Italy)
and
EDOARDO MENTASTI
Department of Analytical Chemistry, University of Turin, Via Giuria 5, Turin (Italy)
(First received June 25th, 1989; revised manuscript received February 22nd, 1990)

ABSTRACT

An ion chromatographic procedure for the determination of plasma oxalate is proposed, in which the ultrafiltered sample is injected into an ion-chromatographic system. Sample processing appears effective in avoiding spontaneous oxalogenesis. Sensitivity (down to 1.0 μmol/l) allows determinations in normal and pathological samples; recoveries from plasma ultrafiltration are 94.6 ± 11.7%. Protein binding was investigated and precautions to improve recoveries from plasma ultrafiltration are proposed. The technique is simple to perform and rapid enough to be useful for routine purposes. Plasma oxalate concentrations from healthy controls averaged 6.75 ± 2.62 μmol/l (mean ± S.D. n = 18); samples from patients with primary hyperoxaluria and chronic renal failure undergoing regular dialysis were also analysed and some of the data obtained are reported and discussed.

INTRODUCTION

The tendency of calcium oxalate salts to precipitate from body fluids has been reported in some cases of end-stage renal disorders and hyperoxaluric syndromes[1]; this finding, which suggests the opportunity for a careful evaluation of calcium oxalate saturation in plasma, requires the accurate determination of plasma oxalate (OX). Most of the techniques for the direct determination of plasma OX yield higher values than the indirect *in vivo* radioisotopic dilution methods, from which mean OX

[a] Presented at the *13th International Symposium on Column Liquid Chromatography, Stockholm, June 25–30, 1989*. The majority of the papers presented at this symposium have been published in *J. Chromatogr.*, Vols. 506 and 507 (1990).

0021-9673/90/$03.50

concentrations in normal plasma are reported to range between 1 and 2 μmol/l[2–5].

Wide ranges of OX concentrations as determined by direct methods from normal plasma have been reported, which is an indication of the instability of native OX. After the earliest work, which yielded OX levels over 20 μmol/l[6,7], reported values progressively decreased and now the ranges found for normal subjects are approaching those obtained by indirect methods.

The enzymatic conversion or the chemical degradation of potential precursors on the one hand and the unfavourable ratio of interfering substances to blood OX on the other mainly account for the above overestimation[8,9]; in addition, improper sample handling may easily promote the degradation of chemical precursors, enhancing the overestimation of the native OX[10].

Enzymic methods, in which oxalate oxidase (EC 1.2.3.4) or oxalate decarboxylase (EC 4.1.1.2) are used, are available[8,11–13]. The former has been used, after plasma ultrafiltration, to convert OX to carbon dioxide and hydrogen peroxide, which can be measured spectrophotometrically by a Trinder-type reaction. The procedure, automated by using immobilized enzyme in a continuous-flow analyser, yields normal plasma OX which averages 2.03 μmol/l[11]. Oxalate decarboxylase, coupled with formate dehydrogenase (EC 1.2.1.2), has been used after precipitation of OX from plasma ultrafiltrate. With this procedure, variations of the NADH concentration, which are related to the OX content, are measured photometrically. The normal OX values averaged[8] 1.25 μmol/l.

Gas chromatographic (GC) methods have been proposed in which plasma OX, extracted by a liquid–liquid procedure, is determined as the trimethylsilyl derivative. Normal plasma OX values averaging 2.8 ± 1.1 (ref. 14) and 4.9 ± 0.8 μmol/l (ref. 15) have been reported.

However, the above techniques are tedious, time consuming and require complex manipulations of samples, so that the development of simpler and more suitable routine methods is desirable. The method reported in the present paper is a much simpler alternative; it is based on ion chromatography and allows the quantification of OX in healthy subjects and patients with chronic renal failure.

Ion chromatography is a widely used and highly sensitive technique for the determination of urinary OX[16,17]. The main problem concerning this technique is the in-column conversion of endogenous ascorbate (ASC) to OX, which can be avoided either by ASC oxidation with iron(III) ions[18] or with ascorbate oxidase[19] or by means of boric acid dilution[20]. The much higher ASC:OX concentration ratio in plasma than urine requires more careful control of the above drawback.

The chromatographic procedure allows both ASC and glyoxylate interferences to be offset both during the sample handling and in the chromatographic step. In addition, the use of specific inhibitors of the enzyme-induced oxalogenesis during plasma collection, which has been proposed previously[13], in our hand is not effective in decreasing the normal range. Samples from normal subjects and patients with chronic renal failure and primary hyperoxaluria have been analysed and some of the data obtained are reported.

EXPERIMENTAL

Reagents

Analytical reagent-grade chemicals and deionized water were used for dilutions and eluents. Sulphuric and hydrochloric acid, sodium carbonate and sodium hydrogencarbonate were purchased from Merck (Darmstadt, F.R.G.), sodium glyoxylate monohydrate from Fluka (Buchs, Switzerland), allopurinol and DL-β-phenyllactic acid from Sigma (St. Louis, MO, U.S.A.) and ascorbic acid and oxalic acid from Carlo Erba (Milan, Italy).

[^{14}C]Oxalic acid 27 mCi/mmol (Amity-Pg Amersham, Milan, Italy) was used for recovery tests. Aliquots were diluted with ethanol to obtain a concentration of 50 μCi/ml; 40 μl of solution were then diluted to 2 ml with water. A 100-μl volume of this solution was used for labelled addition to 1 ml of plasma. PicoFluor (Packard Instruments, Zurich, Switzerland) was used, as a scintillation solution, at a dilution ratio of 60:1 of sample. Radioactivity was measured using a Model 81000 liquid scintillation counter (LKB, Cambridge, U.K.).

A combined inhibitor solution containing allopurinol and boric and DL-β-phenyllactic acids was prepared and used as described elsewhere[13]. The OX stock standard solution was prepared by dissolving 504 mg of oxalic acid dihydrate in 10.0 ml of water and stored at −20°C until used. Working standards of 10 and 100 μmol/l were prepared daily by diluting the above concentrated solution.

Sample handling

Human blood from fasting healthy subjects was obtained by venepuncture using heparinized Vacutainer vessels. Blood from haemodialysed patients was withdrawn by arterio-venous fistulas before and after dialysis. The collections, immediately placed in melting ice, were centrifuged at approximately 1000 *g* for 10 min at 4°C as soon as possible. A 1.0-ml volume of separated plasma was acidified by addition of 40 μl of concentrated hydrochloric acid. The sample was vortex mixed vigorously for 6 min and was transferred to an MPS-1 ultrafiltration unit (Grace Italiana Divisione Amicon, Passirana di Rho, Milan, Italy); ultrafiltration was performed by centrifugation at 4°C at 1500 *g* for 15 min using YMT membranes (Amicon) with a molecular weight cut-off of 30 000 daltons; ultrafiltration allowed the separation of about 100 μl of liquid, which was harversted and diluted five-fold with a 0.3 mol/l boric acid solution and then injected into the chromatograph.

The efficiency of ultrafiltration was tested by radioisotopic dilution. To the separated plasma samples were added 100 μl/ml of the above 1 μCi/ml solution of [^{14}C]oxalic acid and then treated as described. A 50-μl aliquot of sample was mixed with 3.0 ml of scintillation liquid and the emulsion was left overnight at 4°C and then measured for radioactivity. The recovery of [^{14}C]OX from the ultrafiltration step was evaluated by comparing the measured radioactivity of the treated samples with that of the non-ultrafiltered samples.

Chromatography

The chromatographic separation was performed with a QIC liquid chromatograph (Dionex, Sunnyvale, CA, U.S.A.) equipped with a conductimetric detector. Two in-line AS-4A anion separator columns (Dionex, 037041) in conjunction with an

AG-4A guard column (Dionex, 037042) were used as a stationary phase. An automatic injection valve connected with a 200-μl sample loop was used. A sodium carbonate–hydrogen carbonate (2.4 and 3.0 mmol/l) aqueous solution pumped in the column at 2.0 ml/min was used as mobile phase, after accurate degassing.

Periodic replacement of the precolumn and clean-up of separators are essential for the best chromatographic performance. Regeneration was carried out by flushing the separators with 100 ml of 0.2 mol/l sodium hydroxide solution. Columns were ready for analysis after 1 h of conditioning. Eluent conductivity background was suppressed with a cation-exchange membrane (Dionex, 038019) set in-line after the separator. The membrane, in which the eluent flows, is plunged in a counterflow batch of 12.5 mmol/l sulphuric acid flowing at 2.7 ml/min. In the membrane suppressor, eluent and sample anions do not permeate the cation-exchange membrane because of electrostatic exclusion forces, but cations do. Owing to the selective exchange between sodium and hydrogen ions, sodium carbonate and sodium hydrogencarbonate are converted to weakly conducting aqueous carbon dioxide, whereas sodium oxalate is converted to highly conducting oxalic acid. The signal-to-noise ratio is consequently improved. The detector output was set at 100 μS. Oxalate peak heights were measured using a Spectra-Physics SP 4270 plotter/integrator set at an attenuation input ranging from 4 to 32 mV full-scale.

RESULTS

Removal of proteins and macromolecules from the sample was accomplished by plasma ultrafiltration. In addition, some tests were performed in order to investigate and improve the conditions of ultrafiltration with respect to the recovery of OX and the stability of the analyte. The recovery of OX, as tested by isotope dilution, was evaluated as a function of plasma acidification. In particular, plasma samples containing [^{14}C]OX were spiked with various amounts of concentrated hydrochloric acid, vortex mixed for 6 min and subsequently ultrafiltered. The recoveries were substantially quantitative for unacidified plasma and decreased as acidification increased towards a minimum value averaging 56.7%, corresponding to an approximate plasma pH of 3. Further acidification allowed an increase in recovery, reaching up to 94.6% at pH < 1; in addition, a notable increase in precision was observed (Table I).

TABLE I

[^{14}C]OX RECOVERY MEASURED AFTER ULTRAFILTRATION OF PLASMA SAMPLES TREATED AS DESCRIBED IN THE TEXT

Parameter	*Unacidified*	*HCl-acidified (µl HCl/ml plasma)*			
		10	*20*	*30*	*40*
No. of samples	8	9	16	22	161
Mean recovery (%)	105.3	56.7	67.4	71.0	94.6
S.D. (%)	8.4	22.9	16.1	13.2	11.7
Relative S.D. (%)	8.0	40.4	23.9	18.6	12.4

TABLE II

SPONTANEOUS *IN VITRO* OXALOGENESIS IN DELAYED ANALYSIS OF ULTRAFILTRATES FROM THE SAME PLASMA SAMPLE, BOTH ACIDIFIED AND UNACIDIFIED, SPIKED WITH GLYOXYLATE AND ASCORBATE

Delay time (h)	*Oxalate concentration (μmol/l)*				
	Native plasma		*Spiked with 100 μmol/l of glyoxylate, acidified*	*Spiked with 100 μmol/l of ascorbate*	
	Acidified	*Unacidified*		*Acidified*	*Unacidified*
0	6.4	8.5	8.0	–	–
1	7.0	12.2	9.3	7.0	21.4
3	7.7	19.4	–	9.6	32.0

These findings suggest that OX is entirely unbound at physiological pH values. Mild acidification (10 μl of HCl per ml of plasma) enhances the above binding, which can be broken in turn by further acidification ($\geqslant$30 μl of HCl per ml of plasma). This evidence is in agreement with the expected trend of the reciprocal electrostatic affinity occurring as the degree of protonation of both OX and proteins increases. As more satisfactory conditions were obtained from both the untreated plasma and the plasma acidified with 40 μl of HCl/ml, further studies were performed using the above procedures. The ultrafiltration of untreated plasma yielded a large volume of ultrafiltrate, the analysis of which produced well resolved chromatograms, but the OX generation during the preanalysis delay was not negligible. In addition, spikes of ASC sharply increased both the basal OX and the oxalogenesis rate (Table II).

The acidification of plasma inhibited the spontaneous oxidation of ASC (Table II) and suppressed the enzyme-induced production of OX by the immediate denaturation of proteins. Concentrations from normal subjects averaged 6.75 μmol/l, and were thus in fairly good agreement with the results of previous GC[15] and high-performance liquid chromatographic methods[21]. The acidification procedure, even though it suppresses the oxalogenesis at native pH, provides chromatographic traces of worse quality and lower ultrafiltration rates.

Tests were carried out by ultrafiltering untreated plasma and by collecting the ultrafiltrate directly in HCl. Its low concentration (7 μl of 2 mol/l HCl in about 150 μl of final ultrafiltered sample) on the one hand inhibits oxalogenesis and on the other does not reduce the quality of the chromatograms. Nevertheless, the resulting OX concentrations as measured in normal subjects were slightly higher than those obtained by ultrafiltering acidified plasma, indicating that a certain oxalogenesis occurs in the course of the ultrafiltration at physiological pH. Therefore, immediate acidification of plasma with 40 μl of HCl per ml was adopted.

A number of samples were analysed by collecting blood in the presence of a mixture of inhibitors, as suggested in the literature[13], in order to decrease the hypothetical rapid conversion of glyoxylate or glycolate into OX during the sample harvesting. No improvements were observed and this procedure was discarded.

Calibration and sensitivity

The analysis of both untreated aqueous solutions containing oxalic acid in the range 0–100 μmol/l and of treated samples spiked with known amounts (0–100 μmol/l) of oxalic acid produced satisfactory linear responses.

While the chromatographic traces from standards and unacidified plasma permit a minimum detectable concentration of 0.5 μmol/l, the sensitivity of analysis for acidified plasma is limited by a disturbed signal in which OX elutes on a tailing peak. This drawback, possibly due to the fragmentation of metabolites enhanced by acidification with likely production of dicarboxylic acids, could not be avoided by any modification of the chromatographic conditions. However, the minimum detectable concentration was 1.0 μmol/l, which is much lower than the normal range found here. Otherwise, samples from uraemic patients could be easily analysed because of the higher OX content.

Fig. 1 shows three chromatograms, representing analyses of a standard, of plasma from a healthy person and of plasma from a patient on dialysis treatment.

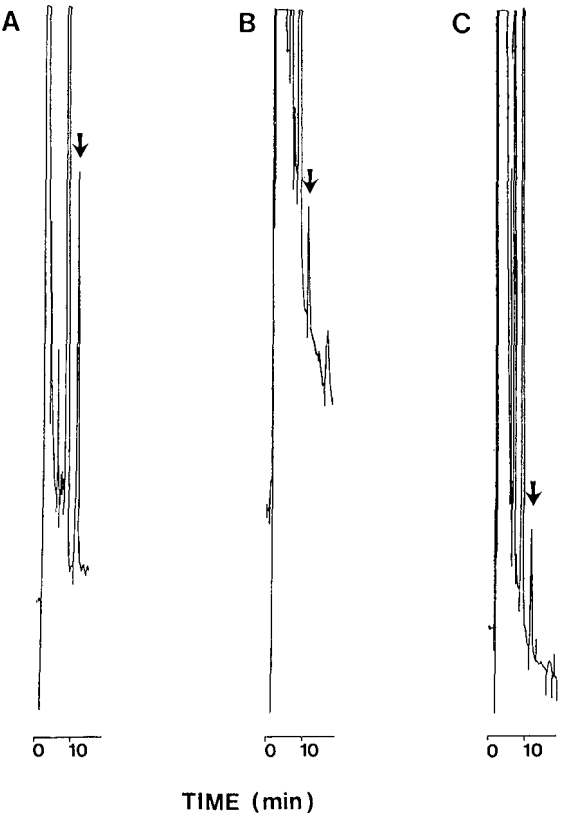

Fig. 1. Typical ion chromatograms for the determination of oxalate under the conditions described in the text. (a) Oxalate standard, 20 μmol/l in water, 4 mV full-scale; (b) plasma sample from a healthy person, 4 mV full-scale; (c) plasma sample from a patient on regular haemodialysis, 16 mV full-scale. Detector sensitivity was set at 100 μS. The arrows show oxalate peaks.

Accuracy and precision

Four ultrafiltrates were analysed both immediately and after storage for 24 h at −20°C. The OX content changed from 12.0 ± 6.9 to 27.1 ± 10.4 μmol/l (mean ± S.D., $p = 0.03$). Even though normal plasma glyoxylate levels would not exceed 0.3 μmol/l, as observed using a previously published method[22], or 2.5 μmol/l as reported by other workers[23], the possible interfering effects of ASC and glyoxylate were tested by spiking plasma with 100 μmol/l of each. The results showed that the sample processing was efficient in avoiding any appreciable overestimation of the measured OX (Table II). More generally, under the proposed conditions, oxalogenesis has to be considered insignificant, provided that the injection is carried out within 2 h (Table II).

As no increase in measured OX was observed when 200 μmol/l of ASC was added just before injection, no significant overestimation can be ascribed to the in-column conversion of native ASC.

Two plasma samples, from a healthy subject and ureamic patient, were analysed four times within the same series. The samples contained OX concentrations averaging 6.8 and 38.8 μmol/l and the relative standard deviation averaged 11.8 and 4.5%, respectively.

The residual tendency for oxalogenesis does not allow the treated samples to be stored and an inter-run precision to be measured. A raw estimate of the between-run precision was obtained by analysing two pre-dialysis samples from fifteen patients withdrawn at subsequent dialysis sessions (range 26.1–75.1 μmol/l). The result, expressed as standard deviation, S.D. $= [(\Sigma d^2)/2n]^{\frac{1}{2}}$, was 3.53 μmol/l.

The ultrafiltration recovery was evaluated in plasma by radioisotopic dilution (Table I). The recovery from the chromatographic step was investigated. The addition of 40 μmol/l of OX to six given ultrafiltrates yielded a mean recovery of 100.4 ± 8.6%.

Clinical results

Samples from 18 apparently healthy adults and 20 patients with chronic renal failure undergoing regular haemodialysis (3–4 h, three times a week) were analysed. The normal OX concentration ranged from 1.42 to 10.70 μmol/l (mean ± S.D. = 6.75 ± 2.62, $n = 18$). Pre-dialysis values averaged 48.1 ± 15.9 μmol/l (mean ± S.D., $n = 20$) and were significantly higher than post-dialysis values ($p < 0.001$) which averaged 18.0 ± 10.1 μmol/l (mean ± S.D., $n = 20$). Samples from three patients with primary hyperoxaluria, two of whom were undergoing regular dialysis treatment for end-stage renal failure, were also investigated. Pre and post-dialysis values for the latter-two were 157.0 and 40.5 μmol/l and 197.6 and 81.4 μmol/l. The third patient, whose renal function was only mildly reduced, had a plasma OX level of 21.4 μmol/l.

CONCLUSIONS

The proposed method is based on the purification of OX by ultrafiltration and subsequent ion-chromatographic assay of the ultrafiltrate. In our hands, ultrafiltration was found to be an efficient procedure for separating the main fraction of proteins, and thus for decreasing the enzyme-induced OX formation. The trend of ultrafilterability as a function of the plasma pH (Table I) suggests, in agreement with previous reports[8], that OX–protein binding cannot be neglected if plasma is moderately acidified. However, further acidification (pH < 1) was found to be

effective in breaking the above binding, allowing quantitative and close recoveries to be obtained.

The immediate acidification allows, first, the protein-containing fractions to be denaturated, making the time required to complete the ultrafiltration less critical, and second, the possible oxalogenesis due to the main interfering compound (*i.e.*, ASC) during the ultrafiltration step to be inhibited.

Results obtained by collecting blood in the presence of specific inhibitors for the enzymic oxidation of glycolate and glyoxylate into OX[13] do not differ significantly from those obtained in the absence of the above inhibition.

In spite of these precautions, the normal range obtained is higher than that reported by using indirect methods[2–5]. The direct methods proposed so far do not provide homogeneous data, which are generally higher than those obtained by *in vivo* isotopic dilution. A few workers have obtained mean values ranging from 1 to 3 μmol/l (refs. 8, 11 and 14) using enzymatic or GC techniques.

On the basis of these considerations, our overestimation could be ascribed to the chromatographic step. Unfortunately, ultrafiltrates incubated with commercially available suspensions of oxalate decarboxylase were unsuitable for chromatographic analysis because of the high saline and the low OX contents. Nevertheless, the above eventuality seems unlikely, as the only known chromatographic interference would be due to ASC, which under the described conditions seems negligible. Moreover, other workers have reported normal ranges for plasma OX to be very close to the values found here[15,21,24]. In any case, no problem seems to exist when the present method is applied to the study of patients with chronic renal failure.

As an example of the clinical usefulness of the determination of OX in plasma, samples were analysed before and after dialysis, and the resulting data were comparable to those obtained by other workers[14,25,26]. The observation that, in our hands, the recoveries of [^{14}C]OX were fairly constant suggests that this step may be considered unnecessary.

Hence, the present method, which requires a minimum volume of blood and is rapid and simple to perform, can be considered as an alternative to the methods proposed previously. Also, it appears to be sensitive, accurate and suitable for routine use, provided that one bears in mind that the analysis cannot be delayed after the blood has been collected.

REFERENCES

1 H. E. Williams, *Kidney Int.*, 13 (1978) 410.
2 A. Hodgkinson and R. Wilkinson, *Clin. Sci. Mol. Med.*, 46 (1974) 61.
3 A. R. Constable, A. M. Joekes, G. P. Kasidas, P. O'Regan and G. A. Rose, *Clin. Sci.*, 56 (1979) 299.
4 P. Boer, J. A. C. Prenen, H. A. Koomans and E. J. Dorhout Mees, *Nephron*, 41 (1985) 78.
5 J. A. C. Prenen, H. Y. Oei, H. A. Koomans and E. J. Dorhout Mees, *Contrib. Nephrol.*, 56 (1987) 18.
6 J. F. B. Barrett, *Biochem. J.*, 37 (1943) 254.
7 P. M. Zarembski and A. Hodgkinson, *Biochem. J.*, 96 (1965) 717.
8 J. Costello and D. M. Landwehr, *Clin. Chem.*, 34 (1988) 1540.
9 N. C. France, E. A. Windleborn and M. R. Wallace, *Clin. Chem.*, 31 (1985) 335.
10 W. W. Borland, C. D. Payton, K. Simpson and A. I. Macdougall, *Nephron*, 45 (1987) 119.
11 G. P. Kasidas and G. A. Rose, *Clin. Chim. Acta*, 154 (1986) 49.
12 M. Sugiura, H. Yamamura, K. Hirano, Y. Ito, M. Sasaki, M. Morikawa, M. Inoue and M. Tsuboi, *Clin. Chim. Acta*, 105 (1980) 393.
13 T. Akcay and G. A. Rose, *Clin. Chim. Acta*, 101 (1980) 305.

14 B. G. Wolthers and M. Hayer, *Clin. Chim. Acta*, 120 (1982) 87.
15 M. Lopez, M. Tuchman and J. I. Sheinmann, *Kidney Int.*, 28 (1985) 82.
16 W. G. Robertson, D. S. Scurr, A. Smith and R. L. Orwell, *Clin. Chim. Acta*, 126 (1982) 91.
17 M. Menon and C. J. Mahle, *Clin. Chem.*, 29 (1983) 369.
18 G. P. Kasidas and G. A. Rose, in P. O. Schwille, L. H. Smith, W. G. Robertson and W. Vahlensieck (Editors), *Urolithiasis and Related Clinical Research*, Plenum Press, New York, 1985, pp. 653–656.
19 M. Petrarulo, O. Bianco, M. Marangella, A. Marchesini and F. Linari, submitted for publication.
20 W. G. Robertson and D. S. Scurr, *Clin. Chim. Acta*, 140 (1984) 97.
21 E. M. Worchester, Y. Nakagawa, D. A. Bushinsky and F. L. Coe, *J. Clin. Invest.*, 77 (1986) 1888.
22 M. Petrarulo, S. Pellegrino, O. Bianco, M. Marangella, F. Linari and E. Mentasti, *J. Chromatogr.*, 432 (1988) 37.
23 K. Koike and M. Koike, *Anal. Biochem.*, 141 (1984) 481.
24 F. E. Cole, K. M. Gladden, V. G. Bennett and D. T. Erwin, *Clin. Chim. Acta*, 139 (1984) 137.
25 B. G. Wolthers, S. Meijer, T. Tepper, M. Hayer and H. Elzinga, *Clin. Sci.*, 71 (1986) 41.
26 I. S. Parkinson, T. Kealey and M. F. Laker, *Clin. Chim. Acta*, 152 (1985) 335.

Journal of Chromatography, 511 (1990) 233–242
Elsevier Science Publishers B.V., Amsterdam

CHROM. 22 411

High-performance liquid chromatographic investigation of the interaction of phenylmercuric nitrate and sodium metabisulphite in eye drop formulations

J.E. PARKIN

School of Pharmacy, Curtin University of Technology, Kent Street, Bentley, Western Australia 6102 (Australia)

(First received November 14th, 1989; revised manuscript received March 5th, 1990)

ABSTRACT

The degradation of phenylmercuric nitrate in the presence of sodium metabisulphite in eye drop formulations has been investigated using a stability-indicating high-performance liquid chromatographic (HPLC) method. HPLC methods have been developed for the quantitation of the principal degradation products (diphenylmercury, benzenesulphonic acid and benzenesulphinic acid) and a mechanism is proposed for their formation. The pharmaceutical significance of the interaction is briefly discussed.

INTRODUCTION

A number of studies have shown that when sodium metabisulphite is added as an antioxidant to ophthalmic products containing phenylmercuric (PM) salts, a loss of PM salts occurs when the product is routinely heat-sterilised[1–6]. These studies afforded conflicting results when products were assessed for antibacterial activity by microbiological procedures, but in all studies where PM salt concentrations were determined by atomic absorption spectrophotometry (AAS)[1,2,5,6] and high-performance liquid chromatography (HPLC)[5], losses of 75–100% PM salt were reported. An exception was the study of Richards *et al.*[2], who quantitated the PM nitrate by AAS using both an air–acetylene technique and a cold-vapour method and found that there was an 80% loss when determined by the air–acetylene technique but mercury levels remained unchanged when the cold-vapour method was employed. They concluded that a complex was formed between the metabisulphite and the PM nitrate during autoclaving which is more refractory in the air–acetylene flame and more difficult to reduce to elemental mercury than aqueous PM nitrate solutions and that this influenced the analytical results.

Despite these observations, the British Pharmacopoeia (1980)[7] contained a number of ophthalmic monographs which incorporated both PM nitrate and sodium

0021-9673/90/$03.50

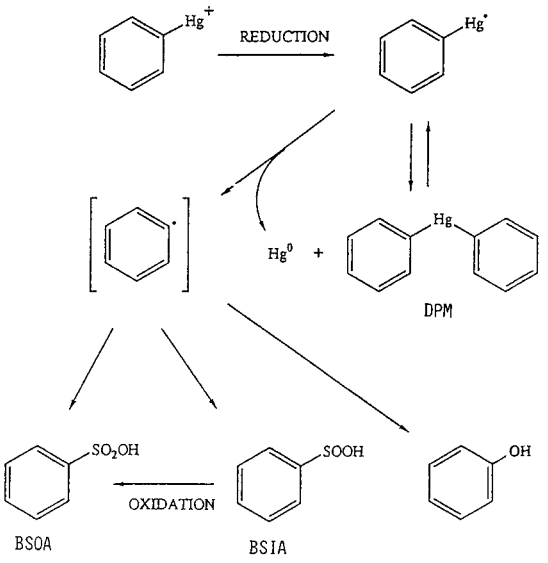

Fig. 1. Proposed route for the degradation of the PM ion in the presence of sodium metabisulphite.

metabisulphite. The current British Pharmacopoeia (1988)[8], in its general monograph on eye drops, contains the statement that "care should be taken to ensure compatability between the antioxidant and the antimicrobial preservative" but does not specifically preclude products containing both these materials; the current Australian Pharmaceutical Formulary and Handbook (1988)[9] lists several ophthalmic products which contain both PM nitrate and sodium metabisulphite.

N-Disubstituted dithiocarbamate complexes have been used to chromatograph and quantitate organomercury and inorganic mercury[10] and the author[10,11] has developed an HPLC assay using these reagents for application to ophthalmic products.

This paper reports an investigation using HPLC of the decomposition following heat-sterilisation of PM nitrate by sodium metabisulphite in simple solution and amethocaine eye drops[9]. The time-course of this decomposition at 100°C is followed with quantitation of PM nitrate and diphenylmercury (DPM), a transient intermediate formed during the degradation. The terminal degradation products following autoclaving at 121°C have also been identified and quantitated and were found to be principally elemental mercury, benzenesulphonic acid (BSOA) and benzenesulphinic acid (BSIA). A mechanism is proposed for the formation of these products (Fig. 1).

EXPERIMENTAL

Materials

PM nitrate (BDH, Poole, U.K.), DPM (Fluka, F.R.G.), amethocaine hydrochloride, BSOA and BSIA as the sodium salt (Sigma, St. Louis, MO, U.S.A.) were used in this study. All other chemicals were analytical-reagent grade.

The morpholine salt of morpholinedithiocarbamate (MDTC) and diethylamine

salt of diethylaminedithiocarbamate (DEADTC) were synthesized as reported previously[11,12]. The MDTC and DEADTC complexing reagents were prepared by dissolving 60 mg of the salts in 75% aqueous acetonitrile for MDTC and acetonitrile for DEADTC (100 ml).

Chromatographic equipment

A liquid chromatograph (Waters Assoc., Milford, MA, U.S.A.), equipped with a 501 pump, 712 WISP injector, 490 variable-wavelength detector and HP 3396A integrator, together with a column of octadecylsilica (Waters Assoc.) 30 cm × 3.9 mm I.D., 10 μm particle size, was used for analysis of the degradation products and of PM nitrate. Injection volumes of 20 μl were used unless otherwise specified.

Spectrophotometric equipment

UV spectra were obtained using an HP 8450 UV–VIS spectrophotometer (Hewlett-Packard, PA, U.S.A.).

Chromatographic procedures

PM and mercury salts were determined by the addition of 1 ml of DEADTC reagent to 1 ml of sample and the resulting complexes submitted to chromatographic analysis using $1 \cdot 10^{-4}$ *M* disodium salt of ethylenediaminetetraacetic acid (Na_2EDTA) in acetonitrile–water (75:25) at a flow-rate of 1.8 ml min^{-1} and monitoring at 258 nm.

DPM in the presence of PM nitrate was determined by the addition of 1 ml of MDTC reagent to 1 ml of sample to complex the PM ion followed by chromatography using $1 \cdot 10^{-4}$ *M* Na_2EDTA in acetonitrile–water (65:35) at a flow-rate of 1.8 ml min^{-1} and monitoring at 225 nm.

BSOA and BSIA were analysed by chromatography using methanol–water (33:67) containing 0.1% (w/v) tetrabutylammonium hydrogensulphate and monitoring at 220 nm.

Phenol was analysed using a mobile phase of methanol–water (40:60) at a flow-rate of 1.5 ml min^{-1} with monitoring at 215 nm.

Kinetic studies

These were performed by adding 200 mg sodium metabisulphite to a solution of PM nitrate (200 ml of $2 \cdot 10^{-4}$ *M*) or amethocaine eye drops APF[9] [200 ml, modified by containing $2 \cdot 10^{-4}$ *M* PM nitrate, equivalent to 0.00634% (w/v) PM nitrate] in a flask with condenser in a boiling water bath. The reaction was equilibrated to temperature prior to the addition of sodium metabisulphite and the solution was kept under nitrogen for the course of the study. Samples of 5 ml were withdrawn at regular intervals, transferred to a vial, cooled on ice and centrifuged for 10 min using a refrigerated centrifuge, and the supernatants were then submitted to HPLC analysis by the chromatographic procedures for PM nitrate and DPM.

Terminal degradation products

Aliquots (10 ml) of the solutions used in the kinetic studies were transferred to 20-ml glass ampoules and autoclaved for 2 h at 121°C. The resulting solutions were transferred to tubes and centrifuged for 30 min. The supernatants were transferred to

second tubes. The residues, which were not visible, were heated at 40°C for 15 min with eight drops of concentrated nitric acid–water (1:1), water was added to 7 ml, saturated sodium acetate was added dropwise to adjust the pH to 4–5 and the solution was made to 10 ml and submitted for analysis for Hg^{II}.

Solutions of PM nitrate (5 ml of $2.5 \cdot 10^{-4}$ *M*) containing sodium metabisulphite (0.2%, w/v) and other materials as specified were sealed in 10-ml glass ampoules and autoclaved for 1.5 h at 121°C. The contents of the ampoules were assayed in the following manner.

(a) For water-soluble inorganic mercury salts and residual PM nitrate following centrifugation for 10 min.

(b) Elemental mercury and insoluble mercury salts were quantitated by the addition of nitric acid (2 ml) to the opened ampoule and digestion at 50°C for 15 min to dissolve the elemental mercury. The cooled solutions were transferred quantitatively to 50-ml volumetric flasks, neutralised to pH 4–5 with saturated sodium acetate solution, diluted to volume with water and submitted to analysis.

(c) Phenol was quantitated following centrifugation of the contents of an ampoule for 10 min.

(d) BSOA and BSIA were analysed by centrifugation of the contents of an ampoule to remove insoluble salts and elemental mercury, followed by analysis. Standards of BSIA as a sodium salt were freshly prepared and for BSOA by preparation of an approximately 0.1 *M* solution in 50% methanol, standardisation of this with 0.1 *M* sodium hydroxide using phenolphthalein indicator and dilution to an appropriate concentration.

Degradation of diphenylmercury

To an ampoule containing 5 ml of 0.1% (w/v) sodium metabisulphite were added metallic mercury (approximately 50 mg) and 50 μl of $1 \cdot 10^{-2}$ *M* DPM in acetonitrile (equivalent to $1 \cdot 10^{-4}$ *M* DPM), and the ampoules were autoclaved at 121°C for 1.5 h. The supernatants were submitted to analysis for PM nitrate, DPM, BSOA and BSIA.

RESULTS AND DISCUSSION

Initial studies demonstrated that DPM was formed as an intermediate in the degradative process, and to assess its importance a kinetic study was performed at 100°C, the concentrations of PM nitrate, DPM and Hg^{II} being monitored. The use of DEADTC as complexing agent allows separate quantitation of the PM nitrate (4.5 min) and Hg^{II} complex (6.1 min) with DPM co-eluting with a minor peak at 3.6 min which is due to the corresponding thiuram disulphide arising from the slow atmospheric oxidation of the DEADTC (Fig. 2)[11]. The method affords a linear response over the range 0–$2.5 \cdot 10^{-4}$ *M* for both PM nitrate ($n = 6$, $r = 0.9998$; coefficient of variation, C.V. = $\pm 0.93\%$ at $0.5 \cdot 10^{-4}$ *M*, $n = 6$) and Hg^{II} ($n = 6$, $r = 0.9996$; C.V. = $\pm 1.80\%$ at $0.5 \cdot 10^{-4}$ *M*, $n = 6$). The DPM thus had to be quantitated using MDTC reagent, the more polar complexes of both the PM ion and Hg^{II} eluting prior to the uncomplexed DPM, and therefore not interfering with the assay (Fig. 3). The method affords a linear response over the range 0–$1 \cdot 10^{-4}$ *M* for DPM ($n = 5$, $r = 0.9999$; C.V. = $\pm 2.9\%$ at $1 \cdot 10^{-5}$ *M*, $n = 6$).

Application of these analytical methods to the PM nitrate–bisulphite solution

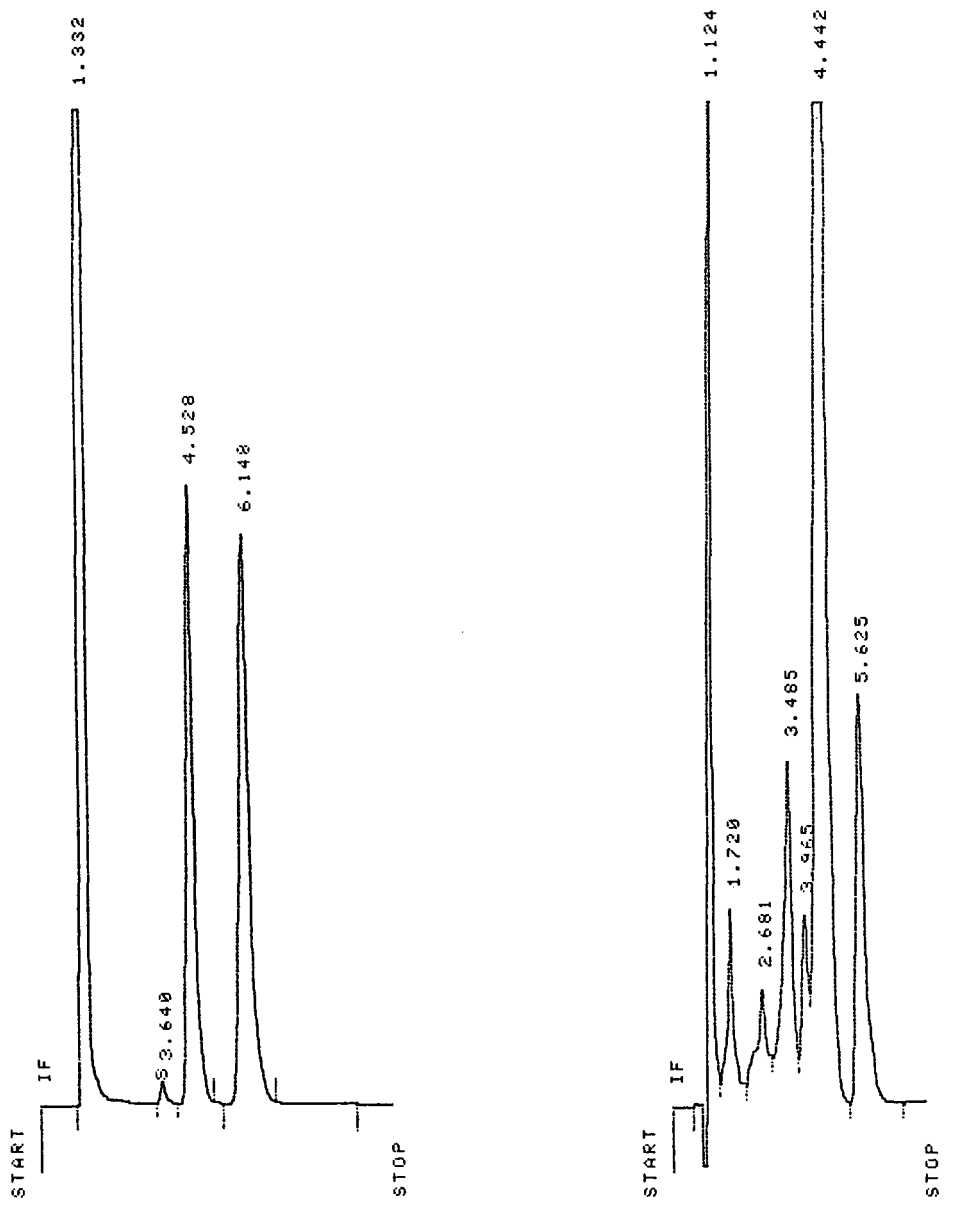

Fig. 2. Chromatogram of a solution of PM nitrate and Hg^{II} acetate, each $1 \cdot 10^{-4}$ *M* (0.064 a.u.f.s., monitoring wavelength 258 nm). Peaks: 1.33 min, excess DEADTC reagent; 3.64 min, DEADTC oxidation product; 4.53 min, PM–DEADTC complex; 6.15 min, Hg–DEADTC complex. Numbers at peaks are retention times in min.

Fig. 3. Chromatogram of a degraded sample of PM nitrate after heating at 100°C for 40 min (0.016 a.u.f.s., monitoring wavelength 225 nm). Peaks: 1.12 min, excess MDTC reagent; 3.48 min, MDTC oxidation product; 3.96 min, Hg–MDTC complex; 4.44 min, PM–MDTC complex; 5.62 min, DPM. The peaks at 1.72 and 2.68 min are unidentified degradation products of the MDTC reagent.

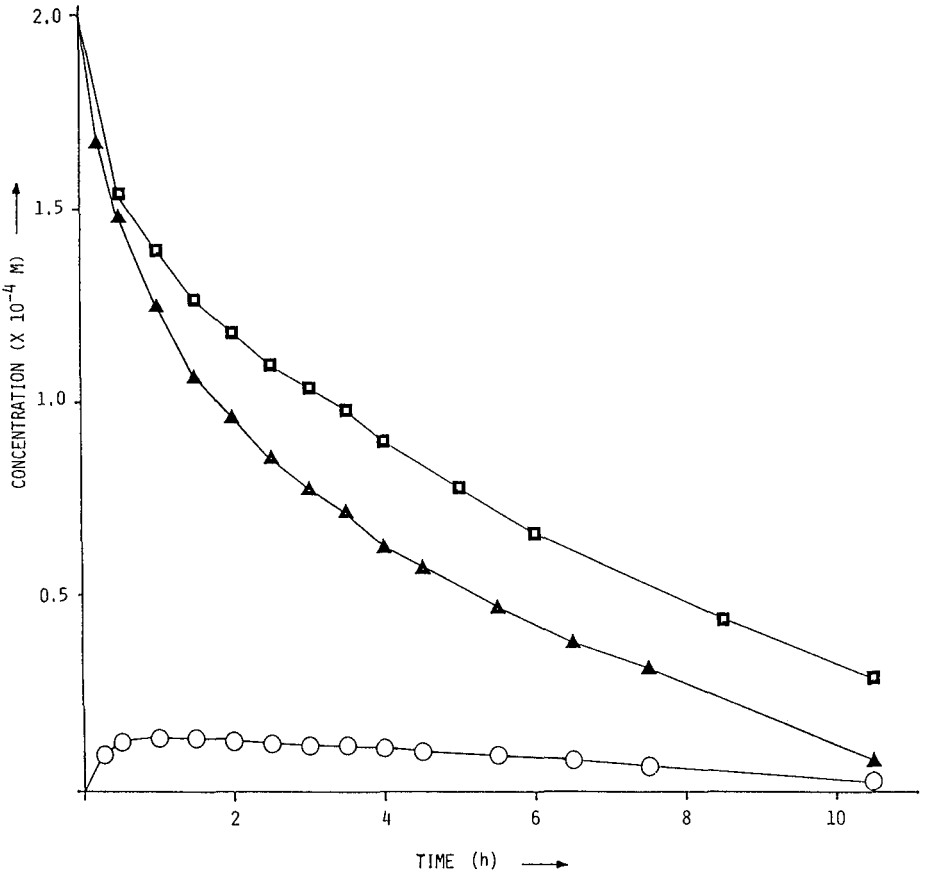

Fig. 4. Concentration of PM nitrate remaining following heating at 100°C with sodium metabisulphite. ◘ = Amethocaine eye drops APF containing $2 \cdot 10^{-4}$ *M* PM nitrate; ▲ = $2 \cdot 10^{-4}$ *M* PM nitrate solution. (○) Concentration of DPM arising from heating the $2 \cdot 10^{-4}$ *M* PM nitrate solution.

showed that at 98–100°C there was a rapid loss of PM nitrate accompanied by the formation of DPM (Fig. 4). Similar results were obtained for the amethocaine eye drops[9]. The DPM was not quantitated for these drops as a minor impurity in the amethocaine co-eluted with the DPM, which could, however, be identified as being present. In all studies the level of soluble mercury salts remained below 2% of total mercury and was not quantitated. In this study no attempt was made to quantitate the insoluble elemental mercury formed during the degradation. PM nitrate solution, in the absence of sodium metabisulphite, when submitted to the same conditions afforded no significant loss ($1.97 \cdot 10^{-4}$ *M*, corresponding to a loss of 1.5% after 10 h).

These observations confirm that PM salts in the presence of metabisulphite undergoes a chemical reaction and that the observations of previous workers arise from a true degradation and not from complex formation affecting the AAS method. The identity of the DPM was confirmed by comparison of its chromatographic retention characteristics with those of an authentic sample in this system, in the solvent

TABLE I

PERCENTAGES OF INORGANIC MERCURY FORMED FOLLOWING AUTOCLAVING OF PHENYLMERCURIC NITRATE SOLUTIONS

Results of two or three experiments followed by the mean percentage in parentheses.

Sample	*Percentage of inorganic mercury*	
	Soluble	*Elemental and insoluble salts*
$2 \cdot 10^{-4}$ *M* PM nitrate[a]	1.5, 1.4 (1.4)	39.3, 42.7 (41.0)
Amethocaine eye drops APF containing $2 \cdot 10^{-4}$ *M* PM nitrate	7.3, 3.4 (5.4)	14.0, 17.0 (15.5)
$2.5 \cdot 10^{-4}$ *M* PM nitrate[b]	1.5, 1.2, 1.0 (1.2)	90.0, 89.6, 84.4 (88.0)

[a] In these studies supernatants were removed by aspiration prior to digestion with nitric acid of the invisible residue.

[b] In this study the total contents of the ampoule were subjected to nitric acid digestion.

system employed for the PM–DEADTC analysis and also using methanol–water (75:25) as a mobile phase. A UV spectrum was obtained of the DPM using a diode-array spectrophotometer in series with the HPLC system and this was superimposable on that of an authentic spectrum of DPM obtained in a similar manner.

Investigation of the species of mercury present following degradation has been investigated by prolonged autoclaving to ensure complete destruction of the PM nitrate and quantitation of the water-soluble and -insoluble fractions. The results are displayed in Table I. Attempts to remove the supernatants following centrifugation and prior to digestion to dissolve elemental mercury resulted in substantial losses whereas digestion of the total contents of an ampoule demonstrated that 88% of total mercury could be accounted for as the Hg^{II} ion.

Studies have also been undertaken into the nature of the degradation products arising from the phenyl portion of the PM nitrate. Preliminary studies indicated that the products of degradation of the PM ion are BSOA and BSIA, and this was confirmed by comparison of retention times with authentic samples in two HPLC systems (33% methanol containing 0.1% tetrabutylammonium hydrogensulphate; 25% acetonitrile containing 0.1% tetrabutylammonium hydrogensulphate) and comparison of UV spectra obtained using a diode-array spectrophotometer in series with the HPLC system with authentic samples.

The BSOA and BSIA were quantitated by HPLC. The system afforded three peaks due to nitrate (3.2 min), BSOA (5.9 min) ($r = 0.9999$ over the concentration range 0–$4.8 \cdot 10^{-4}$ *M*, $n = 5$; C.V. at $2.4 \cdot 10^{-4}$ *M* = $\pm 1.3\%$, $n = 6$) and BSIA (7.4 min) ($r = 0.9999$ over the concentration range 0–$5 \cdot 10^{-4}$ *M*, $n = 5$; C.V. at $2.5 \cdot 10^{-4}$ *M* = $\pm 0.9\%$, $n = 6$) with baseline resolution (Fig. 5). Samples of PM nitrate following prolonged autoclaving with sodium metabisulphite were submitted to analysis for the acids under different conditions (Table II). Only about 75% of the PM nitrate could be accounted for by formation of the acids, and the exact proportion of the two acids varied with the conditions. In sealed ampoules the proportion of products was consistent and when exposed to the atmosphere oxidation occurred of

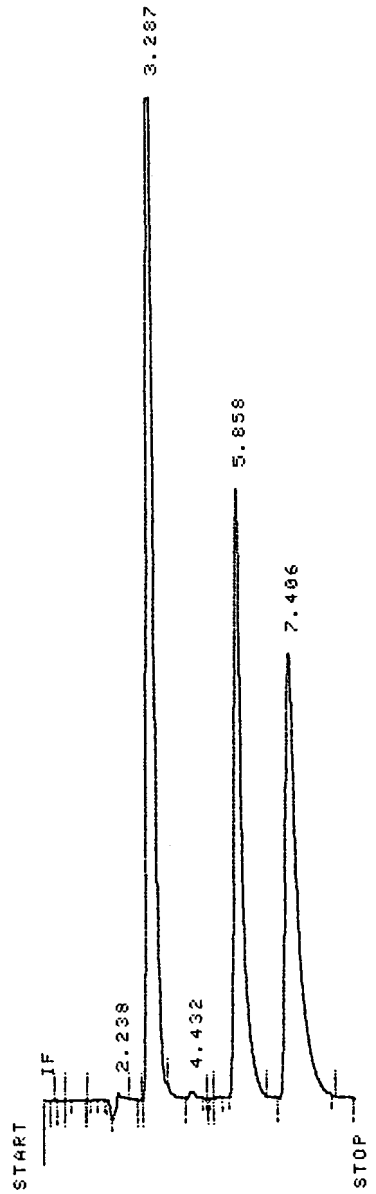

Fig. 5. Chromatogram of a sample of PM nitrate ($2.5 \cdot 10^{-4}$ *M*) autoclaved at 121°C for 2 h (0.064 a.u.f.s., monitoring wavelength 220 nm). Peaks: 3.29 min, nitrate; 5.86 min, BSOA; 7.41 min, BSIA.

the BSIA to BSOA. Sulphinic acids are known to undergo rapid atmospheric oxidation to the corresponding sulphonic acids[13] and this may occur following or together with atmospheric oxidation of the residual sodium metabisulphite. This would account for the increased proportion of BSOA encountered in the loosely stoppered flasks to which oxygen has access at the end of the autoclave cycle. Together

with the BSOA and BSIA approximately 1% of the PM nitrate is degraded to phenol which is just detectable under the conditions used in this study (signal-to-noise ratio = 3).

The most plausible explanation for the transient formation of DPM together with elemental mercury, BSOA and BSIA is that under the extreme conditions of heat sterilisation the bisulphite ion reduces the PM ion to the mercurous form which in turn undergoes disproportionation to DPM and elemental mercury (Fig. 1). It has been previously demonstrated that organomercurous radicals are in equilibrium with dialkyl- and diarylmercury compounds in the presence of metallic mercury via a process of homolytic fission which takes place at the metal surface[14–17]. Homolytic fission of the phenyl–mercury bond of the intermediate organomercurous radical would afford elemental mercury and a reactive phenyl radical, this demercuration reaction probably taking place at the metal surface as for the disproportionation reaction. The phenyl radical could then react with other species in the system to give the range of poducts noted. Bisulphite is known to exist in solution as a complex mixture of species the exact composition of which is influenced by pH, temperature and concentration[18], and reaction with these affords the BSOA and BSIA. When DPM is autoclaved in the presence of sodium metabisulphite and metallic mercury analysis of the product mixture showed the absence of DPM and PM nitrate and the formation of BSOA and BSIA in proportions roughly equivalent to those found in the degradation of PM nitrate solutions (Table II), an observation which supports the proposed mechanism.

The fact that elemental mercury is found in these degradative processes may account for the differing results obtained by Richards *et al.*[2] and other workers[1,5,6] when measuring PM salts by AAS. It is reasonable to suppose that PM nitrate degrades in amethocaine eye drops[9] by a similar mechanism, and upon prolonged autoclaving in the presence of amethocaine hydrochloride (Table II) affords BSOA and BSIA, the change in proportion of acids being probably ascribable to a pH effect on the species in the system arising from the bisulphite[17]. It is obvious from these studies that the amethocaine eye drops[9] are unsatisfactory and that sodium

TABLE II

PERCENTAGES OF PHENYLMERCURY AND DIPHENYLMERCURY CONVERTED TO BENZENESULPHONIC AND BENZENESULPHINIC ACIDS UNDER DIFFERENT CONDITIONS OF AUTOCLAVING

Values are means of three experiments.

Sample	*Sulphonic acid*	*Sulphinic acid*	*Total acids*
PM nitrate in sealed ampoules	39.7	33.0	72.7
PM nitrate in unsealed ampoules[a]	47.0	25.3	72.3
PM nitrate in loosely stoppered flasks	54.3	19.3	73.6
PM nitrate in sealed ampoules plus amethocaine hydrochloride (1%, w/v)	3.7	64.7	68.4
DPM in sealed ampoules[b]	54.6	27.7	82.3

[a] Preceding ampoules exposed to the atmosphere for 2 days and reassayed.
[b] Calculated to the basis of 1 mol of DPM affording 2 mol of acids.

metabisulphite should never be used as an antioxidant together with PM nitrate as an antimicrobial preservative in ophthalmic products.

REFERENCES

1 J. Buckles, M. N. Brown and G. S. Porter, *J. Pharm. Pharmacol.*, 23 (1971) S237.
2 R. M. E. Richards, A. F. Fell and J. M. E. Butchart, *J. Pharm. Pharmacol.*, 24 (1972) 999.
3 R. M. E. Richards and R. J. McBride, *J. Pharm. Pharmacol.*, 24 (1972) 159P.
4 R. M. E. Richards and J. M. E. Reary, *J. Pharm. Pharmacol.*, 24 (1972) 84P.
5 A. J. Collins, P. Lingham, T. A. Burbridge and R. Bain, *J. Pharm. Pharmacol.*, 37 (1985) 123P.
6 A. Hart, *J. Pharm. Pharmacol.*, 25 (1973) 507.
7 *British Pharmacopoeia*, Her Majesty's Stationary Office, London, 1980.
8 *British Pharmacopoeia*, Her Majesty's Stationary Office, London, 1988.
9 *Australian Pharmaceutical Formulary and Handbook*, The Pharmaceutical Society of Australia, Canberra, 14th ed., 1988.
10 J. E. Parkin, *J. Chromatogr.*, 472 (1989) 401; and references cited therein.
11 J. E. Parkin, *J. Chromatogr.*, 407 (1987) 389.
12 A. M. Bond and G. G. Wallace, *Anal. Chim. Acta*, 164 (1984) 223.
13 I. L. Finar, *Organic Chemistry*, Vol. 1, Longman, London, 6th ed., 1976, p. 695.
14 K. P. Butin, A. N. Kashin, A. B. Ershler, V. V. Strelets, I. P. Beletskaya and O. A. Reutov, *J. Organomet. Chem.*, 39 (1972) 30.
15 K. P. Butin, A. B. Ershler, V. V. Strelets, A. N. Kashin, I. P. Beletskaya and O. A. Reutov, *J. Organomet. Chem.*, 64 (1974) 171.
16 K. P. Butin, V. V. Strelets, A. N. Kashin, I. P. Beletskaya and O. A. Reutov, *J. Organomet. Chem.*, 64 (1974) 181.
17 A. N. Kashin, A. B. Ershler, V. V. Strelets, K. P. Butin, I. P. Beletskaya and O. A. Reutov, *J. Organomet. Chem.*, 39 (1972) 237.
18 M. Schmidt and W. Siebert, in J. C. Bailor, H. J. Emeleus, R. Nyholm and A. F. Trotman-Dickenson (Editors), *Comprehensive Inorganic Chemistry*, Vol. 2, Pergamon, Oxford, 1973, pp. 878–880.

Journal of Chromatography, 511 (1990) 243–256
Elsevier Science Publishers B.V., Amsterdam

CHROM. 22 365

Reversed-phase liquid chromatographic column switching for the trace-level determination of polar compounds

Application to chloroallyl alcohol in ground water

E. A. HOGENDOORN, A. P. J. M. DE JONG and P. VAN ZOONEN*
Laboratory of Organic Analytical Chemistry, National Institute of Public Health and Environmental Protection, P.O. Box 1, 3720 BA Bilthoven (The Netherlands)
and
U. A. Th. BRINKMAN
Department of Analytical Chemistry, Free University, De Boelelaan 1083, 1081 HV Amsterdam (The Netherlands)
(First received December 11th, 1989; revised manuscript received January 24th, 1990)

ABSTRACT

Reversed-phase liquid chromatographic (LC) column-switching employing two C_{18} columns was used for the trace-level determination of the polar compound chloroallyl alcohol (CAAL), a key metabolite of the soil sterilant dichloropropene, in ground water. The selectivity of the LC procedure is crucial as CAAL does not possess a chromophoric group and must be detected by UV absorbance at 205 nm. It is shown that the selectivity can be enhanced considerably by the use of a column-switching technique.

A completely automated procedure was developed for the determination of CAAL with a limit of detection (LOD) of 1 ppb (10^9) (signal-to-noise ratio = 3). Recoveries at the 20 ppb level were 103% for *cis*-CAAL [relative standard deviation (R.S.D.) = 3.4%] and 102% for *trans*-CAAL (R.S.D. = 2.5%). Response was linear over more than two decades. The sample throughput is high, as the total time required for the analysis is less than 10 min. If necessary, LODs can be lowered to 0.1 ppb by means of a liquid–liquid extraction combined with a concentration step, resulting in recoveries of 88% (R.S.D. = 4.1%) at a level of 2 ppb.

Confirmation of CAAL and a second metabolite of dichloropropene, chloroacrylic acid (CAAC), was performed by gas chromatography–negative ionization chemical mass spectrometry (GC–NCI-MS), using derivatization procedures to convert CAAL and CAAC into their pentafluorobenzoyl and pentafluorobenzyl derivatives, respectively.

0021-9673/90/$03.50

INTRODUCTION

In a recent review[1], it was stated that precolumn technology is a powerful means for selective sample handling in liquid chromatography (LC). A major advantage of on-line techniques is that sample preparation and clean-up are fully integrated in the chromatographic procedure. Short precolumns (2 × 4.6 mm I.D.) packed with C_{18} material have been used successfully for the trace enrichment of apolar and moderately polar pesticides in water[2–5]. A disadvantage of this method is the poor selectivity, especially in combination with UV detection. The selectivity can be improved by applying more selective electrochemical[2,4] or fluorescence[3] detection. However, the inherent selectivity of these detection techniques restricts them to only a limited number of compounds.

In our previous studies longer C_{18} precolumns (15 × 3.2 mm I.D.) were used, in order to perform an efficient clean-up, with a precise cutting of the relevant fraction to the analytical column for the determination of some fungicides[6] and herbicides[7,8] in extracts of contaminated water. These procedures have a more selective clean-up performance than methods involving preconcentration of large volumes of water on a precolumn, followed by desorption.

When dealing with medium to highly polar compounds, other types of adsorbents are often preferred which possess higher affinities than the C_{18} material for such compounds. For example, polymer PRP-1 precolumns were used for the preconcentration of phenoxyacetic acids in industrial effluents[9,10] and ion-exchange precolumns have been used for trace enrichment of anilines and phenols in surface water[11,12]. The very strong sorbent properties of polymer phases with respect to almost all polar and non-polar organic compounds makes this type of phase less selective than C_{18} materials. The use of ion-exchange precolumns is limited to ionic species.

In this work, we developed a column-switching procedure for the determination of a polar compound in ground water using two C_{18} columns with high separation power, increasing the selectivity by applying the cutting technique and the sensitivity by using large volume injections. It was applied to chloroallyl alcohol (CAAL), which is expected to occur in ground and surface waters as a metabolite of the soil fumigant 1,3-dichloropropene (DPE). DPE is frequently used in certain areas of The Netherlands for the control of nematodes in agriculture, horticulture and ornamental culture. As is known[13–18], *cis*- and *trans*-DPE hydrolyse rapidly to the corresponding CAALs in the presence of water, which in turn may undergo microbial conversion to the acrylic acids. The latter conversion is thought to take place much more slowly. The proliferation of these metabolites depends strongly on their mobility in soil, of which little is still known. However, based on the polarity of these compounds, a high mobility can be expected.

Several gas chromatographic (GC) methods for the determination of CAAL have been described[12–17], but most of them lack sensitivity and/or selectivity and, moreover, most of them are laborious. Reversed-phase LC (UV detection, 210 nm) has been used for the determination of DPE and CAAL at relatively high levels (sub-ppm) in water[19]. This paper describes the development of an automated, sensitive (sub-ppb[a]

[a] Throughout this article, the American billion (10^9) is meant.

TABLE I

STRUCTURAL FORMULAE AND UV CHARACTERISTICS OF DICHLOROPROPENE (DPE), CHLOROALLY ALCOHOL (CAAL) AND CHLOROACRYLIC ACID (CAAC)

Compound	*Structural formula*		λ_{max} *(nm)*	ε_{205} *(l/mol · cm)*
	cis	*trans*		
DPE	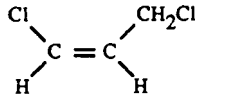	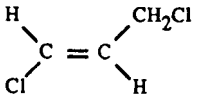	200	15000
CAAL	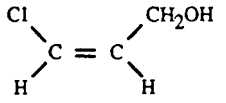	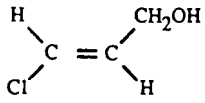	190	10000
CAAC	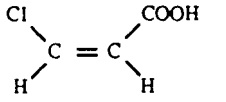	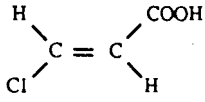	232	12000

level) and selective LC method involving column switching for the determination of CAAL in ground water. GC–mass spectrometric (MS) confirmation techniques were developed for CAAL and chloroacrylic acid (CAAC) in order to confirm the data produced by field studies. The latter methods were based on electron-capture negative chemical ionization (ECNCI) of the pentafluorobenzoyl derivative of CAAL and the pentafluorobenzyl derivative of CAAC, respectively.

The structural formulae of the various compounds and relevant UV characteristics are given in Table I. In this paper, the abbreviations of DPE, CAAL and CAAC indicate the *cis*- and *trans*-isomers, unless stated otherwise.

EXPERIMENTAL

Reagents

1,3-Dichloropropene [a mixture of 49.9% (w/w) *trans*- and 45.8% (w/w) *cis*-DPE], *cis*-chloroallyl alcohol (98.7%, w/w) and *trans*-chloroallyl alcohol (97.5%, w/w) were obtained from Shell (Sittingbourne, Kent, U.K.). *trans*-3-Chloroacrylic acid (99%), *cis*-3-chloroacrylic acid (98%) and triethylamine (99%) were purchased from Janssen Chimica (Beerse, Belgium) and pentafluorobenzoyl chloride, pentafluorobenzyl bromide and dimethylaminopyridine from Pierce (Rockford, IL, U.S.A.). Analytical-reagent grade toluene, hexane, dichloromethane, ethyl acetate and diethyl ether were obtained from Merck (Darmstadt, F.R.G.) and methanol and acetonitrile, both of HPLC grade, from Baker (Deventer, The Netherlands). Analytical reagent grade sodium chloride (NaCl), anhydrous sodium sulphate (Na_2SO_4) and hydrochloric acid (0.1 *M* HCl) were obtained from Merck. De-

mineralized water was purified in a Milli-Q (Millipore, Bedford, MD, U.S.A.) system to obtain LC-grade water for use in eluents and standard solutions.

Equipment

LC instrumentation. The automated LC column-switching system, shown schematically in Fig. 1, consisted of the following components: an ASPI 232-401 autosampler (Gilson, Villiers-le-Bel, France) equipped with two programmable six-port valves and a 200-μl injection loop. The first separation column (SC-1) was a 50 × 3.0 mm I.D. column packed with ChromSpher C_{18}, 5 μm (Chrompack, Middelburg, The Netherlands). An LC-250 binary gradient pump (Perkin-Elmer, Norwalk, CT, U.S.A.) with a helium degassing system was used for solvent delivery (100% water or 100% methanol) to the first LC column. A Model 301 pump (Gilson) was used for delivering methanol–water (5:95, v/v) to the second separation column (SC-2) (100 × 4.6 mm I.D., packed with MicroSpher C_{18}, 3 μm; Chrompack). All flow-rates were set at 1 ml/min. UV detection (205 nm) was performed with an LC-95 (Perking Elmer) detector equipped with a CI-10 integrator (LDC/Milton Roy, Co. Clare, Ireland).

GC–MS instrumentation. GC–MS analyses were performed on a Model 4500 instrument (Finnigan MAT, Sunnyvale, CA, U.S.A.). Ionization of samples was achieved with ECNCI with methane as the moderator gas (0.3 Torr) and 70-eV electrons with a filament emission current of 0.3 mA. The temperature of the source was set at 170°C and the GC–MS interface at 250°C. Multiple-ion detection (MID) was used with a dwell time of 50 ms per ion.

The GC separation was carried out on a 25 m × 0.25 mm I.D. CP Sil-19 CB fused-silica capillary column (d_f = 0.12 μm) obtained from Chrompack. After a splitless injection of 1 μl at an injection temperature of 250°C, the column temperature was programmed from 70°C (held for 2 min) at 8°C/min to a final temperature of 200°C, which was held for 10 min.

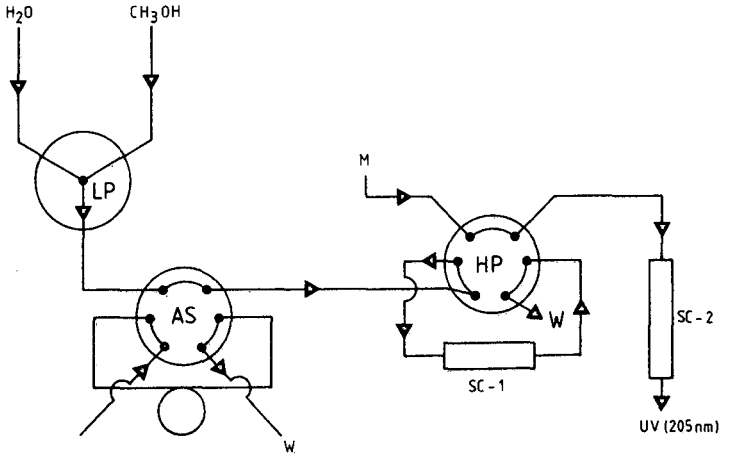

Fig. 1. Scheme of the experimental set-up. AS = Autosampler with a 200-μl loop; LP = low-pressure three-way selection valve; HP = high-pressure six-port valve; SC-1 = 50 × 3 mm I.D. C_{18} precolumn; SC-2 = 100 × 4.6 mm I.D. C_{18} separation column; M = mobile phase, methanol–water (5:95, v/v); flow-rates, 1 ml/min. For the timing of the eluent streams, see Fig. 2 and Results and Discussion.

LC analysis

Direct LC determination of CAAL in water samples (LOD, 1 μg/l). A 200-μl volume of sample was injected onto the first column (SC-1) employing water as the mobile phase (1 ml/min). After clean-up (1.0 min), SC-1 was switched on-line with the second column (SC-2), and the fraction containing CAAL was transferred to SC-2 in 0.8 min with methanol–water (5:95, v/v), the mobile phase for SC-2. Then SC-1 was switched off-line from SC-2 and reconditioned prior to the next injection with 3 ml of methanol followed by 10 ml of water. Depending on the occurrence of interfering peaks, the reconditioning step can be postponed until after about ten samples in order to increase the sample throughput.

LC determination of CAAL in water samples (LOD, 0.1 μg/l). A 100-ml volume of water was transferred to a 250-ml separating funnel. After the addition of 10 g of NaCl, extraction of CAAL was performed twice with 25 ml of diethyl ether by shaking the funnel for 2 min. The combined organic layers were placed in a 250 ml round-bottomed flask together with 2 ml of LC-grade water. The diethyl ether was removed in a rotating film evaporator at ambient temperature. The aqueous residue was transferred to a calibrated tube and the final volume was brought to 2.5 ml with LC-grade water. A 200-μl volume of this solution was injected as described in the previous section.

GC–MS confirmation of CAAL and CAAC

Extraction The same extraction procedure was used for CAAL and CAAC. A 5-ml volume of a water sample was pipetted into a test-tube and, after the addition of 1 ml of 0.1*M* HCl, 200 mg of NaCl and 5 ml of diethyl ether, the tube was shaken vigorously for 5 min. The organic layer was transferred into another tube and carefully evaporated to dryness under a gentle stream of nitrogen at ambient temperature.

Derivatization of CAAL. Toluene (0.5 ml), 10 μl of pentafluorobenzoyl chloride and 50 μl of a dichloromethane solution of dimethylaminopyridine (20 mg/ml) were added to the residue. The tube was closed with a glass stopper and heated for 30 min at 70°C. After cooling to room temperature, 0.5 ml of hexane and 0.5 ml of 0.1 *M* HCl were added and the derivative formed (CAAL–PFBCO) was extracted into the hexane–toluene layer. In this step, the excess of dimethylaminopyridine is largely removed from the sample as its hydrochloride salt. A 1-μl aliquot of the organic phase was injected into the GC–MS system.

Derivatization of CAAC. The residue obtained after extraction was dissolved in 50 μl of acetonitrile, and 10 μl of pentafluorobenzyl bromide and 10 μl of triethylamine were added. The mixture was heated for 10 min at 40°C. The ester formed (CAAP–PFB) was isolated from the reaction mixture by shaking with ethyl acetate (1.0 ml) and 0.1 *M* HCl (0.5 ml). The tube was then centrifuged (1500 *g*) for 1 min and 1 μl of the organic layer was used for GC–MS analysis.

RESULTS AND DISCUSSION

Choice of the method of analysis for CAAL and related compounds

Many polar compounds are difficult to detect in LC because they do not contain a chromophoric group. In this event UV detection at low wavelengths (200–215 nm) sometimes still provides sufficient sensitivity. If this non-selective detection mode has

to provide detection limits in the low-ppb range, a highly selective sample clean-up is required. In low-wavelength UV detection, background absorption plays an important role, especially if the chromatographic procedure involves changes in mobile phase composition. In this study, 205 nm turned out to be a suitable detection wavelength with respect to both sensitivity and low fluctuation of the background absorption on switching of the mobile phases.

In order to investigate the feasibility of a reversed-phase LC (RP-LC) determination of dichloropropene-related compounds, with emphasis on CAAL, the chromatographic behaviour of this compound and CAAC and DPE was studied on 5-μm C_{18} bonded silica material with methanol–water mixtures as eluent. The capacity factors (k') of CAAL and DPE are given in Table II. As expected, even with pure water as eluent, CAAC elutes shortly after t_0 (dead time) from a C_{18} bonded phase. Retention was obtained by using a 0.03 *M* phosphate buffer (pH 2.5); the results are given in Table II. The acrylic acids, however, gave tailing peaks with asymmetry factors at 10% peak height (A_s) of 2.0 (*cis*-CAAC) and 2.5 (*trans*-CAAC), which makes this buffered C_{18} system unsuitable for the trace-level determination of these compounds. The use of a phophate buffer did not influence the chromatographic behaviour of CAAL and DPE in comparison with unbuffered water–methanol systems.

Direct assay of CAAL in ground water

From the data in Table II, it can be seen that some trace enrichment of, *e.g.*, DPE will be possible on C_{18} precolumns, but problems will occur with CAAL as it shows insufficient retention even in a completely aqueous mobile phase. This results in an early breakthrough and excessive band broadening on transfer to the analytical column. In previous applications of column-switching techniques[6–8], limited volumes (100–1000 μl) were injected onto longer C_{18} precolumns (15 × 3.2 mm I.D.). For the present application, it can be estimated that, for example, with 200-μl injections of water samples containing CAAL onto such a large precolumns with a mobile phase of 100% water, only *ca.* 300 μl of mobile phase are available for clean-up before CAAL starts to break through. Moreover, ground-water samples contain relatively high

TABLE II

CAPACITY FACTORS ON A 50 × 3 mm I.D. COLUMN PACKED WITH 5-μm CHROMSPHER C_{18}[a] FOR CAAL AND DPE IN METHANOL–WATER AND FOR CAAC IN METHANOL–PHOSPHATE BUFFER (pH 2.5) MIXTURES

Methanol(%)	*k'*					
	cis-CAAL	*trans-CAAL*	*cis-DPE*	*trans-DPE*	*cis-CAAC*	*trans-CAAC*
0	7.2	7.3	59	55	7.3	17.6
10	3.8	3.9	44	41	3.4	9.9
20	2.4	2.5	23	22	1.7	4.9
30	1.8	1.9	16	15	1.3	3.3
40	1.3	1.4	9.4	8.9	1.0	2.4
50	1.0	1.1	4.7	4.7	–	–

[a] t_0 (Br^-) = 0.16 min.

concentrations of ionic species, which will produce a high UV response at 205 nm in the early part of the chromatogram (solvent peak), so causing interferences in the same part of the chromatogram where the components of interest are eluting.

Obviously, an even larger precolumn has to be selected in order to improve the clean-up performance of the system and, thus, to develop a successful RP-LC column-switching operation for compounds in the polarity range of CAAL. As an alternative, 50 × 3 mm I.D. guard columns packed with 5-μm ChromSphere C_{18} were studied. Such columns, which lie between a precolumn and a full separation column, were used as a first separation column (SC-1) in our further experiments. Because CAAL starts to migrate immediately on SC-1 after injection, the volume of sample introduction was set arbitrarily at 200 μl, in order to have a sufficient clean-up possibility.

To illustrate the problem of the separation of CAAL in ground water, chromatograms (recorded at a high attenuation) from 200-μl injections on SC-1 of a concentrated CAAL standard (200 ng) and a blank ground-water sample are shown in Fig. 2. The chromatograms show that after the 200-μl injection, a clean-up with about 1 ml of solvent can be used before CAAL starts to break through. In experiments with ground-water samples using the column-switching technique described below, it appeared that a flush with 1.0 ml of water after the injection provides a sufficient

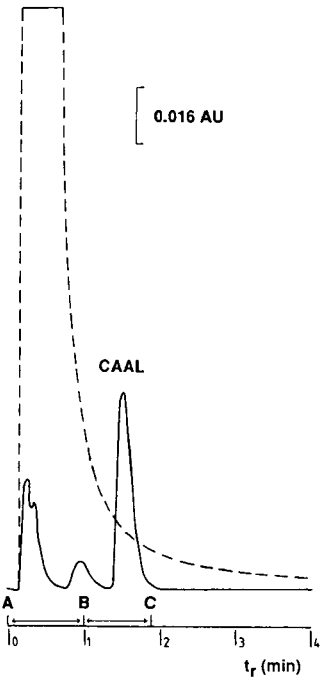

Fig. 2. Chromatograms of 200-μl sample injections on the SC-1 column (conditions as in Fig. 1) illustrating the selection of the column-switching conditions. Solid line, injection of sample containing 1000 ppb *cis*-CAAL in LC-grade water; dashed line, blank ground water sample. A to B, injection (0.2 ml) + clean-up with 0.8 ml of pure water; B to C, desorption of CAAL with 0.8 ml of methanol–water (5:95, v/v) to SC-2 column.

clean-up. With water, CAAL elutes completely from SC-1 within 1.8 ml and therefore after the clean-up a desorption volume of 0.8 ml was selected to transfer the CAAL fraction from the first to the second column.

In order to obtain peak compression and hence an increased sensitivity for CAAL, the mobile phase for the second separation column, *i.e.*, the real separation column, has to contain an organic modifier; 5% methanol in water was selected for use as the mobile phase for the second separation column. Considering the small retention of CAAL on C_{18} bonded silica, a highly efficient second column (SC-2; Fig. 1) should be used to obtain sufficient resolution between CAAL and either early eluting interferences or the baseline disturbance caused by the eluent switch. Several columns with C_{18} bonded phases were tested for their efficiency (expressed as N and A_s) and usefulness (expressed as k') as a second separation column; the results are given in Table III. From these data it can be concluded that the tested 4.6 mm I.D. columns were more efficient than the 3.0 mm I.D. columns. Possibly the larger I.D. of the second column enhances the peak compression caused by the step gradient from 0 to 5% methanol. Because of the shorter time of analysis and the slightly higher k' values, the 100 × 4.6 mm I.D. MicroSpher C_{18} column was preferred as a second separation column. The use of methanol–water (5:95, v/v) instead of pure water results in an enhancement of the peak shape. Compared with pure water, N increases from 3800 to 4800 and A_s decreases from 1.6 to 1.2 with the addition of 5% methanol.

Unfortunately, *cis*- and *trans*-CAAL cannot be separated on any of the four C_{18} bonded phases tested. McCall[19] separated *cis*- and *trans*-CAAL on the polymeric PRP-1 phase. However, his study indicated that the CAAL isomers elute as broad peaks (σ = 1.1 min) with a resolution of only 0.5, which leads to a much lower sensitivity. From an ecotoxicological point of view, separation of *cis*- and *trans*-CAAL is not too important, as the half-life of the conversion of *cis*-DPE into *cis*-CAAL is equal to that of *trans*-DPE into *trans*-CAAL.

The final set-up of the column-switching procedure for the determination of CAAL in water involves the injection of a 200-µl sample, clean-up on a 50 × 3 mm I.D. C_{18} column using water as the mobile phase, followed by desorption of the CAAL

TABLE III

COMPARISON OF C_{18} BONDED PHASE COLUMNS TO BE USED AS A SECOND SEPARATION COLUMN FOR THE DETERMINATION OF CAAL

For conditions, see Fig. 2.

Column dimensions length × I.D. (mm)	*Packing material*	*k'*		N^a	A_s^b
		cis-CAAL	*trans-CAAL*		
100 × 3	ChromSpher C_{18}, 5 µm	4.1	4.2	525	2.6
100 × 3	Hypersil ODS, 5 µm	2.5	2.5	440	2.3
150 × 4.6	Hypersil ODS, 5 µm	7.3	7.3	6380	1.4
100 × 4.6	MicroSpher C_{18}, 3 µm	8.2	8.3	4820	1.2

[a] Plate number calculated as $(t_r/\sigma)^2$, where t_r is retention time and σ is standard deviation, for *trans*-CAAL.

[b] Asymmetry calculated at 10% of the peak height, for *trans*-CAAL.

fraction to a second 100 × 4.6 mm I.D. C_{18} column with methanol–water (5:95, v/v) and UV detection at 205 nm.

Determination of CAAL in ground water. With a 200-μl injection of aqueous sample and UV detection at 205 nm (80% of the maximum UV absorbance at 195 nm), an absolute limit of detection (LOD; signal-to-noise ratio = 3:1) of 0.2 ng of CAAL was obtained, corresponding to an LOD of 1 ppb for the direct assay of CAAL in water. The response for CAAL was linear from 10 to 200 ppb ($r = 0.9996$, $n = 6$). The relative standard deviation (R.S.D.) of the peak height at a level of 40 ppb was 2.3% for *cis*-CAAL ($n = 6$) and 1.7% for *trans*-CAAL ($n = 10$). The R.S.D. of the retention times was 0.45% for both *cis*-CAAL and *trans*-CAAL ($n = 6$). The mean recoveries at a level of 20 ppb of *cis*-CAAL ($n = 5$) and 22 ppb of *trans*-CAAL ($n = 5$) were 103%

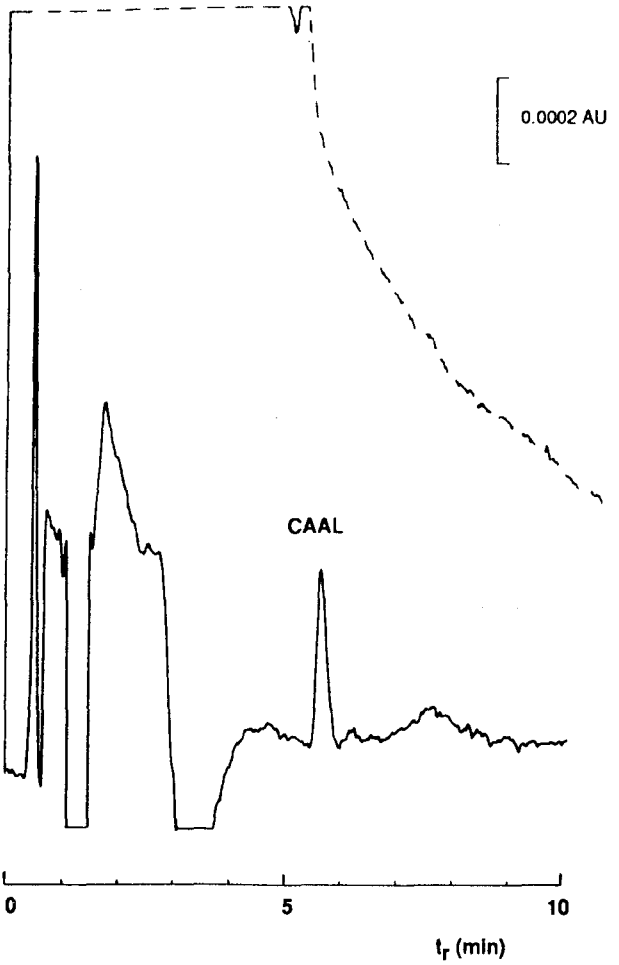

Fig. 3. RP-LC of 200-μl injections of a ground-water sample spiked with 10 ppb of *trans*-CAAL. Solid line, chromatogram obtained using the column-switching procedure; dashed line, chromatogram obtained with the same two columns coupled on-line, but without the column-switching procedure. Mobile phase: methanol–water (5:95, v/v) at 1 ml/min.

(R.S.D. = 3.4%) for *cis*-CAAL and 102% (R.S.D. = 2.5%) for *trans*-CAAL (n = 5). The sample throughput is high; each sample can be analysed within 10 min and for the ground-water samples investigated the washing step of the first column with methanol can be left until after ten injections.

The remarkable gain in selectivity obtained with the present procedure is illustrated in Fig. 3, showing the analysis of ground water spiked with 10 ppb of CAAL with and without column switching. In the latter instance, the same two columns (SC-1 and SC-2) were used but coupled on-line. As stated above, the high UV absorbance in the first part of the chromatogram obtained without column switching is caused mainly by the presence of inorganic ions. A typical conductivity value of this type of ground-water samples is 570 μS/cm, corresponding with a total ion strength of about 7 mmol/l. The anion composition of ground water typically is *ca.* 80% chloride and 20% nitrate. From this it can be estimated that a sample of 200 μl of ground water will contain about 40 μg of Cl^- and 15 μg of NO_3^-. According to Ayers and Gillett[20], the UV detection limit at 205 nm is 30 ng for Cl^- and 0.5 ng for NO_3^-. Consequently, at the wavelength of 205 nm used to detect CAAL, a water sample containing μg/ml levels of these anions will indeed produce a large UV response in the early part of the chromatogram. Multi-dimensional LC obviously is an efficient means of separating large amounts of anions from CAAL, which is not possible with single-column LC.

In a field experiment, according to the set-up of Boumans *et al.*[21], the mobility of CAAL and some pesticides were investigated. With the developed direct assay method, 22 ground-water samples were analysed and residues of CAAL were found in the range from 1 to 118 ppb.

Assay of CAAL in water after diethyl ether extraction and concentration

In order to decrease the LOD for CAAL to 0.1 μg/l, which is the EC tolerance level for pesticides in drinking water, a concentration step is necessary. According to Maddy *et al.*[18], CAAL can be concentrated by liquid–liquid extraction with diethyl ether followed by partial evaporation of the organic extract. For the LC analysis the final solution must consist of pure water. However, it is not possible to remove all of the traces diethyl ether (necessary for the LC analysis) without considerable losses of CAAL. This problem can largely be eliminated by adding a small volume of water to the diethyl ether extract to retain CAAL before the rotating film evaporation takes place. An additional advantage is that the final aqueous solution, after it has been adjusted to the volume required, can be injected directly into the RP-LC system. During the diethyl ether extraction most of the anionic interferences are eliminated and column switching as a clean-up step therefore becomes less urgent. However, the column-switching procedure will prevent the occurrence of later eluting peaks, and so reduce the total time of analysis.

An illustration of the LC analysis after extraction with diethyl ether is shown in Fig. 4, which is a chromatogram of a blank ground water spiked with 1 ppb of CAAL. The recovery of CAAL was tested by adding *cis*- and *trans*-CAAL to ground water at levels of 2 and 20 ppb, respectively. This resulted in mean recoveries of 88% (n = 10; R.S.D. = 4.1%) for *cis*-CAAL and of 87% (n = 10: R.S.D. = 2.7%) for *trans*-CAAL. No significant differences in the recovery at the two levels were found.

Seven ground-water samples were taken from suspected locations and analysed using the present method. None of the samples contained more than 0.1 ppb of CAAL, which is the limit of detection.

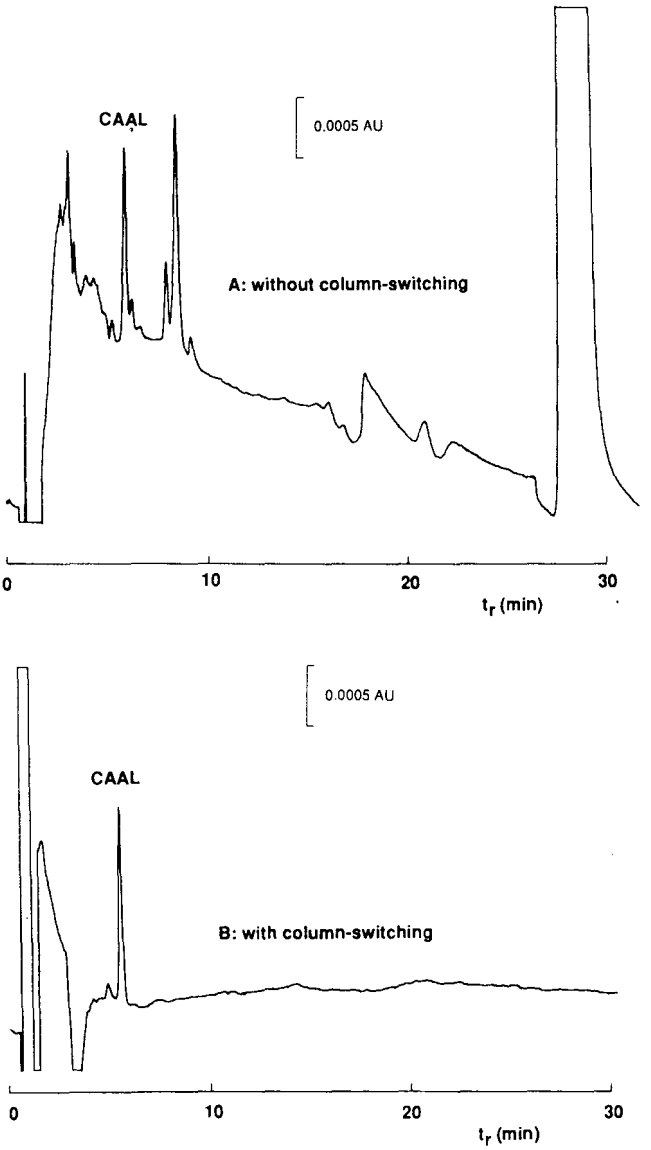

Fig. 4. RP-LC of a blank ground-water sample spiked with 1 ppb of *trans*-CAAL after extraction and concentration with diethyl ether, (A) without and (B) with column switching.

GC–MS confirmation of CAAL and CAAC

If CAAL is found in a drinking-water source, an independent alternative analytical method should be available for confirmation purposes. GC–MS is a very sensitive and selective technique, especially when performed in the ECNCI mode Therefore, a derivatization procedure was developed for CAAL with pentafluorobenzoyl chloride. The use of the strong base dimethylaminopyridine markedly

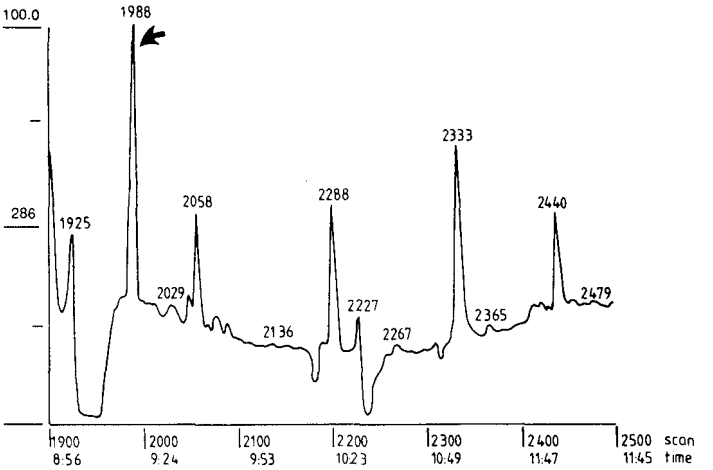

Fig. 5. GC–ECNCI-MS with selected ion detection at *m/z* 286 of a drinking-water sample spiked with 1 ppb of *trans*-CAAL, after extraction and derivatization with pentafluorobenzoyl chloride. Time in min:s.

increases the rate of the reaction, resulting in quantitative (>95%) yields. This was confirmed by residual analysis for free (unreacted) CAAL in the reaction medium by the LC method described here. The derivatives are very stable for several weeks in the organic phase solution when it is stored cool (5°C) and in the dark.

For the confirmation of CAAL, the molecular ion (*m/z* 286) of the pentafluorobenzoyl derivative, its ^{37}Cl isotope (*m/z* 288) and the fragment ions at *m/z* 211 ($PFCOO^-$) and *m/z* 167 (PFB^-) were monitored in the multiple-ion mode. The last two ions are not compound-specific. For positive identification of a peak at the proper retention time, the intensity ratio of the peaks at *m/z* 286 and 288 should be between 0.30 and 0.36, which represents the natural isotope ratio for $^{35}Cl/^{37}Cl$ of 0.33 (±10%).

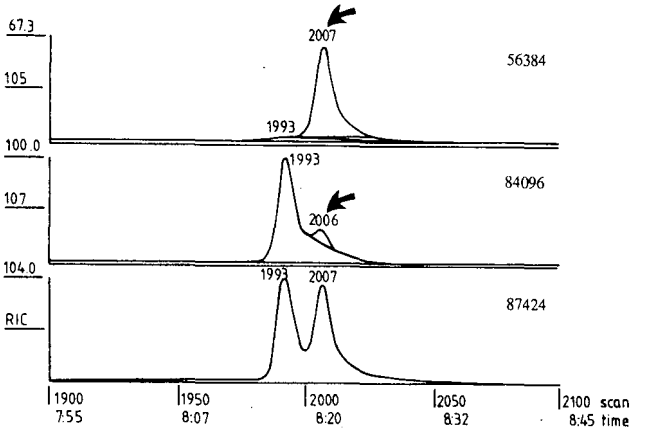

Fig. 6. GC–ECNCI-MS (*m/z* 105 and 107) of the analysis of drinking water spiked with 1 ppb of *trans*-CAAC after extraction and derivatization with pentafluorobenzyl bromide. Time in min:s.

Fig. 5 shows the GC–ECNCI-MS of CAAL in drinking water spiked at the 1 ppb level and indicates that an LOD at this level can easily be obtained.

It is interesting that preliminary experiments with CAAC, for which no proper LC procedure has yet been developed, show that a GC–MS method similar to that for CAAL can serve for identification purposes. In this instance, derivatization is effected with pentafluorobenzyl bromide, yielding the PFB ester[22]. The NCI mass spectrum of the CAAC–PFB derivative shows an intense compound-specific carboxylate anion at *m/z* 105 and 107 (chlorine isotope). The anion is formed by the loss of the PFB moiety from the molecular ion, a well known fragmentation pattern for PFB esters under ECNCI conditions[23]. The intensity ratio of the *m/z* 105 and 107 peaks should, as for CAAL, also be in the range 0.30–0.36. Fig. 6 shows the GC–ECNCI-MS of drinking water spiked with 1 ppb of CAAC, and indicates that the limit of detection of at least 1 ppb was restricted by an interference close to the *m/z* 107 trace and might be considerably improved if a better GC separation could be achieved.

CONCLUSIONS

A sensitive and selective multi-dimensional RP-LC method was developed for the trace-level determination of chloroallyl alcohol, the main metabolite of the pesticide dichloropropene, in drinking and ground waters. Sensitivity was obtained by non-selective UV detection at 205 nm but the selectivity was regained by using a column-switching procedure. The method has a high sample throughput, which makes it useful for screening purposes at a level of 1 ppb. The limit of detection can be reduced to 0.1 ppb by a liquid–liquid extraction with a subsequent evaporation step. The method has been applied to several types of ground- and drinking-water samples. The approach of using a relatively large column with a greater separation power than conventional precolumns for clean-up purposes in determining polar compounds such as CAAL was successful with respect to the overall selectivity of the procedure. The technique has previously been applied to improve the clean-up in the determination of organochlorine pesticides and polychlorinated biphenyls by normal-phase LC[24]. We are currently investigating the applicability of the technique to the trace-level determination of moderately polar and non-polar pesticides. For confirmation purposes a new GC–ECNCI-MS procedure has been developed for both chloroallyl alcohol and chloroacrylic acid, involving extraction and derivatization with fluorine-containing reagents of the analytes. Identification can be achieved down to at least 1 ppb.

ACKNOWLEDGEMENTS

The technical assistance of Mrs. G. den Engelsman is greatly acknowledged. We are indebted to Chrompack (Middelburg, The Netherlands) for their gift and preparation of the 50 × 3 mm I.D. separation columns.

REFERENCES

1 M. W. F. Nielen, R. W. Frei and U. A. Th. Brinkman, in R. W.Frei and K. Zech (Editors), *Selective Sampling Handling and Detection in High-Performance Liquid Chromatography*. Part A (*Journal of Chromatography Library*, Vol. 39A), Elsevier, Amsterdam, 1987, p. 5.

2 C. E. Werkhoven-Goewie, U. A. Th. Brinkman and R. W. Frei, *Anal. Chem.*, 53 (1981) 2072.
3 Low Kun She, U. A. Th. Brinkman and R. W. Frei, *Anal. Lett.*, 17 (1984) 315.
4 M. W. F. Nielen, G. Kroomen, R. W. Frei and U. A. Th. Brinkman, *J. Liq. Chromatogr.*, 8 (1985) 315.
5 M. Akerblom, *J. Chromatogr.*, 319 (1985) 427.
6 C. E. Goewie and E. A. Hogendoorn, *Sci. Total Environ.*, 47 (1985) 349.
7 C. E. Goewie and E. A. Hogendoorn, *J. Chromatogr.*, 410 (1987) 211.
8 E. A. Hogendoorn and C. E. Goewie, *J. Chromatogr.*, 475 (1989) 432.
9 B. Zygmunt, J. Visser, U. A.Th. Brinkman and R. W. Frei, *Int. J. Environ Anal. Chem.*, 15 (1983) 263.
10 R. L. Smith and D. J. Pierzyk, *J. Chromatogr. Sci.*, 21 (1983) 282.
11 M. W. F. Nielen, R. W. Frei and U. A. Th. Brinkman, *J. Chromatogr.*, 317 (1984) 557.
12 M. W. F. Nielen, J. de Jong, R. W. Frei and U. A. Th. Brinkman, *Int. J. Environ. Anal. Chem.*, 25 (1987) 37.
13 C. E. Castro and N. O. Belser, *J. Agric, Food Chem.*, 14 (1966) 69.
14 C. E. Castro and N. O. Belser, *J. Agric, Food Chem.*, 19 (1971) 23.
15 T. R. Roberts and G. Stoydin, *Pestic. Sci.*, 7 (1976) 325.
16 H. van Dijk, *Agro-Eco Systems*, 1(1974) 193.
17 H. van Dijk, *Pestic. Sci.*, 11 (1980) 625.
18 K. T. Maddy, H. R. Fong, J. A. Lowe, D. W. Conrad and A. S. Fredrickson, *Bull. Environ. Contam. Toxicol.*, 29 (1982) 354.
19 P. J. McCall, *Pestic. Sci.*, 19 (1987) 235.
20 G. P. Ayers and R. W. Gillett, *J. Chromatogr.*, 284 (1984) 510.
21 L. M. M. Boumans, D. Wever and E. J. M. Veling, in W. van Duivenbode and H. G. Waegeningh (Editors), *Vulnerability of Soil and Ground Water to Pollutants (Proceedings and Information,* No. 38), CHO-TNO, The Hague, 1987, p. 547.
22 K. A. Waddell, I. A. Blair and J. Welby, *Biomed. Mass. Spectrom.*, 10 (1983) 83.
23 R. J. Strife and R. C. Murphy, *J. Chromatogr.*, 305 (1984) 3.
24 E. A. Hogendoorn, G. R. van der Hoff and P. van Zoonen, *J. High Resolut. Chromatogr.*, 12 (1989) 784.

Journal of Chromatography, 511 (1990) 257–270
Elsevier Science Publishers B.V., Amsterdam

CHROM. 22 412

Packed-column supercritical fluid chromatography–mass spectrometry and supercritical fluid chromatography–tandem mass spectrometry with ionization at atmospheric pressure[a]

ERIC HUANG and JACK HENION*
Drug Testing and Toxicology, Cornell University, 925 Warren Dr., Ithaca, NY 14850 (U.S.A.)
and
THOMAS R. COVEY
Sciex Inc., 55 Glen Cameron Rd., Thornhill, Ontario L3T 1P2 (Canada)
(Received December 12th, 1989)

ABSTRACT

The combination of packed-column supercritical fluid chromatography (SFC) with atmospheric pressure ionization mass spectrometry (SFC–API-MS) is reported. This approach is novel in that the adiabatic expansion of total SFC effluent is subjected to atmospheric pressure chemical ionization (APCI) via a corona discharge with the aid of a heated region around the restrictor. The latter is a laser-drilled stainless-steel pinhole diaphragm which is commercially available, rugged, and easily handled.

Supercritical carbon dioxide was modified with methanol to produce protonated molecular ions via APCI of representative steroids in synthetic mixtures and biological extracts. The separation time for these compounds was within a few minutes so that rapid analyses are possible. The single MS spectra readily indicate the molecular weights of these compounds although little structural information is provided.

In those instances where structural information is desired the technique of tandem mass spectrometry (MS–MS) may be utilized. Thus SFC–MS–MS characterization of trenbolone produced a collision-induced dissociation product ion mass spectrum containing numerous structurally useful fragment ions. SFC–MS–MS analysis of a complex tissue extract fortified with low ppb levels of the same growth-promoting steroid and an internal standard readily revealed the target compound by this technique.

It is suggested that SFC–API-MS is a practical approach to routine SFC–MS. The APCI technique provides reliability and good sensitivity for many classes of compounds while the pinhole diaphragm restrictor is much more rugged and easier to work with than those associated with capillary columns.

[a] Portions of this work were first presented at the *35th ASMS Conference on Mass Spectrometry and Allied Topics, Denver, CO, May 24–29, 1987.*

0021-9673/90/$03.50

INTRODUCTION

Supercritical fluid chromatography (SFC) using bonded stationary phases on either capillary or packed columns has received considerable interest in the last few years. Although there has been some controversy in the literature over whether SFC using capillary or packed columns is preferred, in general most experienced with both techniques admit they each have their own merits and limitations.

The most common detector for capillary SFC has been the flame ionization detector while the UV detector has been favored for packed-column SFC. Each of these modes of detection enjoys acceptance based on ease of use, relatively good sensitivity, wide dynamic range and analytical ruggedness. However, none of the many detectors reported for SFC provide the combination of sensitivity and specificity commonly expected from the mass spectrometer. Although a diversity of reports have appeared which describe the successful combination of SFC with mass spectrometry (MS)[1–3], general acceptance and commercial availability of this desirable combination has lagged expectations.

The majority of the early reports of SFC–MS utilized chemical ionization (CI) instead of the more traditional electron impact (EI). We believe there is good reason for this trend simply because it is much easier to accomplish SFC–MS under CI than EI conditions. In the former the mass spectrometer ion source is operated under pressure conditions which are nearly 1000 times higher than in the latter[4]. This higher gas density in the heated ion source helps transfer heat to vaporize molecules introduced into the mass spectrometer via the adiabatic expansion from the SFC column restrictor. A reagent gas such as methane, isobutane or ammonia is usually admitted which is subjected to primary ionization by high-energy electrons followed by ion–molecule interactions by the ionized excess reagent gas with the analyte molecules[1]. Usually the gas-phase protonation resulting from these processes provides protonated molecular ions with little or no fragmentation. These simple CI mass spectra are of limited value for structural characterization, but readily provide molecular weight determination and relatively good sensitivity.

In contrast to CI experimental conditions, EI ion sources operate under high-vacuum conditions (10^{-5}–10^{-6} Torr) where heat transfer to the analyte, which is necessary for volatilization and subsequent ionization, is very difficult to accomplish. This problem coupled with the additional "gas burden" imposed, for example, by a pressure program during the course of a capillary SFC–MS analysis makes SFC–EI-MS a difficult challenge. Ideally, the EI process requires a constant low pressure in the ion source. Unfortunately, due to the fixed restrictor usually present in such systems the pressure program forces increasingly larger quantities of the expanded mobile phase into the ion source. In fact, since analytes usually elute toward the end of such a pressure program, the conditions in the ion source are at their worse just when they should be at their optimum. Consequently, the limited examples of SFC–EI-MS have not for the most part shown impressive low detection limits especially on "difficult" analytes.

If we remember that SFC with flame ionization detection (FID) appears to work satisfactorily with good reliability and sensitivity perhaps we can consider an alternative approach to SFC–MS. The two obvious facts about the flame ionization detector is that it is maintained at temperatures between 350 and 450°C and it operates

at atmospheric pressure. Thus the tremendous cooling resulting from the supercritical fluid expanding from the restrictor is dealt with by high temperature and gas pressures which facilitate transfer of heat to the analyte. If we could ionize the analyte at atmospheric pressure with sufficient heat for vaporization without thermal degradation then perhaps we could approach FID sensitivities with MS detection. Assuming that ions could be formed, all that remains is a means of sampling them into a vacuum system containing a mass analyzer.

Although these concepts may appear difficult to implement, the task is quite straightforward to accomplish provided a mass spectrometer equipped with an atmospheric pressure ionization (API) ion source is utilized. The focus of this report is to describe how and why SFC–API-MS is perhaps the most logical means of accomplishing routine, high-sensitivity SFC–MS. It is important to note that CI conditions still prevail in this approach, but there are alternative means of providing desired structural information. Also, both capillary- and packed-column SFC are amenable to SFC–API-MS. It is useful to point out that if the API-MS approach can handle SFC flow-rates up to 2 ml/min it can certainly handle the reduced flow-rates of capillary columns. Results of the latter have been accomplished, but will be reported elsewhere.

API-MS is not a new or unproven MS techique. Horning *et al.*[5] reported impressive liquid chromatography (LC)–MS detection limits as early as 1974 while a wide variety of more recent applications and developments have appeared in the last few years[6,7]. The commercial availability of instrumentation used in this work as well as recent developments[8–11] suggests that API techiques will undergo significant developments and be widely applicable in the future. In fact, there is a variety of different ways to form ions at atmospheric pressure.

Historically, ions were formed by emission of β particles from ^{63}Ni foil, but this was later simplified by replacement with a corona discharge which has been utilized in this work. Alternatively, liquids or fluids passing through a capillary held in excess of 3 kV produce charged droplets which emit ions into the gas phase by "ion evaporation". This electrospray approach has been described by ourselves[10] and others[9,11] for the characterization of a wide variety of applications ranging from polar drugs to peptides, proteins and polymers. These approaches to form ions at atmospheric pressure provide unusual flexibility and opportunity for combining separation methods with mass spectrometry. In this report we will focus on packed-column SFC as one example.

EXPERIMENTAL

Chromatography

The packed-column SFC system used in this work was a Hewlett-Packard Model 1084B high-performance liquid chromatography (HPLC) system modified for SFC operation[2]. The variable-wavelength UV detector was equipped with a high-pressure cell and used in-line with the SFC–MS interface in all this work. The exit of the column was disconnected from the conventional backpressure regulator and directed through a 20-μm pinhole centered in a stainless-steel diaphragm restrictor housed in a modified heated pneumatic nebulizer SFC–MS interface (see below). Supercritical fluid conditions were maintained by housing the column in the oven

heated to 80°C while pre-cooled supercritical carbon dioxide (A) was mixed with carbon dioxide doped with 10% methanol (B) and delivered through the column at a flow of 1–2 ml/min. The column used in this work was a standard HPLC column from Shandon (Keystone, State College, PA, U.S.A.) packed with a bonded cyanopropyl stationary phase on 3-μm silica particles (100 × 4.6 mm I.D.). Samples were dissolved in methanol and were injected (5 μl) via a 5-μl loop injector (Model 7125, Rheodyne, Cotati, CA, U.S.A.).

Mass spectrometry

The modified heated pneumatic nebulizer interface was introduced through the standard solids probe inlet of a TAGA 6000E triple quadrupole mass spectrometer equipped with an atmospheric pressure chemical ionization (APCI) source (Sciex, Thornhill, Canada). Packed-column SFC flow-rates ranged from 1 to 2 ml/min while supercritical carbon dioxide doped with varying amounts of methanol was continuously introduced into the APCI source under either SFC–MS or SFC–MS–MS conditions. A probe heater temperature of 500°C was used resulting in a measured vapor temperature of about 125°C at the point where the vapor exits from the quartz liner of the heated pneumatic nebulizer SFC–MS interface (see Fig. 3). Liquid nitrogen boil-off gas was introduced into the interface to effect nebulization at a flow-rate of about 7 l/min. Under full-scan SFC–MS operating mode quadrupole 1 was operated beginning at m/z 200 with quadrupole 3 operating in the rf-only mode. When SFC–MS–MS experiments were undertaken, the mass spectrometer was operated in the full-scan daughter ion or selected reaction monitoring (SRM) modes. Unit resolution (full-width at half maximum = 0.6 dalton) was maintained across the mass range scanned by quadrupole 3 in all collision-induced dissociation (CID) work reported here. Under scanning conditions a scan-rate of 3 s per scan was used while under SRM conditions a dwell time of 100 ms was used. For all MS–MS experiments argon was used as the collision gas with an effective target thickness of approximately

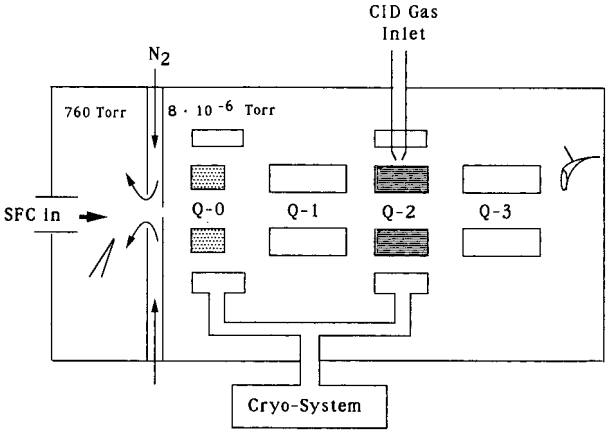

Fig. 1. Simplified diagram of the API tandem triple quadrupole mass spectrometer system used in this work. The API ion source is shown on the left with its associated corona discharge needle. This region is coupled with the the high vacuum system via 100-μm orifice and the nitrogen curtain gas. The vacuum is achieved through a liquid helium cooled cryopump.

$200 \cdot 10^{12}$ atoms/cm^2. The CID experiments were optimized at a laboratory collision energy of 50 eV in order to obtain useful structural information and optimize product ion sensitivity.

The Sciex TAGA 6000E (Fig. 1) is pumped with a two-stage liquid helium cooled cryogenic system. There are two cryoshells, one around the quadrupole lens (Q-0) and the other around the collision cell (Q-2). These cryoshells have a combined pumping speed of more than 60 000 l/s for air. The base vacuum of this system is $5 \cdot 10^{-8}$ Torr, and when the ion sampling orifice is exposed to atmosphere it increases to $7 \cdot 10^{-6}$ Torr. The pitfalls of such a system are that non-condensable gas such as helium cannot be pumped efficiently, and when the cryoshells become saturated, the system needs to be recycled (warmed to room temperature, rough-pumped out, and cooled back down). Recycling takes approximately 10 h and can be done overnight. Usually 50 h of operation are obtained before recycling is required.

Ion extraction with this API-MS system is accomplished through a sampling orifice with an inner diameter of 100 μm (Fig. 2). The atmosphere side of the ion-extraction orifice is bathed with a 0.5–2 l/min flow of dry nitrogen (ultrapure). Without the nitrogen curtain gas ions undergo extensive clustering with water and other polar molecules in the free-jet expansion from atmosphere to high vacuum (see Fig. 2).

Ions are focused into the vacuum via an electrical potential gradient. In positive-ion operation, the corona discharge electrode is operated at 6 kV (constant current control) with the interface plate at 650 V and the orifice at 40 V. When the ions approach the orifice the combination of electrical potential and vacuum pulls them through and into the analyzer. This potential difference can be increased to facilitate CID in the free-jet expansion regin. Low potential differences (20 V or less) impart only enough energy to dissociate hydrogen-bonded clusters and adducts. High potential differences (in excess of 20 V) often fragment molecules and may be used to gain some fragmentation.

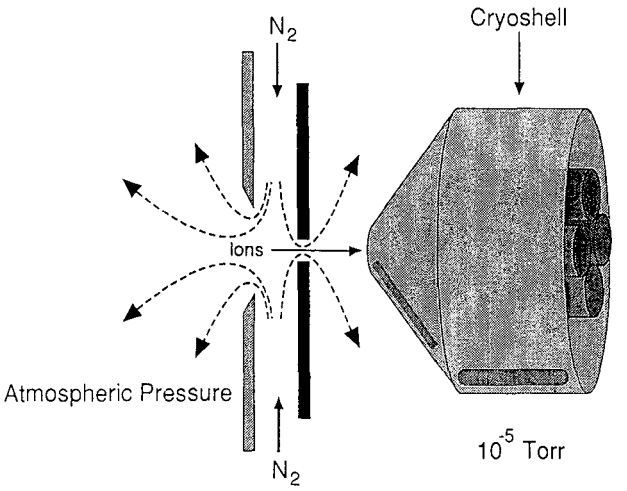

Fig. 2. The API interface which separates the high vacuum mass analyzer system from the API region. Electrical potentials on the lenses focus ions through the ion-sampling orifice and into the mass analyzer.

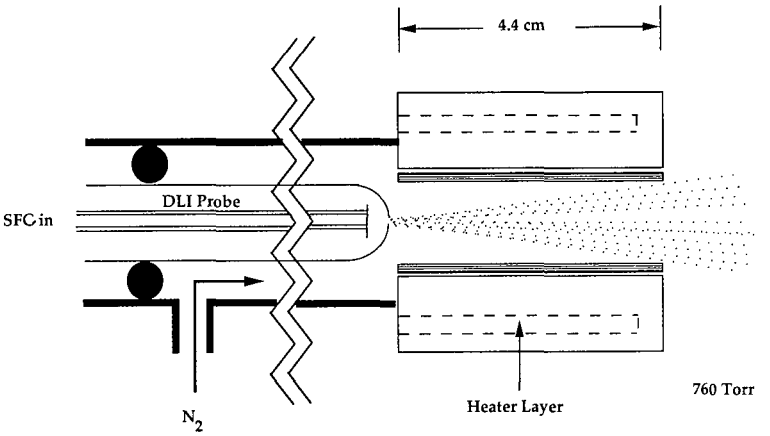

Fig. 3. Combined packed-column SFC restrictor and heated pneumatic nebulizer SFC–MS interface used in this work. The total packed-column SFC effluent passes through the 20-μm pinhole restrictor whereupon adiabatic expansion exposes the analytes to the heated quartz liner region. Following mixing and volatilization by heat the sample is ionized by APCI which is initiated by the corona discharge needle.

The SFC–MS interface

The device or "interface" which can deliver total effluent from the SFC system to the API ion source of the mass spectrometer used in this work is schematically shown in Fig. 3. This system combines the post-column restrictor necessary for maintaining supercritical conditions via a small pinhole diaphragm housed in a direct liquid introduction (DLI) LC–MS probe described previously[13]. This LC–DLI-MS probe was fitted with a 20-μm pinhole diaphragm instead of the 5-μm pinhole used for LC–MS[13]. This probe was held in place via O-rings and housed in an adaptor which placed the probe tip near the opening of a quartz liner maintained at 200°C and allowed co-axial flow of nitrogen nebulizer gas (Fig. 3). The copper heater block which housed the quartz liner was fitted with four cartridge heaters powered by a variable transformer which supplied continuous power to the heaters. Temperature monitoring of this heating block was accomplished via an iron–constantine thermocouple which was also housed in the block. Optimization experiments suggested that a measured temperature of 200°C was adequate to handle the compounds studied in this work. The volatilized analytes eluting from the packed column were ionized via a corona discharge needle maintained at 6 kV (Fig. 1).

The ions formed at atmospheric pressure are then electrically focussed through a 100-μm orifice and through a nitrogen curtain gas into high vacuum conditions (Fig. 2). The nitrogen curtain gas effectively declusters cluster ion adducts with the analyte and minimizes plugging of the small ion-sampling orifice. The small orifice separates the high-vacuum region where the inlet system and ionization region resides. This "decoupling" of the ionization and mass analysis regions provides a flexibility and ease of accomplishing chromatography which is unique from conventional MS systems.

DISCUSSION

APCI

APCI is similar to low-pressure CI in that the analyte of interest must be in the gaseous phase before ionization by ion–molecule reactions can proceed. The ionization process is initiated by an external source of electrons (utilizing β emitters or corona discharge as the primary source). However, because the ions and molecules experience more collisions, APCI is a milder and more efficient process than conventional low-pressure CI. The ionization process of APCI both in positive-ion and negative-ion modes were well documented previously[12]. Under SFC–API-MS experimental conditions, positive reactant ions are formed in ambient air by an electron ionization mechanism and subjected to further collisions to form an equilibrium set of proton hydrates. The analytes in the gas phase then react with these proton hydrates to form protonated molecular ions $(M+H)^+$ and are subsequently mass-analyzed.

Tandem mass spectrometry

The API approach does not directly provide structural information for ionized compounds because little or no fragmentation occurs under the very mild ionization conditions. Although molecular weight information is usually provided, identification of unknown compounds eluting from the SFC system requires plausible fragmentation processes to produce a more useful mass spectrum.

The technique of tandem mass spectrometry (MS–MS) usually involves two mass analyzers in "tandem" and separated by a collision cell[14]. The process involves electrically focussing parent ions such as the protonated molecular ions generated under APCI by the first mass analyzer (Fig. 1, Q-1) into the collision cell. These ions are then subjected to ion–molecule interactions in the collision cell (Q-2) which impart excess energy to the protonated molecular ions. This energy rapidly distributes itself throughout the excited ions and causes breakage of weak bonds resulting in a family of product ions. These ions have different masses than the parent ion and other fragment ions, so another mass analyzer (Q-3) is required to separate these ions. The second mass analyzer produces a full-scan product ion mass spectrum which can be very useful for structural characterization.

When one combines the separation power of SFC with the mixture analysis capability, specificity and sensitivity of tandem mass spectrometry (SFC–MS–MS), we have a very powerful analytical system. In this report we will show how the mild ionization conditions of APCI coupled with the capabilities of MS–MS is a natural combination.

Applications

To illustrate the utility of API for packed-column SFC–MS and SFC–MS–MS we present a few representative examples where these techniques are particularly well-suited. It should be emphasized that compounds of increasing polarity are difficult to chromatograph under SFC conditions even when the mobile phase is modified with methanol or other polar solvents. We suggest that the steroids described below, however, are preferred candidates for SFC and hence SFC–API-MS.

Gas chromatographic (GC) characterization of some steroids either requires

derivatization due to their higher polarity or reduced temperatures due to their thermal instability, while HPLC techniques suffer from occasionally inadequate separation efficiences and longer analysis times. Packed-column SFC, however, provides faster analysis times without derivatization or undue exposure to elevated temperatures. In

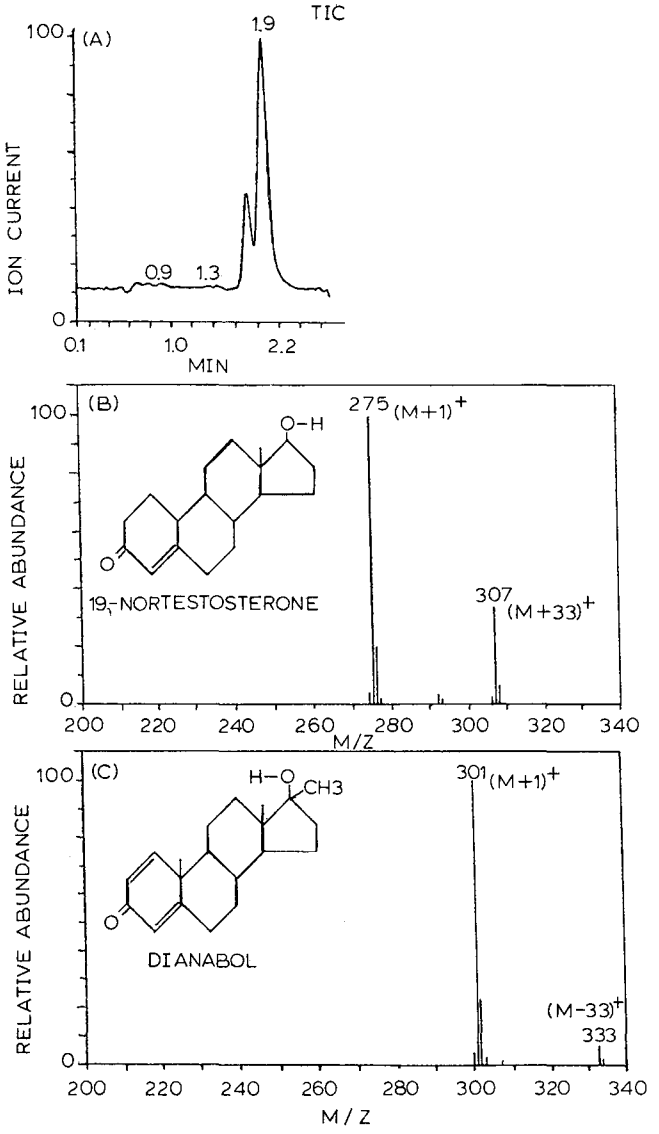

Fig. 4. SFC–API-MS analysis of a synthetic mixture containing 250 and 500 ng of 19-nortestosterone (mol.wt. 274) (B) and Dianabol (mol.wt. 300) (C), respectively. The separation was accomplished on a cyanopropyl column (100 × 4.6 mm I.D.) packed with 3-μm particles using a flow of 1.5 ml/min carbon dioxide–methanol (87:13, v/v) under an operating inlet (outlet) pressure of 3400 (3100) p.s.i. The column was maintained at 80°C and the total effluent was transferred to the API ion source through a 20-μm pinhole restrictor.

the examples of packed-column SFC–MS under APCI conditions described below on both synthetic mixtures and biological extracts the advantages and limitations of this approach will be highlighted.

The on-line packed-column SFI-API-MS analysis of a synthetic mixture

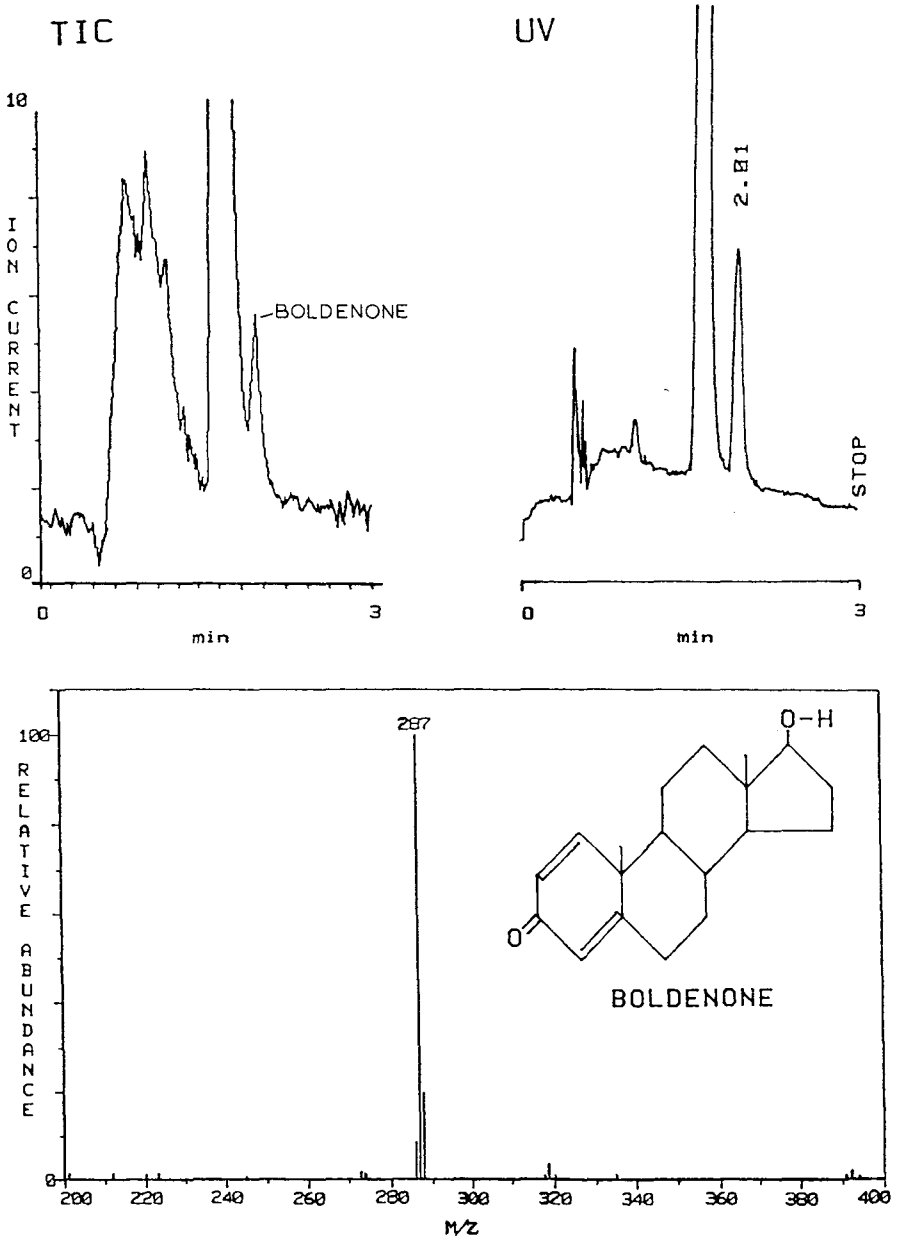

Fig. 5. Packed-column SFC–API-MS analysis of an equine urine extract containing boldenone (mol.wt. 286). Experimental conditions were the same as described for Fig. 4.

containing 250 ng of 19-nortestosterone (mol.wt. 274) and 500 ng methandrostenolone (Dianabol, mol.wt. 300) is shown in Fig. 4. The mass spectrometer was scanned in the single-MS mode from m/z 200 to 500 at a scan-rate of 3 s/scan. The HP 1084B SFC system delivered a 1.5-ml/min flow of carbon dioxide–methanol (87:13, v/v) through a Shandon 3-μm cyanopropyl column (100 × 4.6 mm I.D.) maintained at 80°C. The inlet (outlet) pressure of the column was 3400 (3100) p.s.i. and the total effluent passed through the 20-μm restrictor in the modified DLI probe (Fig. 3). The quartz liner housed in the copper block of the SFC–MS interface (Fig. 3) was maintained at 200°C while the nitrogen make-up gas was set at a flow of 20 standard cubic feet per hour (SCFH).

The total ion current (TIC) from SFC–API-MS analysis of this mixture is shown in Fig. 4A while the corresponding APCI mass spectra for 19-nortestosterone and Dianabol are shown in Fig. 4B and C, respectively. These spectra are dominated by protonated molecular ions which easily provide the molecular weights for these compounds plus adduct ions at $(M+33)^+$ which presumably are proton-bound adducts between the analyte and methanol used as modifier for the carbon dioxide mobile phase. No fragment ions are observed in these mass spectra due to the extremely mild APCI conditions.

Another example of packed-column SFC–MS is shown in Fig. 5 which highlights the rapid and effective means of detecting the anabolic steroid, boldenone, in equine urine. Five microliters of a crude equine urine extract[15] dissolved in methanol were injected under the same SFC–MS conditions as described above for Fig. 4. Fig. 5 shows the corresponding TIC and UV traces from the full-scan SFC–API-MS analysis of the equine urine extract. Note the retention time for boldenone in this experiment is only 2 min, which demonstrates the relatively fast analysis times afforded by packed-column SFC. The unretained endogenous material is adequately resolved from the analyte of interest and the APCI mass spectrum for boldenone shown at the bottom of Fig. 5 readily reveals the $(M+1)^+$ ion at m/z 287 which corroborates its molecular weight of 286 dalton. Forensic confirmation of boldenone in this sample would require structural information in addition to the retenion time and molecular weight information provided by this experiment (see below).

Fig. 6 shows the value of on-line SFC–API-MS–MS analysis of a sample containing the representative anabolic steroid, trenbolone[16]. The TIC and full-scan CID mass spectrum of trenbolone are shown from the analysis of 100 ng trenbolone injected under packed-column SFC–MS conditions identical to those described for Fig. 4. This steroid elutes in 1.2 min and with a collision energy of 70 eV produces the information-rich CID mass spectrum shown in the lower portion of Fig. 6. The m/z 271 ion represents the protonated molecular ion wich corroborates trenbolone's molecular weight of 270 dalton while the abundant fragment ions at m/z 83, 107, 133, 159 and 199 provide structurally important information to facilitate identification of trenbolone in unknown samples.

As a final example of high sensitivity and specificity combined with rapid sample analysis provided by packed-column SFC–MS–MS and APCI we present the data shown in Fig. 7. The upper portion of Fig. 7 shows the UV chromatograms obtained from the analysis of a bovine liver tissue which has been fortified with 20 and 30 ppb[a]

[a] Throughout this paper, the American billion (10^9) is meant.

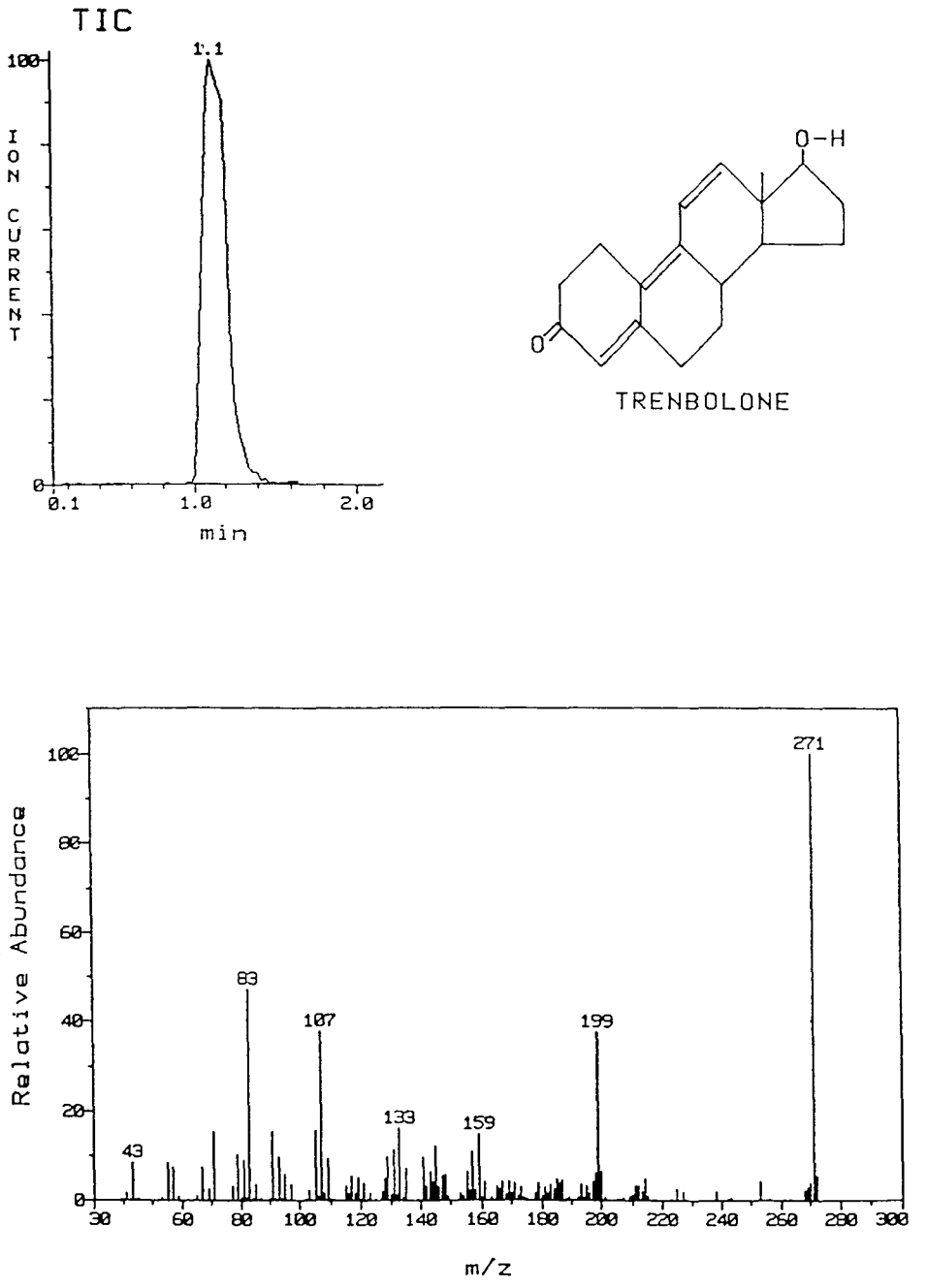

Fig. 6. Packed-column SFC–API-MS–MS analysis of a synthetic standard of the growth promotant, trenbolone (mol.wt. 270). The injected quantity of 100 ng trenbolone produced the TIC (upper portion) and full-scan CID (lower portion) mass spectrum, where the protonated molecular ion at *m/z* 271 was subjected to CID using argon as the collision gas with a collision energy of 70 eV (laboratory frame). SFC experimental conditions were the same as described for Fig. 4.

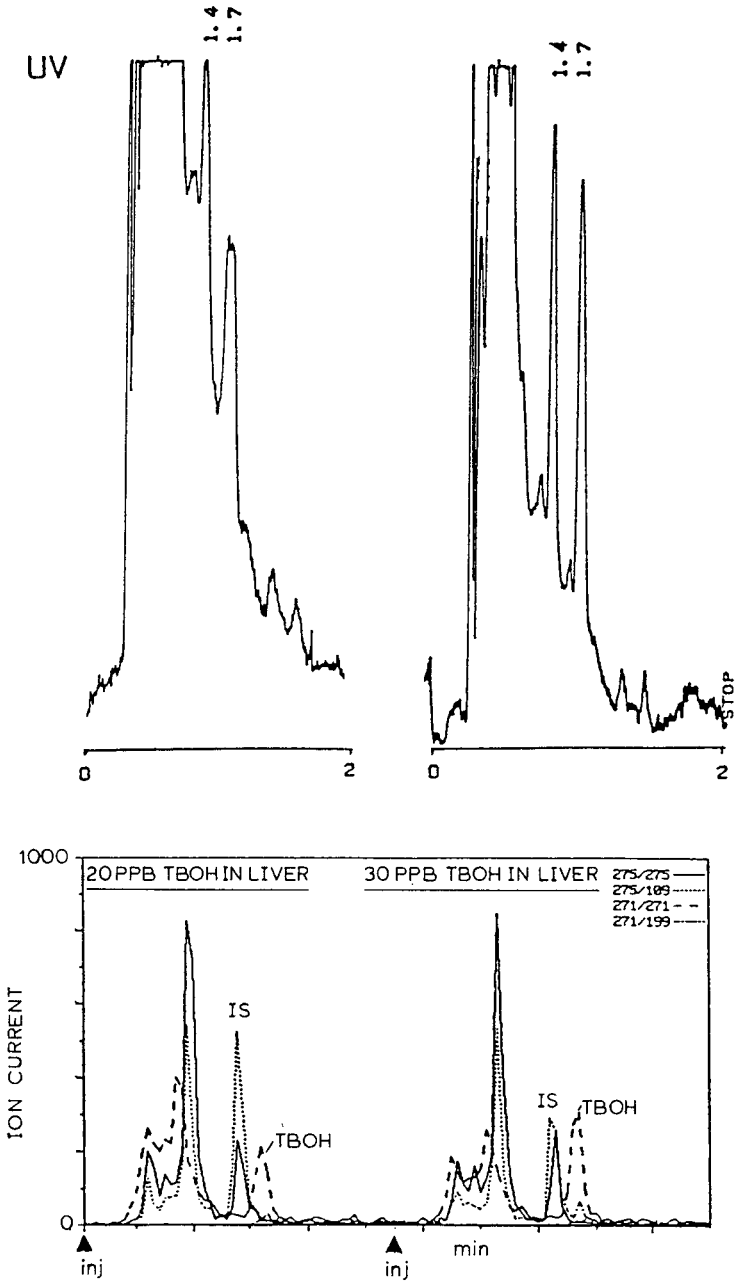

Fig. 7. Packed-column SFC–UV and SFC–API-MS–MS using the SRM mode to detect 20 and 30 ppb, respectively, of trenbolone (TBOH) in a bovine liver tissue homogenate. The internal standard (IS), 19-nortestosterone, was also present at 15 ppb in each sample extract. The experimental conditions were the same as described for Fig. 6.

trenbolone, respectively, and 15 ppb 19-nortestosterone as an internal standard. The liver tissue homogenate was subjected to successive three-phase liquid–liquid extraction followed by liquid–solid extraction as previously reported[16]. A 5-μl volume of the tissue extract was injected under the same conditions as for Fig. 4 and the API-MS–MS system operated in the MS–MS mode under SRM conditions[14]. The SRM experiment is analogous to targeted quantitative GC–selected-ion monitoring (SIM)-MS experiments. The SRM experiment, however, provides an additional element of selectivity due to the mixture analysis capability of tandem mass spectrometry[14].

The internal standard, 19-nortestosterone, and trenbolone are observed at 1.4 and 1.7 min, respectively in the UV chromatograms shown in the upper portion of Fig. 7. The high matrix background signal from the chemically complex tissue extract is evident in both UV chromatograms although both analytes are observed even in the 20-ppb fortified sample. In contrast, however, there is much less interference observed from this matrix in the total selected-ion current profiles shown for these two samples in the lower portion of Fig. 7. This is due to the reduced chemical noise obtained by "selecting" the protonated parent ions and appropriate fragment ions for the internal standard and the target analyte. In this way only these ions are mass-analyzed while all other ions are not observed. This explains the significantly reduced ion current observed in the region where the UV signal is rather high.

The total selected-ion current profiles shown for the 20- and 30-ppb fortified tissue samples shown in the lower portion of Fig. 7 clearly show the separation and detection of the two steroids. In this experiment only the parent ion and the CID fragment ion for each steroid are shown although additional appropriate fragment ions could have been used. These data clearly show differences between the two levels of trenbolone in these samples and could be used for combined qualitative and quantitative analysis of such samples[17]. Particularly evident is the relatively short analysis time under these packed-column SFC–MS–MS conditions where an injection could be made every 2 min. This would allow high sample throughput in suitably equipped laboratories with high sample volume requirements[18].

CONCLUSIONS

Packed-column SFC–MS and SFC–MS–MS analyses under APCI conditions are efficient and rapid means of analyzing chemically complex samples for the determination of unknown and targeted compounds. Sample volumes up to 20 μl may be readily injected onto the column and the elution of relatively polar analytes is not often a problem as can sometimes be the case with capillary SFC columns. The pinhole diaphragm orifice is rugged and commercially available. The corona discharge API system is simple and rugged with near universal response to most analytes. Finally, the API ion source operates at ambient temperature and readily handles packed-column fluid flow-rates up to 2 ml/min so the flexibility of this chromatographic technique may be utilized. It is also a very simple ion source without the cleaning and maintenance problems associated with conventional EI or CI ion sources. The high sample throughput capability of this system could offset the rather high cost of the tandem mass spectrometer system. We suggest that an API ion source with an associated mass analyzer could be the preferred way to accomplish SFC–MS using packed or capillary columns.

ACKNOWLEDGEMENTS

We thank Hewlett-Packard for the generous loan of the modified 1084B SFC system, and the New York State Racing and Wagering Board Equine Drug Testing and Toxicology Program, Sciex Inc., the United States Department of Agriculture Food Safety Inspection Service (FSIS), and the Eastman Kodak Company for financial support. We also thank E. D. Lee for part of the SFC–MS interface design, and Dr. G. A. Maylin, Director of the Laboratory, for his support of this work.

REFERENCES

1 R. D. Smith, H. T. Kalinoski and H. R. Udseth, *Mass Spectrometry Reviews*, Wiley, New York, 1987, p. 445.
2 J. C. Crowther and J. D. Henion, *Anal. Chem.*, 57 (1985) 2711.
3 P. O. Edlund and J. D. Henion, *J. Chromatogr. Sci.*, 27 (1989) 274.
4 D. W. Later, D. J. Bornhop, E. D. Lee, J. D. Henion and R. C. Woebolt, *LC Liq. Chromatogr. HPLC Mag.*, 5 (1987) 804.
5 E. C. Horning, D. I. Carroll, I. Dzidic, K. D. Haegel, M. G. Horning and R. N. Stillwell, *J. Chromatogr. Sci.*, 12 (1974) 725.
6 B. A. Thomson, J. V. Iribarne and P. J. Dziedic, *Anal. Chem.*, 54 (1982) 2219.
7 T. R. Covey, E. D. Lee, A. P. Bruins and J. D. Henion, *Anal. Chem.*, 58 (1986) 1451A.
8 C. M. Whitehouse, R. N. Dreyer, M. Yamashita and J. B. Fenn, *Anal. Chem.*, 57 (1985) 675.
9 M. Mann, C. K. Meng and J. B. Fenn, *Anal. Chem.*, 61 (1989) 1702.
10 A. P. Bruins, T. R. Covey and J. D. Henion, *Anal. Chem.*, 59 (1987) 2642.
11 J A. Olivares, N. T. Nguyen, C. R. Yonker and R. D. Smith, *Anal. Chem.*, 59 (1987) 1232.
12 J. B. French, W. R. Davidson, N. M. Reid and J. A. Buckly, in F. W. McLafferty (Editor), *Tandem Mass Spectrometry*, Wiley, New York, 1983, pp. 357–362.
13 J. D. Henion and T. Wachs, *Anal. Chem.*, 53 (1981) 1963.
14 K. Levsen, in F. W. McLafferty (Editor), *Tandem Mass Spectrometry*, Wiley, New York, 1983, p. 41–66.
15 L. O. G. Weidolf, T. M. P. Chichila and J. D. Henion, *J. Chromatogr.*, 433 (1988) 9.
16 S. S. Hsu and J. D. Henion, *J. Liq. Chromatogr.*, 10 (1987) 3033.
17 P. O. Edlund, L. Bowers, J. Henion and T. R. Covey, *J. Chromatogr.*, 497 (1989) 49–57.
18 T. R. Covey, E. D. Lee and J. D. Henion, *Anal. Chem.*, 58 (1986) 2453.

Journal of Chromatography, 511 (1990) 271–279
Elsevier Science Publishers B.V., Amsterdam

CHROM. 22 446

High-precision sampling of sub-nanogram, low-parts-per-billion solutes from liquids using the dynamic solvent effect

PETER J. APPS[a]
Institute for Chromatography, University of Pretoria, Pretoria 0002 (South Africa)
(First received September 26th, 1989; revised manuscript received March 13th, 1990)

ABSTRACT

The quantitative precision of dynamic solvent-effect sampling from solvent specimens is reported. For sub-nanogram amounts of a range of solutes at a concentration of $5{:}10^9$ the coefficients of variation of peak areas, peak percentage areas and peak-area ratios are consistently below 10%. The dynamic solvent effect allows high-precision sampling of much smaller amounts of solute than do alternative sampling methods.

INTRODUCTION

The dynamic solvent effect is a sampling technique for capillary gas–liquid chromatography which exploits the peculiar chromatographic properties of evaporating solvent films to accumulate quantitatively trace components from either liquid or gaseous specimens. During sampling volatiles are accumulated at the evaporating, upstream edge of a film of solvent held in dynamic equilibrium between evaporation and capillary rise in an axially perforated porous bed[1,2].

The dynamic solvent effect was developed to allow the quantitative analytical capability of the capillary column and its associated detectors to be fully realized for specimens where great dilution or restricted availability limit the total amount of each solute to a few nanograms. Such specimens are most commonly encountered in work on biological[3] or clinical problems.

Dynamic solvent-effect sampling can be applied to either liquid or gaseous specimens. Its quantitative performance with liquid specimens is reported here.

EXPERIMENTAL

Separations were carried out on a Varian 3700 gas chromatograph fitted with a dynamic solvent-effect inlet[2]. The column, produced in-house, was 25 m × 0.3 mm I.D. borosilicate glass, coated with 0.4 μm of methylsilicone. The initial temperature of

[a] Present address: Food Hygiene, Veterinary Research Institute, Onderstepoort 0110, South Africa.

0021-9673/90/$03.50

the inlet and column was 40°C, the inlet was ballistically heated to 220°C after 4 min or 3.5 min, depending on the solvent evaporation time of the concentrator, and the column temperature was programmed at 10°C min^{-1} to 250°C after 7 min, or at 5°C min^{-1} for the Grob mixture[4]. The carrier gas was hydrogen with a linear velocity of 50 cm s^{-1}. Flame ionization detection was used at a sensitivity of 10^{-11} A mV^{-1} and chromatograms were recorded on a Varian 4270 integrator with a full-scale deflection of 2 mV.

The system's qualitative performance was tested by sampling 100 μl of Grob mixture at a concentration of 1:10^8 (*ca.* 1 ng per peak) and 130 μl of a diagnostic test mixture for solvent-effect inlets[5] at a concentration of 5:10^9 (*ca.* 0.65 ng per peak).

The quantitative precision of dynamic solvent-effect sampling from a solvent matrix was tested by running five consecutive samples of the diagnostic test mixture on each of three dynamic solvent-effect concentrators. Pilot studies had already established that errors due to adsorption on containers and volumetric glassware exceeded those due to sampling by the dynamic solvent effect[6], so sampling was consequently carried out directly from a 10-cm^3 stock specimen of test mixture without measuring into other containers. The concentration of the test mixture was 5:10^9. Each sample was obtained by passing 10 cm^3 min^{-1} of palladium-cell-purified hydrogen through a dynamic solvent-effect concentrator dipped into the bulk specimen at 29.6°C. From calibrations of the detector response, based on split injections, *ca.* 0.65 ng of each component was present in each sample, which agreed with the consumption of solution for each sample, determined gravimetrically to be 130 μl.

Standard deviations of peak areas and peak percentage areas (the percentage of the sum of the solute peak areas contributed by a particular peak) were calculated from integrator reports from five consecutive runs, the relative standard deviation being the standard deviation divided by the mean, expressed as a percentage. Standard deviations and relative standard deviations were also calculated for the ratios of areas between pairs of peaks.

The linearity of peak area *vs.* specimen concentration was tested by sampling a series of progressively more dilute test mixture solutions on one concentrator. A 5-cm^3 volume of test mixture at a concentration of 2:10^7 was prepared in *n*-hexane. For each specimen *ca.* 0.5 cm^3 of solution was decanted into a holder that had been rinsed with the same solution to reduce its adsorptive activity. Each specimen was sampled for 10 min (130 μl) with a 10 cm^3 min^{-1} flow of palladium-cell-purified hydrogen at 29.6°C. The residue of the test mixture was then diluted to approximately the original volume with *n*-hexane, and another specimen was sampled and run. To minimize exposure of the test mixture to adsorptive glass surfaces, the amounts of solution and of added hexane at each stage were determined gravimetrically rather than volumetrically. This process was repeated until the smallest chromatographic peaks were *ca.* 200 counts in area (*ca.* 0.065 ng). Peak areas were plotted against calculated concentrations and the straight line giving the best, least-squares fit was calculated.

RESULTS

Except for slight adsorptive activity towards the alcohols of the two test mixtures and the strong base of the Grob mixture, the system was extremely inert (Figs. 1 and 2).

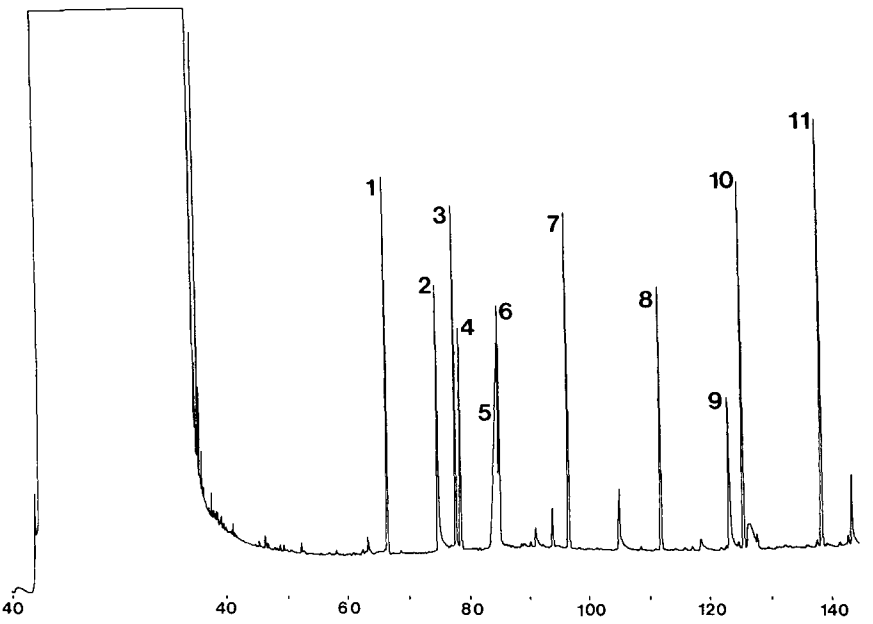

Fig. 1. Chromatogram from 100 μl of $1{:}10^8$ Grob mixture (*ca.* 1 ng per peak) sampled by the dynamic solvent effect and separated on a 25 m × 0.3 mm I.D. methylsilicone (0.4 μm) column. For analytical conditions, see text. Peaks: 1, *n*-decane; 2, *n*-octanol; 3, *n*-nonanal; 4, 2,6-dimethylphenol; 5, ethylhexanoic acid; 6, 2,6-dimethylaniline; 7, *n*-dodecane; 8, methyl decanoate; 9, dicyclohexylamine; 10, methyl undecanoate; 11, methyl dodecanoate. The abscissa is temperature (°C).

Despite the small amounts and dilute solutions involved, dynamic solvent-effect sampling achieved high precisions of peak areas, peak percentage areas and peak-area ratios for all components of the diagnostic test mixture. Except for the dimethylaniline peak, the relative standard deviations of the peak areas and percentage areas were always below 10% even when the results from the three concentrators were pooled. The relative standard deviations of the peak-area ratios were all below 10% (Tables I–VI).

For amounts per peak ranging from *ca.* $6 \cdot 10^{-11}$ g to $2.3 \cdot 10^{-8}$ g, over three orders of magnitude of specimen concentration, the relationship of peak area to specimen concentration was perfectly linear for all except the dimethylaniline and *n*-decanol peaks (Table VII).

DISCUSSION

The results presented here confirm those obtained earlier[6] with 2–3 ng per component at specimen concentrations of $1{:}10^8$.

The external standard method of quantification involves dividing the area of an experimental peak by the area of a peak obtained from an independently determined amount of the same compound[7]. Therefore, the variance of the calculated mass will be the sum of the variances of the peak area and of the estimate of the standard amount.

TABLE I

RELATIVE STANDARD DEVIATIONS OF PEAK AREAS AND PEAK PERCENTAGE AREAS FOR DYNAMIC SOLVENT-EFFECT SAMPLING OF 130 μl FROM A BULK 5:10^9 TEST MIXTURE IN *n*-HEXANE

n = 5 on each of three concentrators. Approximately 0.65 ng per compound.

Compound	*Relative standard deviation (%)*					
	Concentrator 1		*Concentrator 2*		*Concentrator 3*	
	Area	*% area*	*Area*	*% area*	*Area*	*% area*
n-Octane	1.46	1.27	2.70	2.33	2.86	0.87
n-Nonane	1.05	0.33	1.03	0.99	3.38	0.42
2,6-Dimethyl-4-heptanone	0.98	1.46	1.22	0.95	3.75	0.49
n-Decane	1.40	0.75	1.34	0.78	3.43	0.25
p-Cresol	2.75	1.85	0.47	1.87	3.56	0.57
Linalool	1.63	1.01	2.21	1.06	2.84	1.25
Dimethylaniline	2.54	1.90	2.72	2.69	6.12	5.45
n-Dodecane	0.60	0.58	2.47	1.06	3.57	0.26
n-Decanol	1.91	2.74	1.56	0.81	4.87	2.12
Methyl decanoate	0.69	0.39	2.38	1.90	4.11	0.67
n-Tetradecane	0.60	0.58	3.92	2.60	3.96	0.83
n-Pentadecane	1.17	0.81	4.56	3.99	3.48	0.78

TABLE II

COMPARISON OF MEAN PEAK AREAS OF EACH COMPONENT OF A 5:10^9 SOLVENT-MATRIX TEST MIXTURE SAMPLED FROM THE BULK ON EACH OF THREE DYNAMIC SOLVENT-EFFECT CONCENTRATORS AND OVERALL RELATIVE STANDARD DEVIATIONS (R.S.D.) OF PEAK AREAS FROM FIVE SAMPLES ON EACH OF THREE CONCENTRATORS

Compound	*Mean peak area (n = 5)*			*R.S.D. (%)*
	Concentrator 1	*Concentrator 2*	*Concentrator 3*	
n-Octane	3011	2811	2806	4.08
n-Nonane	3044	2786	2617	6.71
2,6-Dimethyl-4-heptanone	3116	2844	2645	7.25
n-Decane	2798	2530	2395	7.03
p-Cresol	3626	3045	3046	9.02
Linalool	2685	2466	2298	6.99
Dimethylaniline	3287	3005	2176	17.61
n-Dodecane	2851	2531	2386	8.07
n-Decanol	3013	2648	2758	6.33
Methyl decanoate	4388	3877	3592	8.96
n-Tetradecane	3265	2879	2651	9.39
n-Pentadecane	4288	3820	3511	9.05

TABLE III

AS TABLE II FOR MEAN PERCENTAGE PEAK AREAS

Compound	*Mean peak % area (n = 5)*			*R.S.D. (%)*
	Concentrator 1	*Concentrator 2*	*Concentrator 3*	
n-Octane	8.057	7.985	8.576	4.96
n-Nonane	7.867	7.904	7.966	1.44
2,6-Dimethyl-4-heptanone	8.009	8.069	8.046	1.07
n-Decane	7.190	7.179	7.286	1.22
p-Cresol	9.047	8.699	9.233	3.16
Linalool	6.917	6.941	6.991	1.49
Dimethylaniline	7.832	8.526	6.622	11.77
n-Dodecane	7.227	7.182	7.259	0.81
n-Decanol	7.852	7.514	8.389	5.41
Methyl decanoate	11.023	10.999	10.924	1.07
n-Tetradecane	8.173	8.165	8.063	1.91
n-Pentadecane	10.804	10.838	10.683	2.38

Internal standardization involves comparison of the areas of two peaks on the same chromatogram[8]; in this instance the relative standard deviations of peak-area ratios (Tables IV–VI) provide a direct measure of the highest available precision. If the dynamic solvent effect is used for sampling, the precision of both techniques will probably be limited by the variance of the estimate of the standard amounts rather than by sampling variations. A good linearity of peak area *vs.* concentration (Table VII) is desirable for both internal and external standardization.

The high precision of the peak-area ratios (Tables IV–VI), even between sub-nanogram amounts of compounds of different chemical character, is a feature of

TABLE IV

RELATIVE STANDARD DEVIATIONS (%) OF PEAK-AREA RATIOS FOR 130 μl OF 5:10^9 TEST MIXTURE SAMPLED BY THE DYNAMIC SOLVENT EFFECT USING CONCENTRATOR 1

Abbreviations in the column headings correspond to the compounds in the first column.

Peaks	C_8	C_9	*8-one*	C_{10}	*pCr*	*Lin*	*DMA*	C_{12}	*10-ol*	*Me-10*	C_{14}	C_{15}
n-Octane	–	1.27	1.41	1.98	2.49	2.03	1.54	1.19	2.91	1.51	1.59	1.91
n-Nonane			0.26	0.88	1.77	1.20	1.94	0.56	2.96	0.59	0.68	0.71
2,6-Dimethyl-4-heptanone				0.70	1.85	1.02	2.01	0.63	2.87	0.49	0.61	0.69
n-Decane					1.67	0.53	2.20	1.24	3.08	0.78	0.95	0.90
p-Cresol						1.82	2.03	2.28	4.55	2.11	2.26	1.93
Linalool							1.98	1.56	3.19	1.12	1.33	1.41
Dimethylaniline								2.24	4.10	2.27	2.46	2.57
n-Dodecane									2.47	0.54	0.48	0.84
n-Decanol										2.47	2.38	2.94
Methyl decanoate											0.24	0.69
n-Tetradecane												0.62
n-Pentadecane												–

TABLE V

AS TABLE IV, USING CONCENTRATOR 2

Peaks	C_8	C_9	*8-one*	C_{10}	*pCr*	*Lin*	*DMA*	C_{12}	*10-ol*	*Me-10*	C_{14}	C_{15}
n-Octane	–	1.99	1.73	2.09	2.09	2.72	3.65	2.54	3.09	2.78	3.93	5.54
n-Nonane			0.31	0.42	0.97	1.14	2.34	1.63	1.44	1.67	3.53	4.62
2,6-Dimethyl-4-heptanone				0.50	1.04	1.47	2.57	1.58	1.51	1.64	3.38	4.58
n-Decane					1.24	1.03	2.22	1.22	1.30	1.29	3.32	4.59
p-Cresol						2.10	2.65	2.38	2.19	2.46	4.28	5.28
Linalool							2.20	0.52	1.40	0.60	3.02	4.61
Dimethylaniline								2.46	2.83	2.64	4.93	6.01
n-Dodecane									1.57	0.45	2.73	4.53
n-Decanol										1.24	2.64	3.48
Methyl decanoate											2.45	4.14
n-Tetradecane												2.58
n-Pentadecane												–

dynamic solvent-effect sampling that has already proved to be valuable in the field of semiochemistry, where the biological properties of a mixture of volatiles depend on their relative concentrations[2].

The literature was surveyed for data on the quantitative performance of sampling systems designed to handle specimens similar to those used here. Disappointingly, quantitative precision is not an aspect of analytical performance that has received general attention[9]. Indeed, it was the exception, rather than the rule, that this type of data accompanied, or even followed, descriptions of sampling techniques. Even among those papers where precision was reported, its interpretation was confounded by a lack of information on the composition of the test specimens employed[10–14]. Studies for which test mixture composition and concentration were reported are presented in Table VIII.

A comparison of the data for the dynamic solvent effect in Tables I–VI with those from other systems in Table VIII reveals that the dynamic solvent effect yields

TABLE VI

AS TABLE IV, USING CONCENTRATOR 3

Peaks	C_8	C_9	*8-one*	C_{10}	*pCr*	*Lin*	*DMA*	C_{12}	*10-ol*	*Me-10*	C_{14}	C_{15}
n-Octane	–	0.98	1.26	1.24	1.14	1.83	6.07	1.15	2.38	1.64	1.71	1.06
n-Nonane			0.33	0.37	0.44	1.43	5.67	0.36	2.01	0.74	1.08	0.80
2,6-Dimethyl-4-heptanone				0.45	0.48	1.59	5.69	0.41	1.91	0.49	1.05	0.95
n-Decane					0.57	1.15	5.35	0.38	2.22	0.76	1.06	0.97
p-Cresol						1.57	5.87	0.64	1.74	0.64	0.98	0.84
Linalool							4.51	1.43	3.26	1.84	1.87	1.81
Dimethylaniline								5.57	7.40	5.82	5.81	6.05
n-Dodecane									2.05	0.65	0.86	0.72
n-Decanol										1.66	1.69	1.74
Methyl decanoate											0.79	1.00
n-Tetradecane												0.68
n-Pentadecane												–

TABLE VII

COEFFICIENTS OF DETERMINATION (r^2) OF THE LINES OF BEST LEAST-SQUARES FIT FOR PEAK AREA *VS.* SPECIMEN CONCENTRATION WHEN TEST MIXTURES WITH CONCENTRATIONS BETWEEN $2{:}10^7$ AND $2.8{:}10^{10}$ WERE SAMPLED BY THE DYNAMIC SOLVENT EFFECT

Compound	r^2	*Compound*	r^2
n-Octane	1.000	2,6-Dimethylaniline	0.999
n-Nonane	1.000	*n*-Dodecane	1.000
2,6-Dimethyl-4-heptanone	1.000	*n*-Decanol	0.995
n-Decane	1.000	Methyl decanoate	1.000
p-Cresol	1.000	*n*-Tetradecane	1.000
Linalool	1.000	*n*-Pentadecane	1.000

a precision at least as high as that provided by other sampling methods. The marked superiority of the dynamic solvent effect lies in its ability to generate such precision with amounts of test solute up to three orders of magnitude smaller than those employed elsewhere, with dilutions up to seven orders of magnitude greater, and with a wide range of test solutes considerably less chromatographically tractable than the hydrocarbons and halocarbons more commonly employed. The only work involving

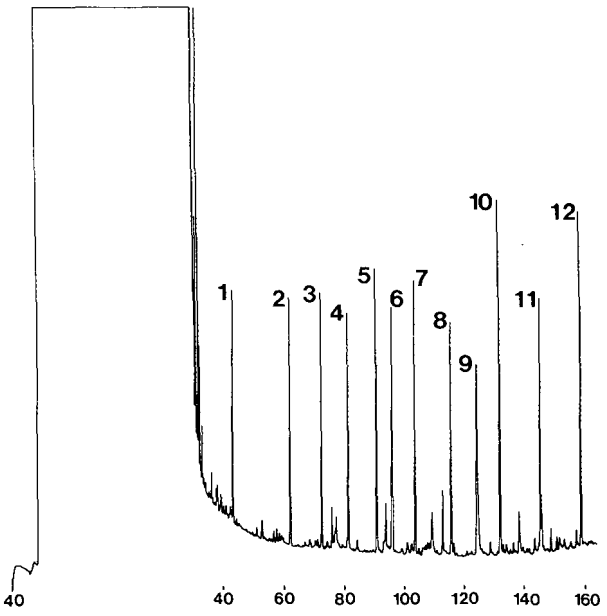

Fig. 2. Chromatogram from 130 μl of $5{:}10^9$ diagnostic test mixture (*ca.* 0.65 ng per peak) sampled by the dynamic solvent effect and separated on a 25 m × 0.3 mm I.D. methylsilicone (0.4 μm) column. For analytical conditions, see text. Peaks: 1, *n*-octane; 2, *n*-nonane; 3, 2,6-dimethyl-4-heptanone; 4, *n*-decane; 5, *p*-cresol; 6, linalool; 7, 2,6-dimethylaniline; 8, *n*-dodecane; 9, *n*-decanol; 10, methyl decanoate; 11, *n*-tetradecane; 12, *n*-pentadecane. The abscissa is temperature (°C).

TABLE VIII

QUANTITATIVE PERFORMANCE OF A VARIETY OF SAMPLING METHODS FOR THE GAS CHROMATOGRAPHIC DETERMINATION OF TRACE COMPONENTS IN SOLVENTS

Techniques are abbreviated as follows: ads = adsorption; ct = cold trapping; ECD = electron-capture detection; FID = flame ionization detection; MS = mass spectrometric detection; NPD = nitrogen–phosphorus detection; oc = on-column injection; ptv = programmed-temperature vaporizer; sl = splitless injection; sp = splitting; TIM = total ion monitoring; vi = valve inlet.

Solutes[a]	*Technique*	*Concentration or mass*	*R.S.D. (%)*	*Ref.*
Alkanes	ptv, FID	10%	0.2–14	16
C_{18}–C_{32} alkanes	ptv, FID	250 ng : 20 μl	0.9–5.2	17
Cl compounds	ptv, ECD	1 ng : 1 μl	2.4–7.0	17
P pesticides	ptv, NPD	1 ng : 5 μl	1.0–2.1	17
Mixed	9c, sl, FID	10–40 ng : 1 μl	0.5–4.2	18
Halocarbons	ads, ct, TIM	200 ng : 1 μl	3–44.4	19
Varian mix	vi, oc, FID	400 ng : 1 μl	0.05–1.9	20
C_8–C_{10} alkanes	vi, ct, sp, FID	500 ng : 0.5 μl	3–6	21
C_{10}–C_{28} alkanes	ptv, FID	240 ng : 0.2 μl	0.7–5.7	22
C_{10}–C_{18} alkanes	oc, FID	44 ng : 0.4 μl	0.5–1.2	23
Alkanes	sp, FID	160–1600 ng	1.7–33.1	24
Alkanes	sp, ptv, FID	160–1600 ng	0.9–6.23	24
Cl pesticides	vi, ECD	16 ppt	4.4	15
Cl pesticides	vi, ECD	40 ppt	2.2–9.5	16
PCBs, PBBs	ads, ct, TIM	75 ng : 100 μl	10–19	25
C_{10}–C_{32} alkanes	oc/sl, FID	0.002%	2–3.1	26
C_{10}–C_{32} alkanes	sp, FID	0.1%	1.5	26
PAHs	ads, ct, FID	0.4–1 μg : 100 μl	1.2 ± 0.6	27
n-Eicosane	oc, FID	15 ng : 1 μl	1.6–4.8	28
C_9–C_{36} alkanes	oc, FID	3.6–10.3%	0.4–9.4	29
Phenols, PAHs	sp, MS	30 ng : 1 μl	13–41	30
C_{18}–C_{32} alkanes	sp/sl, FID	250 ng : 20 μl	0.8–5.2	31
C_{10}–C_{32}	sl/oc, FID	2 : 10^5, 0.2–0.5 μl	0.1–1.5	32
Alkanes	ptv, FID	100 ng : 2 μl	0.5–17.8	33
Ethyl esters	ptv, FID	100 ng : 2 μl	0.8–46.6	33
n-Alcohols	ptv, FID	100 ng : 2 μl	0.5–24.0	33
Carboxylic acids	ptv, FID	100 ng : 2 μl	0.5–19.9	33

[a] PCBs = Polychlorinated biphenyls; PBBs = polybrominated biphenyls; PAHs = polynuclear aromatic hydrocarbons.

comparable specimen volumes and smaller amounts of solute was that by Zlatkis *et al.*[15] in which the specific and highly sensitive electron-capture detector was used.

The linearity of peak area *vs.* specimen concentration for dynamic solvent-effect sampling matches or exceeds that of any other system and should prove adequate for all applied work.

ACKNOWLEDGEMENTS

Funding for this work was provided by grants to Professor V. Pretorius, Director of the Institute for Chromatography. I also thank Egmont Rohwer and Willie Viljoen, and Amanda de Klerk and David Masemula who made the column.

REFERENCES

1 P. J. Apps and V. Pretorius, *J. Chromatogr.*, 471 (1989) 81.
2 P. J. Apps, V. Pretorius, K. H. Lawson, E. R. Rohwer, M. R. Centner, H. W. Viljoen and G. Hulse, *J. High Resolut. Chromatogr. Chromatogr. Commun.*, 10 (1987) 122.
3 P. J. Apps, *Ph.D. Thesis*, University of Pretoria, 1988, pp. 189–288.
4 K. Grob, G. Grob and K. Grob, *J. Chromatogr.*, 156 (1978) 1.
5 P. J. Apps, *Ph.D. Thesis*, University of Pretoria, 1988, pp. 44–47.
6 P. J. Apps, *Ph.D. Thesis*, University of Pretoria, 1988, pp. 110–124 and 129–130.
7 M. L. Lee, F. J. Yang and K. D. Bartle, *Open Tubular Column Gas Chromatography: Theory and Practice*, Wiley, New York, 1984, p. 224.
8 M. L. Lee, F. J. Yang and K. D. Bartle, *Open Tubular Column Gas Chromatography: Theory and Practice*, Wiley, New York, 1984, pp. 222–223.
9 P. Werkhoff and W. Bretschneider, *J. Chromatogr.*, 405 (1987) 87.
10 G. Schomburg, H. Husmann and R. Rittmann, *J. Chromatogr.*, 204 (1981) 85.
11 L. V. Haynes and A. R. Steimie, *J. High Resolut. Chromatogr. Chromatogr. Commun.*, 10 (1987) 441.
12 K. Grob, *Classical Split and Splitless Injection in Capillary Gas Chromatography*, Hüthig, Heidelberg, 1985, pp. 206 and 249.
13 K. Grob and Z. Li, *J. High Resolut. Chromatogr. Chromatogr. Commun.*, 11 (1988) 626.
14 F. J. Yang, A. C. Brown and S. P. Cram, *J. Chromatogr.*, 158 (1978) 91.
15 A. Zlatkis, L. Ghaouli, F. S. Wang and H. Shanfield, *J. High Resolut. Chromatogr. Chromatogr. Commun.*, 7 (1984) 370.
16 E. Loyola, M. Herriaz, G. Reglero and P. Martin-Alvarez, *J. Chromatogr.*, 398 (1987) 53.
17 W. Vogt and K. Jacob, in P. Sandra (Editor) *Sample Introduction in Capillary Gas Chromatography*, Hüthig, Heidelberg, 1985, p. 99.
18 R. P. Snell, J. W. Danielson and G. S. Oxborrow, *J. Chromatogr. Sci.*, 25 (1987) 225.
19 J. F. Pankow, *J. High Resolut. Chromatogr. Chromatogr. Commun.*, 6 (1983) 292.
20 D. H. Steele and D. L. Vassilaros, *J. High Resolut. Chromatogr. Chromatogr. Commun.*, 6 (1983) 561.
21 S. Jacobsson and S. Berg, *J. High Resolut. Chromatogr. Chromatogr. Commun.*, 5 (1982) 236.
22 F. Poy, S. Visani and F. Terrosi, *J. High Resolut. Chromatogr. Chromatogr. Commun.*, 5 (1982) 355.
23 G. Schomburg, H. Husmann and F. Schulz, *J. High Resolut. Chromatogr. Chromatogr. Commun.*, 5 (1982) 565.
24 G. Reglero, M. Herriaz and M. D. Cabezudo, *Chromatographia*, 22 (1986) 333.
25 K. M. Hart and J. F. Pankow, *J. High Resolut. Chromatogr. Chromatogr. Commun.*, 10 (1987) 484.
26 G. Schomburg, H. Husmann, H. Behlau and F. Schulz, in J. Rijks (Editor), *Proceedings of the Vth International Symposium on Capillary Chromatography*, Elsevier, Amsterdam. 1983, p. 280.
27 P. Kirschmer and M. Oehme, *J. High Resolut. Chromatogr. Chromatogr. Commun.*, 7 (1984) 306.
28 M. W. Ogden and H. M. McNair, *J. High Resolut. Chromatogr. Chromatogr. Commun.*, 6 (1983) 550.
29 A. T. G. Steverink and H. Steunenberg, *J. High Resolut. Chromatogr. Chromatogr. Commun.*, 6 (1983) 623.
30 B. N. Colby, P. W. Ryan and J. E. Wilkinson, *J. High Resolut. Chromatogr. Chromatogr. Commun.*, 6 (1983) 72.
31 W. Vogt, K. Jacob, A.-B. Ohnesorge and H. W. Obwexer, *Adv. Chromatogr.*, 114 (1979) 225.
32 G. Schomburg, in P. Sandra (Editor), *Sample Introduction in Capillary Gas Chromatography*, Hüthig, Heidelberg, 1985, p. 55.
33 M. Herriaz, G. Reglero, E. Loyola and T. Herriaz, *J. High Resolut. Chromatogr. Chromatogr. Commun.*, 10 (1987) 598.

Journal of Chromatography, 511 (1990) 281–290
Elsevier Science Publishers B.V., Amsterdam

CHROM. 22 443

Analyses of polychlorinated dibenzo-*p*-dioxins and dibenzofurans and precursors in fly ash samples collected at different points in post-combustion zone of Japanese machida incinerator

K. P. NAIKWADI and F. W. KARASEK*
Department of Chemistry, University of Waterloo, Waterloo, Ontario N2L 3G1 (Canada)
and
H. HATANO[a]
Department of Chemistry, Kyoto University, Kyoto 606 (Japan)
(Received December 14th, 1989)

ABSTRACT

Several samples collected at the post-combustion zone of the Machida incinerator in Japan were analyzed for polychlorinated dibenzo-*p*-dioxins (PCDDs), polychlorinated dibenzofurans (PCDFs), polychlorinated phenols (PCPs) and polychlorinated benzenes (PCBEs). All samples show lower levels of PCDDs and PCDFs in comparison to the levels observed in other samples from various incinerators around the world. The Machida incinerator in Japan shows ten times lower levels of PCDDS/PCDFs than the Ontario incinerator in Canada. Analyses of fly ash samples collected at different points in the post-combustion zone shows higher levels of PCDDs/PCDFs at points near the stack, and decreasing towards the combustion zone. That trend indicates the formation of PCDs/PCDFs in the electrostatic precipitator by catalytic activity of fly ash in addition to their probable formation in the incinerator furnace. Variations in normal operating conditions have no or very little effect on the amount of PCDDs/PCDFs formed. Municipal solid waste in Japan has been separated into combustible and non-combustible materials. Only the combustible materials were incinerated in the Machida incinerator, which is a fluidized bed design with CaO injection into the bed.

INTRODUCTION

A considerable volume of information has been accumulated on polychlorinated dibenzo-*p*-dioxins (PCDDs) and dibenzofurans (PCDFs) in the last two decades. The

[a] Visiting Professor at University of Waterloo during this study.

0021-9673/90/$03.50

chemistry and toxicology of these compounds has been summarized in several reviews and texts[1-10]. The main sources currently of these highly toxic chemicals are herbicides[11], abandoned dump sites of industrial wastes[12] and products of municipal and industrial waste combustion[13,14].

Several publications show that the formation of PCDDs/PCDFs occurs in all municipal incinerators around the world[15-19]. However, there are considerable differences in the levels of PCDDs/PCDFs detected in the fly ash samples from the various incinerators. The formation of PCDDs/PCDFs in municipal solid waste (MSW) incineration has been considered to be a universal phenomenon and all incinerators pose a threat to a clean environment. But this understanding should be reassessed because under certain conditions some incinerators show negligible amounts of PCDDs/PCDFs in the fly ash and fall within the guidelines of environmental agencies. There are several benefits resulting from incineration of municipal waste such as reduction of the need for land filling and the generation of electricity and heat. Since the design and operational conditions of incinerators vary, it is important to analyze the fly ash from different incinerators and determine the operational conditions and factors involved in the formation of PCDDs/PCDFs that can eventually result in safe operation of incinerator with minimum environmental risks from PCDDs/PCDFs.

Work in our laboratories and others has established that the formation of PCDDs/PCDFs occurs by catalytic activity of fly ash[20-27]. Our laboratory has also been involved in analysis of fly ash samples from the different incinerators around the world for more than a decade[28-33]. The results revealed that the lower amounts of native PCDDs/PCDFs were detected in the fly ash sampes from the incinerator at Machida, Japan. Hence, we decided to explore in detail the effect of incinerator operation conditions and treatment of garbage prior to incineration on the formation of PCDDs/PCDFs as well as on the formation of such precursors as polychlorinated benzenes (PCBEs) and polychlorinated phenols (PCPs) in the Machida incinerator. Fly ash samples collected at different points in the post-combustion zone were analyzed to determine the levels of PCDDs/PCDFs at different points. The results from laboratory tests of catalytic activity of fly ash at different temperatures, and amounts of PCDDs/PCDFs detected in fly ash samples collected at different points and temperatures in the post-combustion zone can provide the information for postulation of possible mechanisms of formation PCDDs/PCDFs.

EXPERIMENTAL

Sample collection

Fifteen different fly ash samples were obtained from the Machida incinerator (Japan). Eight samples were collected at the post-combustion zone after electrostatic precipitation (point T in Fig. 1). Another two sets of samples (three each, B1, B2, B3 and C1, C2, C3) were collected at points X, Y and Z simultaneously.

Sample extraction

A 40–60-g portion of fly ash from each sample was separately soxhlet extracted using 350 ml of benzene for 48 h. The fly ash extract was then concentrated to 10 ml by rotary evaporation under aspirator vacuum and then transferred to a 25-ml pear

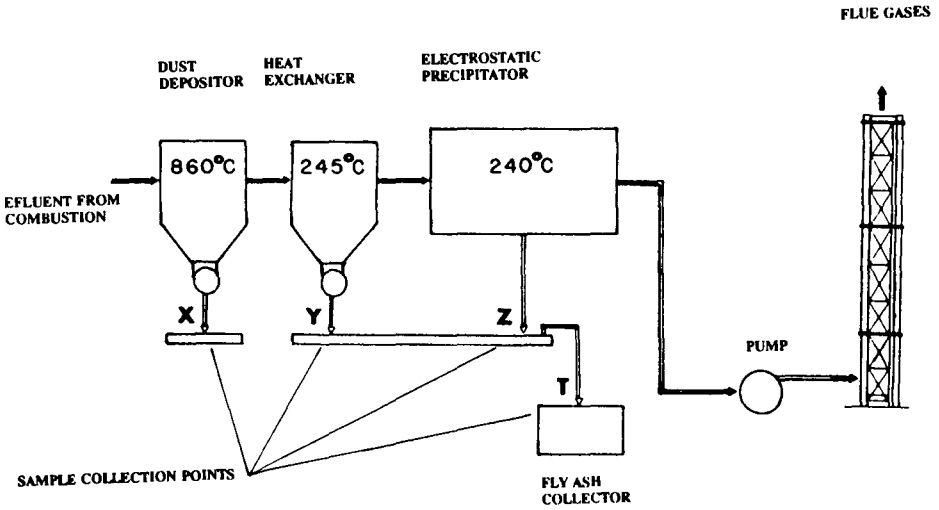

Fig. 1. Post-combustion zone of the Machida incinerator.

shaped flask and reduced to 1 ml by further rotary evaporation, then transferred to a 1-ml Reacti-vial. A final concentration of 150 μl was achieved by blowing a slow stream of high-purity nitrogen across the top of the vial. Exactly the same procedure was used for extraction and concentration of all fifteen samples.

Gas chromatographic (GC) and GC–mass spectrometric (MS) analysis

To estimate the concentration of organic compounds all samples were analyzed on a Hewlett-Packard HP-5880A gas chromatograph equipped with a flame ionization detector and a cool on-column injector. A 30 m × 0.32 mm I.D. DB-5 fused-silica capillary column (J & W Scientific, Rancho Cordova, CA, U.S.A.) was used.

The GC–MS system used was a Hewlett-Packard HP-5887A system equipped with dual [electron impact (EI) and chemical ionization (CI)] ion source and HP-1000 data system. Quantitation of PCBEs, PCPs, PCDDs and PCDFs and PCDFs was carried out using the GC–MS in the selected ion monitoring (SIM) mode. Qualitative identification of compounds in all samples was carried out using GC–MS in electron impact linear (EILIN) mode and probability base matching (PBM) library search of mass spectra for the peaks in total ion current trace (TIC) bases on 70 000 reference mass spectra. Total organic matter in each sample was estimated by using a standard mixture containing aliphatic hydrocarbons, aromatic hydrocarbons, chlorobenzenes, chlorophenols, PCDD and PCDF components. Average response factor area counts per nanogram was used to estimate the total organic matter.

GC conditions used were: injector temperature 50°C; initial temperature 80°C; program rate 4°C/min, to 160°C; then programmed to 300°C at 5°C/min, final time 10 min. The standard mixture used for quantitation of PCDDs, PCDFs, PCBEs and PCPs contains one isomer each of tetra-, penta-, hexa-, hepta- and octachloro-dibenzodioxins and dibenzofurans as well as standard mixture of tetra- to hexa-

chlorobenzenes and tetra- to pentachlorophenols. Three isotope ions (M, M + 2, M + 4 or M + 6) were monitored for tetra- to octachlorodibenzo-*p*-dioxins and dibenzofurans, tri- to hexachlorobenzenes and tri- to pentachlorophenols using GC–EISIM-MS.

Identification of compounds was confirmed using the following criteria: (1) The mass chromatograhic peaks must fall within a retention time "window" established for a specific class of isomers. (2) The mass chromatographic peaks produced by the component must exhibit the appropriate intensities for at least two major ions characteristic of the specific class being monitored. (3) The signal-to-noise ratio should be greater than 3.

Initially the retention windows were determined by using a mixture of PCDDs/PCDFs containing all possible isomers in tetra to octa congeners. For PCBEs and PCPs a single retention window was used where tri- to hexachlorobenzenes and tri- to pentachlorophenols were eluted.

RESULTS AND DISCUSSION

The amount of PCDDs, PCDFs, PCBEs and PCPs present in the eight fly ash samples from the Machida incinerator collected on eight different consecutive days exactly 24 h apart are shown in Table I. The results of the eight samples show that hexa- to octachlorodibenzodioxins and dibenzofurans are present in all samples. However, tetra- and pentachlorinated isomers are either not observed or are in the very low levels of 0.1 to 9 ng/g of fly ash in most of the samples. It should be noted that the levels of the relatively more toxic tetra and penta isomers as well as other PCDD and PCDF isomers in all these samples are extremely low as compared to the samples from other incinerators[20]. Even though the levels of PCDDs and PCDFs in all eight samples are low they are not uniform; sample 7 shows lowest amounts while sample 4 shows the highest levels. A general trend of an increase in the amount of PCDDs and PCDFs from tetra to octa isomers is observed. A comparison of the operating conditions (Table II) during sampling and the PCDDs and PCDFs detected at that time shows no correlation. From this observation it may be concluded that the amount of PCDDs and PCDFs formed depends on some other factors in the incinerators and small variation in normal operating conditions do not have significant effect on PCDDs/PCDFs formed.

The garbage treatment prior to incineration at Machida is different from other incinerators studied. Most of the solids, metallic materials and some plastics are separated from the combustible materials such as paper, wood and household refuse at the Machida incinerator. This may be significant with respect to dioxin formation. One of the mechanisms proposed for the formation of PCDDs and PCDFs is by reactions of molecular precursor species that are present during incineration, resulting in surface catalyzed synthesis of PCDDs/PCDFs on the fly ash via rearrangement, free radical condensation, dechlorination, dehydrogenation, trans-chlorination, isomerization and other similar molecular reactions[12]. From the reaction mechanisms established in organic chemistry, it can be presumed that all above said reactions can occur due to presence of different kinds of metal/metal oxides, inorganic halides and hydroxides formed in the incineration process. Inorganic halides and hydroxides can form in incineration process at high temperatures from traces of mineral acid, moisture and the

TABLE I

AMOUNTS OF PCDDs, PCDFs, PCBEs AND PCPs (ng/g FLY ASH) DETECTED IN MACHIDA FLY ASH SAMPLES

CDD = Chlorodibenzo-*p*-dioxin; CDF = chlorodibenzofuran; CBE = chlorobenzene; CP = chlorophenol.

Compound	*Sample numbers*							
	1	*2*	*3*	*4*	*5*	*6*	*7*	*8*
Dioxins								
Tetra-CDD	ND[a]	ND	0.4	2	ND	0.2	0.6	ND
Penta-CDD	4	ND	2	9	ND	0.7	1	1
Hexa-CDD	21	5	12	38	5	5	3	8
Hepta-CDD	49	13	26	77	18	14	5	29
Octa-CDD	89	19	41	171	37	36	11	56
Total	163	37	81	297	60	55.9	20.6	82
Furans								
Tetra-CDF	2	ND	2	9	0.6	0.5	0.7	1
Penta-CDF	11	5	7	37	4	2	2	5
Hexa-CDF	23	8	11	75	11	7	3	13
Hepta-CDF	62	15	36	177	35	18	12	32
Octa-CDF	87	13	41	181	32	23	9	33
Total	185	41	97	469	82.6	50.5	26.7	84
Chlorobenzenes								
Tri-CBE	4	2	5	28	3	3	2	4
Tetra-CBE	24	17	35	163	15	13	11	16
Penta-CBE	104	44	87	379	524	41	23	53
Hexa-CBE	124	25	71	284	49	40	17	47
Total	252	88	198	854	591	97	53	120
Chlorophenols								
Tri-CP	3	1	2	ND	ND	ND	ND	ND
Tetra-CP	10	4	3	38	1	0.6	0.6	0.3
Penta-CP	11	7	5	149	2	1	ND	0.3
Total	24	12	10	187	3	1,.6	0.6	0.6

[a] ND = Not detected.

small amounts of metals present in garbage.. These compounds could constitute catalysts on the surface of the fly ash produced to enhance the formation of PCDDs/PCDFs. Most of the metallic material is separated in the Machida incinerator prior to incineration, this fact could be one of the major reasons that Machida fly ash shows lower levels of PCDDs and PCDFs than other incinerators.

The amount of PCDDs, PCDFs and the precursors PCBEs and PCPs detected in the eight samples is shown in Table I. There is general trend in all samples where the amount of chlorinated isomers increases with increase in degree of chlorination. The amount of PCBEs detected in all samples is more than four times larger than that of PCPs. The total amount of PCDDs/PCDFs detected in a given sample is greater than the total amount of PCBEs (or sum of PCBEs and PCPs) present in that sample. From the total amount of PCDDs and PCDFs in a given sample as compared to that of total amount of PCBEs and PCPs, it seems that there is a definite correlation between high

TABLE II

INCINERATOR OPERATION CONDITIONS DURING SAMPLE COLLECTION AT MACHIDA

A and B are effluent trains.

Sample	*Garbage megatons/h*	*Dry air flow Nm^3/ton*	*Furnace temperature (°C)*	*Heat generated (kcal/kg)*
1	5.7	10138 (A) 12700 (B)	886	1670
2	5.7	11241 (A) 13136 (B)	835	1620
3	5.7	11265 (A) 13030 (B)	846	1730
4	4.4	13673 (A) 13405 (B)	883	2030
5	4.8	11182 (A) 13432 (B)	903	1920
6	4	13062 (A) 9393 (B)	926	2090
7	3.6	12895 (A) 10010 (B)	825	2260
8	4.2	10967 (A) 13467 (B)	920	2150

levels of PCBEs/PCPs and high levels of PCDDs and PCDFs. From laboratory experiments it is known that chlorophenols can be formed from chlorobenzenes which are precursors in the formation of PCDDs and PCDFs[6]. The reaction route in Fig. 2, shows the formation of PCDDs and PCDFs from PCBEs and PCPs.

The amount of chlorobenzenes formed and their conversions into chlorophenols and finally into PCDDs will depend on the temperature and the presence and amount of catalyst. If reaction I is slower than II, then there will be a lesser amount of PCPs than PCBEs. Since PCDDs and PCDFs are more stable than the chlorobenzenes and chlorophenols, reactions I and II proceed in a forward direction and result in an equal or higher amount of PCDDs and PCDFs formation to that of total PCBEs/PCPs. This is evident from the amount of PCBEs, PCPs, PCDDs and PCDFs observed in samples

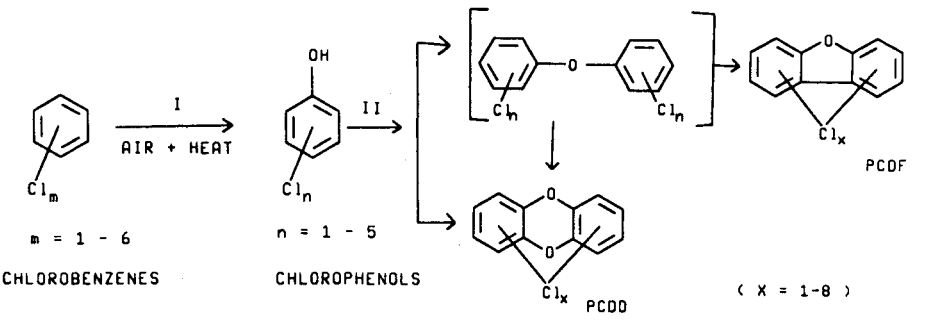

Fig. 2. Possible reaction scheme showing the formation of PCDDs and PCDFs from chlorobenzenes and chlorophenols.

1–8. Although this study is limited to only highly chlorinated benzenes, phenols dibenzodioxins and dibenzofurans, the results do give strong indication that support the surface catalytic mechanism and the formation of PCDDs and PCDFs during incineration of municipal garbage. This mechanism has been proved in laboratory experiments using fly ash and various precursors under various conditions. Attempts to correlate the amount of PCBEs, PCPs, PCDDs and PCDFs formed with that of incinerator operational conditions (Table II) such as amount of garbage, dry air flow, temperature profiles heat generated and dust absorbed during each sampling period were not conclusive.

Incineration processes are very complicated and analysis of fly ash collected at different points in the post-combustion effluent pathways has not been done. Present knowledge of the presence of PCDDs and PCDFs in fly ash is mainly based on the fly

TABLE III

AMOUNTS OF PCDDs, PCDFs, PCBEs AND PCPs (ng/g FLY ASH) DETECTED IN FLY ASH SAMPLES COLLECTED AT DIFFERENT POINTS IN POST-COMBUSTION ZONE OF MACHIDA INCINERATOR

CDD = Chlorodibenzo-*p*-dioxin; CDF = chlorodibenzofuran; CBE = chlorobenzene; CP = chlorophenol.

Compound	*Samples*					
	B1	*B2*	*B3*	*C1*	*C2*	*C3*
Dioxins						
Tetra-CDD	ND[a]	0.1	ND	ND	0.1	ND
Penta-CDD	ND	0.1	ND	ND	ND	ND
Hexa-CDD	ND	0.5	2	ND	0.6	1
Hepta-CDD	ND	0.5	7	ND	0.6	4
Octa-CDD	0.1	0.5	15	ND	0.7	10
Total	0.1	1.7	24	–	2	15
Furans						
Tetra-CDF	ND	0.2	0.3	ND	0.2	0.2
Penta-CDF	ND	0.5	3	ND	0.5	2
Hexa-CDF	ND	0.7	6	ND	0.9	6
Hepta-CDF	ND	0.8	14	ND	1	11
Octa-CDF	0.1	0.5	14	ND	0.6	10
Total	0.1	2.7	37.3	–	3.2	28.2
Chlorobenzenes						
Tri-CBE	2	15	2	1	14	1
Tetra-CBE	0.1	30	4	0.1	24	7
Penta-CBE	0.1	22	12	0.2	22	21
Hexa-CBE	0.1	5	9	0.1	5	13
Total	2.3	72	27	1,4	65	42
Chlorophenols						
Tri-CP	ND	2	2	ND	0.6	0.7
Tetra-CP	ND	1	2	ND	0.6	0.7
Penta-CP	0.1	4	9	0.1	2	3
Total	0.1	7	13	0.1	3.2	4.4

[a] ND = Not detected.

ash collected at the electrostatic precipitator. In our study fly ash was also collected at three different points in the post-combustion zone as shown in Fig. 1. The temperature at position X is higher (850°C) while it is decreased at points Y (245°C) and Z (240°C). The results of quantitation of two sets of samples (Set No. 1: B1, B2 and B3; and Set No. 2: C1, C2 and C3) collected at three different places (X, Y, Z, respectively) are shown in Table III.

For both sets of samples the total amount of PCBEs is in the order of B2 > B3 > B1 (set 1) and C2 > C3 > C1 (set 2). The amount of PCDDs and PCDFs found is in the order of B3 > B2 > B1 and C3 > C2 > C1. The smaller amount of PCBEs, PCDDs and PCDDs and PCDFs in the samples collected at point X could be related to the high temperature at this point. While the difference in amounts of PCBEs and PCDDs/PCDFs in samples collected at point X and Y is more than ten-fold, this difference decreased to less than two-fold in samples collected at point Z. These results can be explained based on the catalytic surface activity of fly ash particles. At point X the precursors concentrations (PCBEs and PCPs) are high, because they are not converted into PCDDs and PCDFs. At point Z, because of probably high catalytic activity due to optimum conditions these precursors are converted to PCDDs and PCDFs. The final result is an increase in PCDDs and PCDFs and a decrease in PCBEs in samples collected at point Z. The amount of PCBEs found in samples C3 and B3 as compared to total PCDDs and PCDFs in these samples are well in agreement with the results of samples 1–8 collected at the same point. This tends to indicate that the most toxic PCDDs and PCDFs congeners in addition to forming in the actual combustion

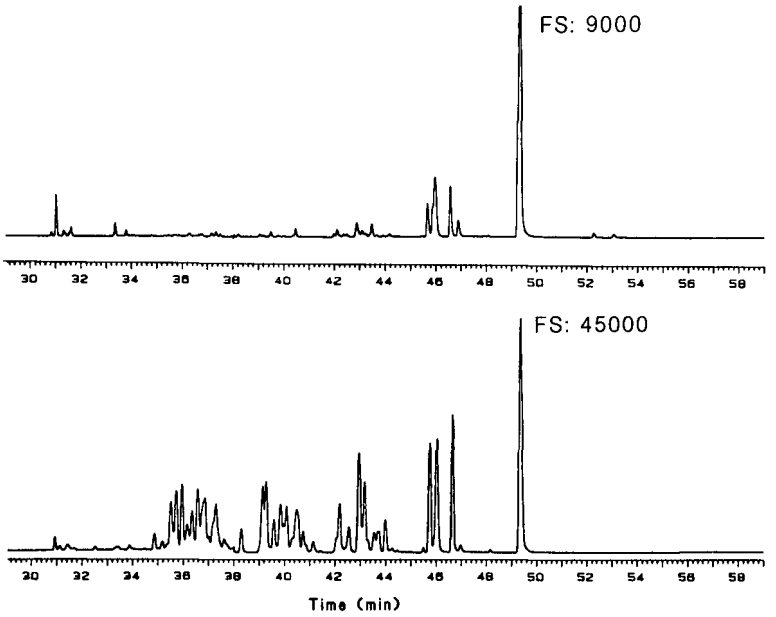

Fig. 3. Reconstructed added mass chromatograms obtained by analyses of (top) Machida sample No. 6 and (bottom) Ontario fly ash under identical GC–MS conditions. For GC conditions see experimental section. FS = full scale.

zones are also forming by surface catalytic activity on fine fly ash particles in the post-combustion zone and in the electrostatic precipitation region.

To determine the correlation of total organic matter (TOM) with that of the PCDDs and PCDFs formed all samples were analyzed using GC–EILIN-MS. The total organic matter in a given sample was estimated by using average response factor in area counts per nanogram for a standard mixture as described in the experimental section. The total organic matter estimated for the B and C series samples is in the order of B3 > B2 > B1 and C3 > C2 > C1 respectively. The lower levels of TOM observed in the order seen above can be correlated with a decrease in temperature. Comparison of the TIC traces of Machida and Ontario fly ash extracts is shown in Fig. 3, where only tetra- to octa-dibenzo-*p*-dioxins and dibenzofurans were monitored using GC–EISIM-MS. Both the TIC traces were drawn on the same scale, indicating high levels of dioxins detected in Ontario fly ash compared to Machida fly ash. In addition to that from the abundances of isomers in each congener group it can be seen that Machida fly ash does not show peaks for the relatively more toxic tetra- and pentadioxins and furans. The preponderance of the octadioxin in the Machida fly ash is apparent.

REFERENCES

1 F. W. Karasek and F. I. Onuska, *Anal. Chem.*, 54 (1982) 309A.
2 C. Rappe, *Environ. Sci. Technol.*, 18 (1984) 78A.
3 M. P. Esposito, H. M. Drake, J. A. Smith and T. W. Owens, *Dioxins, Vol. I, Sources, Exposure, Transport, and Control, EPA-600/2-80-156*, U.S. Environmental Protection Agency, Cincinnati, OH, June 1980.
4 J. R. Gorski, G. Muzi, L. W. Weber, D. W. Pereira, M. J. Iatropoulos and K. Rozman, *Toxicology*, 53 (1988) 19.
5 C. Rappe, G. Choudhary and L. H. Keith (Editors), *Chlorinated Dioxins and Dibenzofurans in Perspective*, Lewis Publishers, Chelsea, MI, 1986.
6 G. G. Choudhry and O. Hutzinger (Editors), *Mechanistic Aspects of the Thermal Formation of Halogenated Organic Compounds Including Polychlorinated Dibenzo-p-dioxins*, Gordon & Breach, London, 1983.
7 G. Choudhary, L. H. Keith and C. Rappe (Editors), *Chlorinated Dioxins and Dibenzofurans in the Total Environment*, Butterworth, London, 1983.
8 L. H. Keith, C. Rappe and G. Choudhary (Editors), *Chlorinated Dioxins and Dibenzofurans in the Total Environment II*, Butterworth, London, 1983.
9 M. A. Kamrin and P. W. Rodgers (Editors), *Dioxins in the Environment*, Hemisphere Publ., Washington, DC, 1985.
10 J. L. Paustenbach, H. P. Shu and F. J. Murray, *Regul. Toxicol. Pharmacol.*, 6 (1986) 284.
11 F. Coulston and F. Pocchiari, *Accidental Exposure to Dioxins: Human Health Aspects*, Academic Press, New York, 183.
12 J. H. Exner, J. D. Johnson, O. D. Ivins, M. N. Wass and R. A. Miller, in J. Exner (Editor), *Detoxication of Hazardous Waste*, Ann Arbor Sci. Publ., Ann Arbor, MI, 1982, p. 269.
13 J. W. A. Lustenhouwer, K. Olie and O. Hutzinger, *Chemosphere*, 9 (1980) 501.
14 R. Bumb, W. Crummett, S. Cutie, J. Gledhill, R. Hummel, R. Kagel, L. Lamparski, D. Miller, T. Nestrick, L. Shadoff, R. Stehl and J. Woods, *Science (Washington, D.C.)*, 210 (1980) 385.
15 D. Mukerjee and D. H. Cleverly, *Waste Manage. Res.*, 5 (1987) 269–283.
16 H. Vogg, M. Metzger and L. Stieglitz, *Waste Manage. Res.*, 5 (1987) 285.
17 J. M. Czuczwa and R. A. Hites, *Environ. Sci. Technol.*, 20 (1986) 195.
18 F. W. Karasek and O. Hutzinger, *Anal. Chem.*, 58 (1986) 633A.
19 A. Yasuhara, H. Ito and M. Morita, *Environ. Sci. Technol.*, 21 (1987) 971.
20 K. P. Naikwadi and F. W. Karasek, in E. Heftmann (Editor), *Chromatography*, Elsevier, Amsterdam, 5th ed., 1991, Ch. 24, in press.

21 H. Y. Tong, D. L. Shore and F. W. Karasek, *Anal. Chem.*, 56 (1984) 2442.
22 G. A. Eicemen, R. E. Clement and F. W. Karasek, *Anal. Chem.*, 51 (1979) 2344.
23 K. P. Naikwadi and F. W. Karasek, *J. Chromatogr.*, 369 (1986) 203.
24 K. P. Naikwadi, A. M. Mcgovern and F. W. Karasek, *Can. J. Chem.*, 65 (1987) 970.
25 F. W. Karasek and L. C. Dickson, *Science (Washington, D.C.)*, 237 (1987) 754.
26 K. P. Naikwadi and F. W. Karasek, *Chemosphere*, 19 (1989) 299.
27 B. Ross, K. P. Naikwadi and F. W. Karasek, *Chemosphere*, 19 (1989) 291.
28 K. P. Naikwadi and F. W. Karasek, in R. E. Clement and R. O. Kagel (Editors), *Proceedings of the 3rd. Chemical Congress of North America (ACS), Toronto, June 1988,* Lwise Publishers, 1989, in press.
29 H. Y. Tong, D. L. Shore and F. W. Karasek, *J. Chromatogr.*, 285 (1984) 423.
30 K. P. Naikwadi, K. P. Hom and F. W. Karasek, *Chemosphere*, 19 (1989) 579.
31 F. W. Karasek, T. S. Thompson and K. P. Naikwadi, *Proceedings Technology Transfer Conference, Ontario Ministry of the Environment, Toronto,* 1988, p. 43.
32 H. Y. Tong and F. W. Karsek, *Chemosphere*, 15 (1986) 1141.
33 K. P. Naikwadi and F. W. Karasek, *Intern. J. Environ. Anal. Chem.*, 38 (1990) 329.

Journal of Chromatography, 511 (1990) 291–302
Elsevier Science Publishers B.V., Amsterdam

CHROM. 22 442

Identification of exposure markers in smokers' breath

SYDNEY M. GORDON
IIT Research Institute, 10 West 35th Street, Chicago, IL 60616-3799 (U.S.A.)
(Received December 14th, 1989)

ABSTRACT

Volatile organic compounds present in the exhaled breath of 26 smokers and 43 non-smokers were evaluated in an effort to identify possible biochemical markers resulting from the exposure to cigarette smoke. The total ion current profiles obtained from gas chromatography–mass spectrometry (GC–MS), which contained about 230 GC–MS peaks, were first analyzed by using standard statistical procedures to select a subset of 22 peaks. The importance of the peaks was ranked using factor analysis, which further reduced the dimensionality of the data, and discriminant analysis served to develop classification functions. One peak, 2,5-dimethyl furan, had sufficient discriminatory power in the GC–MS profiles to allow almost complete differentiation (96% correct classification) between the smokers and non-smokers groups. In addition, several other compounds were able to separate the groups with a high level of accuracy.

INTRODUCTION

The major adverse effects of cigarette smoking on human health (*e.g.*, lung cancer, impaired lung function) are dose-related[1,2]. Although cessation of smoking substantially reduces the risk of lung cancer among smokers, the benefits of smoking reduction programs have to be deduced from unvalidated questionnaires and are therefore sometimes difficult to assess. Hence, independent quantitative markers are needed to validate survey data and monitor compliance behavior.

Of the nearly 4000 individual components identified in cigarette mainstream smoke[3], the uptake of only a few markers has been studied. Biochemical procedures have been developed to measure the concentrations of nicotine, cotinine, thiocyanate, carboxyhemoglobin and carbon monoxide in blood, saliva, expired air and hair[4–11]. While all these procedures register differences between smokers and non-smokers, they are either invasive, analytically complex or non-specific. The potential of alternative methods and the existence of other markers should therefore be explored.

Human breath is an important mode of uptake and elimination of volatile organic compounds (VOCs) in exposed individuals[12]. Numerous studies have demonstrated that breath analysis provides a powerful means of establishing an

0021-9673/90/$03.50

unequivocal diagnosis of exposure and, in some cases, for estimating the extent of exposure[13]. Analysis of exhaled breath, rather than blood or urine, is attractive for two reasons. First, it is non-invasive and therefore preferable for use in studies relying on reasonable levels of response from volunteers among the general public. Second, since breath is a less complex mixture than other body fluids, it is generally more amenable to comprehensive chemical characterization.

Despite the apparent potential offered by breath analysis for diagnosing exposure, its use to date in the objective measurement of exposure to cigarette smoke has been limited. Most earlier work was based on the assumption that only one or two constituents were relevant[4,14]. However, information on concurrent changes in the concentration of several constituents could potentially increase the diagnostic significance of expired air analysis in distinguishing smokers from non-smokers. In a recent study, personal air exposures and exhaled breath concentrations of 25 VOCs were measured by gas chromatography–mass spectrometry (GC–MS) for 200 smokers and 322 non-smokers in New Jersey and California[15–17]. Smokers showed significantly elevated breath concentrations of benzene, styrene, ethylbenzene, *o*-xylene and *m*- + *p*-xylene. The GC–MS data were generated as part of the U.S. Environmental Protection Agency's TEAM (Total Exposure Assessment Methodology) Study, which was statistically designed to measure exposures and corresponding breath levels of about 600 persons in several U.S.A. cities, representing a total population of 700 000 residents[15]. Although measurements were made on 100–200 volatile chemicals in the breath of each participant, the TEAM study focused on only 25 specific compounds. The results obtained by Wallace and co-workers[15–17] for benzene and the other target compounds suggest that there may be other volatile compounds present in exhaled breath that are even more characteristic of smoking activity.

Because of the volume and complexity of the data, as well as the large variations in data commonly found among individuals in a given sample population, special GC–MS data-enhancement procedures together with multivariate statistics (pattern recognition) are needed to extract useful information from the data files and differentiate between smokers and non-smokers. In an earlier investigation[18], we demonstrated the application of these techniques to high resolution GC–MS breath data from lung cancer patients. The method identified several VOCs in the breath of lung cancer patients that had sufficient diagnostic power in the GC–MS profiles to allow almost complete differentiation between them and a group of controls. Similarly, this study has sought to identify exposure markers in the breath of smokers that may be used to distinguish them from non-smokers in non-invasive exposure screens.

EXPERIMENTAL

As the quality assurance laboratory for the TEAM study, we analyzed roughly 20% of all the breath samples collected during the investigation. It was this subset of the complete data base of measured breath VOCs that we evaluated for discriminants between smokers and non-smokers.

Subject selection and characterization

The subjects were selected by the prime contractor (Research Triangle Institute)

TABLE I

CHARACTERISTICS OF PARTICIPANTS

Category		*Number of respondents*
Smoking status	Smoker	26
	Non-smoker	43
Smoked during monitoring period	Yes	26
	No	43
Exposed to tobacco smoke	Yes	37
	No	32

by a three-stage probability sampling design, and were stratified to provide a geographic dispersion of the residences sampled within each municipality[19–23]. The probability sampling methods they used were designed to ensure that the data collected could be used to draw valid statistical inferences concerning the populations sampled. For the present purposes, therefore, the subset population studied is assumed to represent a suitably randomized sample.

After being interviewed by the prime contractor, all participants completed a questionnaire describing their occupations and kept a record of their activities during the monitoring period[19–23]. The data provided the secondary stratification variables of potential occupational exposure and smoking status, as well as age, sex and race. The questionnaire also gave information, *inter alia*, on the number of cigarettes smoked per day, the age at which smoking first started and, where applicable, the age at which smoking stopped. A 24-h activity screener provided information on the use of tobacco during the preceding 24-h period. Table I presents a summary of relevant characteristics of the participants in the sample subset. Of the total, 38% were current smokers, all of whom had smoked during the monitoring period, while 54% had been exposed to tobacco smoke during the preceding 24-h period.

Sample collection and analysis

Sample collection was carried out by the prime contractor and has been described in detail elsewhere[15,22]. Briefly, each participant carried a personal monitor to collect two 12-h air samples and gave a breath sample at the end of the sampling period. Breath samples were collected using a specially designed spirometer and cartridges containing Tenax GC adsorbent to trap the organic vapors for later analysis. These cartridges, which constituted the subset of samples for the present study, were analyzed in our laboratory using a thermal desorption technique followed by combined GC–MS.

Data processing procedures

Using a Digital PDP-11/34 minicomputer and the RSX11M operating system, the raw GC–MS data files were evaluated with an automated spectrum-enhancement algorithm (program CLEANUP) that automatically locates components to yield a set of pure spectra that are free of background contributions and peaks from overlapping

components[24]. Peak matching and file averaging for each sample group were carried out using two more programs (TIMSEK and MAKLOC)[25]. The final reduced data set, consisting of average retention indices and relative concentrations for the components in each sample group, was transmitted to an IBM-compatible personal computer (PC) via an RS-232C serial ASCII interface.

The 26 smokers and 43 non-smokers gave a total of 69 GC–MS profiles and 230 compounds, which served as the primary data base. Because the frequency distributions of exhaled breath values for the TEAM compounds are closer to log normal than normal[15], we applied the Fisher exact test and Mann–Whitney *U* statistics from the BMDPC personal-computer software package[26] to the individual compounds to yield a subset of GC–MS peaks for further analysis. Principal component analysis was used to further reduce the dimensionality of the data, and discriminant analysis provided a suitable classification model. The peaks were identified by comparing their "clean" mass spectra with standard spectra in the PC-based CD-ROM (Compact Disk-Read Only Memory) edition of the Registry of Mass Spectral Data, using the Probability-Based-Matching search program[27].

RESULTS AND DISCUSSION

Broad-spectrum GC–MS analysis of the 69 breath samples identified close to 230 compounds. The average number of compounds identified in the 26 smokers samples was 144 (±27) and 129 (±28) in the 43 non-smokers samples.

Data preparation

The CLEANUP–TIMSEK–MAKLOC algorithms[24,25] provide a powerful and convenient means of enhancing and compositing large groups of complex raw GC–MS data files. The programs produce summary lists of the average relative concentrations and effective retention indices for each sample group of interest. These lists can be used directly to analyze the data further.

The CLEANUP program was used to improve the quality of the mass spectral data by automatically locating and extracting components to produce a set of pure spectra that are free of background contributions and overlapping peaks. Once a clean spectrum was defined by the program, its area was calculated and used to evaluate the relative concentration of the component in the sample by comparing the peak area of that component with the peak area of a standard. The external standard, perfluorobenzene, was added to each Tenax GC cartridge just before analysis.

To match peaks and generate composite GC–MS profiles for non-smokers and smokers, each peak in the profiles was first subjected to retention time scaling (program TIMSEK) to compensate for variations in retention time between individual experiments. The retention times were scaled by converting the raw chromatographic retention data (spectrum scan numbers) into a set of standardized retention indices relative to a set of equally spaced marker peaks that occurred throughout the data base and were easily located. These peaks were initially used to create a reference calibration file that related spectrum scan number to peak position. For all subsequent profiles, the reference peaks were used to calculate an effective retention index scale for the entire profile. The retention scaling program also calculated relative concentrations (*i.e.*, peak area ratios) for each component with respect to the standard.

The peak matching program (program MAKLOC) takes "clean" sets of mass spectral and effective retention index data for each component in a GC–MS profile and makes peak-by-peak comparisons with the corresponding data in associated profiles. To do this, one of the profiles of interest was set up as an historical (standard) library. The program then defined successive time windows, in each of which the unknown spectrum was compared with every reference spectrum in the window of the historical library by performing a relative retention index (RRI) match and a spectrum match. Matching effectiveness was expressed in terms of a score that gave a measure of spectral similarity and RRI proximity. When a satisfactory match occurred, the peak was added to the historical library, and the relative concentration and RRI data for the entry were updated.

The composited data files, which include statistics on the frequency of occurrence and the reproducibility of the average relative concentrations in the two sample groups of interest, were transferred from the PDP-11/34 minicomputer to a spreadsheet in the PC. For those compounds not detected, values were taken to be the average estimated limit of detection. A complete summary of the group data for the smokers' and non-smokers' samples is available on request from the author. The data show the presence of many different chemical classes in the sample groups, including aliphatics, aromatics, halogenated hydrocarbons, alcohols, aldehydes, ethers, esters and ketones. A number of compounds occurred with a frequency of 100% in one of the groups and at least 90% frequency in the other. Of especial interest was the fact that three compounds (1-penten-3-yne, a methyl-1,3-cyclopentadiene isomer and 2,5-dimethyl furan) occurred with high frequency in the breath of the smokers but were entirely absent from, or only occasionally observed in, the non-smokers' breath. Thus, they could serve as marker compounds to distinguish smokers from non-smokers.

Statistical data analysis: peak selection

Given the large number of constituents of human expired air and their complex interrelationships[13], multivariate data analysis provides a more realistic and objective means of extracting useful information from the GC–MS profiles than do piecemeal univariate procedures. However, certain problems complicate the determination of significant differences in the constituents of human expired air between groups of smokers and non-smokers. First, the number of breath samples available for the study is small relative to the number of constituents detected. Second, although multivariate statistical techniques can be effective, they can also identify fortuitous associations that are neither reproducible nor physically meaningful[28]. Generally, it has been shown that, as long as the ratio of the number of samples in the data set (*i.e.*, the GC–MS profiles) to the number of descriptors (*i.e.*, the individual peaks) per sample is greater than 3, then the probability of achieving complete separation due to chance alone is low. Therefore, no more than 23 peaks may be analyzed by multivariate statistics to identify characteristic compounds in the breath of smokers.

For each of the 230 compounds in the smokers and non-smokers samples, χ^2 statistics (Fisher exact test) were used in the univariate case to test smoker–non-smoker differences in terms of the presence or absence of a particular component. A type I error rate of $P < 0.05$ was taken to indicate significance in this initial screen. Then, Mann–Whitney U statistics were computed to test for significant differences in the relative concentrations of each compound between the two groups. This procedure

TABLE II

POTENTIALLY SIGNIFICANT PEAKS BASED ON FISHER EXACT AND MANN–WHITNEY TESTS

Peak No.	*RRI*	*Formula*	*Compound*	*Fisher Exact test*			*Mann–Whitney test*
				Occurrence (%)		*P value*	
				Non-smokers	*Smokers*		*P value*
1	472	C_3H_6O	Acetone	98	88	0.1466	0.0110
2	531	C_5H_6	1-Penten-3-yne	5	77	0.0000	0.0000
3	550	C_5H_8	Cyclopentene	21	62	0.0008	0.0006
4	572	$C_4H_6O_2$	2,3-Butane dione	35	54	0.0979	0.0313
5	577	C_4H_8O	2-Methyl propanal	53	31	0.0553	0.0398
6	590	C_6H_{12}	1-Hexene	74	92	0.0596	0.0000
7	610	C_6H_{12}	Methyl pentene isomer	21	88	0.0000	0.0000
8	622	C_6H_{12}	Methyl pentene isomer	40	88	0.0000	0.0001
9	636	C_6H_8	Methyl-1,3-cyclopentadiene isomer	0	77	0.0000	0.0000
10	640	C_6H_8	Methyl-1,3-cyclopentadiene isomer	0	62	0.0000	0.0000
11	648	C_6H_{10}	Methyl cyclopentene isomer	9	54	0.0001	0.0000
12	649	C_6H_{10}	3-Methyl cyclopentene	19	54	0.0029	0.0006
13	652	C_6H_6	Benzene	100	100	–	0.0716
14	688	C_2HCl_3	Trichloroethylene	81	73	0.3016	0.0393
15	697	C_6H_8O	2,5-Dimethyl furan	0	92	0.0000	0.0000
16	732	C_7H_{16}	Alkane (tentative identification)	51	81	0.0125	0.0345
17	736	C_7H_{10}	Methyl-1,3,5-hexatriene isomer	0	58	0.0000	0.0000
18	789	$C_5H_{12}O$	3-Methyl-1-butanol	16	77	0.0000	0.0000
19	853	C_8H_{10}	Ethyl benzene	100	100	–	0.3187
20	861	C_8H_{10}	*m/p*-Xylene	100	100	–	0.2546
21	878	C_8H_8	Styrene	77	96	0.0305	0.0146
22	884	C_8H_{10}	*o*-Xylene	100	100	–	0.1422

tests the null hypothesis of no difference in the mean concentrations of a compound between the two sample sets. Again, a type I error rate of $P < 0.05$ was assumed to be significant.

Those peaks which were significant by one or more of the tests used, and occurred in at least one of the two sample groups with a frequency greater than 50%, were selected to serve as a starting point for further analysis. The nineteen peaks that satisfied these requirements are listed in Table II. They include the aromatics benzene and styrene, which were found in earlier TEAM studies to be significantly higher in the breath of smokers compared to non-smokers[16,17]. Table II also includes the compounds ethyl benzene and the xylene isomers which, while not satisfying our peak selection requirements, nevertheless exhibited the same behaviour as benzene and styrene in the earlier work.

Multivariate statistical analysis

Before attempting to reduce the dimensionality of the data, a logarithmic transformation was applied to each relative concentration, which substantially reduced the relatively large variance in the raw peak area values. Factor analysis and discriminant analysis were performed on the 22 selected peaks. Factor analysis was

used to rank the peaks according to their importance in describing the data variance, while discriminant analysis served to obtain the optimal separation between the two sample groups from the minimum number of peaks[29,30].

Factor analysis attempts to identify underlying patterns in the samples by describing the variance in the data in as few factors as possible, while still retaining the information content of the originals. The observed variables are placed into linear combinations, and the first factor is the combination that accounts for the largest amount of variance in the sample. Successive factors explain progressively smaller fractions of the total sample variance.

In order to determine the minimum number of factors needed to represent the data, we computed the total variance explained by each factor as well as the cumulative percentage. The results are summarized in Table III. Almost 70% of the total variance is attributable to the first four factors, the remaining eighteen factors together accounting for only 30% of the variance. It therefore appears that the data may be adequately represented by a model based only on the first four factors.

Although the first few factors explain the major portion of the variance, they do not identify the most important individual peaks. To facilitate this identification, we performed factor analysis rotation using the varimax method, which minimizes the number of variables with high loadings on a factor, thus transforming the initial matrix into one that is easier to interpret[29]. Table IV shows the rotated factor loadings for the first four factors. The factor loading matrix has been sorted so that variables with high

TABLE III

TOTAL VARIANCE EXPLAINED BY EACH FACTOR

Factor	*Variance explained*	*Percentage of total variance*	*Cumulative percentage*
1	8.528	38.8	38.8
2	3.902	17.7	56.5
3	1.576	7.2	63.7
4	1.382	6.2	69.9
5	1.086	5.0	74.9
6	1.018	4.6	79.5
7	0.869	4.0	83.5
8	0.670	3.0	86.5
9	0.483	2.2	88.7
10	0.408	1.9	90.6
11	0.404	1.8	92.4
12	0.321	1.5	93.9
13	0.263	1.2	95.1
14	0.237	1.0	96.1
15	0.198	0.9	97.0
16	0.172	0.8	97.8
17	0.140	0.6	98.4
18	0.113	0.6	99.0
19	0.088	0.4	99.4
20	0.061	0.2	99.6
21	0.041	0.2	99.8
22	0.039	0.2	100.0

TABLE IV

ROTATED FACTOR LOADING MATRIX (VARIMAX METHOD)

Peak No.	*RRI*	*Factor*			
		1	*2*	*3*	*4*
17	736	0.928			
10	640	0.874			
2	531	0.861		0.323	
9	636	0.854			
15	697	0.751			
11	648	0.675			−0.381
7	610	0.660		0.486	
6	590	0.600			
22	884		0.916		
19	853		0.915		
20	861		0.873		
13	652		0.736		
3	550	0.358		0.857	
12	649	0.273			0.911
16	732				
5	577				
18	789	0.416			
1	472				
4	572	0.326			
14	688		0.341		
8	622	0.310	0.303	0.299	
21	878		0.519		

loadings on the same factor appear together. Small factor loadings (<0.250) are omitted from the table. Several peaks have large loadings on the same factor, *e.g.*, 17, 10, 9, 15 and 6 on the first factor; 22, 19, 20 and 13 on the second factor, etc. In addition, certain peaks (*e.g.*, 7, 3, 12 and 8) share information over more than one factor. The first factor contains many of the peaks that occurred often in smokers' breath and rarely in non-smokers' breath. The second factor includes all of the aromatic compounds previously found to be at higher concentrations in smokers' breath[16,17].

The minimum number of peaks needed to distinguish between smokers' and non-smokers' samples was ascertained by discriminant analysis, using the peaks determined from the factor technique. In discriminant analysis, group membership of the samples is defined from the beginning, and the variables are linearly combined in such a way that the defined groups are as statistically distinct as possible[26,29,30]. Variables are entered into, or removed from, the analysis on a stepwise basis and the discriminant function maximizes the ratio of the inter-group to intra-group variance at each step. We constructed discriminant functions using the information in Table IV to maximally differentiate smokers from non-smokers, then tested the accuracy of each estimated function both statistically and by examining the concordance between the observed and estimated classifications. A classification accuracy of greater than 80% was considered to be significant.

TABLE V

CLASSIFICATION RESULTS FROM STEPWISE DISCRIMINANT ANALYSIS USING PEAKS HEAVILY LOADED ON A SINGLE FACTOR

Group	*% Correct*[a]	*Number of samples*	*Number misclassified*
Non-smokers	100	43	0
Smokers	89	26	3
Overall:	96		

[a] Peaks 10 and 15 included in discriminant function.

Ideally, the validation of each result should be based on the classification of an independent data set. However, no extra samples were available for independent evaluation and the data set used was not large enough to be randomly split into two groups, one to derive the discriminant function and the other to test it. Consequently, we used the "jackknife" validation procedure in order to estimate misclassification rates and minimize bias[26,30]. In this "leave-one-out" method, each of the samples is left out in turn, the discriminant function is recalculated based on the remaining $(n-1)$ samples, and then the left-out sample is classified. This procedure continues until all samples in the set have been left out and classified once.

Following the approach described by Parrish *et al.*[31], we used the information in Table IV to compare the effect on the overall classification of peaks that are heavily loaded on only one factor as opposed to peaks that share information. Although several peaks were designated from the first category, namely 9, 10, 15 and 17 (factor 1), and 19, 20 and 22 (factor 2), only two (peaks 10 and 15) were selected in the stepwise discriminant analysis. Examination of the data in Table II reveals that peak 15 occurs with high frequency in the smokers' samples while both are completely absent from the non-smokers' samples. Peak 15 exhibits a disproportionate power to discriminate in this case, as indicated by the calculated F-statistic to enter or remove a variable from the discriminant function ($F = 290$ for peak 15; $F = 3.5$ for peak 10)[29,30]. The classification results from the analysis are shown in Table V. The overall percent of samples correctly classified was 96% for both the discriminant model and the jackknifed classification. All of the misclassification involves the smokers group, in which 23 samples are predicted correctly to be members of this group, while three are assigned to the non-smokers group. Further evidence of the dominant role played by peak 15 in discriminating between the two groups is provided by the fact that the same classification results are obtained when only this peak is entered into the analysis.

To establish the discriminatory importance of the remaining peaks heavily loaded on one factor, peak 15 was removed from contention and the discriminant function was recalculated using peaks 9, 10, 17, 19, 20 and 22. The results are summarized in Table VI and show that a jackknifed classification accuracy of 90% was obtained with peaks 9, 10, 20 and 22 selected in the analysis. In this case, the calculated F-values indicate that peak 9 plays a dominant discriminating role followed, to a much lesser extent, by peak 20.

Stepwise discriminant analysis was also performed using peaks that share information, in addition to the peaks that have a high loading on only one factor. The

TABLE VI

SUMMARY OF PEAKS EVALUATED AND JACKKNIFED CLASSIFICATION RESULTS FROM STEPWISE DISCRIMINANT FUNCTION ANALYSIS

Analysis criterion	*Case*	*Peaks considered*[a]	*Peaks selected*[b] *(F-value in parentheses)*	*Overall percentage correctly classified*
High loaded single-factor peaks	1	9, 10, 15, 17, 19, 20, 22	15(290), 10(3.5)	96
	2	9, 10, 17, 19, 20, 22	9(115), 20(5.9), 10(1.3), 22(1.1)	90
High loaded single-factor plus cross-term peaks	3	2, 3, 6, 7, 9, 10, 11, 12, 13, 15, 17, 19, 20, 21, 22	15(290), 10(3.5), 2(1.7), 7(1.0)	96
	4	2, 3, 6, 7, 9, 10, 11, 12, 13, 17, 19, 20, 21, 22	9(115), 7(5.4), 20(5.2), 2(4.8), 17(3.9), 10(2.1), 3(1.7), 22(1.2)	90
Major discriminating peaks selected from cases 1–4	5	2, 3, 7, 9, 10, 15, 17, 20, 22	15(290), 10(3.5), 2(1.7), 7(1.0)	96
Aromatics[c]	6	13, 19, 20, 21, 22	21(7.4), 13(4.1)	61

[a] From data in Table IV (peak numbers identified in Table II).

[b] Using values of 1.0 for *F*-to-enter and remove peaks in BMDPC 7M discriminant analysis program.

[c] Identified in earlier TEAM studies[16,17].

classification results obtained are summarized in Table VI (case 3). Although 15 peaks were considered in the analysis and 4 were selected, peak 15 again displayed an exaggerated power to discriminate and gave an overall classification accuracy of 96%. As before, peak 15 was removed from consideration in order to establish the relative importance of the other compounds, and the discriminant function was recalculated using the remaining 14 peaks. The results are shown in Table VI (case 4) and again reveal the discriminatory importance of peak 9, followed this time by peak 7.

The major discriminating peaks resulting from the analyses described above were thereupon chosen for evaluation, and the results are summarized in Table VI (case 5). Once again, the dominating influence of peak 15 is clearly evident, giving the same classification accuracy (96%) obtained in all of the earlier analyses in which it was one of the peaks considered.

Finally, the discriminant technique was applied to the two groups, using the aromatic peaks (benzene, styrene, ethyl benzene and the xylene isomers) which were found in earlier TEAM studies to be significantly higher in the breath of smokers[16,17]. When the peaks were entered into the analysis, only styrene was selected, and the overall percentage correctly classified decreased to 61%. This suggests that these compounds contain less discriminating information than the compounds discussed above.

Significance of selected compounds

Overall, the breath components which gave the best discrimination between the smokers and non-smokers samples, under the various conditions that were considered, were 2,5-dimethyl furan (peak 15), the methyl-1,3-cyclopentadiene isomers (peaks 9 and 10), *m*/*p*-xylenes (peak 20) and a methyl pentene isomer (peak 7). Of these, 2,5-dimethyl furan plays a dominant role in distinguishing between the two groups.

This compound (2,5-dimethyl furan) has been identified as a major gas-phase constituent of tobacco smoke[32]. It probably arises because of the rich oxygen environment in which the combustion of tobacco takes place, which results in the occurrence of a large number of oxygenated compounds in mainstream smoke. The compound was also previously identified in exhaled breath samples with a 60% occurrence frequency, but was not observed in the corresponding breathing-zone air samples[33]. However, its potential usefulness as a marker of cigarette exposure could not be evaluated from this work, since no distinction was made between smokers and non-smokers.

CONCLUSIONS

The compound 2,5-dimethyl furan and the other major discriminating compounds identified in the present study illustrate the striking power of factor analysis and discriminant analysis to differentiate with a high degree of accuracy between smokers and non-smokers, on the basis of the volatile compounds present in their exhaled breath. Thus, they appear to be effective biochemical markers of smoking, and suggest that the analysis of exhaled breath could provide a reliable non-invasive method for mass screening studies. However, the half-lives of these compounds must be determined before they can be exploited as practical indicators of exposure to smoking. A simple two-parameter time-dependent model has been shown to have some success in estimating biological half-lives of several VOCs[34], and recently a "washout" study was performed over a 10-h period in a pure air chamber which resulted in measured half-lives for tetrachloroethylene and chloroform[35]. Similar measurements are needed on the compounds identified here as potential markers of exposure to cigarette smoke so that a suitable model relating such exposure to body burden can be developed.

ACKNOWLEDGEMENTS

The author thanks Dr. Lance A. Wallace of the U.S. Environmental Protection Agency for providing information from the activity screeners on the smoking habits of the subjects in the study, and Drs. Demetrios J. Moschandreas, Robert G. Gibbons and Lance A. Wallace for reviewing the manuscript. This investigation was supported by PHS grant number 1 R03-CA43959-01, awarded by the U.S. Department of Health and Human Services.

REFERENCES

1 *Surgeon General Report: The Health Consequences of Smoking—Cancer*, U.S. Department of Health and Human Services, Washington, DC, 1982.

2 P. Greenwald and J. W. Cullen, *J. Natl. Can. Inst.*, 74 (1985) 543.

3 M. F. Dube and C. R. Green, *Recent Adv. Tob. Sci.*, 8 (1982) 42.
4 T. M. Vogt, S. Selvin, G. M. Widdowson and S. B. Hurley, *Am. J. Public Health*, 67 (1977) 545.
5 N. Hengen and M. Hengen, *Clin. Chem.*, 24 (1978) 50.
6 P. Hill, N. J. Haley and E. L. Wynder, *J. Chron. Dis.*, 36 (1983) 439.
7 N. J. Haley, C. M. Axelrod and K. A. Tilton, *Am. J. Public Health*, 73 (1983) 1204.
8 N. J. Haley and D. Hoffmann, *Clin. Chem.*, 31 (1985) 1598.
9 R. Pojer, J. B. Whitfield, V. Poulos, I. F. Eckhard, R. Richmond and W. J. Hensley, *Clin. Chem.*, 30 (1984) 1377.
10 M. J. Jarvis, in I. K. O'Neill, K. D. Brunnemann, B. Dodet and D. Hoffmann (Editors), *Environmental Carcinogens—Methods of Analysis and Exposure Measurement, Vol. 9, Passive Smoking*, (*IARC Scientific Publications*, No. 81), International Agency for Research on Cancer, Lyon, 1987, pp. 43–58.
11 H. Muranaka, E. Higashi, S. Itani and Y. Shimizu, *Int. Arch. Occup. Environ. Health*, 60 (1988) 37.
12 B. K. Krotoszynski, G. Bruneau and H. J. O'Neill, *J. Anal. Toxicol.*, 3 (1979) 225.
13 A. Manolis, *Clin. Chem.*, 29 (1983) 5.
14 M. Berlin, J. C. Gage, B. Gullberg, S. Holm, P. Knutsson and A. Tunek, *Scand. J. Work Environ. Health*, 6 (1980) 104.
15 L. A. Wallace, E. D. Pellizzari, T. D. Hartwell, C. M. Sparacino, L. S. Sheldon and H. Zelon, *Atmos. Environ.*, 19 (1985) 1651.
16 L. A. Wallace and E. D. Pellizzari, *Toxicol. Lett.*, 35 (1986) 113.
17 L. A. Wallace, E. D. Pellizzari, T. D. Hartwell, R. Perritt and R. Ziegenfus, *Arch. Environ. Health*, 42 (1987) 272.
18 S. M. Gordon, J. P. Szidon, B. K. Krotoszynski, R. D. Gibbons and H. J. O'Neill, *Clin. Chem.*, 31 (1985) 1278.
19 L. A. Wallace, *Report EPA 600/6-87/002a, Total Exposure Assessment Methodology (TEAM) Study: Summary and Analysis*, Vol. I, U.S. Environmental Protection Agency, Washington, DC, 1987.
20 E. D. Pellizzari, K. Perritt, T. D. Hartwell, L. C. Michael, R. Whitmore, R. W. Handy, D. Smith and H. Zelon, *Report EPA 600/6-87/002b, Total Exposure Assessment Methodology (TEAM) Study: Elizabeth and Bayonne, New Jersey; Devils Lake, North Dakota; and Greensboro, North Carolina*, Vol. II, U.S. Environmental Protection Agency, Washington, DC, 1987.
21 E. D. Pellizzari, K. Perritt, T. D. Hartwell, L. C. Michael, R. Whitmore, R. W. Handy, D. Smith and H. Zelon, *Report EPA 600/6-87/002c, Total Exposure Assessment Methodology (TEAM) Study: Selected Communities in Northern and Southern California*, Vol. III, U.S. Environmental Protection Agency, Washington, DC, 1987.
22 R. W. Handy, D. J. Smith, N. P. Castillo, C. M. Sparacino, K. Thomas, D. Whitaker, J. Keever, P. A. Blau, L. S. Sheldon, K. A. Brady, R. L. Porch, J. T. Bursey and E. D. Pellizzari, *Report EPA 600/6-87/002d, Total Exposure Assessment Methodology (TEAM) Study: Standard Operating Procedures*, Vol. IV, U.S. Environmental Protection Agency, Washington, DC, 1987.
23 R. W. Whitmore, *Atmos. Environ.*, 22 (1988) 2077.
24 R. G. Dromey, M. J. Stefik, T. C. Rindfleisch and A. M. Duffield, *Anal. Chem.*, 48 (1976) 1368.
25 D. H. Smith, M. Achenbach, W. J. Yeager, P. J. Anderson, W. L. Fitch and T. C. Rindfleisch, *Anal. Chem.*, 49 (1977) 1623.
26 *BMDPC: Guide to Using BMDP on the IBM PC*, BMDP Statistical Software, Los Angeles, CA, 1987.
27 *1987 Registry of Mass Spectral Data, CD-ROM Edition*, Wiley Electronic Publishing, New York, 1987.
28 B. K. Lavine, P. C. Jurs, D. R. Henry, R. K. Vander Meer, J. A. Pino and J. E. McMurry, *Chemom. Intell. Lab. Syst.*, 3 (1988) 79.
29 M. J. Norusis, *SPSS/PC+ Advanced Statistics for the IBM PC/XT/AT*, SPSS, Chicago, IL, 1986.
30 D. D. Wolff and M. L. Parsons, *Pattern Recognition Approach to Data Interpretation*, Plenum Press, New York, 1983.
31 M. E. Parrish, B. W. Good, M. A. Jeltema and F. S. Hsu, *Anal. Chim. Acta*, 150 (1983) 163.
32 C. E. Higgins, W. H. Griest and G. Olerich, *J. Assoc. Off. Anal. Chem.*, 66 (1983) 1074.
33 L. A. Wallace, E. Pellizzari, T. Hartwell, M. Rosenzweig, M. Erickson, C. Sparacino and H. Zelon, *Environ. Res.*, 35 (1984) 293.
34 L. A. Wallace, E. Pellizzari, T. Hartwell, H. Zelon, C. Sparacino, R. Perritt and R. Whitmore, *J. Occup. Med.*, 28 (1986) 603.
35 S. M. Gordon, L. A. Wallace, E. D. Pellizzari and H. J. O'Neill, *Atmos. Environ.*, 22 (1988) 2165.

Journal of Chromatography, 511 (1990) 303–315
Elsevier Science Publishers B.V., Amsterdam

CHROM. 22 362

Determination of hydrazine in hydralazine by capillary gas chromatography with nitrogen-selective detection after benzaldehyde derivatization[a]

OLLE GYLLENHAAL*, LENA GRÖNBERG[b] and JÖRGEN VESSMAN
Department of Analytical Chemistry, Pharmaceutical R&D, AB Hässle, S-431 83 Mölndal (Sweden)
(Received November 24th, 1989)

ABSTRACT

A method for the determination of hydralazine substance is described. Hydrazine is derivatized in aqueous media with benzaldehyde to benzalazine. After extraction to an organic phase containing a homologue as marker, the sample is subjected to capillary column gas chromatography with nitrogen-selective detection. A prolonged reaction with 0.1 *M* benzaldehyde of 20 min or more led to an increased level of benzalazine when hydralazine was analysed. An increase was also observed if the aqueous hydralazine sample had been allowed to stand for some time before analysis. The final method involved the use of a 5-min reaction time, fresh solutions and the standard addition principle. The levels of hydrazine found in hydralazine hydrochloride were below 1 ppm (as bases, 1 ng/mg).

INTRODUCTION

Hydralazine (Fig. 1) is a cardiovascularly active compound that has been used as an antihypertensive agent since the 1950s. In combination with β-adrenoreceptor blocking agents the daily dose can be reduced, thus minimizing unwanted side-effects.

Attention has been paid to the presence of hydrazine (Fig. 1) in different drugs

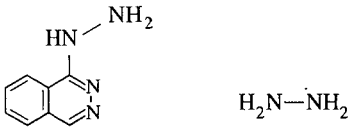

Fig. 1. Hydralazine (left) and hydrazine.

[a] Parts of this work were presented at the *Annual Meeting of the Swedisch Academy of Pharmaceutical Sciences, October 1989.*

[b] Present address: Department of Analytical Chemistry, University of Lund, S-221 99 Lund, Sweden.

0021-9673/90/$03.50

after reports about its mutagenic effects in laboratory animals[1]. Contamination of hydralazine with hydrazine may occur during synthesis or by degradation during storage of the substance or the pharmaceutical formulation.

As hydrazine is a small and polar molecule, most methods for the determination of low concentrations are based on derivatization followed by chromatographic separation of the derivative. Several papers on the determination of hydrazine in different pharmaceutical formulations containing hydrazinic ingredients have been published, including isoniazid[2], phenelzine[3], hydralazine and isoniazid[4] and isocarboxazid[5]. Most of these methods are based on the reaction with an aromatic aldehyde[2–4] (Fig. 2). Attempts to determine hydrazine in hydralazine by liquid chromatography led to irreproducible results, and a gas chromatographic method was therefore developed[4]. The problem with liquid chromatography is interference from the excess of Schiff base formed from the original hydrazinic drug substance itself, which only eluted after several injections as an increasing baseline[4]. This problem can be eliminated by the the use of a short packed disposable column prior to the chromatographic analysis[6].

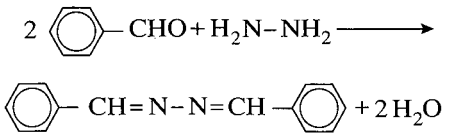

Fig. 2. Reaction of benzaldehyde with hydrazine to give benzalazine.

Gas chromatography for the simultaneous determination of hydrazine and benzylhydrazine in isocarboxamide was at first impossible, as the hydrazone formed was not stable[5], but by derivatization to a pyrazole derivative using a diketone as reagent a stable derivative was obtained[5]. 2-Hydroxy-1-naphthaldehyde has also been used for derivatization followed by UV[7] and fluorimetric[8] detection. Recently a method for the determination of hydrazine and acetylhydrazine in blood after derivatization with pentafluorobenzaldehyde was reported[9].

Some interest in hydrazine determinations has been focused on boiler feedwater, where it is used as an antioxidant. Proposed methods involve the use of electrochemical detection after liquid chromatography of free hydrazine[10] or after salicylaldehyde derivatization[11].

To develop a method for the determination of hyrazine in hydralazine we adopted the gas chromatographic method described by Lovering and co-workers[2–5] (Fig. 3a) with some modifications. These include the use of a capillary column instead of a packed column and a homologue of benzalazine as a marker in the organic phase instead of 5-chloromethyl-2-aminobenzophenone[4].

EXPERIMENTAL

Apparatus

Gas chromatograph. A Varian 3700 gas chromatograph was equipped with a nitrogen–phosphorus-selective detector and a capillary column. To fit the column, the instrument was modified with a Gerstel adaptor at the detector side and a Ger-

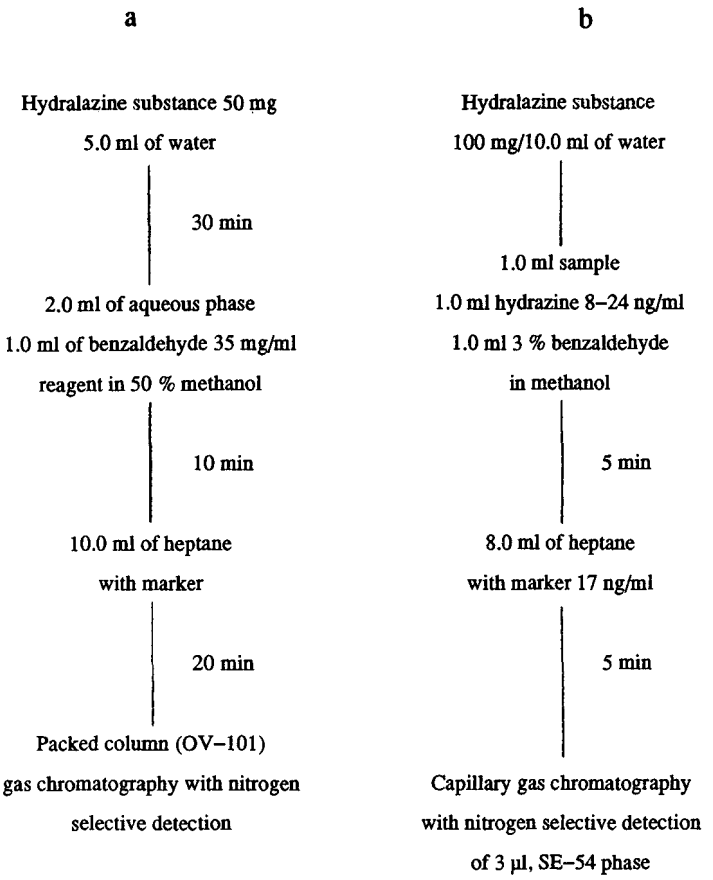

Fig. 3. Schemes for the analysis of hydrazine by gas chromatography with nitrogen-selective detection after derivatization. (a) Previous method[4]; (b) present method.

stel–Swagelock adaptor at the injector side. The fused-silica column (25 m × 0.32 mm I.D.) was coated with SE-54 (0.25 μm). During use *ca.* 20 cm was cut off when required to restore the peak symmetry. Injections were made with the split valve closed. After 2 min it was opened automatically, controlled by a separate unit. It was closed prior to the next injection by a signal from the auxiliary channel of the auto-sampler.

The detector bead voltage was 4 V and the current setting was between 300 and 900 depending on the actual bead probe used and its age. The input current to the detector was adjusted so that a background current of *ca.* 10 mV was obtained.

The instrument temperatures were injector 280°C, detector 300°C and oven 100°C (1 min), increased at 15°C/min to 285°C, which was maintained for 1 or 5 min depending on the type of sample.

The inlet pressure of the nitrogen carrier gas was 100 kPa. Gas flow-rates to the detector were make-up nitrogen 20 ml/min, air 175 ml/min and hydrogen 4.5 ml/min. With a recent detector probe the hydrogen flow-rate was increased to 5.5 ml/min in

order keep the bead working after the solvent had passed, otherwise the "flame" was extinguished and sometimes failed to re-ignite.

Injections. A Varian 8000 autoinjector was used. The auxiliary time facility of the control unit was used to close the split before the next injection. A 3-μl volume was injected throughout. Occasionally the whole injector system was flushed with methanol to prevent precipitation in the tubing by the hydralazine hydrazone from the non-polar heptane phase when the system was at rest. At the same time the syringe piston inlet was cleaned with the same solvent.

Integrator. Chromatograms were recorded and evaluated with a Hewlett-Packard 3390A integrator. Normally peak areas were reported but peak heights gave slightly better precision at low concentrations levels.

The samples were shaken mechanically in an upright position without caps (Ika-Vibrax-VXR; Janke & Kunkel, Staufen, F.R.G.). Up to 36 tubes of 15 ml can be handled simultaneously with this apparatus.

Reagents and chemicals

Hydrazine monohydrochloride (purum; Fluka, Buchs, Switzerland), benzaldehyde (puriss; BDH), 3- and 4-fluorobenzaldehyde (purum; Fluka), benzalazine (Koch-Light Labs., Colnbrook, U.K.), phenylhydrazine, 4-methylbenzaldehyde (*p*-tolualdehyde) (purum, Fluka) and hydralazine hydrochloride (Ciba-Geigy, Basle, Switzerland, batch 37-187-16, s 40 843-2, 870422). Solvents and the buffer salts used were of analytical-reagent grade.

4-Fluorobenzalazine used as a marker was prepared in crystalline form as follows: 4.28 mg of hydrazine hydrochloride was dissolved in 5.0 ml of water + 5.0 ml of methanol, then 50 μl of 4-fluorobenzaldehyde were added and after about 5 min a precipitate formed. After centrifugation the supernatant was decanted and discarded. The yellow crystals were washed twice with 10% aqueous methanol and dissolved in dichloromethane. The solution was placed in a small glass vial, the solvent was evaporated with nitrogen and the crystals obtained were stored in the vial.

Benzaldehyde reagent was prepared by diluting 3.0 ml of the aldehyde to 100.0 ml with methanol. This solution was not kept for more than 1 week.

Determination of hydrazine

Preparation of the samples. Deionized water was used for the preparation of all hydrazine and hydralazine samples. A 63-mg amount of hydralazine hydrochloride was dissolved in 5.0 ml of water (equivalent to 10 mg/ml of hydralazine base). To 2.0 ml of the solution was added 1.0 ml of a 3.0% solution of benzaldehyde in methanol. An Eppendorf repeater pipette was used for addition of the reagent. The mixture was shaken in an upright position for 5 min (before it was found that additional benzalazine was formed in the aqueous phase after about 10 min owing to degradation of the hydralazine Schiff base, the derivatization time adopted at first was 20 min). The reaction mixture was then extracted with 8.0 ml of heptane containing the marker 4-fluorobenzalazine (17 ng/ml). The heptane was dispensed with a Socorex (Renens, Switzerland) 511-10 dispenser.

Both reaction and extraction were performed in 15-ml culture tubes with mechanical shaking. After extraction for 5 min, about 1 ml of the organic upper phase was decanted into a glassvial for autoinjection into the gas chromatograph. A 3.0-μl

volume was injected twice if not stated otherwise. The ratio of peak area or height of benzalazine to that of the marker was calculated and plotted against concentration.

Standard solutions. A hydrazine stock solution (20 μg/ml) was prepared by dissolving 4.28 mg of hydrazine hydrochloride in 100.0 ml of water. The solution was then further diluted to obtain three standard solutions of 8, 16 and 24 ng/ml. These standards were prepared from a fresh stock solution for each analysis. They were used within 30 min and then discarded.

Calibration graphs. For the preparation of the calibration graphs 2.0 ml of each standard solution were analysed as above (duplicates). The derivatization time was 20 min.

Standard addition procedure. For the standard addition procedure the concentration of the hydralazine solution was 20 mg/ml and 1.0 ml of this solution was mixed with 1.0 ml of hydrazine hydrochloride standard solution (0, 8, 16 and 24 ng/ml, as hydrazine). The analysis was performed as described above. The derivatization time was 20 min for the first analyses, and 5 min for the latter ones, for the reason explained below.

RESULTS AND DISCUSSION

Capillary gas chromatography of azines

Capillary columns with neutral or slightly basic characteristics were chosen for the gas chromatography of benzalazine. Symmetrical peaks were observed and normally no carryover of samples in the system was noted. Occasionally, after several injections, the peaks on the SE-54 column showed a tendency to tail. This was eliminated by cutting off the first 20 cm of the column when necessary.

Choice of marker

One intention of this study was to find a more suitable marker for the chromatographic system. Matsui *et al.*[4] used 5-chloro-2-methylaminobenzophenone as an internal standard with a packed column. Preliminary experiments were performed with the azine of tolualdehyde as marker. A drawback with this marker was its difference in retention time compared with benzalazine, *i.e.*, about a 4 min longer time at the rate of 6°C/min and 60 kPa hydrogen inlet pressure. In the present method, with a rate of temperature increase of 15°C/min, the corresponding retention time difference was less than 2 min, which still is considered to be too long. The precision on repeated injections of a solution of the derivatives was 6.5%. In order to improve the accuracy of the chromatographic step a marker with a retention time closer to that of the derivative was desired.

It was found that 3- and 4-fluorobenzalazine both eluted 0.3 min earlier than benzalazine and were stable in heptane for several days. 4-Fluorobenzalazine was chosen as a marker owing to the good precision of the peak response ratios of benzalazine to marker. The relative standard deviation (R.S.D., n = 7–9) was 0.7% compared with 1.5% for the 3-fluoro derivative. This is better than the precision obtained using the azine with tolualdehyde as marker (Table I).

The other two markers tested were based on phenylhydrazine. The benzaldehyde derivative formed had a 0.3 min longer retention time than benzalazine and the R.S.D. was 16% (n = 5). The stability in excess benzaldehyde was poor (about 80%

TABLE I

RETENTION TIMES OF BENZALAZINE AND POSSIBLE MARKERS ON THE SE-54 CAPILLARY COLUMN

Column, 25 m × 0.32 mm I.D. with 0.25-μm SE-54; carrier gas, 100 kPa nitrogen inlet pressure; oven temperature, 100°C for 1 min then increased at 15°C/min; *ca.* 60 pg of each as hydrazine in heptane injected.

Retention time (min)	*Calculated elution temperature, (°C)*	*Compound*	*R.S.D.*[a] *(n = 7–9) (%)*
8.58	214	3-Fluorobenzalazine	1.5
8.61		4-Fluorobenzalazine	0.7
8.90	219	Benzalazine	
9.36		Phenylhydrazine phenylhydrazone	16
10.0	235	Phenylhydrazine tolylhydrazone	–[b]
10.6	244	Tolualdehyde azine	6.5

[a] Based on the peak-area ratio of benzalazine to the actual compound.
[b] Not measured.

loss after 24 h). The poor stability of the hydrazones of phenylalkylhydrazines with benzaldehyde has also been reported by Lovering *et al.*[5]. The retention time for the tolualdehyde derivative of phenylhydrazine was 1.1 min longer than that for benzalazine. The retention times of benzalazine and the different markers are summarized in Table I.

Reaction time

The optimum reaction time for hydrazine with 1% benzaldehyde in aqueous methanol was first investigated for 800 ng/ml aqueous hydrazine solutions. We used 33% methanol because at only 17%[4] droplets of benzaldehyde were present in the solution. The reaction was stopped by the addition of and extraction with heptane. It was found that an extracted and decanted sample was stable for several hours, even if the derivatization was not complete.

A plateau appeared after 15–20 min in the reaction time profile for a hydrazine solution of 800 ng/ml (Fig. 4). When hydralazine hydrochloride was included in the reaction mixture, 5 min seemed to be sufficient (Fig. 5). As no increase in benzalazine was noticed for longer reaction times (20–60 min) in any of these time-course profiles at the level of 800 ng/ml, 20 min was considered to be an adequate but not too long time for the reaction. In the original GC method[4] the derivatization time was 10 min followed by extraction for 30 min (Fig. 3a). Our own experiments showed that 2.5 min was sufficient for quantitative extraction and 5 min was selected for this step.

These conditions were then used for the analysis of aqueous standard solutions of hydrazine hydrochloride. Linear graphs were obtained with the intercept near the origin, *e.g.*, Fig. 6. The precision was acceptable (R.S.D. 8.4% at 20 ng/ml, $n = 9$). However, when standard addition analysis was performed on hydralazine hydrochloride the spread increased. The level of the samples without added hydrazine were often far from the curve. This prompted us to re-evaluate the reaction conditions in the actual low concentration range encountered. When hydrazine was added at 20 ng/ml, a significant increase in the benzalazine formed after a reaction time of about

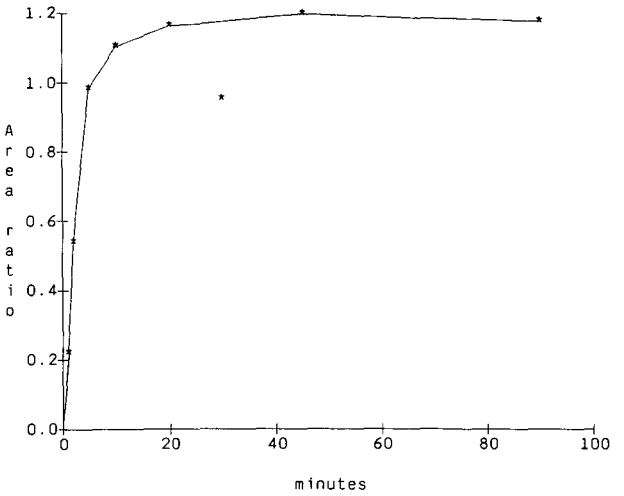

Fig. 4. Reaction time profile: formation of benzalazine from hydrazine hydrochloride, 800 ng/ml as base, with 1% benzaldehyde (0.098 *M*).

10 min was observed (Fig. 7). This increase can be explained either by degradation of the hydralazine Schiff base to hydrazine followed by condensation with benzaldehyde, or by a direct reaction of benzaldehyde with the Schiff base. A similar pathway has been proposed for the reaction of the acetone hydrazone of hydralazine with pyruvic acid[12]. The high hydrazine concentration used earlier of 800 ng/ml might explain why an increase in benzalazine was not observed for longer reaction times in the first rection time profiles. A plateau appeared between 2.5 and 7.5 min in most profiles at 20 ng/ml, and then benzalazine increased irregularly with time. The duration of the plateau was shortened when the samples were not shaken during the

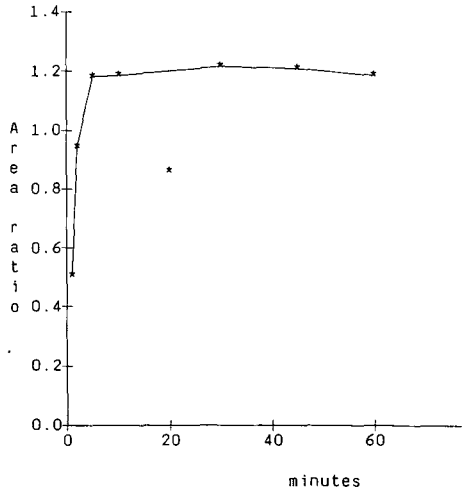

Fig. 5. Reaction time profile: formation of benzalazine from hydrazine hydrochloride, 800 ng/ml as base, with 1% benzaldehyde (0.98 *M*) in the presence of hydralazine hydrochloride, 20 mg/ml (as base).

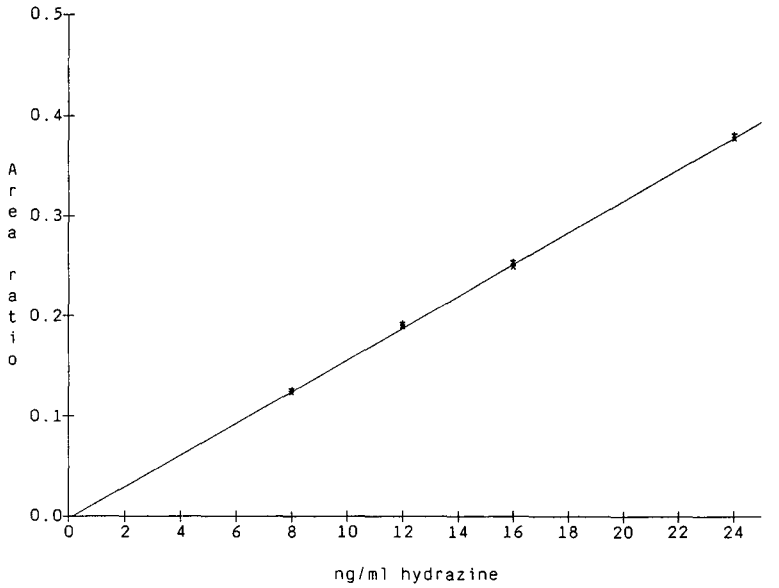

Fig. 6. Calibration graph for the determination of aqueous hydrazine hydrochloride. Marker concentration: 17 ng/ml in heptane (as hydrazine). Each point on the curve is the mean of two injections. Regression equation: $y = 0.016x + 0.0036$ ($r = 0.99993$).

reaction. The reason for this could be that the precipitation of the hydralazine Schiff base was now slower in the reaction tubes. Dissolved Schiff base can be expected to decompose at a faster rate when in solution than if it is present as crystals.

These results prompted a reduction in the derivatization time to 5 min, which was used for all further determinations. It can be concluded that if the actual reaction

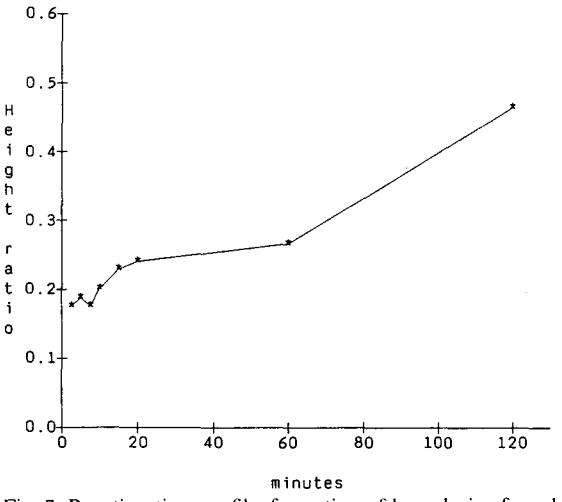

Fig. 7. Reaction time profile: formation of benzalazine from hydrazine hydrochloride, 20 ng/ml as base, with 1% benzaldehyde (0.098 *M*) in the presence of hydralazine hydrochloride, 20 mg/ml (as base).

time is too short this will only affect the slope of the standard addition curve and not the intercept on the abscissa. On the other hand, if the reaction time is too long benzalazine will be formed in equal amounts in all samples from hydralazine and the curve thus moves up parallel to the theoretical curve and the intercept on the abscissa thus increases. This will lead to falsely high levels of hydrazine. The final method is outlined in Fig. 3b.

Stability of solutions and derivatives formed

Hydrazine solutions. A solution containing 20 ng/ml decomposed by 6% during 2 h and by 50% during 24 h, as can be seen in Fig. 8. Even the hydrazine stock solution (20 μg/ml) was found to be unstable. A loss of about 46% was observed after 2 weeks at room temperature in the dark.

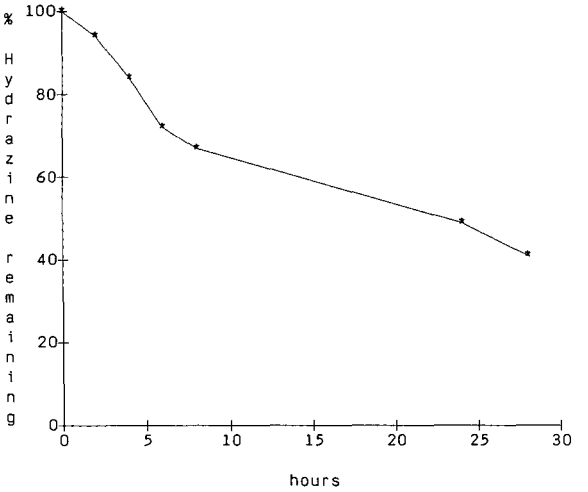

Fig. 8. Time course for the decomposition of a diluted hydrazine solution given as a percentage of the orginal concentration. A stock solution of hydrazine hydrochloride was diluted to 20 ng/ml (as base), from which 2.0-ml duplicates were withdrawn and analysed after reaction with benzaldehyde for 20 min.

Matsui *et al.*[2] reported that the stability of the dihydrochloride was superior to that of the sulphate or hydrate for their calibration standard of concentration 24 μg/ml. The stock standard solution was used during the day of its preparation and the working standards prepared by dilution were used immediately.

Hydralazine solution. A 10 mg/ml aqueous hydralazine solution was shown to decompose. After 1 h an increase in hydrazine as benzalazine of 21% was observed, and after 5 hours it was *ca.* 200%. The time course is illustrated in Fig. 9. This instability has been mentioned elsewhere[2].

Benzalazine. Butterfield *et al.*[3] reported that benzalazine is not stable in the pH 3.5 aqueous reaction medium used when hydrazine sulphate was the starting material. Significant decomposition started after 20 min with benzaldehyde in unbuffered media. With hydrazine dihydrochloride as the starting material the benzalazine formed was stable for at least 35 min[2].

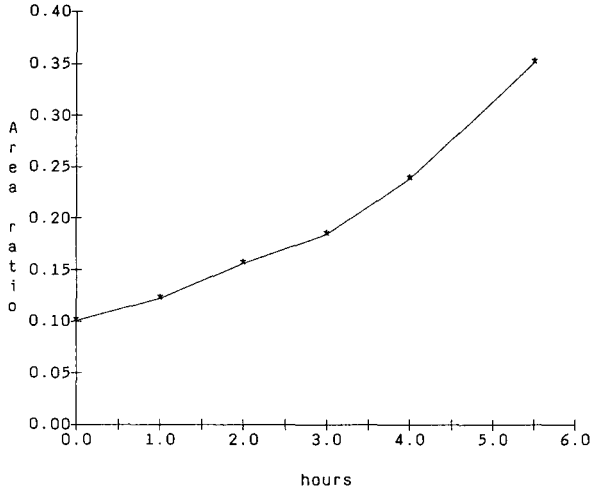

Fig. 9. Time course for the formation of hydrazine in an aqueous hydralazine hydrochloride solution, 10 mg/ml (as base). Duplicates of 2.0 ml were withdrawn and analysed by reaction with benzaldehyde for 20 min followed by extraction.

When investigating liquid chromatography with mass spectrometry (LC–MS) as a possible technique for the determination of hydrazine in hydralazine, the reaction with benzaldehyde was performed with a dodecadeuterated benzalazine marker present. This deuterated compound was partly converted to benzalazine[13], indicating that transfer or exchange of the aldehyde moiety can occur. This observation was investigated further and confirmed by an experiment in which the transformation of

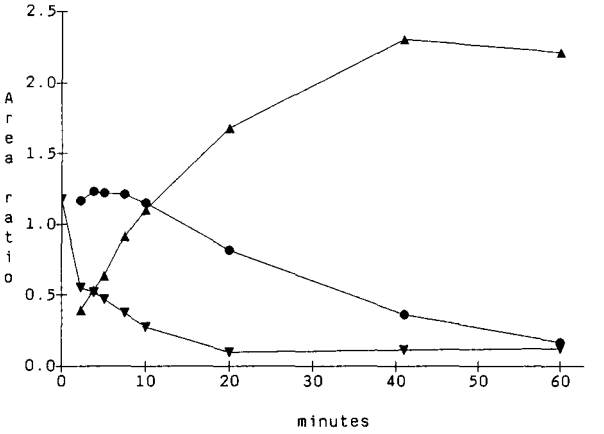

Fig. 10. Time course for the transformation of benzalazine to an azine with tolualdehyde (0.011 *M*). Benzalazine (60 μg) was dissolved in 3.0 ml of methanol and 6.0 ml of buffer (pH 3.0) (ionic strength = 0.05, phosphate). Just before time zero, one 0.5-ml sample was withdrawn and extracted with 1.5 ml of heptane containing 100 ng/ml of the marker. At time zero, 10 μl of tolualdehyde were added, the tube was kept agitated and samples were withdrawn at suitable time intervals for analysis as described. ▼, Benzalazine; ●, mixed azine derivative; ▲, azine with tolualdehyde.

benzalazine to an azine with tolualdehyde was studied. The time course is shown in Fig. 10. The actual concentration of the aldehyde was reduced to 0.1% as with the standard 1% concentration of reagent the exchange was virtually instantaneous. Even with this lower concentration only 50% of the initial benzalazine concentration remained after 2 min. Simultaneously the mixed azine has its maximum at about 4 min Fig. 10). Similar transformation has been reported when benzalazine was mixed with pentafluorobenzaldehyde at pH 5.2[14] using a molar ratio of 1:20. Here the reaction was slower, 50% of benzalazine remaining after 2 h.

Hydralazine Schiff base. Formation of additional benzalazine from the hydralazine Schiff base in the heptane phase (after extraction) seemed to be serious in the presence of the aqueous phase. The initial benzalazine content was doubled after 5 h. However, once the separated heptane phase was decanted into a glass vial, the derivative was found to be stable for several days. Repeated analyses of decanted samples gave a benzalazine-to-marker ratio within 5%. This indicates that the benzaldehyde reagent mainly remained in the aqueous phase and/or that a protic solvent is required for the transformation.

Reaction yield and precision of the method

The quantitative reaction yield for the derivatization of aqueous hydrazine solutions was about 86% for 12 ng/ml and 94% for 24 ng/ml. References were heptane solutions of pure benzalazine of about the same concentrations with respect to hydrazine. The precision of analysis was determined by analysing ten samples of derivatized and extracted hydrazine (20 ng/ml). The amount of benzalazine injected was 98 pg, and the R.S.D. of the area count ratio of benzalazine to that of the marker was 7.7% (6.5% for $n = 9$).

Analysis of hydralazine batches

Owing to the low levels of hydrazine found in preliminary determinations the standard addition principle was considered to give more accurate values than calculation from calibration graphs. The levels of hydrazine in ppm found in different hydralazine batches 1–2 years old are presented in Table II. An example of a standard addition curve is presented in Fig. 11 and a series of representative gas chromatograms are shown in Fig. 12. The levels found were in the range 0.3–0.4 ppm. These values are near the limit of quantification with the present method.

TABLE II

HYDRAZINE IN HYDRALAZINE SAMPLES

Analysis by standard addition of hydrazine and a reaction time of 5 min with benzaldehyde.

Sample code	*Source*	*Hydrazine (ppm)*
A = 064675 01	Ciba-Geigy	0.27
B = 063495 01	Ciba-Geigy	0.39
H = 072069 01	Ciba-Geigy	0.34
F	See *Reagents and chemicals* section	0.29

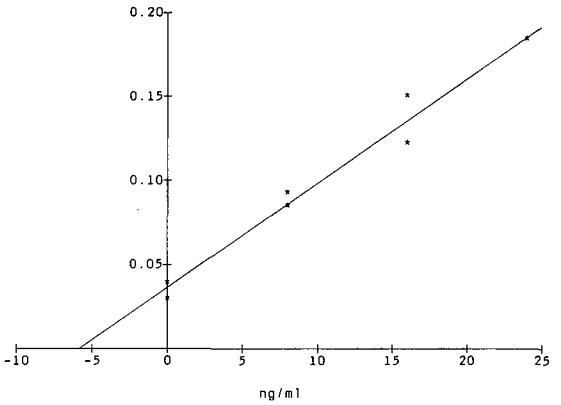

Fig. 11. Standard addition curve for hydrazine in hydralazine hydrochloride, batch F, 20 mg/ml (as base). Each point on the curve is the mean of two injections. Regression equation: $y = 0.0082x + 0.026$ ($r = 0.9234$). Concentration found: 5.8 ng/ml, which corresponds to 0.29 ppm.

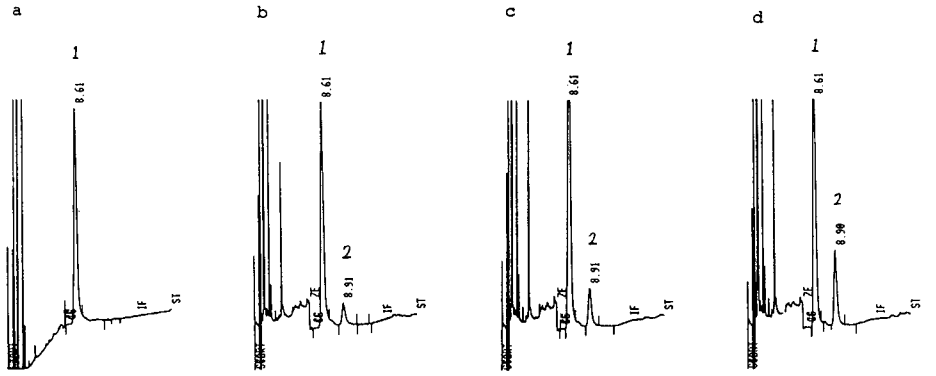

Fig. 12. Gas chromatograms with nitrogen-selective detection after analysis of hydralazine, 20 mg/ml. (a) Blank; (b) no hydrazine; (c) 8 ng/ml of hydrazine added; (d) 24 ng/ml of hydrazine added. Peaks: 1 = 4-fluorobenzalazine (marker), 17 ng/ml as hydrazine; 2 = benzalazine. Chart speed: 0.2 cm/min, and 2.0 cm/min from 8.5 min. SE.54 column. For other details, see Experimental.

ACKNOWLEDGEMENTS

We express our gratitude to Mr. Lars Johansson for capillary column support and to M. Jean-Pierre Callens for technical assistance during part of this work.

REFERENCES

1 *Evaluation of Carcinogenic Risk of Chemicals to Man* (*IARC Monographs No. 4*), International Agency for Research on Cancer, Lyon, 1974, p. 127.
2 F. Matsui, D. L. Robertson and E. G. Lovering, *J. Pharm. Sci.*, 72 (1983) 948.
3 A. G. Butterfield, N. M. Curran, E. G. Lovering, F. F. Matsui, D. L. Robertson and R. W. Sears, *Can. J. Pharm. Sci.*, 16 (1981) 15.

4 F. Matsui, A. G. Butterfield, N. M. Curran, E. G. Lovering, R. W. Sears and D. L. Robertson, *Can. J. Pharm. Sci.*, 16 (1981) 20.
5 E. G. Lovering, F. Matsui, D. L. Robertson and N. M. Curran, *J. Pharm. Sci.*, 74 (1985) 105.
6 S.-O. Jansson, personal communication.
7 J. Mañes, P. Campillos, G. Font, H. Martre and P. Prognon, *Analyst (London)*, 112 (1987) 1183.
8 J. Mañes, M. J. Gimeno, J. C. Moltó and G. Font, *J. Pharm. Biomed. Anal.*, 6 (1988) 1023.
9 K. H. Schaller and J. Lewalter, *Fresenius Z. Anal. Chem.*, 334 (1989) 712.
10 K. Ravichandran and R. P. Baldwin, *Anal. Chem.*, 55 (1983) 1782.
11 P. E. Kester and N. D. Danielsson, *Chromatographia*, 18 (1984) 125.
12 M. Iwaki, T. Ogiso and Y. Ito, *J. Pharm. Sci.*, 77 (1988) 280.
13 L. Grönberg and K.-E. Karlsson, unpublished work, 1988.
14 Y.-Y. Liu, I. Schmeltz and D. Hoffmann, *Anal. Chem.*, 46 (1974) 885.

Journal of Chromatography, 511 (1990) 317–323
Elsevier Science Publishers B.V., Amsterdam

CHROM. 22 404

Trace determination of lower volatile fatty acids in sediments by gas chromatography with chemically bonded FFAP columns

CORNELIS A. HORDIJK, ILSE BURGERS, GERARDINA J. M. PHYLIPSEN and THOMAS E. CAPPENBERG*

Limnological Institute, Vijverhof Laboratory, Rijksstraatweg 6, 3631 AC Nieuwersluis (The Netherlands)

(First received November 21st, 1989; revised manuscript received March 5th, 1990)

ABSTRACT

A capillary gas–liquid chromatography method was developed for the quantification of free lower volatile fatty acids (LVFA) in freshwater sediments. The method is based on the application of water-resistant FFAP (free fatty acid phase) columns and splitless injection. An important feature is the ability to determine LVFA directly at picomole levels in 1–3 μl of water without sample extraction, clean-up or derivatization. Continuous saturation of the carrier gas with formic acid is superfluous, making this method compatible with mass-selective detection. Detection limits of 0.2 pmol can be obtained for propionate with mass-selective detection and 1 pmol for acetate with flame ionization detection. The ability to study LVFA metabolism using stable isotope tracers is discussed. The method allows the measurement of well defined concentration profiles (4–70 μM) in sediment pore waters and is a good alternative to existing techniques for determining trace amounts of LVFA in very small volumes of organic-rich matrices.

INTRODUCTION

Lower volatile fatty acids (LVFA) such as acetate and propionate, generated during diagenesis of organic matter, play a key function in aquatic ecosystems as precursors of methanogenesis and respiration[1–3]. Respiration in meso-eutrophic lakes is limited mainly to the top few centimeters of the sediment–water interface[4] while methanogenesis occurs in deeper strata, making spatial differences in LVFA metabolism with sediment depth expected. A study of natural concentration profiles of LVFA and their actual turnover rates will lead to a better understanding of complex interactions between fermentative and respiratory processes. A knowledge about the actual conversion of LVFA to carbon dioxide and methane in freshwaters is still limited, however, owing to the lack of analytical methods[2] for measuring low LVFA concentrations (4–70 μM) routinely in very small sample volumes of porewater.

0021-9673/90/$03.50

Gas–liquid chromatography (GLC) is routinely applied to the determination of LVFA of food[5], clinical[6], atmospheric[7] and waste-water samples[8]. Ion-exclusion chromatography (IEC) is a alternative for determining LVFA in relatively clean matrices such as Antarctic ice water[9], but trace measurements in sediments can be complicated by interfering peaks[10]. To analyse sediments by IEC requires sample clean-up methods such as vacuum distillation[11] or ultrafiltration[12]. In an earlier study we determined LVFA, including formate and lactate, after derivatization to a fluorophore[2]. Detection limits below 100 fmol can be achieved but complex sample pretreatment is required[2]. For determining volatile acids only, GLC without derivatization or sample purification is preferable for its speed and simplicity[13].

Recently, FFAP-CB (free fatty acid phase chemical bond; Varian) capillary columns have been introduced[15]. These columns tolerate aqueous injections, making them very suitable for the determination of hydrophilic LVFA. Capillary columns facilitate the application of mass-selective detectors and consequently the use of stable isotopes to trace metabolic processes as discussed in this paper.

EXPERIMENTAL

Apparatus

A Hewlett-Packard Model 5890 gas chromatograph with a split–splitless injection port, a 90 × 4 mm I.D. glass liner and a flame ionization detector was used. The capillary columns were a 10 m × 0.53 mm I.D. column coated with 1-μm FFAP-CB wax (Hewlett-Packard) and a 25 m × 0.32 mm I.D. column coated with 0.33-μm FFAP-CB wax (Chrompack, Middelburg, The Netherlands). Chromatographic conditions are given in Table I. The column was primed daily by ten injections of 1.0% formic acid (Suprapur; Merck, Darmstadt, F.R.G.) in Milli-Q water.

TABLE I

CHROMATOGRAPHIC CONDITIONS FOR THE DETERMINATION OF LVFA USING 25 m × 0.32 mm I.D. AND 10 m × 0.53 mm I.D. CAPILLARY FFAP-CB COLUMNS

Programme	*Column I.D. (mm)*		
	0.32 (FID)	*0.32 (MS)*	*0.53 (FID)*
Injector temperature	225°C	150°C	150°C
Detector temperature	260°C	250°C	200°C
Isothermal period	80°C (1.10 min)	80°C (1.10 min)	70°C (1.10 min)
First ramp rate	15°C min^{-1}	15°C min^{-1}	10°C min^{-1}
Isothermal period	105°C (1.00 min)	105°C (1.00 min)	105°C (0.25 min)
Second ramp rate	10°C min^{-1}	15°C min^{-1}	n.d.
Isothermal period	140°C (1.00 min)	140°C (1.00 min)	n.d.
Purge on time	1.1 min	1.1 min	1.1 min
Purge off time	2.5 min	2.5 min	4.8 min
Gases (ml min^{-1})			
Carrier gas (He)	4	4.5	20
Make up gas (He)	35	27	20
Septum vent	1	1	1
Purge vent	30	30	30

For peak identification, a C_1–C_{10} fatty acid mixture (Supelco, Bellefonte, PA, U.S.A.) and gravimetric standards (Suprapur; Merck) were analysed with an HP 5970 mass-selective detector, to which a 25 m × 0.32 mm FFAP (Chrompack) column was linked. Samples (0.5 μl) were introduced by splitless injection. Chromatographic conditions are included in Table I; the vacuum in the mass-selective detector was below $8 \cdot 10^{-5}$ Torr and the ionization energy was 70 eV. During elution, continuous scans were made from m/z 44 to 550. The mass spectral data were processed with an HP-300 computer to trace molecular ions (M^+) or specific fragments originating from LVFA. Sediment and stable isotope analysis were performed by selective ion monitoring (SIM).

Sediment analysis

Undisturbed sediment cores were taken with a Jenkin sampler from Vechten, a 10-m deep lake with a clay-rich anoxic sediment[1]. Samples of 0.35 g were drawn by syringe through 2.8-mm holes (covered with Scotch tape No. 471) in the acrylic glass sampling core. The samples were centrifuged at 1000 *g* for 5 min in 0.4-ml polypropylene sampling tubes (Emergo, The Netherlands). The supernatant was separated and frozen for storage. Before injection, 100 μl of supernatant were adjusted with 1 μl of 50% formic acid (Suprapur; Merck). A volume of 3 μl was injected in duplicate or triplicate into the gas chromatograph. Calibration was done by external standardization with gravimetric standards (0–50 μM) of acetate (Suprapur; Merck), [$^2H_3$]acetate (99.5% pure; Aldrich, Beerse, Belgium) and propionate (analytical-reagent grade; J. T. Baker, Philipsburgh, NY, U.S.A.) in Milli-Q water, acidified with 0.5% (v/v) formic acid. The glass insert in the injector needs regular cleaning; pushing a wetted ball of crumpled paper though the insert is usually sufficient to pick up deposits.

RESULTS

With FFAP-CB, good separation of acetate and propionate from other LVFA was achieved (Figs. 1 and 2). Only intense molecular ion peaks of acetate (m/z 60 and 61), propionate (m/z 73–77) and butyrate (m/z 88) were recovered in scans of the fatty acid mixture. Other LVFA were identified by their retention times and interpretation of related spectra. Formate (m/z 44–46) was not recovered in the ion chromatograms. [$^2H_3$]Acetate signals (m/z 63) were of same intensity as those of unlabelled acetate.

Sediment samples (natural pH 7.5–8; 5–10 mequiv l^{-1} HCO_3^-) require acidification (pH < 4.5) to improve volatilization and suppress adsorption in the instrument. At pH 4.5–5.5 the peak heights were already 70% lower. New columns require 0.5% formic acid acidification, but contaminated columns need a higher concentration. Only the acetate blank was affected by formic acid addition; an increase in formic acid concentration by 0.5% leads to a *ca.* 2 μM rise in the acetate blank. With 0.5% formic acid, the acetate blanks for Milli-Q water (1.5–4 μM) were similar to those previously found (2–5 μM[2]). The reproducibility improved with increasing concentration (Table II), column diameter and with injection volume [0.53 mm I.D. column and 25 μM: 0.5 μl, 10.5%; 3 μl, 1.2%; 5 μl, 0.6% (n = 5)]. With the 0.32 mm I.D. column the relationship between injection volume and peak height was linear up to 8 μl (r = 0.993) and with the 0.53 mm I.D. column until at least 5 μl (r = 0.997) for acetate.

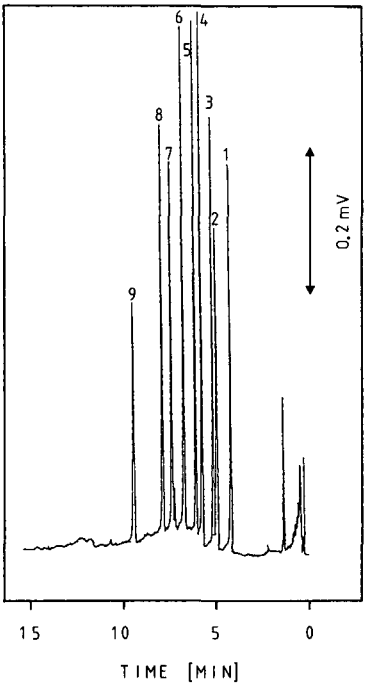

Fig. 1. Chromatogram of a mixture of volatile fatty acids (Supelco; 3 μl 100 μM or 300 pmol each) by GLC with a 25 m × 0.32 mm I.D. FFAP column and FID. Peaks: 1 = acetic acid; 2 = propionic acid; 3 = isobutyric acid; 4 = butyric acid; 5 = valeric acid; 6 = isovaleric acid; 7 = capronic acid; 8 = isocapronic acid; 9 = heptanoic acid.

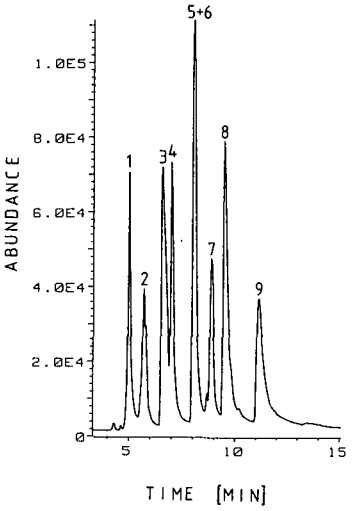

Fig. 2. Composed ion chromatogram of a mixture of volatile fatty acids (0.6 μl, 100 μM or 60 pmol each) by GLC on a 25 m × 0.32 mm I.D. FFAP column and MS processed in the SIM mode. The ion chromatogram was composed by summation of intensities of ions of m/z 45 and 60. Peaks as in Fig. 1.

TABLE II

RELATIONSHIP BETWEEN RELATIVE STANDARD DEVIATION, CONCENTRATION (n = 10) AND COLUMN DIAMETER FOR ACETATE ANALYSIS WITH SPLITLESS INJECTION (3 μl) AND FID

Standards were made in Milli-Q water (blank 3 μM) which was acidified with 0.5% formic acid.

Concentration (μM)	*Relative standard deviation (%)*	
	0.32 mm I.D. column	*0.53 mm I.D. column*
0	19	7
5	14	9
10	8	4
25–100	8	3

The detection limits, defined as a signal change equal to three times the signal-to-noise ratio, were 1–3 pmol for flame ionization detection (FID), and 0.2–0.7 pmol for mass-selective detection (MS) (Table III). Acetate calibration graphs [signal obtained by summation of ABU (abundance units or relative intensity) for m/z 45 and 60) were linear from 20 to 400 pmol (r = 0.947). Below 20 pmol the curves flatten. The [$^2H_3$]acetate (m/z 63; r = 0.998) and propionate calibration graphs (m/z 45 and 75; r = 0.957) were linear from 0.2 to 400 pmol.

DISCUSSION

Capillary FFAP-CB columns can be applied to the trace determination of LVFA (<200 pmol) in aqueous samples. Gross sediment sample sizes of 300 μl can be processed with ease as only 3 μl of centrifugate are needed for GLC. Continuous

TABLE III

COMPARISON OF DETECTION LIMIT, LINEAR RANGE AND SENSITIVITY OF THE DETERMINATION OF ACETATE AND PROPIONATE BY GLC

The signal of acetate was composed of m/z 45 and 60 and that of propionate m/z 45 and 74.

Detection	*Column I.D. (mm)*	*Detection limit (pmol)*	*Linear range*		*Sensitivity (attenuation 32)*[a]
			pmol	*r*	
Acetate					
FID	0.32	1	0–150	0.990	5.7 μV pmol^{-1}
FID	0.53	1	0–125	1.000	6.7 μV pmol^{-1}
MS	0.32	0.2	30–400	0.947	261 ABU pmol^{-1}
Propionate					
FID	0.32	3	n.d.	n.d.	4.7 μV pmol^{-1}
FID	0.53	2.5	0–125	0.999	5.8 μV pmol^{-1}
MS	0.32	0.7	0–400	0.957	86 ABU pmol^{-1}

[a] ABU, abundance units.

saturation of the carrier gas with formic acid vapour to suppress ghosting[2,13,14] was unnecessary. Sample pretreatment requires no purification or concentration step, thereby avoiding losses due to ineffective extraction or freeze-drying[2]. Derivatization of LVFA in pore water requires excess of reagent, as part of the reagent will be neutralized by dissolved organic carbon[2]. Addition of an excess of reagent implies that reproducibility of the reagent blanks rather than the detection limit of the derivative determines the accuracy at trace levels. Lactate, for example, does not appear as an impurity in reagents and can be well determined as a derivative. Acetate, however, is a common contaminant in reagents and solvents[2]. Using the FFAP-CB column, reagent interference is circumvented and only the instrument blank limits the linear dynamic range in which acetate can be accurate determined (Table II). The absence of a reagent label has for MS a second advantage that stable isotope signals originate only from isotope in the LVFA molecules themselves. Note that ^{13}C in aromatic reagent labels can contribute considerably to "blank" signals.

The practical advantages of using stable isotope labelling instead of radioactive isotopes[3] are obvious. Stable isotope tracers can be used for fieldwork or in ordinary laboratories without special licenses. We previously applied on-line gas proportional counting of radioactively labelled LVFA[3]. In the proportional counter most of the chromatographic resolution was lost, which is not the case with MS (Fig. 2). Similar MS chromatograms of free LVFA (Fig. 2) have, to our knowledge, not yet been published. Of the LVFA, only formate (m/z 44–46[16]) could not be detected by MS or FID and derivatization or other techniques[2,10,17] may be required for this compound.

Sediment analysis

Profiles of free acetate concentrations measured in 1988 and 1989 in sediment porewater from Lake Vechten (Fig. 3) regularly showed similarly shaped concentration profiles to those observed in 1978[4] and 1983[2], but the peaks in the profiles

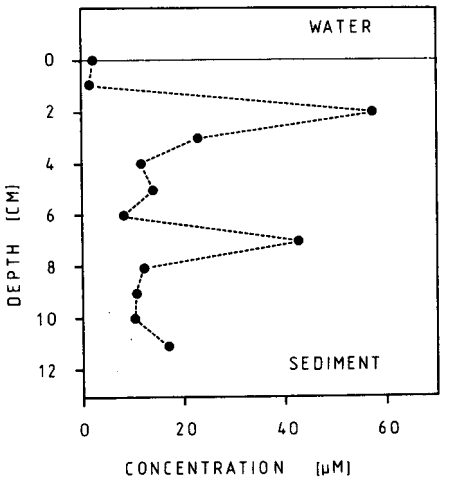

Fig. 3. Profile of free acetate concentration with sediment depth in pore water collected in Lake Vechten on April 24th, 1989.

measured with the FFAP-CB column were much sharper. Although changes in LVFA metabolism in the lake cannot be excluded, the lower concentrations found in 1978 and 1983 can be ascribed to dilution effects due to the larger sample sizes (5–10 ml instead of 0.35 ml) used in previously applied techniques. The sharp sediment acetate peaks obviously reflect intense acetogenesis under well defined metabolic conditions. The acetate peak just below the sediment–water interface can be explained by respiratory and/or diffusion processes[2,3]; the peak at -6 cm, however, hints at as yet unexplained fermentative processes. To unravel these processes, [$^2H_3$]acetate can be used as a tracer.

In conclusion, GLC on capillary FFAP columns is a good alternative to existing techniques for the determination of trace amounts of acetate and higher homologues in small sample volumes of organic-rich matrices such as sedimental porewater.

ACKNOWLEDGEMENTS

We thank Hewlett-Packard (The Netherlands) and Chrompack (The Netherlands) for the opportunity to test several types of capillary columns. We also thank our colleagues R. D. Gulati and M. E. Sierszen for helpful reviews of the manuscript.

REFERENCES

1 T. E. Cappenberg, *J. Microbiol. Serol.*, 40 (1974) 285.
2 C. A. Hordijk and T. E. Cappenberg, *Appl. Environ. Microbiol.*, 46 (1983) 361.
3 T. E. Cappenberg and E. Jongejan, in *Environmental Biogeochemistry and Geobiology*, Vol. 1, Ann Arbor Sci. Publ., Ann Arbor, MI, 1978, p. 129.
4 C. A. Hordijk, M. Snieder, J. J. M. van Engelen and T. E. Cappenberg, *Appl. Environ. Microbiol.*, 53 (1987) 217.
5 D. L. Schooley, F. M. Kubiak and J. V. Evans, *J. Chromatogr. Sci.*, 23 (1985) 385.
6 B. Schatowitz and G. Gercken, *J. Chromatogr.*, 425 (1988) 257.
7 K. Kawamura, L.-L. Ng and I. R. Kaplan, *Environ. Sci. Technol.*, 19 (1985) 1082.
8 A. Yasuhara, *Agric. Biol. Chem.*, 51 (1987) 2259.
9 C. Saigne, S. Kirchner and M. Legrand, *Anal. Chim. Acta*, 203 (1987) 11.
10 D. J. Kieber, G. M. Vaughan and K. Mopper, *Anal. Chem.*, 60 (1988) 1654.
11 J. E. Tyler and G. H. Dirbin, *J. Chromatogr.*, 105 (1975) 71.
12 H. M. Chen and C. H. Lifschitz, *Clin. Chem.*, 35 (1989) 74.
13 G. C. Cochrane, *J. Chromatogr. Sci.*, 13 (1975) 440.
14 M. H. Henderson and T. A. Steedman, *J. Chromatogr.*, 244 (1982) 337.
15 G. Gaspar and J. de Zweeuw, *Analusis*, 16 (1988) 54.
16 G. P. Happ and D. W. Steward, *J. Am. Chem. Soc.*, 74 (1952) 4404.
17 I. Mueller-Harvey and R. J. Parkes, *Estuarine Coastal Shelf Sci.*, 25 (1987) 567.
18 K. Tanaka and J. S. Fritz, *J. Chromatogr.*, 361 (1986) 151.

Journal of Chromatography, 511 (1990) 325–332
Elsevier Science Publishers B.V., Amsterdam

CHROM. 22 413

Degradation and analysis of commercial polyoxyethylene glycol mono(4-alkylphenyl) ethers

J. SZYMANOWSKI*
Technical University of Poznań, Institute of Chemical Technology and Engineering, Pl. M. Sklodowskiej-Curie 2, 60-965 Poznań (Poland)
and
P. KUSZ and E. DZIWIŃSKI
Institute of Heavy Organic Synthesis "Blachownia", 47-225 Kędzierzyn-Koźle (Poland)
(Received December 1st, 1989)

ABSTRACT

Commercial polyoxyethylene glycol mono(4-alkylphenyl) ethers having different degrees of ethoxylation were degraded in the presence of acetyl chloride and anhydrous iron(III) chloride. Compounds formed from polyoxyethylene chains can be easily and precisely determined and their contents can be used to calculate the average degree of ethoxylation.

INTRODUCTION

In a previous study[1], the degradation of model oligooxyethylene glycol mono(4-alkylphenyl) ethers was investigated and used to determine the average degree of alkylphenol ethoxylation. Good agreement between the average degrees of ethoxylation determined by means of degradation and by direct analysis was observed.

The composition of commercial products is usually much more complex than that studied previously[1]. In most instances nonylphenol is used as one reagent and contains several components, including different types of compounds and different isomers of the nonyl group. Up to now, their structures have not been determined. The average degree of ethoxylation is usually higher than that considered in our previous work[1]. Depending on the value of this average degree of ethoxylation, direct analysis gives results that more or less deviate from the actual values or it may even be impossible to analyse such products.

The aim of this work was to study the degradation of commercial polyoxyethylene glycol mono(4-alkylphenyl) ethers in the presence of an excess of acetyl chloride and anhydrous iron(III) chloride[2] and the application of this degradation to determine the average degree of alkylphenol ethoxylation.

0021-9673/90/$03.50

EXPERIMENTAL

The commercial polyoxyethylene glycol mono(4-alkylphenyl) ethers used were Rokafenol N-5 (NZPO "Rokita", Brzeg Dolny, Poland) and Lutensol AP-4, Lutensol AP-9 and Lutensol AP-14 (BASF, Ludwigshafen, F.R.G.). Analytical-reagent grade acetyl chloride (Fluka, Buchs, Switzerland) and anhydrous iron(III) chloride (POCh, Gliwice, Poland) were also used.

The degradation and chromatographic analyses were carried out according to the methods described previously[1].

Chromatographic columns (0.9 m × 2.7 mm I.D.) filled with silicone resin OV-101 (3%) on Chromosorb G AW DMCS (60–80 mesh) were used for the direct analysis of commercial polyoxyethylene glycol mono(4-alkylphenyl) ethers. The temperature of these columns was 100°C for 1 min, then raised to 320°C at 8°C/min. Chromatographic columns (0.9 m × 2.7 mm I.D. and 1.6 m × 2.7 mm I.D.) filled with silicone resin OV-17 (3%) on Chromosorb G AW DMCS (60–80 mesh) and with Carbowax 20M–TPA (terminated with terephtalic acid) (12%) on Chromosorb W AW DMCS (80–100 mesh) were used for the analyses of degradation products. Their temperatures were 80°C and 100°C for 1 min, then raised to 290°C and 220°C at 6°C/min and 5°C/min, respectively.

The average degree of ethoxylation and the degree of degradation were calculated in the same way as for oligooxyethylene glycol mono(4-*tert.*-octylphenyl) ethers[1].

RESULTS AND DISCUSSION

Chromatograms of Lutensol AP-4, Rokafenol N-5 and Lutensol AP-9 are given in Figs. 1–3. They were separated as broad peaks according to the increased numbers of oxyethylene groups. Their compositions and retention indices are given in Table I. Separation was good but only up to the homologue containing ten oxyethylene units.

TABLE I

RETENTION INDICES AND CONTENTS OF SUCCESSIVE HOMOLOGUES

Silicone resin OV-101.

No. of oxyethylene groups	*Retention index, I_p*	*Content (wt.-%)*		
		Lutensol AP-4	*Rokafenol N-5*	*Lutensol AP-9*
0	1668–1737	0.14	1.03	0.95
1	1929–2067	2.10	6.85	1.31
2	2170–2284	15.56	17.66	1.85
3	2416–2540	26.52	22.66	5.46
4	2680–2789	25.93	20.51	11.98
5	2909–3027	17.48	14.60	18.18
6	3153–3258	8.78	9.64	21.09
7	3371	2.68	5.13	19.68
8	3640	0.32	1.57	14.14
9	3881	–	0.20	4.78
10	4135	–	0.15	0.58

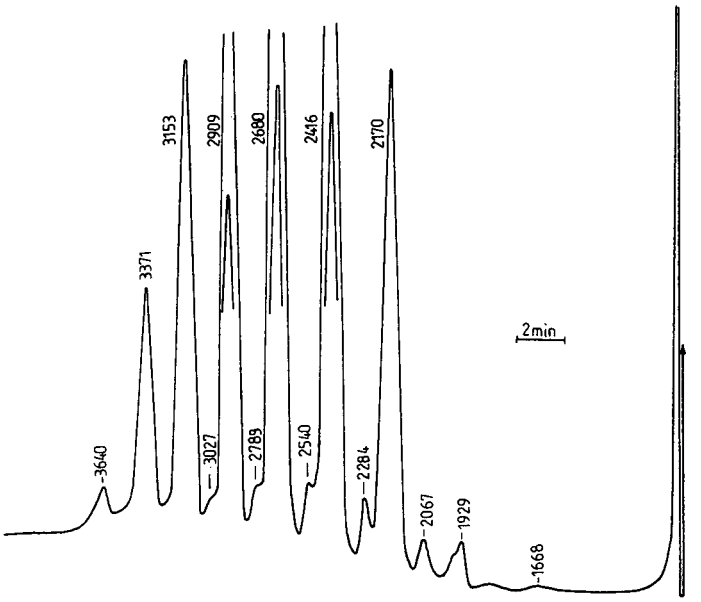

Fig. 1. Chromatogram of Lutensol AP-4 (acetate derivatives, OV-101). Numbers at peaks are retention indices.

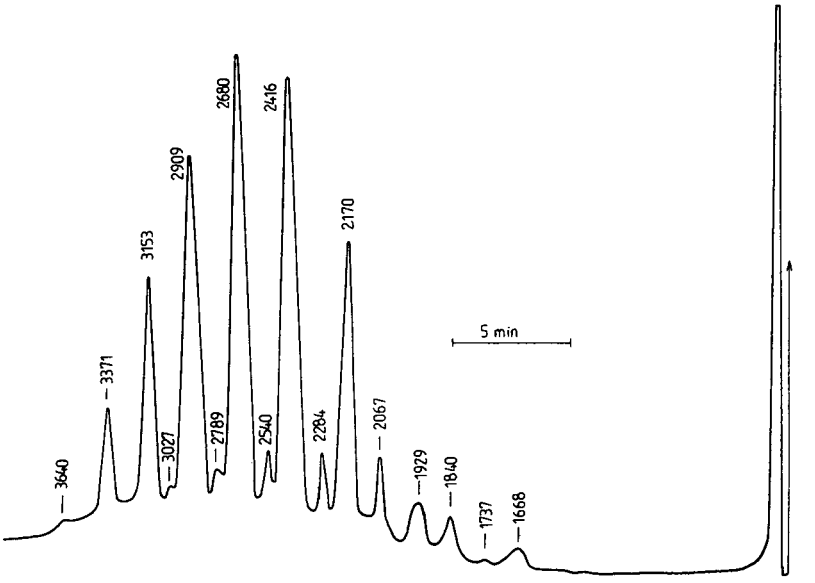

Fig. 2. Chromatogram of Rokafenol N-5 (acetate derivatives, OV-101).

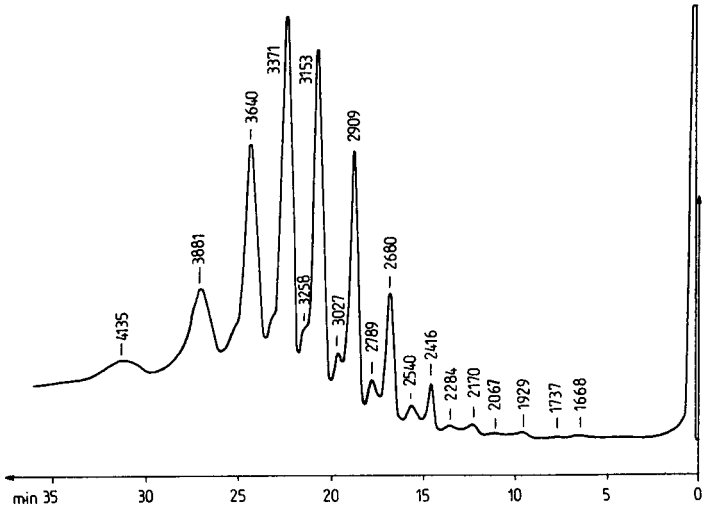

Fig. 3. Chromatogram of Lutensol AP-9 (acetate derivatives, OV-101).

Lutensol AP-14 contains higher homologues than those present in previous preparations and it elutes from the column only to the extent of about 2%, hence it was impossible to analyse it directly). Its degradation was complete at 150°C after 30 min (Fig. 4). Under these conditions the degradation of other commercial preparations investigated was also complete and the peaks of the initial components were not observed on the chromatograms. The chromatograms of the degradation products of Lutensol AP-9 shown in Figs. 5 and 6 demonstrate the completeness of degradation and the similarity of the degradation products to those identified previously[1].

2-Chloroethyl acetate (I_p = 1318 on Carbowax 20M–TPA) is the main product formed by the degradation of the polyoxyethylene chains. 1,2-Dichloroethane (I_p =

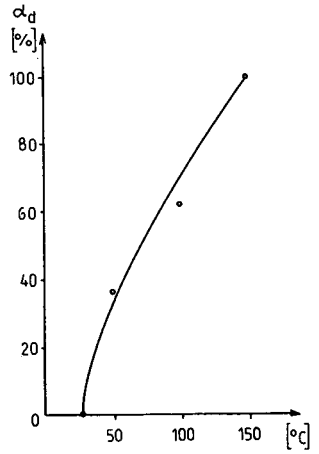

Fig. 4. Effect of temperature on degree of degradation (α_d) of Lutensol AP-14 (30 min).

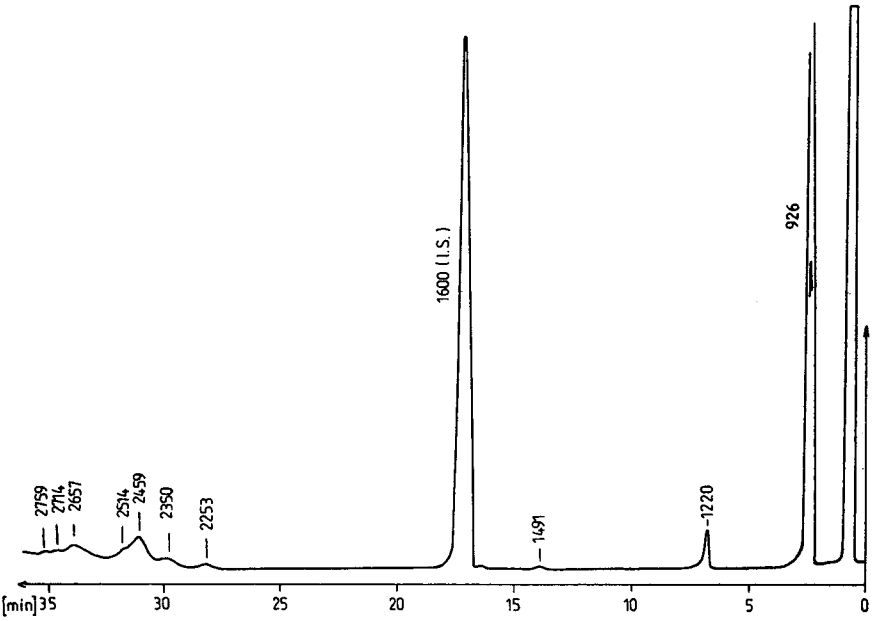

Fig. 5. Chromatogram of the degradation products formed from Lutensol AP-9 (silicone resin OV-17). I.S. = Internal standard.

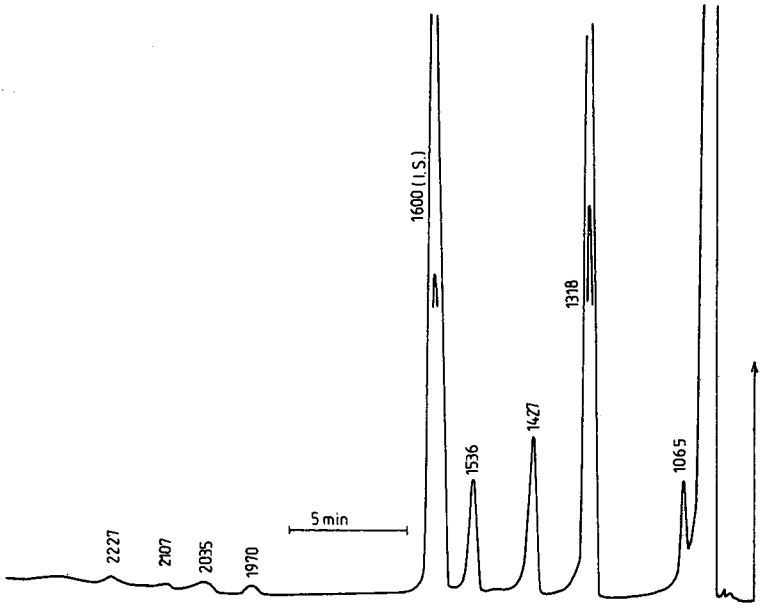

Fig. 6. Chromatogram of the degradation products formed from Lutensol AP-9 (Carbowax 20M–TPA).

TABLE II

COMPOSITION OF DEGRADATION PRODUCTS

Type of compound[a]	*Component*	*Retention index*		*Content (wt.-%)*			
		Carbowax 20M–TPA	*OV-17*	*Lutensol AP-4*	*Rokafenol N-5*	*Lutensol AP-9*	*Lutensol AP-14*
I	1,2-Dichloroethane	1065	745	2.33	1.08	7.05	2.83
	2-Chloroethyl acetate	1318	926	34.69	33.61	43.32	64.30
	Bis(2-chloroethyl) ether	1536	1220	4.96	4.48	7.83	1.41
	Dioxyethylene glycol diacetate	1970	1491	0.21	2.67	–	2.12
II	Volatile components	–	2253–2759	4.38	2.98	2.43	2.46
	High-boiling resins	–	–	53.43	55.18	42.97	26.88

[a] I and II denote components obtained from polyoxyethylene chains and alkylphenyl groups, respectively.

1065), bis(2-chloroethyl) ether (I_p = 1536) and dioxyethylene (I_p = 1970) are formed in small amounts. Acetic acid (I_p = 1427) is formed from acetyl chloride and γ-pyrone derivatives (I_p = 2035, 2107 and 2227) are formed from acetic acid, as discussed previously[3].

Alkylphenyl groups form mainly unidentified high-molecular-mass resins and only small amounts of low-molecular-mass compounds are formed which elute from the chromatographic column (I_p = 2253, 2350, 2459, 2514, 2657, 2714 and 2759 on silicone resin OV-17). Their mass spectra are not specific enough to identify them, as a result of their different and branched alkyl groups. Their contents cannot be determined and the average degree of ethoxylation can be calculated only from the contents of products formed by the degradation of the polyoxyethylene chains and the mass of the starting sample, assuming the appropriate average molar mass for a hydrophobic alkylphenyl group.

The contents of the separated components are given in Table II and the average degrees of alkylphenol ethoxylation obtained are presented in Table III. The values obtained by direct analysis are significantly lower than those obtained by degradation. These differences depend on the average degree of ethoxylation, and increase as the latter increases. They are not caused by the presence of polyoxyethylene glycols, the content of which is below 1%. For Rokafenol N-5 and Lutensol AP-9 these diferences are about 10 and 24%, respectively. For Lutensol AP-14 the average degree of ethoxylation could be only determined by means of degradation.

CONCLUSIONS

Commercial polyoxyethylene glycol mono(4-alkylphenyl) ethers containing several different components can be easily degraded in the presence of an excess of acetyl chloride and anhydrous iron(III) chloride. Compounds obtained by the degradation of the polyoxyethylene chains can be easily identified and their contents can be precisely determined. These values can be further used to calculate the average degree of alkylphenol ethoxylation.

TABLE III

AVERAGE DEGREE OF ALKYLPHENOL ETHOXYLATION

A and *B* denote values obtained by direct analysis and by means of degradation, respectively.

Parameter	*Lutensol AP-4*		*Rokafenol N-5*		*Lutensol AP-9*		*Lutensol AP-14*	
	A	*B*	*A*	*B*	*A*	*B*	*A*[a]	*B*
Degree of ethoxylation (individual results)	3.73	3.96	3.37	3.53	6.25	7.45		12.12
	3.48	3.47	3.33	3.37	5.41	6.70		11.87
	3.65	3.50	3.18	3.44	5.32	6.79		11.90
	3.41	3.47	3.33	3.67	5.41	6.90		12.16
	3.41	3.89	3.18	3.99	5.34	6.59		12.25
Average	3.54	3.65	3.28	3.60	5.55	6.88		12.05
Standard deviation	0.14622	0.24530	0.09094	0.24515	0.3564	0.33531		0.16288
Confidence limits ($\alpha = 0.05$)	±0.20	±0.34	±0.13	±0.34	±0.55	±0.47		± 0.23
Average differences:								
$B - A$	0.11		0.32		1.33		–	
$\frac{B-A}{A} \cdot 100(\%)$	3.10		9.76		23.96		–	

[a] Determination impossible.

REFERENCES

1 J. Szymanowski, P. Kusz, E. Dziwiński and Cz. Latocha, *J. Chromatogr.*, 502 (1990) 407.
2 P. Waszeciak and H. G. Nadeau, *Anal. Chem.*, 36 (1964) 764.
3 J. Szymanowski, P. Kusz and E. Dziwiński, *J. Chromatogr.*, 455 (1988) 131.

Journal of Chromatography, 511 (1990) 333–339
Elsevier Science Publishers B.V., Amsterdam

CHROM. 22 382

Electric properties of photoaffinity-labelled pancreatic A-subtype cholecystokinin

J. JIMÉNEZ[a], M. DUFRESNE, S. POIROT, N. VAYSSE and D. FOURMY*
INSERM U 151, Bat L3, Avenue Jean Poulhès, CHU Rangueil, 31054 Toulouse Cédex (France)
(First received December 11th, 1989; revised manuscript received February 6th, 1990)

ABSTRACT

Although the isoelectric point of a protein is very important, electric focusing of intrinsic membrane proteins in polyacrylamide or agarose gels often fails. The recently introduced Bio-Rad Rotofor cell allowed isoelectric focusing of such a protein, cholecystokinin (CCK) receptor. Both the isoelectric point and the molecular weight (M_r) of pancreatic CCK receptor were determined. For this purpose, membrane CCK receptor was photoaffinity labelled by a cleavable agonist probe, subsequently prepurified on immobilized wheat germ agglutinin and analysed by sodium dodecyl sulphate polyacrylamide gel electrophoresis and isoelectrofocusing in solution in the presence of Nonidet P-40. CCK receptor was identified at M_r 85 000–100 000, whereas its deglycosylated product was shifted to M_r 42 000. Further, the isoelectric points of the glycosylated and deglycosylated forms of CCK receptor were pH 4.8 and 4.3, respectively. A knowledge of the isolelectric point should help in characterizing better CCK receptor heterogeneity and/or in purifying CCK receptor proteins.

INTRODUCTION

Cholecystokinin (CCK) is a major neurohormonal peptide with effects on various tissues within the gut[1] and the nervous system[2]. CCK receptor subtype diversity as revealed by pharmacological studies is now well established[3]. However, the molecular basis of such a diversity remains unclear. Rat pancreatic CCK receptor, which is of A-subtype, has been pharmacologically and functionally characterized[4]. Its biochemical knowledge was provided essentially by sodium dodecyl sulphate polyacrylamide gel electrophoresis (SDS-PAGE) analysis of affinity-labelled membrane proteins using radioiodinated CCK probes. In particular, CCK-8 based probes covalently linked to CCK receptor through their N-terminus[5] or C-terminus[6] led to the identification of a glycoprotein of molecular weight (M_r) 85 000–95 000 having a

[a] Present address: Department of Medical Biochemistry and Molecular Biology, School of Medicine, University of Seville, Avda. Sanchez Pizjuan 4, 41009 Seville, Spain.

0021-9673/90/$03.50

protein core of M_r 42 000[7]. Recently we synthesized and characterized a cleavable ligand which was used to photoaffinity label CCK receptor with minor modification of its structure[8]. The probe was [^{125}I]azidosalicylaminodithiopropionate-(Thr^{28},-Nle^{31})-CCK-25-33, [^{125}I]ASD-(Thr^{28},Nle^{31})-CCK-25-33, the peptide moiety of which was released from photoaffinity-labelled CCK receptor by reduction.

In an effort to design a purification strategy for pancreatic CCK receptor, we determined the isoelectric point of its glycosylated and deglycosylated photoaffinity-labelled forms. This new criterion should provide a better understanding of the molecular nature of CCK receptor and thus facilitate its purification.

To achieve isoelectric focusing of CCK receptor, several methods were tried, including focusing in polyacrylamide and agarose gels. As none of them yielded a satisfactory amount of focused CCK receptor, we decided to use the Rotofor cell[9].

EXPERIMENTAL

Membrane preparation

Enriched pancreatic plasma membranes were prepared from male Wistar rats by homogenization of 24 pancreases in 0.3 *M* sucrose according to the method described previously[5].

Photoaffinity labelling of CCK receptor

The synthesis of the photoactivatable ligand [^{125}I]ASD-(Thr^{28},Nle^{31})-CCK-25-33 and its binding to pancreatic membranes were described previously[8]. Briefly, binding of [^{125}I]ASD-(Thr^{28},Nle^{31})-CCK-25-33 (100 p*M*) to plasma membranes (5–10 μg) was carried out at 22°C for 60 min in HEPES buffer (50 m*M*, pH 7.0) containing 115 m*M* NaCl, 5 m*M* $MgCl_2$, 0.01% soybean trypsin inhibitor, 0.1% bacitracin, 1 m*M* ethylene glycol tetraacetate, 0.1 m*M* phenylmethylsulphonyl fluoride and 0.2% bovine serum albumin. Membranes were centrifuged and resuspended in cold buffer without albumin for a 5-min photolysis under a 125-W mercury lamp. Photoaffinity-labelled membranes were solubilized at 4°C for 1 h in binding buffer containing 5% Nonidet P-40. Soluble membrane proteins were recovered by ultracentrifugation at 100 000 *g* for 30 min.

Lectin prepurification of CCK receptor

As the yield of photoaffinity labelling was relatively low (4% of initial binding on membranes), we enriched the membrane proteins in photoaffinity-labelled CCK receptor by taking advantage of its glycosylation. Chromatography on immobilized wheat germ agglutinin (WGA) was performed according to Rosenzweig *et al.*[10]. Retained glycoproteins were eluted with 0.5 *M* N-acetylglucosamine. Fractions corresponding to the radioactive peak were ultraconcentrated (Centricon 30, Amicon) and, to avoid protein aggregation, free sulphydryl groups were carboxymethylated with iodoacetic acid as described by Waxdal *et al.*[11]. Finally, proteins were precipitated with methanol–chloroform–water (4:1:3)[12] and dried under vacuum. Alternatively, aliquots of CCK receptor eluted from the wheat germ agglutinin column were directly subjected to isoelectric focusing and SDS-PAGE.

Isoelectric focusing of CCK receptor

A Rotofor cell (Bio-Rad Labs.) was used[9]. The focusing medium was composed of a solution containing 2% Nonidet P-40, 1.5% (w/v) of ampholytes (1%, pH 3.5–9.5, and 0.5%, pH 2.5–4.5, Ampholines, LKB). The electrode solutions were 0.1 *M* NaOH and 0.1 *M* H_3PO_4. Focusing was achieved at 4°C in two steps: (i) prefocusing at 12 W constant power for 1 h, then the Nonidet P-40 solubilized sample was loaded into the chamber; (ii) isoelectric focusing at 12 W constant power for 3 h. The contents of the focusing chamber were collected for pH and radioactivity determinations as recommended by Bio-Rad Labs. Fractions corresponding to the focused radioactive peak were ultraconcentrated for subsequent SDS-PAGE analysis.

Other methods

Prepurified and isoelectric focused CCK receptor were analysed by SDS-PAGE in a 10% acrylamide gel according to Laemmli[13]. Apparent molecular masses were calculated using prestained standard proteins (Bethesda Research labs.). Deglycosylation of CCK receptor was performed by treating precipitated proteins (10-50 μg) with 50 μl of dried trifluoromethane sulphonic acid (TFMSA) for 5 min at 0°C according to the modified method of Edge *et al.*[14]. The reaction was stopped by adding 500 μl of iced 1 *M* Tris solution. Deglycosylated proteins were recovered and desalted by ultrafiltration (Centricon 10, Amicon).

RESULTS

Photoaffinity labelling and prepurification of CCK receptor

Photoaffinity labelling of pancreatic plasma membranes with [^{125}I]ASD-(Thr^{28},Nle^{31})-CCK-25-33 identified a component migrating as a broad band at M_r 85 000–100 000 in SDS-PAGE. The covalent labelling of this component was removed by incubating [^{125}I]ASD-(Thr^{28},Nle^{31})-CCK-25-33 with the membranes in the presence of 10^{-6} *M* CCK prior to photolysis (Fig. 1, lanes 1 and 2). Treatment with dithiothreitol prior to electrophoresis did not affect the labelling pattern (not shown). This confirms data obtained with other probes[5,6] and establishes that the cleavable probe [^{125}I]ASD-(Thr^{28},Nle^{31})-CCK-25-33 specifically identified CCK receptor. Photoaffinity-labelled CCK receptor was fully retained on immobilized wheat germ agglutinin and eluted with N-acetyl-β-D-glucosamine[8]. Using such a lectin affinity chromatography provided a purification rate of 17–20-fold from starting membrane proteins, and yielded prepurified CCK receptor samples of specific activity 0.7 μCi/mg proteins. Prepurified CCK receptor was identified again at M_r 85 000–100 000 (Fig. 1, lane 3).

Isoelectric focusing of photoaffinity-labelled CCK receptor

Previous attempts to focuse CCK receptor in either polyacrylamide or agarose gels failed. These results were attributed to the biochemical nature of CCK receptor, an integral membrane protein which is glycosylated and probably very hydrophobic. As an alternative, we performed focusing in solution in the presence of 2% Nonidet P-40. As illustrated in Fig. 2, prepurified CCK receptor was focused as a single radioactive peak at pH 4.8 ± 0.1 (n = 5). The content of this peak was identified as being CCK receptor which migrated at M_r 85 000–100 000 in SDS-PAGE (Fig. 2,

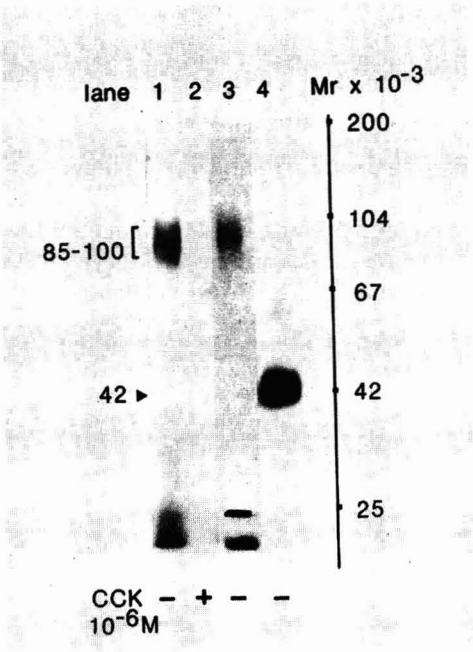

Fig. 1. SDS-PAGE of photoaffinity-labelled CCK receptor. Membranes photoaffinity labelled by [^{125}I]ASD-(Thr^{28},Nle^{31})-CCK-25-33 (lanes 1 and 2) and wheat germ agglutinin-prepurified CCK receptor (lane 3) were identified at M_r 85 000–100 000. This M_r was shifted to 42 000 after TFMSA deglycosylation (lane 4).

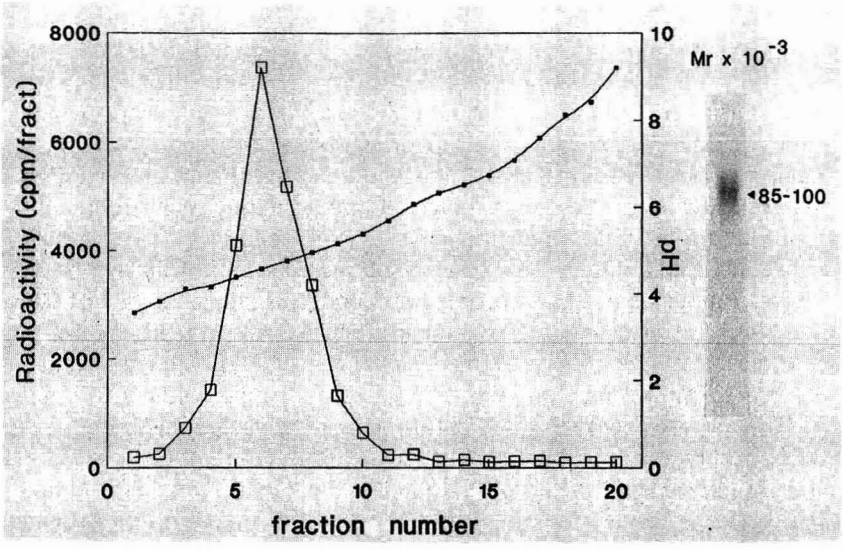

Fig. 2. Isoelectric focusing of photoaffinity-labelled CCK receptor. An aliquot of wheat germ agglutinin-prepurified CCK receptor (50 μg of proteins, 50 000 cpm) was electrically focused in 2% Nonidet P-40 solution for 3 h. The focusing pH was 4.8 ± 0.1 (n = 5). Right: SDS-PAGE of an aliquot of the focused radioactivity showing CCK receptor at M_r 85 000–100 000.

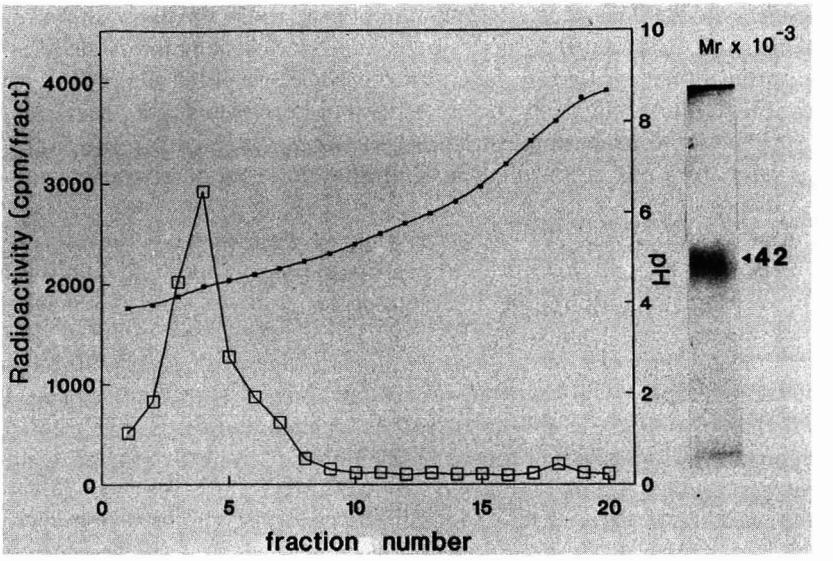

Fig. 3. Isoelectric focusing of deglycosylated photoaffinity-labelled CCK receptor. An aliquot of wheat germ agglutinin-prepurified CCK receptor (50 μg of proteins, 50 000 cpm) was precipitated, treated at 4°C with 50 μl of TFMSA for 5 min and submitted to isoelectric focusing. The focusing pH was 4.3 ± 0.1 (n = 3). Right: SDS-PAGE of the focused radioactivity showing deglycosylated CCK receptor at M_r 42 000.

right). We evaluated whether reduction and carboxymethylation affected the electric properties of CCK receptor by focusing chemically unmodified CCK receptor. We found the focusing pH to be 5.0 (n = 2).

In another set of experiments, we chemically deglycosylated prepurified CCK receptor. A component of M_r 42 000 was obtained (Fig. 1, lane 4), demonstrating that removal of carbohydrates from CCK receptor decreased its apparent mass by 60%, as already achieved by endoglycosidase-F treatment of affinity-labelled membrane CCK receptor[7]. Moreover, we evaluated whether these carbohydrates also contribute to the electric charge of the receptor protein. As shown in Fig. 3, chemically deglycosylated CCK receptor was focused at pH 4.3 ± 0.1 (n = 3). Analysis of the content of this radioactive peak demonstrated a component of M_r 42 000 (Fig. 3, right), confirming deglycosylation of CCK receptor.

Finally, we determined the focusing pH of the small chemical residue of the probe ([^{125}I]ASD) which remained on the photoaffinity-labelled receptor. [^{125}I]ASD was focused at pH 4.1 ± 0.1 (n = 5) (not shown), which is close to the isoelectric point of the receptor protein core. This result indicates that only a weak charge modification occurred on CCK receptor protein by affinity labelling with [^{125}I]ASD-(Thr^{28},Nle^{31})-CCK-25-33 and that the isoelectric point of photoaffinity-labelled CCK receptor is representative of that of the native receptor.

DISCUSSION

Since its first introduction, isoelectric focusing, especially when used in two-dimensional electrophoresis, has been applied extensively to the problems of charac-

terizing macromolecules. There have been a number of studies involving hormone receptors where isoelectric focusing is used to yield the isoelectric point of the receptor and as a purification step[15]. More generally, the isoelectric point of a protein is a physico-chemical characteristic as important as its molecular weight. It provides informations on the amino acid composition of the protein, permits the selection of optimum pH values for purification and helps in the development of separation methods based on charge.

In an effort to design a purification strategy for pancreatic CCK receptor, we determined its isoelectric point. For this purpose, numerous methods and conditions of isoelectric focusing were tested but without success. For instance, when using isoelectric focusing in polyacrylamide gel (PAGIF), only a very small amount of CCK receptor was able to enter the gel rod. Attempts with agarose gels revealed that migration of CCK receptor did occur but was so slow that CCK receptor could not reach reproducible pH values before the agarose gel melted and/or the pH gradient drifted dramatically. All solutions proposed in the literature to resolve the problems encountered were tested, but none significally improved the results. We speculatively attributed the inability of CCK receptor focusing either to its high hydrophobicity and/or to the high degree of glycosylation. In addition, in spite of the presence of SDS, CCK receptor is detected as an unusual very broad band in SDS-PAGE. Such abnormal migration may be due both to hydrophobicity and to the degree and /or heterogeneity of glycosylation, as suggested recently[16].

To circumvent these difficulties, we used the Rotofor cell, which consists of a cylindrical focusing chamber divided into twenty compartments by polyester membranes. Because of the absence of a gel matrix, the proteins easily migrate through the membranes to their focusing pH and are obtained in solution with a high recovery[17]. Using this apparatus we focused photoaffinity-labelled pancreatic CCK receptor and its deglycosylated product at pH 4.8 ± 0.1 and 4.3 ± 0.1, respectively.

This study demonstrated that removing the glycoside moiety of CCK receptor shifted its M_r from 85 000–100 000 to 42 000 but weakly decreased its isoelectric point (4.3 *versus* 4.8). Consequently, the 60% decrease in M_r found in SDS-PAGE is unlikely to be due to a charge effect. Further, the results indicated that the acidic property of CCK receptor is more relevant to the amino acid composition of the protein than to the sialic acids ending carbohydrate chains[6].

During the preparation of this paper, Duong *et al.*[18] reported on the purification of CCK receptor. They used chromatography on the strong cation exchanger Mono-S (Pharmacia) as a first step. At their experimental pH of 6.5, a Mono-S column should retain basic proteins but not CCK receptor. The only explanation for this result lies either in a non-specific interaction of CCK receptor with the Sepharose-S matrix or in the interaction of a large aggregate containing several basic proteins in addition to CCK receptor.

The isoelectric point of CCK receptor is a new biochemical characteristic provided by this study that may be used for establishing the molecular basis of CCK receptor heterogeneity and for setting up an additional purification step on the basis of the electric properties of CCK receptor. On the other hand, the Rotofor cell should be helpful in determining the isoelectric point of membrane proteins without decreasing their biological activity.

ACKNOWLEDGEMENTS

This work was supported by Region Midi-Pyrénées No. 001 777 and by CEE contract ST2J-001-3-F(CD). We thank A. M. Remaury for typing the manuscript.

REFERENCES

1 V. Mutt, in J. G. Glass (Editor), *Gastrointestinal Hormones*, Raven Press, New York, 1980, p. 69.
2 J. E. Morley, *Life Sci.*, 30 (1982) 479.
3 J. T. Jensen, T. V. Schrenck, D. H. Yu, S. A. Wank and J. D. Gardner, in J. Hughes, G. Dockray and G. Woodruff (Editors), *Anatomy and Biochemistry, Receptors, Pharmacology and Physiology*, Ellis Horwood, Chichester, 1989, p. 150.
4 H. Sankaran, I. D. Goldfine, C. W. Deveney, K. Y. Wong and J. A. Williams, *J. Biol. Chem.*, 255 (1980) 1853.
5 R. K. Pearson and L. J. Miller, *J. Biol. Chem.*, 262 (1987) 869.
6 S. P. Powers, D. Fourmy, H. Gaisano and L. J. Miller, *J. Biol. Chem.*, 263 (1988) 5295.
7 R. K. Pearson, L. J. Miller, E. M. Hadac and S. P. Powers, *J. Biol. Chem.*, 262 (1987), 13850.
8 D. Fourmy, P. Lopez, S. Poirot, J. Jimenez, M. Dufresne, L. Moroder, S. P. Powers and N. Vaysse, *Eur. J. Biochem.*, 185 (1989) 397–403.
9 N. B. Egen, W. Thormann, G. E. Twithy and M. Bier, *Electrophoresis*, 83 (1984) 547.
10 S. A. Rosenzweig, L. D. Madison and J. D. Jamieson, *J. Cell Biol.*, 99 (1984) 1110.
11 M. J. Waxdal, W. H. Konigsberg, W. L. Henley and G. M. Edelman, *Biochemistry*, 7 (1968) 1959.
12 D. Wessel and V. I. Flügge, *Anal Biochem.*, 138 (1984) 141.
13 U. K. Laemmli, *Nature (London)*, 227 (1970) 680.
14 A. S. B. Edge, C. R. Faltynefe, L. Hof, L. E. Reichert and P. Weber, *Anal. Biochem.*, 118 (1981) 131.
15 L. Lilly, B. Eddy, J. Schaber, C. M. Fraser and J. C. Venter, in J. C. Venter and L. C. H. Harrison (Editors), *Receptor Purification procedures*, Alan R. Liss, New York, 1984, p. 77.
16 U. G. Klueppelberg, S. P. Powers and L. J. Miller, *Biochemistry*, 28 (1989) 7124.
17 N. B. Egen, M. Bliss, M. Mayersohn, S. Owens, L. Arnold and M. Bier, *Anal. Biochem.*, 172 (1988) 488.
18 L. T. Duong, E. M. Hadac, L. J. Miller and G. P. Vlasuk, *J. Biol. Chem.*, 264 (1989) 17990.

Journal of Chromatography, 511 (1990) 341–352
Elsevier Science Publishers B.V., Amsterdam

CHROM. 22 464

Hadamard transform photothermal deflection densitometry of electrophoretically blotted proteins

PATRICK J. TREADO, LINDA M. BRIGGS and MICHAEL D. MORRIS*
Department of Chemistry, University of Michigan, Ann Arbor, MI 48109-1055 (U.S.A.)
(First received December 12th, 1989; revised manuscript received March 22nd, 1990)

ABSTRACT

Hadamard transform spatial multiplexing techniques are applied to laser densitometry in order to prevent the photo-induced degradation of sensitive materials. Photochemical and thermal degradations can often occur in point focused scanning laser densitometry. In spatial multiplexing, the excitation source is defocused and efficiently distributed throughout the sample, reducing local power density. In this paper, we describe the application of Hadamard transform spatial multiplexing to transverse photothermal deflection spectroscopy (PDS). Proteins western blotted on nitrocellulose membrane are line imaged using the Hadamard transform PDS densitometer. For comparison, the blots are imaged with a high-dynamic-range video densitometer.

INTRODUCTION

Protein or western blotting[1] involves the transfer of electrophoretically resolved proteins to an immobilizing membrane. Proteins are transferred without loss of resolution to the surface of a nitrocellulose or other membrane and become accessible to a variety of probes including antibodies[2]. Immunodetection is highly specific and capable of high sensitivity (30 pg of protein). Protein blotting provides a rapid screen for detection of a gene product in a foreign host. The technique is rapid since isolation and purification of the protein does not preclude identifying it.

In addition, multiple blots can be made from a single gel if necessary for application of different detection schemes. For example, stain of total protein, or highly specific immunoassays can be performed. Also, blots have archival properties. Under certain conditions proteins blotted on nitrocellulose retain activity and can be probed as late as several months after initial immobilization. These advantages have made protein blotting an attractive technique.

Densitometry of proteins in gels is well-developed. Measurement of proteins separated by gel electrophoresis in mini-gels or separated by isoelectric focusing requires at least moderate spatial resolution (100–250 μm) in order to detect and

0021-9673/90/$03.50

quantify closely spaced bands. Most scanning laser densitometers and video cameras can fulfill the spatial requirements. Spatial resolution in conventional laser densitometers is determined by the diameter of the focused laser beam. In video systems, spatial resolution is determined by magnification of the imaging optics. Video imaging does provide two-dimensional capability, but many inexpensive cameras lack adequate sensitivity to quantify faint bands. Laser transmission densitometers often suffer from the same problem.

A commercially available charge-coupled device (CCD) system has been employed for imaging of proteins on two-dimensional polyacrylamide gels[3,4]. The commercial system employs a high dynamic range, cryogenically cooled CCD camera. Despite the excellent performance, the instrument's expense limits widespread applicability for routine protein densitometry. Another two-dimensional imaging technique, electronic autofluorography, has been described[5]. The method detects scintillation light or fluorescence with sensitivity comparable to autoradiographic methods, but spatial resolution is poor at 400 μm.

Photothermal lensing techniques also provide 0.5–1 ng sensitivity for gel densitometry[6–9]. A photothermal lens is the refractive index gradient formed by heat evolution from a light absorbing sample[10,11]. By probing this gradient with a laser and monitoring its positional change or its intensity after passage through the gradient, sensitive indirect absorption measurements can be made. Schlieren optics is an alternative method for measuring the refractive index gradients within protein bands. This technique has been applied to densitometry of unstained proteins as a real time monitor of protein separation in gels[12]. The method has poor sensitivity, 0.5 μg, and is limited to transmissive samples only.

Conventional thermal lensing is also limited to transmissive samples, but a variant, transverse photothermal deflection spctroscopy (PDS)[13], can be used for detection of samples on opaque substrates used in thin-layer chromatography (TLC)[14] or protein blotting.

Laser densitometry is performed with PDS by either translating the sample through the pump laser or by raster scanning the pump laser across the sample. Another indirect absorption technique, photoacoustic spectroscopy (PAS), has been applied to densitometry of proteins[15] on gels. This technique provides high spatial resolution, 50–100 μm, but only moderate sensitivity with a detection limit of 0.2 μg.

Under conditions of tight focussing for high spatial resolution and high laser power for increased sensitivity analytes can undergo photophysical or photochemical transformations. These effects can range from coagulation of colloidal stains resulting in subtle absorbance shifts to gross thermal decomposition of the stained or unstained protein.

To avoid the high laser power densities of point focused laser imaging, Hadamard spatial multiplexing has been applied to both PAS[16] and transverse PDS[16–20]. In practice, the excitation source is defocused and coded with an n element Hadamard mask before sample illumination. The power density is reduced by at least a factor of $\sqrt{n/2}$ relative to a scanning laser densitometer at comparable spatial resolution and total laser power. In addition to a reduction in power density, these techniques allow one- and two-dimensional imaging with point detectors.

Most densitometry methods were originally developed for detection of proteins in gels. Video cameras operated in reflectance mode can be used for blots. Most other

transmission based techniques require a transparent or translucent matrix and are not easily modified for densitometry of proteins on opaque blotting substrates.

In this communication, we describe the application of Hadamard transform PDS imaging to densitometry of blotted proteins. Transverse photothermal densitometry may ultimately become the principle of a sensitive, inexpensive densitometer capable of quantifying proteins on opaque substrates. The Hadamard multiplexing allows use of higher laser power than point scanning, to maximize sensitivity or minimize measurement time.

For comparison to photothermal densitometry, we have performed video densitometry using a high dynamic range, low light level CCD camera. The CCD is cryogenically cooled and has 14 bits of dynamic range. A device of this sophistication is not typically employed for routine protein densitometry. However it should serve as a rigorous standard against which to compare the photothermal system.

More conventional and lower cost video densitometry systems employ 8-bit dynamic range cameras. With dynamic range expansion techniques, the effective range can be increased to 11 bits[21]. If Hadamard transform photothermal densitometry can compare favorably with the 14-bit CCD camera, then the photothermal system should have a significant performance advantage over conventional video densitometry system.

EXPERIMENTAL

Fig. 1 is a diagram of the Hadamard transform photothermal deflection densitometer. A continuous wave Nd-YAG laser (Quantronix, Smithtown, NY, U.S.A.; Model 416), frequency doubled at 532 nm, was used to irradiate the sample. The Nd-YAG laser beam shaping optics were similar to those used previously[19]. A one-dimensional telescope was used to expand and roughly collimate the beam for presentation to the one-dimensional Hadamard mask. The pump beam was modulated at 13 Hz with a mechanical chopper. The spatially encoded beam was

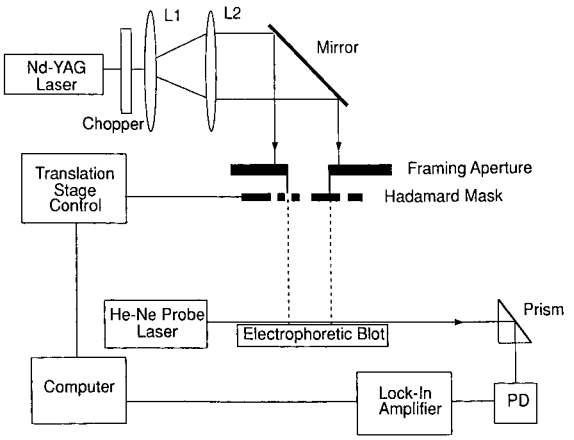

Fig. 1. Hadamard transform transverse photothermal deflection densitometer. Nd–YAG source; L1 = lens 1 (–50-mm focal length) and L2 = lens 2 (150-mm focal length): cylindrical telescope; He–Ne probe; PD: photodiode.

framed by an aperture having a width equal to the number of active resolution elements, n, times the width of a single element, d. The power delivered to the sample was approximately 20 mW. The generated refractive index gradients were probed by a He–Ne laser (Uniphase, Sunnyvale, CA, U.S.A.; Model 1101P) which was parallel to the line defined by the collimated pump beam and to the sample surface. The probe beam was detected by a position sensing photodiode. The photothermal signal was demodulated with a lock-in amplifier (Princeton Applied Research, Princeton, NJ, U.S.A.; Model 5209).

The one-dimensional Hadamard mask used in this study had 127 active elements, each element was 150 μm wide. The mask was generated as a photographic negative on high contrast film mounted between glass plates[18].

The mask was translated mechanically using a stepping motor drive (New England Affiliated Technologies, Lawrence, MA, U.S.A.; Model TM-200-SM) having 10-μm resolution. An AT level computer (Zenith, St. Joseph, MI, U.S.A.; Model Z-248) equipped with a 12-bit analog-digital converter board (MetraByte, Taunton, MA, U.S.A.; Model DAS-16) was used for instrument control and data acquisition. The fast Hadamard transform, implemented in Turbo Pascal, was used for transformation of data from the 127-element mask.

Video densitometry was performed with a slow-scan charge-coupled device (CCD) camera (Photometrics, Tucson, AZ, U.S.A.; Series 200). The CCD is a cryogenically cooled (–110.0°C) detector suitable for low-light level imaging with 14 bits of dynamic range. Blot images were taken under tungsten illumination with a 50-mm focal length camera lens. For image processing and display the video image is transferred to a MacIntosh IIcx computer (Apple Computer, Cupertino, CA, U.S.A.) and displayed on the computer monitor using the public domain image processing program *Image* (Wayne Rasband, National Institutes of Health, Building 36, Room 2A-03, Bethesda, MD 20892, U.S.A.). For publication, the MacIntosh video monitor is photographed.

The protein samples used in this study were low-range molecular weight standards and plastocyanin, a small blue copper protein (10 500 daltons) isolated from spinach chloroplasts. The molecular weight standards are: phosphorylase B (97 400 daltons), bovine serum albumin (66 200 daltons), ovalbumin (45 000 daltons), carbonic anhydrase (31 000 daltons) and soybean trypsin inhibitor (21 500 daltons).

The proteins were separated using sodium dodecyl sulphate (SDS)–polyacrylamide gel electrophoresis[22] (Bio-Rad, Richmond, CA, U.S.A., Miniprotein II) in 10–17% gradient gels with 5% stacking gel. The gel thickness was 0.5 mm and sample wells were 3 mm wide. Electrophoresis was carried out at room temperature for 1 h, 30 mA constant current.

Proteins were transferred electrophoretically to a nitrocellulose substrate (Schleicher and Schuell, Keene, NH, U.S.A.) for 1 h at 240 mA. A cooling coil was employed. The molecular weight standards were stained by India ink. Plastocyanin was immunoassayed by first washing the nitrocellulose membrane in a 1:1000 dilution of antiserum for 1 h, followed by a second wash in the IgG enzyme conjugate protein A alkaline phosphatase. Polyclonal antibodies to purified spinach plastocyanin were developed by immunizing rabbits with multiple interdermal injections[23].

The protein A alkaline phosphatase is visualized by Nitroblue tetrazolium chloride–5-bromo-4-chloro-3-indolyl phosphate *p*-toluidene salt (NBT–BCIP) color

development. Charasteristic purple bands were generated. The developed blots were fixed by treatment with EDTA.

RESULTS AND DISCUSSION

Fig. 2 shows images of 1 μg of electrophoretically blotted spinach plastocyanin.

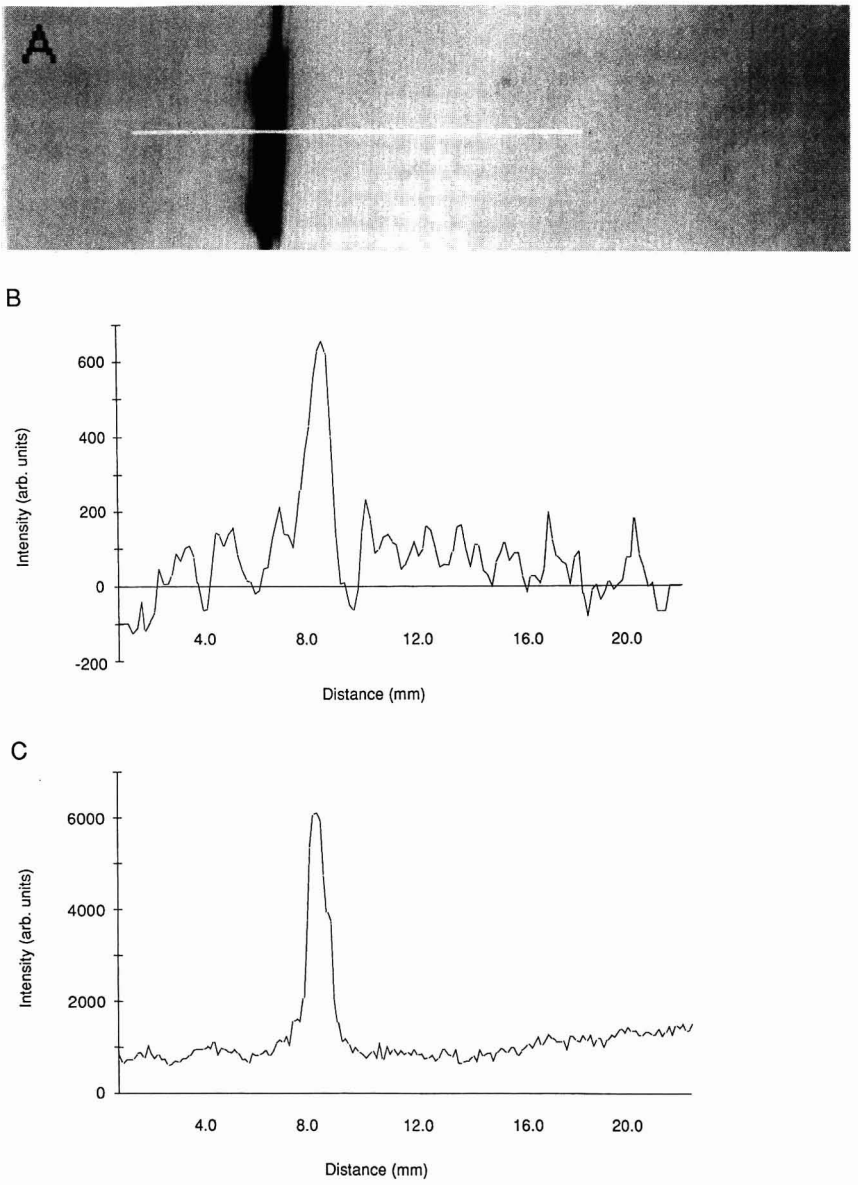

Fig. 2. Images of 5-μg spinach plastocyanin on nitrocellulose. NBT–BCIP color development. (A) CCD camera image: white line is region where photothermal densitometry performed; (B) Photothermal electropherogram: 1 min. acquisition; (C) Video electropherogram: plot of video data within white line.

Fig. 2A was acquired with a slow-scan CCD camera. Fig. 2B is a Hadamard transform photothermal densitometry plot of the plastocyanin in the region defined by the white line of Fig. 2A. The one-dimensional photothermal image was acquired using the 127-element mask. The dimensions of the projected mask pattern were 2.3 cm by 0.075 cm, to yield a pixel of 0.018 by 0.075 cm. With laser power of 25 mW the power density at the sample was approximately 0.072 W/cm^2. This compares with a power density of

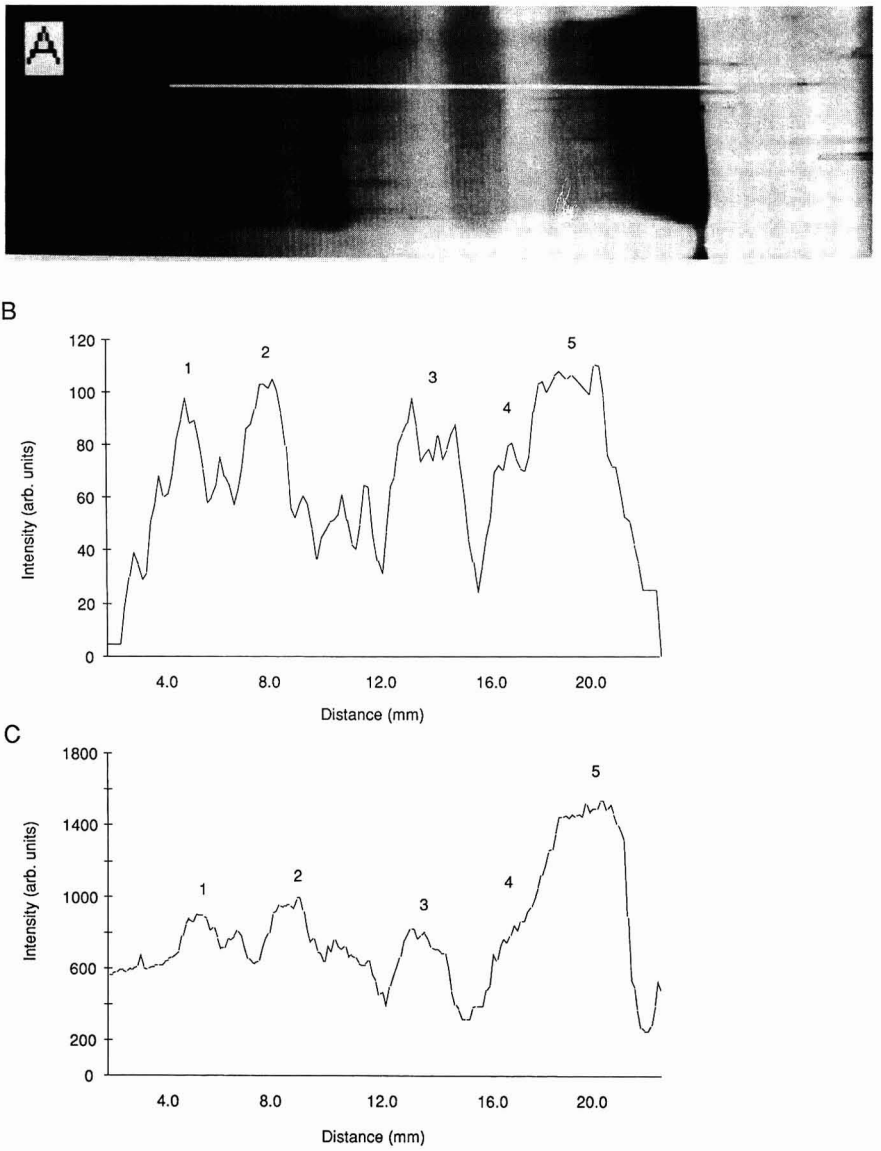

Fig. 3. Images of 5-μg each low-range molecular weight standards. India ink stained total protein. Band 1 = phosphorylase B; 2 = bovine serum albumin; 3 = ovalbumin; 4 = carbonic anhydrase and 5 = soybean trypsin inhibitor. (A) CCD camera image: white line is region where photothermal densitometry performed; (B) photothermal electropherogram; (C) video electropherogram.

77.16 W/cm^2 generated by a conventional focused laser densitometer with 0.018 cm diameter spot size and 25 mW laser power. The multiplexed system reduces the power density by over three orders of magnitude. The size of the projected mask aperture at the sample, 180 μm, indicates approximately 0.1 mrad divergence in the illumination beam. Calibration was performed using USAF 1951 standard resolution targets[18]. Spatial resolution of 180 μm was enough to adequately resolve the protein bands. Protein bands were separated in general by 1 mm or more. The image was acquired using a lock-in time constant of 0.1 sec.

Fig. 2C is a densitometry plot of the same plastocyanin band. The image is a one-dimensional plot of the video data in the region where the photothermal image was taken. The band structure correlates well in both images. The photothermal image has poorer signal-to-noise ratio than the video due to several factors.

Because the probe laser is vertically positioned as close to the substrate surface as possible in order to probe the region of maximum refractive index change, photothermal deflection spectroscopy is sensitive to surface deformations in the substrate. Surface obstructions can deflect the probe beam, generating artifacts in the image. The poorer signal-to-noise ratio in fig. 2A is caused in part by sensitivity to surface deformations in the nitrocellulose substrate. These surface artifacts could be reduced by raising the probe beam relative to the substrate but at a cost to overall sensitivity. For imaging of materials on rough surfaces a trade-off between signal sensitivity and susceptibility to surface defects must be made. Storing the protein blots flat between glass plates would reduce the surface deformation artifacts.

In addition to the surface deformation contribution to the photothermal background, there is a multiplex disadvantage. The multiplex disadvantage[24] is the redistribution throughout the data set of noise from isolated high intensity features. Random fluctuations in the probe beam due to air currents are seen as noise spikes in the raw image data. These spikes are than randomly distributed throughout the transformed data set, effectively degrading the signal-to-noise performance. Smoothing of the image reduces the background noise, but at a cost to sensitivity.

Fig. 3 shows images of 5.0 μg quantity each of low-range molecular weight standards. Band 1 is phosphorylase B; 2: bovine serum albumin; 3: ovalbumin; 4: carbonic anhydrase; 5: soybean trypsin inhibitor. The blot was stained with India ink. Fig. 3A was obtained with the CCD video system. The electropherogram in Fig. 3B was obtained with the Hadamard transform photothermal densitometer taken in the region defined by the white line in Fig. 3A. Fig. 3C is a video electropherogram taken from the same region as the photothermal image. Carbonic anhydrase and soybean trypsin inhibitor are barely resolved in the video image but are distinct in the photothermal image.

Fig. 4 demonstrates that the sensitivity of the photothermal technique is approximately the same as video densitometry. The blot imaged in Fig. 4 has protein bands overexposed to India ink, generating a high background and smearing the protein bands. Fig. 4A is a video image of the molecular weight standards. Fig. 4B is a photothermal electropherogram of the white region of Fig. 4A. Despite the overexposure and poor separation of the proteins the photothermal technique can adequately resolve the bands. In contrast, Fig. 4C, a video electropherogram of the blot, is very poorly resolved. Note in particular the phosphorylase B band and the bovine serum albumin band which appear smeared into a single band in the video plot but are adequately imaged with the photothermal densitometer.

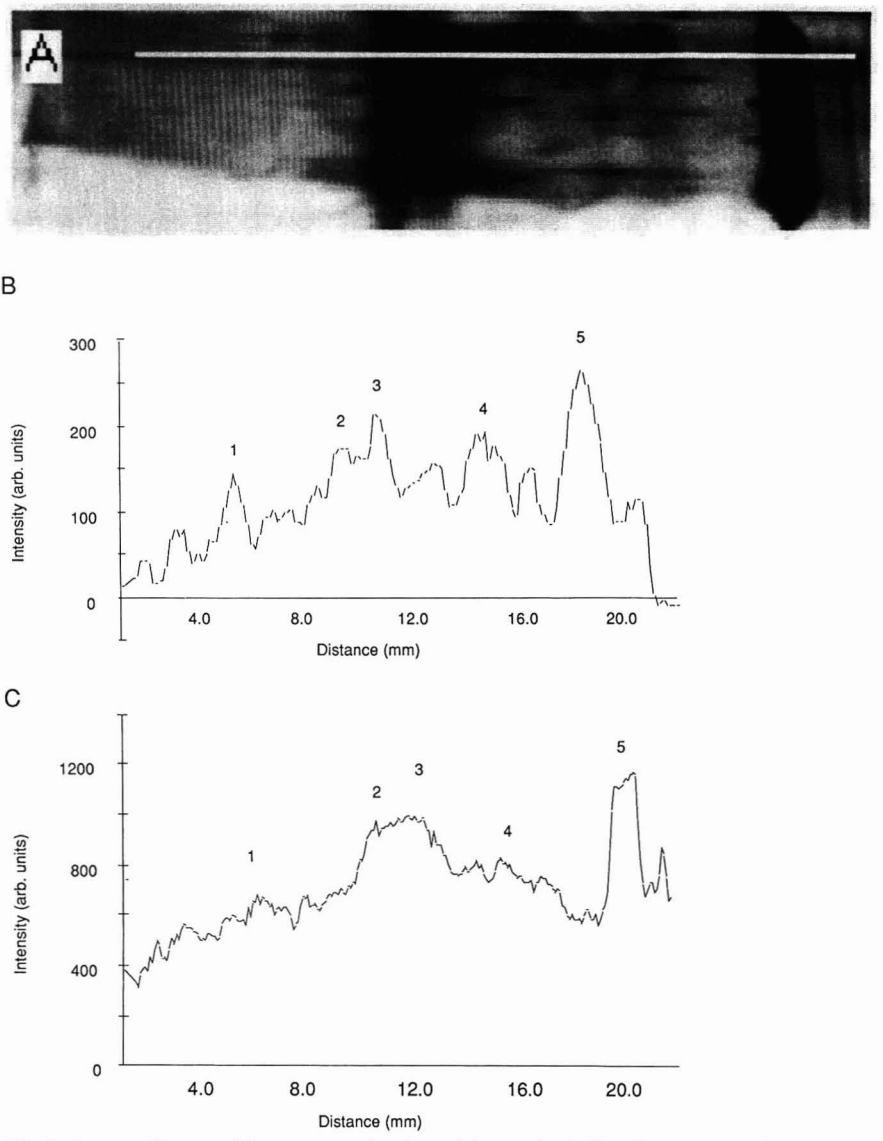

Fig. 4. Images of 5-μg each low-range molecular weight standards. Protein overexposed to India ink. Bands: 1 = phosphorylase B; 2 = bovine serum albumin; 3 = ovalbumin; 4 = carbonic anhydrase and 5 = soybean trypsin inhibitor. (A) CCD camera image: white line is region where photothermal densitometry performed; (B) photothermal electropherogram; (C) video electropherogram.

Densitometry techniques, in general, give a direct measure of the stain associated with a particular protein, not of the protein itself. Because different proteins will take up a particular stain to varying degrees quantitative measurements are difficult. Fig. 3 and 4 demonstrate this problem. An amount of 5 μg of each molecular weight standard has been separated, yet the peak areas are not identical for the individual proteins. In order to make quantitative measurements, experimental parameters must be controlled carefully and comparisons must be made between individual protein systems.

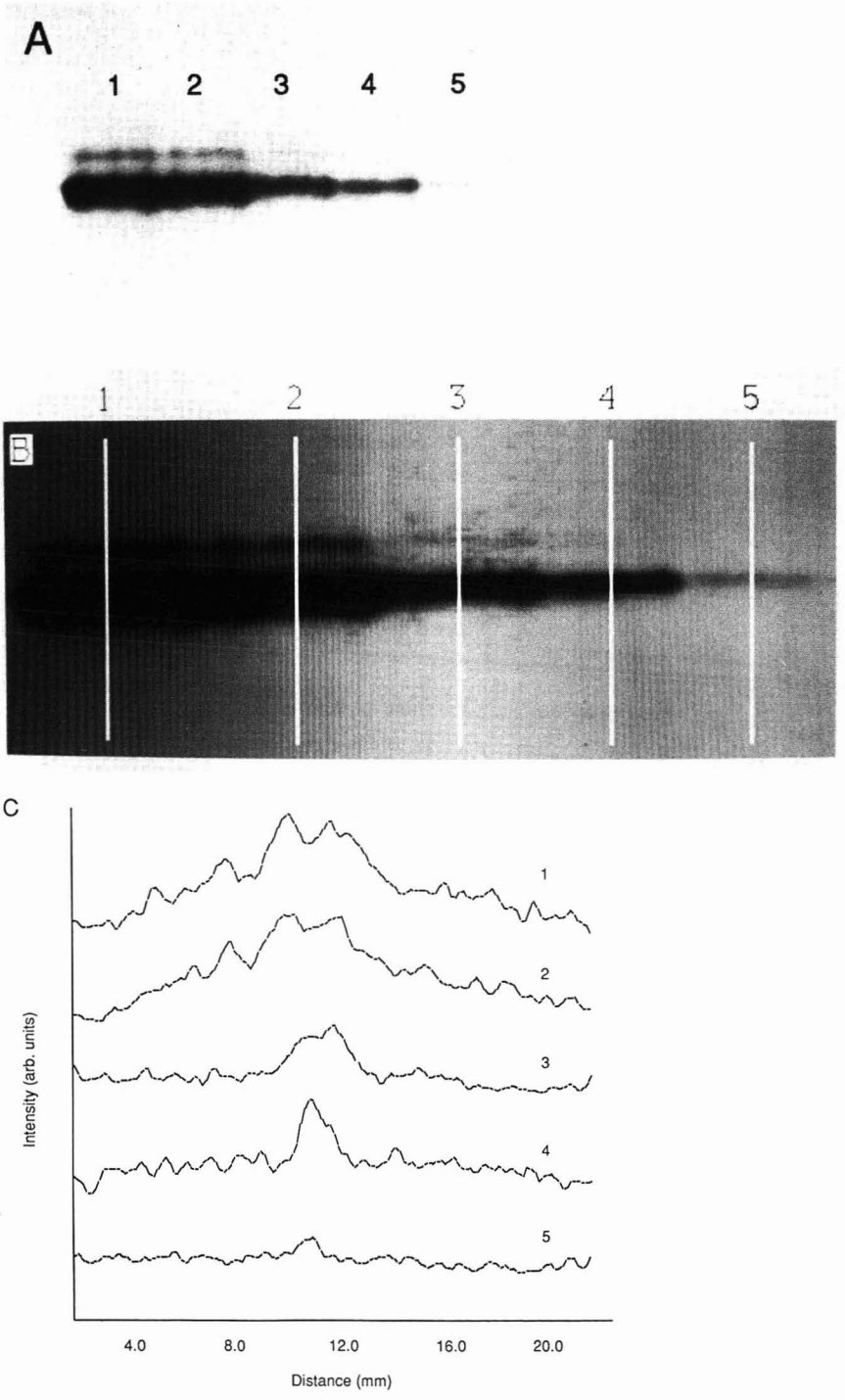

Fig. 5. Spinach plastocyamin concentration study blot. Lane 1 = 1 μg; 2 = 500 ng; 3 = 100 ng; 4 = 50 ng and 5 = 10 ng. NBT–BCIP color development. (A) 35-mm camera photograph of blot; (B) CCD camera image: white lines are regions where photothermal densitometry performed, top of video image corresponds to left of electropherograms; (C) photothermal electropherograms.

Quantitative protein determinations were made under controlled conditions for spinach plastocyanin using the photothermal and video densitometers. The blot containing the varying concentrations was quantitatively imaged by video and by the photothermal method. For qualitative comparison the concentration standard blot was photographed with a conventional 35-mm film camera as well. A photograph of the blot is shown in Fig. 5A. Spinach plastocyanin at concentrations of 1 μg, 500 ng, 100 ng, 50 ng and 10 ng are shown in lanes 1–5, respectively. Fig. 5B is the CCD video image of the spinach plastocyanin bands. The two-dimensional images compare favorably. For presentation purposes a direct photograph of the blot is as good as the photograph of the CCD image displayed on the video monitor. The conventional photograph is purely qualitative unless subjected to subsequent densitometry. The CCD image is already available for digital analysis and enhancement.

The white lines of Fig. 5B correspond to the regions where the photothermal image was acquired. The top of the video image corresponds to the left of the photothermal plots. Fig. 5C shows the photothermal electropherograms of the same bands as in 5A and 5B.

Fig. 6 is a plot of the normalized concentration response of both densitometry systems. The upper curve, a plot of the photothermal response, is a plot of integrated peak area *versus* plastocyanin concentration. The video response, shown in the lower curve, is a plot of integrated band area *versus* plastocyanin. Both calibration curves exhibit linear response below 100 ng of protein. The photothermal response is in agreement with previous photothermal densitometry studies[8]. The sensitivity of both systems is comparable, but the photothermal system has approximately a factor of two worse signal-to-noise performance than the CCD camera. The photothermal densitometer is approximately equivalent to a 13-bit video camera. With the immunochemical protocol used here the plastocyanin detection limit is approximately

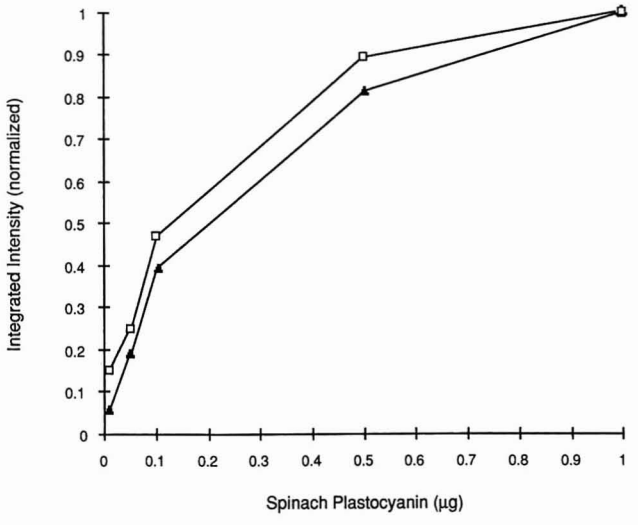

Fig. 6. Concentration response of photothermal and video densitometers. ▲ = Video densitometer and □ = Hadamard transform PDS. Photothermal curve: a plot of integrated peak intensity *vs.* spinach plastocyanin concentration. Video curve: a plot of integrated band intensity *vs.* plastocyamin.

5 ng with the photothermal system and approximately 3 ng with the high dynamic range video camera. Lower detection limits can be obtained by longer color development, but only at the expense of linear dynamic range.

Video based techniques are in general faster than photothermal densitometry. Video systems comprised of a camera and 8-bit frame grabber can acquire an image at several frames a second. High-speed image acquisition allows the possibility of signal averaging for enhanced signal-to-noise performance.

Currently our photothermal system is limited to imaging one lane a minute. Our image acquisition time could be reduced significantly with modifications to the instrument. Presently, acquisition time is limited by the lock-in time constant, 0.1 s. Reducing noise in the system would reduce the time constant and subsequently the acquisition time.

Two significant noise sources are present in our system. The first is the presence of air currents which cause random fluctuations in the probe beam position. By more effectively shielding the entire experiment from the lab environment, air currents can be minimized. A second source of noise comes from the He–Ne probe laser pointing and amplitude instability. Diode lasers should provide more stable performance. With a quieter system the lock-in time constants could be reduced to 0.03 s. Image acquisition time of 20 s per lane should be readily achievable.

CONCLUSION

Hadamard transform photothermal densitometry provides line images of photosensitive materials at high sensitivity using a point detector. It is more sensitive than conventional video densitometry using 8-, 10- or 12-bit cameras. Only the most sensitive cryogenically-cooled slow-scan CCD cameras can provide better sensitivity, but at greater cost and complexity. Although we have used laser excitation, transverse photothermal deflection signals can be excited with incoherent sources as well. A low-cost arc lamp and broad band filter could be used for sample illumination in our system. With stained proteins, monochromaticity is not essential. Another useful extension of this technique would be to employ multichannel detection to allow image acquisition across an extended region of the protein band. Multichannel detection would allow spatial averaging to reduce effects of local fluctuations in the blot surface or band structure without increasing measurement time.

ACKNOWLEDGEMENTS

This work was supported in part by DOE Grant DE-FG02-89ER13996, in part by PHS Grant GM37006 and in part by an ACS Analytical Division Fellowship sponsored by Dow Chemical to P.J.T. L.M.B. thanks Professor V. Pecoraro for research assistantship support through NSF grant No. 022829.

REFERENCES

1 H. Towbin, *Proc. Natl. Acad. Sci. U.S.A.*, 76 (1979) 4350–4354.
2 A. T. Andrews, *Electrophoresis*, Clarendon Press, Oxford, 1986.
3 C. D. Mackay, in M. J. Dunn (Editor), *Electrophoresis '86*, VCH, Weinheim, 1986, 720–722.
4 P. Jackson, V. E. Urwing and C. D. Mackay, *Electrophoresis*, 9 (1988) 330–339.

5 J. B. Davidson, in V. Neuhoff (Editor), *Electrophoresis '84*, VCH, Weinheim, 1984, 235–252.
6 K. Peck and M. D. Morris, *Anal. Chem.*, 58 (1986) 2876–2879.
7 K. Peck and M. D. Morris, *Anal. Chem.*, 58 (1986) 506–507.
8 K. Peck, T. Demana and M. D. Morris, *Appl. Theor. Electrophor.*, 1 (1989) 41–41–45
9 B. J. Jager, R. J. G. Carr and C. R. Goward, *J. Chromatogr.*, 472 (1989) 331–335.
10 J. P. Gordon, R. C. C. Leite, R. S. Moore, S. P. S. Porto and J. R. Whinnery, *J. Appl. Phys.*, 36 (1965) 3–6.
11 J. A. Sell (Editor), *Photothermal Investigations of Solids and Fluids*, Academic Press, New York, 1989.
12 T. Takagi, P. F. Rao and Y. Sato, in C. Schafer-Nielsen (Editor), *Electrophoresis '88*, VCH, Weinheim, 1988, 344–354.
13 M. D. Morris and K. Peck, *Anal. Chem.*, 58 (1986) 811A–822A.
14 T. I. Chen and M. D. Morris, *Anal. Chem.*, 56 (1984) 19–21.
15 H. Köst, U. Möller, S. Schneider and H. Coufal, in H. Harai (Editor), *Electrophoresis '83*, Walter de Gruyter, Berlin, 1984, 495–502.
16 H. Coufal, U. Moller and S. Schneider, *Appl. Opt.*, 21 (1982a) 116–120.
17 F. Fotiou and M. D. Morris, *Appl. Spectrosc.*, 40 (1986) 704–706.
18 F. Fotiou and M. D. Morris, *Anal. Chem.*, 59 (1987) 185–187.
19 F. Fotiou and M. D. Morris, *Anal. Chem.*, 59 (1987) 1446–1452.
20 P. J. Treado and M. D. Morris, *Appl. Spectrosc.*, 42 (1988) 1487–1493.
21 S. Inoué, *Video Microscopy*, Plenum Press, New York, 1986.
22 U. K. Laemmli, *Nature (London)*, 227 (1970) 680–685.
23 J. L. Vaitukaitis, *Methods Enzymol.*, 73 (1981) 46–52.
24 T. Hirschfeld, *Appl. Spectrosc.*, 30 (1976) 234–236.

Journal of Chromatography, 511 (1990) 353–358
Elsevier Science Publishers B.V., Amsterdam

CHROM. 22 471

Note

Normal-phase chromatography and post-column colorimetric detection of abamectin-8,9-oxide

R. J. DEMCHAK* and J. G. MacCONNELL

Agricultural Research & Development, Merck & Co., Inc., Hillsborough Road, Three Bridges, NJ 08887 (U.S.A.)

(First received December 12th, 1989; revised manuscript received March 9th, 1990)

The avermectins[1] are a class of macrocyclic lactone, natural products. They have generated much interest as a broad-spectrum anthelmintic (ivermectin) and as an acaricide/insecticide (abamectin or avermectin B_1). The 8,9,10,11-diene chromophore of avermectin B_1, which is the basis for its UV detection at 245 nm in reversed-phase high-performance liquid chromatography (HPLC), contributes[2] to the rapid degradation of the avermectins in the environment[3]. Thus, attempts to prolong their activity have involved the synthetic modification of the diene[4].

Recent work has shown that the 8,9-oxide of avermectin B_1 (structure 1, Fig. 1) can be easily synthesized[5], is biologically active[6] and is chemically more stable[7] than the parent compound, avermectin B_1. However, the lack of the diene chromophore produces an analytical problem. Abamectin-8,9-oxide can be detected at 210 nm, but in the presence of formulation excipients this wavelength has a low specificity for the analyte. One course of action is to separate the analyte from the excipients and utilize reversed-phase HPLC with UV detection at 210 nm. We present an alternative for detecting abamectin-8,9-oxide and similar analytes, namely, normal-phase HPLC with no separation of analyte and excipients and with post-column detection at 570 nm. Post-column reactions have been used to detect several pesticides, including carbamates[8,9] and glyphosate[10]. Additionally, they have been useful for the analysis of drugs in animal feeds[11,12].

We recently discovered a novel color reaction between trichloroacetic acid (TCA) and several avermectins[13]. The reaction conditions for abamectin-8,9-oxide are similar to those in the colorimetric determination of vitamin A[14,15], despite that the former contains no conjugated double bonds whereas the latter contains five conjugated double bonds. The reaction between TCA and abamectin-8,9-oxide forms the most intense colors in chlorinated solvents and requires a few minutes of mild heating, which is not necessary with vitamin A. The reaction is inhibited, to varying extents, by typical solvents used in reversed-phase HPLC, *i.e.*, water, acetonitrile, tetrahydrofuran and alcohols.

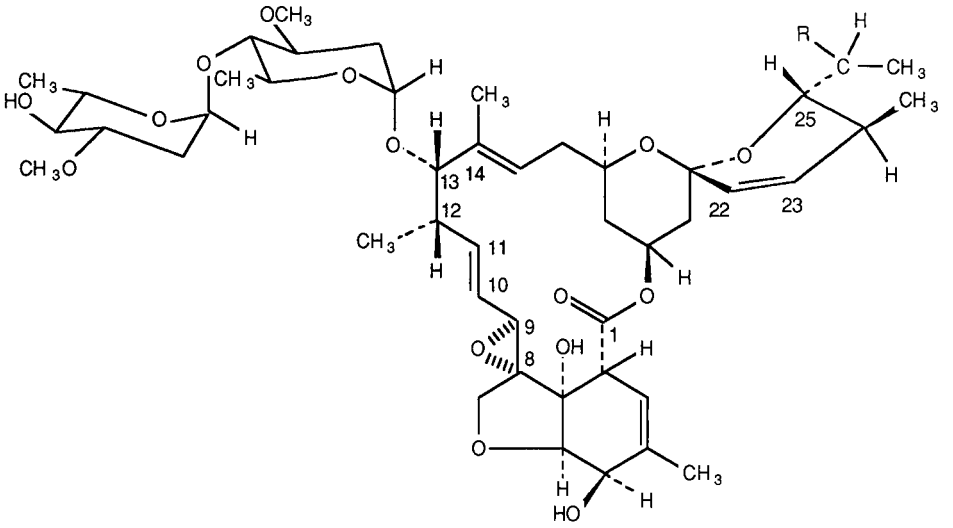

Fig. 1. Structure I (abamectin-8,9-oxide). B_{1a} component: R = C_2H_5 ($\geqslant$ 80%); B_{1b} component: R = CH_3 ($\leqslant$ 20%).

EXPERIMENTAL

The HPLC apparatus consisted of an LDC Constametric III pump, a Kratos Spectroflow 757 dual-lamp (deuterium and tungsten) detector, a Micromeritics 725 autoinjector connected to a Valco EC6W valve and a Nelson Analytical data system with XTRA-CHROM software. The silica column was 25 cm × 4.6 mm, packed with 3-μm Hypersil (Keystone Scientific). The post-column reaction system (PCRS) consisted of a Kratos Spectroflow 400 pump and a Kratos Model 525 dual-oven heating unit. The reaction coils were constructed from PTFE PFA tubing (0.020 in. × 1/16 in.) that had been made with a melt process (Zeus Industries). Two knitted reaction coils, each 2.5 ml in volume and the maximum allowed by the apparatus, were fabricated and connected in series. All solvents were HPLC grade and the TCA (Fisher), 2-naphthalenesulfonic acid 1-hydrate (NSA) (Kodak) and 3-hydroxypropionitrile (Aldrich, Gold Label) were used without further purification.

The mobile phase consisted of 1.1% (v/v) 3-hydroxypropionitrile in a 5:2 (v/v) mixture of 1-chlorobutane–1,2-dichloroethane. The 3-hydroxypropionitrile was more soluble in 1,2-dichloroethane than in 1-chlorobutane and this blend yielded a modifier concentration that was close to saturation. The PCRS reactant solution consisted of 5% TCA (w/v) in 1,2-dichloroethane, which was then saturated with NSA ($\sim$500 ppm). Both the mobile phase and PCRS reactant solution were filtered through a 0.2-μm PTFE filter (Millipore) prior to use. No attempts were made to eliminate water from these solutions, other than to minimize its introduction by using a previously unopened bottle of TCA.

The abamectin-8,9-oxide was dissolved in the mobile phases at a nominal concentration of 100 ppm. The solutions used to demonstrate linearity were made by diluting the 100 ppm solution with mobile phase.

RESULTS

Fig. 2 depicts the visible absorption spectra for one concentration of abamectin-8,9-oxide under different reaction conditions, in 1-cm cuvettes. The amount of color formation is directly proportional to the concentration of TCA, and the maximum absorption decreases (curves 2 and 3) as one reduces the level of TCA from 10 to 5%. However, 5% TCA solutions that are saturated with NSA or 4-biphenylsulfonic acid yield essentially the same absorption maximum as that with 10% TCA. The higher absorbance at 400 nm in curve 1 is not due to the absorption from the NSA itself; it is due to a change in the nature of the chromophore(s).

The HPLC conditions were chosen so as to achieve a sensitivity comparable to that in UV detection and to minimize wear-and-tear on the instrumentation. For example, the Tefzel coils originally supplied with the Kratos PCRS were subject to leakage with the halogenated solvents, and TCA is a very corrosive reagent. The custom-fabricated PTFE PFA coils were more robust, and use of NSA lowered the TCA concentration. The coil volume of 5 ml was the maximum allowed by the apparatus, so adequate sensitivity was achieved by raising the temperature.

Fig. 3 depicts the normal-phase chromatography of an abamectin-8,9-oxide solution (100 ppm in mobile phase) with detection at 210 nm using a typical mobile phase. There was no separation between the B_{1a} and B_{1b} components at a retention time of 28–29 min. Fig. 4 displays the chromatography obtained for a similar abamectin-8,9-oxide solution (100 ppm in mobile phase) with post-column reaction detection at 570 nm using the tungsten lamp. Based upon the flow-rates and coil volumes, the reaction time was 3–4 min. At retention times of 34–37 min there was near baseline separation of the B_{1a} and B_{1b} components. The B_{1a} component eluted before the B_{1b} component, which is opposite to the elution order in reversed-phase HPLC. The response shown in Fig. 4 is linear (correlation coefficient = 0.9996) over the range 20–100 ppm, and one can easily detect 1.0 μg (20 ppm × 50 μl) of analyte.

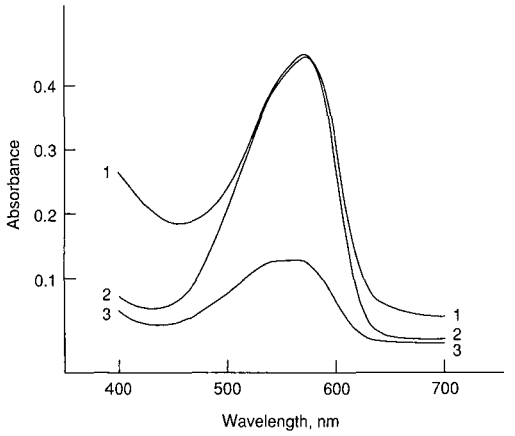

Fig. 2. Color formation with abamectin-8,9-oxide after 5 min at 50°C. Curve 1: 1 ml of abamectin-8,9-oxide (75 ppm in mobile phase) + 0.5 ml of 5% TCA, saturated with NSA. Curve 2: 1 ml of abamectin-8,9-oxide (75 ppm in mobile phase) + 0.5 ml of 10% TCA. Curve 3: 1 ml of abamectin-8,9-oxide (75 ppm in mobile phase) + 0.5 ml of 5% TCA.

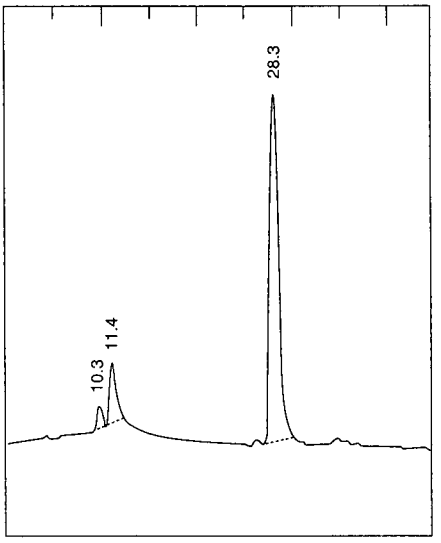

Fig. 3. Abamectin-8,9-oxide with UV detection at 210 nm. HPLC conditions: mobile phase, cyclohexane–isopropyl alcohol (90:10); flow-rate, 0.5 ml/min; column temperature, 30°C; PCRS solution, mobile phase flowing at 0.5 ml/min; PCRS temperature, ambient; loop size, 50 μl; detector sensitivity, 0.02 a.u.f.s. Numbers at peaks indicate retention times in min.

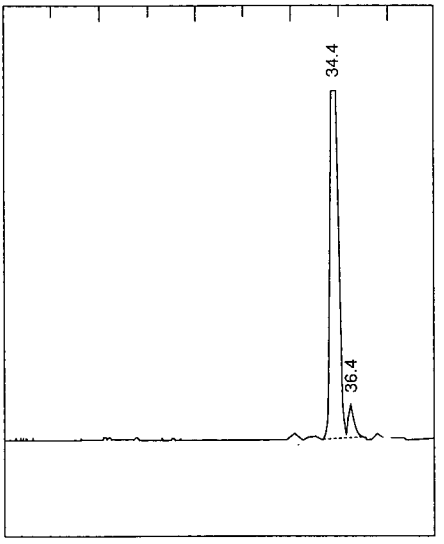

Fig. 4. Abamectin-8,9-oxide with detection at 570 nm, after post-column reaction. HPLC conditions: mobile phase, 1.1% 3-hydroxypropionitrile in 1-chlorobutane-1,2-dichloroethane (5:2); flow-rate, 1.0 ml/min; column temperature, 30°C; PCRS solution, 5% TCA in 1,2-dichloroethane saturated with NSA flowing at 0.5 ml/min; PCRS temperature, 45°C; loop size, 50 μl; detector sensitivity, 0.02 a.u.f.s.

DISCUSSION

The nature of the chromophore that is formed in these reactions merits some discussion. Although abamectin-8,9-oxide is a much larger molecule than vitamin A, not all of the avermectin structure is necessary for color formation. In fact, structure 2 (Fig. 5) shows an avermectin fragment, kindly supplied by Dr. S. Hanessian[16], that also gives a color reaction. Color formation with fragments frequently occurs at ambient temperatures. In contrast, 22,23-dihydroavermectin B_1 (ivermectin), lacking the double bond at C-22–C-23, does not undergo this color reaction. Now, it has been shown[17] that under strongly acidic conditions, the C-22–C-23 double bond participates in the opening of the neighboring ketal functionality. Also, the silyl-protecting groups would be removed from structure 2 under these conditions. Since small amounts of sulfonic acids catalyze the reaction, thus implying some elimination step(s), one can at least speculate on the formation of some chromophore similar to that which occurs in the reaction of TCA with vitamin A. No reaction products of this color formation have been isolated; however, this is also true of the long-studied vitamin A color reaction. The end result of the work is that one has a post-column procedure that is highly specific for avermectin-like structures.

The development of the mobile phase used in the colorimetric detection of abamectin-8,9-oxide deserves some explanation. It has been stated in the literature[18,19] that a silica surface is modified by adsorption of a polar solvent from a typical hydrocarbon mobile phase. One view is that the modifier is adsorbed much more strongly than the analyte, and does not compete with it for adsorption sites[20]. However, Scott[21] has shown that there are conditions under which an analyte does displace a polar solvent used as a modifier. The advantage of this latter concept is that it is easier to understand how modifier composition can affect chromatographic selectivity. Our experience is that a mobile phase that contains a nitrile modifier such as 3-hydroxypropionitrile provides better resolution for the avermectin components than does a typical alcohol–hydrocarbon mobile phase. The major advantage of 3-hydroxypropionitrile over other nitrile modifiers, such as 3,3′-oxydipropionitrile or glutaronitrile, is that it does not have to be purified for most chromatography with UV detection. We suspect that a nitrile-deactivated silica will be a useful alternative to an alcohol-deativated silica in many instances.

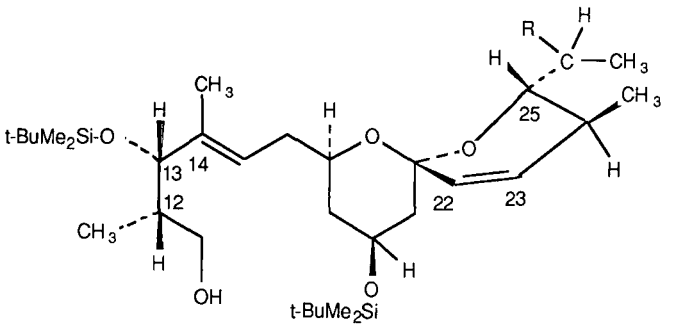

Fig. 5. Structure 2. B_{1a} component: R = C_2H_5; t-Bu = *tert.*-Butyl; Me = methyl.

ACKNOWLEDGEMENTS

The authors thank Dr. S. Hanessian for the sample of the material shown in structure 2. The authors appreciate the assistance of Messrs. D. Parriott and S. Kuczek of Applied Biosystems for the knitting of the PFA tubing and the fabrication of the reaction coils.

REFERENCES

1 W. C. Campbell (Editor), *Ivermectin and Abamectin*, Springer-Verlag, New York, 1989.
2 H. Mrozik, P. Eskola, G. F. Reynolds, B. H. Arison, G. M. Smith and M. H. Fisher, *J. Org. Chem.*, 53 (1988) 1820.
3 Y. Iwata, J. G. MacConnell, J. E. Flor, I. Putter and T. M. Dinoff, *J. Agric. Food Chem.*, 33 (1985) 467.
4 T. L. Shih, H. Mrozik, J. Ruiz-Sanchez and M. H. Fisher, *J. Org. Chem.*, 54 (1989) 1459.
5 H. H. Mrozik, *U.S. Pat.*, 4 530 921 (1985).
6 R. A. Dybas, N. J. Hilton, J. R. Babu, F. A. Preiser and G. J. Dolce, in A. L. Demain, G. A. Somkuti, J. C. Hunter-Cevera and H. W. Rossmoore (Editors), *Novel Microbial Products for Medicine and Agriculture*, Elsevier, 1989, Ch. 23, p. 203.
7 J. G. MacConnell, R. J. Demchak, F. A. Preiser and R. A. Dybas, *J. Agric. Food Chem.*, 37 (1989) 1498.
8 H. A. Moye, S. J. Scherer and P. A. St. John, *Anal. Lett.*, 10 (1977) 1049.
9 R. T. Krause, *J. Chromatogr. Sci.*, 16 (1978) 281.
10 H. A. Moye, C. J. Miles and S. J. Scherer, *J. Agric. Food Chem.*, 31 (1983) 69.
11 J. T. Goras and W. R. Lacourse, *J. Assoc. Off. Anal. Chem.*, 67 (1988) 701.
12 M. R. Lapointe and H. Cohen, *J. Assoc. Off. Anal Chem.*, 71 (1988) 480.
13 R. J. Demchak and J. G. MacConnell, *194th American Chemical Society National Meeting, New Orleans, LA, 1987*, Abstracts.
14 R. F. Bayfield, *Anal. Biochem.*, 39 (1971) 282.
15 G. B. Subramanyam and D. B. Parrish, *J. Assoc. Off. Anal. Chem.*, 59 (1976) 1125.
16 S. Hanessian, A. Ugolini, P. J. Hodges and D. Dubé, *Tetrahedron Lett.*, 27 (1986) 2699.
17 H. Mrozik, P. Eskola, B. H. Arison, G. Albers-Schönberg and M. H. Fisher, *J. Org. Chem.*, 47 (1982) 489.
18 L. R. Snyder, *Anal. Chem.*, 46 (1974) 1384.
19 H. Engelhardt, *J. Chromatogr. Sci.*, 15 (1977) 380.
20 D. L. Saunders, *J. Chromatogr.*, 125 (1976) 163.
21 R. P. W. Scott, *Adv. Chromatogr.*, 20 (1982) 167.

Journal of Chromatography, 511 (1990) 359–366
Elsevier Science Publishers B.V., Amsterdam

CHROM. 22 393

Note

Determination of flavins in dairy products by high-performance liquid chromatography using sorboflavin as internal standard

N. BILIC* and R. SIEBER
Federal Dairy Research Institute, Schwarzenburgstrasse 161, 3097 Liebefeld-Berne (Switzerland)
(First received July 21st, 1989; revised manuscript received February 12th, 1990)

Riboflavin, riboflavin-5-phosphate (flavin mononucleotide, FMN) and flavin adenine dinucleotide (FAD) are the principal forms of vitamin B_2. A variety of methods are available for their assays[1–3]. Microbiological methods and rat growth assay for riboflavin are not suitable for common laboratory applications[1]. Competetive protein binding assays are only specific for riboflavin[4]. Fluorimetric methods have been widely used because they are sensitive, rapid and applicable to the assay of individual flavins[3].

New developments in this area include assays of flavins by high-performance liquid chromatography (HPLC) with fluorescence detection. Applications of reversed-phase separation to the determination of riboflavin in various foods have been reviewed[5,6]. Assays for individual flavins in blood have been reported recently[7–9]. Important requirements are mild extraction procedures to prevent hydrolysis of both FAD and FMN.

HPLC assays for flavins or riboflavin have been carried out without use of internal standards and correction for losses in the extraction and in the chromatography was difficult or impossible. An internal standard must share structural and chromatographic properties with the flavins of interest, so as to co-purify them during the extraction and isolation procedures.

In this work we used sorboflavin as an internal standard for the assay of natural flavins by HPLC. It contains a glucityl side-chain on the isoalloxazine ring, in contrast to the ribityl chain in riboflavin. In our HPLC system, sorboflavin is well resolved and eluted between FMN and riboflavin. The substance is not commercially available, but can be prepared in the laboratory. Further a mild extraction procedure for flavins is presented, based on solubilization of the protein content followed by solid-phase extraction. Flavin losses due to coprecipitation, as observed in previous procedures, are largely avoided.

0021-9673/90/$03.50

EXPERIMENTAL

Apparatus

The HPLC system consisted of precision-flow metering pumps (Beckman Model 100A), a Supelco LC-18 7.5 cm × 4.6 mm I.D. column with a 3-μm packing, a 5μl loop, a Shimadzu C-R1A data processor and a Merck–Hitachi Model F1000 fluorescence spectrophotometer for HPLC applications equipped with a 12-μl flow cell. The excitation and emission wavelengths were set at 450 and 530 nm, respectively. The mobile phase was delivered at 1 ml/min. A Carl Zeiss PMQ II spectrophotometer was used to measure the absorption of flavin standard solutions.

Reagents and chemicals

Chemicals were of analytical reagent grade except acetonitrile (HPLC grade). Riboflavin, FMN monosodium salt and FAD disodium salt were from Merck. Water and deionized and doubly distilled.

Stock reagents and materials were 4 *M* urea, 1.5 *M* H_3PO_4, 10 and 12% aqueous formic acid, 1 *M* KH_2PO_4 (stored in a refrigerator) and silica gel C_{18}, 40–60 μm particle size, in ethanol (20 g in 80 ml).

The following reagent solutions were prepared prior to use: a solution for extraction of flavins consisting of 6% formic acid and 2 *M* urea (formic acid–urea), eluent for the extraction column [methanol–10% formic acid (1:4, v/v)] and mobile phase for HPLC, consisting of 14% acetonitrile in 100 m*M* KH_2PO_4, titrated to pH 2.9 with 1.5 *M* H_3PO_4.

Synthesis and purification of sorboflavin

The preparation of sorboflavin is based on the procedures described by Karrer and Benz[10] for riboflavin and by Berger and Lee[11] for arylamide-N-glycosides, but adapted for our laboratory without facilities for hydrogenation under both high pressure and temperature.

Methanol (200 ml) and a magnetic stirring bar were placed in a 250-ml boiling flask containing both 1 m*M* 4,5-dimethyl-*o*-phenylenediamine and 1 m*M* D-glucose. The mixture was refluxed for 8 h with stirring. The condenser was removed briefly in order to add 50–100 mg of allylpalladium (II) chloride as a hydrogenation catalyst. A stream of hydrogen, flowing through the fluid at 50 ml/min, was set up using PTFE tubing (1/8 in. O.D. × 2.1 mm I.D.) attached between the hydrogen bottle and the fluid (down the inside of the condenser). Refluxing under the hydrogen flow continued for 8–10 h. The fluid was cooled and filtered through a 0.45-μm PTFE membrane to remove the palladium. After evaporation of the solvent, 200 ml of glacial acetic acid and 10 m*M* alloxan were added to the residue and the mixture was stirred for 1 h at 50–60°C. The solvent was removed by evaporation. The residue containing sorboflavin was dissolved in 50–100 ml of water. Sorboflavin was purified on silica gel C_{18} (40–60 μm) packed in an Allihn filter tube to half the volume. The adsorbent was conditioned with ethanol and washed with water. The sorboflavin solution was loaded onto the adsorbent and passed through using suction. Non-flavin compounds and sorboflavin were eluted with 10 and 20% ethanol, respectively.

The sorboflavin obtained may be sufficiently pure for HPLC applications. If necessary, further purification may be carried out as described for flavin standard

solutions (see below). Using butanol–formic acid–water (77:10:13, v/v/v) as a solvent in paper chromatography, sorboflavin gave $R_F = 0.136$, in agreement with earlier observations[12].

Flavin standard solutions

Riboflavin (0.1 mg), FMN monosodium salt (0.15 mg) and FAD disodium salt (0.2 mg) were dissolved in 1 ml of water and separated on a 25 cm × 8 mm I.D. column filled with silica gel C_{18} (10 μm) using linear gradient elution at 2 ml/min [mobile phase A, 50 m*M* KH_2PO_4 (pH 5.5); mobile phase B, ethanol; gradient from 0 to 50% B in 30 min]. Measuring the absorbance at 450 nm, the major peak of each flavin was identified, collected and diluted with water to obtain an absorbance of about 0.3 (corresponding to concentrations of about 30 μM). The final concentration of each flavin was calculated using the molar absorptivity of $12.1 \cdot 10^3$ for both riboflavin and FMN and $11.3 \cdot 10^3$ for FAD[7]. Each standard solution was stored in 1-ml aliquots at −20°C. On the day of use, a 1 μM standard solution was prepared by transfering aliquots of purified flavin solutions into a 1-ml screw-capped volumetric flask (Pierce), followed by addition of 50 μl of sorboflavin solution (absorbance 0.2 at 450 nm) and dilution to volume with water.

Extraction of flavins

Solid-phase extraction columns were made on the day of use by filling filtration tubes (containing frits only) with 0.75 ml of silica gel C_{18} in ethanol, suspended by magnetic stirring. The ethanol was allowed to drain. A 1-cm glass microfibre circle (GF/D grade: Whatman) was placed on the adsorbent and gently pressed. The packing was rinsed with 2 ml of water.

A 1-g amount of cheese or 1 ml of milk was homogenized in or mixed with, respectively, 19-ml of formic acid–urea. Whole milk powder (0.2 g) was added to 10 ml of formic acid–urea and stirred for 30 min. The solutions were centrifuged to remove the fat. A 2-ml aliquot was mixed with 50 μl of sorboflavin solution (absorbance 0.2 at 450 nm) and passed through an extraction column, without application of pressure or vacuum. The packing was washed with 2 ml of 10% formic acid. The flavins were eluted by passing 1 ml of methanol–formic acid at a slow rate using a Vis-1 Single SPE Tube processor (Supelco) to provide gentle air pressure. The eluate was filtered and analysed by HPLC within 1 h.

RESULTS AND DISCUSSION

Reversed-phase HPLC with isocratic elution on a 7.5 cm × 4.6 mm I.D. column, filled wit a 3-μm packing, is effective for analysis of the flavins. Further advantages include short retention times, ranging from 1.2 to 2.9 min, in comparison with 8–20 min reported for riboflavin using other procedures[7–9]. Typical chromatograms of flavin standards and of flavins extracted from cheese are shown in Fig. 1. Because of both the short retention times and isocratic elution, the sample throughput can be fairly high. Also, clean-up of flavin extracts helps to prolong the column life considerably. The chromatograms in Fig. 1 were obtained on a column used for more than 500 separations.

The fluorescence intensity of flavins is pH dependent[3]. FAD exhibits a lower

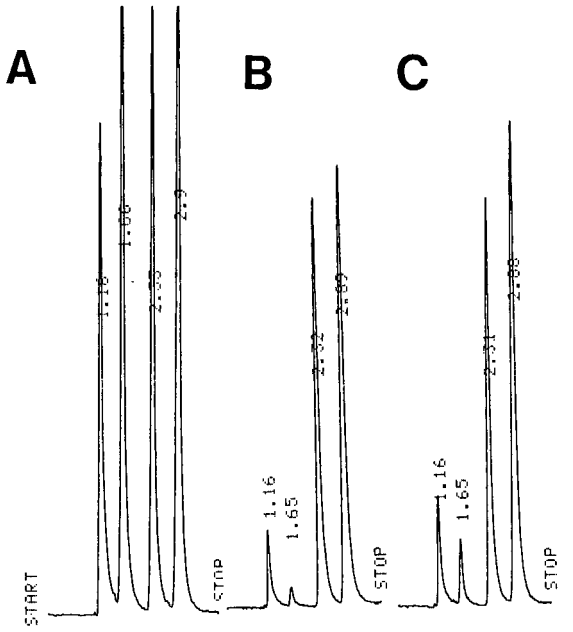

Fig. 1. Typical chromatograms of (A) flavin standards, each at a concentration of 1 μM, with retention times of 1.16, 1.66, 2.33 and 2.9 min for FAD, FMN, sorboflavin and riboflavin, respectively; (B) flavins extracted from 2 ml of a 5% Gruyère cheese homogenate; (C) flavins extracted from the same homogenate spiked with flavins, 100 pM each. Elution at 1 ml/min; injection volume, 5 μl; recording attenuation, 8 mV full-scale. For other conditions, see text. Numbers at peaks indicate retention times in min.

fluorescence efficiency than both FMN and riboflavin. A mobile phase of pH 2.9 was chosen to provide for the maximum fluorescence of FAD and for 85% of the maximum fluorescence of the two other flavins. We believe this to be a good compromise, allowing the analysis of all the flavins at low levels. The ionic strength of the mobile phase (100 mM KH_2PO_4) is important for separating FAD and FMN. At lower ionic strength, their peaks may overlap.

The determination of FAD by HPLC requires that the extraction procedure be sufficiently mild to prevent hydrolysis of the flavin to FMN. Exposure to both mineral acids and alkali should be avoided. Extraction with ice-cold trichloroacetic acid is possible if performed rapidly[1]. However, this procedure may destroy 4–5% of the FAD[13]. Other methods utilize extraction with acetonitrile at pH 7 or with 5% ammonium chloride at pH 5.5 and 80°C for 15 min[7,9]. Under such conditions, the protein precipitate formed may adsorb up to 17–20% of the riboflavin[8,9].

Our approach to the extraction of flavins includes a step to solubilize the protein content, which consists of poorly soluble casein. When this material is dissolved, the flavins are extracted by solid-phase extraction.

Formic acid was considered as a possible solvent for the present purposes, as it is known as a good solvent for peptides. Further, formic acid is perhaps the best solvent for riboflavin, dissolving 100 times as much riboflavin as water[14]. However, in our attempts to avoid hydrolysis of FAD, only dilute formic acid was used. It was soon shown that neither 5 nor 10% formic acid can dissolve casein or a piece of cheese

without the formation of a precipitate, unless supplemented by urea. A solution at pH 2 was adopted, containing both 6% formic acid and 2 *M* urea. It readily dissolves the required material and gives no precipitate on centrifugation at 4000 *g*.

A number of solvents were tried to desorb the flavins from an extraction column. It was observed by chance that methanol–formic acid is a very effective eluent for flavins. For instance, it is superior to methanol–0.15 *M* H_3PO_4 (Table I). By passing 1 ml of methanol–formic acid, more than 90% of the flavins were recovered in the eluate, in comparison with 20% or less using methanol–phosphoric acid. The reasons for these differences are not clear. Possibly higher protonation of the isoalloxazine ring at lower pH plays a role[14]. When the phosphoric acid had been replaced with 50 m*M* KH_2PO_4 (pH 5.5), the desorption rates of flavins remained almost unchanged (not shown). Eluents containing either phosphoric acid or phosphate buffer require a higher percentage of methanol (30% or more) for effective desorption of flavins. Consequently, eluates with 30% methanol may distort the FAD peak shape and shorten the column life.

Both FAD and FMN were examined for their stabilities in either methanol–formic acid or formic acid–urea. Each medium was spiked with either flavin and allowed to stand at ambient temperature in the dark for 24 h, then analysed by HPLC (Fig. 2). The fluids were filtered and analysed by HPLC without prior extraction. In methanol–formic acid, 8% of the FAD hydrolysed to FMN in 24 h. In another experiment (not shown), 9% of the FAD decomposed to FMN in the same period. These rates of FAD hydrolysis are very low, and may be neglected if flavin extracts are analysed within 1 h as proposed here. In formic acid–urea, the FAD was almost fully recovered, with trace amounts of FMN that could not be measured with the

TABLE I

DESORPTION RATES AND RECOVERIES OF FLAVINS FROM EXTRACTION TUBES.

A 2-ml volume of formic acid–urea was spiked with 1 n*M* each, of FAD, FMN and riboflavin, followed by addition of 50 µl of sorboflavin (absorbance 0.2 at 450 nm) and passed through an extraction tube. The adsorbent was washed with 2 ml of 10% formic acid. Volumes of 0.5 ml of either eluent were sequentially passed through the tube, collected and analysed by HPLC for flavin recovery.

Eluent	*Eluate No.*	*Recoveries of flavins in 0.5 ml of eluates (%)*			
		FAD	*FMN*	*Sorboflavin*	*Riboflavin*
Methanol–10% formic acid (1:4, v/v), pH 1.60	1	70	60	57.2	45.8
	2	22.9	33.3	37.1	46.1
	3	2.7	3.9	5.1	8
	Total:	95.8	97.2	99.4	99.9
Methanol–0.15 *M* H_3PO_4 (1:4, v/v), pH 1.85	1	4.7	3.3	1,3	0
	2	17.4	12.5	12.1	3.1
	3	21	18.5	22	9.2
	4	18	18.5	24	13.5
	5	12.8	16.6	19	17
	6	8	12	13	16.5
	7	4.3	7.3	7	13
	8	2.1	4.6	3.1	9.9
	Total:	88.3	93.3	101.5	82.2

TABLE II

DETERMINATION OF FLAVINS IN 2-ml ALIQUOTS OF CHEESE HOMOGENATES AND MILK DILUTIONS WITH AND WITHOUT ADDITION OF FLAVINS

The flavins (100 p*M* each) were added in a 100-μl volume.

No.	*Sample*	*Amounts of flavins measured (pM)*		
		FAD	*FMN*	*Riboflavin*
1	Aliquots of milk without addition of flavins ($n=8$)	32.9 ± 5	22.7 ± 4	427 ± 20
	Aliquots of milk with addition of flavins ($n=8$)	137 ± 11	128 ± 20	526 ± 18
	Recoveries of flavins added	104.1%	105.3%	99.0%
2	Aliquots of Sbrinz cheese homogenate without addition of flavins ($n=8$)	135 ± 19	19,6 ± 2	1300 ± 60
	Aliquots of Sbrinz cheese homogenate with addition of flavins ($n=8$)	237 ± 12	119 ± 11	1401 ± 28
	Recoveries of flavins added	102%	100.4%	101%
3	Aliquots of Gruyère cheese homogenate without addition of flavins ($n=8$)	163 ± 24	Not detected	1301 ± 30
	Aliquots of Gruyère cheese homogenate with addition of flavins ($n=8$)	255 ± 28	102 ± 10	1408 ± 36
	Recoveries of flavins added	92%	102%	98%

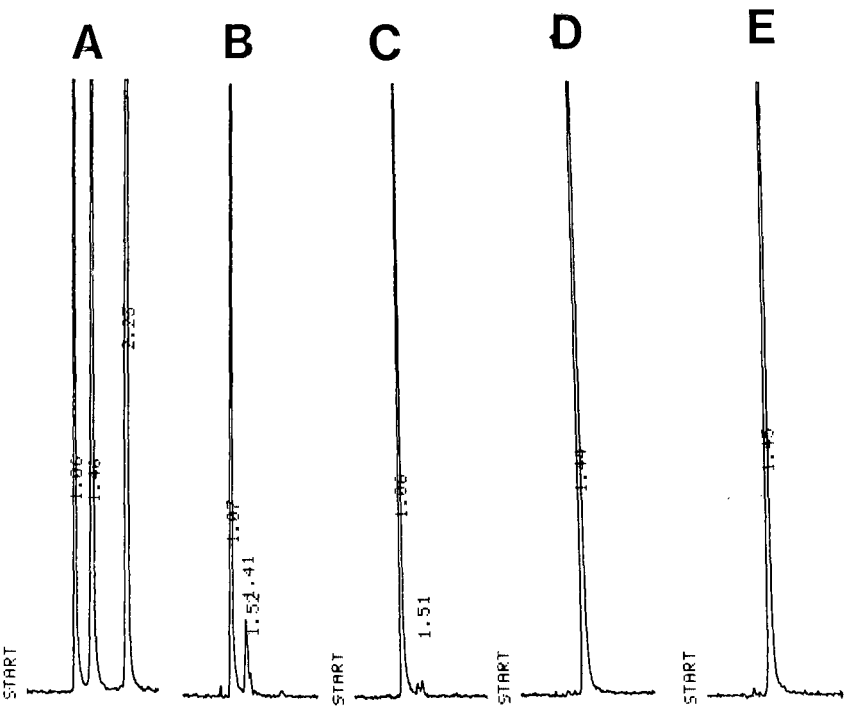

Fig. 2. Analysis of 1 μM flavin solutions. (A) FAD, FMN and riboflavin prepared in water and analysed within 2 h; (B) FAD in formic acid–methanol and (C) FAD in formic acid–urea analysed 24 h after preparation; (D) FMN in formic acid–methanol and (E) FMN in formic acid–urea analysed 24 h after preparation. Recoveries: (B) 94.4% as FAD and 8.5% as FMN, (C) 96.6% as FAD and (D) 98% and (E) 101% as FMN. The mobile phase contained 15% acetonitrile.

instrumental setup. In this case, hydrolysis rates of FAD may be guessed to be *ca.* 1% in 24 h or less, and may also be neglected. The FMN was shown to be stable in both media.

Recoveries of flavins for the whole procedure were checked in two ways. First, 2-ml aliquots of a 5% homogenate of Gruyère cheese were spiked with different amounts of each flavin to obtain 0.1, 0.2, 0.3, 0.4 and 0.5 μM concentrations. The results were evaluated using linear regression. The calculated slopes were multiplied by 100 to obtain percentage recoveries, which were 105.8, 99.7 and 100.2% for FAD, FMN and riboflavin, respectively. In the second approach, fixed amounts of flavins, 100 pM each, were added to 2-ml aliquots of either 5% cheese homogenates or 5% dilutions of milk in formic acid–urea. The flavin recoveries, given in Table II, are in the ranges 92–104% for FAD, 100–105% for FMN and 98–101% for riboflavin.

Both the within- and between-assay precisions of the method were tested on a cow milk containing all the flavins of interest. The milk was defatted by centrifugation and stored in aliquots at −20°C until the day of analysis. The results are given in Table III. The relative standard deviations are about 6% for both FAD and riboflavin and 12% for FMN; the low concentration of FMN might be a reason for the high value.

TABLE III

PRECISION OF THE ASSAY

Parameter	*pM in 2-ml aliquot of milk (mean ± S.D.)*		
	FAD	*FMN*	*Riboflavin*
Within-assay ($n=8$)	52.4 ± 3.4	17.8 ± 3	395 ± 25
Relative standard deviation	6.5%	11%	6,3%
Between-assay ($n=17$)	50.5 ± 3	15.1 ± 1.7	419 ± 28
Relative standard deviation	5.9%	12%	6.7%

At a signal-to-noise ratio of 3, the detection limits were calculated to be about 3 nmol/l for FAD and 2.5 nmol/l for both FMN and riboflavin.

The present procedure seems to be reliable for measuring the flavins in dairy material. The recovery and precision are within acceptable limits. The reliability is based on the use of sorboflavin as the internal standard, formic acid–urea as a good solvent for both the protein matrix and the flavins and methanol–formic acid as good solvent for desorption of the flavins.

Sorboflavin is stable in the procedure, readily soluble in aqueous solutions and exhibits spectral properties similar to those of natural flavins. The use of sorboflavin does not prolong the chromatography time, as its peak emerges between those of natural flavins. However, when stored at 4°C for 6 months or longer, sorboflavin may exhibit an new peak emerging shortly after riboflavin. This is of no consequence for the assay.

REFERENCES

1 J. Koziol, *Methods Enzymol.*, 43 (1971) 253.
2 W. N. Pearson, in P. György and W. N. Pearson (Editors), *The Vitamins*, Vol. 7, Academic Press, New York, 1967, p. 99.
3 S. Udenfriend, *Fluorescence Assay in Biology and Medicine*, Academic Press, New York, 1962.
4 S. E. Lotter, M. S. Miller, R. C. Bruch and H. B. White, *Anal. Biochem.*, 125 (1982) 110.
5 M. A. Marletta and D. R. Light, in A. P. De Leenheer, W. E. Lambert and M. G. M. De Ruyter (Editors), *Modern Chromatographic Analysis of the Vitamins*, Marcel Dekker, New York, Basle, 1985, p. 413.
6 P. M. Finglas and R. M. Faulks, *J. Micronutr. Anal.*, 3 (1987) 251.
7 H. Ohkawa, N. Ohishi and K. Yagi, *Biochem. Int.*, 4 (1982) 187.
8 A. J. Speek, F. van Schaik, J. Schrijver and W. H. P. Schreurs, *J. Chromatogr.*, 228 (1982) 311.
9 A. Lopez-Anaya and M. Mayersohn, *J. Chromatogr.*, 423 (1987) 105.
10 P. Karrer and F. Benz, *Helv. Chim. Acta*, 18 (1935) 426.
11 L. Berger and J. Lee, *J. Org. Chem.*, 11 (1946) 84.
12 W. Forter and P. Karrer, *Helv. Chim. Acta*, 36 (1953) 1530.
13 V. Massey and B. E. P. Swoboda, *Biochem. Z.*, 338 (1963) 474.
14 T. Wagner-Jauregg, in W. H. Sebrell, Jr. and R. S. Harris (Editors), *The Vitamins*, Vol. 5, Academic Press, New York, 1972, p. 3.

Journal of Chromatography, 511 (1990) 367–372
Elsevier Science Publishers B.V., Amsterdam

CHROM. 22 401

Note

Determination of 10-camphorsulphonates in pharmaceutical formulations by high-performance liquid chromatography

C. PIERRON*, J. M. PANAS, M. F. ETCHEVERRY and G. LEDOUBLE
Laboratoire de Chimie Analytique, Faculté de Pharmacie, 51096 Reims Cédex (France)
(First received October 17th, 1989; revised manuscript received February 23rd, 1990)

Salts of 10-camphorsulphonic acid (CSA) are used in pharmaceutical preparations as an aqueous soluble form of camphor. The most frequently found are camphorsulphonates of sodium, codeine, piperazine, ephedrine and ethylmorphine, which are used in tablets, suppositories, oral drops, syrups and injections. A specific study of their determination in pharmaceutical forms has not yet been reported.

10-Camphorsulphonic acid has been used as a counter ion in reversed-phase chromatography[1–5]; (+)- and (−)-antipodes of 10-camphorsulphonic acid have been used for the separation of enantiomeric amines or amino alcohols by ion-pair formation[6–10], and themselves have been separated by the same procedure with chiral amines[11,12]. These separations of optical isomers require the use of low-polarity solvents, which are often incompatible with commercial dosage forms (syrups, injections, oral drops) containing water, and which therefore cannot be used.

Moreover, the raw material for the preparation of camphorsulphonates for medical use is synthetic camphor, a mixture of optical isomers. Our problem was to find a method for use in routine work that would achieve a separation suitable for quantification without the separation of enantiomers. The low absortivity of camphorsulphonic acid and of camphorsulphonates requires the use of a UV-absorbing counter ion. In these systems, the counter ion has a double function: to permit the separation in a reversed-phase system (now the most popular mode of liquid chromatography) and to improve the detection at the measured wavelength.

We chose phenethylammonium as a UV-absorbing counter ion with a high molar absortivity because it is known to yield good sensitivity, linearity and precision in the quantification of alkylsulphonate ions[13,14]. This chromatographic system has also been well described in several other papers[15–20].

The purpose of this paper is to present a method for the determination of 10-camphorsulphonates in commercial dosage forms. The developed method is based on ion-pair reversed-phase high-performance liquid chromatography (RP-HPLC) using phenethylammonium as a highly UV-absorbing counter ion.

0021-9673/90/$03.50

EXPERIMENTAL

Apparatus

The high-performance liquid chromatograph used was a Waters Assoc. 6000 A equipped with a U6K universal injector, a Waters Assoc Lambda-Max M480 detector and a Hewlett-Packard 3390 A recorder–integrator. The column used was a μBondapak C_{18} (30 cm × 3.9 mm I.D.; 10 μm) (Waters Assoc.).

Chemicals and reagents

All solvents and chemicals were of analytical-reagent or reagent grade and were used without further purification. (1*R*)-(−)-10-Camphorsulphonic acid, (1*S*)-(+)-10-camphorsulphonic acid and 2-phenethylamine were purchased from Aldrich (Strasbourg, France). Racemic 10-camphorsulphonic acid, perchloric acid, phenol (internal standard) and methanol were obtained from Prolabo (Paris, France).

Chromatographic conditions

The mobile phase was 2.5 m*M* 2-phenethylamine in water containing 50% (v/v) methanol. The pH of the aqueous solution was adjusted to 3.00 (±0.05) with dilute perchloric acid before adding methanol. The mobile phase was filtered through a 0.45-μm Millipore filter before use. The temperature was 20–25°C and the flow-rate was 1.0 ml min^{-1}. Before commencing the day's analysis, mobile phase was pumped through the column for 1 h at 1 ml min^{-1} to establish stable baseline conditions. The UV detector was set at 260 nm, the chart speed was 1 cm min^{-1} and the volume injected was 10 μl.

Preparation of standards

A stock solution of (1*S*)-(+)-10-camphorsulphonic acid was prepared by dissolving an accurately weighed amount of 464.6 mg of CSA into enough mobile phase to obtain a final volume of 100.0 ml (20 m*M* solution).

To prepare the stock solution of the internal standard, an accurately weighed amount of 22.5 mg of phenol was dissolved and diluted with mobile phase to 20.0 ml (12 m*M* solution).

Serial dilutions of the stock solution of (+)-10-camphorsulphonic acid and phenol (as constant internal standard) were prepared and diluted with the mobile phase.

Calibration solutions were prepared in the range 1–15 m*M* of (+)-10-camphorsulphonic acid and each contained 0.6 m*M* of phenol.

Preparation of samples

Depending on the theoretical amount of camphorsulphonate present in the sample, the volume of mobile phase has to be adjusted to obtain a concentration similar to that of one of the calibration solutions; the volume of stock solution of internal standard (phenol) has to be adjusted correspondingly.

Tablets. The tablets were broken and extracted under magnetic stirring with mobile phase for 10 min, the suspension was centrifuged and the supernatant was collected in a volumetric flask, then the bottom layer was stirred once more with the mobile phase for another 10 min. The supernatants were combined, the internal

TABLE I

INTRA-ASSAY VARIATION FOR THREE CONCENTRATIONS OF CSA

CSA concentration (mM)	*Standard deviation of peak-area ratios (n = 5)*	*Relative standard deviation (%) (n = 5)*
1	0.00261	1.09
9	0.0167	0.88
15	0.0275	0.77

standard solution was added to the volumetric flask and the mixture was diluted with mobile phase. The solution was filtered through paper before use.

Suppositories. The suppositories were dissolved in mobile phase by heating at 60°C for *ca.* 15 min in a water-bath, then cooled to separate the mass of excipient. The liquid phase was collected and the mass was extracted once more for 15 min. The combined solutions were filtered through paper; all the glassware was washed with mobile phase and the internal standard solution was added. The resulting solution was diluted to volume with mobile phase.

Liquids. All liquid forms (syrups, oral drops, injections) were merely diluted with the mobile phase and the appropriate volume of internal standard solution was added.

Linearity, precision and sensitivity

The peak-area ratios of 10-camphorsulphonic acid to the internal standard (phenol) were calculated in the 1–15 m*M* range. The calibration graph was plotted as peak-area ratio *versus* CSA concentration. The results of linear regression analysis were slope 0.799, intercept −0.013 and correlation coefficient $r = 0.9998$ ($n = 10$).

The precision of the proposed method was evaluated by assaying repeated injections using three concentrations (1, 9 and 15 m*M*) of CSA. The within-day variation was investigated by five replicate analyses for each concentration; the results are shown in Table I. The inter-assay variation was determined by replicate analyses of the three concentrations over a 5-day period (Table II). The assays showed good precision at low and high concentrations. The average reproducibility was greater than 99% in the intra-assay and close to 98% in the inter-assay mea-

TABLE II

INTER-ASSAY VARIATION OVER A 5-DAY PERIOD

Replicate analyses of three samples containing 1.9 and 15 m*M* CSA.

CSA concentration (mM)	*Standard deviation of peak-area ratios*	*Relative standard deviation (%)*
1	0.00605	2.55
9	0.0471	2.39
15	0.0677	1.95

surements. Under the analytical conditions, the limit of detection (corresponding to a signal-to-noise ratio of *ca.* 4:1, with an injection volume of 10 μl) was 0.2 μg (absolute amount).

RESULTS AND DISCUSSION

Influence of optical isomers

To determine the possible influence of rotatory power on determinations, we prepared by accurate weighing and dilution three solutions of 10-camphorsulphonic acid [(+), (−) and racemic (±)] and two solutions with sodium camphorsulphonates from natural and synthetic camphor. The comparison between capacity factors (k') and peak areas showed total similarity between the responses of the various optical antipodes (enantiomers) and mixtures. Therefore, we shall henceforth refer to camphorsulphonates and 10-camphorsulphonic acid without specifying the rotatory power.

Influence of pH

CSA is a strong acid, fully dissociated even at pH < 3, and therefore the effect of pH on separation can be neglected. We chose the mobile phase pH so that phenethylamine would be ionized enough (into phenethylammonium) to favour ion-pair formation without damage to the column. Hence, in accordance with Bidlingmeyer[13], it was deemed preferable to adjust the pH of the water solvent before mixing it with the organic solvent. The acid used was perchloric acid, which improves peak shapes[1]. Fig. 1 is an illustration of the influence of pH on ion-pair formation. Here the solute and the UV-absorbing counter ion have opposite charges and the solute peak is positive after the "system peak", well known in this chromatographic system. This is in accordance with principles presented in several papers[10–15,17,18,20].

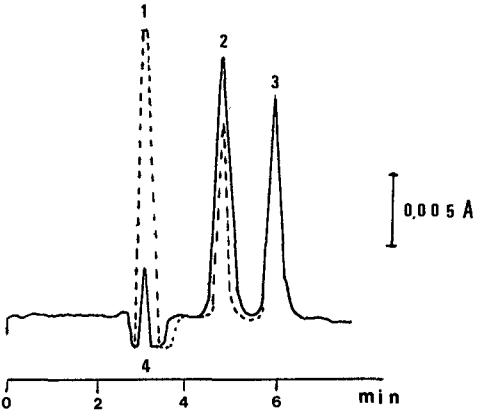

Fig. 1. Influence of pH on ion-pair formation of CSA with 2.5 m*M* phenethylamine. 1 = Perchlorate system peak; 2 = CSA; 3 = internal standard (phenol); 4 = phenethylamine system peak. Dashed line, pH = 5; solid line, pH = 3.

TABLE III

RESULTS FOR 10-CAMPHORSULPHONATES IN VARIOUS COMMERCIAL DOSAGE FORMS

Results are averages of three consecutive analyses, expressed as 10-camphorsulphonic acid

Commercial formulation	*Salt*	*CSA content*		*Percentage of label claim determined*
		Manufacturer's label claim	*Found (mg)*	
Tablet A	Codeine	10.92 mg/tablet	10.89	99.7
Suppository B	Na	18.27 mg/suppos.	18.29	100.1
Syrup C	Codeine Ethylmorphine Ephedrine Piperazine	4.85 mg/ml	4.89	100.8
Syrup D	Na Thiamine	13.55 mg/ml	13.38	98.7
Oral drops E	Piperazine	102.0 mg/ml	105.5	103.4
Injection F	Piperazine	102.13 mg/ml	102.21	100.1

Influence of other variables on the capacity factor

As generally occurs in reversed-phase chromatography, with increasing methanol content the capacity factor k' decreases. Sachok et al.[14], Denkert *et al.*[17] and others[15,16] have thoroughly investigated the influence of counter-ion concentration. Here, when the phenethylamine concentration changes from 1 to 3 mM, the capacity factor increases from 1.74 to 2.24. We chose a phenethylamine concentration of 2.5 mM because good separations were obtained in a reasonable time. It will be noted that the capacity factor is not influenced by the nature of the camphorsulphonate cation.

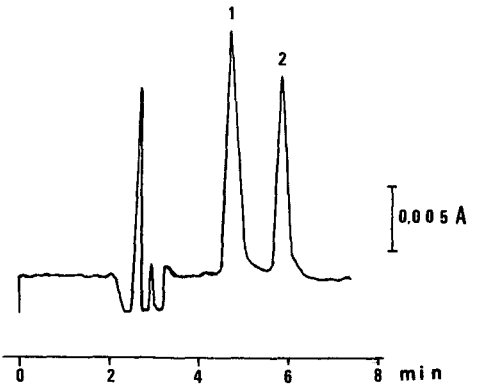

Fig. 2. Example of separation of camphorsulphonate as an ion pair with phenethylammonium in a commercial formulation (injection F). 1 = CSA; 2 = internal standard (phenol).

Applications

The method was applied to six commercial pharmaceutical formulations: two solid forms (tablets A, suppository B) and four liquid forms (syrups C, and D, oral drops E and injection F). The results (means of three replicates) are reported in Table III; they show a good correlation between the labelled and found amounts of CSA. An example a chromatogram is presented in Fig. 2.

CONCLUSIONS

Ion-pair RP-HPLC with a UV-absorbing counter ion can be applied to salts of 10-camphorsulphonic acid in commercial pharmaceutical preparations without interfering with the nature of the cation. Separation can be carried out by simply dissolution in the mobile phase for solid forms, or by simple dilution with mobile phase for liquid forms. Because camphorsulphonates are highly water soluble, this simple method is limited to formulations with a camphorsulphonate concentration sufficient to produce by dilution a solution in the range 1–15 m*M*.

REFERENCES

1 R. Gloor and E. L. Johnson, *J. Chromatogr. Sci.*, 15 (1977) 413–423.
2 E. Tomlinson, T. M. Jefferies and C. M. Riley, *J. Chromatogr.*, 159 (1978) 315–358.
3 W. Lindberg, E. Johansson and K. Johansson, *J. Chromatogr.*, 211 (1981) 201–212.
4 G. Szepesi, M. Gazdag and R. Ivancsics, *J. Chromatogr.*, 241 (1982) 153–167.
5 A. Bartha, G. Y. Vigh, H. Billiet and L. De Galan, *Chromatographia*, 20 (1985) 587–590.
6 C. Pettersson and G. Schill, *J. Chromatogr.*, 204 (1981) 179–183.
7 C. Pettersson and G. Schill, *Chromatographia*, 16 (1982) 192–197.
8 G. Szepesi, M. Gazdag and R. Ivancsics, *J. Chromatogr.*, 244 (1982) 33–48.
9 H. K. Lim, M. Sardessai, J. W. Hubbard and K. K. Midha, *J. Chromatogr.*, 328 (1985) 378–386.
10 C. Pettersson and G. Schill, *J. Liq. Chromatogr.*, 9 (1986) 269–290.
11 C. Pettersson and K. No. *J. Chromatogr.*, 282 (1983) 671–684.
12 C. Pettersson, *J. Chromatogr.*, 316 (1984) 553–567.
13 B. A. Bidlingmeyer, *J. Chromatogr. Sci.*, 18 (1980) 525–539.
14 B. Sachok, S. N. Deming and B. A. Bidlingmeyer, *J. Liq. Chromatogr.*, 5 (1982) 389–402.
15 N. Parris, *J. Liq. Chromatogr.*, 3 (1980) 1743–1751.
16 J. Crommen, *J. Chromatogr.*, 193 (1980) 225–234.
17 M. Denkert, L. Hackzell, G. Schill and E. Sjögren, *J. Chromatogr.*, 218 (1981) 31–43.
18 L. Hackzell and G. Schill, *Chromatographia*, 15 (1982) 437–441.
19 J. R. Larson, *J. Chromatogr.*, 356 (1986) 379–381.
20 J. Crommen, G. Schill, D. Westerlund and L. Hackzell, *Chromatographia*, 24 (1987) 252–260.

Journal of Chromatography, 511 (1990) 373–378
Elsevier Science Publishers B.V., Amsterdam

CHROM. 22 483

Note

Chromatographic evaluation of boldine and associated alkaloids in Boldo

T. J. BETTS
School of Pharmacy, Curtin University of Technology, GPO Box U 1987, Perth, W. Australia 6001 (Australia)

(Received January 8th, 1990)

In 1988, Pietta *et al.*[1] recorded high-performance liquid chromatographic (HPLC) assays of some alkaloids, and thin-layer chromatographic (TLC) studies of Boldo extracts from *Peumus boldus* Molina leaves, a herb from Chile with a reputation for urinary and liver treatment. They devised a reversed-phase HPLC method using an amine-phosphate buffer reported as containing about 85% acetonitrile as mobile phase, which after a "clean-up" procedure gave at 270 nm a chromatogram (illustrated) with six peaks, only three of which (not including the major one!) they named. Their thin-layer chromatography (TLC) method used 25% diethylamine in chloroform on silica gel F_{254}.

In the course of some studies of several commercial samples of Boldo, I reviewed and modified the procedures of Pietta *et al.*[1], and my observations and results are given below.

Alkaloids which have been recorded from Boldo are boldine, isocorydine and nor-isocorydine, N-methyllaurotetanine[2] and laurotetanine, and isoboldine[3] (see Fig. 1). Boldine occurs in two other plant genera along with some of these above-mentioned aporphine alkaloids[4,5].

EXPERIMENTAL

Apparatus

A Laboratory Data Control HPLC 7800 system with Constametric pumps, UV Spectromonitor III 1204A, accessory control module, computer chromatography control module, and recorder/printer was applied.

Materials

Boldo herb (mostly leaf) and Boldo extract commercial samples from various European manufacturers were used. Boldine alkaloid (crystallised with a molecule of chloroform) was obtained from Sigma.

0021-9673/90/$03.50

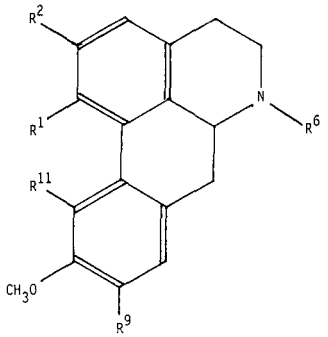

R^1	R^2	R^6	R^9	R^{11}	
CH_3O	HO	CH_3	HO	H	boldine
HO	CH_3O	CH_3	HO	H	isoboldine (diphenols)
CH_3O	CH_3O	CH_3	HO	H	N-methyllaurotetanine
CH_3O	CH_3O	H	HO	H	laurotetanine
CH_3O	CH_3O	CH_3	H	HO	isocorydine
CH_3O	CH_3O	H	H	HO	nor-isocorydine

Fig. 1. Structures.

Methods

HPLC. Reversed-phase Spherisorb S5 ODS S1 columns 4.9 or 4.6 mm I.D. were used at 30°C. A 20-μl injection loop was applied. The detector was set at 304 nm.

Solvent system 1, for quick review of an extract, with some peak overlapping, was isocratic, with 77.4% acetonitrile in water, containing 0.05% diethylamine, and the pH brought below 4 by the addition of dilute phosphoric acid; flow-rate 0.8 ml/min. Six peaks appear between 5 and 10 min (Fig. 2b).

Solvent System 2, for accurate boldine analysis, was initially isocratic, with 16.3% acetonitrile in water, containing 0.2% diethylamine, and the pH below 4, as above. After 8 min at a flow-rate of 2.1 ml/min the acetonitrile content was increased linearly to 28.0% at 11 min elapsed time, then left isocratically until 18 min. After 5 min a series of six peaks appeared, designated U to Z, with V corresponding to reference boldine (Fig. 2a).

Evaluation of alkaloids. Boldine was evaluated by HPLC peak area against a solution of about 6 mg% reference boldine in acetonitrile (73.28% of the weight taken due to chloroform of crystallisation). This was stable over several weeks if stored away from light. Other peaks were evaluated as though they were boldine, which is of course, somewhat inaccurate. Results are given in Table I.

Extraction of Boldo herb or extract. Exactly 1 g is percolated (leaf, in filter

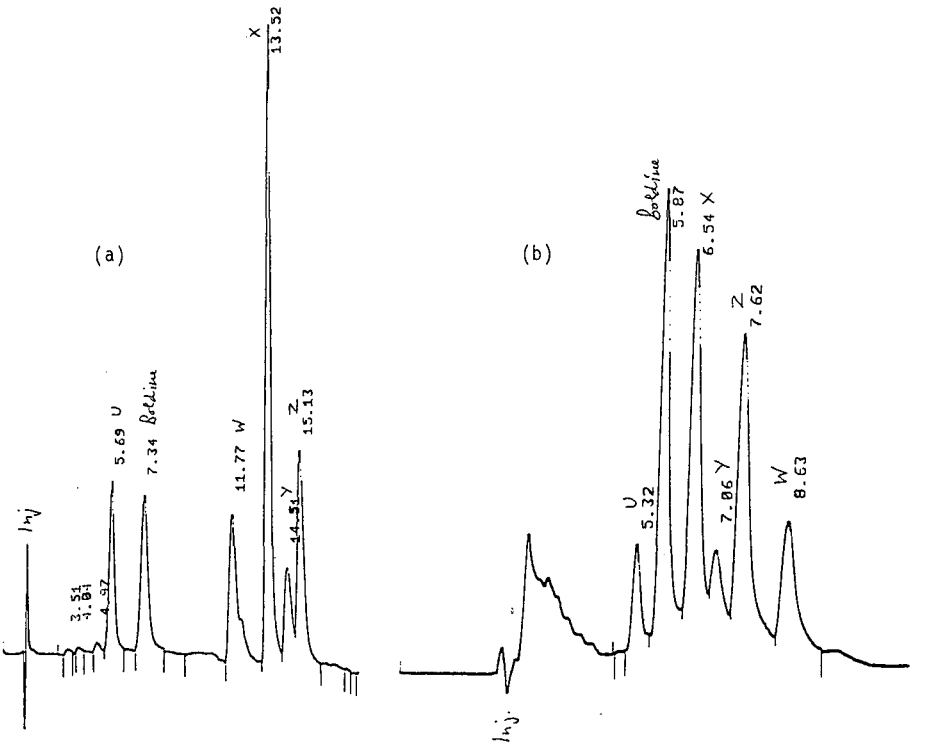

Fig. 2. HPLC traces of processed Boldo. (a) Solvent system 2 (programmed from 16.3 to 28% acetonitrile in water) used on Boldo leaf B. (b) Solvent system 1 (isocratic with 77% acetonitrile in water) used on Boldo extract H. The deduced identity of peaks is given in Table I. The numbers at the peaks indicate retention times in min.

paper) or rubbed with a spatula (commercial extract) in nearly boiling dilute hydrochloric acid. After cooling, this is exhausted of interfering pigments by careful shaking with a solvent mix of equal parts of ethyl acetate and carbon tetrachloride (discarded). The residual aqueous extract is made alkaline with ammonia and carefully extracted with fresh solvent mix, which is evaporated to dryness. The residue is taken up in acetonitrile (exactly 10 ml) for HPLC assay. For TLC study the residue is used in concentrated form.

TLC. A two-dimensional system was devised, using silica gel plates with fluorescent (254 nm) indicator. The first-direction solvent consisted of equal parts of methanol and ethyl acetate which elutes pigment to about R_F 0.8, with a complex main alkaloidal spot R_F 0.5–0.6, followed by traces of minor spots. The second-direction solvent was 5% diethylamine in ethyl acetate (which avoids amine interaction with halogenated solvents). Boldine is most polar and so slow moving, R_F 0.20 or less. Two other strong spots ahead of boldine at R_F 0.35 and 0.70 should be N-methyllaurotetanine and isocorydine (-N-oxide? — due to the large surface area of the TLC plate), respectively, according to other studies[1,6] using diethylamine systems.

TABLE I

mg% BOLDINE AND OTHER BOLDO ALKALOIDS (CALCULATED AS BOLDINE FROM PEAK AREAS AT 304 nm) IN BOLDO SAMPLES

Letters U–Z refer to chromatographic peaks in Fig. 1. They are provisionally identified by their chromatographic responses. Letters A-H refer to different samples. Numbers 1 and 2 refer to solvent systems (see text).

	Boldo leaf "whole" samples												*Commercial extracts*			
	A		*B*		*C*		*D*		*E*		*F*		*G*		*H*	
	2	*1*	*2*	*1*	*2*	*1*	*2*	*1*	*2*	*1*	*2*	*1*	*2*	*1*	*2*	*1*
Boldine	4	6	6	6	8	8	9	9	9	9	13	14	27	27	8	10
U Isoboldine?	3	3	5	5	4	4	6	6	5	5	13	13	5	5	1	2
X Laurotetanine?	16	16	16	18	14	14	22	22	27	26	62	57	23	23	8	10
Z N-Methyllaurotetanine?	14	15	7	8	7	8	20	22	17	17	27	27	22	21	9	10
Y Isocorydine?	6	6	3	4	4	6	13	12	15	15	9	10	9	8	3	3
W Isocorydine-N=O?	4	11	7	3	6	6	13	13	14	17	14	14	6	12	2	4
Total	47		44		43		83		87		138		92		31	
% Boldine	8.5		13.6		18.6		10.8		10.3		9.4		29.3		25.8	
% "Laurotetanines"	64		52		49		51		51		64		49		55	
% "Isocorydines"	21		23		23		31		33		17		16		16	

Minor spots scattered over the plate nearer the start point should be relatively polar other diphenolic substances and nor-alkaloids. Visualisation is by fluorescence quenching of the plate background viewed in UV at 254 nm, and subsequent darkening of the spots to slaty-brown on standing in daylight or UV light. A reaction to Dragendorff's or iodoplatinate reagents can be obtained, but this is not as sucessful as the slow darkening in daylight; the plate can best be viewed the following day. The phenolic reaction sequence of ferric chloride solution followed by potassium ferricyanide spray is a better method of detection.

The relatively high polarity of boldine compared to the other alkaloids was confirmed by reversed phase TLC using Whatman KC_{18} F plates, with solvent methanol–acetonitrile–water–diethylamine (55:5:40:0.2) (with pH brought below 4 with dilute phosphoric acid). Boldine has an R_F just below 0.30, followed by other alkaloidal spots, these being strongest at R_F about 0.15.

DISCUSSION

The only possible way to obtain a reversed-phase HPLC result like that illustrated by Pietta *et al.*[1] is to use a solvent mix with about 16% acetonitrile instead of the 85% they quote. In other words, their quoted proportions of acetonitrile to watery component need reversing. The gap between their boldine peak 1 and peak 2 only occurs with low percentages of acetonitrile in the solvent, as also for their later peaks with long retention times. Their mysterious major peak just after their peak 2, which they make no reference to at all, is clearly an artefact introduced by their use of Sep-Pak C_{18} cartridges for "clean-up", as it is absent from their unpurified Boldo extract chromatogram. If an HPLC solvent mix close to that given by Pietta *et al.*[1] is used, and the flow-rate adjusted to give the retention time for boldine that they record (about 6 min) then all the later peaks are eluted and the chromatogram finished in about 11 min, not the 25 min shown by them.

Pietta *et al.*[1] note that the Boldo alkaloids "exhibit different UV absorption maxima, and (their) determination was carried out at 270 nm which represents the best compromise". This wavelength in fact only suits the 11-hydroxy alkaloids such as isocorydine (see Fig. 1) and not the others like boldine, which have absorption maxima at about 283 and 303 nm. Using 270-nm detection has deflated the results for boldine and those alkaloids without an 11-hydroxy group, which hardly seems desirable.

My work was performed at 304 nm, where there is a slightly lower intensity peak for boldine than at 283 nm[7], but it is less likely to interference from various other constituents, including ascaridole[8] from the volatile oil. By using detection at both 304 and 269 nm it was possible to recognise the 11-hydroxy alkaloids by their higher peaks shown at the shorter wavelength. This applied to peaks designated W and Y by me, which were thus noted as members of the isocorydine group. W revealed behaviour unlike any other peak from Boldo extracts, in that it shifted position in the sequence of peaks to overlapping X and Y at solvent concentrations of about 40–60% acetonitrile, and to coming after Z in 77% acetonitrile. Isocorydine is recorded as susceptible to oxidation, and so I suspected that it was isocorydine-N-oxide, leaving Y as isocorydine itself. If this is correct, peak 2 of Pietta *et al.*[1] which they called "isocorydine" is actually its N-oxide. They "isolated" this substance (and N-

methyllaurotetanine) "by preparative TLC" without any identification, and the large surface area of a TLC adsorbent can readily catalyse oxidation.

Thus a diphenolic alkaloidal boldine early peak V was identified using authentic alkaloid, and a late peak Y characterised as monophenolic isocorydine. This is an appropriate sequence for a reversed-phase system, with the less polar monophenolic being retained longest on the non-polar column. Thus the small peak(s) U ahead of boldine should also be diphenolic(s) like isoboldine and later peaks X and Z should be monophenolics of the (non-11-hydroxy)laurotetanine type. N-Methyllaurotetanine will be less polar than the nor-alkaloid and so should be retained longer by the non-polar column (Z), leaving X as laurotetanine itself. This does not correspond to the peak 3 designated by Pietta *et al.*[1] as "N methyllaurotetanine" (I believe it to be iso-corydine) but their reliance on UV detection at 270 nm hints that their peak 3 (and also 2) are 11-hydroxy alkaloids.

Boldine, from Table I (and Fig. 1) is clearly a minor alkaloid in both the Boldo herb samples and commercial extracts. It forms 8.5 to 18.6% of the total leaf alkaloids, and about 25–30% of the extracts. It is interesting that commercial processing (probably by hot-water extraction) increases the proportion of boldine. However, put in this manner, the proportion of boldine really depends on the total amount of other alkaloids there. Total alkaloids calculated as boldine form 43–138 mg% of the leaf samples and 31–92 mg% of the extracts. Extract H, at least, has thus undergone a preferential loss of non-boldine constituents, which is perhaps desirable, as the other alkaloids may not assist the physiological effects of boldine. For three commercial extracts, Pietta *et al.*[1] found 8, 14 and 16 mg% boldine. In 1983, by titrimetry, total alkaloids of 53 and 68 mg% were recorded, with boldine forming 13 and 19% of the total. These values agree with my results.

From my limited observations, there may be at least two chemical forms of Boldo herb, one with total alkaloids of 40–50 mg%, and the other with double or treble this. It seems desirable to look for Boldo leaf with at least 8 mg% boldine, which forms at least one-tenth of the total alkaloids (to limit excessive amounts of these other substances). Commercial extracts should show an increased boldine content, which forms greater than a quarter of the total alkaloids. This is best monitored by using HPLC solvent system 1 (isocratic, and quick) supported by two dimensional TLC.

ACKNOWLEDGEMENT

This work was performed in the Technical Services Laboratory of William Ransom and Son, PLC, Hitchin, Hertfordshire, U.K. I am grateful for the opportunity to undertake research there during 1989, as part of an Outside Study Programme.

REFERENCES

1 P. Pietta, P. Mauri, E. Manera and P. Ceva, *J. Chromatogr.*, 457 (1988) 442.
2 A. Ruegger, *Helv. Chim. Acta*, 42 (1959) 754.
3 D. W. Hughes, K. Genest and W. Skakum, *J. Pharm. Sci.*, 57 (1968) 1023, 1619.
4 K. W. Bentley, *Nat. Prod. Rep.*, 4 (1987) 688.
5 K. W. Bentley, *Nat. Prod. Rep.*, 5 (1988) 278.
6 K. Genest and D. W. Hughes. *Can. J. Pharm. Sci.*, 3 (1968) 84.
7 J. C. Craig and S. K. Roy, *Tetrahedron*, 21 (1965) 395.
8 H. Krug and B. Borkowski, *Naturwissenschaften*, 52 (1965) 161.

Journal of Chromatography, 511 (1990) 379–383
Elsevier Science Publishers B.V., Amsterdam

CHROM. 22 478

Note

Comparison of the EASI-EXTRACT immunoaffinity concentration procedure with the AOAC CB method for the extraction and quantitation of aflatoxin B_1 in raw ground unskinned peanuts

MAGDA CARVAJAL[a]
Cancer Research Unit, Department of Biology, University of York, Heslington, York YO1 5DD (U.K.)
FRANCIS MULHOLLAND[b]
Microtest Research Ltd., University Road, Heslington, York YO1 5DU (U.K.)
and
R. COLIN CARNER*
Biocode Ltd., University Road, Heslington, York YO1 5DE (U.K.)
(First received September 27th, 1989; revised manuscript received March 13th, 1990)

Aflatoxins are secondary metabolites of the moulds *Aspergillus flavus* and *parasiticus* from the chemical group difuranocoumarins. They are potent carcinogens, teratogens, mutagens and toxins and pose a severe hazard to animal and human health[1–6]. The most potent of the four naturally occurring aflatoxins is aflatoxin B_1 (AFB_1). Aflatoxins have been found as contaminants of numerous crops including peanuts, cereals, figs, maize etc.

Official first action AOAC methods have been prepared for the analysis of aflatoxins in peanuts, one of the most commonly contaminated crops. The CB Method I[7] is recommended for analysing aflatoxins in raw and processed peanut products but it is our experience that for routine testing most laboratories pursue some variant of this procedure. Hence, it is often not possible to establish if a particular aflatoxin level found in food is an accurate reflection of the true value. The CB method is time consuming, uses large volumes of solvent and often is affected by interfering substances during the final thin-layer chromatography (TLC) analysis.

To circumvent these problems antibody methods are now beginning to be routinely used for aflatoxin analysis because of their exquisite sensitivity and specificity[8–13]. We have found, that for complex food matrices, enzyme-linked immunoad-

[a] Present address: Botany Department, Institute of Biology, National Autonomous University of Mexico, Ap.Postal 70-233, 04510 Mexico D.F., Mexico.
[b] Present address: AFRC Institute of Food Research, Reading Laboratory, Shinfield, Reading RG2 9AT, U.K.

0021-9673/90/$03.50

sorbent assay (ELISA) methods suffer from the disadvantage of non-specific inhibition leading to false positives as well as an inability to quantitate accurately each of the four naturally occurring aflatoxins. It is for these reasons that we have examined a commercial immunoaffinity column for the routine assay of aflatoxins and compared this with the AOAC CB method[7]. We present the results of this comparison here.

EXPERIMENTAL

Materials

Commercial immunoaffinity columns were purchased (EASI-EXTRACT® columns for total quantitative aflatoxin analysis — TD110, Oxoid Ltd., Basingstoke, U.K., manufactured and developed by Biocode Ltd., Heslington, U.K.; EASI-EXTRACT is a trademark of Biocode). AFB_1 and Celite were obtained from Sigma (Poole, U.K.) and silica gel 60 extra pure mesh 70–230 and DC Alufolien Kieselgel 60 Merck TLC plates from BDH (Poole, U.K.). All other chemicals were of laboratory reagent grade.

Spiking of ground peanuts with aflatoxin B_1

A standard solution of AFB_1 at a concentration of 10 μg/ml in dimethyl sulphoxide (DMSO) was prepared using UV spectrophotometry. This was used to prepare 100 and 500 ng/ml solutions by dilution in chloroform for spiking ground peanut samples. The latter were prepared by grinding raw, skinned peanuts obtained from a local health food store in a coffee grinder so that they would pass through a medium sieve. An amount of 480 g of the ground peanuts were aliquoted as detailed in Fig. 1.

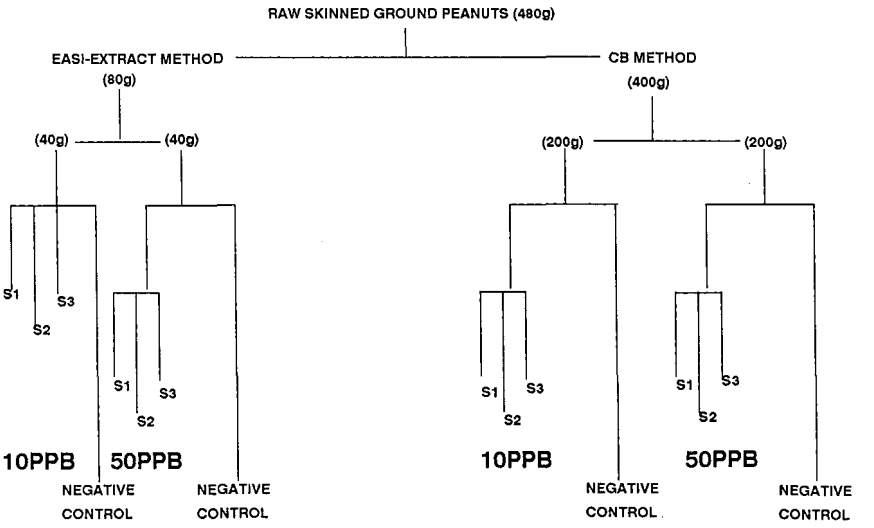

Fig. 1. Spiking and extraction scheme used in this study. S1, S2, S3 and the negative control were equal weight aliquots that were extracted as separate samples, *i.e.* for the EASI-EXTRACT procedure, 10 g and the AOAC method, 50 g.

Samples were spiked with AFB_1 at the levels indicated and the mycotoxin recovered using the EASI-EXTRACT or CB methods (see below).

Recovery of aflatoxin B_1 from spiked ground peanuts

EASI-EXTRACT immunoaffinity chromatography. An amount of 10 g of spiked ground peanut sample was blended using a Ultra-Turrax homogeniser (Janke and Kunkel from Sartorius, Belmont, U.K.) for 2 min in 20 ml acetonitrile–water (3:2, v/v) and then centrifuged at 860 *g* for 10 min. The supernatant was recovered and 4 ml taken and diluted with 92 ml of phosphate-buffered saline (PBS; potassium chloride 0.2 g, potassium dihydrogen orthophosphate 0.2 g, disodium hydrogen orthophosphate 1.16 g, sodium chloride 8 g, made up to 1 l with distilled water, pH 7.4). This was passed through the EASI-EXTRACT column by means of a 50-ml disposable syringe such that the liquid emerged from the nozzle in a steady stream in which individual drops were visible. The column was washed with 10 ml PBS to remove any contaminating matter and the bound AFB_1 recovered by eluting with 2 ml acetonitrile. The solvent was removed by blowing down with nitrogen and the resulting AFB_1 dissolved as described below prior to TLC.

AOAC CB method. An amount of 50 g of spiked peanut sample was placed in a flask with chloroform (250 ml), distilled water (25 ml) and Celite (25 g) and the flask shaken on a wrist action shaker for 30 min. The resulting extract was filtered through Whatman 41 filter paper and processed as per the official AOAC first action CB method[7]. The final chloroform solution was evaporated under nitrogen prior to TLC analysis.

Thin-layer chromatography

The dried down AFB_1 was redissolved in 200 μl chloroform for the EASI-EXTRACT samples and 200 μl of benzene–acetonitrile (98:2, v/v) for the CB recovered samples. Aliquots were spotted onto precoated aluminium backed silica gel plates which had been activated for 120 min at 100°C prior to sample application. Samples of standard AFB_1 solutions were spotted onto the same plates in order that comparisons could be made in fluorescence intensity between these standards and the recovered spiked samples. The plates were developed in acetone–chloroform (1:9, v/v) and air-dried before visualisation of the spots under a UV lamp (365 nm). Three spots, applied by microsyringe, from each spiked sample, negative controls and external standards (1, 2.5, 5, 7.5 and 10 ng applied to the plate) were used to quantitate recovery. Where the sample spot fluorescence fell between standards the mean of the two standards was used for calculation purposes. Where the match could not easily be made the chromatography run was repeated using more appropriate concentrations of either standard or sample. All procedures were performed by the same analyst. Quantitation was confirmed by a second person who was unaware of the sample or standard codes.

RESULTS AND DISCUSSION

As far as we are aware there are no published reports on comparing immunoaffinity procedures to recover AFB_1 from spiked ground peanut samples with official AOAC methods. In Table I we detail the results obtained using the two procedures.

TABLE I

COMPARISON OF THE RECOVERY OF AFB_1 FROM SPIKED GROUND PEANUTS USING THE AOAC CB METHOD OR BY IMMUNOAFFINITY CHROMATOGRAPHY USING EASI-EXTRACT COLUMNS

n = Number of samples analysed; S.D. = standard deviation; C.V. = coefficient of variation; EE = EASI-EXTRACT columns.

Method	*Spike concentration (μg/kg)*	*n*	*Recovery (%)*	*S.D.*	*C.V.*
CB	10	39	82.0	17.0	20.7
	50	36	84.1	14.9	17.7
EE	10	34	93.0	12.6	13.6
	50	27	95.5	11.4	12.0

For the CB method we were able to recover 82.0% for the 10-ppb[a] sample and 84.1% for the 50-ppb spiked sample.

For the EASI-EXTRACT immunoaffinity procedure we were able to recover 93.0% AFB_1 from the 10-ppb spiked sample and 95.5% for the 50-ppb sample. These values are significantly higher than the CB method ($p < 0.05$). The coefficients of variation are also lower than those obtained for the CB method indicating the lower variability of the immunoaffinity procedure.

Beside the higher recoveries using the antibody method there is a considerable saving in time of analysis compared with the CB method. Extraction for the former method involves merely blending for 2 min compared with 30 min for the CB method. Much smaller volumes of solvent are required compared with the CB method and there is no intermediary clean up step using silica gel column chromatography. Finally because the antibody recovers AFB_1 specifically there are no interfering spots on the TLC plate enabling easier and more accurate quantification.

We have examined the use of the EASI-EXTRACT columns to recover the other three naturally occurring aflatoxins *viz.* AFB_2, AFG_1 and AFG_2 and have found similar percentage recoveries as those described above for AFB_1 (data not presented). It is our opinion that immunoaffinity clean up columns provide an extremely useful method to improve aflatoxin quantification and accuracy. Whilst the cost of the columns is substantially higher than silica gel columns the savings in time, solvents and the elimination of false-positives because of the specificity of the antibody more than makes up this cost difference. Similar findings to these have been reported for the use of immunoaffinity columns to recover AFM_1 from milk[14] and cheeses[15].

ACKNOWLEDGEMENTS

M.C. would like to thank the British Council, the International Agency for Research on Cancer, Lyon, France and the National Council of Science and Technology of Mexico (CONACYT) for grants given to help fund this research.

[a] Throughout the article the American billion (10^9) is meant.

REFERENCES

1 W. F. Busby, Jr. and G. N. Wogan, in C. E. Searle (Editor), *Aflatoxins in Chemical Carcinogens, Vol. 2, (ACS Monograph Series,* No. 182), American Chemical Society, Washington, DC, 1984, pp. 945–1136.
2 J. D. Groopman, L. G. Cain and T. W. Kensler, *CRC Crit. Rev. Toxicol.,* 19 (1988) 113–145.
3 R. C. Garner and C. N. Martin, in P. L. Grover (Editor), *Chemical Carcinogens and DNA,* CRC Press, Boca Raton, FL, 1979, pp. 187–225.
4 E. L. Louchler, M. M. Teeter and M. D. Whitlow, *J. Biomol. Struct. Dyn.,* 5 (1988) 1237–1257.
5 W. H. Butler, M. Greenblatt and W. Lijinsky, *Cancer Res.,* 29 (1969) 2206–2211.
6 F.-S. Yeh, M. C. Yu, C.-C. Mo, S. Lo, M. J. Tong and B. E. Henderson, *Cancer Res.,* 49 (1989) 2506–2509.
7 *Official Methods of Analysis,* AOAC, Arlington, VI, 14th ed., 1984, pp. 477–500.
8 J. J. Langone and H. Van Vunakis, *J. Natl. Cancer Inst.,* 56 (1976) 591–595.
9 F. S. Chu and I. Ueno, Appl. Environ. Microbiol., 31 (1977) 1125–1128.
10 D. Lawellin, D. W. Grant and B. K. Joyce, *Appl. Environ. Microbiol.,* 34 (1977) 94–96.
11 P. Sizaret, C. Malaveille, R. Montesano and C. Frayssinet, *J. Natl. Cancer Inst.,* 69 (1982) 1375–1381.
12 F. S. Chu, T. S. L. Fan, G.-S. Zhang, Y.-C. Xhu, S. Faust and P. L. McMahon, *J. Assoc. Off. Anal. Chem.,* 70 (1987) 854–857.
13 D. L. Park, B. M. Miller, L. P. Hart, G. Yang, J. McVey, S. W. Page, J. Pestka and L. H. Brown, *J. Assoc. Off. Anal. Chem.,* 72 (1989) 326–332.
14 D. N. Mortimer, J. Gilbert and M. J. Shepherd, *J. Chromatogr.,* 407 (1987) 393–408.
15 M. Sharman, A. L. Patey and J. Gilbert, *J. Chromatogr.,* 474 (1989) 457–461.

Journal of Chromatography, 511 (1990) 384–389
Elsevier Science Publishers B.V., Amsterdam

CHROM. 22 468

Note

Heptafluorobutyrylation of trichothecenes using a solid-phase catalyst[a]

S. R. KANHERE and P. M. SCOTT*
Food Research Division, Bureau of Chemical Safety, Food Directorate, Health Protection Branch, Health and Welfare Canada, Ottawa, Ontario K1A 0L2 (Canada)
(First received December 28th, 1989; revised manuscript received March 27th, 1990)

Non-macrocyclic trichothecenes known to be produced by species of *Fusarium* and certain other fungal genera now number over 80 (ref. 1). However, only a few have been detected as naturally occurring contaminants of grains and other agricultural commodities[2]. Deoxynivalenol (DON) and nivalenol (NIV), which are type B trichothecenes possessing a conjugated 8-carbonyl group (I, Fig. 1), and the type A trichothecenes T-2 toxin (T-2), HT-2 toxin (HT-2) and 4,15-diacetoxyscirpenol (DAS), which lack the 8-carbonyl group (II, Fig. 1), are the main ones found.

Gas chromatography (GC) with electron-capture detection (ECD) or mass spectrometric (MS) detection has been used by many laboratories for the determination of trichothecenes in grains and feeds, with heptafluorobutyrylation and trimethylsilylation being the most commonly used derivatization procedures[3,4]. Heptafluorobutyrate (HFB) derivatives of trichothecenes were first applied to the determination of T-2 and DAS, which react very readily at room temperature with heptafluorobutyrylimidazole (HFBI)[5], and then to DON[6] which requires heating with this reagent for 1 h at 60°C. HFB derivatives of related trichothecenes, including HT-2, verrucarol, 4- and 15-acetoxyscirpendiol (monoacetoxyscirpenol, MAS), NIV and fusarenon X, have also been formed with HFBI[6–12]. We have, however, recently noted deterioration of one brand of HFBI: after storage of the distilled reagent for one month at −8°C, the capillary GC background due to reagent blank showed a marked increase.

A second reagent used for heptafluorobutyrylation of trichothecenes is heptafluorobutyric anhydride (HFBA) with 4-dimethylaminopyridine (4-DMAP) or trimethylamine as catalysts dissolved in an organic solvent[13–15]. Derivatization of DON proceeds faster at 60°C than with HFBI[13]. Polymer-bound 4-(*N*-benzyl-*N*-methylamino)pyridine has been used as a catalyst for acetylation of linalool with acetic anhydride[16]. The convenience of an insoluble solid catalyst encouraged us to investigate its use in heptafluorobutyrylation of trichothecenes with HFBA.

[a] Presented at the *103rd Annual International Meeting of the Association of Official Analytical Chemists, St. Louis, MO, U.S.A., Sept. 25–28, 1989.*

0021-9673/90/$03.50

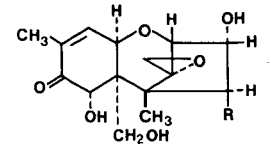

I

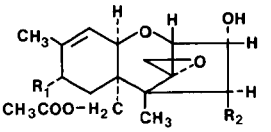

II

Fig. 1. Chemical structures of nivalenol (NIV) (I, R = OH), deoxynivalenol (DON) (I, R = H), 15-acetoxyscirpendiol (15-MAS) (II, $R_1 = H$; $R_2 = OH$), 4,15-diacetoxyscirpenol (DAS) (II, $R_1 = H$; $R_2 = OCOCH_3$), HT-2 toxin (HT-2) [II, $R_1 = (CH_3)_2CHCH_2COO$; $R_2 = OH$] and T-2 toxin (T-2) [II, $R_1 = (CH_3)_2CHCH_2COO$; $R_2 = OCOCH_3$].

EXPERIMENTAL

Standards and reagents

DON, 3-acetyl-DON and 3,15-diacetyl-DON were from the Plant Research Centre (Agriculture Canada, Ottawa, Canada), NIV was purchased from Wako Chemicals (Dallas, TX, U.S.A.) and HT-2 and DAS were purchased from Makor Chemicals (Jerusalem, Israel); T-2 was from the U.S. Department of Agriculture (Peoria, IL, U.S.A.) and 4- and 15-MAS were from C.P. Gorst-Allman (Council for Scientific and Industrial Research, South Africa). Stock solutions of trichothecene standards were prepared in chloroform–methanol (3:1) and stored in the freezer. HFBA was purchased from Pierce (Rockford, IL, U.S.A.) and "dimethylaminopyridine" on polystyrene [polymer-bound 4-(*N*-benzyl-*N*-methylamino)pyridine, 1.6 mmol "DMAP" per g resin] from Fluka (Buchs, Switzerland). Testosterone was from U.S.P.C. (Rockville, MD, U.S.A.); testosterone bis-HFB was prepared using HFBA and acetone as previously described[17].

Derivatization

Stock solutions of trichothecenes were evaporated under nitrogen in a 4-ml screw-cap vial to give 1 μg of each trichothecene. HFBA (50 μl) and toluene–acetonitrile (80:20) (450 μl) were added, the vial was capped (PTFE-lined insert) and the contents were mixed for 30 s on a vortex mixer. A 10-mg amount of "DMAP" on polystyrene was added and the capped vial heated in a sand bath for 2 h at 90°C. After cooling to room temperature, a 40-μl aliquot of the liquid phase was evaporated to dryness under nitrogen in a 1.8-ml screw-cap vial, and 1.6 ml *N*-hexane, containing 50 ng/ml testosterone bis-HFB[17] as internal quantitation standard, was added. The reaction was also studied at 22° and 60°C and with only 25 μl HFBA.

Gas chromatography

Capillary GC was carried out on Varian Model 3700 or Model 3400 gas chro-

matographs equipped with on-column capillary injectors (either at 23°C or programmed from 50 to 200°C), 1 m × 0.5 mm I.D. deactivated fused-silica retention gap, make-up gas conversion adapter, J & W Scientific DB-1701 fused-silica capillary column (15 m × 0.33 mm I.D., 0.25 μm film thickness) and ^{63}Ni electron-capture detector (at 300°C). Column temperature programmes were: Varian 3700: 70°C (2 min), 30°C/min to 175°C (2 min), 2°C/min to 220°C (10 min); Varian 3400: 50°C (1 min), 50°C/min to 175°C (5 min), 3°C/min to 220°C (10 min). The carrier gas was helium (*ca.* 2 ml/min) and the make-up gas was nitrogen (*ca.* 27 ml/min). Attenuation was $64 \cdot 10^{-12}$ A/mV. Chromatograms were recorded and peaks integrated on a Spectra-Physics SP4270 computing integrator or Shimadzu C-R6A Chromatopac data processor; chart speed was 5 mm/min.

Gas chromatography–mass spectrometry

A VG Analytical 7070 EQ mass spectrometer was operated in the electron-impact mode at 70 eV and interfaced with a Varian 6000 gas chromatograph, equipped with an on-column injector and a J & W Scientific DB-5 column (30 m × 0.25 mm I.D., 0.25 μm film thickness); the temperature was programmed from 70°C (1 min) at 50°C/min to 170°C (5 min), then at 3 or 5°C/min to 220°C.

RESULTS AND DISCUSSION

Use of polymer-bound "DMAP" as an insoluble solid catalyst for derivatization of trichothecenes with HFBA has the advantage that no aqueous washing step is necessary. An aliquot of derivatizing solution is taken leaving behind the solid catalyst, and the excess reagent and solvent are readily removed by evaporation. By comparison, washing with aqueous sodium bicarbonate solution, water or phosphate buffer is required with HFBA/4-DMAP[13–15] or HFBI[5–12]. The time course of the reaction at 90°C for six trichothecenes with HFBA/polymer-bound "DMAP" is shown in Fig. 2. As expected from the literature on heptafluorobutyrylation with HFBI, the type B trichothecenes NIV and DON react more slowly than type A trichothecenes. A reaction time of 90 min was considered necessary to ensure complete derivatization of all the trichothecenes under the conditions described in the Experimental section. Initial studies established that a toluene/acetonitrile ratio of 80:20 afforded better miscibility of the HFBA than a 95:5 ratio. Use of 25 μl HFBA instead of 50 μl resulted in slower reaction of NIV and DON (data not shown).

Partial heptafluorobutyrylation of NIV and DON was evident at lower temperatures and shorter reaction times. The chromatogram of a 60°C/20 min reaction mixture obtained using the polymer-bound catalyst (Fig. 3) indicates longer retention times for NIV tris-HFB and DON bis-HFB in relation to those of the fully derivatized trichothecenes (NIV tetrakis-HFB and DON tris-HFB). By comparison, such conditions of temperature and time (60°C/20 min)[13] give complete derivatization of DON and NIV with 4-DMAP as catalyst. After 1 min at room temperature (with the polymer-bound catalyst), NIV tetrakis-HFB and DON tris-HFB were not yet formed and these mild reaction conditions were used to prepare NIV tris-HFB and DON bis-HFB for GC–MS confirmation (Fig. 4). These partial derivatives ($M^+ = 900$ and 688, respectively) have not been previously reported. It is presumed that the unreacted hydroxyl group is the 7-hydroxyl group, which would be expected to be more

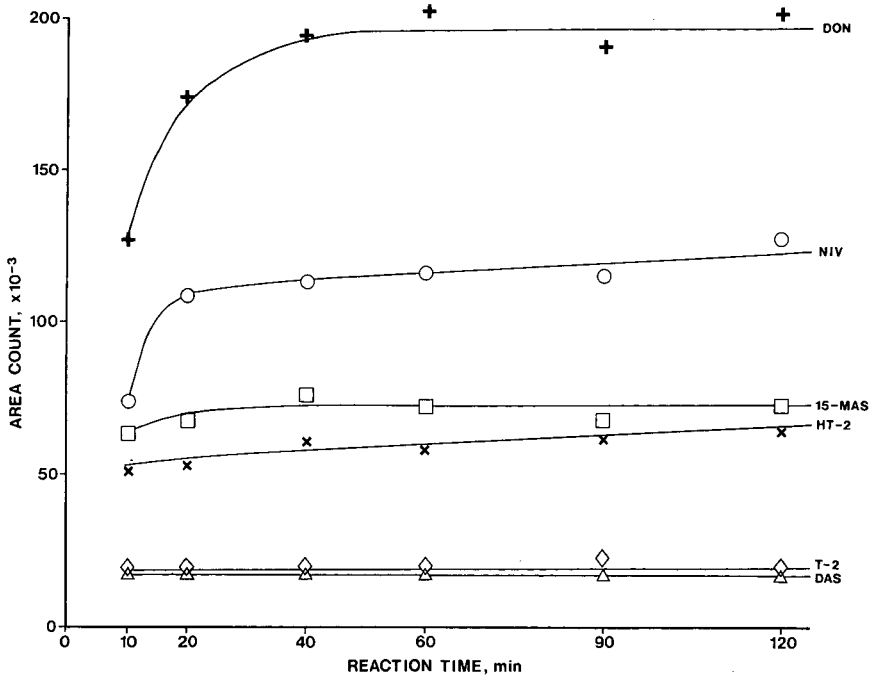

Fig. 2. Rates of reaction of trichothecenes (DON, NIV, 15-MAS, HT-2, T-2 and DAS) with HFBA (50 μl) in the presence of polymer-bound "DMAP" at 90°C.

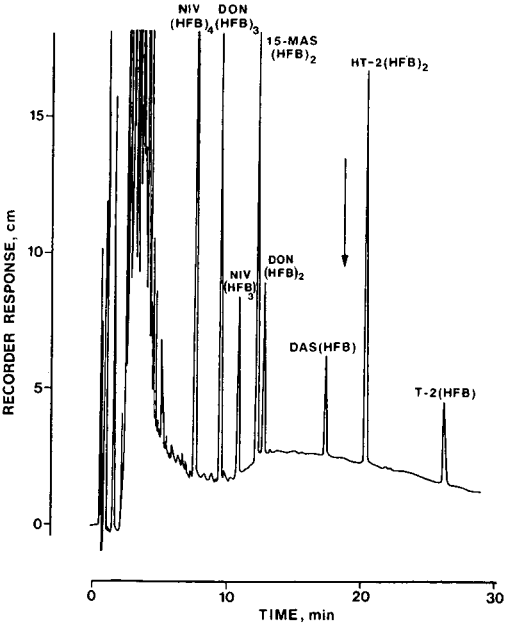

Fig. 3. Gas chromatogram (Varian 3400) of trichothecene HFB derivatives, showing incomplete derivatization of NIV and DON as indicated by presence of NIV tris-HFB and DON bis-HFB. Other marked peaks are fully derivatized trichothecenes: NIV tetrakis-HFB, DON tris-HFB, 15-MAS bis-HFB, DAS HFB, HT-2 bis-HFB and T-2 HFB. Arrow shows retention time of testosterone bis-HFB internal standard. Reaction with HFBA/polymer-bound "DMAP" at 60°C after 20 min.

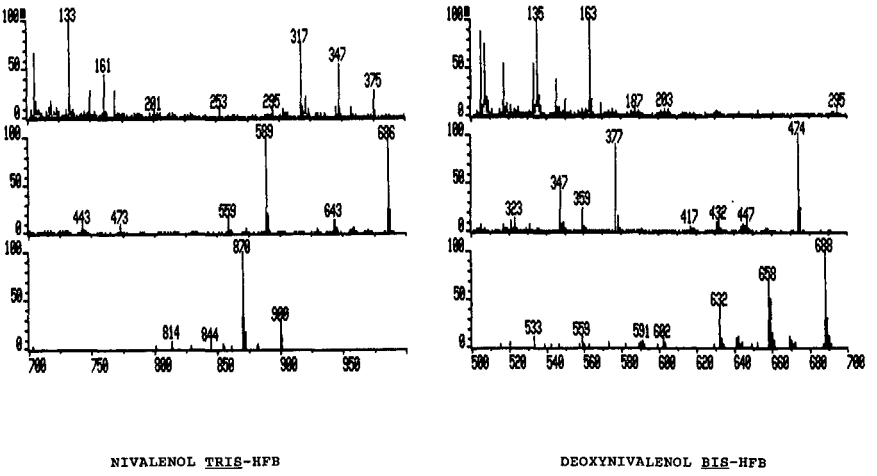

Fig. 4. Mass spectra of NIV tris-HFB and DON bis-HFB separated by GC following derivatization with HFBA/polymer-bound "DMAP" at 22°C for 1 min.

difficult to derivatize than the 3- and 15-hydroxyl groups on account of the possibilities of steric hindrance and hydrogen bonding to the 8-carbonyl group. In a comparative reaction model, the 7-hydroxyl group in DON or 3-acetyl-DON does not react under partial acetylation conditions with a limited amount of acetic anhydride[18,19]. In further support of this less reactive 7-hydroxyl group, we found that (like DON) 3-acetyl-DON and 3,15-diacetyl-DON formed only minor amounts of the fully reacted HFB derivative after 10 min at room temperature. Incomplete trifluoroacetylation and trimethylsilylation of NIV and DON have also been observed[20–22]. NIV tris-trimethylsilyl contained an unreacted 7-hydroxyl group based on nuclear magnetic resonance spectroscopic evidence[21]. However, formation and identification by GC–MS of two DON bis-trimethylsilyl derivatives[20], at least one of which must have a derivatized 7-hydroxyl group, indicates that regiospecificity of trimethylsilylation of DON may differ from that of acylation.

Several types of internal standards have been used in GC of trichothecenes[3,5,8,10,11,14,15]; some have been added to the sample before extraction, others before derivatization and others after derivatization (as a derivatized internal standard or an underivatized compound such as methoxychlor). After examination of a number of steroid heptafluorobutyrates, we propose testosterone bis-HFB as a post-derivatization internal standard for trichothecene HFB derivatives to correct for instrumental variations. Its retention time is conveniently between those of DAS and HT-2 HFB derivatives (Fig. 3), it contains fluorine rather than chlorine, whose ECD responses may not vary proportionately, and it can be prepared[17] and stored as a stock solution in hexane for at least 2 weeks at room temperature. GC–MS ($M^+ = 680$) confirmed its identity.

ACKNOWLEDGEMENT

The authors thank W. F. Sun for GC–MS analyses.

REFERENCES

1 J. F. Grove, *Nat. Prod. Rep.*, 5 (1988) 187.
2 P. M. Scott, in V. R. Beasley (Editor), *Trichothecene Mycotoxicosis: Pathophysiologic Effects*, Vol. I, CRC Press, Boca Raton, FL, 1989, p. 1.
3 J. Gilbert, in M. O. Moss and J. E. Smith (Editors), *The Applied Mycology of Fusarium*, Cambridge University Press, Cambridge, 1984 p. 175.
4 P. M. Scott, *J. Assoc. Off. Anal. Chem.*, 65 (1982) 876.
5 T. R. Romer, T. M. Boling and J. L. MacDonald, *J. Assoc. Off. Anal. Chem.*, 61 (1978) 801.
6 P. M. Scott, P.-Y. Lau and S. R. Kanhere, *J. Assoc. Off. Anal. Chem.*, 64 (1981) 1364.
7 H. Cohen and M. Lapointe, *J. Assoc. Off. Anal. chem.*, 67 (1984) 1105.
8 S. Steinmeyer, R. Tiebach and R. Weber, *Z. Lebensm.-Unters.-Forsch.*, 181 (1985) 198.
9 P. M. Scott, S. R. Kanhere and E. J. Tarter, *J. Assoc. Off. Anal. Chem.*, 69 (1986) 889.
10 R. M. Black, R. J. Clarke and R. W. Read, *J. Chromatogr.*, 388 (1987) 365.
11 T. Krishnamurthy, M. B. Wasserman and E. W. Sarver, *Biomed. Environ. Mass Spectrom.*, 13 (1986) 503.
12 P. M. Scott, G. A. Lombaert, P. Pellaers, S. Bacler, S. R. Kanhere, W. F. Sun, P.-Y. Lau and D. Weber, *Food Addit. Contam.*, 6 (1989) 489.
13 G. M. Ware, A. Carman, O. Francis and S. Kuan, *J. Assoc. Off. Anal. Chem.*, 67 (1984) 731.
14 R. Kostiainen and A. Rizzo, *Anal. Chim. Acta*, 204 (1988) 233.
15 B. Yagen, M. Bialer and A. Sintov, *J. Chromatogr.*, 343 (1985) 67.
16 M. Tomoi, Y. Akada and H. Kakiuchi, *Makromol. Chem., Rapid Commun.*, 3 (1982) 537.
17 L. A. Dehennin and R. Scholler, *Steroids*, 13 (1969) 739.
18 T. Yoshizawa, T. Shirota and N. Morooka, *J. Food Hyg. Soc. Jpn.*, 19 (1978) 178.
19 J. F. Grove, A. J. McAlees and A. Taylor, *J. Org. Chem.*, 53 (1988) 3860.
20 C. E. Kientz and A. Verweij, *J. Chromatogr.*, 355 (1986) 229.
21 Y. Nakahara and T. Tatsuno, *Chem. Pharm. Bull.*, 21 (1973) 1267.
22 J. Gilbert, J. R. Startin and C. Crews, *J. Chromatogr.*, 319 (1985) 376.

Journal of Chromatography, 511 (1990) 390–395
Elsevier Science Publishers B.V., Amsterdam

CHROM. 22 396

Note

Poly(styrene–dimethylsiloxane) block copolymer as a stationary phase for capillary gas chromatography

PEIFEN ZHU, MEILING YE and LIANGHE SHI*
Institute of Chemistry, Academia Sinica, Beijing 100080 (China)
and
HUWEI LIU and RUONONG FU
Department of Chemical Engineering, Beijing Institute of Technology, Beijing 100081 (China)
(First received November 14th, 1989; revised manuscript received February 19th, 1990)

Poly(styrene–dimethylsiloxane) block copolymers with different ratios of the two chain segments, synthesized by anionic[1] or radical polymerization[2], have been used as surface-active agents[3] and stabilizers for non-aqueous dispersion[4]. It was reported that this kind of copolymer has good electrical properties and unexpected climatic resistance[5]. The synthesis and properties of the block copolymer have been carefully studied by many researchers in recent years. The use of this copolymer as a stationary phase for capillary gas chromatography (GC), however, has not been reported. On the other hand, polysiloxanes constitute the vast majority of stationary phases in capillary GC, and siloxane-type copolymers such as poly(silarylene–siloxane)[6] are considered to be thermally stable at high temperatures. Buijten and co-workers[7,8] prepared poly(silarylene–methylphenylsiloxane) and cyanosilicones and coated them on fused-silica capillary columns. These stationary phases exhibited high thermal stability and satisfactory chromatographic performance[9,10].

In this study, two batches of poly(styrene–dimethylsiloxane) A–B block copolymers were used as stationary phases in capillary columns and promising results were obtained. It is indicated that fused-silica capillary columns coated with these copolymers could be used routinely with temperature programming up to 290°C.

EXPERIMENTAL

Analysis of stationary phases

Poly(styrene–dimethylsiloxane) (PSDMS) block copolymers were obtained from Dow Corning and their properties are listed in Table I. Molecular weights and glass transition temperatures (T_g) were measured with a Knauer membrane osmometer (Type 01.00) and a Perkin-Elmer differential scanning calorimeter (DSC-2), respectively. The content of styrene segments was determined with a Hitachi 340 UV spectrophotometer and decomposition temperatures were evaluated with a Perkin-Elmer TGS-2 thermogravimetric analyser.

0021-9673/90/$03.50

TABLE I

PROPERTIES OF POLY(STYRENE–DIMETHYLSILOXANE) BLOCK COPOLYMERS

Copolymer	*Molecular weight ($\bar{M}_n$)*	*Content of styrene (%)*	*Glass transition temperature (°C)*	*Decomposition temperature (°C)*[a]
PSDMS-1	24 500	12	70–72	335
PSDMS-2	41 300	23	80–82	320

[a] Temperature giving a weight loss of 5%.

Coating procedure

Fused silica tubes of I.D. 0.22 mm (Yongnian Optical Fibre Factory) were purged with dry nitrogen at 250°C for 2.5 h before coating so as to remove residual nitric and hydrochloric acids, which were adsorbed on the inside wall of the capillaries. The tubes were then coated statically with the copolymers mentioned above solvated in methylene chloride, as described previously[11].

Column testing

Column testing was carried out with an SP-2305 gas chromatograph (Beijing Analytical Instrument Factory) with flame ionization detection (FID) and a GC-5A instrument (Shimadzu) with FID and a modified column system[12]. Nitrogen was used as the carrier gas in all instances. The test mixtures were (i) Grob's test mixture, (ii) a mixture of C_{10}–C_{28} *n*-alkanes and (iii) a positional isomer mixture of nitrotoluene (NT) and dinitrotoluene (DNT) and also trinitrotoluene (TNT). A Model CDMS-1B chromatographic data processor (Shanghai Institute of Computing Technology) was utilized to handle the data for the quantitative analysis of DNT isomers.

RESULTS AND DISCUSSION

Three fused-silica capillary columns were prepared with these copolymers and their properties are given in Table II. The coating experiment showed that these copolymers are easy to coat on the fused-silica tubes. Fig. 1 illustrates representative chromatograms of Grob's test mixture on these columns. From this it can be seen that these columns have acceptable inertness, although the theoretical plate number is

TABLE II

PROPERTIES OF THE FUSED-SILICA CAPILLARY COLUMNS

TPN = Theoretical plate number; k' = capacity factor.

Column No.	*Stationary phase*	*Column length (m) × I.D. (mm)*	*Cloumn temperature (°C)*	*Test compound*	*TPN*[a] *(n/m)*	k'
1	PSDMS-1	9 × 0.22	120	*n*-C_{12}	1345	3.52
2	PSDMS-2	9 × 0.22	160	*n*-C_{12}	2059	1.14
3	PSDMS-2	21 × 0.22	130	*n*-C_{12}	2674	3.57

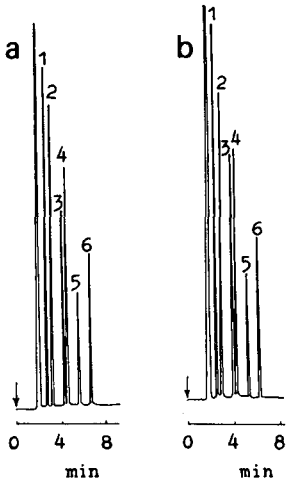

Fig. 1. Gas chromatograms of Grob's test mixture on (a) column 1 and (b) column 2 in an SP-2305 gas chromatograph. Column temperature, 140°C; injection temperature, 350°C. Peaks: 1 = *n*-octanone; 2 = *n*-octanol; 3 = 2,4-dimethylaniline; 4 = *n*-dodecane; 5 = 2,6-dimethylphenol; 6 = *n*-tridecane.

relatively poor (below 3000/m). This may be because the fused-silica tubes were not deactivated and the stationary phases were not immobilized.

According to the differential scanning calorimetric and thermogravimetric experiments (Table I), the T_g of the block copolymer is lower than that of styrene homopolymer (about 100°C). This is also shown in Fig. 2 by the linear relationship between log t'_R (adjusted retention time) and the reciprocal of column temperature (T_c) within the range 80–160°C. The height equivalent to a theoretical plate (H) as a function of carrier gas flow-rate (u) for these columns corresponds to the Van Deemter equation, as illustrated in Fig. 3. Table III gives the retention indices of several samples on these columns at 120 and 130°C. Therefore, it can be concluded that styrene–dimethylsiloxane A–B block copolymers share a common chromatographic behaviour with other polysiloxane stationary phases.

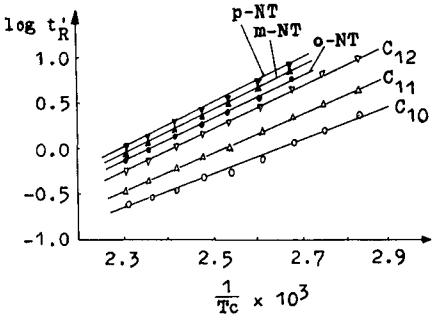

Fig. 2. Relationship between log t'_R and the reciprocal of column temperature ($1/T_c$) for isomers of NT and C_{10}–C_{12} *n*-alkanes on column 2 in an SP-2305 chromatograph. Carrier gas flow-rate, 30 cm/s; make-up gas flow-rate, 45 ml/min; injection temperature, 350°C; detector temperature, 250°C.

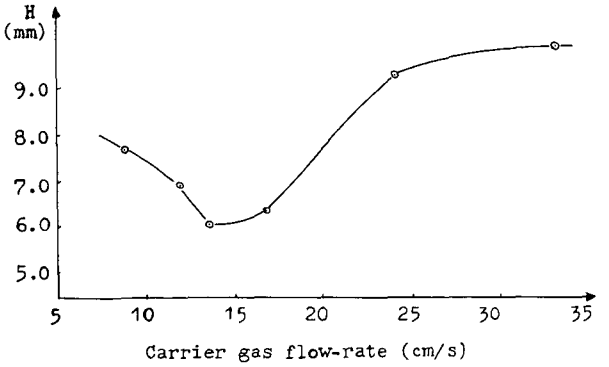

Fig. 3. Van Deemter curve for column 2 at 120°C in an SP-2305 gas chromatograph with FID.

As an example of applications, isomers of NT, DNT and TNT were separated on the above three columns, and typical chromatograms are shown in Fig. 4. Significantly, the isomers of NT and DNT can be satisfactorily separated on a column as short as 9 m within 7 min and TNT on a 21-m column within 10 min. These results are much better than those given by columns coated with SE-54 (ref. 12) and OV-101 (ref. 13), on which 2,3- and 2,4-DNT cannot be completely separated, and by a column coated with OV-225 (ref. 14), which is difficult to prepare with fused-silica tubes and has the drawback of long analytical times, although complete separation of these isomers can be obtained. These results show that the selectivity of the PSDMS block copolymer towards polar compounds is improved because of the introduction of a polystyrene chain in the polydimethylsiloxane backbone. Hence, columns coated with PSDMS block copolymers could be applied in the separation of positional isomers of compounds such as benzenes substituted with different polar groups. Table IV gives the quantitative results for a practical DNT sample on column 2. The reproducibility and accuracy are acceptable and potential applications of this type of columns are expected.

As shown in Fig. 4, the columns coated with PSDMS block copolymers can be used up to 268°C, indicating that these new stationary phases are thermostable. To investigate further the stability of these columns, a mixture of *n*-alkanes was injected after column conditioning at 270°C for 30 h and a representative chromatogram is shown in Fig. 5. It is found that these columns could be used with temperature

TABLE III

RETENTION INDICES OF DIFFERENT COMPOUNDS ON PSDMS

DMA = Dimethylaniline; DMP = dimethylphenol.

Column No.	T_c *(°C)*	*n-Octanone*	*n-Octanol*	*2,4-DMA*	*2,6-DMP*
1	120	1017	1094	1177	1256
2	120	1018	1085	1179	1256
3	130	1026	1100	1168	1263

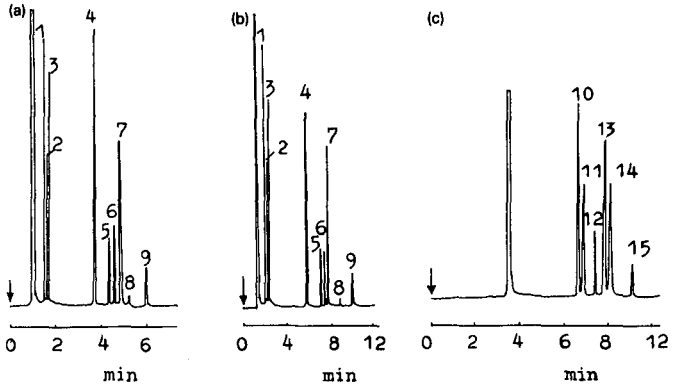

Fig. 4. Gas chromatograms of (a) NT and DNT on column 1 at 180°C with a carrier gas flow-rate of 17.0 cm/s; (b) NT and DNT on column 2 at 166°C with a carrier gas flow-rate of 17.0 cm/s; and (c) TNT on column 3 at 268°C with a carrier gas flow-rate of 12.0 cm/s. Peaks: 1 = *o*-NT; 2 = *m*-NT; 3 = *p*-NT; 4 = 2,6-DNT; 5 = 2,5-DNT; 6 = 2,3-DNT; 7 = 2,4-DNT; 8 = 3,5-DNT; 9 = 3,4-DNT; 10 = 2,4,6-TNT; 11 = 2,3,6-TNT; 12 = 2,3,5-TNT; 13 = 2,4,5-TNT; 14 = 2,3,4-TNT; 15 = 3,4,5-TNT.

TABLE IV

QUANTITATIVE ANALYSIS OF A PRACTICAL DNT SAMPLE

The results are means of six runs, calculated by peak-area normalization. Column temperature, 172°C; injection temperature, 350°C; detector temperature, 250°C; carrier gas flow-rate, 16.0 cm/s.

Isomer	*2,6-DNT*	*2,5-DNT*	*2,4-DNT*	*3,5-DNT*	*3,4-DNT*
Content (%)	12.38	0.65	78.15	3.41	4.40
Standard deviation (%)	0.2791	0.0227	0.1973	0.1775	0.1473
Relative standard deviation (%)	2.086	3.492	0.252	5.206	3.348

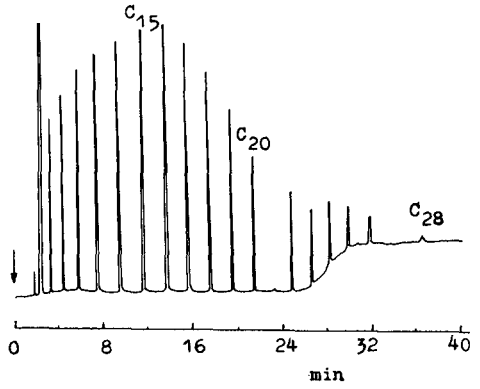

Fig. 5. Gas chromatogram of *n*-alkanes. Column temperature, programmed from 120 to 290°C at 6°C/min; injection temperature, 350°C; carrier gas flow-rate, 18.8 cm/s.

programming up to 290°C and the baseline drift is very slight. The thermal stability would be further improved by cross-linking or immobilization of the stationary phase on the column. Further studies are in progress.

CONCLUSIONS

PSDMS A–B block copolymers can be used as stationary phases for capillary GC. The columns, which are easily coated with these copolymers, are thermally stable at elevated temperature up to 280°C. For the separation of different polar substances, they may serve as potential stationary phases in capillary column GC for laboratory and industrial analysis.

ACKNOWLEDGEMENT

The authors express their gratitude to Dr. J. C. Saam of Dow Corning for providing the block copolymer samples.

REFERENCES

1 J. W. Dean (General Electric), *U.S. Pat.*, 3 760 030, (1973).
2 J. V. Crivello, J. L. Lee and D. A. Conlon, *J. Polym. Sci., Part A*, 24 (1986) 1251.
3 G. L. Gaines, Jr. and G. W. Bendex, *Macromolecules*, 5 (1972) 82.
4 J. S. Higgins, *Polymer.*, 21 (1980) 627.
5 J. C. Saam, A. H. Ward and F. W. C. Fearon, *Polym. Prepr. Am. Chem. Soc. Div. Polym. Chem.*, 13 (1972) 524.
6 P. R. Dvornic and R. W. Lenz, *Polymer*, 24 (1983) 763.
7 J. Buijten, L. Blomberg, S. Hoffmann, K. Markides and T. Wannman, *J. Chromatogr.*, 301 (1984) 265.
8 K. Markides, L. Blomberg, S. Hoffmann, J. Buijten and T. Wannman, *J. Chromatogr.*, 302 (1984) 319.
9 A. Bemgard, L. Blomberg, M. Lymann, S. Claude and R. Tabacchi, *J. High Resolut. Chromatogr. Chromatogr. Commun.*, 10 (1987) 302.
10 A. Bemgard, L. Blomberg, M. Lymann, S. Claude and R. Tabacchi, *J. High Resolut. Chromatogr. Chromatogr. Commun.*, 11 (1988) 881.
11 H. Liu, A. Zhang, Y. Jin and R. Fu, *J. High Resolut. Chromatogr.*, 12 (1989) 537.
12 H. Liu, R. Fu, Z. Guan and L. Tian, *J. Chromatogr.*, 462 (1989) 376.
13 A. Hashimoto, H. Sakino, E. Yamagami and S. Tateishi, *Analyst (London)*, 105 (1980) 787.
14 H. Lu, X. Liu, J. Niu, R. Fu and H. Liu, *Huaxue Shiji*, 11 (1989) 16.

Journal of Chromatography, 511 (1990) 396–401
Elsevier Science Publishers B.V., Amsterdam

CHROM. 22 363

Note

Automated multiple development high-performance thin-layer chromatographic analysis of natural phenolic compounds

EMILIA MENZIANI
Department of Pharmaceutical Sciences, University of Ferrara, Via Scandiana 21, I-44100 Ferrara (Italy)
BARBARA TOSI and ANGELO BONORA
Institute of Botany, University of Ferrara, Via Porta Mare 2, I-44100 Ferrara (Italy)
and
PIERLUIGI RESCHIGLIAN and GAETANO LODI*
Department of Chemistry, University of Ferrara, Via Borsari 46, I-44100 Ferrara (Italy)
(Received January 18th, 1990)

Phenolic compounds are widespread plant secondary metabolites, the flavonoids being the largest group. However, simple monocyclic phenols, phenylpropanoids and phenolic quinones are also frequently encountered[1].

Liquid chromatography, both column[2–10] and planar[11–19], has proved to be the most useful technique for the analysis of phenolic compounds. In the gradient elution mode, high-performance liquid chromatography (HPLC) has been most widely used and the intrinsic problem of gradient elution optimization in the HPLC separation of multi-component phenolic compounds mixtures has already been discussed[20]. However, once a recent plate development concept known as the automated multiple development (AMD) technique[21–24] has been properly characterized, planar chromatography may play a more important role in the analysis of complex mixtures. The most important feature that allows the successful application of AMD with high-performance thin-layer chromatography (HPTLC) in complex mixtures analysis is the possibility of carrying out the separation process using a gradient development mode. Further, multi-development is known to produce a band reconcentration effect[25] which allows spots to migrate over considerable distances without appreciable band broadening. Both gradient development and the band reconcentration effect act in the direction of improving the spot capacity, *i.e.*, allowing homogeneous spreading over a single chromatogram of many compounds which might belong to different polarity ranges[26].

An application of the AMD–HPTLC procedure to phenolic compounds separation was reported by Ebel *et al.*[27], who showed that this approach is suitable for the analysis of coumarins in multi-component extracts of medicinal plants.

In this paper a basic approach to an optimized AMD–HPTLC experimental procedure and its ability to separate several classes of natural phenolic compounds is

0021-9673/90/$03.50

presented. *Chamomilla recutita* extracts were chosen as chamomile flowers are a well known natural source of phenolic compounds (flavonoids, coumarins, phenolcarboxylic acids) spanning a wide chemical polarity range[28].

EXPERIMENTAL

Merck 5641 silica gel 60 HPTLC precoated plates, 10 × 20 cm, without fluorescence indicator, twice prewashed with methanol were used. The solvents employed were methanol, ethanol, ethyl acetate, dichloromethane and *n*-hexane of HPLC grade (Carlo Erba, Milan, Italy). Formic acid (puriss.) was purchased from Fluka (Buchs, Switzerland).

The selected phenolic compounds used as standards were obtained from Extrasyntese (Genay, France). They were used as received and dissolved in ethanol or ethanol–ethyl acetate (1:1) to give 100–200 ppm solutions. The selected standards represent the most important phenolic compounds in chamomile, *i.e.*, coumarins, phenolcarboxylic acids, flavones, flavonols and glycosides. They are listed in Table I.

TABLE I

PHENOLIC COMPOUNDS USED AS STANDARDS

No.	*Compound*	R_F[a]
1	Herniarin (7-methoxycoumarin)	0.94
2	Ferulic acid (4-hydroxy-3-methoxycinnamic acid)	0.86
3	Umbelliferone (7-hydroxycoumarin)	0.81
4	Isorhamnetin (3,4′,5,7-tetrahydroxy-3′-methoxyflavone)	0.75
5	Apigenin (4′,5,7-trihydroxyflavone)	0.69
6	Caffeic acid (3,4-dihydroxycinnamic acid)	0.60
7	Luteolin (3,4′,5,7-tetrahydroxyflavone)	0.55
8	Quercetin (3,3′,4′,5,7-pentahydroxyflavone)	0.50
9	Fisetin (3,3′,4′,7-tetrahydroxyflavone)	0.42
10	Myricetin (3,3′,4′,5,5′,7-hexahydroxyflavone)	0.38
11	Apigenin 7-O-glucoside	0.29
12	Luteolin 7-O-glucoside	0.23
13	Hyperoside (quercetin 3-α-D-galactoside)	0.18
14	Chlorogenic acid [3-(3,4-dihydroxycinnamoyl)quinic acid]	0.13
15	Rutin {quercetin-3-O-[6-(α-L-rhamnosyl)-D-glucose]}	0.09

[a] Values obtained in this work.

Preparation of extracts

The source material was a commercial aqueous alcoholic extract of chamomile flowers. A 1-g amount of this sample was suspended in 10 ml of water acidified with hydrochloric acid to pH 2–3. It was extracted successively with three 20-ml portions of ethyl acetate. The aqueous phase was discarded and the organic phase filtered through anhydrous sodium sulphate and evaporated to dryness under reduced pressure (at 40–50°C). The residue was dissolved in 2 ml of ethanol–ethyl acetate (1:1) and the resulting solution was used for AMD analysis.

Sample application

Standards and sample solutions were applied to the plates either as spots with a Pt–Ir capillary or as 10-mm wide bands with a Linomat IV (Camag, Muttenz, Switzerland) (3 μl; delivery speed 4 s/μl).

Detection

Fluorescence detection was used at an excitation wavelength of 360 nm. Coumarins and phenolcarboxylic acids give an inherent bluish fluorescence. The flavonoids were derivatized by dipping the developed plates in a 4% aqueous aluminium sulphate solution[15]. After 10-min exposure to UV light they showed yellow fluorescent spots that were stable for several weeks. The derivatized plates were scanned with a Camag Scanner II equipped with a Merck–Hitachi Chromato-Integrator. Fluorescence was induced at 360 nm with a mercury vapour lamp. Emission was measured through a cut-off filter (400 nm).

Development

The AMD system (Camag) and its operating conditions have been described in detail elsewhere[21–24]. Briefly, an HPTLC plate is subjected to a stepwise gradient development in an enclosed chamber. The developing solvent mixture is prepared in a gradient mixer from the solvent components in separate bottles. Between developments, the mobile phase is removed from the developing chamber and the plate is dried under vacuum and then conditioned in an atmosphere of controlled composition. The parameters to be specified for an AMD run are the solvent composition in each feeding bottle, the number of development steps, the drying times between steps, the development times (determining the run distance) for each step and the preconditioning conditions.

The experimental AMD parameters used in this study were as follows: number of steps, 15; drying times, 6 min for the first four steps, then 4 min for the remaining steps, with the exception of the last step (10 min); preconditioning, nitrogen bubbled through water was the conditioning atmosphere; and preconditioning time, 15 s for each step. The filling of the feeding bottles and the development times are reported in Table II and Fig. 1, respectively.

TABLE II

OPTIMIZED SOLVENT COMPOSITION USED IN THE AMD EXPERIMENTS

Obtained using the instructions for the Camag AMD system (1986).

Component	*Starting with step No.*			
	1	*2*	*6*	*11*
	Use bottle No.			
	1	*2*	*3*	*4*
Methanol	70.5	23.5	9.4	100
Dichloromethane	25	74	90	–
Water	4.5	1.5	0.6	–
Formic acid	1	1	1	–

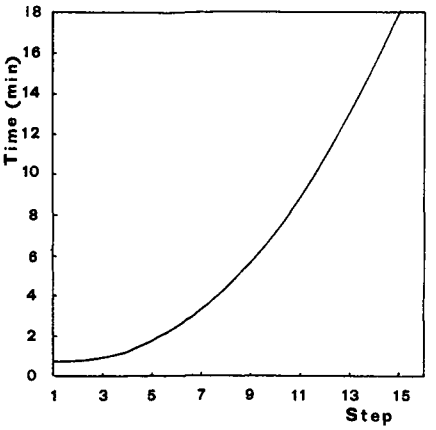

Fig. 1. Development time determining the running distance for each step.

RESULTS

The AMD gradient optimization was carried out on mixtures of the selected standards listed in Table I. As a starting point of the optimization, a "universal gradient" was chosen, *i.e.*, an AMD gradient that started with a very polar solvent and changed its composition, passing through a central or "basic" solvent of medium polarity and ending with a non-polar solvent[24]. Among the possible eluents spanning the overall polarity range, methanol was chosen as the strongest (most-polar) starting solvent and *n*-hexane as the weakest (non-polar), final solvent. As dichloromethane showed the best selectivity with respect to other medium-polarity solvents, *e.g.*, ethyl acetate or diethyl ether, it was used as a basis component. These general gradient conditions were gradually modified on the basis of trial-and-error experiments. First, formic acid was added to minimize the ionization of the weakly acidic compounds under examination. Water was added afterwards as a tailing suppressor for the most polar compounds. This last gradient-adjustment step required mixing of the starting, high-polarity solvent (methanol) with the medium-polarity eluent (dichloromethane) as water and formic acid actually acted as high solvent strength components as well. Finally, in the optimizing procedure, the non-polar gradient component (*n*-hexane) was eliminated because, under our conditions, it caused only a broadening of the developed bands. Hence, the final optimized gradient composition started (see Table II) from methanol–dichloromethane–water–formic acid (70.5:25:4.5:1) and proceeded gradually through 15 steps ending with pure dichloromethane (Fig. 2).

Owing to the relatively high concentration of non-volatile modifiers in the solvent, careful adjustment of plate drying times between each development step was carried out. It was observed that dryings shorter than the optimized ones (see Experimental) produced more diffuse, broadened bands, while longer drying times caused marked tailing.

In Table I the average R_F values of the standards obtained by means of three optimized AMD runs are reported. The selected phenolic compounds are separated

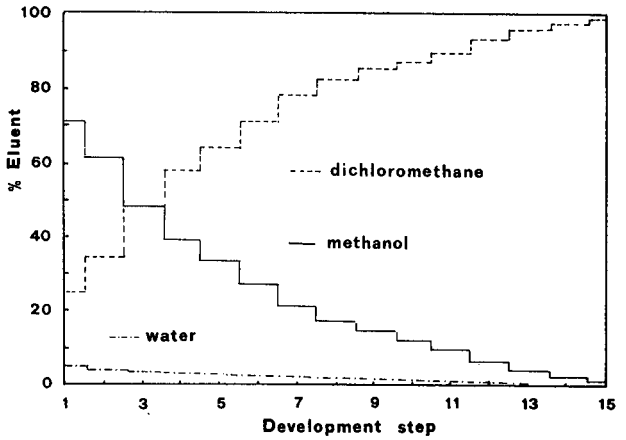

Fig. 2. Solvent composition obtained for each step for the optimized gradient.

and well distributed on the layer. The flavonoids isorhamnetin, luteolin and quercetin, for which poor separations have been obtained using various TLC systems[13], are well separated here. The polarity range of the standards spans from the low/–medium-polarity herniarin to highly polar rutin. It can be seen that inside each compound class the group contribution to the retention[11] follows trends that have been already observed in both silica gel and paper chromatography[11,13]. Hence the order of R_F values reported in previous work is still valid, *i.e.*, $ROCH_3 > ROH > R(OH)_n >$ RO–sugar.

Once the gradient for the selected standards had been optimized, it was employed for the analysis of the chamomile extract. The results are reported in Fig. 3. A regular distribution of the bands is observed, making further gradient optimization no longer necessary. Some components of the sample were identified by comparison

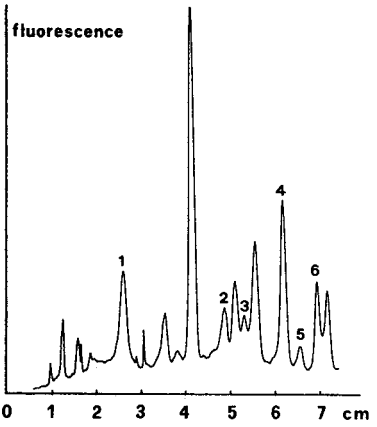

Fig. 3. Densitogram of the chamomile sample. The separation was obtained with the optimized gradient shown in Fig. 2. Peaks: 1 = apigenin 7-O-glucoside; 2 = caffeic acid; 3 = apigenin; 4 = umbelliferone; 5 = ferulic acid; 6 = herniarin.

between their retentions and the R_F values of the reference compounds and by standard addition. However, control of their purity has not yet been achieved. This aspect together with quantitative implications will be subject of further studies.

In conclusion, the AMD–HPTLC approach appears to be appropriate for the analysis of phenolic compounds because of its enhanced screening possibilities with respect to traditional TLC techniques. Further, gradient development on silica gel plates may be useful for the analysis of natural extracts as it often allows simpler clean-up procedures.

REFERENCES

1 J. B. Harborne, *Phytochemical Methods*, Chapman & Hall, London, 1984, p. 37.
2 L. W. Wulf and C. W. Nagel, *J. Chromatogr.*, 116 (1976) 271.
3 C. Redaelli, L. Formentini and E. Santaniello, *Planta Med.*, 42 (1981) 288.
4 K. Hostettmann and M. Hostettmann, in J. B. Harborne and T. J. Mabry (Editors), *The Flavonoids: Advances in Research*, Chapman & Hall, London, 1982, p. 1.
5 F. Villeneuve, G. Abravanel, M. Moutounet and G. Alibert, *J. Chromatogr.*, 234 (1982) 131.
6 K. Vande Casteele, H. Geiger and C. F. Van Sumere, *J. Chromatogr.*, 258 (1983) 111.
7 J. M. Andersen and W. B. Pedersen, *J. Chromatogr.*, 259 (1983) 131.
8 J. B. Harborne and M. Boaerdley, *J. Chromatogr.*, 299 (1984) 377.
9 J. B. Harborne, in E. Heftman (Editor), *Chromatography, Part B: Applications (Journal of Chromatography Library*, Vol. 22B), Elsevier, Amsterdam, 1986, p. 40.
10 D. J. Daigle and E. J. Conkerton, *J. Liq. Chromatogr.*, 11 (1988) 309.
11 E. C. Bate-Smith and R. G. Westall, *Biochim. Biophys. Acta*, 4 (1950) 427.
12 E. Stahl and P. J. Schorn, *Hoppe-Seyler's Z. Physiol. Chem.*, 325 (1961) 263.
13 K. Egger, in E. Stahl (Editor), *Thin Layer Chromatography*, Springer, Berlin, 1969, p. 686.
14 A. Hiermann and Th. Kartnig, *J. Chromatogr.*, 140 (1977) 322.
15 P. P. S. Schmid, *J. Chromatogr.*, 157 (1978) 217.
16 A. Hiermann, *J. Chromatogr.*, 174 (1979) 478.
17 M. Vanhaelen and R. Vanhaelen-Fastré, *J. Chromatogr.*, 187 (1980) 255.
18 H. Wagner, S. Bladt and E. M. Zgainski, *Plant Drug Analysis*, Springer, Berlin, 1984.
19 D. Heimler, *J. Chromatogr.*, 366 (1986) 407.
20 F. Dondi, Y. D. Kahie, G. Lodi, P. Reschiglian, M. Remelli and C. Bighi, *Anal. Chim. Acta*, 191 (1986) 261.
21 K. Burger, *Fresenius' Z. Anal. Chem.*, 318 (1984) 228.
22 D. E. Jaenchen, in R. E. Kaiser (Editor), *Proceedings of the IIIrd International Syposium on Instrumental HPTLC (Würzburg)*, Institut für Chromatographie, Bad Dürkheim, 1985, p. 71.
23 K. Burger and H. Tengler, in R. E. Kaiser (Editor), *Planar Chromatography*, Hüthig, Heidelberg, 1986, p. 193.
24 D. E. Jaenchen, *J. Liq. Chromatogr.*, 11 (1988) 1941.
25 J. A. Perry, K. W. Haag and L. J. Glunz, *J. Chromatogr. Sci.*, 11 (1973) 447.
26 C. F. Poole and S. K. Poole, *Anal. Chem.*, 61 (1989) 1257A.
27 S. Ebel, H.-J. Bigalke and S. Voelkl, in H. Traitler, A. Studer and R. E. Kaiser (Editors), *Proceedings of the IVth International Symposium on Instrumental HPTLC (Selvino)*, Institut für Chromatographie, Bad Dürkheim, 1987, p. 113.
28 R. Kunde and O. Isaac, *Planta Med.*, 37 (1979) 124.

Journal of Chromatography, 511 (1990) 402–403
Elsevier Science Publishers B.V., Amsterdam

CHROM. 22 444

Letter to the Editor

Influence of pressure on the maximum production rate in preparative liquid chromatography

Sir,

The influence of the available inlet pressure on the production rate in preparative chromatography is an important practical problem. It is critical that the users understand it properly. Snyder and Cox[1] have recently published a paper discussing the optimization of the experimental conditions for maximum production rate in preparative chromatography, in the touching band case. In this pedestrian reformulation of the classical treatment by Knox and Pyper[2], these authors make the following commentary: "Golshan-Shirazi and Guiochon[3] pointed out that there is an optimum pressure for a given preparative separation, which is true but misleading. Their optimum pressure corresponds to the case when the reduced velocity $\nu \ll 3$, which is never a good choice in practice [*i.e.*, this case corresponds to lower N_0 (column plate number for a small sample) and longer run time]. In any case, pressures larger than their "optimum" can in principle always be used to achieve higher production rate by using larger particles (so as to increase ν). Of course practical considerations of various kinds impose very definite limits on maximum pressure". This statement prompts *two* comments on our part.

First, in our referenced paper[3], at the bottom of p. 1376, we have written: "It is seen [in Fig. 6c] that the production rate increases steadily with increasing pressure at which the equipment can operate, provided the optimum column is used". Similar comments can be found in other places, all underlining the gain in production rate associated with operating the column at high velocities and trading a reduction in the column efficiency for a decrease in the cycle time. In other words, our conclusions are precisely the opposite of what Snyder and Cox have incorrectly stated as being in our work.

To correct the record:

(i) The maximum production rate which can be achieved for any given separation increases with increasing available inlet pressure. This is illustrated in Fig. 6c of ref. 3. However, the optimum values of the column length, particle size, mobile phase velocity and sample size which permit the achievement of this maximum production rate vary also with the available pressure.

(ii) For a given column (*i.e.*, constant column length and particle diameter), there is an optimum inlet pressure, since there is an optimum mobile phase velocity[3]. The lowest value of ν considered in Tables V–XI of ref. 3 is 55, a number considerably larger than the $\nu \ll 3$ misquoted by Snyder and Cox[1]. Fig. 11 of ref. 3 shows that, for a given column, the production rate increases with increasing ν up to 100, where the plot stops.

0021-9673/90/$03.50

(iii) In practice, for most separations and for a given value of the inlet pressure, the optimum value of v is very high, often several hundred. This result has been obtained by theoretical analysis of the solutions of the mass balance equations of chromatography[3], as well as by a Simplex optimization of the experimental conditions[4].

Secondly, we have always believed in the promise: "Then you will know the Truth, and the Truth will make you free"[5], a promise which applies well to science. It is difficult to understand how a truth may be misleading, unless it is presented deviously so as to mislead the reader as occurred in ref. 1. In their classical paper, Knox and Pyper[2] noted that their approach neglected the competition between the mixture components for interaction with the stationary phase. The authors of the present paper[1] suggest optimum conditions which are incorrect since we know that components interact in accordance with the displacement and tag-along effects[6,7], with experimental proof in refs. 8 and 9.

We are at a loss to understand the origin of the factual error made in ref. 1 and regret that the review process was unable to catch it.

SADRODDIN GOLSHAN-SHIRAZI
and GEORGES GUIOCHON*

**Department of Chemistry, University of Tennessee, Knoxville, TN 37996-1600 and Division of Analytical Chemistry, Oak Ridge National Laboratory, Oak Ridge, TN 37831-6120 (U.S.A.)*

1 L. R. Snyder and G. B. Cox, *J. Chromatogr.*, 483 (1989) 85.
2 J. H. Knox and H. M. Pyper, *J. Chromatogr.*, 363 (1986) 1.
3 S. Golshan-Shirazi and G. Guiochon, *Anal. Chem.*, 61 (1989) 1368.
4 S. Ghodbane and G. Guiochon, *Chromatographia*, 26 (1989) 53.
5 John, 8:32
6 G. Guiochon and S. Ghodbane, *J. Phys. Chem.*, 92 (1988) 3682.
7 S. Golshan-Shirazi and G. Guiochon, *J. Phys. Chem.*, 93 (1989) 4143.
8 J. Newburger and G. Guiochon, *J. Chromatogr.*, 484 (1989) 153.
9 A. M. Katti and G. Guiochon, *J. Chromatogr.*, 499 (1990) 5.

(Received February 7th, 1990)

Journal of Chromatography, 511 (1990) 404–405
Elsevier Science Publishers B.V., Amsterdam

CHROM. 22 482

Letter to the Editor

Influence of pressure on the maximum production rate in preparative liquid chromatography

Reply to the letter of S. Golshan-Shirazi and G. Guiochon

Sir,

We welcome the opportunity to comment on the letter of Golshan-Shirazi and Guiochon[1] with respect to our previous paper[2]. These authors cite a specific passage from ref. 2 and then proceed to generalize on the remainder of that article. Concerning the specific passage (which deals with their own published work[3]), we can say that (a) the passage represents a misinterpretation on our part of Fig. 6 for ref. 3, and (b) this error was further compounded by an intuitive —but totally wrong— analysis of the misinterpretation. Unfortunately two "wrongs" did not make a "right". We are also surprised that this obvious error was not caught during inhouse reviews or its subsequent processing by three outside reviewers for the journal. However, the text in question appears in ref. 2 as a footnote which in no way compromises the remaining discussion or conclusions of that paper.

The more important issue raised by Golshan-Shirazi and Guiochon deals with the pertinence of our treatment[2] for separations which involve "... the competition between the mixture components for interaction with the stationary phase". They assume that the existence of this competition invalidates the various conclusions reached by Knox and Pyper[4] in their elegant treatment of preparative liquid chromatographic separation as a function of sample weight and volume, column efficiency and mobile phase strength. We disagree with this conclusion.

We have reported modeling studies[5] and supporting experimental data[6] which treat the case of the 2-compound sample in preparative liquid chromatography. This work shows for moderately overloaded columns (and consequent "touching band" separations as discussed by Knox and Pyper[4]) that sample interaction leads to a significant increase in allowable sample size *vs.* the case where interaction effects are ignored. This in turn increases the predicted production rate (grams per hour of purified product) by a constant factor (so-called "blockage effect") for a given value of the separation factor α), but it has little affect on the optimum value of the plate number N (for maximum production rate). For this case, therefore, the treatment of ref. 2 is still appropriate; our conclusions with regard to production rate as a function of column conditions, maximum allowable pressure, etc. are still valid.

We have since extended the conclusions of refs. 5 and 6 (see also ref. 7) to the case of more heavily overloaded separations —where the two bands leaving the col-

0021-9673/90/$03.50

umn overlap more or less extensively[8]. Again we find that interaction effects lead to higher sample loadings than are predicted in the absence of interaction, but the effect on conditions for maximum production rate is parallel to that shown by Knox and Pyper[4] for touching-band separations with no interaction. Thus, for recovery of a certain fraction of product charged to the column (50, 95 or 99%), a larger sample weight can be separated and a lower plate number is required. However, the optimum choice of column conditions (particle size, column length, flow-rate) is still understandable in terms of the treatment of ref. 2. These optimum column conditions depend on two factors: the value of α for the separation in question and the desired recovery of purified product.

The simplifications suggested by the Knox-Pyper treatment[4] have since been found[9] to provide a comparable picture of preparative liquid chromatographic separations that use gradient elution. However, these advances in our understanding of preparative liquid chromatography necessarily involve some compromise. A more rigorous treatment as developed by Guiochon and his collaborators in several dozen recent papers should in principle be more accurate for specific cases. Our aim has instead been the uncovering of more general (and more approximate) recommendations that can facilitate the practical development of liquid chromatography methods for preparative separation. Similar differences in approach characterize much of chromatography; practical chromatographers have generally benefitted from both the complex, rigorous treatment and its simplified, more approximate counterpart. We welcome quantitative comparisons of these two approaches, so that any limitations of the simplified treatment can be made known.

LC Resources Inc., 3182C Old Tunnel Road, Lafayette, CA 94549 (U.S.A.) L. R. SNYDER

ProChrom Inc., 5622 W 73rd Street, Indianapolis, IN 46278 (U.S.A.) and G. B. COX

1 S. Golshan-Shirazi and G. Guiochon, *J. Chromatogr.*, 511 (1990) xxx,
2 L. R. Snyder and G. B. Cox, *J. Chromatogr.*, 483 (1989) 85.
3 S. Golshan-Shirazi and G. Guiochon, *Anal. Chem.*, 61 (1989) 1368.
4 J. H. Knox and H. M. Pyper, *J. Chromatogr.*, 363 (1986) 1.
5 J. E. Eble, R. L. Grob, P. E. Antle and L. R. Snyder, *J. Chromatogr.*, 405 (1987) 1.
6 J. E. Eble, R. L. Grob, P. E. Antle, G. B. Cox and L. R. Snyder, *J. Chromatogr.*, 405 (1987) 31.
7 L. R. Snyder, G. B. Cox and P. E. Antle, *Chromatographia*, 24 (1987) 82.
8 L. R. Snyder, J. W. Dolan and G. B. Cox, *J. Chromatogr.*, 483 (1989) 63.
9 L. R. Snyder, J. W. Dolan and G. B. Cox, *J. Chromatogr.*, in preparation.

(Received March 21st, 1990)

Author Index

Erratum

J. Chromatogr., 504 (1990) 391–401

Page 391, Summary, third sentence should read

"The individual truxillines were characterized via high-performance liquid chromatography–diode array detection, capillary gas chromatography–electron capture detection, capillary gas chromatography–electron ionization mass spectrometry and capillary supercritical fluid chromatography–flame ionization detection."

Page 395, 4th text line, "tritium" should read "3-H".

PUBLICATION SCHEDULE FOR 1990

Journal of Chromatography and Journal of Chromatography, Biomedical Applications

MONTH	J	F	M	A	M	J	J	A	S
Journal of Chromatography	498/1 498/2 499	500 502/1	502/2 503/1 503/2 504/1	504/2 505/1	505/2 506 507 508/1	508/2 509/1 509/2 510	511 512 513	514/1 514/2 515	The publication schedule for further issues will be published later
Cumulative Indexes, Vols. 451–500		501							
Bibliography Section		524/1		524/2		524/3		524/4	
Biomedical Applications	525/1	525/2	526/1	526/2 527/1	527/2	528/1 528/2	529/1	529/2 530/1	530/2

INFORMATION FOR AUTHORS

(Detailed *Instructions to Authors* were published in Vol. 478, pp. 453–456. A free reprint can be obtained by application to the publisher, Elsevier Science Publishers B.V., P.O. Box 330, 1000 AH Amsterdam, The Netherlands.)

Types of Contributions. The following types of papers are published in the *Journal of Chromatography* and the section on *Biomedical Applications:* Regular research papers (Full-length papers), Notes, Review articles and Letters to the Editor. Notes are usually descriptions of short investigations and reflect the same quality of research as Full-length papers, but should preferably not exceed six printed pages. Letters to the Editor can comment on (parts of) previously published articles, or they can report minor technical improvements of previously published procedures; they should preferably not exceed two printed pages. For review articles, see inside front cover under Submission of Papers.

Submission. Every paper must be accompanied by a letter from the senior author, stating that he is submitting the paper for publication in the *Journal of Chromatography*. Please do not send a letter signed by the director of the institute or the professor unless he is one of the authors.

Manuscripts. Manuscripts should be typed in double spacing on consecutively numbered pages of uniform size. The manuscript should be preceded by a sheet of manuscript paper carrying the title of the paper and the name and full postal address of the person to whom the proofs are to be sent. Authors of papers in French or German are requested to supply an English translation of the title of the paper. As a rule, papers should be divided into sections, headed by a caption (*e.g.*, Summary, Introduction, Experimental, Results, Discussion, etc.). All illustrations, photographs, tables, etc., should be on separate sheets.

Introduction. Every paper must have a concise introduction mentioning what has been done before on the topic described, and stating clearly what is new in the paper now submitted.

Summary. Full-length papers and Review articles should have a summary of 50–100 words which clearly and briefly indicates what is new, different and significant. In the case of French or German articles an additional summary in English, headed by an English translation of the title, should also be provided. (Notes and Letters to the Editor are published without a summary.)

Illustrations. The figures should be submitted in a form suitable for reproduction, drawn in Indian ink on drawing or tracing paper. Each illustration should have a legend, all the *legends* being typed (with double spacing) together on a *separate sheet*. If structures are given in the text, the original drawings should be supplied. Coloured illustrations are reproduced at the author's expense, the cost being determined by the number of pages and by the number of colours needed. The written permission of the author and publisher must be obtained for the use of any figure already published. Its source must be indicated in the legend.

References. References should be numbered in the order in which they are cited in the text, and listed in numerical sequence on a separate sheet at the end of the article. Please check a recent issue for the layout of the reference list. Abbreviations for the titles of journals should follow the system used by *Chemical Abstracts*. Articles not yet published should be given as "in press" (journal should be specified), "submitted for publication" (journal should be specified), "in preparation" or "personal communication".

Dispatch. Before sending the manuscript to the Editor please check that the envelope contains three copies of the paper complete with references, legends and figures. One of the sets of figures must be the originals suitable for direct reproduction. Please also ensure that permission to publish has been obtained from your institute.

Proofs. One set of proofs will be sent to the author to be carefully checked for printer's errors. Corrections must be restricted to instances in which the proof is at variance with the manuscript. "Extra corrections" will be inserted at the author's expense.

Reprints. Fifty reprints of Full-length papers, Notes and Letters to the Editor will be supplied free of charge. Additional reprints can be ordered by the authors. An order form containing price quotations will be sent to the authors together with the proofs of their article.

Advertisements. Advertisement rates are available from the publisher on request. The Editors of the journal accept no responsibility for the contents of the advertisements.

For Superior Chiral Separation

The finest from DAICEL……

Why look beyond DAICEL? We have developed the finest CHIRALCEL, CHIRALPAK and CROWNPAK with up to 17 types of HPLC columns, all providing superior resolution of racemic compounds.

NEW CHIRALPAK AS

NEW CHIRALPAK AD

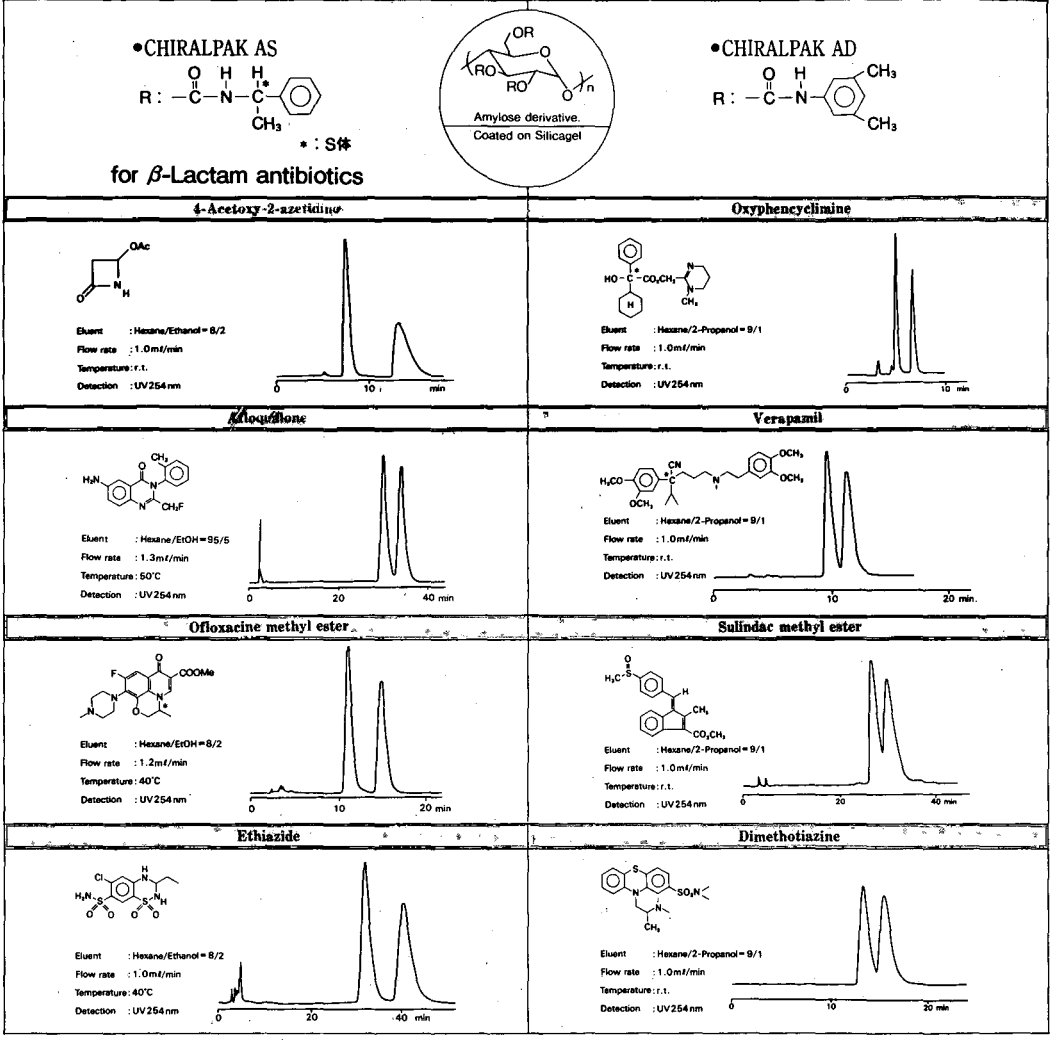

■Separation Service

- A pure enantiomer separation in the amount of 100g~10kg is now available.
- Please contact us for additional information regarding the manner of use and application of our chiral columns and how to procure our separation service.

DAICEL CHEMICAL INDUSTRIES, LTD.

8-1, Kasumigaseki 3-chome, Chiyoda-ku, Tokyo 100, Japan Phone: 03 (507) 3151 FAX: 03 (507) 3193

DAICEL(U.S.A.), INC.
Fort Lee Executive Park
Two Executive Drive, Fort Lee,
New Jersey 07024
Phone: (201) 461-4466
FAX: (201) 461-2776

DAICEL(U.S.A.), INC.
23456 Hawthorne Blvd.
Bldg. 5, Suit 130
Torrance, CA 90505
Phone: (213) 791-2030
FAX: (213) 791-2031

DAICEL(EUROPA)GmbH
Oststr. 22
4000 Düsseldorf 1, F.R. Germany
Phone: (211) 369848
Telex: (41) 8588042 DCEL D
FAX: (211) 364429

DAICEL CHEMICAL(ASIA)PTE. LTD.
65 Chulia Street #40-07
OCBC Centre, Singapore 0104
Phone: 5332511
FAX: 5326454